
Experimental and Kinetic Studies of the *Escherichia coli* Glucuronylsynthase:

An Engineered Enzyme for the Synthesis of Glucuronides

A thesis submitted for the degree of Doctor of Philosophy of

The Australian National University

by

Shane M. Wilkinson



THE AUSTRALIAN NATIONAL UNIVERSITY

Research School of Chemistry

Australian National University

September 2010

Declaration

This thesis is a summary of work carried out in the School of Chemistry, The University of Sydney and the Research School of Chemistry, Australian National University, under the supervision of Dr Malcolm McLeod between August 2006 and August 2010. This thesis contains no material which has been accepted for the award of any degree in any university. No other person's work has been used without due acknowledgement and every effort has been made to acknowledge previously published material. This thesis contains less than 100,000 words in accordance with Australian National University guidelines.

Sections of original work described in this manuscript have been published in peer-reviewed scientific journals, namely:

“Escherichia coli Glucuronylsynthase: An Engineered Enzyme for the Synthesis of β -Glucuronides” Wilkinson, S. M.; Liew, C. W.; Mackay, J. P.; Salleh, H. M.; Withers, S. G.; McLeod, M. D. *Org. Lett.* **2008**, *10*, 1585.

Shane Wilkinson

Acknowledgements

To begin, I would like to thank my supervisor Dr Mal McLeod for all his support and giving me the opportunity to work on such an interesting and challenging project. He has been a brilliant mentor, colleague and friend whose chemical knowledge knows no boundaries. He would always be thinking about the project and continually developing new angles to take the research. I remember first approaching him at Sydney University in the hunt for an Honours project. During the interview he asked the question, "What are you looking for in a project?" to which my reply was "Something incorporating biochemistry and organic chemistry". Unbeknownst to me, he had just returned from a sabbatical at UBC to initiate the glucuronylsynthase project. It was surely fate that brought us together.

My research involving molecular biology could have been done if not for the assistance of Prof. Stephen Withers (UBC), Prof. Joel Mackay (USyd) and Prof. David Ollis (ANU) and their research groups. My project would not exist if it were not for Prof. Stephen Withers and his research group. I thank him for his discovery of glycosynthases and his research group for constructing the genetic material to express the glucuronylsynthase. I would like to thank the Mackay (USyd) and Ollis (ANU) labs for their hospitality and provision of resources for the protein expression which would not normally be present in a standard chemistry laboratory.

My chemical research could not have been complete without the aid of technical staff at Sydney University and ANU involved with operating machinery or servicing the storerooms. In particular, I would like to thank Kelvin Picker (USyd) and Tony Herlt (ANU) for passing on their extensive knowledge of HPLC which I will find priceless in years to come. I thank Ian Luck (USyd), Chris Blake (ANU) and Gottfried Otting (ANU) for their NMR expertise (especially Gottfried who operates the 800 MHz NMR with such grace and ease he would have a spectrum on screen before I type my first command!). I accredit the elucidation of my crystal structures to Tony Willis (ANU).

I thank the various funding organisations for their generous assistance; in particular, I thank Sydney University and ANU for awarding me a PhD

scholarship. This was generously supplemented by the RSC, Agnes Campbell benefaction (USyd), Alan Sargeson benefaction (ANU) and the Royal Australian Chemical Institute (RACI). Certain compounds were generously donated by the National Measurement Institute and NSW Horse Racing Forensic laboratories.

My thanks go out to the McLeod Research group, both past and present. In particular, I would like to thank those group members who have aided my advancement in the project. These colleagues include Dr Morgan Watson (who joined the group in my final year of the project to perform the biological tasks associated with the project) and Luke Pasfield (who aided my studies with the steroid solubility).

To the other group members, I thank them for their technical support, companionship, and “regular” coffee breaks which made the three and a half years in the lab an enjoyment. Thank you Joey for passing on your words-of-wisdom, instilling good lab practices and cleanliness (I will enforce these practices in future occupations) and your futile attempt to restore normality in the lab. Dwain for passing on your “words-of-wisdom”, defining the lab “rules” and teaching me proper etiquette. I thank Belinda (for her seemingly endless supply of sugar treats for the lab which kept my productivity at hyperactive levels), Rhiannon (for having dinner on the table after a late night in the lab despite my assurance earlier that day that I would get home early enough to cook a roast dinner), Luke (for his involvement in the project and weekly Rugby goss) and Masruri (for his interesting insight to chemistry and life in Indonesia). Lastly, I would like to thank my good friend and “adopted” McLeod member Andrew for his willingness to always go out of his way to lend a hand and his unmerciful training regime (the gym won’t be the same without you big guy!).

Thank you to all my friends at USyd and the RSC for your daily interactions and chemical input. I am sure our paths will cross once again at future conferences and travels. Thank you to my “non-chemistry” friends whom have put up and understood my absence over this busy period (I promise to catch up with you all soon!). A huge thanks goes to my family, especially my parents, who have supported me throughout my university life and ensured that my visits home were not without the bare necessities (home-cooked dinners, clean clothes, adequate sleep) during this busy time.

And finally to my partner Alexandra, whose love and support throughout my study has been amazing. You remained by my side even when my research took me interstate and understood the importance of the time I spent researching. I am certain you no longer trust my judgement of time when it comes to chemistry. There were numerous accounts when I would say, “I would be home in about an hour” only to work through the door many, many hours later! I promise to make up for those hours with interest. Four years is short in comparison to the future ahead of us.

Abstract

The *E. coli* glucuronylsynthase is a glycosynthase enzyme derived from *E. coli* β -glucuronidase. It catalyses the conjugation of a glucopyranuronic acid unit to an alcohol acceptor. These glucuronide conjugates are important markers for doping in sports drug testing and drug metabolism in pharmaceutical trials. Up till now, the optimal glucuronylsynthase reaction conditions were unknown which may have reduced the previously reported yields.

This thesis covers the development and optimisation of the glucuronylsynthase-mediated glucurylation reaction. This was achieved by determining the enzyme kinetics associated with the glucuronylsynthase enzyme and devising a synthetic strategy to overcome the water solubility issues associated with steroidal substrates.

HPLC-UV was used to monitor and quantitate the components of the glucuronylsynthase reaction required for enzyme kinetic analysis. This HPLC assay was used to determine the kinetic parameters (K_m , k_{cat}) of the α -D-glucuronyl fluoride **51** donor and a range of acceptor substrates. Substrate inhibition and product inhibition were observed during these kinetic investigations and inhibition constants are determined in each case.

The optimised glucuronylsynthase-mediated reaction conditions were also determined using HPLC-UV. Different variations (pH, temperature, enzyme concentration, substrate concentration/equivalents) were altered and their effect on enzyme activity and product yield determined by HPLC-UV. Improved reaction rates and yield were observed in the glucuronylsynthase reactions involving phenol **52** and DHEA O-(carboxymethyl)oxime **116** when applying optimised conditions.

To overcome the poor water solubility of steroidal substrates, carboxymethylamine **115** was condensed to the ketone of DHEA **55** and testosterone **7** to synthesise ionisable oxime analogues with greatly enhanced water solubility. This provided greater yields of the steroid glucuronide conjugates compared to the direct glucuronylsynthesis of the parent steroids. Greater enzyme efficiency was also achieved due to more concentrated

reaction volumes being used. The oxime moiety was cleaved under mild titanium(III) hydrolysis to complete the synthesis of the steroid glucuronide conjugate in high overall yields in three steps. Application of this steroid solubilisation strategy on a half gram scale was demonstrated.

A solid-phase extraction procedure was adapted to a small library of steroids to isolate a variety of purified steroid glucuronides. This screen illustrated the broad application of the enzyme and served as a trial for a larger screen of substrates. The combination of the optimised methodology and screening procedures sets the foundation to expand the substrate repertoire for the glucuronylsynthase reaction.

Upon reviewing the glucuronylsynthase procedure and alternate means of glucuronylation, the glucuronylsynthase procedure compares well, and is better than these alternative procedures in many ways. This includes an experimental procedure that is easy to set-up, mild and applicable to a broad range of substrates. Other attributes include a short and simple donor synthesis and the absence of by-products (to date) which allows high isolated yields and purity.

Table of contents

Declaration.....	ii
Acknowledgements.....	iii
Abstract.....	vi
Table of contents	viii
Abbreviations and acronyms	x
Symbols and units.....	xiii
Nomenclature.....	xvi
~ CHAPTER 1 ~ INTRODUCTION.....	1
1.1 Drug metabolism.....	2
1.2 Glucuronides in sports drug testing.	3
1.3 Glucuronides in pharmaceuticals.	5
1.4 Glucuronides in agriculture.	6
1.5 Current methods of glucuronylation.....	7
1.6 β -Glucuronidase enzyme.....	11
1.7 Glycosynthases and the genetically-modified β -glucuronidase enzyme	14
1.8 Early results	16
1.9 Project proposal.....	20
~ CHAPTER 2 ~ THE GLUCURONYLSYNTHASE SYSTEM.....	22
2.1 Overview	23
2.2 The recombinant <i>E. coli</i>	23
2.3 Glucuronylsynthase crystal structure.....	30
2.4 Synthesis of the ammonium 1-deoxy-1-fluoro α -D-glucopyranuronate (α -D-glucuronyl fluoride).....	33
2.5 Expanding the scope of the glucuronylsynthase methodology	35
~ CHAPTER 3 ~ ENZYME KINETICS	48
3.1 Introduction to enzyme kinetics	49
3.2 Glycosynthase kinetic assays.....	58
3.3 ^1H NMR assay	60
3.4 Isothermal titration calorimetry.....	66
3.5 HPLC-UV	72
3.6 Reaction optimisation	90
3.7 High-throughput assays.....	96
3.8 Conclusions from enzyme kinetics	107
~ CHAPTER 4 ~ STEROID SOLUBILISATION STRATEGY.....	109
4.1 Introduction	110
4.2 Glucuronylsynthesis of steroids.....	110
4.3 DHEA derivatives.....	113
4.4 De-oximation of the <i>O</i> -(carboxymethyl)oxime	123

4.5	Investigation the reaction variables of the DHEA O-(carboxymethyl)oxime glucuronylsynthase reaction.....	130
4.6	Product inhibition.....	135
4.7	Solubility strategy with testosterone.....	147
4.8	Conclusions.....	156
~ CHAPTER 5 ~ EXTENSION OF THE GLUCURONYLSYNTHASE METHODOLOGY TO OTHER STEROIDS.....		159
5.1	Introduction.....	160
5.2	Effects of additives on the glucuronylsynthase reactions	160
5.3	Additives Conclusion	168
5.4	Expansion of the steroid library	169
~ CHAPTER 6 ~ CONCLUSIONS AND FUTURE WORK.....		177
6.1	Comparative study	178
6.2	Conclusions.....	190
6.3	Future work	192
~ CHAPTER 7 ~ EXPERIMENTAL		195
7.1	General Experimental.....	196
7.2	Glucuronylsynthase expression	201
7.3	Synthesis of α -D-glucuronyl fluoride 51	210
7.4	Revised glucuronylsynthase reactions.....	213
7.5	Large scale glucuronylsynthase reaction.....	219
7.6	Kinetic resolution of racemic <i>trans</i> -2-methylcyclohexanol 39	220
7.7	^1H NMR assay	223
7.8	Isothermal titration calorimetry (ITC) assay	224
7.9	HPLC-UV assay	225
7.10	Reaction optimisation	234
7.11	In vitro chromo-ablative assay for directed evolution.....	236
7.12	In vitro fluoride-selective assay for directed evolution	241
7.13	Steroid glucuronylsynthase reactions	243
7.14	DHEA Derivatives.....	246
7.15	Kinetics with DHEA O-(carboxymethyl)oxime.....	253
7.16	Steroid solubility strategy with testosterone.....	257
7.17	Effect of additives on the glucuronylsynthase reactions	260
7.18	SPE methodology.....	261
~ CHAPTER 8 ~ NMR SPECTRA		273
~ CHAPTER 9 ~ X-RAY CRYSTAL DATA		313
9.1	Crystal structure of $\text{C}_6\text{H}_{12}\text{FNO}_6$ — mcl0801	314
9.2	Crystal structure of $\text{Na}_2\text{C}_{27}\text{H}_{37}\text{NO}_{10}\cdot\text{CH}_3\text{OH}$ — mcl0901	323
~ CHAPTER 10 ~ REFERENCES		339
~ CHAPTER 11 ~ PUBLICATIONS ARISING FROM THIS WORK.....		352

Abbreviations and acronyms

1FglucA – α -D-glucuronyl fluoride **51**

Ac - acetyl

ANU – Australia's National University

Bn – benzyl

bp – boiling point

brsm – based on recovered starting materials

CMO-DHEA – dehydroepiandrosterone O-(carboxymethyl)oxime **116**

CMO-DHEA Gluc - dehydroepiandrosterone O-(carboxymethyl)oxime
 β -D-glucuronide **118**

DCC - Dicyclohexylcarbodiimide

DCM - dichloromethane

DDM – *n*-dodecyl β -maltoside

decomp. - decomposition

DHEA – dehydroepiandrosterone **55**

DIPEA - diisopropylethylamine

DMAP – 4-dimethylaminopyridine

DMF – *N,N*-dimethylformamide

DMSO - dimethylsulfoxide

E. coli – *Escherichia coli*

E413 – glutamate residue at the 413th position of *E. coli* β -glucuronidase

E504A – genetically-modified *E. coli* β -glucuronidase with the glutamate residue at the 504th position replaced by alanine through site-directed mutation.

E504G – genetically-modified *E. coli* β -glucuronidase with the glutamate residue at the 504th position replaced by glycine through site-directed mutation.

E504S – genetically-modified *E. coli* β -glucuronidase with the glutamate residue at the 504th position replaced by serine through site-directed mutation.

ELISA – enzyme-linked immunosorbent assay

equiv. - equivalents

ESI – electron spray ionisation
Et – ethyl
GUS – WT β -glucuronidase
HPLC – high performance liquid chromatography
HRMS – high resolution mass spectrometry
IPTG – Isopropyl β -D-thiogalactopyranoside **81**
IR – infra-red
ITC – isothermal titration calorimetry
LB – Luria-Burtani media
LC-MS – liquid chromatography mass spectrometry
lit. – literature value
LRMS – low resolution mass spectrometry
MAX – mixed-mode anion exchange
*m*CPBA - *m*-chloroperoxybenzoic acid
Me – methyl
mp – melting point
MTPA – α -methoxy- α -trifluoromethyl- α -phenylacetyl
NMR – nuclear magnetic resonance
NOESY - nuclear overhauser effect spectroscopy
PDA – photodiode array detector
PEG – polyethylene glycol
Ph - phenyl
*p*NPG – *p*-nitrophenyl β -D-glucuronide
pyr - pyridine
ret – retention time
 R_f – retention factor
RT – room temperature
SDS – sodium dodecyl sulfate
SDS-PAGE – sodium dodecyl sulfate – polyacrylamide gel electrophoresis
SPE – solid phase extraction
t-BOC - *N-tert*-butoxycarbonyl
t-BuOH - *tert*-butanol

TEA – triethylamine
TEMED - *N,N,N',N'*-tetramethylethylenediamine
TEMPO - 2,2,6,6-tetramethylpiperidine-1-oxyl
Tf – triflate
THF - tetrahydrofuran
TLC – thin layer chromatography
TMS – trimethylsilyl
TMU - *N,N,N',N'*-tetramethylurea
TX-100 – Triton X-100
UBC – University of British Columbia
UDP - uridine 5'-diphospho
UGT – uridine 5'-diphospho glucuronosyltransferase
USyd – University of Sydney
UV – ultraviolet spectrum
WAX – weak anion exchange resin
WT – wildtype strain

Symbols and units

$^{\circ}\text{C}$ – degrees Celcius

ΔH – binding enthalpy

δ – chemical shift

$\Delta\delta$ – difference in chemical shift

λ_{em} – emission maximum

λ_{ex} – excitation maximum

\AA - Angstrom

a – concentration of first substrate

au – arbitrary units

b – concentration of second substrate

c – defines the shape of the sigmoidal curve of an isotherm ($= e_t \times K_a$)

d – days

e – concentration of enzyme

e_0 – initial concentration of enzyme

e_t – total enzyme concentration

g – gram

g – acceleration due to gravity

h = hour

Hz - hertz

i – inhibition concentration

$i_{0.5}$ – inhibition concentration that halves the velocity

xJ – NMR coupling constant where x defines the number of bonds between the two atoms. Undefined x values represent vicinal coupling constants.

K - Kelvin

K_A – association constant

kB – kilobases

k_{cat} – catalytic turnover

k_{cat}^{app} – catalytic turnover

k_{cat}/K_m – substrate specificity constant

K_D – dissociation constant

kDa – kiloDalton

K_{iA} – dissociation constant of first substrate

K_{iB} – dissociation constant of second substrate

K_{ic} – competitive inhibition constant

K_{iu} – uncompetitive inhibition constant

K_m – Michaelis constant, concentration to achieve $\frac{1}{2}V_{max}$

K_m^{app} – apparent Michaelis constant

K_{mA} – Michaelis constant of first substrate

K_{mB} – Michaelis constant of second substrate

kPa - kilopascal

K_{si} – substrate inhibition constant

L – litre

M – molar (moles per litre)

mg – milligram

MHz – megahertz

min - minutes

mL - millilitre

mM – millimolar

mm - millimetres

mmol – millimoles

mol – moles

MPa - megapascal

mV - milliVolt

nM – nanomolar

nm - nanometres

nmol - nanomoles

ppm – parts per million

q – heat released/absorbed

rpm – revolutions per minute

R^2 – co-efficient of determination in linear regression

s – second

μcal - microcalories

μL – microlitre

μM – micromolar

μm - micrometer

μmol - micromoles

μs - microseconds

V – volts

v - volume

v – velocity

v_0 – initial velocity

v/v – volume per volume

V_{max} – maximum velocity of the enzyme

$V_{\text{max}}^{\text{app}}$ – apparent maximum velocity of the enzyme

w/w – weight per weight

w/v – weight per volume

Nomenclature

This thesis follows the nomenclature outlined by the IUPAC guidelines. However, a summary of the carbohydrate and steroid nomenclature used in this thesis is provided below.

Carbohydrate nomenclature

The numbering for monosaccharides begins at the aldehyde carbon if drawn in a Fisher projection (Figure i). The symbols “D” and “L” refers to the configuration of the highest-numbered centre of chirality (which usually forms the bridging oxygen in the cyclic form). When the oxygen is positioned to the right of the Fisher projection (as drawn on C5 of Figure i), the carbohydrate is classed as a “D” sugar. The “L” sugar is the enantiomer of the “D” sugar.

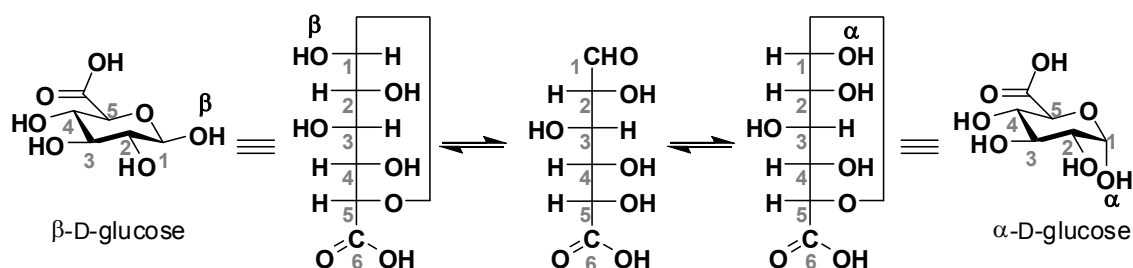


Figure i. Numbering of straight-chain and cyclic D-glucuronic acid.

The stereochemistry at the C1 carbon (anomeric carbon) is defined by the Greek letter “ α ” or “ β ” depending on its stereochemistry relative to the highest-numbered stereogenic centre in the Fisher projection. Substituents with a *cis* arrangement to the highest-numbered centre of chirality are classed α -anomers, whereas a *trans* arrangement provides the β -anomer (Figure i). The remaining stereocentres are also assessed by their relative stereochemistry (*cis/trans*) to the highest-numbered centre of chirality. However, the amalgamation of their stereochemistry is defined by trivial names. For example, the name glucose is given to the monosaccharide with the stereochemistry *2-cis,3-trans,4-cis* relative stereochemistry to the C5 carbon

The term “pyran” refers to the 6-membered cyclic configuration. When a carboxylic acid replaces the primary alcohol on the C6 of glucose, the systematic names change from glucose to glucuronic acid, glucoside to glucosiduronic acid, and glucosyl to glucosyluronic acid. Furthermore, the

carboxylate anion and esters of glucuronic acid are referred to as glucuronates. For simplicity reasons, the term *glucopyranosiduronic acid* will be shortened to *glucuronide* and *glucosyluronic acid* shortened to *glucuronyl*.

Steroid nomenclature

The numbering of positions and rings of steroids is depicted in Figure ii. With the structure drawn as depicted in Figure ii, any substituents drawn below the plane of paper (dashed bonds) are termed α (alpha) whilst substituents drawn above the plane of paper (thick wedge) are termed β (beta).

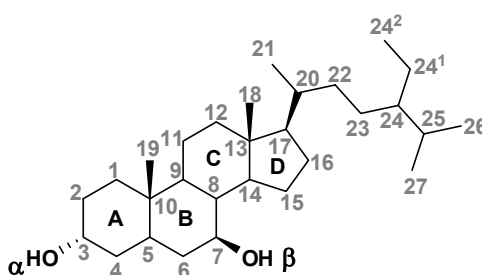


Figure ii. Numbering of the positions and rings of the steroid backbone.

There are names given to some core steroid nuclei (Figure iii). These names are used to describe the backbone of the steroid structure which is then modified to include the functional groups attached to that backbone analogous to standard IUPAC hydrocarbon nomenclature. A small range of steroid nuclei consisting of various C17 side-chains also exist (e.g. pregnane, cholane, cholestane, etc) but are excluded from this nomenclature summary as they will not be mentioned in this thesis.

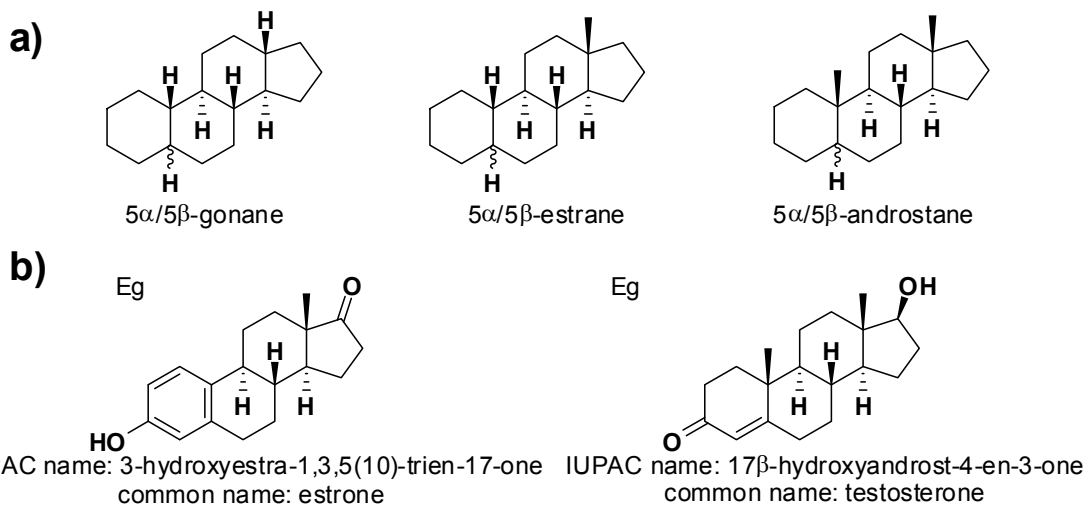


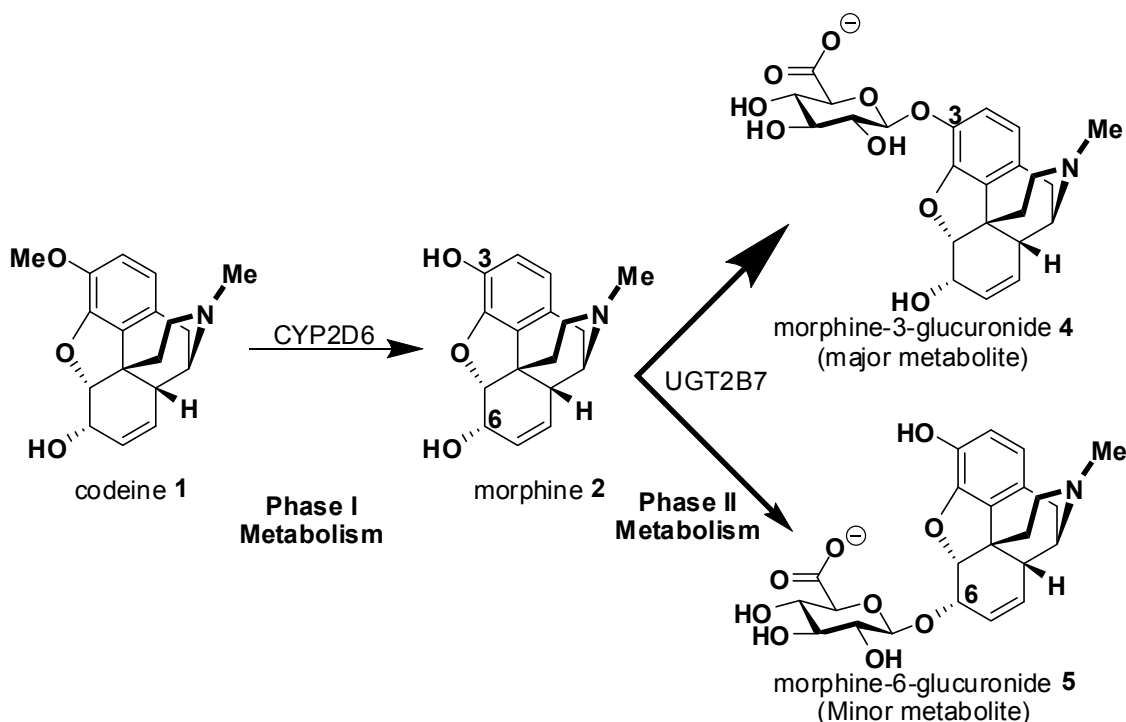
Figure iii. a) Some common steroid nuclei and b) examples of their use.

~ Chapter 1 ~

Introduction

1.1 Drug metabolism

Exogenous and endogenous molecules are eliminated from the body principally by excretion in urine. The hydrophilicity of a molecule is a major factor determining its rate of elimination from the body *via* urine - an aqueous medium. Hydrophilic drugs such as amphetamines, which possess a protonated amine at physiological pH, can be excreted in urine without undergoing metabolism. However, hydrophobic compounds, such as steroids, are less likely to enter into the aqueous medium and will remain in the body. These molecules will undergo metabolism by the body to increase the drug's hydrophilicity and allow renal excretion. This process is commonly known as *biotransformation*.



Scheme 1.1: Metabolism of codeine 1 to morphine 2 and its respective glucuronide metabolites (4 and 5).

Biotransformation can occur throughout the body, but the vast majority is carried out at the smooth endoplasmic reticulum of the liver cells (hepatocytes). Hydrophobic drugs can diffuse through the hepatocyte cell walls where they can be acted upon by an array of metabolising enzymes. There exist two classes of biotransformation. The first class is known as *phase I* metabolism and involves the chemical modification of the parent compound by such means as oxidation,

reduction and/or hydrolysis. For example, codeine **1** is metabolised by the cytochrome P450 enzyme (CYP2D6) to the more bioactive morphine **2** molecule (Scheme 1.1).

The second class of biotransformation, *phase II*, involves the conjugation of a drug to an endogenous molecule. The three primary conjugates are D-glucuronic acid **3**, sulfate, and glutathione. At physiological pH, these molecules are charged, so upon conjugation they enhance the drug's hydrophilicity, leading to its excretion from the body. The most common phase II conjugation is with D-glucuronic acid (Figure 1.1) **3** (pK_a 2.96), known as *glucuronylation*. Glucuronylation in humans is catalysed by uridine 5'-diphosphoglucuronosyltransferases (UGTs): a super-family of enzymes, comprised of many isoforms.¹ UGTs are able to conjugate activated glucuronic acid to an array of functional groups including alcohols, carboxylic acids, amines and thiols. Morphine **2** can undergo phase II metabolism by UGT2B7 (an isoform of UGT), on its phenol or hydroxyl substituent to form two different glucuronide metabolites: morphine-3-glucuronide **4** and morphine-6-glucuronide **5** respectively (Scheme 1.1).²

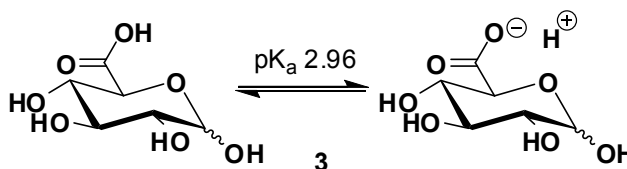


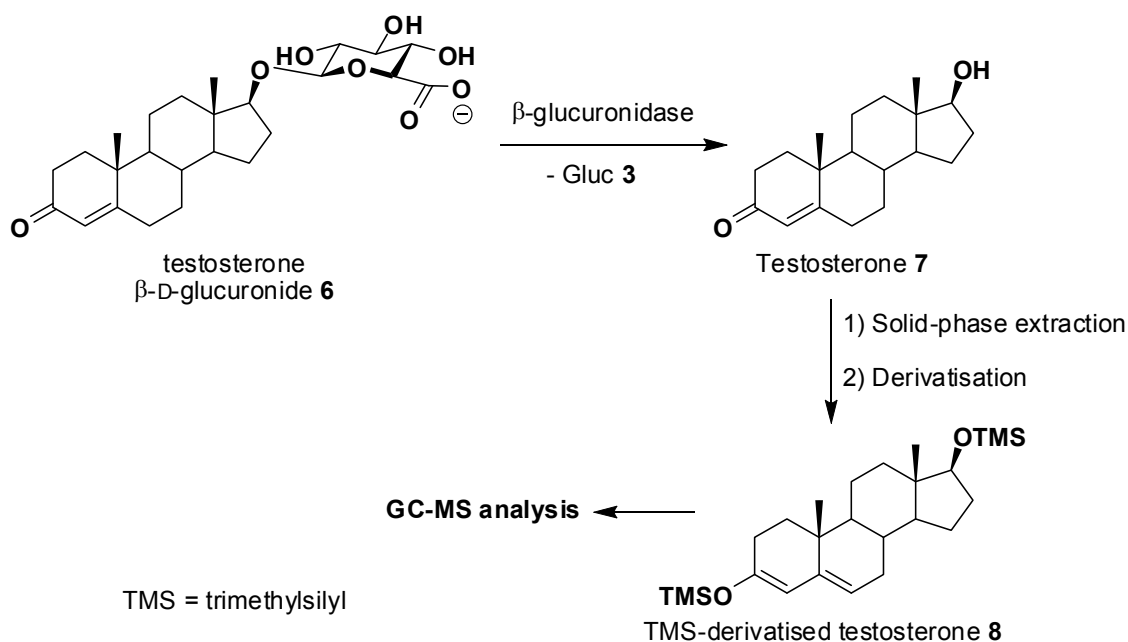
Figure 1.1: The pK_a of D-glucuronic acid **3**.³

1.2 Glucuronides in sports drug testing.

The use of drugs in an attempt to enhance sporting performance is known as “doping”. The World Anti-Doping Agency (WADA) was formed in 1998 to unify the standards on drug analysis following a large police drug raid at the Tour de France that exposed the degree of doping in sport. Its mission is to create a “level playing field” in sports, and educate athletes about the health risks involved with doping. Sport drug testing laboratories, such as the Australian Sports Drug Testing Laboratory (ASDTL) at the National Measurement Institute, screen for performance-enhancing drugs using the standards set down by WADA.

Introduction

Testing is predominately performed on urine samples in which most hydrophobic performance-enhancing drugs would have undergone phase I and/or phase II metabolism. Drugs such as anabolic androgenic steroids are predominately excreted as glucuronide metabolites.⁴ Direct analysis of these glucuronides proves difficult. Due to their instability towards heat, gas chromatography – mass spectroscopy (GC-MS) cannot be directly applied for analysis. Liquid chromatography – mass spectroscopy (LC-MS) avoids the heat, but requires an additional liquid-phase micro-extraction sample clean-up prior to analysis.⁵ Additionally, there is not always a glucuronide reference material available to validate LC-MS results. Therefore, the most commonly adopted protocol (Scheme 1.2) involves hydrolysis of the metabolites (such as testosterone β -D-glucuronide **6**) back to the parent compound (testosterone **7**), utilising *E. coli* β -glucuronidase, then derivatisation to the corresponding silyl ether **8** and analysis by gas chromatography/mass spectrometry using electron impact ionisation (GC-EIMS).⁶



Scheme 1.2. Steps required for the analysis of steroid glucuronides by GC-MS.

An inefficient work-up, such as an incomplete enzymatic hydrolysis, reduces the quantity of detectable hydrolysed drug and provides the laboratories with an underestimate of the degree of doping found from the athlete's urine sample. To solve this problem, known quantities of glucuronide reference materials (in particular isotope-labelled materials) can be added at the initial step and then

utilised to monitor the loss of material associated with each work-up step. The extent of the loss can provide information on the original concentration of metabolites prior to the work-up procedures. This provides the drug testing laboratory with a more accurate account of the degree of doping.

1.3 Glucuronides in pharmaceuticals.

All new pharmaceutical drugs must undergo various clinical trials before they can be approved by the respective pharmaceutical advisory board to be sold as a treatment. One of the trials each drug must pass is the toxicity assessment. The toxicity assessment examines how the parent compound is absorbed, metabolised and excreted, and aims to identify toxic effects in a broad range of situations.⁷ This study is required for various reasons. The first, and most important reason, is to assess any potential health risks that a drug, or any of its metabolites, may have on the body. The second reason is to assess a drug's pharmacokinetics which refers to the study of a drug's distribution throughout the body. It considers the half-life of the drug, its blood-lipid distribution (known as volume of distribution), the best means of administration, as well as its elimination or clearance from the body. Pharmacokinetics is vital in determining the maximum tolerated (toxic) dose, minimum therapeutic dose, and to design an effective dose regime (i.e. single dose or repeated doses over time).

In order to study the elimination or clearance of a drug from the body, extensive investigation must be undertaken to characterise and quantify every possible metabolite. As the drug under investigation is a new compound, no information or reference materials would be available for its metabolites. This investigation would be simplified if reference metabolites, such as glucuronides, could be obtained and be used as a comparison in their studies.

Codeine **1** is a well-characterised drug in terms of pharmacokinetics. Codeine **1** is converted to the more bioactive morphine **2** through phase I metabolism. Morphine **2** can then undergo glucuronylation to form two different glucuronide metabolites (Scheme 1.1). Glucuronylation of the phenol produces morphine-3-glucuronide **4**, which accounts for two-thirds of morphine **2** recovered in urine.⁸ Morphine-3-glucuronide **4** is a potent antagonist of morphine **2** and so accumulation of this metabolite reduces the efficacy of morphine **2**.⁹

Introduction

Glucuronylation of the hydroxyl substituent produces morphine-6-glucuronide **5**, which is present at 10% of the concentration of morphine-3-glucuronide **4** in plasma.⁸ Morphine-6-glucuronide **5** is pharmacologically active and displays greater agonistic properties for the μ 1 opioid receptor than morphine **2** itself, increasing the efficacy of morphine **2**.⁸ The example case- study of codeine **1** highlights the importance of metabolite monitoring in clinical trials. By quantifying the metabolites and their associated bioactivity, a therapeutic dose regime can be accurately designed.

1.4 Glucuronides in agriculture.

Monitoring of agricultural products is an ever-increasing field due to continual pressure placed on the standards required for the food we eat. In an attempt to increase cattle size, some farmers feed their cattle muscle-building androgens, or estrogens (that direct the body's resources into muscle development instead of the reproductive cycle). In 1988, the European Union (EU) placed a ban on the importation of hormone-treated meat. Concerns rose that the hormone-packed meat may disrupt the hormone levels of its consumers. Additionally, EU-funded studies have raised the concern that hormones are metabolised by cattle and the urine-excreted metabolites can run-off and contaminate waterways and/or other food sources.¹⁰ This ban has increased the demand for hormone glucuronide reference materials as EU importers screen meat for evidence of hormone-enhanced cattle. Similarly, cattle exporters, such as Australia and the USA, need to screen their exports to Europe to ensure hormone concentrations are below the EU standards to avoid costly rejections. Glucuronide metabolites are monitored in these screens.

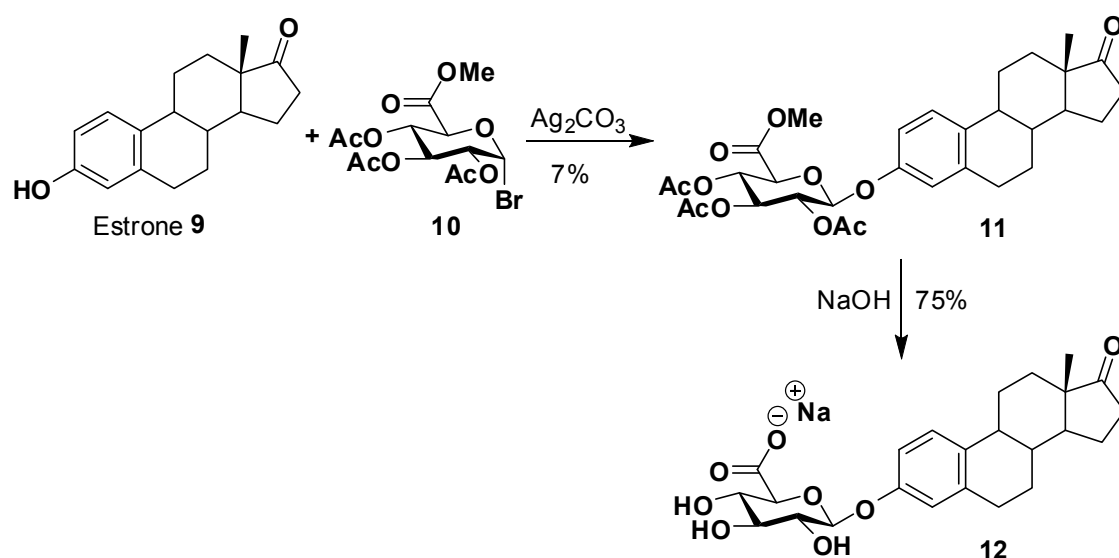
Another area of concern in agriculture is the presence of pesticide and herbicide residues. Pesticides are sprayed on the crops that cattle eat, as well as directly onto the cattle to treat parasites. These pesticides can also run-off to contaminate other food sources and waterways. As a result, meat, vegetation and waterways are screened for pesticides and their associated metabolites (such as glucuronides). Agencies such as Australia's National Measurement

Institute monitor these levels to ensure that the public are not exposed to high levels of these toxic compounds.

1.5 Current methods of glucuronylation

It is apparent from sections 1.1-1.4 that the monitoring of glucuronides is important in a wide variety of fields. Glucuronide standards are an essential commodity in the validation of glucuronide metabolites. However, these standards are often difficult and/or expensive to obtain, if they exist at all. The underlying reason is the absence of an efficient glycosylation method.¹¹ Low yields are frequently obtained due to the low reactivity between the glycosyl donor and the glycosyl acceptor (such as the secondary alcohol functions in the steroid moiety).

One of the oldest and still most commonly utilised glucuronylation procedures is the Koenigs-Knorr method (Scheme 1.3).¹² It involves the glucuronylation of an acceptor alcohol/phenol (e.g. estrone **9**) with a protected α -glycosyl halide (e.g. methyl 2,3,4-tri-*O*-acetyl- α -D-glucopyranosyluronate bromide **10**) in the presence of a heavy metal salt, Lewis acid or phase-transfer catalyst.¹³⁻²⁰

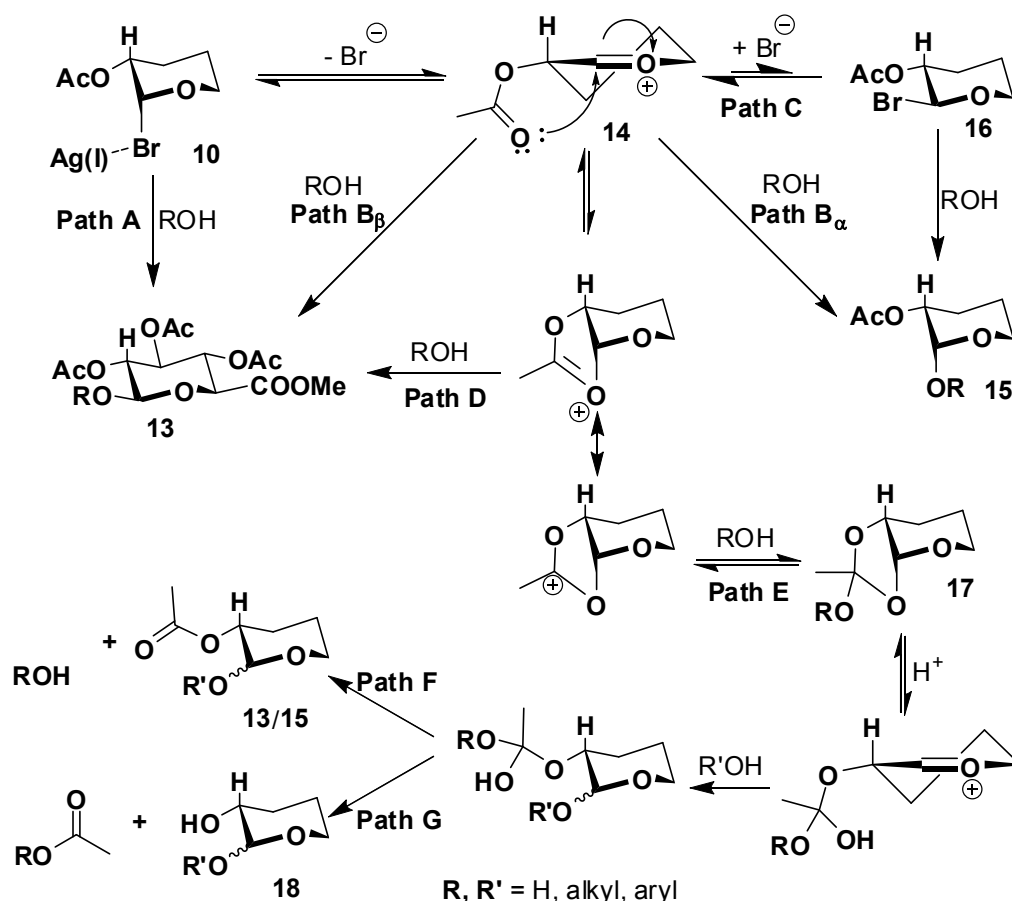


Scheme 1.3: Methyl 2,3,4-tri-*O*-acetyl- α -D-glucopyranosyluronate bromide (**10**) is coupled to estrone (**9**) via Koenigs-Knorr method. Subsequent deacetylation of the protected estrone glucuronide (**11**) produces the estrone 3- β -D-glucuronide (**12**).

There are many disadvantages associated with the Koenigs-Knorr method. Of most concern is the likely formation of by-products. The majority of Koenigs-Knorr reactions are only stereoselective due to the multiple pathways possible

Introduction

in the reaction (Scheme 1.4).²¹ The protected β -glucuronide product **13** can form from the S_N2 mechanism with the α -glucuronyl halide **10** (Path A) or through a S_N1 mechanism that occurs via an oxocarbenium intermediate **14** (Path B $_{\beta}$). The α -glucuronide product **15** can occur as a result of a S_N1 mechanism (Path B $_{\alpha}$) or via a β -glucuronyl halide intermediate **16** (Path C).



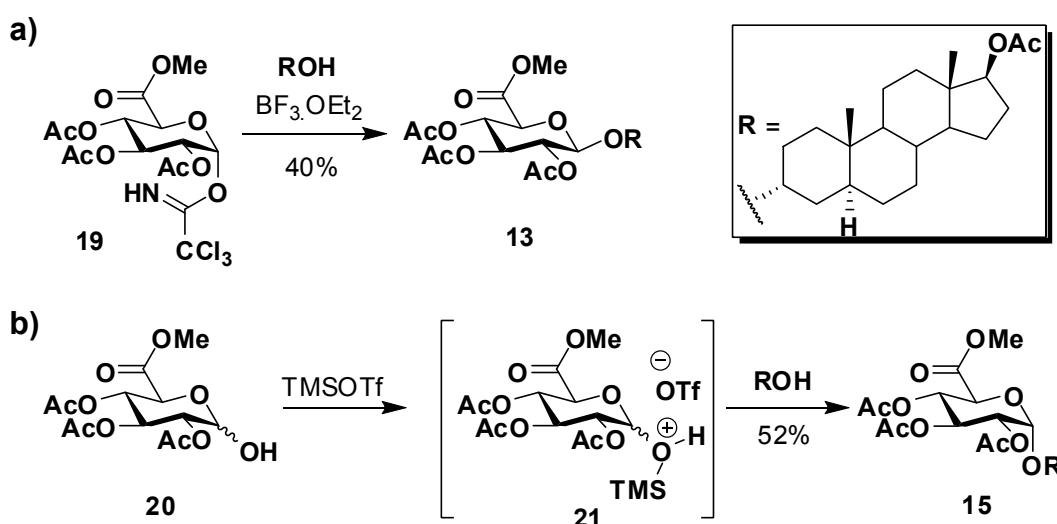
Scheme 1.4. The mechanistic pathways for the Koenigs-Knorr reaction. Substituents at the 3, 4, and 5-position are omitted for clarity.

The use of acyl-protecting groups helps stabilise the glucuronyl halide **10** and promotes β -glucuronide product **13** formation through anchimeric assistance (Path D).²² However, this anchimeric assistance provides additional pathways that lead to an ortho ester by-product **17** (Path E). This ortho ester **17** can be isolated or may hydrolyse upon acid work-up to yield an anomeric mixture of glucuronide product **13** & **15** (Path F) and/or the 2-deacetylated by-product **18** (Path G).

Another drawback to the Koenigs-Knorr reaction is the poor reactivity of the glycosyl halides which require harsh reaction conditions and activation by metal

salts which are generally toxic, expensive and moisture-sensitive. Lastly, reactions are performed with protected glucuronyl donors **10**, so the additional hydrolysis step required to remove the protecting groups will reduce the overall yield of the glucuronide conjugates.

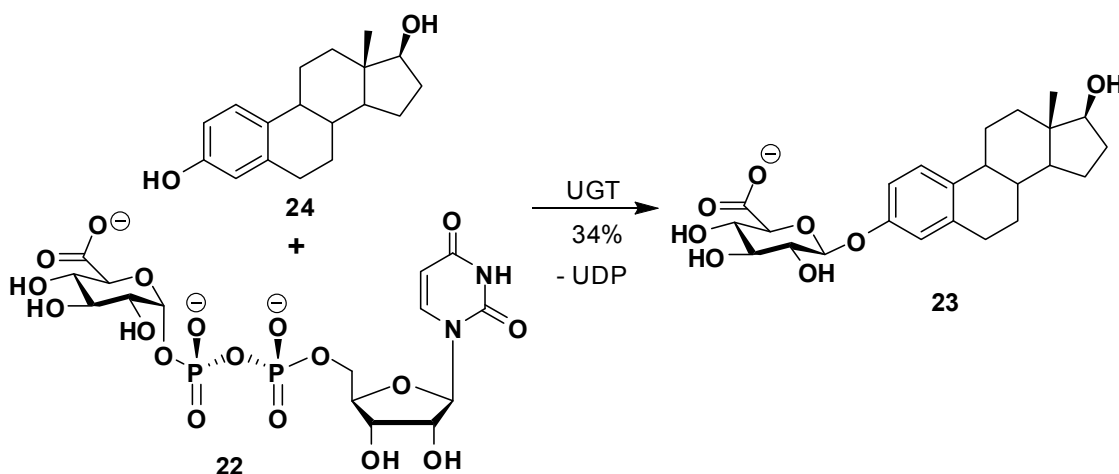
Since the discovery of the Koenigs-Knorr reaction in 1901, there has been a development of several novel chemical-based glucuronylation reactions. They are somewhat related to the Koenigs-Knorr reaction with the most significant variation involving the use of alternative glucuronyl donors. The substitution of the glycosyl halide **10** for a trichloroacetimidate **19** may achieve high glycosylation yields under mild Lewis acid catalysis (Scheme 1.5a).^{11,18,23-27} Alternatively, the 1-hydroxyl glucuronyl donor **20** can be converted to the activated 1-O-silylated glucuronyl donor **21** *in situ* by the addition of trimethylsilyl triflate (Scheme 1.5b).^{11,18,28} Another strategy for glucuronide synthesis is to use the above-mentioned glycosylating methods with a glucose unit. The corresponding glucoside is then selectively oxidised using TEMPO to its consequent glucuronide.^{29,30} Glucuronides yielding *O*-acyl linkages have also been synthesised by using either the Mitsunobu reaction^{31,32} or through a direct and selective esterification³³. These variations have improved yields and expanded the range of glucuronylation procedures available to synthetic chemists.



Scheme 1.5. The glucuronylation of 3 α ,17 β -dihydroxy-5 α -androstane 17-acetate with a) trichloroacetimidate (**19**) provides preferentially the β -glucuronide product (**13**) whereas b) the triflate procedure produces predominately α -glucuronide product (**15**).¹⁸

Introduction

Enzyme-mediated glucuronylation avoids the stringent reaction conditions of the Koenigs-Knorr method (and its variants) and utilises unprotected and activated glucuronic acid substrates to allow a one-step glucuronylation. The wild-type glucuronidase enzyme can be used by exploiting its transglycosylation mechanism (detailed in a later chapter in Scheme 1.8).³⁴⁻³⁷ A glucuronyl donor is generally a glucuronide with a good beta-linked leaving unit such as 4-nitrophenol. The glucuronyl acceptor is required in high concentrations to compete with water for the glycosyl-enzyme intermediate but improvements to the glucuronyl donor have been made in this area with the development of chemical rescue³⁸ and glycosyl azides.³⁹ The major drawback to this procedure is that the transglycosylation product is also a substrate for hydrolysis which often results in low yields.



Scheme 1.6: UGT-mediated glucuronylation of estradiol (24).

The UGTs are a family of eukaryotic membrane-bound enzymes that catalyse the transfer of the glucuronic acid moiety of uridine 5'-diphospho- α -D-glucuronic acid (UDP-glucuronic acid) **22** to a variety of acceptors. For example, estradiol 3- β -D-glucuronide **23** has been synthesised by the UGT-mediated glucuronylation of estradiol **24** (Scheme 1.6).⁴⁰ Its existence as a membrane-bound enzyme causes difficulty in its expression and the practicality of its application in reactions. Animal sacrifice is often required to obtain the UGT enzymes. Additionally, many isoforms of UGTs exist, for example the reported number UDP-glucuronosyltransferase isoforms for humans is fifteen and for rats it is fourteen.^{41,42} Each isoform exhibits substrate specificity for a different class

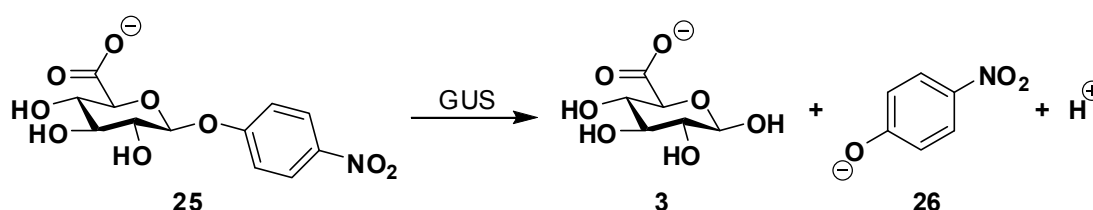
of drug/steroid. However, all isoforms require the addition of UDP-glucuronic acid **22** as the glucuronyl donor, which is an unstable and expensive substrate.

These factors combine to form a very costly and time-consuming glucuronylation. However, the mild, one-step reaction and stereospecific outcome of enzyme-mediated glucuronylation makes it an attractive method.

1.6 β -Glucuronidase enzyme

The β -glucuronidase enzyme (E.C. 3.2.1.31) belongs to a class of glycoside hydrolysing enzymes known as glycosidases. They exist in a range of animals (e.g. humans, dogs, rats), plants (e.g. rye, rhubarb, tobacco) and micro-organisms (e.g. *Escherichia coli*, *Clostridium*, *Staphylococcus*).^{43,44} The species of interest in this study is *Escherichia coli* (*E. coli*). *Escherichia coli* has a fully defined genome⁴⁵ and well-established handling procedures, so genome manipulation, cell growth and protein expression are well understood.

The *E. coli* β -glucuronidase exists as a homotetramer with each subunit consisting of 603 amino acids and weighing 68.5 kDa each.⁴⁶ Investigations have proven that the enzyme has optimal activity at pH 7.5.⁴⁷ The activity of the enzyme (Units) and enzyme kinetics (K_m and V_{max}) can be measured by the hydrolysis of *p*-nitrophenyl β -D-glucuronide **25** (Scheme 1.7).⁴⁸ The released *p*-nitrophenolate **26** absorbs strongly in the visible light spectrum (405 nm) and can be monitored over time by spectrophotometry.



Scheme 1.7: The hydrolysis of *p*-nitrophenyl- β -D-glucuronide (**25**) by β -glucuronidase (GUS).

The crystal structure for *E. coli* β -glucuronidase was not available at the time this study was performed. A model has been proposed by Matsumura *et. al.* using the known human β -glucuronidase crystal structure.⁴⁹ It is a reasonable comparison to make considering the orthologue is ~50% identical in amino acid sequence and exhibits identical activity (K_m 0.2 mM *E. coli*.⁵⁰ vs. 0.2 mM

Introduction

human⁵¹ for *p*-nitrophenyl- β -D-glucuronide **25**). The model depicts several amino acid residues that may form the binding pocket inside the active site that may be responsible for the enzyme's specificity for glucuronides. Intermolecular hydrogen bonding to the glucuronic acid residue is observed through aspartic acid 163 (D163), tyrosine 468 (Y468), tryptophan 549 (W549), arginine 562 (R562), and asparagine 566 (N566). Additionally, the close proximity of the protonated lysine 568 (K568) residue to the glucuronyl carboxylate may provide an ionic interaction that defines the enzyme's high specificity for glucuronides. Two glutamate residues (E504 and E413) are in close range of the anomeric carbon.

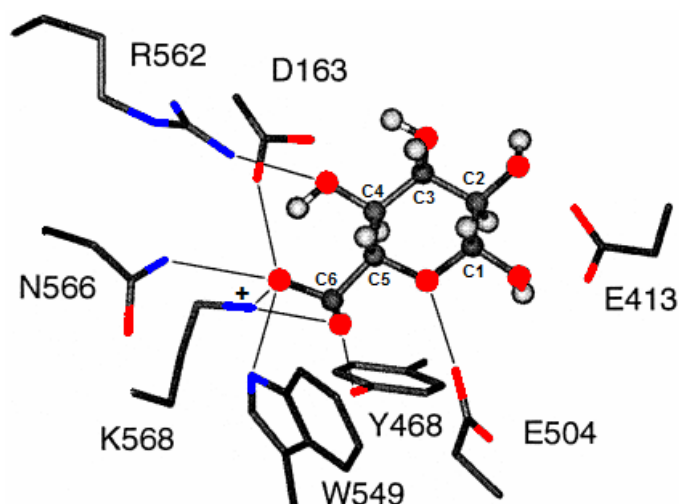
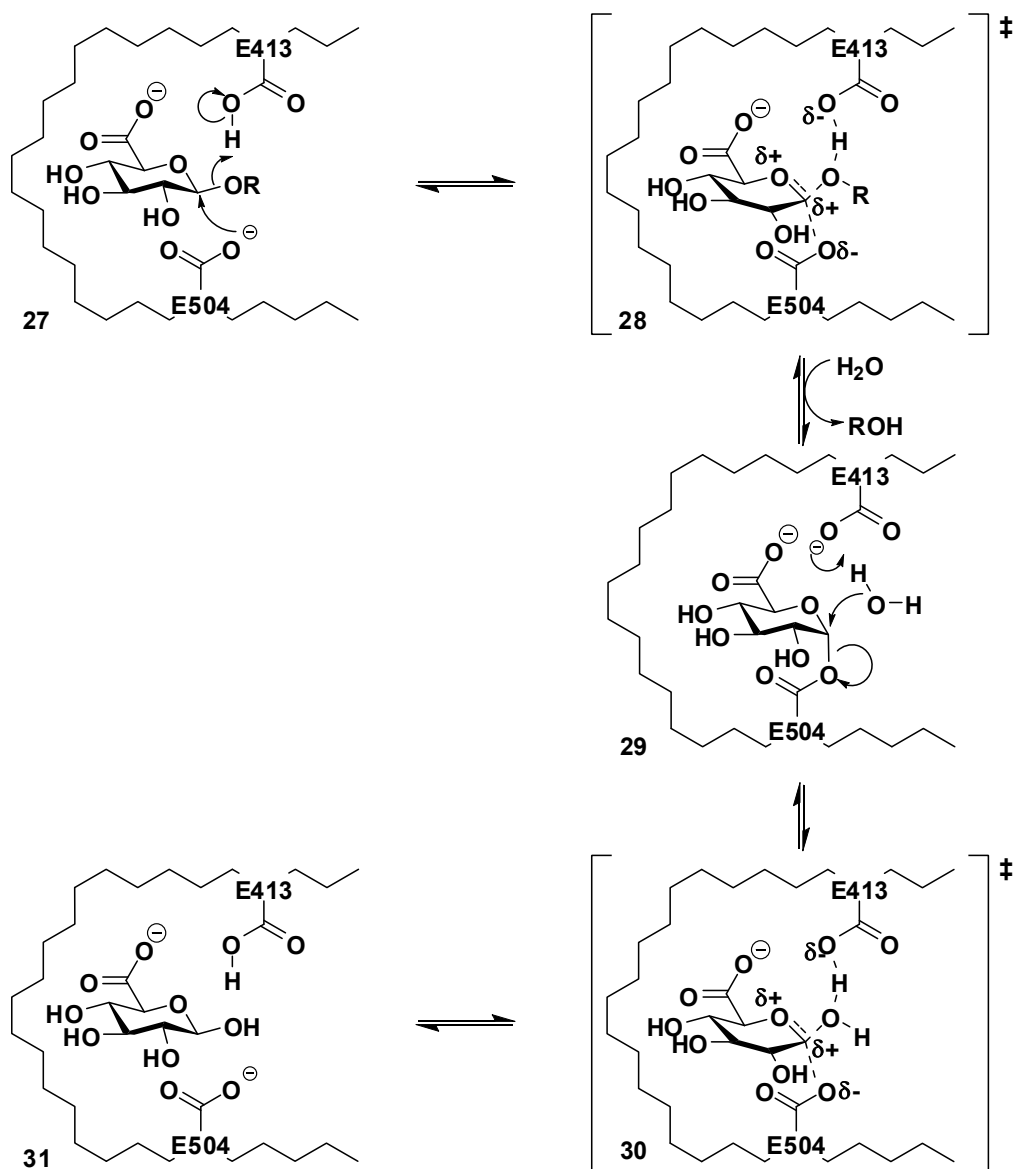


Figure 1.2: The hypothesised binding of glucuronic acid 3 to the active site of *E. coli* β -glucuronidase. This model has been adapted from Matsumura and Ellington's model of *E. coli* based on the human sequence and quaternary structure.⁴⁹ Fine lines indicate intermolecular hydrogen bonding within 3Å.

The mechanism of action for β -glucuronidase (Scheme 1.8) has been well characterised and is analogous for both prokaryotes and eukaryotes.⁵² The active site consists of two strategically positioned glutamic acid residues: the glutamate 504 residue (E504) and the glutamate 413 residue (E413). These work mutually to provide general acid/base and nucleophilic catalysis *via* a S_N2 -like mechanism with a transition state demonstrating substantial oxocarbenium-ion-like character. The mechanism begins with an S_N2 nucleophilic attack by the carboxylate anion of E504 on the anomeric carbon of the glucuronide **27**. This is catalysed by E413 which acts as a general acid and protonates the departing glycosidic oxygen of **27**.



Scheme 1.8: β -glucuronidase mechanism of action.

This mechanism also has S_N1 character due to the oxygen in the ring donating electrons to the electron-deficient anomeric carbon of **28**. Departure of the aglycon residue results in α -glycosyl enzyme intermediate **29**. Water enters the active site and performs a nucleophilic attack on the anomeric carbon to displace the E504 residue in another S_N1/S_N2 hybrid mechanism **30**. This is catalysed by the E413 carboxylate anion which acts as a general base. D-Glucuronic acid **3** is released from **31** with overall retention of configuration and the enzyme prepared for another cycle of hydrolysis.

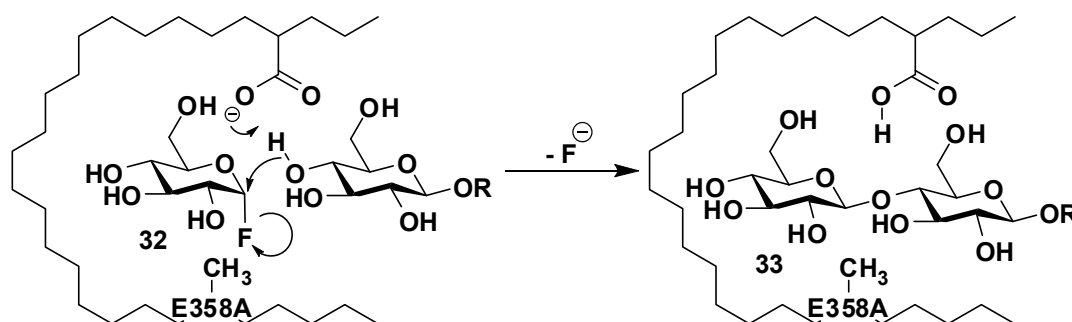
The mechanism (Scheme 1.8) is completely reversible which means the nucleophilic attack on the anomeric carbon in the glycosyl enzyme intermediate

Introduction

29 by an alcohol can generate a β -transglycosylated product. However, this transglycosylated product will not accumulate, as it is a substrate for β -glucuronidase, and will eventually undergo the hydrolysis mechanism.

1.7 Glycosynthases and the genetically-modified β -glucuronidase enzyme

In 1998, Withers *et al.* reported the first of what would be a series of engineered β -glycosidase enzymes that could synthesise β -glycosidic linkages.⁵³ Because of their ability to synthesise β -glycosidic linkages in the absence of the reversing hydrolytic pathway they were dubbed “glycosynthases”.⁵³ Through site-directed mutagenesis, the nucleophilic glutamate residue E358 of the β -glycosidase enzyme from *Agrobacterium sp.* was converted to alanine. The result was a mutant enzyme that was unable to function *via* the normal hydrolytic pathway. However, when the mutant enzyme was supplied with α -D-glucosyl fluoride donor **32** and an appropriate glucoside acceptor residue, the fluoride was displaced and a 1 \rightarrow 4 β -glycosylation occurred to produce oligosaccharides (such as cellobiosides **33** or longer-chained oligosaccharides) (Scheme 1.9).

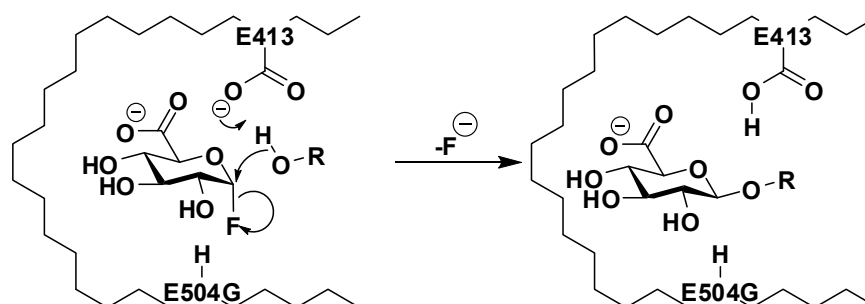


Scheme 1.9: Mechanism of action for the *Agrobacterium sp.* β -glycosynthase.

The α -D-glucosyl fluoride-enzyme complex mimics the glycosyl enzyme intermediate (i.e. analogous to **29**) by providing a good leaving group during glycosylation. The reverse mechanism (fluorination) is essentially absent since the fluoride ion is not bound strongly to the enzyme and will be dispersed into the medium following glycosylation. Additionally, the newly formed glycoside **33** has a poor anomeric leaving group and will not be displaced by poor nucleophiles such as a fluoride ion.

Since the *Agrobacterium* sp. glycosynthase in 1998, a variety of glycosynthases from a range of β -glycosidases have been developed by numerous groups from around the world.⁵⁴⁻⁵⁶ The mutants thus far have been utilised to synthesise oligosaccharides (such as **33**). Of particular importance to this project is a recently engineered enzyme, *E. coli* β -glucuronidase, which was developed as a glycosynthase (or more specifically – a glucuronylsynthase) but failed to catalyse oligosaccharide synthesis in preliminary trials with a range of carbohydrate acceptors.

Withers developed four *E. coli* β -glucuronidase mutants to be utilised in this project. The glucuronylsynthase enzymes were prepared through the site-directed mutagenesis of the native *E. coli* β -glucuronidase gene. The nucleophilic glutamate residue (E504) was replaced by either an alanine (E504A), glycine (E504G), or serine (E504S) residue. The fourth mutant is a wild-type (WT) species prepared from the unmodified native β -glucuronidase gene (i.e. retention of the E504 glutamate residue). All differ from native β -glucuronidase due to an added poly-histidine tag. β -Glucuronidase-deficient strains of *E. coli* were transformed with plasmids bearing the codon of one of the four genetically-modified β -glucuronidase enzymes.

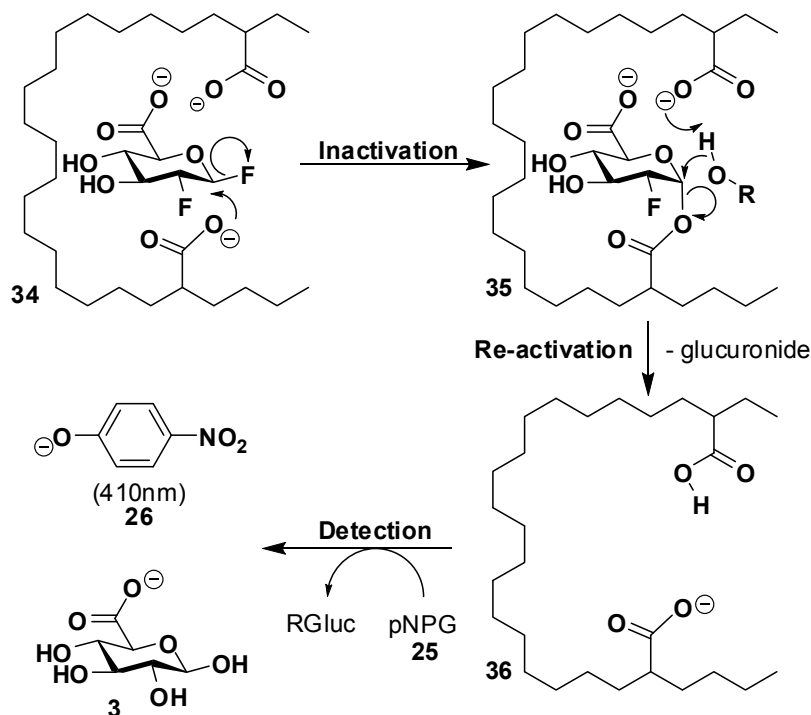


Scheme 1.10. General mechanism for the *E. coli* β -glucuronylsynthase

The mechanism of the *E. coli* β -glucuronylsynthase (Scheme 1.10) is anticipated to operate analogously to the common mechanism of other glycosynthases. Hence, the substitution of the nucleophilic E504 residue to a non-nucleophilic residue disables the hydrolytic pathway. Upon addition of the glycosyl fluoride, the glycosyl-enzyme intermediate is imitated (analogous to **29**). The E413 residue still exists to fulfil its role as a general acid-base which aids glucuronylation. The absence of the hydrolytic pathway means the glucuronide products can accumulate.

1.8 Early results

The investigation of enzyme-mediated glucuronylation of biologically important alcohols began in early 2005 by Dr. Malcolm McLeod of the University of Sydney, in collaboration with Prof. Steven G. Withers of the University of British Columbia in Canada. Following the unsuccessful oligosaccharide synthesis by the glucuronylsynthases, their research focused on discovering what sort of aglycons would be susceptible to glucuronylation by the glucuronylsynthase enzyme. This study incorporated the development of a library of acceptor compounds that were screened to identify “hits” in the *Jan screen*. The Jan screen (Scheme 1.11) involved the inactivation of the WT β -glucuronidase enzyme with 2-deoxy-2-fluoro- β -D-glucuronyl fluoride **34**. Transglycosylation of the inactivated β -glucuronidase enzyme **35** with an accepting alcohol re-activates the β -glucuronidase enzyme **36**. Formation of reactivated β -glucuronidase enzyme **36** was monitored by the release of the *p*-nitrophenolate **26** chromophore from the hydrolysis of *p*-nitrophenyl β -D-glucuronide (*p*NPG) **25**. A successful transglycosylation was a promising first step that suggested the acceptor alcohol may undergo glucuronylation in a glucuronylsynthase reaction.



Scheme 1.11: Successful transglycosylation in a Jan Screening.

Twelve (**37** -**50**) out of the ninety-six alcohols screened gave significant enzyme reactivation after one hour (Figure 1.3).⁵⁷ The alcohols 2-methylcyclohexanol (**38** and **39**) and 4-methylcyclohexanol (**40** and **41**) were used as a diastereomeric mixture. None of the 54 carbohydrates trialled showed any evidence of reactivation. The twelve alcohol substrates (**37-50**) were trialled in small scale glucuronylation reactions with the three glucuronylsynthase (E504A, E504G and E504S) and α -D-glucuronyl fluoride **51**. The formation of glucuronides was monitored by TLC and the products were confirmed by LC-MS.

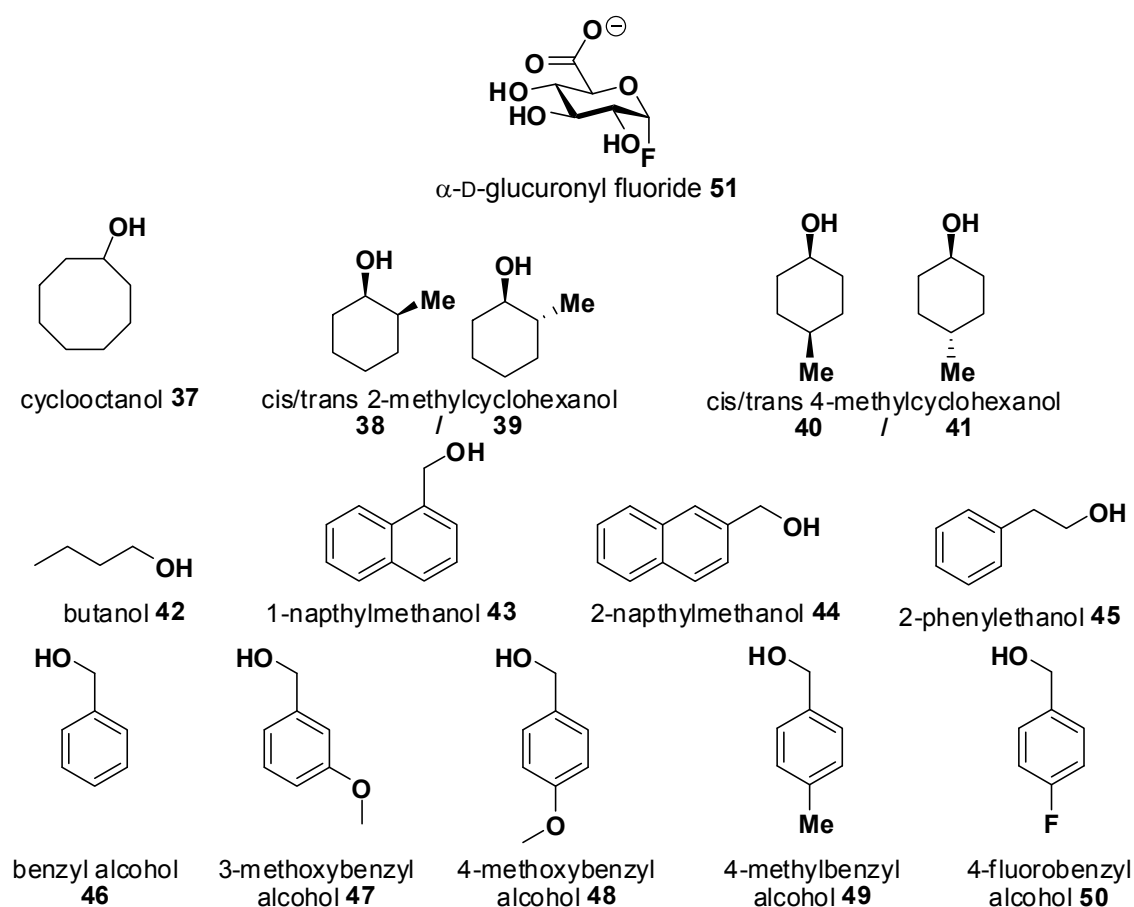


Figure 1.3: Successful hits from the Jan screening of the WT.

In late 2005, three glycosynthases (E504A, E504G, and E504S) were successfully expressed and isolated at the University of Sydney.⁵⁸ McLeod's small scale glucuronylation reactions were successfully repeated and confirmed by LC-MS. The small scale study also determined that the glycine mutant (E504G) was the more active mutant. This observation is hypothesised to be due to the absence of a side chain on the glycine residue. Additional

Introduction

candidates for glucuronylation were also trialled, including a range of phenols (**52-54**) and steroids (**7, 9, 55 -62**; Figure 1.4).⁵⁸

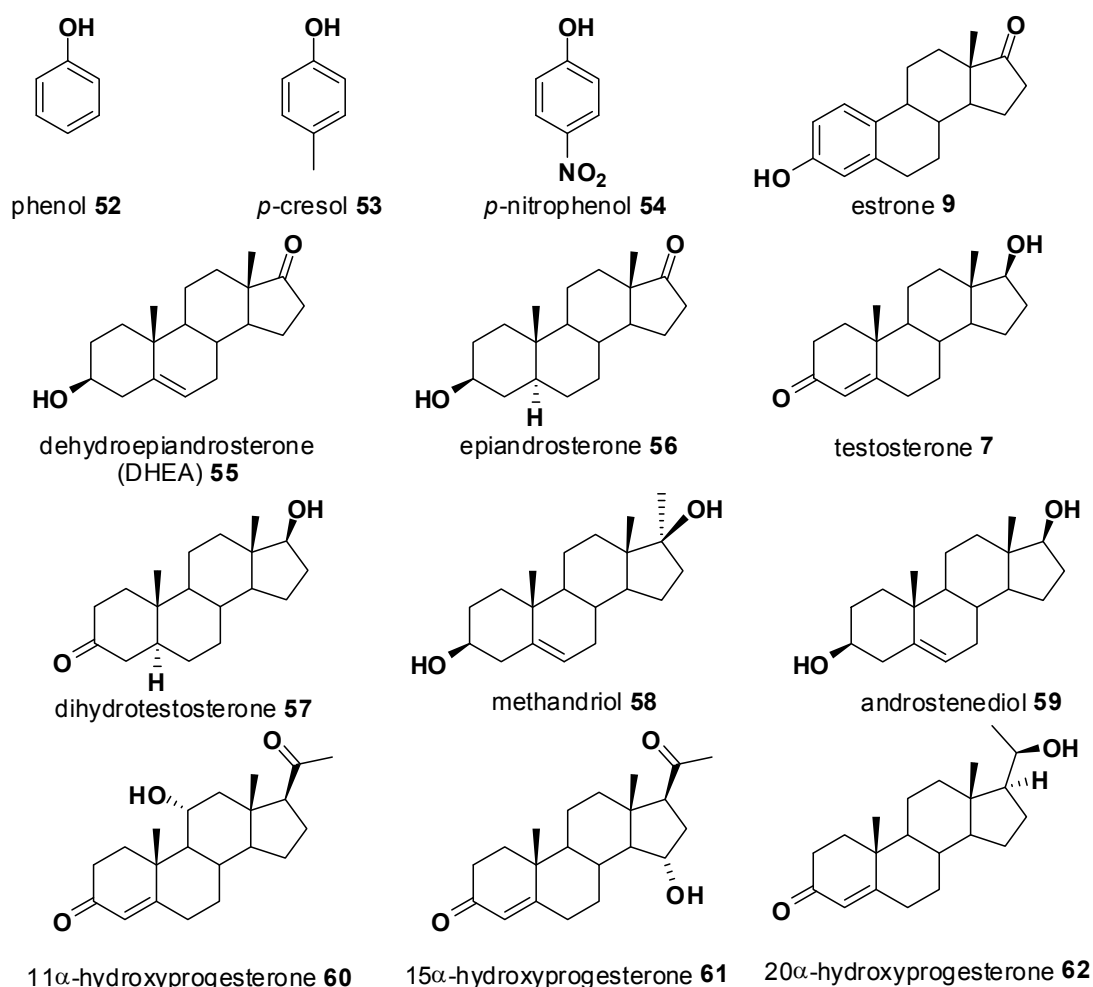


Figure 1.4: Additional substrates trialled in glucuronylsynthase reactions.

Phenol **52** was more reactive than *p*-cresol **53** which was more reactive than *p*-nitrophenol **54**. It is speculated that the pKa of phenols plays a role in its nucleophilicity and therefore reactivity. Alternatively, the binding site of the enzyme may not accommodate a negatively-charged acceptor and therefore prohibit the phenolate ion from entering the binding site.

The 3 β -hydroxy steroids (**55** and **56**) showed a good aptitude towards glucuronylation by the E504G glucuronylsynthase. The 17 β -hydroxy steroids (**7** and **57**) showed moderate propensity towards glucuronylation with the E504G enzyme. Surprisingly, the 3 β ,17 β -dihydroxy steroids (**58** and **59**) displayed no formation of mono or di-glucuronide products. Progesterone analogues with variously positioned alcohols (**60**, **61** and **62**) and estrone **9** showed no spots by TLC but tentative signals by electron spray ionisation mass spectrometry (ESI-

MS). The difference in reactivity was rationalised as steric hindrance for the 17 β -hydroxy and progesterone analogues and poor nucleophilicity by estrone **9**. No reasonable rationale could be offered for the dihydroxy steroids.

The twelve alcohols (**37-50**) identified by McLeod plus phenol **52** and dehydroepiandrosterone (DHEA) **55** were scaled up on a 20 mg scale so that a yield can be determined and thorough characterisation could be performed on the glucuronide products (**63 -77**, Table 1.1).

Table 1.1: Alcohols subjected to glucuronylation by glucuronylsynthase.

Entry	R (product no.)	Additive ^a	Yield (%)	Entry	R (product no.)	Additive	Yield (%) ^b
a	63	-	60	i	71	-	84 (38)
b	64	A	66 ^c	j	72	B	39
c	65	A	37 ^c	k	73	-	40
d	66	A	44	l	74	B	67
e	67	B	53	m	75	B	42 (30)
f	68	-	93	n	76	-	13
g	69	-	47	o	77	- ^d C ^d	5 26
h	70	A	71				

^a Reactions were performed using α -D-glucuronyl fluoride **51** (1.2 equiv.), E504G glucuronylsynthase (0.1 mg mL⁻¹) in 50 mM sodium phosphate buffer, pH 7.5 unless otherwise stated. Reaction additives include A: DMSO (12.5% v/v), B: DMSO (25% v/v), C: DDM (2.2% w/v). ^b Yield in parentheses denotes the yield obtained from the alanine glucuronylsynthase (E504A) under analogous reaction conditions. ^c Product was isolated as a mixture of diastereomers. ^d Saturated acceptor (1.4 mg mL⁻¹), E504G (0.2 mg mL⁻¹) and 100 mM sodium phosphate buffer, pH 7.5 was used.

Introduction

Dimethylsulfoxide (DMSO) was required as a co-solvent to dissolve the more hydrophobic alcohols (entries b, c, d, e, h, j, l, m), yet the enzyme showed robust qualities by remaining active in DMSO concentrations of up to 25% v/v (entries e, j, l, m). The steroid DHEA **55** was only sparsely soluble in DMSO, so the detergent *n*-dodecyl β -maltoside (DDM) was utilised to avoid a significant drop in activity by subjecting the enzyme to higher concentrations of DMSO. Although complete dissolution was still not attained, DDM was better at dissolving DHEA **55** without the denaturing effects DMSO poses at greater concentrations.

An initial investigation into the optimised glucuronylsynthase reaction conditions was also visited prior to this research.⁵⁸ Using the WT enzyme as a model system, a range of co-solvents and detergents (at various concentrations) were investigated as additives to aid the solubility of hydrophobic substrates.⁵⁸ The effect that each additive had on the hydrolysis of *p*-nitrophenyl- β -D-glucuronide **25** (Scheme 1.7) in relation to the control sample (no additives) suggested their affect with glucuronylsynthases. This study suggested DMSO, DDM and Amidosulfobetaine-14 (ASB-14) had the least impact on reducing enzyme activity. Whilst this study is a good indication to the relative affect these additives may have on the glucuronylsynthases, their actual effect is still undetermined. An assay is required to monitor the activity of the glucuronylsynthase so that a direct correlation can be drawn between the experimental variables and enzymatic activity.

1.9 Project proposal

Following on from my Honours research, the ultimate goal for this research will be to identify the optimal reaction conditions to maximise product yield for the glucuronylsynthase reactions. To attain this goal, an assay to quantitatively measure the kinetics and activity of the glucuronylsynthase enzyme will need to be developed. The ideal assay would directly detect product formation in a continuous manner. The experimental variables of pH, concentration and temperature will be optimised to achieve the maximum yield.

Another objective will be aiming at broadening the application of the glucuronylsynthase reactions. In the past, the glucuronides of simple acceptor substrates (identified from the Jan screen) have been synthesised to establish the functionality of the glucuronylsynthase. By demonstrating the enzyme's application in industries, such as the pharmaceutical industry, it will expand the potential use in the synthesis of phase II glucuronide metabolites. The ultimate role of this enzyme is for the synthesis of steroid glucuronides which are in high demand in the sports testing laboratories. The development of high yielding reactions with steroids, that rival the alternate means of glucuronylation, is essential for the future applications of this enzyme.

The development of a direct assay will assist in observing the enzyme kinetics and provide the information required to seek the optimal reaction conditions. Success with a range of steroid and pharmaceutical substrates will demonstrate the diversity of this technique's application. A combination of high yielding glucuronylation and universal application will see the glucuronylsynthase enzyme become an asset in the industrial synthesis of glucuronide metabolites.

~ Chapter 2 ~

**The
glucuronylsynthase
system**

2.1 Overview

The primary development of the glucuronylsynthase methodology has been researched and successfully applied to the glucuronylation of a library of simple alcohols and a select range of steroids (Table 1.1).^{57,58} The methodology was developed from general chemical and biochemical procedures as well as those reported for other glycosynthase systems. A more thorough investigation into the methodology may improve reaction yields and provide a greater understanding of the glucuronylsynthase system. The optimisation of the glucuronylsynthase system was performed at all levels: from the expression of the glucuronylsynthase enzyme and the synthesis of the α -D-glucuronyl fluoride **51** donor through to the reaction conditions of the glucuronylsynthase reactions.

2.2 The recombinant *E. coli*.

The construction of the glucuronylsynthase gene was developed in the Wither's group through site-directed mutagenesis of the *E. coli* β -D-glucuronidase enzyme.⁵⁷ The glucuronylsynthase enzyme was expressed from a gene sub cloned into a Novagen[®] pET-28a(+) vector (Figure 2.1) at the *NdeI* and *XhoI* cloning sites.⁵⁷ The pET-28a(+) vector also carries the kanamycin **78** resistance gene, T7lac promoter, and an N-terminal His-Tag extension. The β -glucuronidase deficient *E. coli* lysogenic cell line GMS407(DE3) was used to host this plasmid to ensure glucuronylsynthase expression that was free of wild-type activity.⁵⁹

Using this expression system, the glucuronylsynthase enzyme has been achieved in good yields ($\sim 40 \text{ mg L}^{-1}$ culture).⁵⁸ However, for each step of the expression (e.g. transformation, cell lysis), alternative biochemical techniques are available. It was of particular interest if an alternative technique may provide a more efficient and higher yielding method to obtain the glucuronylsynthase enzyme. The optimum expression, isolation and purification techniques for the glucuronylsynthase enzyme are discussed.

The glucuronylsynthase system

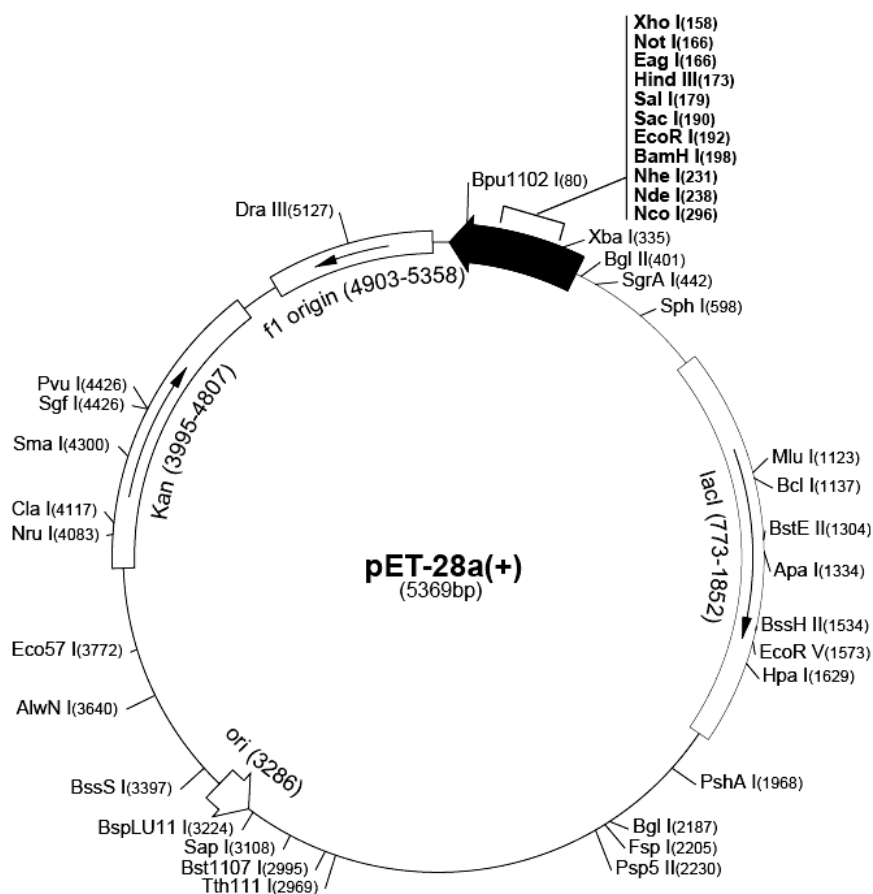


Figure 2.1. pET-28a(+) vector map reproduced from Novagen.⁶⁰

2.2.1 Transformation

The first step of the glucuronylsynthase expression involved the transformation of the *E. coli* cells with the pET-28a vector bearing the glucuronylsynthase gene. Two common procedures were available to perform this feat. The first method was a chemical heat-shock transformation.^{61,62} Upon an instant rise in temperature (4 °C to 42 °C) in a calcium-rich media, the plasmid penetrates the host cells. This method was the original transformation procedure used, prior to this research, to transform the host strain with the vector.

An alternative technique is electroporation which also achieved successful transformation. An electric current is used to increase the permeability of the bacteria cell wall and allow plasmid penetration.⁶³ By visual observation, both transformation procedures achieved transformation with equivalent efficiency. The choice of transformation procedure is therefore at the researcher's discretion.

2.2.2 Selection

Following transformation, the successful transformants must be identified and isolated. Selection of the transformed *E. coli* was performed on Luria Burtani (LB) agar media containing kanamycin **78** and 5-bromo-4-chloro-3-indolyl β -D-glucuronide (X-gluc) **79**. Kanamycin **78** is an aminoglycoside antibiotic that inhibits the 30s ribosomal subunit and prevents translation of protein. The pET-28a(+) carries the gene for kanamycin kinase, an enzyme capable of deactivating kanamycin **78** through phosphorylation to allow the host cell to survive in the presence of this antibiotic. A selection process was achieved by growing cells in kanamycin-enriched media whereby only successful transformants bearing kanamycin **78** resistance survived.

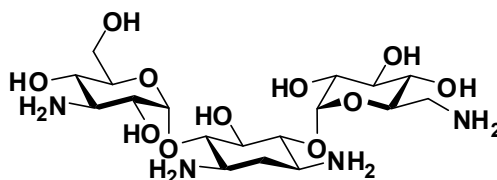
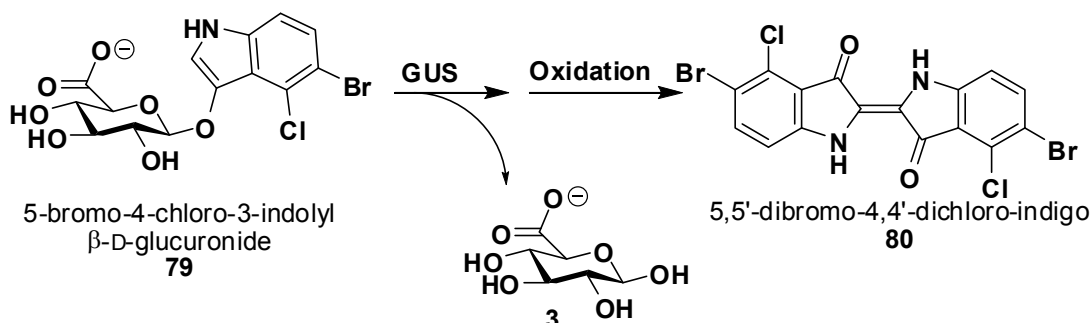


Figure 2.2. The aminoglycoside antibiotic kanamycin **78**

In the presence of wild-type β -glucuronidase, X-Gluc **79** is hydrolysed to the enol 5-bromo-4-chloroindoxyl and, through dimerisation and oxidation (in the presence of oxygen), forms the blue ($\epsilon_{\text{max}} = 615\text{nm}$) 5,5'-dibromo-4,4'-dichloro-indigo dye **80** (Scheme 2.1). As a result, any cells expressing wild-type β -glucuronidase would grow with blue discolouration. X-Gluc **79** therefore provided a second selection process based on glucuronidase functionality. Successful transformation of the glucuronylsynthases into the GMS407(DE3) strain produced white colonies that survived on LB media containing kanamycin **78** and X-gluc **79**.



Scheme 2.1. Use of X-gluc **79** for the selection of functional β -glucuronidase (GUS).

The glucuronylsynthase system

2.2.3 Induction

Once the successful transformants had been identified, a culture was grown from a single colony, and the over-expression of the glucuronylsynthase enzyme was commenced. The pET-28a(+) plasmid regulates the expression of glucuronylsynthase using an amalgamation of two well-characterised transcription regulators: the *lac* operon (specifically *lacUV5*) and the strong T7 bacteriophage transcription system (Figure 2.3). The *lac* operon acts as an expression “brake” and is derived from the regulation of β -galactosidase.⁶⁴

The *lac* repressor protein, a tetrameric DNA binding protein, is expressed from the *lacI* gene from the genome and the plasmid. It binds to the *lac* operator site (*lacO*) present in the DE3 gene of the genome (T7 RNA polymerase expression) and the T7 promoter on the plasmid (glucuronylsynthase expression).

When bound, the *lac* repressor protein represses T7 RNA polymerase expression at the genome and blocks the binding of any polymerase to the plasmid (“brake” applied), preventing transcription of the glucuronylsynthase gene.

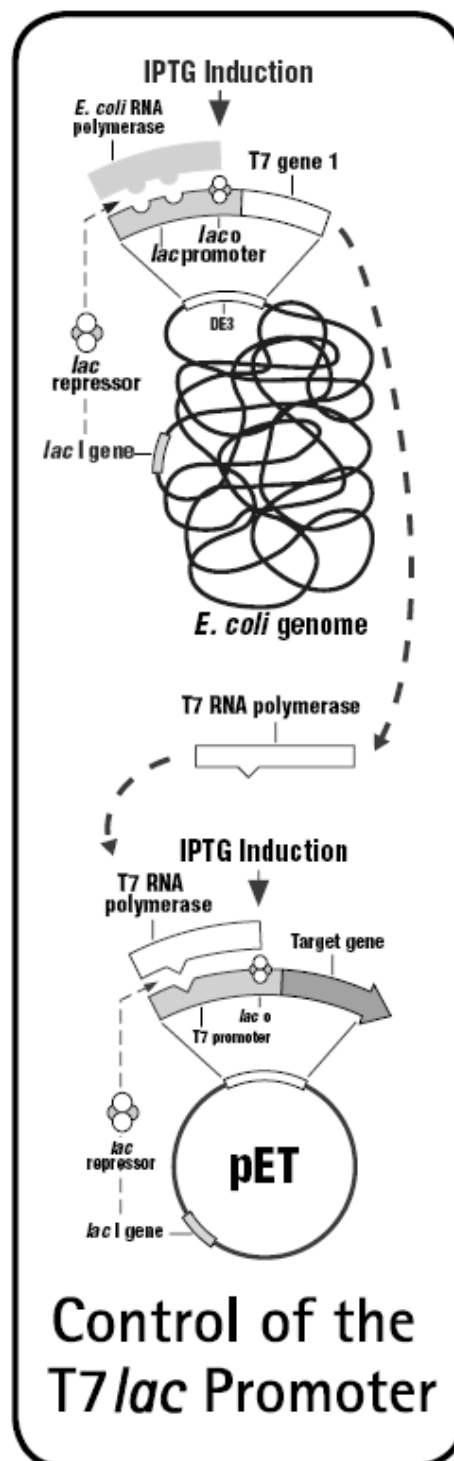


Figure 2.3 The induction of the pET-28a(+) vector in λ DE3 lysogens. Image reproduced from Novagen.⁶⁵

The glucuronylsynthase system

Isopropyl β -D-1-thiogalacto-pyranoside (IPTG) **81** (Figure 2.4) binds to the repressor protein, altering its conformation and releasing it from the *lacO* sites to allow expression of the T7 RNA polymerase (“brake” lifted). T7 RNA polymerase expressed from the DE3 gene (in the *E. coli* genome) will strongly bind to the un-repressed T7 promoter region on the plasmid and subsequently transcribe the glucuronylsynthase gene.

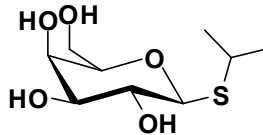


Figure 2.4. Isopropyl β -D-1-thiogalactopyranoside (IPTG) **81**

The T7 transcription system is derived from the T7 bacteriophage, a bacterial virus. The T7 RNA polymerase is highly selective and active such that when cells are fully induced, almost all of the cell's resources are converted to targeted gene expression; the desired product can comprise more than 50% of the total cell protein a few hours after induction.⁶⁵ Its high selectivity and activity makes it an expression “accelerator”. The removal of the lac repressor protein combined with the strong binding of the T7 RNA polymerase metaphorically “lifts the brake and applies the acceleration” to over-express the glucuronylsynthase enzyme.

From the selection plates (kanamycin **78** and X-gluc **79**), 0.5 L cultures were grown in LB media containing kanamycin **78**, and cells were induced with IPTG **81** once the optical density (OD_{600nm}) reached ~0.7. An aliquot from each culture was taken prior to and after induction (Figure 2.5) and subjected to sodium dodecyl sulfate – polyacrylamide gel electrophoresis (SDS-PAGE), a technique that resolves protein based on molecular weight. Over-expression of the glucuronylsynthase gene was confirmed by an intense band in the post-induction sample coinciding with the mass of the enzyme (68.5 kDa). Post-induced cells were centrifuged and the cell pellet stored at -80 °C until needed.

The glucuronylsynthase system

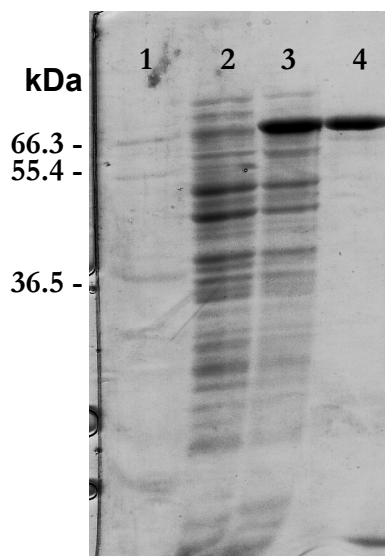


Figure 2.5. SDS-PAGE gel from glucuronylsynthase induction. Lane 1 is a protein standard marker with indicated band sizes; lane 2 is the cell culture pre-induction; lane 3 is the cell culture 3 h after IPTG 81 induction; lane 4 is the purified protein.

2.2.4 Purification

The final step of the glucuronylsynthase production involved the isolation of the pure enzyme from the bacterial cells. The pET-28a(+) plasmid encodes for a hexa-histidine extension (His-tag) and thrombin recognition site on the *N*-terminus of the expressed enzyme. This protein fusion link was exploited in the enzyme's purification. The nitrogen in the imidazole ring of histidine coordinates strongly to nickel (II) ions (Figure 2.6) to allow affinity-based purification.

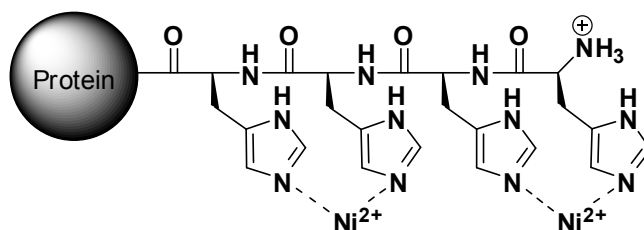


Figure 2.6: Poly-histidine tail co-ordinated to Ni²⁺ ions.

Purification began by first lysing the bacterial cells. Previously, cellular disruption was performed by a series of freeze-thaw cycles in liquid nitrogen.⁵⁷ Having recently gained access to a French pressure cell press, the yields on glucuronylsynthase enzyme have risen from 18 mg of protein per gram of cells (utilising freeze-thaw) to 20-25 mg of protein per gram of cells (French press). The over-expression of glucuronylsynthase is therefore calculated to be at least 2.5% w/w of cell mass.

The crude cell extract was loaded onto a HisTrap™ column (GE Healthcare) consisting of nickel sepharose media. The column was washed with a

buffered saline solution containing a dilute concentration of imidazole. Glucuronylsynthase bound tightly to the resin-bound nickel due to its poly-histidine tail whilst the remainder of the cell extract was washed from the column. This could be visualised by a strong UV absorption during this washing step. Imidazole also binds strongly to nickel and competes with the histidine residues. The concentration of imidazole was slowly increased over a gradient to displace glucuronylsynthase from the Histrap™ column. Amicon® centrifugation filter units were used to concentrate the enzyme fractions and change the eluting solution to phosphate buffer by ultrafiltration. The centrifugation filter units have a molecular weight cut-off of 10 kDa allowing the glucuronylsynthase (68 kDa) to remain in the cartridge.

A thrombin recognition sequence exists in the linker region between the poly-histidine tail and the enzyme. Thrombin is highly specific endo-peptidase and can be used for the cleavage of the poly-histidine tag from the enzyme. This is useful in cases where the poly-histidine tail may hinder enzyme activity and/or infer incorrect structural conformation.^{66,67} Fortunately, previous studies on the His-tagged wild-type glucuronidase showed no impediment on wild-type activity.⁵⁸ As a result, the glucuronylsynthase was used with the His-tag still appended.

2.2.5 Plasmid amplification

A fresh transformation was performed for every batch of enzyme expressed and stocks of plasmid were needed to avoid the laborious steps involved in re-cloning another plasmid. NEB5α strain of *E. coli* was used to host the amplification due to its genotype giving it high permeability and low plasmid degradation. It contains genotypes such as *recA1* (a recombination deficiency to avoid recombination of homologous sequences into the bacterial genome), *endA1* (elimination of non-specific endonuclease expression) and *hsdR17* (removal of a native restriction enzyme to avoid foreign DNA degradation). The NEB5α cells were transformed via electroporation and grown to a 2 mL culture from a single transformed colony. The plasmid was extracted from the cell pellet using a QIAprep Spin Miniprep Kit (Qiagen) to yield 100 μL of plasmid.

The glucuronylsynthase system

The isolated plasmid was sequenced to ensure the infallible duplication of the plasmid and the glucuronylsynthase gene. A single digestion (XhoI) and double digestion (NdeI and XhoI) was performed on the plasmid at the gene insertion sites with the digestion fragments analysed by SDS-PAGE (Figure 2.7). For the single digestion, a single band was observed ~7 kB corresponding to the pET28a(+) plasmid (~5.4 kB) bearing the glucuronylsynthase gene (~1.8 kB). For the double digestion, two bands were observed. One band is observed at 6 kB and corresponds to the empty pET-28a(+) plasmid (~5.4 kB) and the other band occurs at 1.8 kB which corresponds well with the glucuronylsynthase gene (~1.8 kB). Sequencing the plasmid has confirmed that the glucuronylsynthase gene still exists in the plasmid for future transformations.

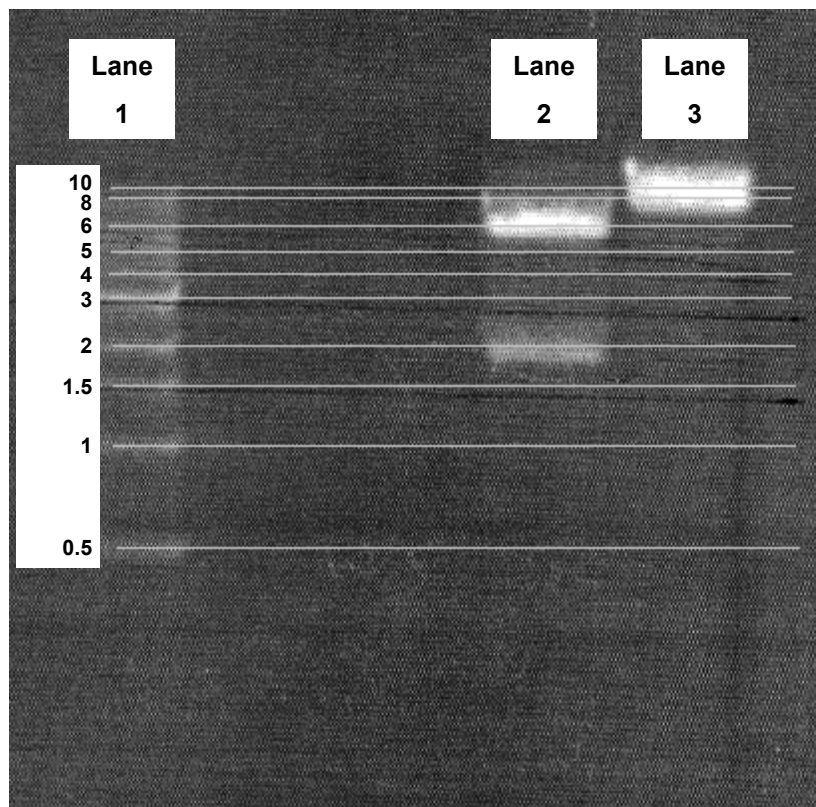


Figure 2.7: SDS-PAGE of the double digestion (lane 2) and single digestion (lane 3) of the pET-28a plasmid against a 1 kB DNA ladder standard (Lane 1).

2.3 Glucuronylsynthase crystal structure

From the introduction, the β -glucuronidase enzyme is used extensively in industry and molecular biology. Yet, despite its widespread application, at the time of this publication, no crystal structure has been obtained. A model has been proposed by Matsumura *et. al.* using the known human β -glucuronidase

crystal structure (Figure 1.2).⁴⁹ Whilst this model predicts the amino acid residues that may participate in binding of the glucuronic acid moiety, the residues responsible for the variation of aglycon substrate specificity are not known. It may also be difficult to use this model to rationalise aglycon specificity considering the different roles that β -glucuronidase plays in humans versus *E. coli*. Human β -glucuronidase has a specific role of hydrolysing the β -linked D-glucuronic acid **3** residues from the non-reducing termini of glycosaminoglycans oligosaccharides.⁶⁸ In *E. coli*, β -glucuronidase has a universal role of removing β -glucuronic acid **3** residues from almost any metabolite as an energy source for the cell. The universal role of *E. coli* β -glucuronidase suggests the tertiary structure of the aglycon binding region would differ from the human β -glucuronidase structure. The crystal structure of the *E. coli* β -glucuronidase would provide more information behind the promiscuous activity of this enzyme and, in future, allow the evaluation of changes involved in mutagenic studies, such as site-direct mutagenesis and directed evolution.

An attempt to grow a crystal of glucuronylsynthase was performed with a library of known crystallising conditions. A series of microbatch crystallisations in 96-well plates were performed using Hampton Research[®] Crystal Screen[™] (Hampton Research, Laguna Hills, CA), Hampton Research[®] Index Screen[™] (Hampton Research, Laguna Hills, CA) and QIAGEN[®] PEGS Suite[™] (QIAGEN Sciences, Germantown, MD). For each crystallising solution, three wells were used. The first well contained the enzyme only, the second well contained the enzyme and α -D-glucuronyl fluoride **51** and the third well contained the enzyme and *p*-nitrophenyl- β -D-glucuronide **25**. Screens were conducted with α -D-glucuronyl fluoride **51** and *p*-nitrophenyl- β -D-glucuronide **25** in the hope of obtaining a substrate-bound crystal.

Out of the 864 crystallising conditions trialled, only ten conditions displayed possible crystal formation (crystal photographs are attached in section 7.2.16). Out of this ten, two crystallising solutions exhibited crystals in more than one well. In the presence of Tris (0.1 M, pH 6.9), mono-sodium phosphate monohydrate (0.49 M), and di-potassium phosphate (0.91 M), rod-clusters

The glucuronylsynthase system

were observed for the enzyme in the presence of α -D-glucuronyl fluoride **51** and *p*-nitrophenyl β -D-glucuronide **25**. In the presence of tri-ammonium citrate (1.8 M, pH 7.0), plate-like crystals were observed in the wells containing the glucuronylsynthase alone and in the presence of α -D-glucuronyl fluoride **51**.

Table 2.1: Formulation for the scaled up crystallisation attempts of glucuronylsynthase.

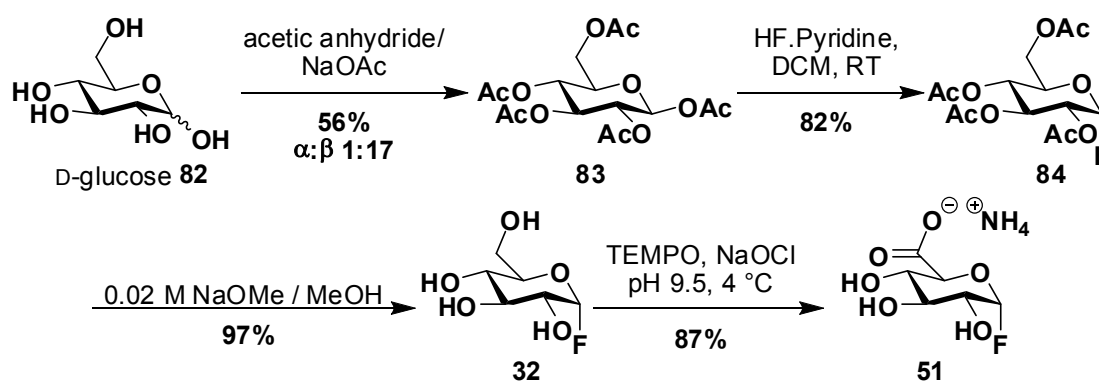
Crystal attempt	Crystallising formulation	Conditions		
		E504G only	E504G + 350 mM 1FGlucA 51	E504G + 10 mM pNPG 25
1	Tris (0.1 M, pH 9.6), NaH ₂ PO ₄ .H ₂ O (0.45-0.55 M), K ₂ HPO ₄ (0.75–1 M)	<input checked="" type="checkbox"/>	<input checked="" type="checkbox"/>	<input checked="" type="checkbox"/>
2	Na ₂ HPO ₄ (0.175-0.225 M), PEG 3350 (16-26% w/v)	<input checked="" type="checkbox"/>	<input checked="" type="checkbox"/>	<input checked="" type="checkbox"/>
3	Mg(HCO ₂) ₂ (0.175-0.225 M), PEG 3350 (16-26% w/v)	<input checked="" type="checkbox"/>	<input checked="" type="checkbox"/>	<input checked="" type="checkbox"/>
4	HEPES (0.075-0.125 M, pH 7.5), PEG 3350 (19-29% w/v)	<input checked="" type="checkbox"/>	<input checked="" type="checkbox"/>	<input checked="" type="checkbox"/>
5	Tris (0.1 M, pH 8.5), CaCl ₂ .H ₂ O (0.175-0.225 M), PEG 400 (24-34% w/v)	<input checked="" type="checkbox"/>	<input checked="" type="checkbox"/>	<input checked="" type="checkbox"/>

The growth of crystals large enough for x-ray diffraction was attempted using the hanging-drop method in 24-well plates. Out of the ten promising crystallising conditions, five crystallising solutions were selected and repeated on a larger scale (Table 2.1). This selection was based on the appearance of crystals grown in the microbatch crystallisation screen. Eighteen wells were used to crystallise the enzyme using various ratios of the crystallisation

formulation. The remaining 6 wells were omitted of enzyme in a blank run to rule out inorganic crystallisation. No crystals were observed from any of the scaled up crystallisations. Repeating the conditions using batch crystallisation (as used in the screens) might be more successful. The tri-ammonium citrate was not trialled in the scaled up crystallisations as the formula consisted of a single component. Given the results in the crystallisation screen, it should be investigated in future attempts by varying the concentration or pH of the solution.

The methodology for glucuronylsynthase expression has been investigated and improved with only a slight modification from the initial protocol used. A 40% improvement in enzyme yield was seen when the cell lysis method was altered from a freeze-thaw technique to a French-cell press technique. However, the appropriate crystallisation condition to grow sizable crystals for x-ray crystal analysis is still under investigation. With the development of the methodology for glucuronylsynthase expression complete, the methodology for the α -D-glucuronyl fluoride **51** donor synthesis was optimised.

2.4 Synthesis of the ammonium 1-deoxy-1-fluoro α -D-glucopyranuronate (α -D-glucuronyl fluoride)



Scheme 2.2: Synthesis of α -D-glucuronyl fluoride **51**

The ammonium 1-deoxy-1-fluoro α -D-glucopyranuronate (α -D-glucuronyl fluoride) **51** required for glucuronylsynthase reactions has previously been synthesised (Scheme 2.2).⁵⁸ With each attempt at the synthesis, some reaction yields have improved and the conditions for these optimised reactions are detailed in the experimental. To summarise the synthetic sequence,

The glucuronylsynthase system

D-glucose **82** is selectively per-acetylated as the β -anomer **83**, then fluorinated with hydrogen fluoride at room temperature. The α -anomer **84** is the thermodynamic product in the fluorination reaction.⁶⁹ A simple transesterification with methoxide removes the acetyl groups which is followed by a selective TEMPO oxidation of the primary alcohol of **32**.

A TEMPO oxidation is usually performed in the presence of stoichiometric sodium chlorite and catalytic sodium hypochlorite to avoid chlorination by-products which tend to occur with aromatic substrates.⁷⁰ With no aromaticity in the molecule, the TEMPO oxidation was conducted with stoichiometric quantity of sodium hypochlorite and in the absence of sodium chlorite. No chlorinated by-products were observed. Purification was achieved by ion-exchange chromatography with Dowex® anion exchange resin and ammonium bicarbonate. The fractions were combined and lyophilised on a freeze-drier until most of the ammonium bicarbonate had decomposed.

Crystallisation was achieved with 70% aqueous ethanol with acetone required in some cases to aid crystallisation. The X-ray crystal structure was obtained (Figure 2.8) and shows the relative stereochemistry of the sugar **51**. The crystal unit depicts an extensive network of hydrogen bonding exists between the species (omitted in Figure 2.8 for clarity).

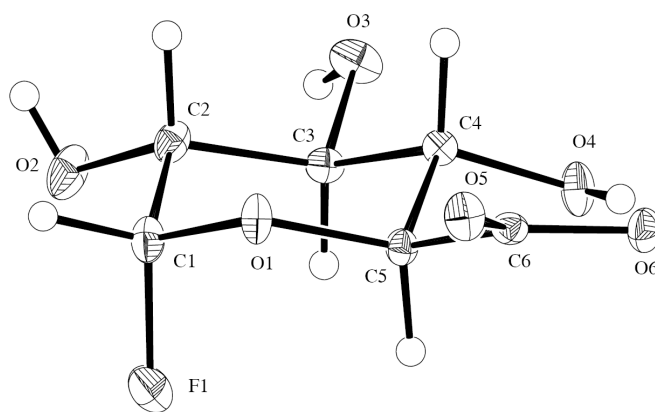


Figure 2.8. Crystal structure of 1-deoxy-1-fluoro α -D-glucopyranuronate **51** anion with labelling of selected atoms. Anisotropic displacement ellipsoids show 30% probability levels. Hydrogen atoms are drawn as circles with small radii. The CIF is reported in appendix 2.

The synthesis of the ammonium 1-deoxy-1-fluoro α -D-glucopyranuronate (α -D-glucuronyl fluoride) **51** has not been altered from its previous synthetic sequence. However, improvements to the work-up procedures, particularly in

the isolation of the final α -D-glucuronyl fluoride **51**, have improved the overall yield of the glycosyl donor. The α -D-glucuronyl fluoride **51** can be synthesised in 39% from D-glucose **82** or 69% from the penta-acetylated glucose **83**. The single crystal x-ray structure obtained for α -D-glucuronyl fluoride **51** validates the synthesis and relative stereochemistry of this molecule.

The core components of the glucuronylsynthase reaction are the glucuronylsynthase enzyme and α -D-glucuronyl fluoride **51**. The protocols outlining their optimised production have been outlined for the glucuronylsynthase methodology. The next agenda was to optimise and improve yields in the glucuronylsynthase reactions and expand the substrate repertoire for this enzyme.

2.5 Expanding the scope of the glucuronylsynthase methodology

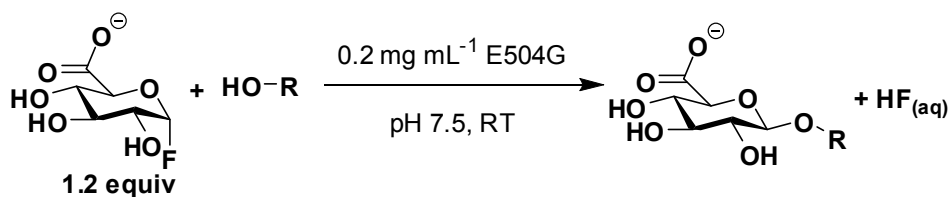
2.5.1 Defining the glucuronylsynthase reaction protocol

In the past, glucuronylsynthase reactions were performed with no formalised protocol to follow. The substrate would be used as concentrated as possible with DMSO to aid solubility where required. It was time to research the optimised conditions and define the reaction protocol for the glucuronylsynthase reaction. A selection of the alcohols subjected to glucuronylsynthesis during my Honours research (Table 1.1) were retested with different reaction conditions to verify reproducibility and improved yields. A range of results were achieved consisting of both improved and inferior yields (Table 2.2). In each case, double the glucuronylsynthase concentration (0.2 mg mL^{-1}) of my Honours research (0.1 mg mL^{-1}) was used unless otherwise stated.

Some reactions were performed with multiple variations making it difficult to pinpoint the exact variable responsible for the reaction yield. However, there were a couple of trends that stood out. When DDM is used to aid solubility, the yield is improved in most cases (*trans*-4-methylcyclohexanol **41** being the exception). This may be due to reduced enzyme inactivation especially when the detergent is substituted for harsh co-solvents like DMSO.

The glucuronosyltransferase system

Table 2.2. Revised glucuronosyltransferase reactions.



R	Previous yield (%) ^a	New yield (%) ^a	Altered conditions
	67 ^b	41	half the substrate concentration, E504G increased to 0.4 mg mL ⁻¹ , DMSO concentration reduced to 5%
	37 ^b	60	half the substrate concentration, DMSO concentration reduced to 10%
	44 ^c	21	25% DMSO replaced by 0.5% DDM
	47	58	none
	84	64	double the substrate concentration
	40	50	quarter the substrate concentration, 0.5% DDM used
	39 ^c	45	half the substrate concentration, 25% DMSO replaced by 2% DDM
	42 ^c	48	25% DMSO replaced by 1% DDM
	13	31	E504G increased to 0.4 mg mL ⁻¹

^a Reactions were performed using α -D-glucuronyl fluoride 51 (1.2 equiv.), E504G glucuronosyltransferase (0.1 mg mL⁻¹) in 50 mM sodium phosphate buffer, pH 7.5 unless otherwise stated. ^b 12.5% DMSO used. ^c 25% DMSO used.

Increasing enzyme concentration also seemed to improve the yield for *cis*-2-methylcyclohexanol **38** and phenol **52**. The improvement in yield is likely due to more enzyme available to turnover such a slow reaction. It is also interesting to see that by doubling the concentration of 3-methoxybenzyl alcohol **47** we reduce the yield by 20%, yet when we reduce the concentration, such as for 4-fluorobenzyl alcohol **50** or 4-methoxybenzyl alcohol **48**, an improved yield is observed. Standard Michaelis-Menten enzyme kinetics predicts that an increase to the substrate concentration should increase the rate of reaction (limited to the enzyme's maximum velocity) which would be advantageous to the yield. However, this is not the case and with the optimum reaction variables still undetermined, a glucuronylsynthase reaction protocol could not be defined. An enzyme kinetic study was required to better assess the individual reaction variables. But before an enzyme kinetic study was undertaken, the scope of the glucuronylsynthase methodology was explored with the demonstration of reaction scalability.

2.5.2 Scalability of glucuronylsynthase

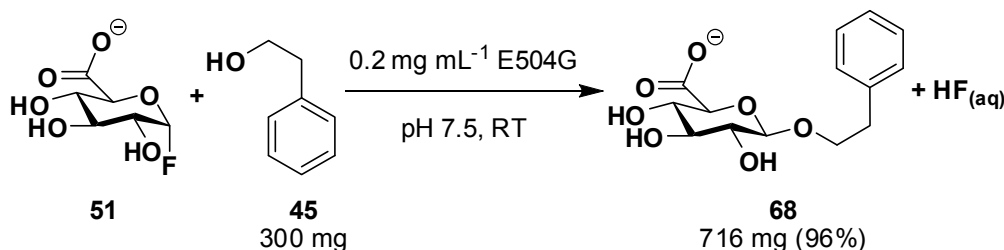
The most contemporary procedure for glucuronide synthesis incorporates uridine 5'-diphosphoglucuronosyltransferases (UGTs) to catalyse glucuronylation.⁴⁰ However, its existence as a membrane-bound enzyme causes difficulty in its expression and the practicality of its application in reactions. Typically, reactions involving UGTs are restricted to <10 mg scales.

The glucuronylsynthase enzyme exists as globular homotetramer; allowing ease of handling and large-scale expression. In past investigations, glucuronylsynthase reactions were performed on 20 mg scales for analytical purposes.⁵⁸ To assess the application of glucuronylsynthase on a large scale reaction, 5 mg of enzyme was used to convert 300 mg (2.5 mmol) of 2-phenylethanol **45** to its corresponding glucuronide **68** (Scheme 2.3) in 96% yield (718 mg). This yield is equivalent to that obtained with a 20 mg scale reaction (93%) and was achieved with only 0.003 mol% of enzyme.

The capability to scale up the reaction (fifteen fold in this case) with no change in yield illustrates the practicality of large scale glucuronylsynthase reactions for application in industry. With glucuronylsynthase reaction

The glucuronylsynthase system

scalability successfully demonstrated, it was time to expand the scope of the glucuronylsynthase methodology by investigating the enantioselectivity of the glucuronylsynthase enzyme.



Scheme 2.3. Large scale glucuronylsynthesis of 2-phenylethanol 45.

2.5.3 Enantioselectivity of the glucuronylsynthase enzyme

A large range of enzymes are known to be enantioselective. Whilst no literature exists on the stereoselectivity of native β -glucuronidase, it would be an interesting study to determine if the glucuronylsynthase has any preference towards one enantiomer of a chiral acceptor. Reviewing the fifteen substrates explored during my Honours research (Table 1.1), two substrates (*cis*-2-methylcyclohexanol **38** and *trans*-2-methylcyclohexanol **39**) were reacted as a mixture of enantiomers (Figure 2.9). In previous studies, the glucuronide of *trans*-2-methylcyclohexanol **39** was synthesised in the highest yield out of the two substrates (Table 1.1). As a result, the enantioselectivity of the glucuronylsynthase enzyme towards *trans*-2-methylcyclohexanol **39** was examined in more depth through the use of a Mosher's auxiliary in an attempt to identify and quantify the enantiomers.

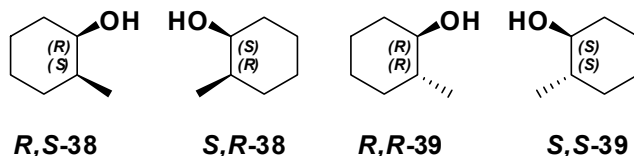
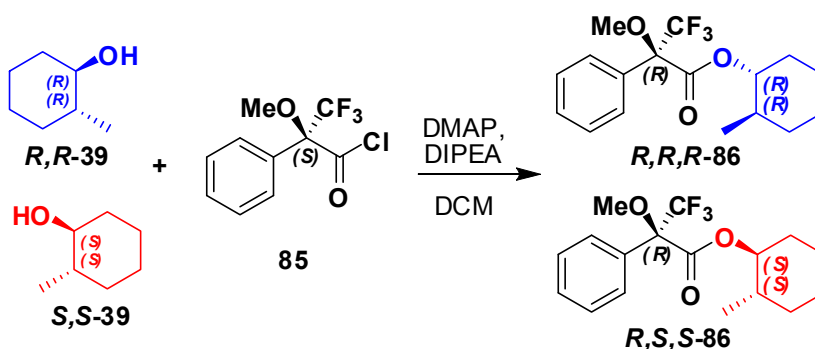


Figure 2.9: The enantiomers of *cis*-2-methylcyclohexanol **38** and *trans*-2-methylcyclohexanol **39**.

To begin, the enantiomeric ratio of the commercially-supplied *trans* alcohol **39** was determined. Excess (*S*)-(+)- α -methoxy- α -trifluoromethylphenylacetyl chloride **85** was generated in situ then added to the *trans*-alcohol **39** to create a diastereomeric mixture of the *trans*-2-methylcyclohexyl (*R*)-3,3,3-trifluoro-2-methoxy-2-phenylpropanoate (*trans* Mosher ester) **86** (Scheme 2.4).⁷¹



Scheme 2.4: The Mosher esterification of (\pm)-*trans*-2-methylcyclohexanol **39**.

The chemical shift relating to the methyl on the cyclohexyl ring is resolved by ^1H NMR and was used to quantify each diastereomer (Figure 2.10). For the *trans* Mosher esters **86**, one methyl shift occurs at 0.94 ppm and the other at 0.78 ppm. The NMR analysis showed an equivalent ratio of diastereomers for the *trans* Mosher esters **86** which suggested that the *trans* 2-methylcyclohexanol **39** was supplied as a 1:1 mixture of enantiomers.

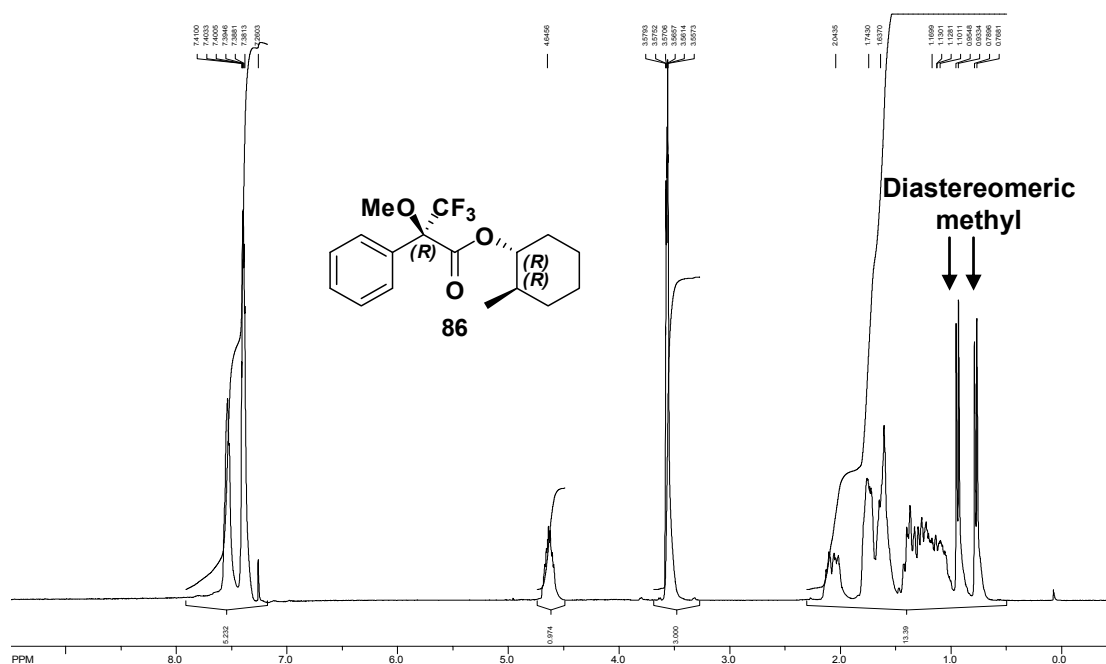


Figure 2.10: ^1H NMR spectrum (300 MHz, CDCl_3) of the *trans* Mosher esters **86** made from commercial *trans*-2-methylcyclohexanol **39**.

The methyl resonance in the ^1H NMR was also used to determine the absolute configuration of the *trans* Mosher esters **86**. Analysing the Dale-Mosher model for the *trans* Mosher esters **86**, it is predicted that the methyl of the *S,S-trans* Mosher ester R,S,S -**86** would exist further upfield from the methyl of the *R,R-trans* Mosher esters ester R,R,R -**86** due to the shielding by

The glucuronylsynthase system

the phenyl ring (Figure 2.11).⁷² This model suggests that the methyl resonance at 0.94 ppm should be assigned as the *R,R-trans* Mosher ester ***R,R,R-86*** and the 0.78 ppm as the *R,S,S-trans* Mosher ester ***R,S,S-86***. However, this is not consistent with literature, which assigns the methyl of ***R,S,S-86*** further downfield relative to the ***R,R,R-86*** methyl resonance.^{73,74} The assignment of the *trans* Mosher esters **86** in the literature were based on the optical rotation of the alcohol **39** prior to esterification. An extensive ¹³C study on Mosher esters by Lemière noted that the Mosher's ester for 2-substituted cyclohexanols did not fit the Dale-Mosher model.⁷⁵ The proximity of the methyl group to the Mosher's auxiliary is hypothesised to impose steric interactions that distort the Dale-Mosher conformation.

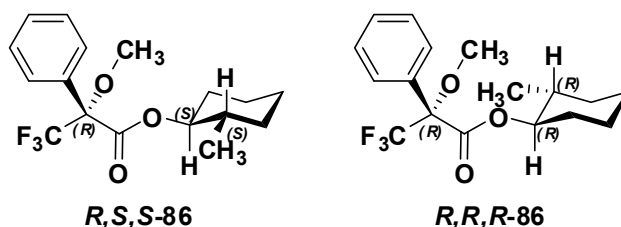


Figure 2.11. Dale-Mosher conformations of (*R*)-MTPA esters of *trans*-2-methylcyclohexanols **86**.

In light of this literature inconsistency, we hoped to determine the absolute configuration of the *trans* Mosher esters **86** by separating them by HPLC, removing the Mosher auxiliary and assigning the absolute configuration of the *trans*-alcohol **39** based on optical rotation. Normal phase HPLC was used on the *trans* Mosher esters **86** but baseline separation could not be achieved (Figure 2.12). Attempts at isolating the two diastereomers **86** by preparative HPLC was unsuccessful with the two isomers co-eluting from the column. Alternative HPLC conditions need to be further investigated so that the diastereomers **86** can be isolated. As a result of this, the literature data reported by Hirata was used to assign the absolute configuration of the *trans* Mosher esters **86**.⁷³

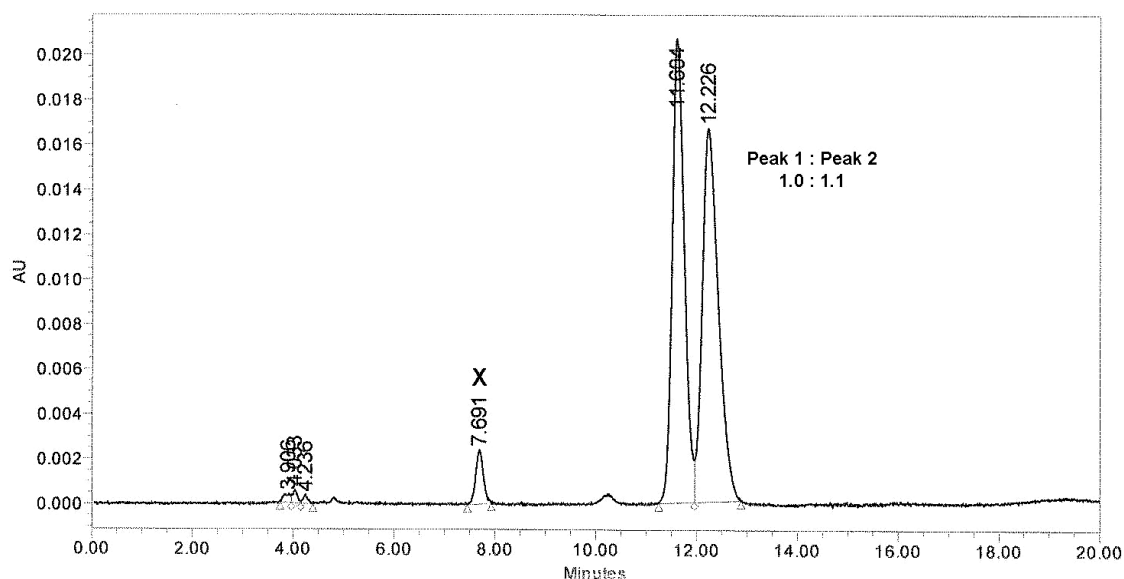
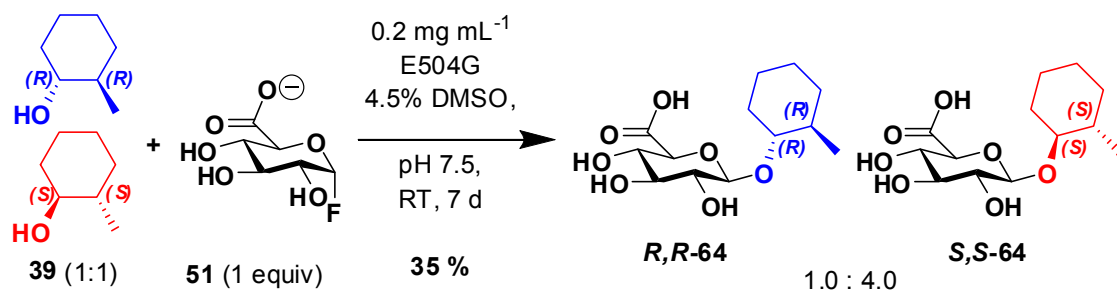


Figure 2.12: HPLC chromatogram (260 nm) of the *trans* Mosher ester **86** made from commercial supply.

A glucuronylsynthase reaction was performed on the racemic mixture of *trans*-2-methylcyclohexanol **39** with the glucuronide product **64** isolated from flash chromatography in 35% yield (Scheme 2.5). The ^1H NMR illustrated a clear selectivity for the reaction of one enantiomer over the other (Figure 2.13 and Figure 2.14). There is a significant shift in some of the pyranose protons (Figure 2.13). The H12 and H11 protons are clearly separated and have a chemical shift difference ($\Delta\delta$) of 0.022 ppm and 0.029 ppm respectively. The H10 and H9 protons also show diastereomeric resonances, however the extent of their separation is obstructed. The H1 proton of the two diastereomeric glucuronides **64** achieves baseline separation. However, the environment for the major isomer is obscured by the H9 environment.



Scheme 2.5. Glucuronylsynthase reaction on racemic *trans*-2-methylcyclohexanol **39**.

The majority of the alkyl protons in the cyclohexanyl ring appear as broad multiplets in the ^1H NMR spectrum (Figure 2.14). The exception to this being

The glucuronylsynthase system

the two doublets that correspond to the methyl protons (H7). The two resonances ($\Delta\delta = 0.064$ ppm) provide an estimated diastereomeric ratio of 1.0 : 4.0. Unfortunately, another proton environment arises between these two peaks which did not allow baseline integration of the two environments. However, another set of isolated diastereomeric resonances were present in the spectrum. The H2 protons appear at ~ 2.1 ppm and are separated ($\Delta\delta = 0.051$ ppm) with baseline separation. The ratio of their integration provided a diastereomeric ratio (1.0 : 4.2.) equivalent to that calculated for the methyl (H7) environments.

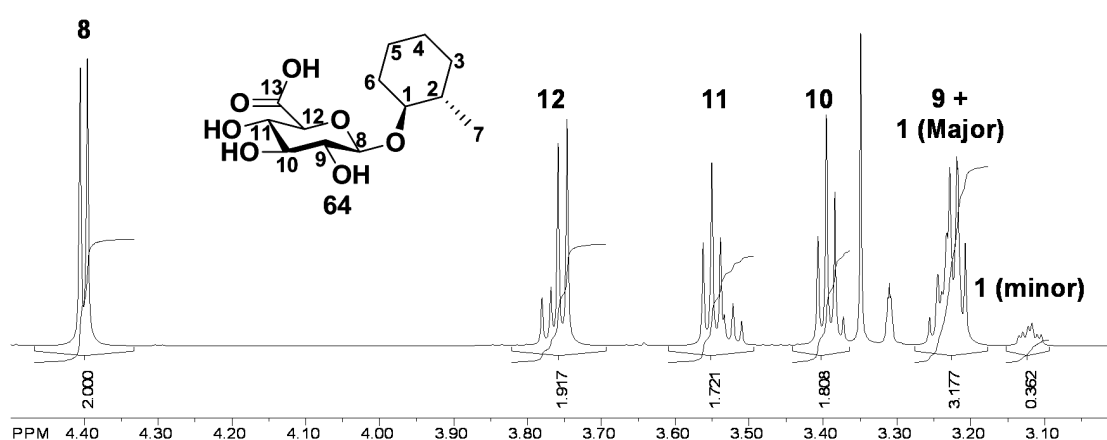


Figure 2.13. 4.5-3.0 ppm region of the ^1H NMR (800 MHz, MeOD) spectrum of *trans*-2-methylcyclohexyl β -D-glucuronide 64 depicting the diastereomeric protons in the pyranosyl ring.

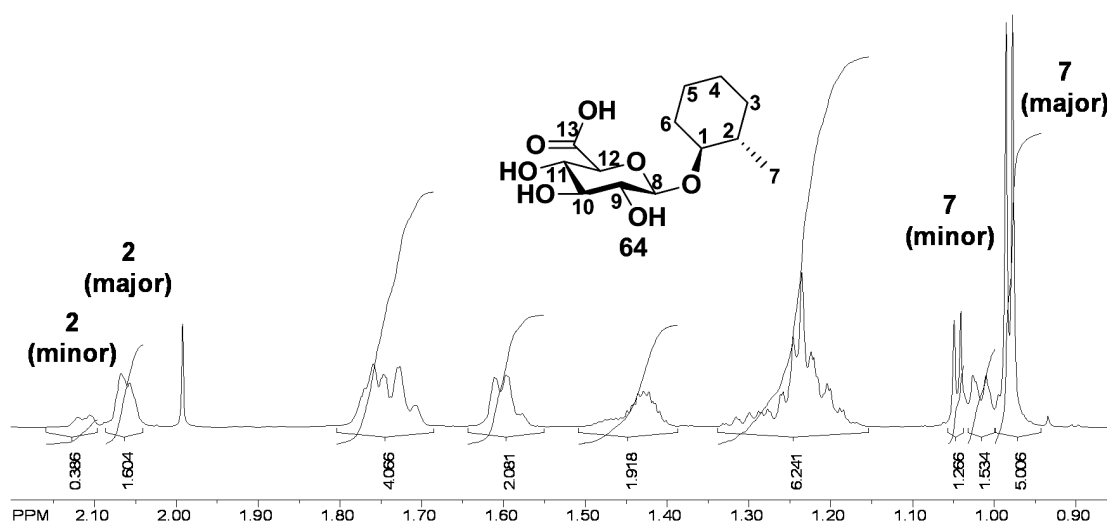
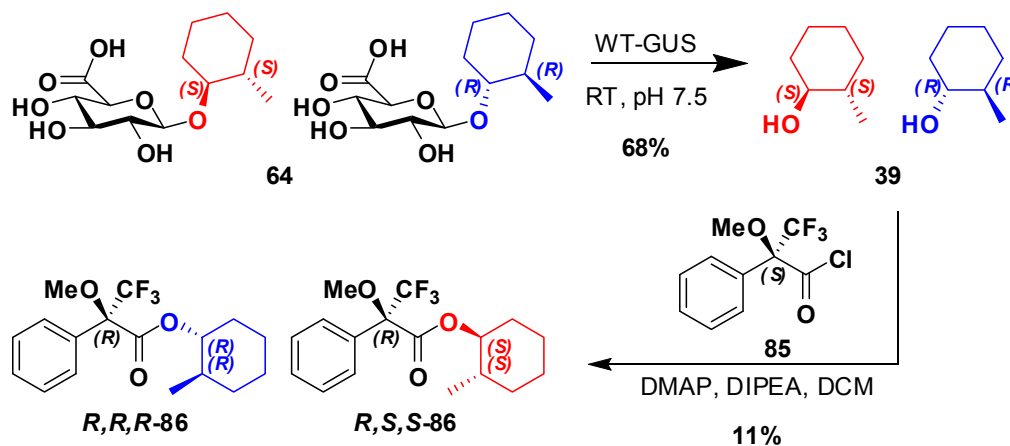


Figure 2.14. 2.2-0.85 ppm region of the ^1H NMR spectrum of *trans*-2-methylcyclohexyl β -D-glucuronide 64 depicting the diastereomeric protons in the cyclohexanyl ring.

The ^1H NMR of *trans*-2-methylcyclohexyl β -D-glucuronide **64** provides the diastereomeric ratio of the reaction, but no information regarding the absolute configuration of the major diastereomer. To determine the stereochemistry of the major diastereomer, the purified glucuronide **64** was dissolved in phosphate buffer and subjected to enzymatic hydrolysis by wild-type β -glucuronidase (Scheme 2.6). The free *trans*-alcohol **39** aglycon was extracted with ethyl acetate to yield 67% recovery from the glucuronide **64**. The unaccounted mass (5.8 mg, 33%) was likely due to the evaporation of the volatile alcohol **39** during the drying process. The aglycons were converted to the *trans* Mosher esters **86** under analogous conditions used for the starting material. Unfortunately, there was not enough material to make the (S)-Mosher ester as well.



Scheme 2.6. Mosher's esterification of the glucuronide aglycons (**39**).

The ^1H NMR spectrum for the *trans* Mosher esters **86** of the hydrolysed product **39** showed a significant difference in the integration of the methyl chemical shifts. The methyl shift at 0.94 ppm predominates over the other methyl shift just visible at 0.78 ppm (Figure 2.15). Whilst the NMR spectrum is not clean enough to accurately integrate the two methyl environments, visually there is a dramatic decrease in one of the diastereomeric species.

The difference of the two diastereomeric methyl shifts ($\Delta\delta = \delta[(R)\text{-MTPA ester of (+)-alcohol}] - \delta[(R)\text{-MTPA ester of (-)-alcohol}]$) was equal to the $\Delta\delta$ value of 0.161 reported by Hirata.⁷³ The major methyl peak at 0.94 ppm implies that the *R,S,S-trans* Mosher ester **R,S,S-86** is the major diastereomer and therefore the (1*S*,2*S*)-*trans*-2-methylcyclohexyl β -D-glucuronide **S,S-64**

The glucuronylsynthase system

was the major product (4 : 1) from the glucuronylsynthesis of a racemic mixture of *trans*-2-methylcyclohexanol **39** (Scheme 2.5).

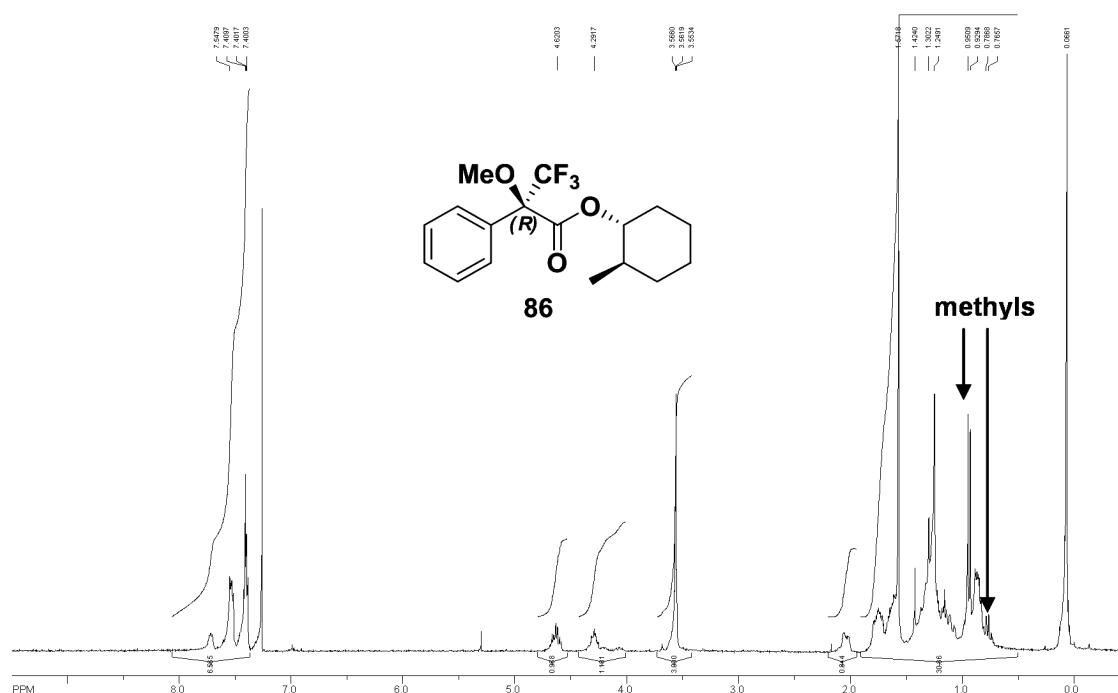


Figure 2.15: ¹H NMR spectrum (300 MHz) of the *trans* Mosher esters **86** made from the hydrolysed product **39**.

Future investigations should aim at isolating and characterising the individual *trans* Mosher esters **86** and determining the rotation of the hydrolysed alcohols **39**. Most concerning in this study was the low conversion (11%) of hydrolysed alcohol **39** converted to the *trans* Mosher esters **86**. Such a low yield with a 1 : 4 ratio of alcohols **39** could produce the expected minor Mosher's ester as the major product through kinetic resolution. This uncertainty could be avoided in future studies by the synthesis and analysis of the (*S*)-Mosher esters.

A repeat study using an alternative racemic substrate would also be insightful. From the experience gained in this study, a non-volatile substrate would be recommended so that it can be sufficiently dried without loss to evaporation. This would allow more accurate determination of sample mass and may also improve yields, especially in the esterification step whereby water decomposes the MTPA acid chloride **85**.

This glucuronylsynthase enantioselectivity would arise from different reaction rates between the two enantiomers which is based on the substrate fitting in the active site of the enzyme. This provides some information about the

binding pocket of glucuronylsynthase and β -glucuronidase. Generating a list of diastereomeric ratios from a library of enantiomers would be useful in mapping out the space of the binding pocket and deducing structure-activity relationships.

This enantiomeric study has proven that the glucuronylsynthase enzyme is selective for one enantiomer of *trans*-2-methylcyclohexanol **39** over the other. This is the first reported study detailing the enantioselectivity of β -glucuronidase. The diastereomeric glucuronides **64** were produced in a glucuronylsynthase reaction in a 1 : 4 ratio. However, with the possibility of kinetic resolution during the esterification, the major diastereomer could not be definitely assigned as the (1*S*,2*S*)-*trans*-2-methylcyclohexanyl β -D-glucuronide **S,S-64**. Whilst not selective enough for synthetic purposes, this enantiomeric study has expanded the scope of the glucuronylsynthase methodology. The development of the glucuronylsynthase methodology was continued by expanding the substrate library for this enzyme.

2.5.4 Novel substrates for glucuronylsynthesis

Up until this point, the glucuronylsynthase has successfully attached a glucuronyl residue to a selection of simple alcohols and a small library of steroids. But for the glucuronylsynthase enzyme to be implemented in industry, it needs to accommodate larger and structurally more complex molecules.

As discussed in the introduction (chapter 1.1), enzymes in our body convert codeine **1** into morphine **2** and then subsequently one of two morphine glucuronides (Scheme 1.1). Codeine **1**, morphine **2** and chloramphenicol **87** were generously donated by the National Measurement Institute to trial with the glucuronylsynthase enzyme. Morphine **2** and its methylated analogue, codeine **1**, have analgesic properties whilst chloramphenicol **87** is an antibiotic. Morphine **2** and chloramphenicol **87** are synthetically interesting substrates due to the presence of two possible sites of glucuronylation. The trends from previous studies predict the more reactive and less hindered alcohols are favoured. Hence, the allylic alcohol of morphine **2** and the primary alcohol of chloramphenicol **87** are predicted to be the probable sites of glucuronylation.

The glucuronylsynthase system

Unfortunately, no product could be seen by TLC for all three substrates. This observation was supported by a negative result in the electron-spray ionisation mass spectrum (ESI-MS). Perhaps under optimised conditions, the glucuronide product(s) would be observed.

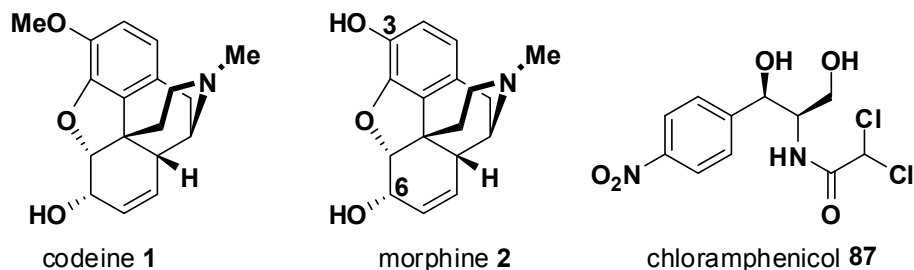


Figure 2.16. Pharmaceutical substrates trialed with the glucuronylsynthase.

The mechanism of glucuronylsynthase is essentially an enzyme-mediated S_N2-like nucleophilic reaction (Scheme 1.10). It was of great interest to determine if an alternative class of nucleophiles would react in a similar manner. Given the impressive yield of 2-phenylethanol **45**, identical reaction conditions were tested on 2-phenylethylamine **88** and 2-phenylethanethiol **89** (Figure 2.17). Unfortunately the respective *N*-linked and *S*-linked glucuronides could not be visualised by TLC or confirmed by ESI-MS.

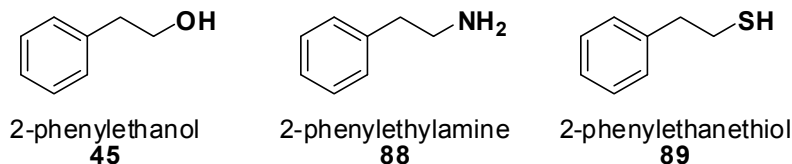


Figure 2.17. Different classes of substrates attempted with the glucuronylsynthase enzyme

The reaction with 2-phenylethanethiol **89** went cloudy suggesting probable protein denaturation. Thiols are reducing agents and at such a high concentration (100 mM) may have reduced the disulfide bonds of cysteine to cause protein denaturation. Comparing the pK_a of the three substrates, 2-phenylethanol **45** (~16), 2-phenylethylamine **88** (30-40, protonated 10-11) and 2-phenylethanethiol **89** (10-11), the amine would be charged at the reaction pH of 7.5. The ammonium species has no lone pairs and is no longer a nucleophile for the reaction. Furthermore, if the *N*-glycoside was formed, the corresponding hemiacetal may be unstable in aqueous solution and hydrolyse readily. This means that phenylethylamine **88** may act as a donor despite no product formation observed. So it is proposed that alcohols and phenols are

the only class of nucleophiles capable of reacting at the active site of glucuronylsynthase. For this particular example, the thiol **89** proved to be too reactive and caused enzyme inactivation whilst no glucuronide product was observed for the cationic amine species **88**. This result meant that the glucuronylsynthase substrate library could not be expanded to include the use of alternative nucleophiles or the pharmaceutical substrates demonstrated in this study.

Optimisation and expansion of the glucuronylsynthase methodology has been discussed in this chapter. The production of the glucuronylsynthase enzyme and synthesis of α -D-glucuronyl fluoride **51** has been optimised and both can be achieved in high yields. Expanding the scope of the glucuronylsynthase enzyme was demonstrated with a large scale synthesis of 2-phenylethanol **45** and the enantioselectivity towards *trans* 2-methylcyclohexanol **39** arising from kinetic resolution. Unfortunately, attempts at expanding the substrate repertoire of glucuronylsynthase were unsuccessful at this point of time. The glucuronylsynthesis of few pharmaceutical substrates did not produce any products. Furthermore, attempts at improving yields of known glucuronylsynthase reactions produced both positive and negative results. A more thorough investigation of these reactions through an enzyme kinetic study may shed some light on improving the yields of glucuronylsynthase reactions.

~ Chapter 3 ~

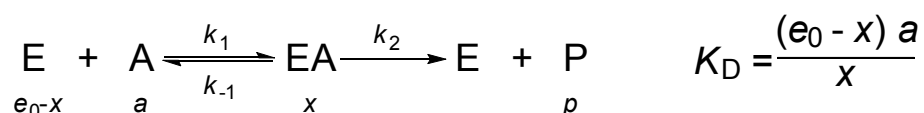
Enzyme kinetics

3.1 Introduction to enzyme kinetics

Before the details of the assay development are discussed, it is essential that the fundamentals of enzyme kinetics are known and that the assumptions that will be made in this research are outlined.

3.1.1 The Michaelis-Menten equation

In 1913, Michaelis and Menten proposed that the mechanism of an enzyme be represented by a reversible first step prior to product formation (Scheme 3.1).⁷⁶ This equilibrium is assumed to occur fast enough to be represented by an equilibrium constant for substrate dissociation (K_D). The instantaneous concentrations of enzyme (e) and substrate (a) can be calculated stoichiometrically from their initial concentrations minus the concentration of the enzyme-substrate complex (x). Respectively, $e = e_0 - x$ and $a = a_0 - x$. The concentration of the enzyme-substrate complex (x) is assumed to be limited by the concentration of enzyme (e_0) with the substrate concentration (a_0) usually much greater than e_0 and therefore much greater than x . So the concentration of the substrate can be assumed as $a = a_0$ with good accuracy.



Scheme 3.1. Michaelis-Menten's enzyme mechanism. Font in italics represent the terms used in the kinetic equations.

Arranging the dissociation constant in terms of x :

$$x = \frac{a e_0}{K_D + a} \quad (1)$$

The second step of the reaction is a simple first-order reaction determined from the concentration of enzyme-substrate complex (x) and the reaction rate constant k_2 . Its rate is given by:

$$v = k_2 x = \frac{k_2 a e_0}{K_D + a} \quad (2)$$

Enzyme kinetics

Briggs and Haldane (1925) extended this work by re-defining the change in the enzyme-substrate complex concentration (x) in terms of substrate dissociation *and* the rate of product formation (k_2). It can be defined as:

$$\frac{dx}{dt} = k_1 e a - k_{-1} x - k_2 x \quad (3)$$

Briggs and Haldane proposed that a steady state would be reached during the reaction in which the concentration of intermediate was constant.⁷⁷ This means that $dx/dt = 0$:

$$k_1(e_0-x)a - k_{-1}x - k_2x = 0 \quad (4)$$

Re-arranged in terms of substrate-enzyme complex concentration (x):

$$x = \frac{k_1 e_0 a}{k_{-1} + k_2 + k_1 a} \quad (5)$$

The reaction rate (v) for product formation is a simple first-order reaction dependent on the concentration of the substrate-enzyme complex concentration (x) with a rate constant of k_2 . Substituting (5) for x :

$$v = k_2 x = \frac{k_1 k_2 e_0 a}{k_{-1} + k_2 + k_1 a} = \frac{k_2 e_0 a}{\frac{k_{-1} + k_2}{k_1} + a} \quad (6)$$

Equation (6) may be re-written in its more general form as the *Michaelis-Menten equation*:

$$v = \frac{k_{\text{cat}} e_0 a}{K_m + a} \text{ or } \frac{V_{\text{max}} a}{K_m + a} \quad (7)$$

where k_{cat} is the catalytic constant, K_m is the Michaelis constant and V_{max} is the limiting rate. The rate equation (7) is almost identical to the equation derived by Michaelis and Menten (equation 2) with the exception of the constants used in the denominator (i.e. K_D vs. K_m). The latter is seen as an improvement to the original Michaelis-Menten approach and has been adopted into kinetic analyses ever since.

The V_{max} is the product of k_{cat} and e_0 ($V_{\text{max}} = k_{\text{cat}} \times e_0$) and is dependent on enzyme concentration (e_0). The catalytic constant (k_{cat}) is equal to k_2 for

simple mechanisms obeying Michaelis kinetics. As the concentration of substrate A approaches infinity ($a \rightarrow \infty$), the velocity of the reaction approaches V_{\max} ($v \rightarrow V_{\max}$):

$$v = \frac{k_{\text{cat}} e_0 a}{K_m + a} \quad \begin{array}{l} \text{as } a \rightarrow \infty \\ a \gg K_m \end{array} \quad v = \frac{k_{\text{cat}} e_0 a}{a} = k_{\text{cat}} e_0 \quad (8)$$

Similarly, K_m is a fundamental property of the enzyme and equates to $(k_{-1} + k_2)/k_1$ under simple single substrate kinetics. *Via* mathematical means, it has been proven to be the concentration of substrate required to achieve half the limiting rate:

$$\text{when } a = K_m, \quad v = \frac{k_{\text{cat}} e_0 a}{a + a} = \frac{k_{\text{cat}} e_0}{2} = \frac{1}{2} V_{\max} \quad (9)$$

The curve defined by equation (7) is a rectangular hyperbola that spans from the origin to the asymptote $v = V_{\max}$ (Figure 3.1).

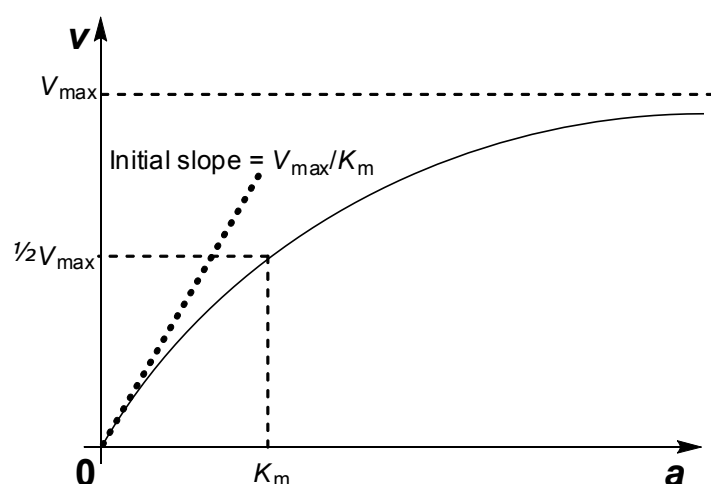


Figure 3.1. Dependence of initial rate v on the substance concentration a for a reaction obeying the Michaelis-Menten equation.

At the initial tangent to this curve, where the concentration of substrate (a) is small, the velocity (v) is directly proportional to the substrate concentration (a):

$$\begin{array}{l} \text{as } a \rightarrow 0 \\ a \ll K_m \end{array} \quad v \approx \frac{k_{\text{cat}} e_0 a}{K_m} = \frac{V_{\max} a}{K_m} \quad (10)$$

The gradient of this initial slope is therefore determined by the parameters V_{\max}/K_m . The term V_{\max} is dependent on enzyme concentration ($V_{\max} = k_{\text{cat}} \times e_0$) and so dividing by the initial enzyme concentration determines the fundamental parameter k_{cat}/K_m . The parameter k_{cat}/K_m is given the term

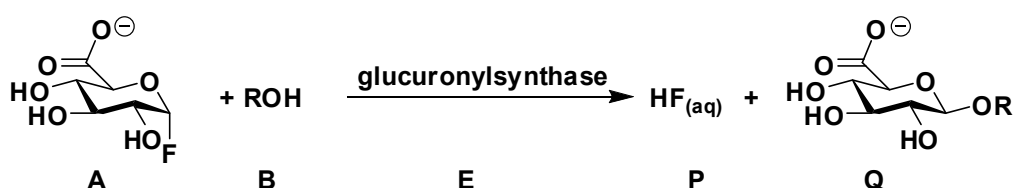
Enzyme kinetics

specificity constant and it indicates how well a substrate is turned-over by the enzyme. Substrates that have low K_m values and/or high turnover numbers (large k_{cat} values) will have a high specificity constant which results in a steep initial slope for the initial velocity vs. concentration plot for a given e_0 value. The specificity constant provides the means of contrasting the specificities of different substrates for an enzyme.

The k_{cat} , K_m and k_{cat}/K_m constants are not dependent on reaction variables such as enzyme/substrate concentration and are therefore fundamental parameters that define an enzyme reacting with a given substrate. These parameters will be determined in the enzyme kinetic study to profile and better understand the mechanism of the glucuronylsynthase enzyme. The Michaelis-Menten equation (7) has been derived to analyse the enzyme kinetics for a single-substrate reaction. The glucuronylsynthase reaction is a two-substrate reaction which follows more complicated rate equations.

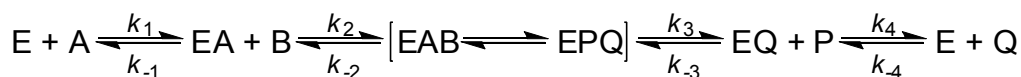
3.1.2 Two-substrate kinetics

The glucuronylsynthase reaction is a two-substrate reaction (Scheme 3.2) which has a mechanism more complicated than the initial mechanism proposed by Michaelis and Menten (Scheme 3.1). In general terms, there are three different mechanisms proposed for enzymatic reactions containing two substrates that will be discussed in this review. In fact, the actual number of mechanisms observed in nature is much greater as many variations are observed to occur.⁷⁸



Scheme 3.2. The bimolecular glucuronylsynthase reaction with letter assignments for schematic representations.

The first mechanism is known as the “ordered bi bi” reaction according to Cleland nomenclature or compulsory-order ternary complex mechanism (Scheme 3.3).⁷⁹ In this mechanism, the substrates must enter in a specific sequence and the products also released in a specific order.



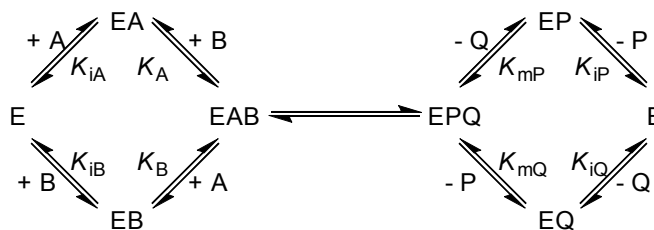
Scheme 3.3. Ordered bi bi enzyme mechanism.

Using King-Altman analysis⁸⁰, the complex rate equation in terms of kinetic constants can be derived for the ordered bi bi mechanism. For initial reaction rates, the concentration of products is deemed negligible such that $P = Q = 0$. The rate equation in terms of kinetic constants takes the form:⁸¹

$$v = \frac{V_{\max} a b}{K_{iA} K_{mB} + K_{mB} a + K_{mA} b + a b} \quad (11)$$

where V_{\max} is the limiting velocity of the enzyme, a and b are the concentration of the two substrates, K_{mA} and K_{mB} are the Michaelis constants for the respective substrates and K_{iA} is the true dissociation constant of A (k_{-1}/k_1).

The second type of mechanism is the "random bi bi" mechanism according to Cleland nomenclature or random-order ternary complex mechanism (Scheme 3.4).⁷⁹ In this mechanism, the substrates can bind to the enzyme in any order and products can also be released in any order.



Scheme 3.4. Random bi bi mechanism.⁸¹

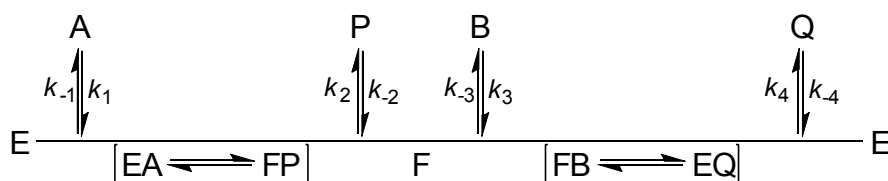
The scheme depicts the dissociation constant for each complex formed rather than rates. The King-Altman analysis of this mechanism is lengthy and for simplicity, its basic rate equation given in terms of kinetic constants is:⁸¹

$$v = \frac{\frac{V_{+ab}}{K_{iA}K_{mB}} - \frac{V_{-pq}}{K_{mP}K_{iQ}}}{1 + \frac{a}{K_{iA}} + \frac{b}{K_{iB}} + \frac{p}{K_{iP}} + \frac{q}{K_{iQ}} + \frac{ab}{K_{iA}K_{mB}} + \frac{pq}{K_{mP}K_{iQ}}} \quad (12)$$

When the initial rate is monitored, the concentration of products (p and q) are assumed negligible ($p = q = 0$) and the rate equation conveniently simplifies to the same rate equation (11) used for the ordered bi bi mechanism.

Enzyme kinetics

The third general mechanism is the “ping pong” mechanism according to Cleland nomenclature or substituted enzyme mechanism. In this mechanism (Scheme 3.5), the first product leaves before the second substrate binds and the enzyme goes through an activated intermediate (F). This mechanism describes the hydrolysis mechanism of the wild-type glycosidase (Scheme 1.8) whereby the glycosyl-enzyme intermediate (29) can be labelled the activated intermediate (F). On mechanistic grounds, it is expected that the glycosynthase proceeds by the binding of the two substrates prior to the first product release (Scheme 1.9).⁵⁴ The glycosynthase does not become involved as an activated intermediate and only mediates a single substitution with inversion of stereochemistry. As a result, this mechanism will not be considered and its rate equation will not be presented.



Scheme 3.5. The ping pong mechanism

Equation (11) can be re-arranged to make the concentration of substrate A (a) a factor (equation 13). If the concentration of substrate B (b) is kept constant, the congregation of constants can be combined to give *apparent* kinetic parameters and the relationship takes the form of the single substrate Michaelis-Menten equation:

$$v = \frac{\left[\frac{V_{\max} b}{K_{mB} + b} \right] a}{\left[\frac{K_{iA} K_{mB} + K_{mA} b}{K_{mB} + b} \right] + a} = \frac{V_{\max}^{\text{app}} a}{K_{mA}^{\text{app}} + a} \quad (13)$$

The apparent values are an approximation to the actual V_{\max} and K_{mA} values. The V_{\max}^{app} is proportional to the true value of V_{\max} with respect to $b/(K_{mB}+b)$. As K_{mB} must be greater than zero, it suggests that the V_{\max}^{app} will always be an underestimate of the true value of V_{\max} ($V_{\max}^{\text{app}} < V_{\max}$) for all moderate values of b . K_m^{app} is defined by multiple parameters and can be either an overestimation or underestimation of the true K_m .⁸²

However, if the concentration of substrate B is large ($b > 10 \times K_m$), the terms in equation (11) that do not contain b are assumed negligible (i.e. $K_{iA}K_{mB}$ and $K_{mB}a \ll b$).⁸¹ Equation (11) will simplify down to a simple pseudo-single substrate Michaelis-Menten model with true kinetic parameters:

$$\text{From (11), } v = \frac{V_{\max} a b}{b(K_{mA} + a)} = \frac{V_{\max} a}{K_{mA} + a} \quad (14)$$

The parallel equation can be used to find the kinetic parameters for substrate B when the concentration of substrate A (a) is saturating.

3.1.3 Practical aspects of kinetic studies.

It is valuable to describe the practical aspects of enzyme kinetics so that accurate results can be achieved and translated in terms of the theory discussed. The monitoring of the initial rate of the reaction is crucial for determining the kinetic parameters using the rate equations discussed. At the initial rate of the reaction, the concentration of the product and change in substrate concentration is deemed negligible. These assumptions were factored into the derivation of the rate equation.

The enzyme activity is dependent on several experimental factors. These include temperature, pH and enzyme concentration. These factors need to be identical for each reaction monitored so that changes in the reaction rate are solely due to substrate concentration. When considering the pH for a reaction to monitor, the enzyme's optimum pH should be used if known. Enzymes tend to have bell-shaped activity vs. pH curves (Figure 3.2).⁸¹ If the reaction is performed on the slope of this bell-curve, the slightest pH difference can cause a significant shift in activity.

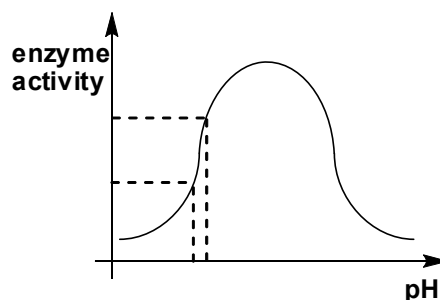


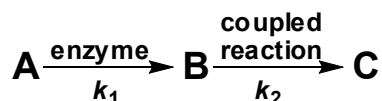
Figure 3.2. The typical enzyme activity vs. pH bell-curve. Dotted lines represent the large change in activity in response to a small change in pH on the slope of the curve.

Enzyme kinetics

Enzyme activity is usually proportional to temperature, but some enzymes may be unstable at certain temperatures. A constant temperature that is stable for the enzyme must be used throughout the kinetic study.

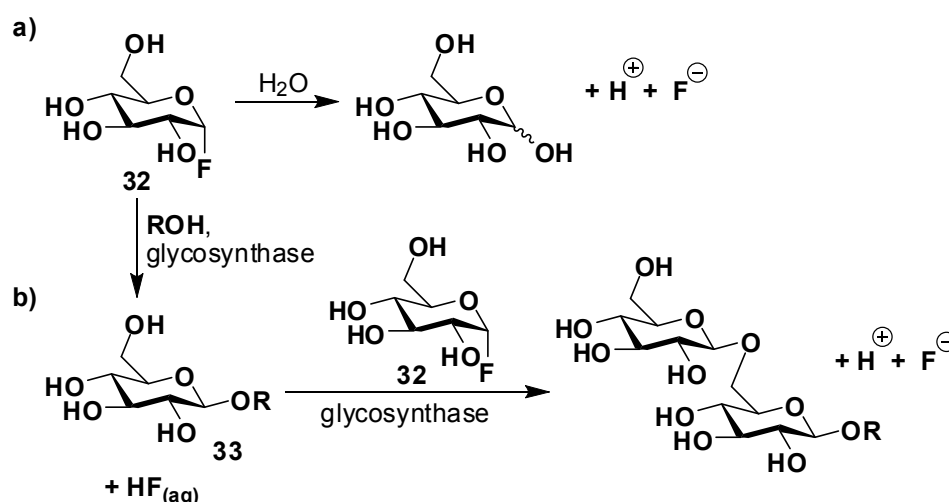
The enzyme stability can also be a factor of enzyme concentration. Many enzymes are more stable at high concentrations than at low, in a phenomenon known as enzyme inactivation.⁸¹ Some enzymes form quaternary structures (e.g. by β -glucuronidase forms a homotetramer) which often provide a greater enzyme stability.⁸³⁻⁸⁵ Enzyme activity may differ between the monomeric and associated forms through allosteric-like regulation between the subunits.^{86,87} At low concentrations of enzyme, the enzyme may be in equilibria between its monomeric and quaternary forms which could cause deviations from the linearity in activity. The linear relationship between enzyme activity and enzyme concentration should be demonstrated to prove enzyme inactivation is not an issue. However, if present, the enzyme concentration needs to be identical in every assay so that the initial rates can be accurately compared.

The initial rate can be monitored using one of three possible assays. A *continuous* assay involves the reaction being continuously monitored by an automated recording apparatus. This is the preferred method as the reaction remains untouched throughout the assay. However, it can sometimes be difficult to incorporate the required reaction conditions with the recording apparatus, for example reactions requiring extreme temperatures or pressures. A *discontinuous* assay is performed when portions of the reaction are removed at intervals and analysed to determine the extent of the reaction. This assay can tolerate reactions with more demanding reaction conditions as aliquots are removed from the reaction vessel to be analysed. However, the removal (and possible dilution) of samples can introduce errors to the kinetic experiment through instrumental and human error. The final assay is the *coupled* assay which is only used when a continuous or discontinuous assay is not possible. It involves monitoring a reaction that occurs in response to the product(s) formed in the enzyme reaction of interest (Scheme 3.6). This is an indirect determination of product formation (B) and uses the assumption that the reaction rate of the coupled reaction (k_2) is faster than the enzyme reaction of interest (k_1).



Scheme 3.6. The coupled assay

The direct or indirect monitoring of product is also an important aspect. An assay that directly monitors product formation is ideal as it eliminates side reactions that may contribute to the component that is monitored. Monitoring the release of fluoride ions in the glycosynthase reactions is an example of monitoring indirect product formation. The release of fluoride ions can be attributed to multiple side-reactions such as the hydrolysis of the glycosyl donor (Scheme 3.7a). A blank reaction in the absence of alcohol acceptor would need to be performed for each reaction to account for glycosyl fluoride donor hydrolysis.



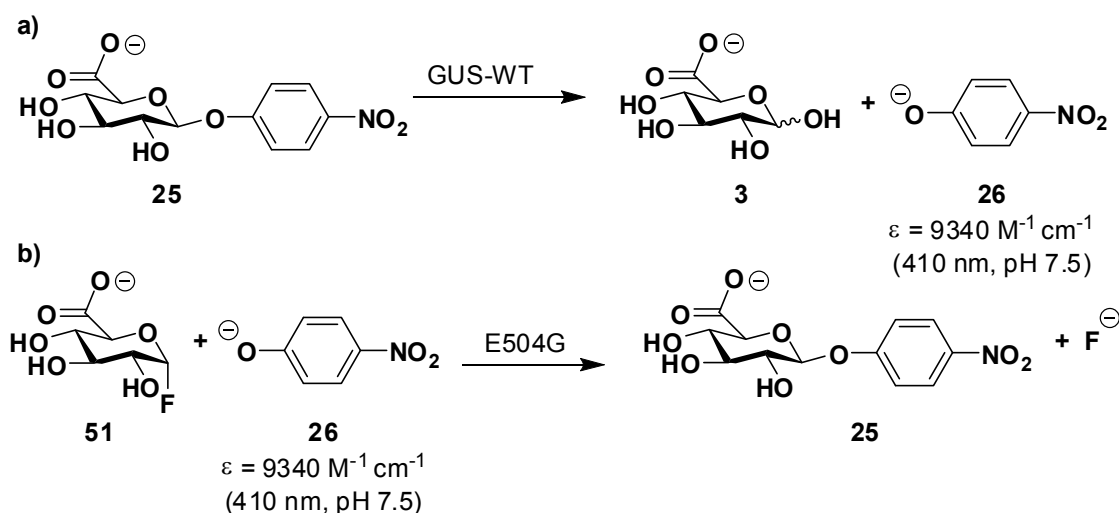
Scheme 3.7. The release of fluoride ion from glucosyl fluoride 32 by a) hydrolysis and b) oligomerisation.

Additionally, any oligomer formation, which can occur for most glycosynthases, would also contribute towards the fluoride concentration (Scheme 3.7b). The presence of multiple acceptors and donors with different affinities would complicate the kinetic analysis. Whilst oligomerisation has not been observed with glucuronylsynthase, the preparation of blank reactions essentially doubles the work load.⁵⁸ Ultimately, the direct observation of the glucuronide product would simplify the kinetic analysis and eliminate the need to perform additional controlled reactions. These theoretical and practical aspects were considered in the search for an assay to monitor the glucuronylsynthase reactions.

3.2 Glycosynthase kinetic assays

3.2.1 Introduction

The glucuronylsynthase reactions performed with varied reaction conditions (Table 2.2) illustrated unusual trends in yield. It was obvious that a more systematic study behind the effect of each of these variations needed to be implemented. This would involve elucidating the kinetic parameters for the substrates used, the catalytic rates of the reactions and the effect each reaction variable had on these parameters. The first step of the enzyme kinetic study was to identify a suitable assay. For the wild-type β -glucuronidase enzyme, a simple continuous chromogenic assay is used to assess enzymatic activity. A chromophore is cleaved from its glucuronyl residue by the enzyme which can be detected spectrophotometrically (Scheme 3.8a). The reverse chromo-ablative reaction (Scheme 3.8b) could be utilised for glucuronylsynthase except past examples have shown low reactivity towards phenols with the reaction rate being many magnitudes lower than the wild-type counter-part. Furthermore, the substrates tested would have to contain a chromophore, which is absent in most of the substrates used to date. The kinetic parameters of other glycosynthases have been determined primarily by fluoride-selective potentiometry.



Scheme 3.8. a) Hydrolysis of *p*-nitrophenyl β -D-glucuronide 25 by wild-type glucuronidase and b) glucuronylsynthesis of *p*-nitrophenyl- β -D-glucuronide 25 by glucuronylsynthase.

3.2.2 Fluoride-selective potentiometry

There are many different types of glycosynthases developed from a range of different organisms utilising a plethora of sugar donors and acceptors. However, there is one aspect that is common to all and that is the release of fluoride from the glycosyl fluoride donor. It is for this reason that fluoride-selective potentiometry is the most commonly utilised assay for glycosynthase reactions.⁸⁸⁻⁹⁸

The latest fluoride selective electrodes do not suffer significant interference from other anions and will detect fluoride concentrations in the low micromolar range (1.0×10^{-6} M).⁹⁹⁻¹⁰² Nevertheless, there are multiple drawbacks associated with this method that should be addressed. As discussed in the practical aspects of an assay (refer to section 3.1.3), the monitoring of fluoride is an indirect measurement of product formation which would require additional testing of blank reactions. The main concern with ion selective electrodes is the degree of drift over time, with most electrodes requiring recalibration every 2 hours. This is adequate time to determine initial velocities but means monitoring a glucuronylsynthase reaction over days would require constant recalibration and introduce errors. Further to this, the calibration curve is not always linear over the concentration range monitored and estimations may be needed which introduce further errors.

Another major disadvantage of fluoride selective potentiometry is response time in reading low concentrations of fluoride ions. Some procedures recommend up to a minute to obtain an accurate reading which is unsuitable for kinetic studies where the fluoride concentration is continuously changing. A work around would involve removing aliquots of the reaction in a discontinuous manner. This would provide further problems as an adequate volume (generally millilitres) is required to cover the probehead. This means either a dilution is required, reducing the detection limit of the assay, or large aliquots of a sizeable reaction would need to be taken.

Another factor of concern is the incompatibility of the probe with certain solvents which may dissolve the membrane of the junction. Unlike the majority of glycosynthases which operate with highly hydrophilic donors and acceptors, the glucuronylsynthase functions with lipophilic acceptors i.e. alkyl alcohols,

Enzyme kinetics

benzyl alcohols and steroids. The effect of detergents or co-solvents to aid solubility needed to be tested but their implementation may cause damage to the electrode.

Fluoride selective potentiometry has been successfully applied to many glycosynthase kinetic studies, but the drawbacks and errors disclosed here suggest an alternative assay was required. So a different glycosynthase assay was explored.

3.3 ^1H NMR assay

3.3.1 General discussion

No glycosynthase assays to date have reported the use of NMR as a means of detection. With a Bruker 800 MHz NMR spectrometer at my disposal, proton NMR spectroscopy could be used to identify and quantify the various reaction components in a time-efficient manner with most samples requiring only a single scan. Multiple samples were analysed simultaneously in a *continuous* assay through the use of an autosampler while the temperature was maintained at 21 °C by a probe heater.

The glucuronylsynthesis of 2-phenylethanol **45** was used to initiate the study due to its high yield and water solubility. The glucuronylsynthase enzyme was used at five times its normal concentration (1.0 mg mL^{-1}) so that an appreciable reaction rate was observed. By using the “Jump and Return” sequence, developed by Plateau and Guéron, the samples did not have to be prepared in completely deuterated materials.¹⁰³ Only 10% deuterium oxide was required in the final solution for locking purposes, making sample preparation quick and simple. Seven reactions were analysed simultaneously; differing only by substrate concentration to ensure all factors, such as enzyme activity, were identical for the kinetic study.

The acquired spectrum resembles a sine curve with an inflexion point at the water peak to suppress its presence (Figure 3.3). Baseline correction and peak integrations were applied at the regions 5.9-5.4 ppm (anomeric proton of α -D-glucuronyl fluoride **51**), 4.5-4.3 ppm (anomeric proton of the glucuronide product **68**) and 3.1-2.7 ppm (benzylic protons of 2-phenylethanol **45** and the

glucuronide product **68**). The benzylic protons of 2-phenylethanol **45** and the glucuronide **68** are isolated in the spectra and their combined integration remains constant throughout the reaction. The integration of this region was therefore used as an internal standard in the integration of the ^1H NMR spectra.

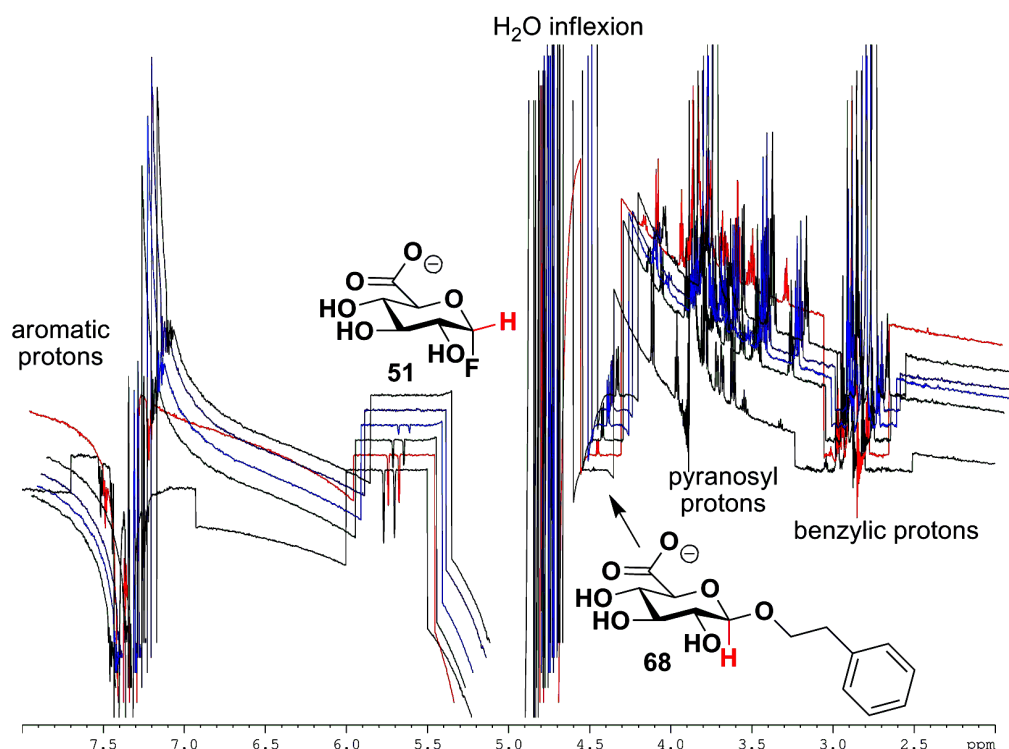


Figure 3.3: Stacked ^1H NMR spectra for a single glucuronylsynthesis reaction of 2-phenylethanol **45** (100 mM) with α -D-glucuronyl fluoride **51** (2.4 mM) and E504G (1 mg mL $^{-1}$) over a 2 h timescale. Spectra are colour-coded as black: $t = 0$ min, red: $t = 26$ min, green: $t = 51.5$ min, blue: $t = 75.5$ min, purple: $t = 98$ min, navy blue: $t = 124$ min. The respective regions have been labelled with text or represented by a red-highlighted proton.

3.3.2 Kinetics of α -D-glucuronyl fluoride **51**

An enzyme kinetic study was initiated by first determining the kinetic parameters for the α -D-glucuronyl fluoride **51** donor. The concentration of 2-phenylethanol **45** was kept constant at 100 mM – the limit of its solubility in a phosphate buffered solution. Because of this restricted solubility, the enzyme was not saturated with 2-phenylethanol **45** and meant that only the apparent kinetic parameters could be determined for α -D-glucuronyl fluoride **51** according to equation (13). Seven reactions with varied concentrations of α -D-

Enzyme kinetics

glucuronyl fluoride **51** (500 mM, 239 mM, 119 mM, 59.7 mM, 23.9 mM, 11.9 mM and 2.40 mM) were used. It was remarkable to see the time course plots (product formation vs. time) display equivalent velocities (Figure 3.4). The initial velocities were linear ($R^2 > 0.98$) in the region below 10% conversion. The reaction containing 2.4 mM α -D-glucuronyl fluoride **51** went to completion within the two hour timescale. This can be observed in Figure 3.4 by a plateau of product formation.

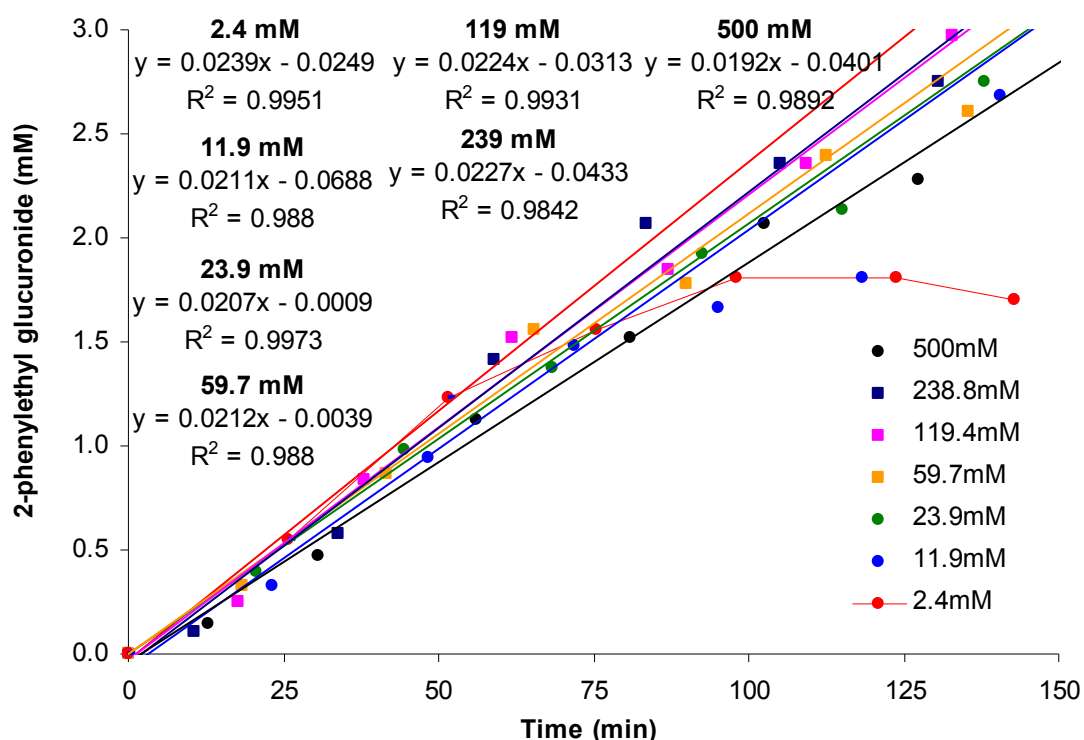


Figure 3.4: Time course plots of varying α -D-glucuronyl fluoride **51** donor with constant glucuronylsynthase (1.0 mg mL^{-1}) and sub-saturating 2-phenylethanol **45** acceptor (100 mM) obtained by 800 MHz ^1H NMR experiments (21 $^\circ\text{C}$, 50 mM phosphate buffer, pH 7.5, 10% D_2O). Linear plots are lines of best fit for the initial velocity (<10% conversion). R^2 values for the initial velocity were calculated using linear regression analysis.

When the initial velocities of these reactions are plotted against the α -D-glucuronyl fluoride **51** concentration, it provided a horizontal straight line in the initial velocity vs. concentration plot (Figure 3.5). This suggested the glucuronylsynthase was approaching the $V_{\text{max}}^{\text{app}}$ in this range of α -D-glucuronyl fluoride **51** concentrations tested and that the K_m^{app} for α -D-glucuronyl fluoride **51** is below the lowest concentration (2.4 mM) tested. This

is not unusual with strong affinities being reported for glycosynthases such as *Humicola insolens* endoglucanase E197A (0.87 mM)⁹⁰, *Bacillus licheniformis* 1,3-1,4- β -glucanase (1.36 mM)¹⁰⁴ and *Streptomyces sp.* β -glucosidase (1.7 mM)¹⁰⁵ towards their α -glycosyl fluoride donor.

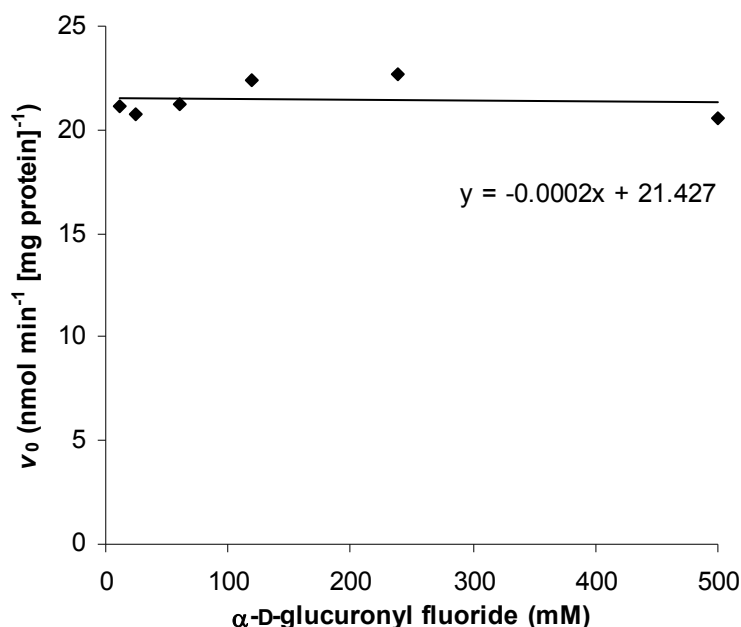


Figure 3.5. Initial velocity vs. concentration plot of varying α -D-glucuronyl fluoride **51** donor with constant sub-saturating 2-phenylethanol **45** acceptor (100 mM) and glucuronylsynthase (1.0 mg mL⁻¹) obtained by 800 MHz ¹H NMR experiments (21 °C, 50 mM phosphate buffer, pH 7.5, 10% D₂O).

A repeat of this assay with lower α -D-glucuronyl fluoride **51** concentrations (50 μ M, 100 μ M, 250 μ M, 500 μ M, 1 mM and 2.5 mM) was performed but no conclusions could be reached due to the poor signal-to-noise ratio at these dilute concentrations. The results from this study suggest that the apparent Michaelis constant (K_m^{app}) is less than 2.4 mM which is below the detection limit of the NMR technology used. In contrast, it appears the apparent limiting velocity (V_{max}^{app}) of the reaction was approached in the concentration range explored. The initial velocities of the reactions monitored appear to form the plateau of the initial velocities vs. concentration plot suggesting an approximate V_{max}^{app} of 21 nmol min⁻¹ [mg protein]⁻¹.

3.3.3 Kinetics of 2-phenylethanol **45**

NMR studies were then used to instigate the kinetic study of the acceptor alcohol, 2-phenylethanol **45**. The concentration of α -D-glucuronyl fluoride **51**

Enzyme kinetics

was kept constant at 100 mM. From the kinetic study of α -D-glucuronyl fluoride **51** (refer to section 3.3.2), the proposed K_m^{app} (and K_m) is less than 2.4 mM so the enzyme would have been saturated at this concentration. This saturating concentration of α -D-glucuronyl fluoride **51** would provide the conditions ($a \gg K_m$) that determine the true kinetic parameters for 2-phenylethanol **45** according to equation (14). Seven samples with varied concentrations of 2-phenylethanol **45** (100 mM, 75 mM, 50 mM, 25 mM, 10 mM, 5 mM and 1 mM) were used. Unlike the velocities observed in the α -D-glucuronyl fluoride **51** study, the initial velocities for 2-phenylethanol **45** varied with substrate concentration (Figure 3.6). After 2 hours, the product was only just visible in the NMR spectrum for the reaction containing 1 mM of 2-phenylethanol **45**. This once again highlights the poor sensitivity of this technique. Nevertheless, good linear regression values were achieved for the more concentrated samples.

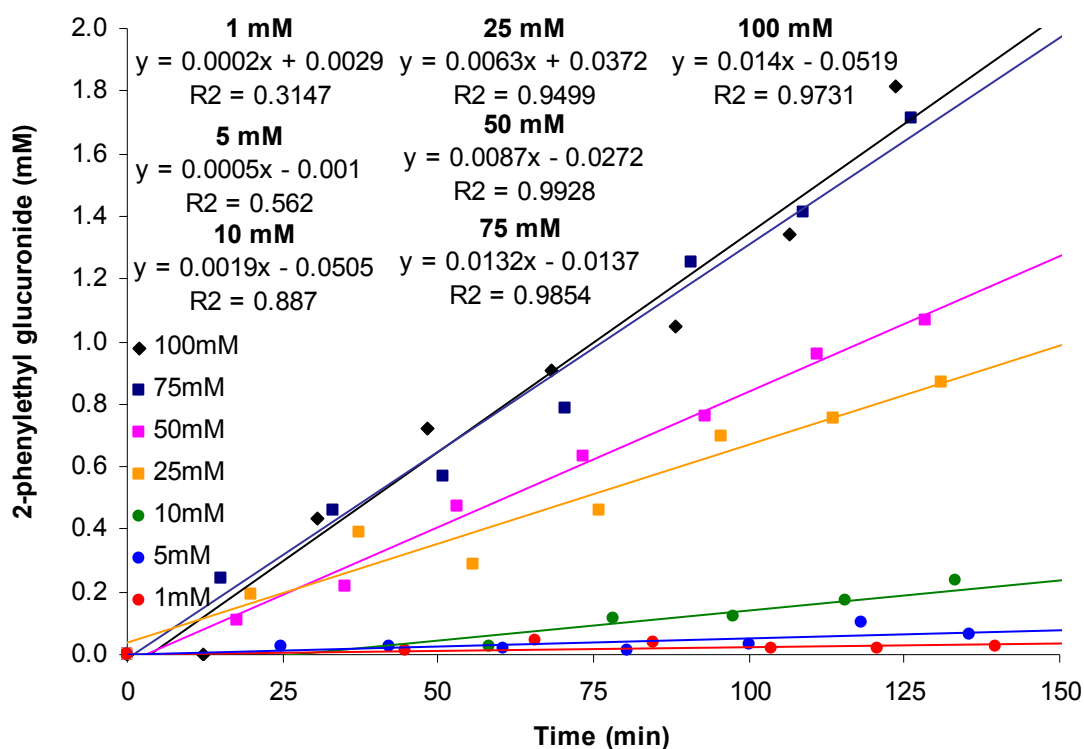


Figure 3.6. Time course plots of varying 2-phenylethanol **45** acceptor with constant glucuronylsynthase (1.0 mg mL^{-1}) and saturating α -D-glucuronyl fluoride **51** acceptor (100 mM) obtained by 800 MHz ^1H NMR experiments ($21 \text{ }^\circ\text{C}$, 50 mM phosphate buffer, pH 7.5, 10% D_2O). Linear plots are lines of best fit for the initial velocity (<4% conversion). R^2 values for the initial velocity were calculated using to linear regression analysis.

Plotting the velocities against the 2-phenylethanol **45** concentrations produces a hyperbolic curve indicative of Michaelis-Menten kinetics (Figure 3.7). Data fitting software was used to estimate the Michaelis-Menten parameters. The Michaelis constant (K_m) for 2-phenylethanol **45** was extrapolated as 109.5 mM and the limiting velocity (V_{max}) as 29.7 nmol min⁻¹ [mg protein]⁻¹. The affinity for 2-phenylethanol **45** (with saturating α -D-glucuronyl fluoride **51**) is quite weak in comparison to the proposed sub-millimolar α -D-glucuronyl fluoride **51** binding affinity. In fact, according to the estimated kinetic values, the Michaelis constant (K_m 109.5 mM) is never reached due to the insolubility of this substrate at higher concentrations. So at the best, the extrapolated value is still only an approximation of the real K_m . The V_{max} was extrapolated as 29.7 nmol min⁻¹, which is larger than the V_{max}^{app} (21 nmol min⁻¹ [mg protein]⁻¹) estimated from the α -D-glucuronyl fluoride **51** study. This is expected considering V_{max}^{app} is an underestimation of the true value of V_{max} (refer to section 3.1.2). The V_{max} equates to a very slow catalytic turnover (k_{cat}) of 0.034 s⁻¹.

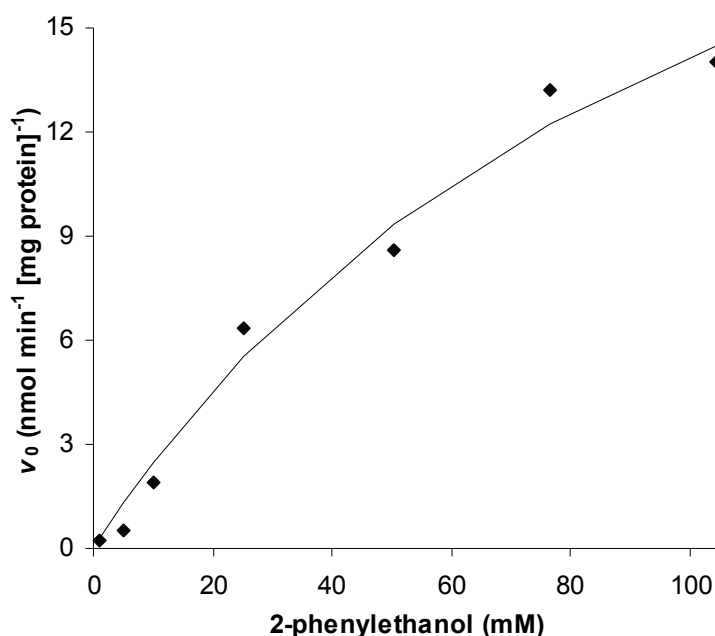


Figure 3.7. Initial velocity vs. concentration plot of varying 2-phenylethanol **45** acceptor with constant saturating α -D-glucuronyl fluoride **51** donor (100 mM) and glucuronylsynthase (1.0 mg mL⁻¹) obtained by 800 MHz ¹H NMR experiments (21 °C, 50 mM phosphate buffer, pH 7.5, 10% D₂O). Curve represents Michaelis-Menten fit from extrapolated parameters (K_m 109.5 mM, V_{max} 29.7 nmol min⁻¹ [mg protein]⁻¹).

Enzyme kinetics

Taking the slope of the initial velocities vs. concentration plot at low concentrations, the substrate specificity (k_{cat}/K_m) was determined as $0.30 \text{ M}^{-1} \text{ s}^{-1}$. This value, when compared to the substrate specificity values of other alcohol acceptors with glucuronylsynthase, will give a relative indication of how well each substrate is recognised and how efficiently it is converted to its glucuronide by the enzyme.

3.3.4 Conclusion

Proton NMR has been proven to be a practical means of monitoring the glucuronylsynthase reaction in a continuous manner. The anomeric protons of the reaction components are generally isolated and can be integrated to quantify the conversion of a reaction. The successful application of this assay was applied to 2-phenylethanol **45**. It was determined to bind weakly to the glucuronylsynthase (K_m 109.5 mM) under conditions of saturating glucuronyl donor **51** and incapable of approaching its limiting velocity (V_{max} $29.7 \text{ nmol min}^{-1} [\text{mg protein}]^{-1}$) due to solubility restraints. The α -D-glucuronyl fluoride **51** donor is predicted to bind tightly the glucuronylsynthase enzyme ($K_m < 2.4 \text{ mM}$) but a value was not determined due to the poor sensitivity of this technique. The proton NMR assay is applicable to glucuronylsynthase reactions and may be extended to other glycosynthase reactions. With the current NMR technology, the assay is limited to binding affinities down to the millimolar region.

3.4 Isothermal titration calorimetry

3.4.1 Background

Isothermal titration calorimetry (ITC) is not used to establish kinetic parameters but does determine the thermodynamic parameters associated with a ligand binding to its host. It uses heat measurement to indicate the extent to which a ligand-binding site is saturated. The technique is relatively new, with the first applications conducted 44 years ago to solve chemical equilibria.¹⁰⁶ It was followed closely by the first biochemical binding study and enzyme kinetic study.^{107,108} However, it is not until possibly the past decade that the calorimetric technology has become suitable for the routine use in

characterising the thermodynamics of biochemical interactions.^{109,110} Current ITC technology is sensitive enough to detect 0.1 μcal (10 μcal accurately).¹¹¹ This allows the determination of binding constants as large as 10^8 - 10^9 M^{-1} .

ITC works by the incremental addition of ligand or substrate into a solution of the enzyme in a constant temperature (isothermal) cell. Heat is applied or removed to retain a constant temperature and this energy applied or withdrawn is directly proportional to the amount of binding. As the system reaches saturation, the heat signal diminishes until only heats of dilution are observed. The optimised binding data for a single-site binding enzyme should resemble a sigmoidal curve that follows the equation:

$$q = v \Delta H e_t \frac{K_A a}{1 + K_A a} \quad (15)$$

where q is the heat produced/absorbed, v is the volume of the cell, ΔH is the binding enthalpy per mole of the ligand, e_t is the total enzyme concentration, K_A is the binding constant and a is the concentration of ligand.¹¹² The shape of the sigmoidal curve is greatly affected by the size of the enzyme concentration (e_t) and the binding constant (K_A) in a parameter termed as the “ c ” value.¹⁰⁹ The “ c ” value is defined as the enzyme concentration multiplied by the binding constant ($c = e_t \times K_A$). A “ c ” value of 0 provides a horizontal line, and as “ c ” increases, the sigmoidal curve emerges until $c \rightarrow \infty$, which has a vertical inflexion like a step (Figure 3.8). For the accurate determination of the binding constant K_A , a “ c ” value of 10-100 is recommended.

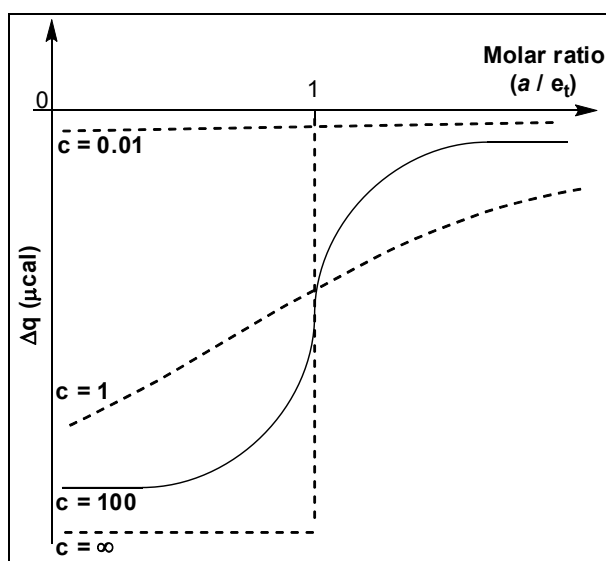


Figure 3.8. Simulated binding isotherms for various values of the parameter c . The desirable curvature ($c = 100$) is depicted as continuous curve.

3.4.2 Binding constant of α -D-glucuronyl fluoride **51**

The substrate (α -D-glucuronyl fluoride **51**) was dissolved in an identical batch of phosphate buffer used to dialyse the enzyme to eliminate heats of ionisation (or protonation) caused by different salt and pH levels. It was degassed prior to its addition to the ITC syringe. The enzyme concentration was determined by spectroscopic methods and degassed prior to its addition to the isothermal cell set at 21 °C. Beginning with a glucuronylsynthase concentration of 50 μ M (3.4 mg mL⁻¹), titration with different concentrations of α -D-glucuronyl fluoride **51** was performed until the correct curvature in the thermogram was obtained.¹⁰⁹ The ideal sigmoidal curvature was never obtained with only the latter half of the sigmoidal curve (demonstrating binding-site saturation) only ever achieved. When lower concentrations of α -D-glucuronyl fluoride **51** were added, the binding site did not achieve saturation and the slow initial uptake (giving rise to a sigmoidal curve) was still not observed. The best curvature was achieved with 3 mM of α -D-glucuronyl fluoride **51**, which provided data points that approached saturating conditions (Figure 3.9).

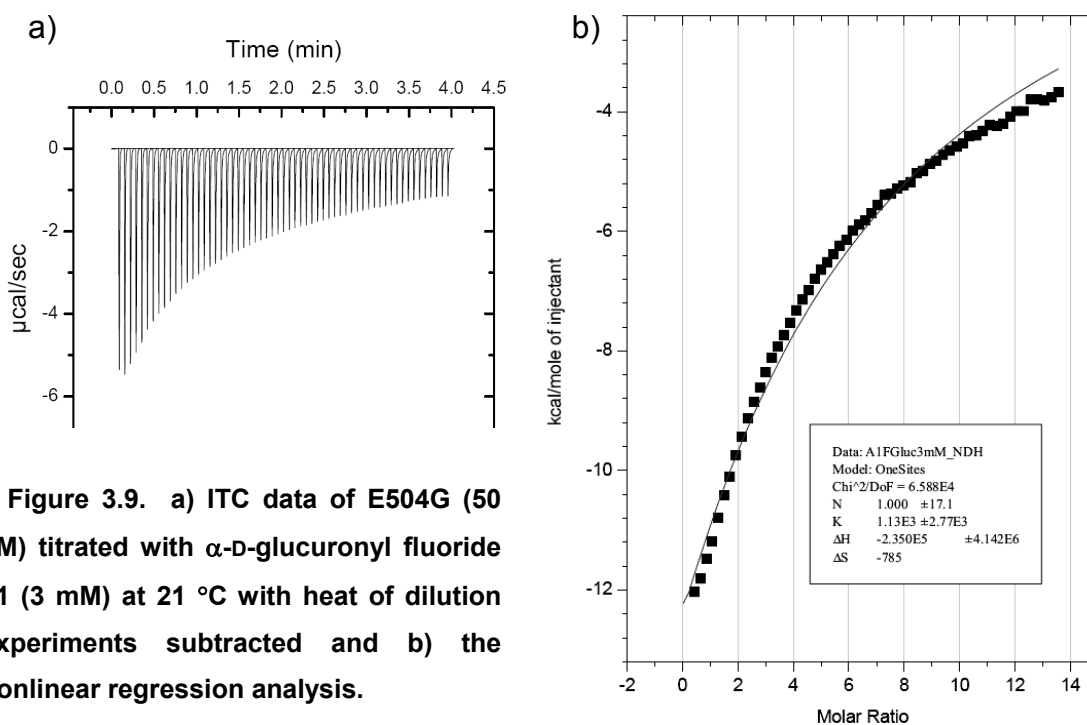


Figure 3.9. a) ITC data of E504G (50 μ M) titrated with α -D-glucuronyl fluoride **51** (3 mM) at 21 °C with heat of dilution experiments subtracted and b) the nonlinear regression analysis.

A repeat of this titration was performed with the absence of enzyme to determine temperature changes contributed from heat of dilution. The negative energy applied to the system implies that the binding of α -D-

glucuronyl fluoride **51** to glucuronylsynthase is an exothermic event. Non-linear regression fits of this data to equation (15) provided large errors with the binding constant (K_A) calculated as $1130 \pm 2770 \text{ M}^{-1}$. Taking the inverse of this value, we obtain a dissociation constant (K_D) of $0.2 \pm 0.4 \text{ mM}$.

One of the major causes for this error was from the poor signal response provided by the system. The maximum signal ($5 \mu\text{cal s}^{-1}$) obtained from titration did not pass the recommended threshold for accuracy of $10 \mu\text{cal s}^{-1}$. So the titration was repeated with $125 \mu\text{M}$ (8.5 mg mL^{-1}) of glucuronylsynthase and 6.7 mM α -D-glucuronyl fluoride **51**. An identical thermogram was obtained with larger responses (Figure 3.10). The non-linear regression fit had smaller errors and calculates the binding constant (K_A) as $780 \pm 30 \text{ M}^{-1}$.

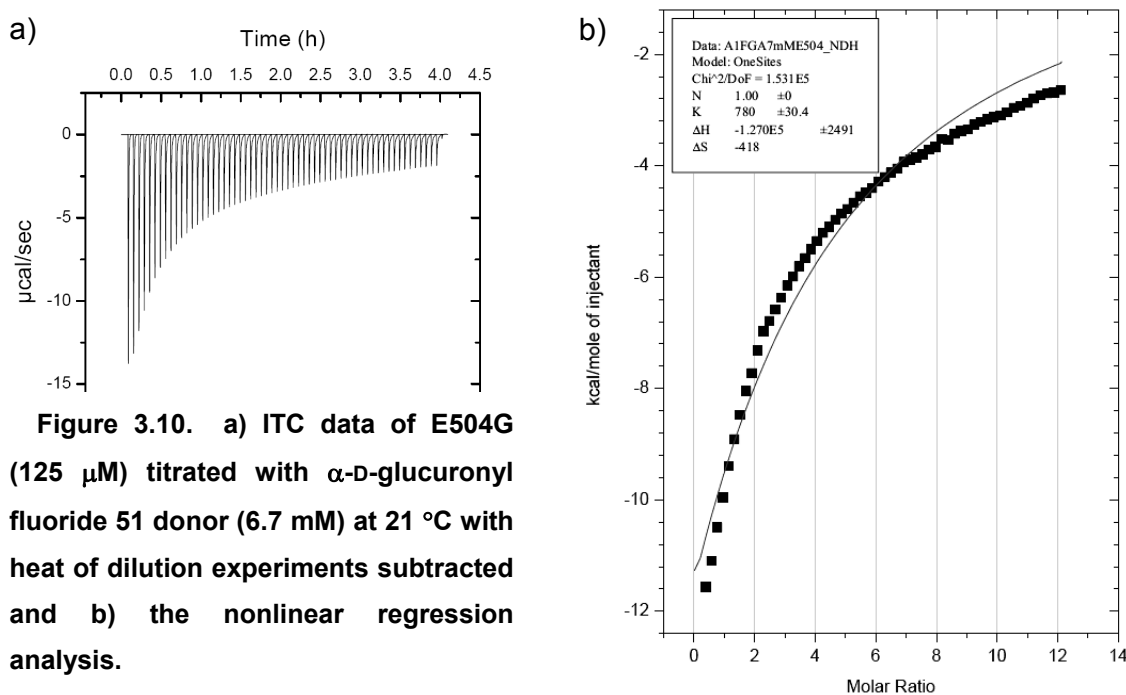


Figure 3.10. a) ITC data of E504G ($125 \mu\text{M}$) titrated with α -D-glucuronyl fluoride **51** donor (6.7 mM) at $21 \text{ }^\circ\text{C}$ with heat of dilution experiments subtracted and b) the nonlinear regression analysis.

Taking the inverse of this value, we obtain a dissociation constant (K_D) of $1.28 \pm 0.03 \text{ mM}$. The dissociation constant (K_D) is an approximation of the Michaelis constant (K_m) with the actual K_m being of greater value for a single substrate mechanism.¹¹³ However, Cook and Cleland demonstrate how the dissociation constant (K_D) can be greater *or* smaller estimation of the real K_m value in a two substrate mechanism.⁸² This implied that the K_m of α -D-glucuronyl fluoride **51** resides in the low mM region in line with the previously mentioned glycosynthase literature examples.^{90,104,105} However, the accuracy

Enzyme kinetics

of this value is questionable given the “c” parameter for this titration ($c = 0.1$) is below the recommended “c” values of 10-100. From these figures, a titration using glucuronylsynthase one hundred times more concentrated (850 mg mL^{-1}) is required for an acceptable result. Such a concentrated sample is unviable and an alternative assay was required to determine the binding affinity of α -D-glucuronyl fluoride **51**.

3.4.3 Binding constant for 2-phenylethyl β -D-glucuronide **68**

The glucuronide products formed in the glucuronylsynthase reactions are substrates for the wild-type glucuronidase. With glucuronylsynthase differing from glucuronidase by a single amino acid, it is likely that the glucuronide product may have some affinity towards the glucuronylsynthase binding site. To determine the extent of this equilibrium, the 2-phenylethyl β -D-glucuronide **68** was titrated against glucuronylsynthase ($48.5 \text{ }\mu\text{M}$) using ITC. Titrating with a millimolar solution produced a titration curve that depicted no trace of saturation even occurring. The titration was stopped prematurely and repeated with a 10 mM solution of 2-phenylethyl β -D-glucuronide **68**. This showed some sign of saturation occurring, but the signal response was too low ($<0.2 \text{ }\mu\text{cal s}^{-1}$) so the titration was also stopped prematurely. In contrast, when a 100 mM concentration of 2-phenylethyl β -D-glucuronide **68** was titrated against glucuronylsynthase, an endothermic thermogram was observed. This suggested that the response from substrate binding was still not measurable and that only the heat of dilution was providing a response. A heat of dilution control experiment would have provided the net calorimetric response that substrate binding exerted. However, this was not performed due to the small overall response in the titrations ($\sim 5 \text{ }\mu\text{cal s}^{-1}$) suggesting the response from substrate binding was still minute. Whilst inconclusive, this study implies that the binding affinity of 2-phenylethyl β -D-glucuronide **68** to glucuronylsynthase is very weak and that a highly concentrated batch of enzyme ($>30 \text{ mg mL}^{-1}$) would be required to obtain an adequate response required to determine the binding constant (K_A).

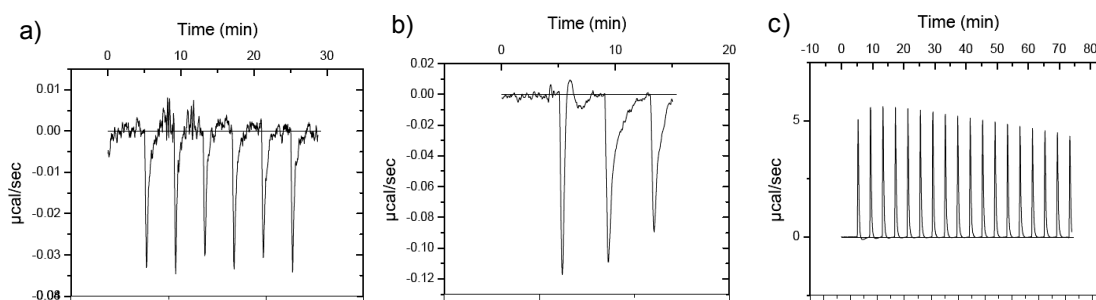


Figure 3.11. Raw ITC data of E504G (48.5 μM) titrated with 2-phenylethyl $\beta\text{-D}$ -glucuronide **68** at a) 1 mM; b) 10 mM; and c) 100 mM at 21 $^{\circ}\text{C}$.

3.4.4 Conclusions

Isothermal titration calorimetry demonstrated the saturation of glucuronylsynthase with $\alpha\text{-D}$ -glucuronyl fluoride **51** by measuring the heat associated with its exothermic binding interaction. A binding constant (K_A) of $780 \pm 30 \text{ M}^{-1}$ was calculated from its titration. However, the accuracy of this value is questionable given the signal response and the “c” value (0.1) were both below their recommended thresholds. From the data obtained, glucuronylsynthase would be required at one hundred times the concentration for an acceptable binding constant result. Such a concentration is unfeasible, and even if possible, demands high quantities of precious enzyme. The titration of 2-phenylethyl $\beta\text{-D}$ -glucuronide **68** encountered equivalent threshold problems. No binding constant was calculated due to low signal response.

Complications are envisaged for the binding of the acceptor alcohols to glucuronylsynthase. Under a 2-substrate enzyme system, two possible models could exist: the random-order ternary-complex mechanism or the compulsory-order ternary complex mechanism (refer to section 3.1.2). In each case, the binding would be different with and without the presence of $\alpha\text{-D}$ -glucuronyl fluoride **51**. In the presence of $\alpha\text{-D}$ -glucuronyl fluoride **51** and the acceptor alcohol, a glucuronylsynthase reaction will produce a glucuronide product, fluoride ion and a proton. These products may alter the binding studies by binding to the enzyme or alter the reaction temperature through the heat of reaction, dilution and/or ionisation. Heat from reactions have been monitored by ITC to determine enzymatic parameters, but requires reaction completion within 30-60 min.¹¹¹ Well outside the timeframe required for a glucuronylsynthase reaction (days).

Enzyme kinetics

A repeat of the binding study using glucuronylsynthase as concentrated as possible may provide adequate results for the binding of α -D-glucuronyl fluoride **51** and the glucuronide products, but is unlikely to define the binding constant for the acceptor alcohols. Furthermore, the sample preparation was an arduous task to eliminate interference resulting from heat of dilutions. Overall, ITC appeared to be an unsuitable assay for the glucuronylsynthase system.

3.5 HPLC-UV

3.5.1 Background

HPLC has been successfully applied in literature as a means to determine the enzyme kinetics of glycosynthases.^{104,105,114} HPLC is a discontinuous assay by definition, as samples are removed from the reaction over intervals. However, HPLC in conjunction with an autosampler provides automation that can be associated with a continuously sampled assay. Multiple detectors are available to directly monitor and quantify the product(s) of the reactions. As discussed previously (refer to section 3.1.3), this simplifies kinetic analysis by focusing on the reaction of interest.

Yang *et al* utilised LC-MS to determine the kinetic parameters of their glycosynthase.¹¹⁵ A past group member attempted to repeat the LC-MS work with the glucuronylsynthase.¹¹⁶ His work was successful in that the individual reaction components could be separated and identified by ESI-MS, but the response of the ESI was easily interfered by variations in buffer concentration making it difficult to accurately quantify the reaction components. This procedure is extremely sensitive with the reaction mixture being too concentrated for a direct injection. Aliquots had to be manually removed from the reaction and diluted prior to LC-MS analysis which introduces numerous means for errors to occur.

A repeat of the assay using HPLC with a photodiode array detector (PDA) was developed to eliminate the interferences encountered with the ESI-MS detector. The reaction was directly injected without dilution from a thermostat-

controlled autosampler to eliminate human error and provide efficiency through automation.

3.5.2 Development of the HPLC-UV assay

Initial studies looked at the development of an assay that would separate the components in the 2-phenylethanol **45** glucuronylsynthase reaction. A solution containing 2-phenylethanol **45**, α -D-glucuronyl fluoride **51** and 2-phenylethyl β -D-glucuronide **68** was used to simulate the glucuronylsynthase reaction and to hone in on the optimised conditions. An isocratic mobile phase of 23% aqueous acetonitrile containing 0.1% trifluoroacetic acid provided adequate separation of the reaction components within a 10 min run time. The trifluoroacetic acid was important to achieve good resolution on the C18 column by ensuring the protonation of the glucuronide. Pure samples of 2-phenylethanol **45**, α -D-glucuronyl fluoride **51** and 2-phenylethyl β -D-glucuronide **68** were analysed by the HPLC assay to verify retention times (ret). The α -D-glucuronyl fluoride **51** was UV silent, but the 2-phenylethanol **45** (ret 7.2 min) and 2-phenylethyl β -D-glucuronide **68** (ret 4.2 min) had an UV maximum at 260 nm.

3.5.3 Internal standard

To perform an accurate comparison between each injection, an internal standard was introduced to the glucuronylsynthase reaction. A library of potential internal standards was created from simple chemicals found within the lab and were assessed on 3 factors. The first selection criterion was to omit any alcohols or phenols to avoid any chance of glucuronylation. The second requirement was the presence of UV activity to allow PDA detection. The final condition needed a retention time within (or close to) the 10 min run time developed for the 2-phenylethanol **45** glucuronylsynthase reaction without overlapping the peaks of interest. Nineteen compounds were subjected to the HPLC assay with their retention time and UV maxima reported in Table 7.1.

Six compounds (1,2-naphthoquinone-4-sulfuric acid **90**, 2-methoxybenzoic acid **91**, 4-methoxybenzoic acid **92**, 3,4-dimethoxybenzoic acid **93**, 2-nitrobenzoic acid **94** and 3-nitrobenzoic acid **95**) satisfied all of the previously mentioned requirements.

Enzyme kinetics

The 2-methoxybenzoic acid **91** was chosen as the potential internal standard due to its retention time approximately midway between the two peaks of interest. A study was then performed to ensure no change in enzymatic activity was observed as a result of 2-methoxybenzoic acid **91** being present in the glucuronylsynthase reaction. A solution of 2-phenylethanol **45** (100 mM) and α -D-glucuronyl fluoride **51** (100 mM) was divided into two HPLC vials. To the first vial, 2-methoxybenzoic acid **91** (final concentration 1 mM) was added and to the second vial, an equal volume of phosphate buffer (the control). An equal aliquot of enzyme was added to each and the reaction monitored simultaneously by the developed HPLC assay. The glucuronide product peak area was plotted against time for both reactions (Figure 3.12) with a linear relationship ($R^2 > 0.99$) observed over the studied time frame for each reaction.

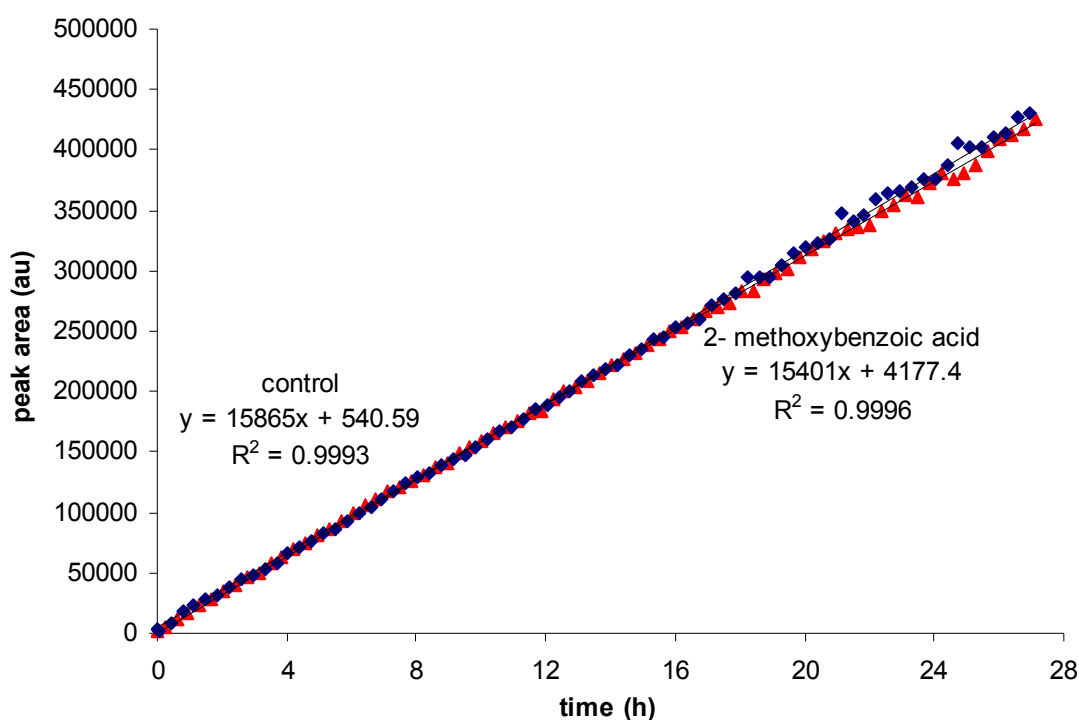


Figure 3.12. Reaction profiles for the glucuronylsynthase reaction between 2-phenylethanol **45** acceptor (100 mM) with α -D-glucuronyl fluoride **51** donor (100 mM) in the presence of 2-methoxybenzoic acid **91** (\blacktriangle) and its absence (\blacklozenge) (21 °C in 100 mM phosphate buffer, pH 7.5). Linear plots and R^2 values were calculated using linear regression analysis.

The reaction without 2-methoxybenzoic acid **91** (the control) provided an initial velocity of 15,865 arbitrary units (au) min^{-1} whilst the reaction containing

1 mM 2-methoxybenzoic acid **91** (internal standard) provided an initial velocity of 15,401 au min⁻¹ (97% of control). When the data points for the reaction with 2-methoxybenzoic acid **91** are corrected for the internal standard, the linear regression value improves even further to a value of 0.9999. This demonstrates the positive effect an internal standard has on data accuracy. The small deviation in velocity (<3% of control) was considered low and so 2-methoxybenzoic acid **91** was deemed not to effect the glucuronysynthesis of 2-phenylethanol **45**. Due to its intense absorption at 296 nm, retention time and inert nature, 2-methoxybenzoic acid **91** was used as an internal standard, at a concentration of 0.5 mM, in all the following HPLC assays.

The HPLC assay is a quick and simple assay for the glucuronysynthase enzyme. Temperature and injection times are all automated due to a thermostat-controlled autosampler which also allows the possibility to monitor multiple reactions at once. The optimised conditions (23% aqueous acetonitrile + 0.1% trifluoroacetic acid) have provided a quick 10 min run time for the 2-phenylethanol **45** example. An internal standard, 2-methoxybenzoic acid **91**, was identified and proven not to interfere with the reaction. The HPLC-UV assay had been successfully developed for the kinetic investigations on glucuronysynthase.

3.5.4 Kinetics of α -D-glucuronyl fluoride **51**

The commencement of enzyme kinetics focused on the kinetic parameters of the α -D-glucuronyl fluoride **51** donor. The first step in determining the kinetic parameters for α -D-glucuronyl fluoride **51** was to develop a calibration curve to relate the glucuronide product concentration with UV response. The 2-phenylethyl β -D-glucuronide **68** was synthesised by glucuronysynthesis and standard solutions were made between 0 - 50 μ M in 100 mM phosphate buffer, pH 7.5 with 0.5 mM internal standard.

Initially, an injection volume of 5 μ L was used, but the signal-to-noise ratio was poor for dilute samples so the injection volume was increased to 25 μ L. However, the area of the glucuronide peak did not increase proportionally by five fold, and the solvent front appeared larger with the increasing concentration of glucuronide standard. It appeared that the 0.1%

Enzyme kinetics

trifluoroacetic acid in the mobile phase was not strong enough to buffer the 25 μL injection. As a result, a large portion of the glucuronide product **68** remained de-protonated, which did not retain on the reverse-phase column and was subsequently eluted with the solvent front. To overcome this problem, the 0.1% trifluoroacetic acid in the mobile phase was replaced with 100 mM phosphate buffer at pH 2. This new solvent system imposed no change in retention time for the individual reaction components and was strong enough to buffer the large 25 μL injections. Furthermore, using phosphate buffer over trifluoroacetic acid allowed spectral monitoring down to 210 nm which was otherwise masked by the trifluoroacetic acid absorbance. The absorbance at 211 nm was stronger than the absorbance at 260 nm for 2-phenylethanol **45**, which improved the sensitivity of the assay. The absorbance at 211 nm is due to the carboxylic acid functionality. This meant that the glucuronylsynthase reactions of UV silent alcohols could now be monitored by the developed HPLC assay.

The calibration curve of 2-phenylethyl β -D-glucuronide **68** was obtained by the injection of known concentrations (0 - 50 μM) to the improved HPLC assay. A linear response ($R^2 > 0.99$) in peak area, with respect to the 2-phenylethyl β -D-glucuronide **68** concentration, was observed (Figure 7.2). The calibration curves, for the glucuronides of all the substrates tested in the HPLC kinetic study, were obtained in an identical fashion.

Kinetic measurements for α -D-glucuronyl fluoride **51** were commenced with a fixed, kinetically sub-saturating concentration of 2-phenylethanol **45** acceptor (107 mM) due to limited solubility of this substrate in the aqueous buffer. Fourteen separate reactions with various concentrations of α -D-glucuronyl fluoride **51** (0-100 μM) were monitored with the HPLC assay at 21 $^{\circ}\text{C}$. The reactions rates varied with concentration and when plotted against the concentration of α -D-glucuronyl fluoride **51**, it resembled a curve expected for Michaelis-Menten kinetics (Figure 3.13).

Attempts to fit this data to the two-substrate kinetic model (equation 11), using Kleidograph data-fitting software, produced large errors. It is recommended that many more data points are required to extrapolate accurate

values from an equation with four unknown parameters. Given that the concentration of 2-phenylethanol **45** concentration remains constant throughout the study, the data points were fitted to the simplified two substrate rate equation (13). This resulted in the elucidation of apparent kinetic parameters with significantly lower errors than the previous fit. The K_m^{app} was calculated as $15.0 \pm 1.1 \mu\text{M}$ and is low relative to other glycosynthase enzymes.^{91,92,105,115} The $V_{\text{max}}^{\text{app}}$ was extrapolated as $20.3 \text{ nmol min}^{-1} [\text{mg protein}]^{-1}$ which denotes a slow $k_{\text{cat}}^{\text{app}}$ of $0.023 \pm 0.001 \text{ s}^{-1}$.

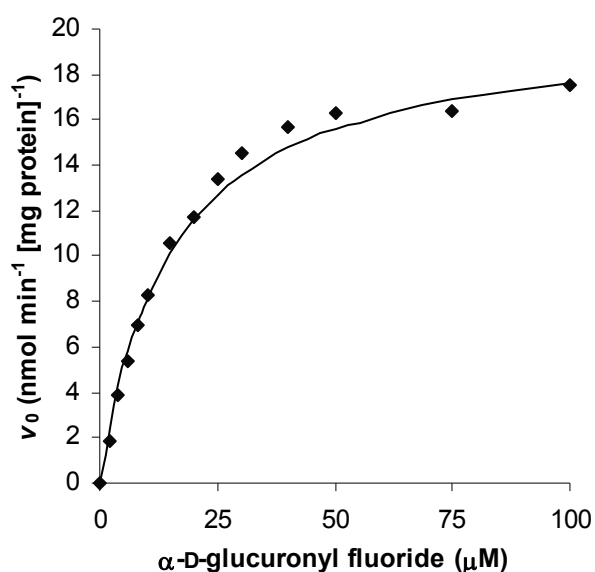


Figure 3.13. Initial velocity vs. concentration plot of varying $\alpha\text{-D-glucuronyl fluoride 51}$ donor with constant sub-saturating (107 mM) 2-phenylethanol **45** acceptor (21 °C, 100 mM phosphate buffer, pH 7.5). The line represents the data fitted (least-squares) to the Michaelis-Menten equation.

The apparent substrate specificity was determined from the initial slope of the initial velocity vs. concentration curve where substrate concentration is low as indicated in equation (10). The apparent k_{cat}/K_m from the initial slope was determined as $1.0 \times 10^3 \text{ M}^{-1} \text{ s}^{-1}$ which is comparable to other glycosynthases with their glycosyl donor that range in literature from $0.003\text{-}1050 \text{ M}^{-1} \text{ s}^{-1}$.⁸⁸⁻⁹⁷ The glucuronylsynthase enzyme exhibited strong and highly specific binding of its glycosyl donor, but demonstrated a turnover much lower than glycosynthase examples in the literature. The low k_{cat} for this reaction leaves considerable scope for improving the catalytic efficiency of this enzyme system.

3.5.5 Kinetics of 2-phenylethanol **45**

An analogous study to the previous one was used to determine the kinetic parameters of 2-phenylethanol **45**. The concentration of α -D-glucuronyl fluoride **51** was kept at a constant concentration of 1 mM which is greater than ten times K_m^{app} as recommended by kinetic literature ($>66 \times K_m^{\text{app}} = 15 \mu\text{M}$). By definition, the enzyme is considered saturated with α -D-glucuronyl fluoride **51** and the two substrate rate equation (11) can be simplified to the pseudo-single substrate model (equation 14). Consequently, the true kinetic parameters for 2-phenylethanol **45** could be determined.

Ten reactions with a varied concentration of 2-phenylethanol **45** (0-107 mM) were analysed with the HPLC assay. Under these conditions the acceptor alcohol did not saturate the enzyme due to the limited aqueous solubility of the acceptor alcohol. Nevertheless, when the initial velocities were plotted against the concentration of 2-phenylethanol **45** acceptor, the beginning of a curve depicting Michaelis-Menten kinetics was observed (Figure 3.14). The magnitude and curvature of this curve was very similar to the initial velocity vs. concentration curve obtained from the NMR kinetics of 2-phenylethanol **45** (Figure 3.7).

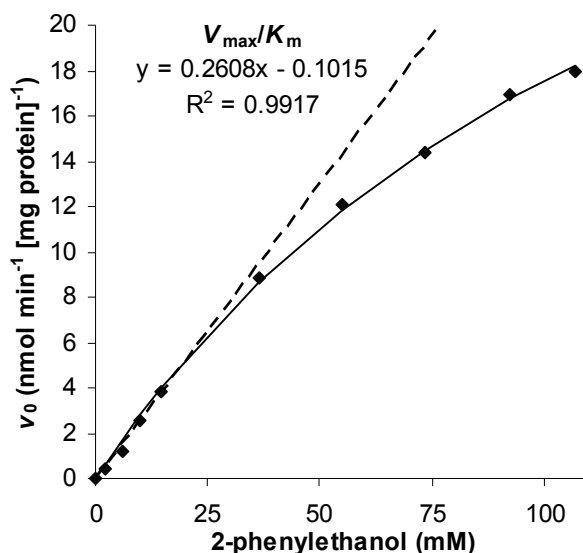


Figure 3.14. Initial velocity vs. concentration plot of varying 2-phenylethanol **45** acceptor with constant saturating (1 mM) α -D-glucuronyl fluoride **51** donor (21 °C, 100 mM phosphate buffer, pH 7.5). Continuous line represents data fitted (least squares) to the pseudo-single substrate rate equation (14) and the broken line represents the initial slope of the curve used for k_{cat}/K_m calculations ($n = 5$) with its linear regression analysis denoted as R^2 .

Fitting the data to the pseudo-single substrate model (equation 14), a K_m of 140 ± 10 mM and a V_{max} of $42.8 \text{ nmol min}^{-1} [\text{mg protein}]^{-1}$ denoting a k_{cat} of $0.049 \pm 0.003 \text{ s}^{-1}$. The kinetic parameters were of similar magnitude to that determined by NMR experiments (K_m 109.5 mM, k_{cat} 0.034 s^{-1}) obtained at the same temperature, but using 100 mM of α -D-glucuronyl fluoride **51**. Similar to the NMR experiments, the calculated K_m (144 mM) is never reached due to solubility restrictions and its accuracy questionable as it is an extrapolated value.

This large difference in binding affinity provides information regarding the enzyme mechanism. A literature survey compiled by Davis *et al* revealed that the Michaelis-Menten ratio (K_{mB}/K_{mA}) strongly correlates to either ordered or random bi bi mechanisms.¹¹⁷ Their survey suggested that a threshold of $K_{mB}/K_{mA} > 10$ denotes an ordered bi bi reaction. The binding affinity ratio for 2-phenylethanol **45** ($K_m = 144$ mM) and α -D-glucuronyl fluoride **51** ($K_m^{app} = 15$ mM) is calculated as 9600 suggesting that the glucuronylsynthase reaction operates via an ordered bi bi mechanism. Despite the α -D-glucuronyl fluoride **51** parameter being an apparent value, it is improbable that the true Michaelis-Menten constant would alter the ratio to within the threshold of 10 reported by Davis *et al*.

The V_{max}^{app} is an underestimation of the V_{max} (refer to section 3.1.2) and by definition, the k_{cat}^{app} is an underestimation of the true k_{cat} value. It is therefore no surprise that the k_{cat} determined in this kinetic study is of similar magnitude but slightly greater than the k_{cat}^{app} of 0.023 s^{-1} determined in the α -D-glucuronyl fluoride **51** kinetic study. Assuming saturating donor and acceptor concentrations, the k_{cat}^{app} or turnover number for this system is low relative to other glycosynthases.

The slope of the initial velocity vs. concentration plot (Figure 3.14) provided an estimated substrate specificity (k_{cat}/K_m) of $0.30 \text{ M}^{-1} \text{ s}^{-1}$. This value is identical to the substrate specificity value determined from the NMR kinetic study. The similar results produced from the NMR and HPLC assays for the 2-phenylethanol **45** glucuronylsynthase reaction helps validate the kinetic parameters determined for 2-phenylethanol **45**. However, the HPLC assay is

Enzyme kinetics

easier to perform and provided greater sensitivity which was essential in successfully determining the kinetic parameters of α -D-glucuronyl fluoride **51**. The HPLC assay was then used to determine the kinetic parameters of other alcohol acceptors.

3.5.6 Kinetics of 3-methoxybenzyl alcohol **47**

The expansion of the enzyme kinetic investigation with glucuronylsynthase was continued with 3-methoxybenzyl alcohol **47** due to its reasonable solubility in water. To commence, a calibration curve was created so that the 3-methoxybenzyl β -D-glucuronide **71** concentration could be related to UV response.

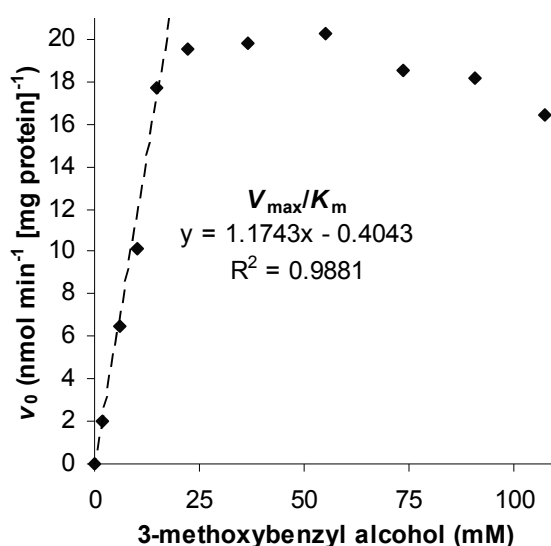
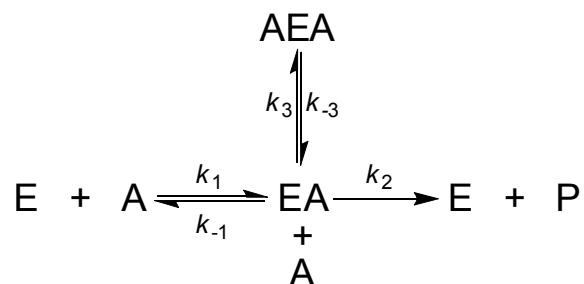


Figure 3.15. Initial velocity vs. concentration plot of varying 3-methoxybenzyl alcohol **47** acceptor with constant saturating (1 mM) α -D-glucuronyl fluoride **51** donor (21 °C, 100 mM phosphate buffer, pH 7.5). Broken line represents the initial slope of the curve used for k_{cat}/K_m calculations ($n = 5$) with its linear regression analysis denoted as R^2 .

Eleven reactions were monitored at 21 °C with a saturating concentration of α -D-glucuronyl fluoride **51** (1 mM) and varied concentrations (0 – 107 mM) of 3-methoxybenzyl alcohol **47**. The initial velocities of these reactions were plotted against their respective concentration of 3-methoxybenzyl alcohol **47**, but Michaelis-Menten kinetics were not observed (Figure 3.15). The data at low substrate concentrations resembled Michaelis-Menten kinetics, but the initial velocity at higher concentrations appeared to drop off. The entire experiment was repeated only to achieve identical results. The reduction in

initial velocity at high substrate concentrations is indicative of substrate inhibition. In light of this discovery, the enzyme mechanism had to be re-modelled to incorporate substrate inhibition.

Considering the single substrate mechanism, a second substrate molecule (A) may bind to the enzyme-substrate complex (EA) to produce the inactive complex AEA (Scheme 3.9).



Scheme 3.9. Single substrate mechanism with substrate inhibition

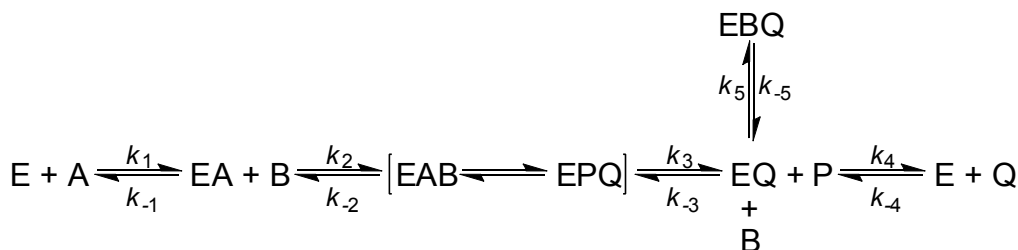
As the concentration of A increases, the enzyme-substrate complex is pushed down an additional dead-end pathway that reduces the concentration of EA and lowers the velocity of product formation. The rate equation for this model is as follows:

$$v = \frac{V_{\max} a}{K_m + a + a^2 / K_{si}} \quad (16)$$

where K_{si} is the equilibrium constant of the substrate inhibition pathway (k_{-3}/k_3) and V_{\max} and K_m satisfy the usual definitions of the Michaelis-Menten parameters. As the concentration of A (a) becomes large, the effect of the term a^2 reduces the reaction velocity towards zero rather than V_{\max} . This term creates a decrease in velocity at higher substrate concentrations instead of a plateau of velocity associated with standard Michaelis-Menten kinetics. The maximum of the initial velocity vs. concentration curve for a system with substrate inhibition occurs at $a^2 = K_m K_{si}$.⁸¹ The equation also shows that at low concentrations of A ($K_{si} > a$, therefore $a^2/K_{si} \rightarrow 0$), the rate equation simplifies to Michaelis-Menten kinetics. The same occurs if only weak inhibition exists ($K_{si} \gg a$, therefore $a^2/K_{si} \rightarrow 0$).

The glucuronylsynthase has been proposed to operate via the ordered bi bi mechanism whereby substrate inhibition is denoted by a dead-end pathway (Scheme 3.10).

Enzyme kinetics



Scheme 3.10. The ordered bi bi mechanism with a dead-end path. A dead-end step (interconversion of EQ to EBQ in this example) is always at equilibrium in the steady state.

A two-substrate model that undergoes substrate inhibition by substrate B follows the rate equation:⁸¹

$$v = \frac{V_{\max} a b}{K_{iA} K_{mB} + K_{mB} a + K_{mA} b + a b + a b^2 / K_{siB}} \quad (17)$$

where a and b are the concentrations of substrates A and B, K_m and V_{\max} are defined as the Michaelis-Menten constants, K_{iA} is the substrate dissociation constant (k_{-1}/k_1) and K_{siB} is the strength of inhibition by substrate B which approximates (but does not equal) to k_{-5}/k_5 . Parallel to the single substrate equation, the term b^2 drives the velocity towards zero at high concentrations of B instead of V_{\max} .

Taking out the factor a from the denominator, we get:

$$v = \frac{V_{\max} a b}{a \left(\frac{K_{iA} K_{mB}}{a} + K_{mB} + \frac{K_{mA} b}{a} + b + \frac{b^2}{K_{siB}} \right)} \quad (18)$$

From (18), it can be shown in saturating conditions of a , the two-substrate equation with substrate inhibition simplifies to the single substrate equation with substrate inhibition:

$$\text{As } a \rightarrow \infty, \frac{K_{iA} K_{mB}}{a} \text{ \& } \frac{K_{mA} b}{a} \rightarrow 0, \text{ so } v = \frac{V_{\max} b}{K_{mB} + b + b^2 / K_{siB}} \quad (19)$$

The 3-methoxybenzyl alcohol **47** glucuronylsynthase reaction monitored by HPLC contained a saturating concentration of α -D-glucuronyl fluoride **51**. Therefore, rate equation (19) was used to model the data and determine the kinetic parameters for 3-methoxybenzyl alcohol **47**. The data appears to fit

well to the equation ($R^2 > 0.97$), but considerable errors (45-66%) were found with the kinetic parameters. The K_m was determined as 43 ± 25 mM, the V_{max} as 64 ± 29 nmol min⁻¹ [mg protein]⁻¹ and the K_{si} was 41 ± 27 mM. The weak binding affinity once again demonstrated the stronger binding affinity of the carbohydrate moiety in glucuronides. The ratio K_{mB}/K_{mA}^{app} was calculated as 287 which supports an ordered bi bi mechanism.

The calculated V_{max} equates to a slow catalytic turnover (k_{cat}) of 0.073 s⁻¹. Conversely, only a third of this velocity was ever observed with a maximum observed velocity of 20 nmol⁻¹ min⁻¹ [mg protein]⁻¹ ($k_{cat} = 0.023$ s⁻¹) from the initial velocity vs. concentration plot (Figure 3.15). This velocity occurred at 55 mM which corresponded well with the calculated concentration ($a^2 = K_m K_{si}$) of 42 mM.

The substrate specificity (k_{cat}/K_m) was calculated as 1.8 M⁻¹ s⁻¹ using the calculated parameters. Given the error associated with these values, the slope of the initial velocity vs. concentration curve at very low substrate concentration was used. A substrate specificity of 1.3 M⁻¹ s⁻¹ was determined which corresponds well with the calculated value. The k_{cat}/K_m value for 3-methoxybenzyl alcohol **47** (1.3 M⁻¹ s⁻¹) is greater than 2-phenylethanol **45** (0.3 M⁻¹ s⁻¹) which implies 3-methoxybenzyl alcohol **47** is favoured as a substrate by the glucuronylsynthase enzyme.

The calculated strength of inhibition (K_{si}) is less than the Michaelis-Menten constant suggesting that 3-methoxybenzyl alcohol **47** provides greater binding through inhibition rather than reaction turnover. However, this can not be affirmed given the large errors associated with both of these kinetic parameters. It is recommended that more data points are acquired to accurately fit the data to the rate equation which consists of 3 unknown kinetic parameters. Alternatively, the proposed model does not correspond to the actual mechanism associated with this system. The adoption of alternate model of inhibition may lead to a better fit to the data.

3.5.7 Kinetics of 4-fluorobenzyl alcohol 50

The kinetic parameters of another acceptor alcohol were explored with 4-fluorobenzyl alcohol **50** subjected to HPLC enzyme kinetics. Once again, the

Enzyme kinetics

glucuronide standard was synthesised by glucuronylsynthesis and used to generate a calibration curve for 4-fluorobenzyl β -D-glucuronide **73**. Twelve reactions were monitored at 21 °C with a saturating concentration of α -D-glucuronyl fluoride **51** (1 mM) and varied concentrations (0 – 107 mM) of 4-fluorobenzyl alcohol **50**. The initial velocities of these reactions were plotted against their respective concentration of 4-fluorobenzyl alcohol **50**, to resemble a curve similar to that obtained for 3-methoxybenzyl alcohol **47**. The curve also showed substrate inhibition at high substrate concentrations (Figure 3.16).

The α -D-glucuronyl fluoride **51** was used at a saturating concentration so the pseudo-single substrate with substrate inhibition rate equation (equation 19) was used to model the data. A good fit ($R^2 > 0.98$) was obtained for the curve, but once again the errors associated with the kinetic parameters were still unacceptable (33-46%). The V_{\max} was calculated as $27 \pm 9 \text{ nmol min}^{-1} [\text{mg protein}]^{-1}$, the K_m as $45 \pm 19 \text{ mM}$ and the K_{si} as $24 \pm 11 \text{ mM}$. The calculated V_{\max} provides a catalytic turnover of $k_{\text{cat}} 0.031 \text{ s}^{-1}$. However only 0.0085 s^{-1} was observed at a concentration of 37 mM of 4-fluorobenzyl alcohol **50**. The theoretical concentration of maximum velocity ($a^2 = K_m K_{si}$) of 33 mM agreed closely to the observed value.

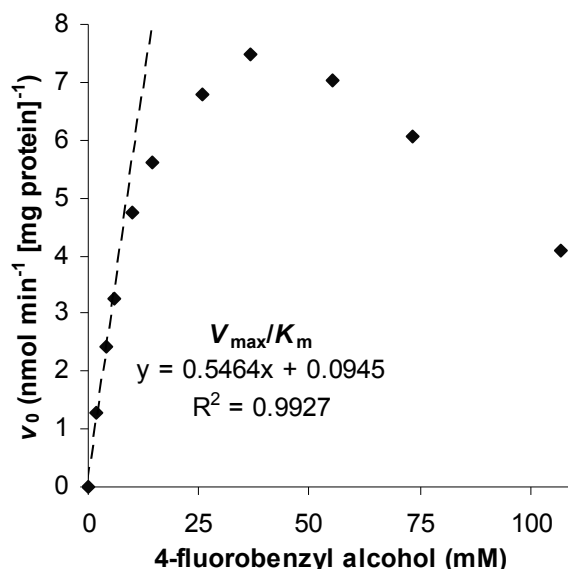


Figure 3.16. Initial velocity vs. concentration plot of varying 4-fluorobenzyl alcohol **50** acceptor with constant saturating (1 mM) α -D-glucuronyl fluoride **51** donor (21 °C, 100 mM phosphate buffer, pH 7.5). Broken line represents the initial slope of the curve used for k_{cat}/K_m calculations ($n = 4$) with its linear regression analysis denoted as R^2 .

The large K_{mB}/K_{mA}^{app} ratio of 3000 once again denotes an ordered bi bi system for the glucuronylsynthase reaction. Using the slope of the kinetic curve at very low substrate concentration, the substrate specificity (k_{cat}/K_m) was determined as $0.62 \text{ M}^{-1} \text{ s}^{-1}$. The substrate specificity determined from the calculated kinetic parameters is $0.69 \text{ M}^{-1} \text{ s}^{-1}$ and agrees closely to the observed value. This substrate specificity value suggests the 4-fluorobenzyl alcohol **50** is more favoured by the glucuronylsynthase enzyme than 2-phenylethanol **45** but not as favoured as 3-methoxybenzyl alcohol **47**.

Once again, the strength of inhibition (K_{si} 24 mM) is smaller than the Michaelis-Menten constant (K_m 45 mM) which suggests inhibitory binding is greater than productive binding. But this is a tentative result given the large errors associated with both kinetic parameters once again. These errors demonstrate the inaccuracies associated with fitting a small set of data to a complex rate equation with so many unknowns. Alternatively, the proposed model (Scheme 3.10) may need to be altered to suit the true mechanism for the glucuronylsynthase system and lead to a better fit to the data. But with all the datasets tested so far being restricted by the solubility of the acceptor substrate solubility, the study was continued by exploring the kinetics of the more water soluble substrate, phenol **52**.

3.5.8 Kinetics of phenol **52**

The alcohol substrates tested thus far have had poor water solubility and a full picture of the kinetic curve is yet to be obtained. Phenol **52** has been shown to form glucuronides with the glucuronylsynthase and has a greater solubility in water than all of the acceptor alcohols tested so far. Furthermore, the yields obtained from phenol **52** in glucuronylsynthase reactions are significantly smaller than achieved for acceptor alcohols. The kinetic parameters for phenol **52** were explored in the hope of obtaining a kinetic curve over a greater substrate concentration and to understand phenol's moderate glucuronide yield.

A calibration curve was developed for phenyl β -D-glucuronide **76** in an identical fashion as previous kinetic studies. The less hydrophobic product

Enzyme kinetics

meant the solvent system had to be altered to 18% acetonitrile in 100 mM sodium phosphate buffer, pH 2.0 to provide a retention time of 4.2 min.

Fourteen glucuronylsynthase reactions were monitored by the altered HPLC assay (18% acetonitrile) at 21 °C. The α -D-glucuronyl fluoride **51** was used at a saturating concentration of 1 mM and phenol **52** was varied (0-240 mM). When the initial velocity was plotted against the concentration of phenol **52**, the presence of substrate inhibition was again observed (Figure 3.17). This time however, a large enough concentration of substrate was achievable to visualise complete reaction inhibition.

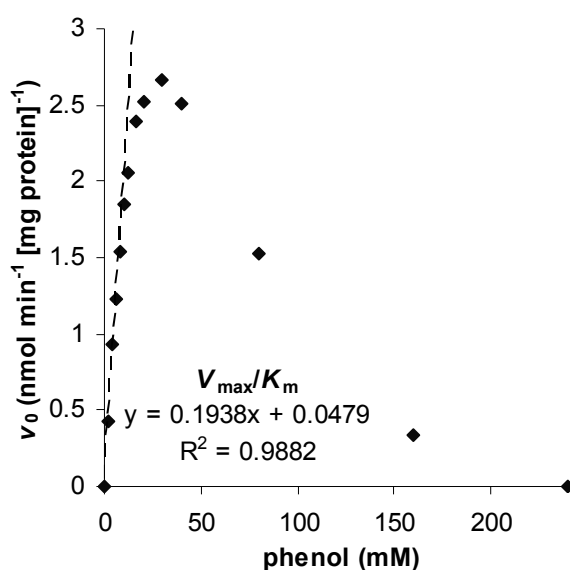


Figure 3.17. Initial velocity vs. concentration plot of varying phenol **52** acceptor with constant saturating (1 mM) α -D-glucuronyl fluoride **51** donor (21 °C, 100 mM phosphate buffer, pH 7.5). Broken line represents the initial slope of the curve used for k_{cat}/K_m calculations ($n = 5$) with its linear regression analysis denoted as R^2 .

An attempt to fit this data to the pseudo-single substrate model with substrate inhibition (equation 19) was a little less accurate ($R^2 > 0.95$) than attempts with previous acceptor alcohols. The extrapolated kinetic parameters comprised of high errors (10-80%) with the V_{max} estimated as 5 ± 4 nmol min⁻¹ [mg protein]⁻¹, the K_m as 20 ± 2 mM and the K_{si} as 34 ± 9 mM. The large K_{mB}/K_{mA}^{app} ratio (1,333) is consistent with an ordered bi-bi mechanism.

The catalytic turnover is k_{cat} 0.0061 s⁻¹ from the calculated V_{max} value. As anticipated from experimental observations, this was the slowest glucuronylsynthase reaction monitored. The maximum observed catalytic

turnover was only half of the theoretical turnover with a value of 0.0030 s^{-1} . This occurred at a concentration of 30 mM which corresponds well with calculated concentration ($a^2 = K_m K_{si}$) of 26 mM.

The substrate specificity (k_{cat}/K_m) determined from the slope of the kinetic curve at very low substrate concentration was $0.22 \text{ M}^{-1} \text{ s}^{-1}$ which is similar with the value of $0.31 \text{ M}^{-1} \text{ s}^{-1}$ determined from the calculated kinetic parameters. The Michaelis-Menten constant (K_m) is the lowest reported for the acceptor species yet the catalytic turnover is the slowest of the acceptor species. It is evident that the slow catalytic turnover of phenol **52** is responsible for it be the less favoured substrate for the glucuronylsynthase enzyme in terms of substrate specificity. The sluggish reaction rate and low substrate specificity is likely the cause of the low yields associated with the glucuronylsynthesis of phenol **52**.

3.5.9 Conclusions

The kinetic parameters of the α -D-glucuronyl fluoride **51** donor and a few of the acceptor alcohols have been successfully determined by HPLC kinetic studies (Table 3.1). The data demonstrated pseudo-single substrate Michaelis-Menten kinetics for the reaction between α -D-glucuronyl fluoride **51** donor and 2-phenylethanol **45**. For α -D-glucuronyl fluoride **51**, the concentration of 2-phenylethanol **45** was kept at a constant, sub-saturating concentration so that apparent kinetic parameters were determined. For the acceptor aglycons, the α -D-glucuronyl fluoride **51** was kept at a constant, saturating concentration so estimates of the true kinetic parameters were determined (Table 3.2). With the exception of 2-phenylethanol **45**, the acceptor alcohols demonstrated substrate inhibition. Attempts of fitting the data to a pseudo-single substrate model with substrate inhibition returned large errors. Either more data points are needed to solve the multiple unknown parameters in the complex rate equation or an alternative model needs to be derived to fit the glucuronylsynthase mechanism. Despite the large errors associated with the calculated kinetic parameters (Table 3.2), they do provide a reasonable estimation especially with regards to the substrate specificity

Enzyme kinetics

constants. The calculated values matched those determined from the slope very closely. The K_m values on the other hand, were less reliable.

Table 3.1. Summary of *observed* kinetic parameters for the substrates of glucuronylsynthase at 21 °C in 50 mM sodium phosphate, pH 7.5.

Substrate	Max k_{cat} (s^{-1})	Concentration at max v_0 (mM)	k_{cat}/K_m ($M^{-1} s^{-1}$) ^a
α -D-glucuronyl fluoride 51	0.020 ^b	N/A ^c	1.0×10^3
2-phenylethanol 45	0.021	N/A ^c	0.30 ± 0.02
3-methoxybenzyl alcohol 47	0.023 ^d	55 ^d	1.3 ± 0.09
4-fluorobenzyl alcohol 50	0.0085 ^d	37 ^d	0.62 ± 0.04
phenol 52	0.0030 ^d	30 ^d	0.22 ± 0.01

^a) determined from the slope of the initial velocity vs. concentration plot at low substrate concentration. Errors were determined using linear regression analysis; ^b) apparent kinetic parameter; ^c) maximum v_0 never achieved; ^d) substrate inhibition observed.

Table 3.2. Summary of *calculated* kinetic parameters from data fitting for the substrates of glucuronylsynthase at 21 °C in 50 mM sodium phosphate, pH 7.5. Errors were determined using a non-linear regression analysis.

Substrate	K_m (mM)	K_{si} (mM)	k_{cat} (s^{-1})	Conc. at max v_0 (mM) ^d	k_{cat}/K_m ($M^{-1} s^{-1}$)
α -D-glucuronyl fluoride 51 ^a	0.015 ± 0.001	N/A	0.023 ± 0.01	N/A	1500
2-phenylethanol 45 ^b	140 ± 10	N/A	0.049 ± 0.003	N/A	0.34
3-methoxybenzyl alcohol 47 ^c	43 ± 23	41 ± 27	0.073 ± 0.03	42	1.7
4-fluorobenzyl alcohol 50 ^c	45 ± 19	24 ± 11	0.031 ± 0.01	33	0.69
phenol 52 ^c	20 ± 2	34 ± 9	0.0061 ± 0.005	26	0.31

^a) apparent parameters calculated from the pseudo-single substrate model (equation 13); ^b) parameters calculated from the pseudo-single substrate model (equation 14), ^c) parameters calculated from the pseudo-single substrate model with substrate inhibition (equation 16); ^d) calculated from $a^2 = K_m K_{si}$

The significant difference in estimated Michaelis constants (K_m) observed for the α -D-glucuronyl fluoride **51** donor and 2-phenylethanol **45** acceptor substrates is noteworthy. Despite the degree of error associated with the remaining acceptors, their approximated K_m values are still three orders of magnitude greater than the α -D-glucuronyl fluoride **51** donor. This may reflect the binding interactions for glucuronide substrates at the WT β -glucuronidase and the role of this enzyme in *E. coli*, the producing organism. *Escherichia coli* is an enteric organism that employs a glucuronide transporter/ β -glucuronidase enzyme system to harvest the glucuronide residue as a carbon source from biliary metabolites excreted in the gut.¹¹⁸ These glucuronide conjugates are formed from a wide variety of xenobiotic and some endogenous compounds. For this reason the primary recognition of the glucuronide conjugate by β -glucuronidase is expected for the target carbohydrate moiety over the variable aglycon portion. The kinetic data reported for β -glucuronidase mediated hydrolysis provides some support for this analysis. A K_m 0.2 mM was reported for the *E. coli* β -glucuronidase mediated hydrolysis of *p*-nitrophenyl- β -D-glucuronide **25** and estriol 3- β -D-glucuronide that contain significantly different aglycon residues.¹¹⁹ The substrate promiscuity of this enzyme has been exploited in the field of analytical chemistry for the de-conjugation of glucuronide metabolites. For the glucuronylsynthase, this is reflected in tight binding and a low apparent K_m for the α -D-glucuronyl fluoride **51** donor (K_m^{app} 15.0 ± 1.1 μ M) and weaker binding and a much higher estimated K_m for the alcohol acceptors ($K_m > 20$ mM). As for the catalytic rate of the enzyme, it is possibly at the lower end of the range in the glycosynthase family.

The kinetic properties of 2-phenylethanol **45** are interesting. The absence of substrate inhibition (in the concentrations studied) may be linked to the high yields associated with its glucuronylsynthesis. These high yields are achieved despite the 2-phenylethanol **45** being one of the least preferred substrates according to substrate specificity (k_{cat}/K_m) values (Table 3.1). This goes against the trend expressed by the other aglycons whereby their glucuronylsynthesis yields parallel their substrate specificity values (Table 3.3).

Enzyme kinetics

Table 3.3. Correlation of substrate specificity values and glucuronysynthesis yields

Substrate	k_{cat}/K_m ($\text{M}^{-1} \text{s}^{-1}$) ^a	Yield from glucuronylation reaction (%) ^b
2-phenylethanol 45	0.30 ± 0.02	96 ^c
3-methoxybenzyl alcohol 47	1.3 ± 0.09	84 ^d
4-fluorobenzyl alcohol 50	0.62 ± 0.04	40 ^c
phenol 52	0.22 ± 0.01	13 ^c

^a determined from the initial slope of the initial velocity vs. concentration plot. ^b reaction conditions: 1.2 equiv α -D-glucuronyl fluoride **51**, 0.2 mg mL⁻¹ E504G, RT, 50 mM sodium phosphate buffer, pH 7.5. ^c substrate concentration 100 mM. ^d substrate concentration 50 mM.

Using the substrate at its maximum concentration does not increase the catalytic turnover for the majority of acceptor alcohols due to substrate inhibition. This provides a rationale for one of the trends observed in the series of glucuronysynthase reactions listed earlier in the research (Table 2.2). It was observed that when the substrate concentration was increased from 50 mM to 100 mM for 3-methoxybenzyl alcohol **47**, the yield is reduced. Conversely, when the concentrations of 4-fluorobenzyl alcohol **50** and 4-methoxybenzyl alcohol **48** were reduced in the reactions, an improved yield was obtained. It is proposed that substrate inhibition may have been hindering these reactions which caused the discrepancies in yields. If a more dilute substrate concentration was used, the effect of substrate inhibition would be reduced. This would increase the initial velocity of the reaction which may lead to improved glucuronide yields. Another strategy of improving the glucuronysynthase yields may lie in optimising other reaction variables.

3.6 Reaction optimisation

In an attempt to improve the catalytic activity and yield in the glucuronysynthase reactions, a selection of reaction variables were altered and their effect on reaction velocity and yield were monitored by HPLC.

3.6.1 Effect of pH

The effect of pH on the hydrolysis mechanism of the WT glucuronidase has been reported.¹²⁰ An optimal pH range of 5-8.5 was determined with an optimum of ~7. However, the mechanism of glucuronylsynthase is different and an alternative pH may favour this reaction.

The effect of pH was studied using the glucuronylsynthase reaction with 2-phenylethanol **45**. Nine identical reactions were set up with a sub-saturating concentration of 2-phenylethanol **45** and saturating concentration of α -D-glucuronyl fluoride **51**. The pH of each reaction was varied by one pH unit over a wide range of pH values (3.0 - 11.0). The initial velocity of the reactions was monitored at 21 °C and then the reactions were incubated without agitation at 21 °C for 5 days before another injection was made to determine the reaction yield.

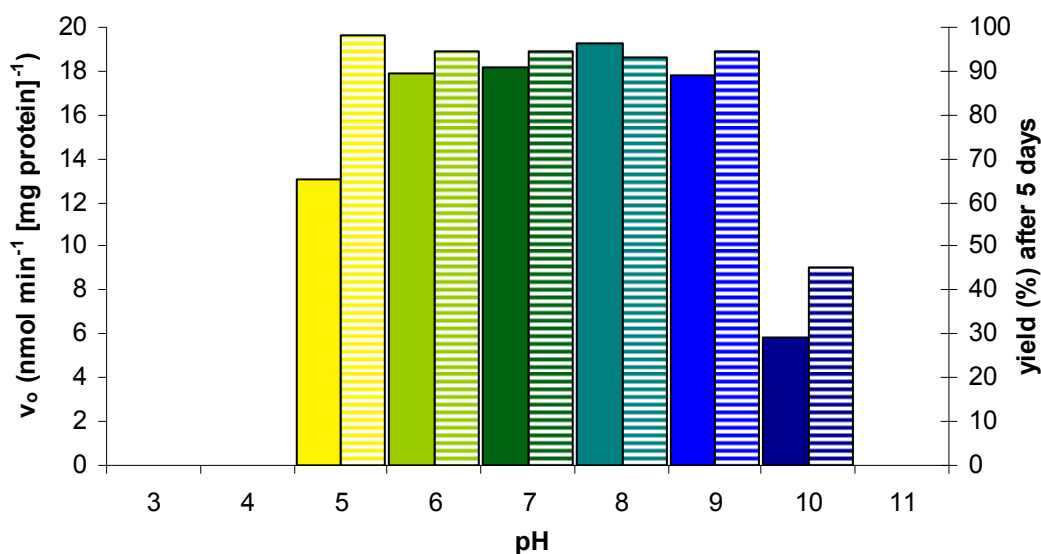


Figure 3.18. Dependence of initial rate (v_0 ; solid bars) and final yield (%; lined bars) on pH for reaction of 2-phenylethanol **45** acceptor (100 mM) and α -D-glucuronyl fluoride **51** donor (1 mM), (21 °C, 50 mM buffer).

An equivalent initial velocity was observed over the pH range 6-9 (Figure 3.18) which shares an equivalent optimum range reported for the wildtype β -glucuronidase. An average velocity of 18.3 nmol min⁻¹ [mg protein]⁻¹ was observed over this range which is the equivalent velocity observed in the kinetic study of 2-phenylethanol **45** with identical concentrations but a pH of 7.5 (Figure 3.14). Reduced activity is observed at pH 5 and 10 with no product

Enzyme kinetics

formation observed outside of this pH range suggesting the enzyme is inactive or has denatured.

After 5 days, the reactions in the pH range of 5-9 all achieved equivalent yields (93-98%). It is interesting to see that the reaction at pH 5 achieved the same yield as the reactions in the optimum pH range despite it having a reduced initial velocity. The other slow reaction at pH 10 only achieves a yield of 45%. The reactions that showed no initial activity (pH 3, 4 and 11) also produced no product after 5 days confirming absolutely no detectable enzyme activity at these pH levels. Like the wild-type glucuronidase, the glucuronylsynthase has a broad pH range with an equivalent pH optimum of 7-8. The glucuronylsynthase reactions are already performed at pH 7.5 so no further optimisation could be achieved by altering the pH. Progress was then made at optimising another reaction variable.

3.6.2 Effect of temperature.

An increased temperature is known to increase reaction rates of both enzymatic and non-enzymatic processes. However, thermal stability can be an issue for substrates, products or the enzyme. The glucuronylsynthase reaction was evaluated at several temperatures (4, 11, 18, 24, 30, 37 °C) at a saturating concentration of α -D-glucuronyl fluoride **51** donor (90 mM) and sub-saturating concentration of 3-methoxybenzyl alcohol **47** acceptor (89 mM). With the reaction of 2-phenylethanol **45** achieving near quantitative conversion, the acceptor alcohol was substituted to 3-methoxybenzyl alcohol **47** (a lower yielding glucuronide) to determine if increasing temperature had a positive effect on yield. A reduced enzyme concentration (0.02 mg mL⁻¹), relative to typical synthesis experiments (0.2 mg mL⁻¹), was used to allow the observation of initial rates and more keenly assess the influence temperature had on overall yield.

Similar to the pH investigation, two measurements of enzyme activity were taken for each temperature value. Firstly, the initial rate (v_0) of reaction was determined and as expected showed an increase of initial rate with temperature (Figure 3.19a). The reactions were incubated in the HPLC thermostatted autosampler at their respective temperature during their analysis

before being transferred to their thermostat-controlled storage. The reactions were incubated for 13 days at their respective temperature and analysed once again by HPLC after day 4 and day 13 to assess the yield of product formed (Figure 3.19b).

A yield of 1-10% only is achieved due to enzyme concentration being a tenth of what is typically used in a synthetic application. It is worthy to note the increase in yield even after day 13 which demonstrates the ruggedness of this enzyme. However, the reactions maintained at 30 °C and 37 °C gave similar yields after 13 days suggesting that the higher initial reaction rate observed at the higher temperature is attenuated over time by a higher rate of enzyme inactivation.

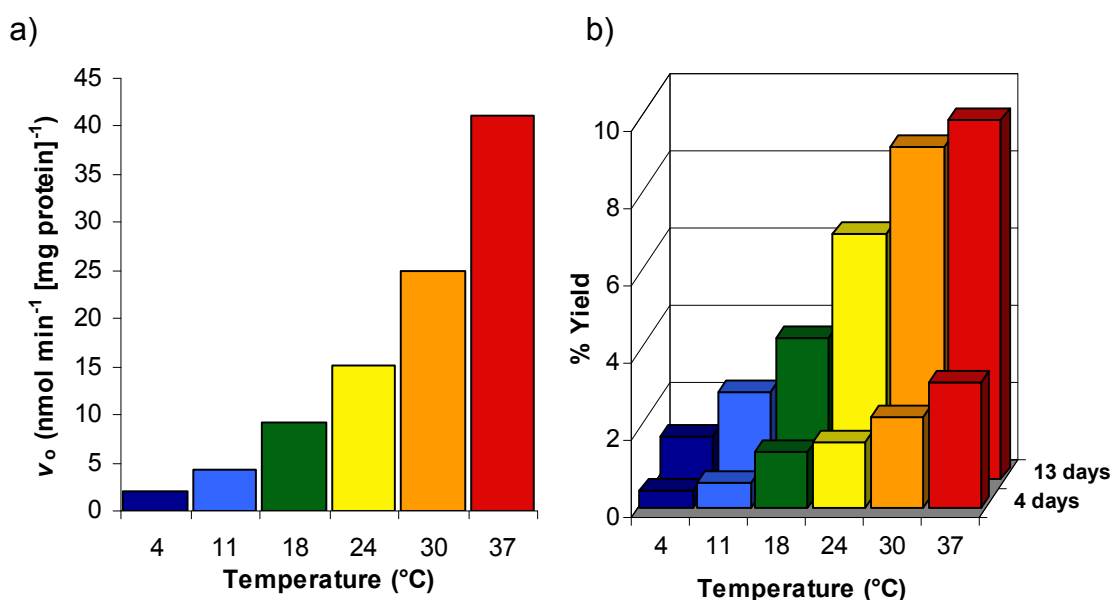


Figure 3.19. Dependence of a) initial rate (v_0) and b) yield (%) on temperature for reaction of 3-methoxybenzyl alcohol 47 acceptor (89 mM) and α -D-glucuronyl fluoride 51 donor (90 mM), (50 mM sodium phosphate buffer, pH 7.5).

Previously, the glucuronylsynthase reactions have been performed at room temperature over 3-5 days. But according to the results of this investigation, a 3 fold increase in velocity is achieved if the reaction is performed at 37 °C rather than at 24 °C. Looking at the activity over time, the enzyme is very stable at 37 °C over the length of time required for a glucuronylsynthase reaction (4 days). It is only if extended reaction times are required that enzyme inactivation may become an issue. It was therefore determined that

Enzyme kinetics

glucuronylsynthase reactions should be incubated at 37 °C to promote faster reactions that may lead to improved yields.

The low yields observed in these reactions were due to the low concentration of enzyme used. But there was no evidence to suggest that the activity observed in the kinetic assays was proportional to the activity in a synthetic application given the tremendous difference (10-fold) in enzyme concentration used. It was obvious that an enzyme concentration study was necessary.

3.6.3 Effect of enzyme concentration on enzyme activity

The *E. coli* β -glucuronidase quaternary structure is comprised of four identical subunits (homotetramer).¹²⁰ The formation of a quaternary structure is enzyme concentration dependent which can lead to deviations in activity through its association-dissociation equilibria or allosteric regulation. An investigation to determine the linearity between enzyme activity assayed in the kinetic experiments and the synthetic applications, where concentrations vary by over 10 times, was completed.

The measurement of enzyme activity in response to enzyme concentration was determined using the glucuronylsynthesis of 2-phenylethanol **45** (94 mM) with the α -D-glucuronyl fluoride **51** donor (1 mM) in the presence of various concentrations of glucuronylsynthase (0.026 - 1.93 mg mL⁻¹). A perfectly linear response ($R^2 > 0.99$) in relation to enzyme concentration was observed for the absolute reaction velocity (Figure 3.20, **◆**). This suggested that no variation in the enzyme's activity, as a result of allosteric regulation, was observed in the concentration ranges studied. Comparing the relative velocities with respect to enzyme concentration, an equivalent velocity of 17 nmol min⁻¹ [mg protein]⁻¹ is observed throughout (Figure 3.20, **■**) demonstrating the catalytic equivalence across all enzyme concentrations.

The results of this study show that the activity demonstrated in the kinetic experiments can be compared to those conducted on a synthetic scale. With most of the reaction variables now investigated, it was of great interest to see what effect these optimised conditions had on a synthetic application.

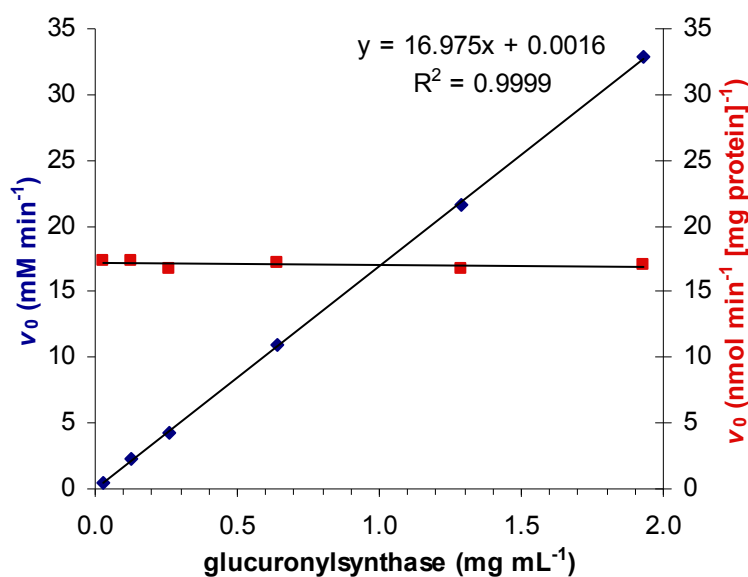


Figure 3.20. Dependence of initial rate on glucuronylsynthase concentration for the reaction of 2-phenylethanol **45** acceptor (94 mM) and α -D-glucuronyl fluoride **51** donor (1 mM) in 50 mM phosphate buffer, pH 7.5 at 21 °C. The initial velocity is shown as absolute velocity (\blacklozenge) as $\mu\text{M min}^{-1}$ and relative velocity (\blacksquare) to the amount of enzyme ($\text{nmol min}^{-1} [\text{mg protein}]^{-1}$). R^2 was determined using linear regression analysis.

3.6.4 Optimised synthesis of phenyl β -D-glucuronide **76**

The optimum reaction conditions have been determined for most of the reaction variables (substrate and enzyme concentration, pH and temperature). These optimum conditions were combined and used in the glucuronylsynthesis of phenol **52**. The previous glucuronylsynthesis of phenol **52** obtained the phenyl β -D-glucuronide **76** in only 13% yield.⁵⁸ This yield was obtained by reacting 100 mM of phenol **52** in the presence of 0.1 mg mL^{-1} of glucuronylsynthase at room temperature ($\sim 25 \text{ }^\circ\text{C}$). Alterations to this reaction included the dilution of phenol **52** to 40 mM, incubating the reaction at $30 \text{ }^\circ\text{C}$ and using five times the concentration of glucuronylsynthase. According to the plot of initial velocity vs. phenol concentration (Figure 3.17), a reaction with 40 mM phenol **52** has twice the velocity of a reaction performed with 100 mM of phenol **52** due to substrate inhibition at higher concentrations. Using these optimised conditions, the phenyl β -D-glucuronide **76** was obtained in 43% yield; over three times the yield from the un-optimised reaction. A review of previously synthesised glucuronides is yet to be completed. Given the

Enzyme kinetics

remarkable improvement in yield for the synthesis with phenol **52**, a review of other alcohol acceptors is warranted.

3.6.5 Summaries and conclusions

Improving the catalytic turnover and overall yield in the interim has been achieved by understanding the kinetic behaviour of the substrates and scrutinising the reaction variables (pH, temperature, and enzyme concentration). The glucuronylsynthase is robust and kept full activity over a wide range of pHs (6-9). Thermal stability is also noteworthy with improved activity achieved at higher temperatures and very little enzyme inactivation observed. Reactions at 37 °C are now recommended to achieve reactions rates three times that of the preceding reactions performed at room temperature. Enzyme concentration dependent allosteric regulation has also been ruled out with an identical catalytic rate observed across all concentrations of enzyme. Combining these optimised conditions for the glucuronylsynthase reaction of phenol **52**, the yield of the glucuronide product was improved three-fold. Further studies are needed to assess the improvements on both previous and new acceptor alcohols. Of particular interest is the reaction with steroids, a fundamental goal of this project.

3.7 High-throughput assays

In addition to an enzyme kinetic assay, a high-throughput assay for glucuronylsynthase activity was also investigated. This research was performed in conjunction with a molecular biologist with the aim of developing a screen suitable for directed evolution.

Directed evolution is not uncommon amongst glycosynthases. To date, there have been four types of high throughput screening applied to glycosynthases. These include chemical complementation, enzyme-coupled spectrophotometry, pH-dependent assays and enzyme-linked immunosorbent assay (ELISA).

3.7.1 Chemical complementation

Chemical complementation was developed by the Cornish group and involves transcriptional modification brought about by glycosynthase

activity.¹²¹⁻¹²³ In their system, a molecule of dexamethasone is linked to a molecule of methotrexate via an oligosaccharide linkage (Figure 3.21). The oligosaccharide linkage is formed via a glycosynthase reaction with a genetically-modified *endo*-glucosidase. Dihydrofolate reductase binds to the methotrexate moiety and the glucocorticoid receptor binds to the dexamethasone moiety. The dihydrofolate reductase is fused to a DNA binding domain, which binds to a specific DNA binding site upstream from the LEU2 gene. The glucocorticoid receptor is fused to an activation domain which up-regulates the transcription of the LEU2 genes. When the oligosaccharide linker is fused through a glycosynthase reaction, the activation domain is “locked” in position to promote the transcription of the LEU2 gene. The LEU2 gene is an essential gene in the biosynthesis of leucine and its up-regulation allows cells to grow in leucine-deficient media. A novel selection criterion is achieved by relating glycosynthase activity to cell survival. This makes this assay a high throughput *selection* as opposed to a *screen* as only mutants with appreciable glycosynthase activity will survive.

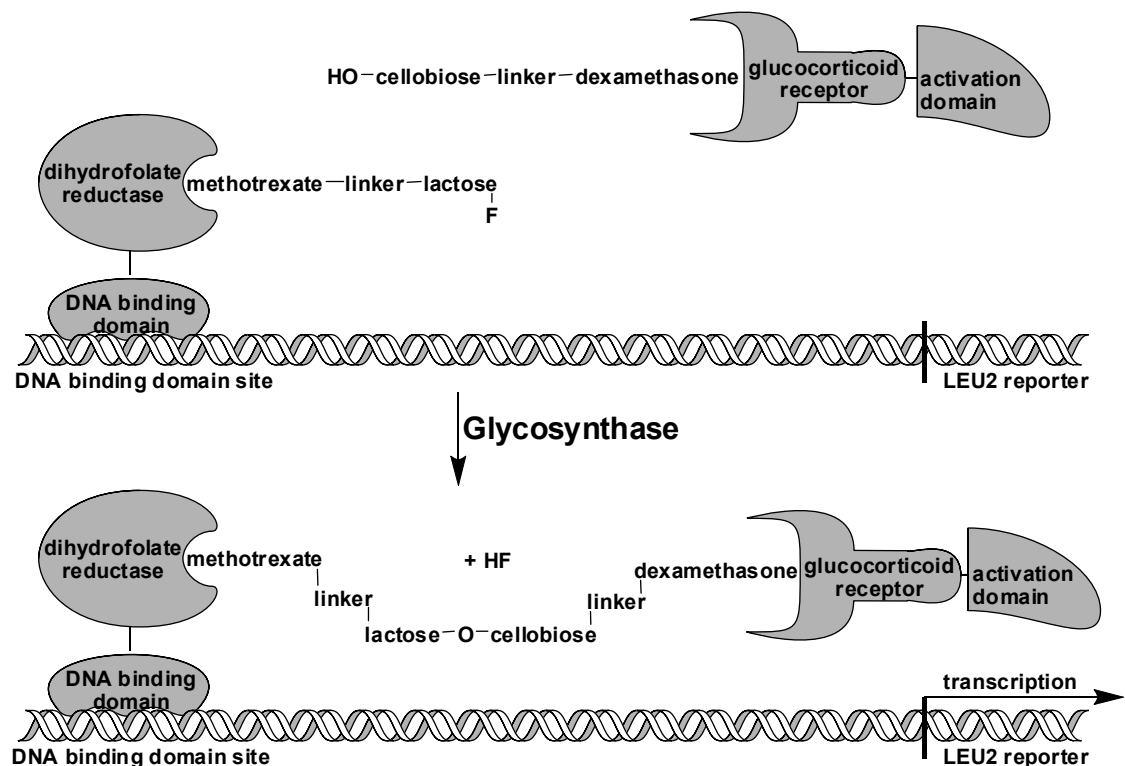
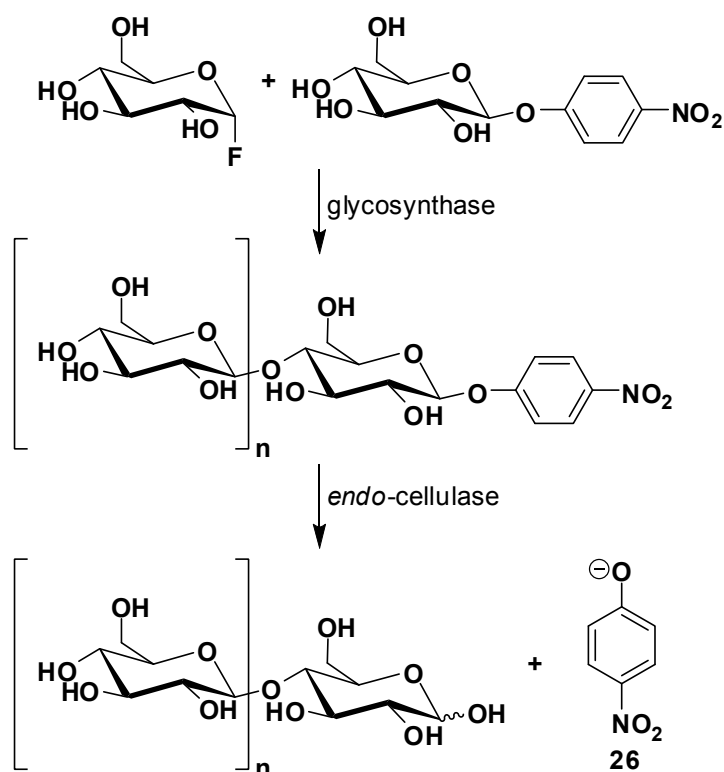


Figure 3.21. Cornish’s chemical complementation model. Formation of the glycosidic bond via a glycosynthase reaction up-regulates LEU2 transcription.

Enzyme kinetics

Chemical complementation is an ingenious and complex model as a high throughput selection for glycosynthase activity. Unfortunately, the system relies on oligosaccharide formation through the use of an *endo*-glycosynthase. The β -glucuronidase enzyme (and therefore the glucuronylsynthase enzyme) is an *exo*-glycosidase meaning it can only cleave (form) glycosidic bonds at the terminal glycoside. This makes chemical complementation unsuitable for the glucuronylsynthase high throughput screen.

3.7.2 Enzyme-coupled spectrophotometric assay

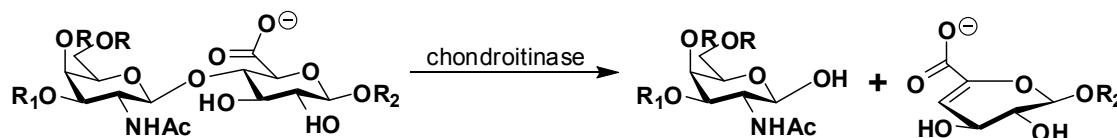


Scheme 3.11. An example of a glycosynthase reaction coupled with *endo*-cellulase to hydrolyse the 4-nitrophenolate (26) chromophore in an enzyme-coupled high throughput glycosynthase screen. $n = 1$ or 2 .¹²⁴

The enzyme-coupled spectrophotometric assay was developed in the Withers group and is based on the hydrolysis of a fluorescent or colorimetric tag from the glycosynthase product.^{96,124} It involves the reaction of a glycosyl fluoride donor with a glycoside acceptor bearing a chromophore. An *endo*-glycosidase, that recognises the newly formed oligosaccharide, hydrolyses the glycosidic bond linking the chromophore which can be measured spectrophotometrically (Scheme 3.11). The hydrolysis step is usually of many

magnitudes faster than the glycosynthase step, so the glycosynthesis is the rate-determining step. The rate of fluorescence or colour formation is therefore directly related to the glycosynthase activity.

Similar to chemical complementation, this assay relies on the formation of an oligosaccharide which has not been observed for the glucuronylsynthase enzyme. Further to this, the only known enzyme to cleave oligosaccharides bearing glucuronyl residues is chondroitinase.¹²⁵ Chondroitinase cleaves the 1-4 linkage between hexosamines and glucuronic acid **3** residues of the polysaccharide chondroitin via an elimination mechanism (Scheme 3.12).¹²⁶ Chondroitinase is unlikely to be coupled with the glucuronylsynthase enzyme as the glucuronylsynthase product would have to contain a 4-O-linked chromophore. This product would be improbable to synthesise from a glucuronylsynthase reaction and the absence of the hexosamine means it is highly unlikely to be recognised by chondroitinase. This makes the enzyme-coupled assay unsuitable for the glucuronylsynthase high throughput screen.



Scheme 3.12. The general reaction of chondroitinase.

3.7.3 “Chromo-ablative” Assay

Spectrophotometric assays are sensitive and simple to run and typically involve the hydrolysis of a masked chromophore. The spectrophotometric assay can not be applied directly to the glucuronylsynthase system due to it being a glycosidic-bond forming reaction. Nor can it be applied in an indirect manner such as the enzyme-coupled assay mentioned previously. But the reverse reaction that removes the spectrophotometric signal through bond formation is applicable. The glucuronylsynthase activity would be monitored by the quenching of fluorescence or removal of colour via glucuronide conjugation. Being the reverse reaction to the chromogenic (colour-producing) assay, we coined the term *chromo-ablative* (colour-destroying) assay.

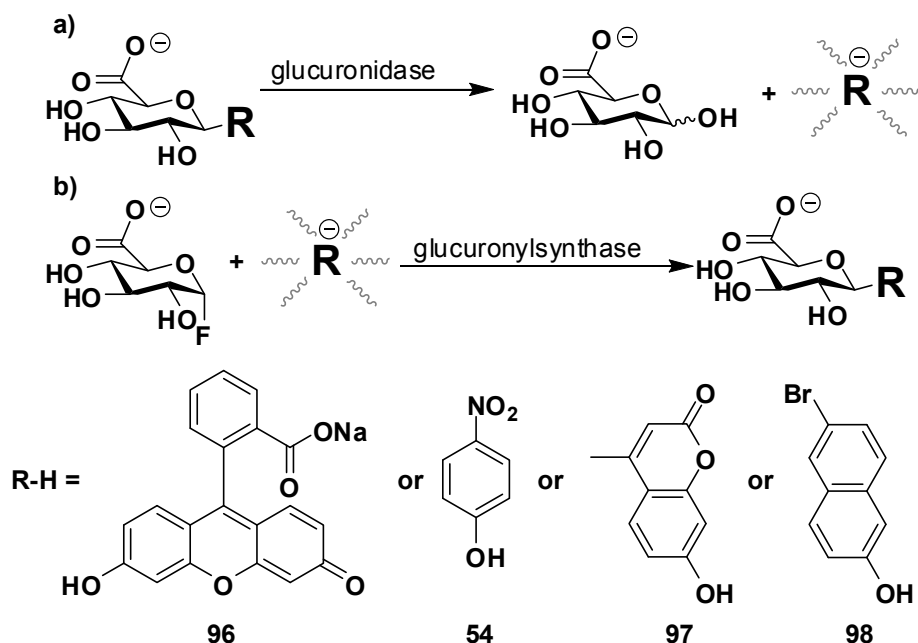
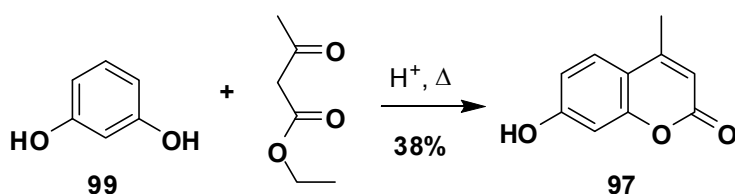


Figure 3.22. a) spectrophotometric assay of glucuronidase by the release of a chromophore and b) chromo-ablative assay of glucuronylsynthase through the quenching of a chromophore. Some examples of chromophores are given for R.

Fluorescein **96**, *p*-nitrophenol **54**, 7-hydroxy-4-methylumbelliferone **97** and 6-bromo-2-naphthol **98** are known chromophores (Figure 3.22) that were subjected to small scale glucuronylsynthase to verify that the glucuronide is formed. The 7-hydroxy-4-methylumbelliferone **97** dye was synthesised in-house via a Pechmann condensation with resorcinol **99** (Scheme 3.13).¹²⁷ A new spot was visualised on TLC for the glucuronylsynthase of 7-hydroxy-4-methylumbelliferone **97** and 6-bromo-2-naphthol **98** only. All four crude reactions were also analysed by LC-MS ESI with a strong signal corresponding to the correct mass for the glucuronide conjugates of 7-hydroxy-4-methylumbelliferone **97** and 6-bromo-2-naphthol **98** only.



Scheme 3.13. Synthesis of 7-hydroxy-4-methylumbelliferone **97** via a Pechmann condensation.

The 4-methylumbellifer-7-yl β -D-glucuronide **100** and 6-bromo-2-naphthyl β -D-glucuronide **101** were synthesised on a larger scale and obtained in good yields (41% and 69% respectively) when compared to the yield obtained from

phenol **52** (31%, Table 2.2). A chromo-ablative assay was initiated by first determining the excitation and emission maximum for 7-hydroxy-4-methylumbelliferone **97** ($\lambda_{\text{ex}} = 389 \text{ nm}$, $\lambda_{\text{em}} = 447 \text{ nm}$) and 6-bromo-2-naphthol **98** ($\lambda_{\text{ex}} = 257 \text{ nm}$, $\lambda_{\text{em}} = 367 \text{ nm}$) in phosphate buffer, pH 7.5 under ambient conditions. Calibration curves of the two chromophores were obtained and were near linear ($R^2 > 0.94$) up to their solubility limit. Individual glucuronosyltransferase reactions on the two chromophores were performed inside quartz cuvettes and monitored by fluorescence every ten minutes over 2 days in a continuous assay. Blank reactions lacking glucuronosyltransferase were also performed to verify fluorescent quenching was due to the glucuronosyltransferase reaction. After twelve hours, the fluorescence of 7-hydroxy-4-methylumbelliferone **97** had been quenched by 80% through its glucuronosyltransferase-mediated conjugation with α -D-glucuronyl fluoride **51** (Figure 3.23). An unusual rise in fluorescence was observed over the first hour for 6-bromo-2-naphthol **98** (Figure 3.24). A likely cause may be due to inadequate mixing of the substrate. Nevertheless, an equivalent quenching of fluorescence was observed over time, albeit at a lower rate than 7-hydroxy-4-methylumbelliferone **97**. The concentration of 7-hydroxy-4-methylumbelliferone **97** (0.5 mM) was 2.5 times that of 6-bromo-2-naphthol **98** (0.2 mM) which may partially account for the variation in reaction rates.

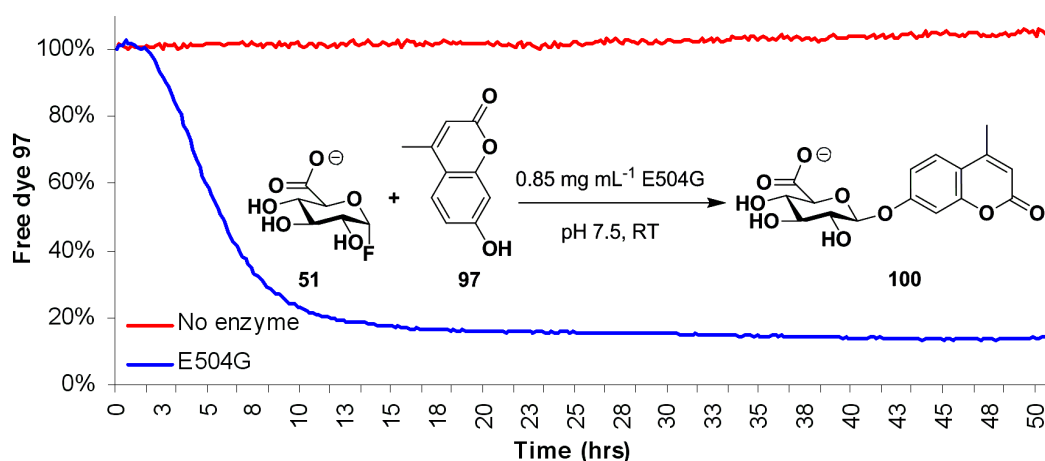


Figure 3.23. *In vitro* fluorescent monitoring of 7-hydroxy-4-methylumbelliferone **97** in a glucuronosyltransferase reaction.

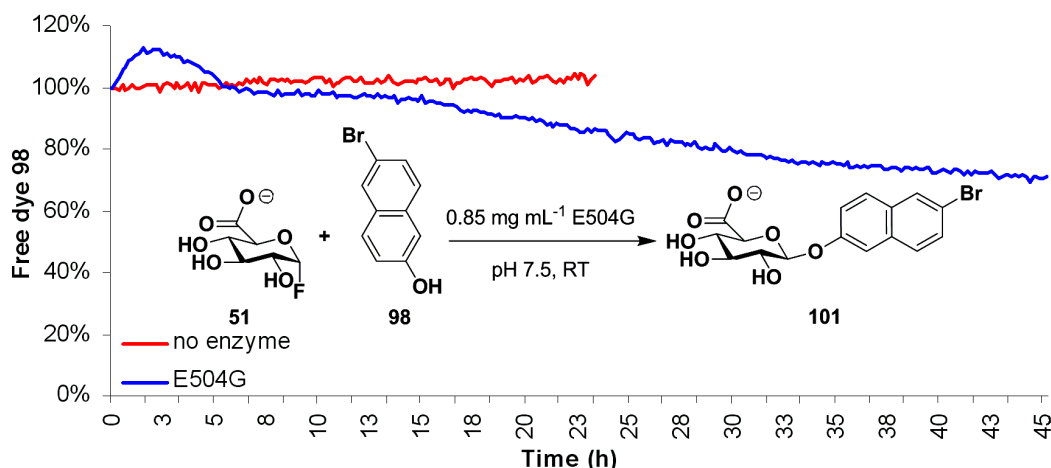


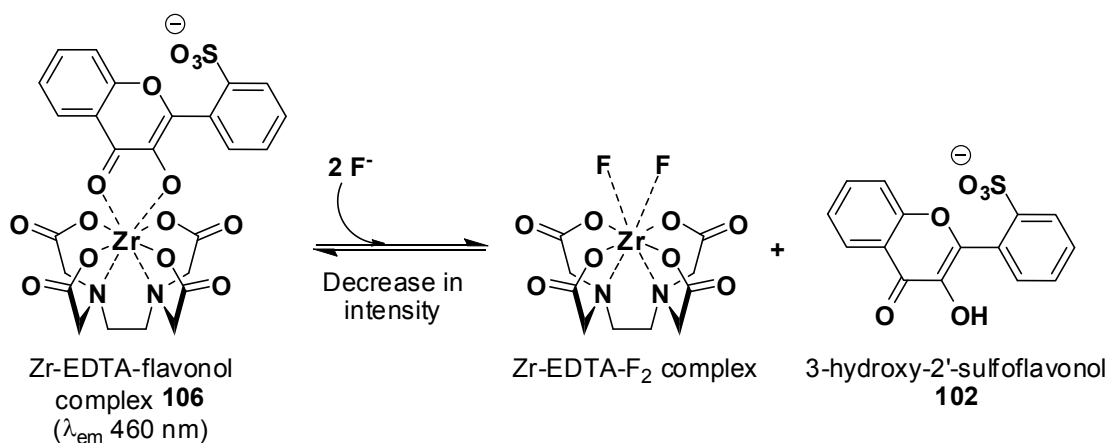
Figure 3.24. *In vitro* fluorescent monitoring of 6-bromo-2-naphthol **98** in a glucuronylsynthase reaction.

In vitro, the chromo-ablative assays were successfully proven to work due to high concentrations of purified enzyme available. However, the assays were never trialled *in vivo*. The screens would be performed with cell lysate which contains dilute concentrations of crude glucuronylsynthase. This would suggest significantly slower reactions would be observed which may introduce errors such as false positives through signal drifting. Additionally, the assay relies on monitoring the small reduction of fluorescence from an initially intense source of fluorescence. This is difficult to measure compared to measuring the small development of fluorescence from an environment free of fluorescence. As a final point, directed evolution may only result in the evolution of a new glucuronylsynthase specific towards 7-hydroxy-4-methylumbelliferone **97** or 6-bromo-2-naphthol **98**. Improved glycosynthase activity in the directed evolution screens would not necessarily suggest improved universal glycosynthase activity e.g. towards steroids. So this assay was placed aside for a more universal screening assay to be developed.

3.7.4 Fluoride-selective assay

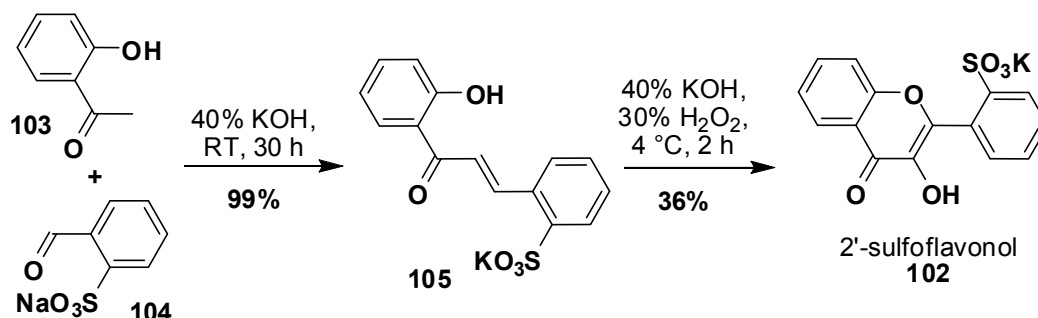
Fluoride selective potentiometry is the most common glycosynthase kinetic assay, primarily for its universal application in all glycosynthases regardless of the acceptor alcohol or products formed. Its application on a high throughput screen, however, would be impractical. Fortunately, there are alternative means to detect fluoride ions. Fluoride binds strongly to tetravalent zirconium

and ligand-exchange assays have been developed for the detection of fluoride.¹²⁸⁻¹³⁰ The complex of zirconium (IV) and flavonol emits a blue fluorescence (λ_{em} 460 nm) that can be quenched in the presence of fluoride ions via ligand exchange in a chromo-ablative manner.¹³¹ The earlier flavonol-zirconium methods required low pHs and organic solvents to promote hydrogen bonding and dissolve the hydrophobic flavonol ligand. Such conditions would mean an inconvenient discontinuous assay. Recently, the highly water-soluble 2'-sulfoflavonol **102** was used as the zirconium(IV) ligand in neutral, aqueous conditions (Scheme 3.14).¹³² This work was investigated as possible high throughput screening assay for glucuronylsynthase with expansion to all glycosynthases.



Scheme 3.14. Ligand exchange reaction of Zr-EDTA-flavonol with fluoride ion.

The 2'-sulfoflavonol **102** was synthesised from *o*-hydroxyacetophenone **103** and sodium 2-formylbenzenesulfonate **104** via an Aldol condensation followed by an oxidative cyclisation of the 2'-hydroxychalcone-2-sulfonate **105** (Scheme 3.15). The final flavonol **102** product was isolated as the potassium salt from reverse-phase flash chromatography.



Scheme 3.15. Synthesis of 2'-sulfoflavonol **102**

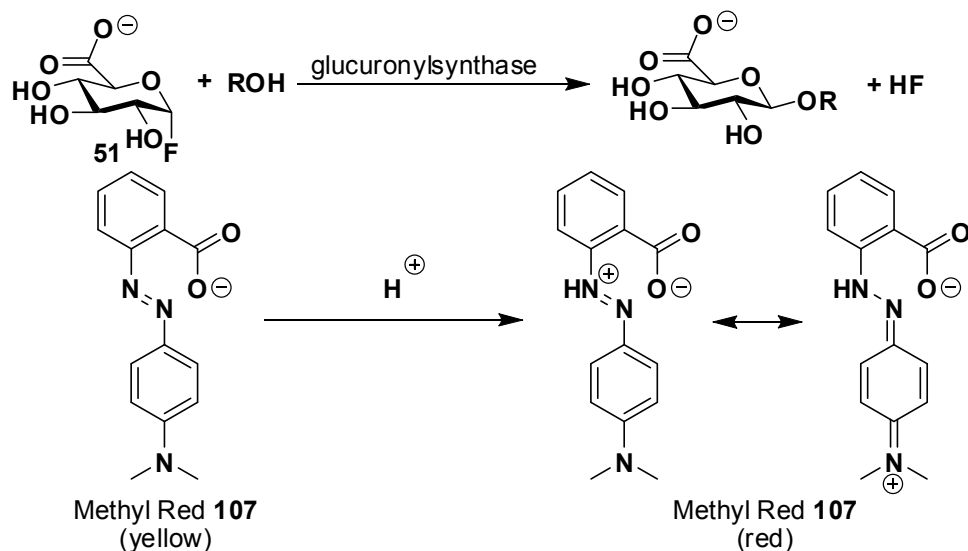
Enzyme kinetics

The Zr-EDTA-flavonol complex **106** was created *in situ* during the high throughput screening in the molecular biology lab. The assay was able to detect the release of fluoride ions down to 200 nM, with the *in vitro* experiments showing an appreciable decrease in fluorescence over time.¹³³ Unfortunately, when the assay was applied with cell lysate, it appeared that the non-enzymatic hydrolysis of the α -D-glucuronyl fluoride **51** donor (Scheme 3.7a) was increased in the cell lysate and interfered with the assay. The minute amount of glucuronylsynthase activity in the mutants made it difficult to set apart a positive result from background hydrolysis.¹³³ This assay is a novel means of high throughput screening applicable to all glycosynthases where a glycosyl fluoride donor is utilised and an appreciable catalytic turnover is achieved. This assay was inadequate for the current glucuronylsynthase activity and alternative assays were explored until a more active generation of mutants were created.

3.7.5 pH-Dependent assay

The pH-dependent assay was developed by Shoham *et al* and is a universal assay applicable to all glycosynthases.¹³⁴ It exploits the fact that hydrogen fluoride is produced from all glycosynthase reactions so that when little to no buffer is applied, the pH of the reaction will drop. Using common pH indicators, the reaction progress can be monitored by eye or more accurately through spectrophotometry (Scheme 3.16). This assay was explored as a glucuronylsynthase high throughput assay using 1 mM phosphate buffer and Methyl Red **107** as the pH indicator. The assay was successful *in vitro*, but when applied with cell lysate, the same problems experienced with the zirconium flavonol assay were encountered. The minute amount of glycosynthase activity in the mutants made it difficult to set apart a positive result from background hydrolysis.¹³³ Furthermore, there was a lag time before the pH started to drop due to additional buffering from the cell lysate. The assay reported by Shoham *et al* was successful for their glycosynthase system due to an appreciable parent glycosynthase activity (k_{cat} 1.3 s⁻¹). This catalytic turnover is over 50 times faster than the fastest reported glucuronylsynthase reaction (k_{cat} 0.023 s⁻¹ involving 3-methoxybenzyl alcohol **47**). An appreciable

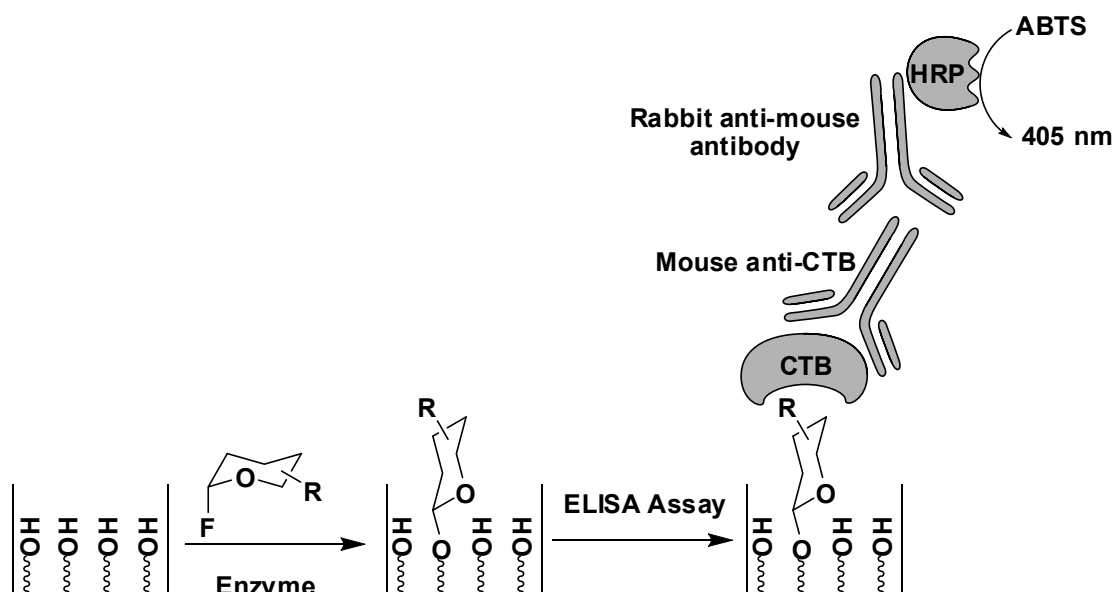
glucuronylsynthase activity needs to be achieved by initial directed evolution studies before this assay is viable as a glucuronylsynthase high throughput assay.



Scheme 3.16. Detection of HF production in the glucuronylsynthase by Methyl Red 107.

3.7.6 ELISA assay

An enzyme-linked immunosorbent assay (ELISA) relies on the recognition of the glycosynthase products by a specifically developed anti-body. An enzyme-coupled assay would then be used to detect anti-body binding. This assay was demonstrated by Withers and Hancock for their glycosynthase-inspired glycophospholipid-synthesising enzyme.^{91,135} The glycophospholipid-synthesising enzyme attaches the glycosyl donor to a membrane-attached acceptor (Scheme 3.17). Cholera toxin B subunit (CTB) is added which specifically binds to the membrane-bound glycophospholipid products. The plates are washed and mouse anti-CTB is added to bind to the CTB. The plates are washed once again and rabbit anti mouse antibody fused with horseradish peroxidase binds to the mouse anti-body. The horse radish peroxidase will oxidise 2,2'-azino-bis(3-ethylbenzothiazoline-6-sulfonic acid) (ABTS) in the presence of peroxide which can be measured at 405 nm.



Scheme 3.17. ELISA assay for the glycosyltransferase synthesising glycosynthase. CTB = Cholera toxin B subunit, HRP = horseradish peroxidase, ABTS = 2,2'-azino-bis(3-ethylbenzthiazoline-6-sulphonic acid).

The glycosyltransferase synthesising glycosynthase shares similar attributes to the glucuronosyltransferase enzyme: both attach a glycosyl fluoride donor to a variety of non-carbohydrate acceptors. The ELISA assay may be applicable to the glucuronosyltransferase system. ELISA assays have already been developed for a small library of steroid glucuronides, including pregnanediol 3-glucuronide,¹³⁶ pregnanetriol 3 α -glucuronide,¹³⁷ and estrone 3- β -D-glucuronide **12**¹³⁸. Unfortunately no highly specific ELISA assays seem to exist for the glucuronides of anabolic steroids such as testosterone **7**, nandrolone and tetrahydrogestrinone. Although previous work in the group has seen the development of an ELISA assay for the detection of non-conjugated anabolic steroids.^{139,140} It is plausible to develop an ELISA assay, similar to Withers and Hancock, whereby an antibody fused with horseradish peroxidase binds to another antibody that is selective for a steroid glucuronide of choice. The development of such an ELISA assay is complex task as it requires the development of antibodies and so more simple assays were considered first.

3.7.7 Conclusions

Multiple high through-put screening assays have been mentioned and, at the time of this publication, are currently undergoing trials with cell lysate. Some screens, such as the pH-dependent and fluoride-selective assays failed when

the assay was performed with cell lysate. This is likely due to the low glucuronylsynthase activity in cell lysate. This is not due to the enzyme concentration in the cell, but due to the slow catalytic turnover of the enzyme. However, options are still open with the chromo-ablative and ELISA assay yet to be trialled with cell lysate. The chromo-ablative assay has been developed *in vitro* but the ELISA assay is still a concept. The ^1H NMR and HPLC assays developed for kinetic investigations are unsuitable for high throughput screening due to the arduous task of preparing such a large sample set. The search for a successful high through-put screen is on-going.

3.8 Conclusions from enzyme kinetics

A HPLC assay was developed to monitor the kinetics of the glucuronylsynthase reactions. Unlike the ITC and ^1H NMR assays, the samples did not have to be prepared in a special manner for analysis and provided the greatest sensitivity of all the kinetic assays attempted. The results from the kinetic investigation (Table 3.1 and Table 3.2) found that α -D-glucuronyl fluoride **51** bound strongly to the glucuronylsynthase enzyme (K_m^{app} 15 μM) whilst the accepter alcohols exhibited weak binding ($K_m > 20 \text{ mM}$). This large difference in Michaelis constants reflects the binding interactions of the wild-type β -glucuronidase enzyme whereby the preferential recognition of the carbohydrate residue allows the hydrolysis of D-glucuronic acid **3** from a wide variety of aglycons.

This large difference in Michaelis-Menten constants also suggested that the glucuronylsynthase operated under an ordered bi bi enzyme mechanism. The rate equation for this model fitted the kinetic data very well for α -D-glucuronyl fluoride **51** and 2-phenylethanol **45**. However, the kinetic investigation of 3-methoxybenzyl alcohol **47**, 4-fluorobenzyl alcohol **50** and phenol **52** showed substrate inhibition. An attempt at fitting the data to a model with substrate inhibition generated kinetic parameters with a moderate degree of uncertainty. Either more data points are required to accurately solve the multiple unknown kinetic parameters of the current model or an alternative model needs to be derived for the glucuronylsynthase system.

Enzyme kinetics

The catalytic turnovers determined from the kinetic study are less than desirable ($k_{\text{cat}} < 0.023 \text{ s}^{-1}$ observed). The low catalytic turnover suggested the application of directed evolution to more active glucuronylsynthase enzyme. A range of high-throughput screens were proposed for the study but the poor activity of the current glucuronylsynthase made it difficult to monitor the enzyme activity in cell lysate by the chromo-ablative, pH-dependent and fluoride-selective assays. Alternative options are still available (for example, the ELISA assay) and work, in conjunction with a molecular biologist, is still on-going.

The activity of the glucuronylsynthase was improved marginally through the optimisation study of the reaction variables. Increasing the temperature of the glucuronylsynthase reactions to 37 °C will increase the reaction rate three fold. No improvement in activity could be achieved by pH with the optimum pH (pH 7.5) was already used in reaction. A linear relationship was observed between enzyme activity and enzyme concentration, ruling out any deviations of activity as a result of quaternary structure equilibria or allosteric regulation. With the optimised reaction conditions determined and a better understanding of the glucuronylsynthase mechanism (i.e. substrate inhibition is possible), the research was redirected back towards expanding the repertoire of the glucuronylsynthase library. With the ultimate goal of this research to synthesise steroid glucuronides for analytic standards; the investigation of steroidal substrates was commenced.

~ Chapter 4 ~

Steroid

solubilisation

strategy

4.1 Introduction

An initial attempt at expanding the glucuronylsynthase methodology was unrewarding. Unsystematic modifications to the variables of the glucuronylsynthase reaction were performed in the hope identifying a trend (refer to section 2.5.1). Furthermore, novel substrates were subjected to glucuronylsynthase reactions with no known experimental protocol to follow (refer to section 2.5.4). A deeper understanding of the glucuronylsynthase reaction was gained from enzyme kinetic studies. The kinetic aspects of the enzyme, recognition of substrate inhibition and optimum reaction variables were determined from this systematic approach.

With this knowledge in hand, the extension of the glucuronylsynthase methodology was recommenced by expanding the substrate library once again. With the ultimate goal of synthesising steroid glucuronides as analytical standards, the glucuronylsynthase methodology for steroids was explored.

Previous attempts at synthesising steroid glucuronides via glucuronylsynthase reactions produced low yields and identified the low water solubility of the steroidal substrates as a major issue.⁵⁸ The solubility of steroids in the aqueous media will be addressed in this study along with the optimised conditions to achieve high yields of steroid glucuronide conjugates from glucuronylsynthase reactions.

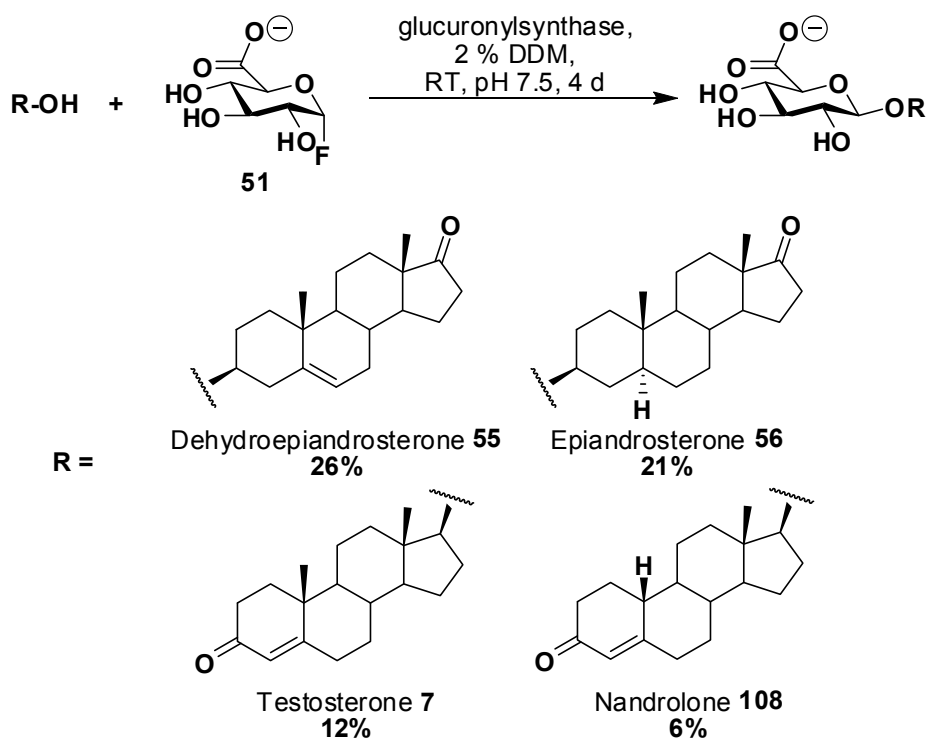
4.2 Glucuronylsynthesis of steroids

The majority of the glucuronylsynthase research performed to date has investigated simple alcohols. The only steroid glucuronide isolated in milligram quantities prior to this research has been that derived from DHEA **55**.⁵⁷ DHEA **55** is very hydrophobic and had to be dissolved in 2% w/v of the detergent DDM to synthesise the DHEA β -D-glucuronide **77** in 26% yield (Scheme 4.1). This yield was low but still significant considering literature states that the Koenigs-Knorr procedure yields **77** in 20% yield over two steps.²⁰ The glucuronylsynthase achieved the desired product **77** in a mild, single step reaction that allowed essentially complete recovery of starting

material **55**. Further to this, it was performed prior to the knowledge of the optimised glucuronylsynthase conditions.

A few additional steroids were subjected to small scale glucuronylsynthesis prior to this research and demonstrated likely product formation in accordance to the ESI-MS analysis.⁵⁸ Due to the scale of these reactions, the glucuronide products of epiandrosterone **56**, testosterone **7**, and nandrolone **108** could not be confirmed by a complete characterisation nor could a yield be placed on these reactions. To commence the steroid methodology study, it was of great importance to determine the yield of these glucuronylsynthase reactions and confirm the glucuronide products from these reactions.

On a 40 mg scale, epiandrosterone **56** yielded 21% of the glucuronide product **109** using identical reaction conditions to that applied to the DHEA **55** synthetic scale glucuronylsynthesis (Scheme 4.1). Under the mild conditions, the unconsumed epiandrosterone **56** was essentially fully recovered (76%). This yield is similar to the yield obtained from DHEA **55** (26%); which is consistent given their structural similarities.



Scheme 4.1. Glucuronylsynthesis of a selection of steroids

The glucuronide formation of the 17 β -hydroxy steroids was less obvious in the small scale investigation and this was consistent with low yields obtained

Steroid solubilisation strategy

by the preparative scale reactions. The glucuronides of testosterone **7** and nandrolone **108** were obtained in 12% and 6% respectively (Scheme 4.1). Nandrolone **108** was completely soluble at 10 mM with 2% DDM whilst testosterone **7** was not fully dissolved at 5 mM in 2% DDM. It appears that increased solubility did not necessarily provide a greater yield as only half the yield of nandrolone β -D-glucuronide **110** (6%) was formed in comparison to testosterone β -D-glucuronide **6** (12%). Two possibilities are hypothesised. The first theory is that the small structural difference of the methyl group is playing an important role in the correct binding in the enzyme. For example, the A ring of nandrolone **108** is subtly more planar than testosterone **7**. This may encourage the incorrect binding of the less sterically-demanding A ring into the binding site instead of the D ring required for a glucuronylsynthase reaction to take place.

The alternative hypothesis relates to the findings of the kinetic experiments (chapter 3.5). Substrate inhibition was discovered for the majority of acceptor alcohols tested in the kinetic studies. The nandrolone **108** concentration (10 mM) was almost double the concentration of the other steroids (5-6 mM) and so the presence of substrate inhibition may have affected the yield of the glucuronylsynthase reaction.

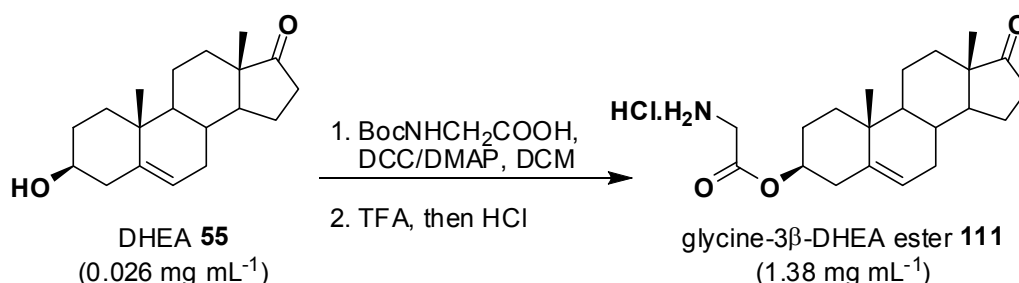
Which ever the cause for the reduced yield, there was one factor that all reactions suffered from. All reactions were very dilute due to the poor water solubility of steroids. The dilute reactions meant greater quantities of precious enzyme were needed to achieve enzyme concentrations that provided an appreciable reaction rate. A more concentrated reaction would require less enzyme, but may encounter substrate inhibition if existing for this class of substrates. This could be explored through HPLC kinetic assays; however the first step was to discover a suitable method of making the steroids more soluble in water.

The detergent DDM was used to aid in the solubility of the steroid in the above examples. It was used to prevent the denaturing effects associated with the use of co-solvents as determined in previous studies.⁵⁸ This study also detailed that DMSO is deemed the best co-solvent due to its conservation of enzyme activity and enzyme stability over time. So a glucuronylsynthase

reaction with DHEA **55** using DMSO as a co-solvent was performed to compare its use against the detergent DDM. DHEA **55** was not very soluble in the DMSO solution with only a 5 mM concentration achievable with a 25% v/v DMSO solution. Nevertheless, this was subjected to glucuronidation, using analogous reaction conditions applied to the DDM reaction, to achieve the DHEA β -D-glucuronide **77** in 17% yield. The high concentration of detergents and co-solvents required to get the steroid even slightly more concentrated is a trade-off against enzyme inactivation. It was concluded that additives did not significantly aid the solubility of the steroids. An alternative approach may be to temporarily modify the steroid to make itself more water soluble.

4.3 DHEA derivatives

Improving the aqueous solubility of steroids with additives proved futile so a new strategy to install a modifier onto the steroid might prove more successful. This modifier would have to increase the aqueous solubility of the steroid without hindering the glucuronidation reaction and be easily cleaved in the presence of a glucuronide moiety. The chemical modification of steroids to improve water solubility has already been reported previously with an example demonstrating the interconversion of the alcohol in DHEA **55** to an ionisable species.¹⁴¹ In this example, DHEA **55** was made over 50 times more soluble in a saline solution by coupling glycine to the alcohol of DHEA **55** (Scheme 4.2). The primary amine of the glycine 3β -DHEA ester **111** is easily protonated to create an ionised species that enhances water solubility.



Scheme 4.2. Improved solubility of DHEA **55** through the esterification with glycine.¹⁴¹

A similar concept was envisaged for this research that would leave the alcohol untouched for glucuronidation reactions by manipulating an

Steroid solubilisation strategy

alternative region of the steroid. Using DHEA **55** as the model substrate, its only functionality aside from the alcohol is an alkene bond and a ketone. Modification of the ketone seemed the best choice given it is positioned on the opposite side of the steroid to the point of glucuronylation, and the large choice of ketone derivatives available.

A simple, mild and reversible reaction is the condensation of a primary amine with a ketone to form an imine product.¹⁴² The imine is usually hydrolysed under aqueous acidic conditions to reform the ketone. Imines alone are too labile and would hydrolyse *in situ* in the aqueous media of the glucuronylsynthase reactions. Hydrazones and oximes, on the other hand, are made in a similar manner but are more resistant towards hydrolysis. Hydrazone and oxime analogues were synthesised in the hope of improving the water solubility of DHEA **55**.

4.3.1 Hydrazone analogues of DHEA **55**

Hydrazone analogues of DHEA **55** were synthesised in the hope that the nitrogen alpha to the imine instils resistance to hydrolysis and solubility through a cationic species (Figure 4.1).

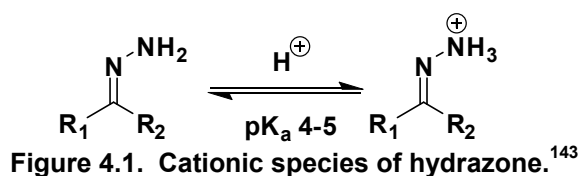
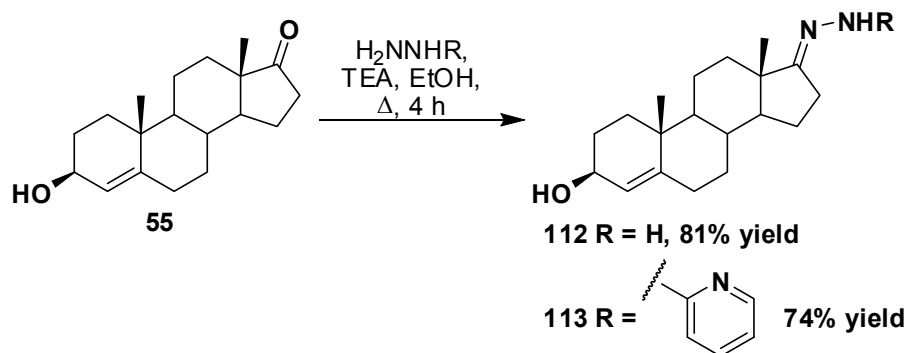


Figure 4.1. Cationic species of hydrazone.¹⁴³

DHEA **55** was refluxed with hydrazine to yield the DHEA hydrazone **112** in 81% (Scheme 4.3).¹⁴⁴ The NMR spectra (attached in example spectra) for the DHEA hydrazone **112** looked very similar to the DHEA **55** spectra with some minor differences. A broad singlet is present at 4.76 ppm which was assigned to the NH₂ protons in the ¹H spectrum (*d*₆-DMSO). The interconversion of the ketone to a hydrazone is observed as an upfield shift in the ¹³C spectrum with the C17 carbon going from a carbonyl (221 ppm) to an imine (166 ppm).



Scheme 4.3. Synthesis of DHEA hydrazone analogues 112.

A second hydrazone analogue of DHEA **55** was synthesised using 2'-pyridyl hydrazine using identical reaction conditions. The DHEA 2'-pyridylhydrazone analogue **113** was obtained in 74% yield as a single diastereomer. This isomer is assumed to be the *E*-isomer due to steric interactions associated with the methyl at the C13 position. There is no previously reported data for the DHEA 2'-pyridylhydrazone **113** with this synthesis being the first reported. The ^1H and ^{13}C NMR spectra (attached in example spectra) exhibited only one diastereomer. The introduction of the hydrazone is evident by the clearly defined aromatic segment in the ^1H and ^{13}C spectra and the upfield shift of the C17 carbon to 163 ppm. The addition of the 2'-pyridyl group to DHEA **55** was expected to aid solubility by introducing a heteroatom that could undergo hydrogen-bonding. The substitution of benzene rings for pyridine is a common strategy in reducing the lipophilicity of drugs in medicinal chemistry. In addition, pyridine has a $\text{p}K_{\text{a}}$ of 5.2 suggesting that a small proportion of the protonated form may exist in the glucuronylsynthase reaction pH of 7.5 and enhance this analogue's solubility in water.

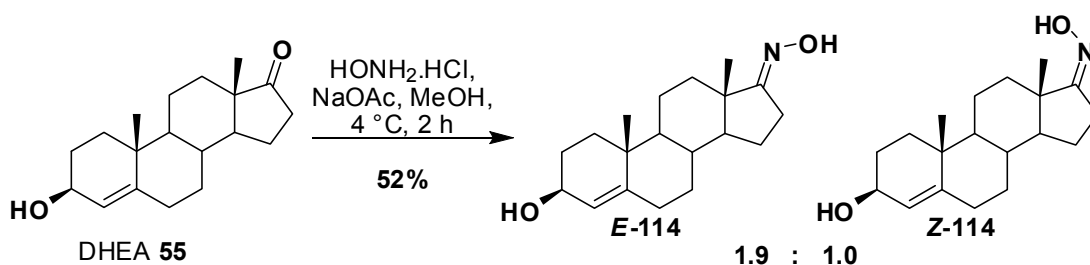
The solubility of DHEA **55** and its analogues were determined by the continuous dilution of a known sample at room temperature until complete dissolution was determined by eye. DHEA **55** had a low solubility of 0.02 mM in 100 mM phosphate buffer, pH 7.5. Formation of the DHEA hydrazone **112** improved the solubility of DHEA **55** five fold to 0.1 mM whereas the DHEA 2'-pyridylhydrazone **113** was only soluble to 0.05 mM. It was concluded that the hydrophobicity of the aromatic ring and low $\text{p}K_{\text{a}}$ value was responsible for its lack of solubility. With only minor enhancements to the solubility of DHEA

Steroid solubilisation strategy

produced by the hydrazone groups, the synthesis of oxime analogues was investigated.

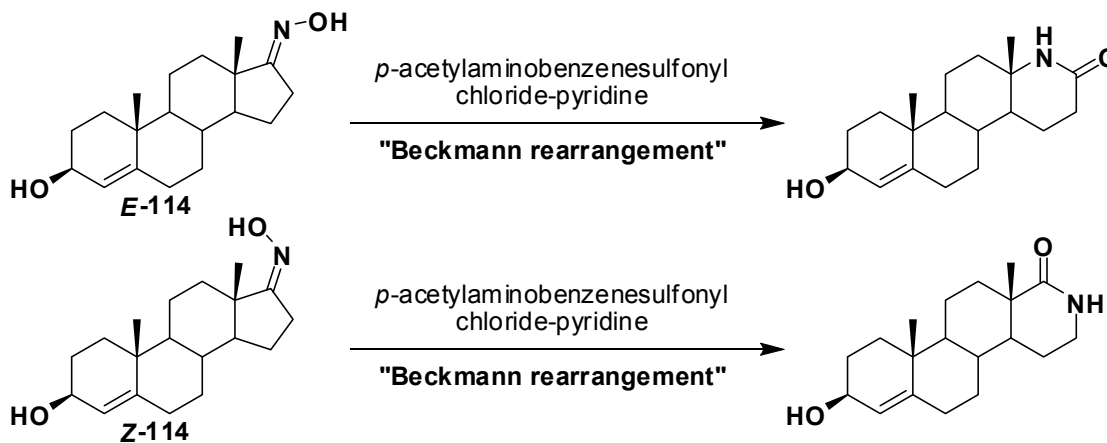
4.3.2 Oximes analogues of DHEA 55

The successful synthesis of DHEA hydrazones provided DHEA analogues that did not show significantly enhanced solubility. The synthesis of some DHEA oxime analogues were investigated in the hope of greater success. The first synthesised DHEA oxime analogue was the simple unsubstituted DHEA oxime **114** (NMR spectra attached in example spectra). DHEA **55** was added to a basic solution of hydroxylamine to produce the DHEA oxime **114** (Scheme 4.4) in a 52% yield as a mixture of *E* and *Z* diastereomers (1.9 : 1.0 respectively).¹⁴⁵



Scheme 4.4. Synthesis of DHEA oxime 114

The assignment of the isomers was based on the IR spectrum which was compared to work performed by Göndös *et al.*¹⁴⁶ Göndös separated the two isomers on alumina and provides the melting points and IR spectra of both isomers. In his publication, the stereochemistry of each isomer was determined via the Beckmann rearrangement which leads to two different and easily distinguishable lactams (Scheme 4.5).



Scheme 4.5. Beckmann rearrangement on the DHEA oxime 114 diastereomers

The O-H stretch in the IR is 3250 cm^{-1} for the *E*-isomer and 3310 cm^{-1} for the *Z*-isomer. The imine stretch (C=N) is reported as 1671 cm^{-1} for the *E*-isomer and 1636 cm^{-1} for the *Z*-isomer. The IR spectrum of the diastereomeric mixture of DHEA oximes **114** we synthesised gave an O-H stretch at 3252 cm^{-1} and a C=N stretch at 1679 cm^{-1} which strongly suggested that the *E*-isomer **114** was the predominant isomer.

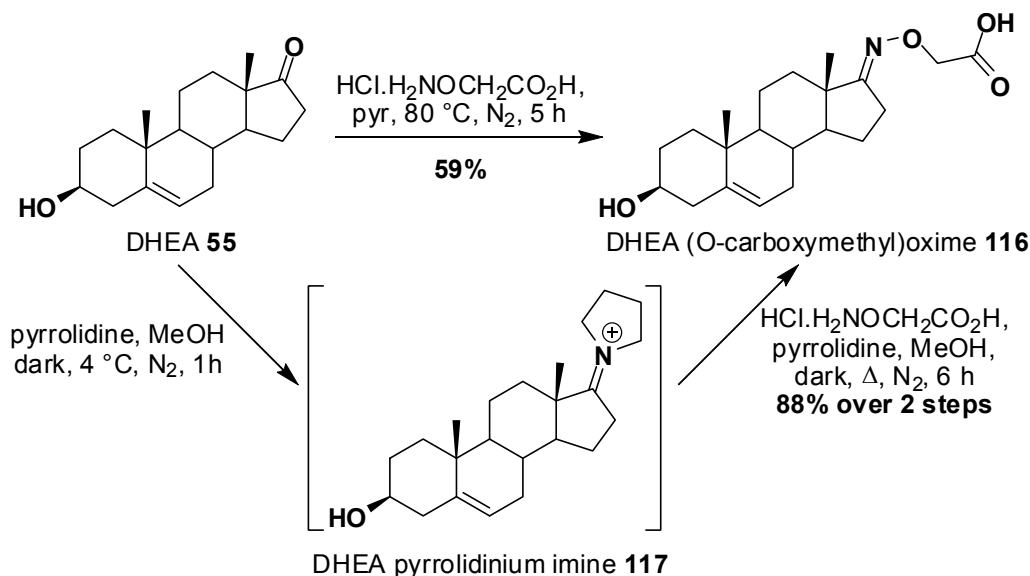
A second oxime analogue was synthesised with a similar ionisable functional group strategy that was applied to the hydrazone synthesis. DHEA **55** was reacted with carboxymethylamine hemihydrochloride **115** to form the DHEA O-(carboxymethyl)oxime **116**. The carboxylic acid attached to the end of this oxime has a pK_a of $\sim 2\text{-}3$ meaning the carboxylate anion would prevail and provide enhanced water solubility in the glucuronylsynthase reactions performed at pH 7.5.

First attempts at the oxime synthesis involved refluxing the two substrates in pyridine for 5 hours but only yielded 59% of the DHEA O-(carboxymethyl)oxime **116** (Scheme 4.6).¹⁴⁰ The yield is reasonable, but when it is considered that two more steps are yet to follow (i.e. glucuronylation and de-oximation), a low yield at the start of a linear sequence would vastly reduce the overall yield of synthesising DHEA β -D-glucuronide **77**. An alternative synthesis was attempted that involved the addition of pyrrolidine to DHEA **55** prior to the addition of carboxymethylamine hemihydrochloride **115**.¹⁴⁷ The pyrrolidine activated the carbonyl as an iminium intermediate **117** which reacts more readily with the carboxymethylamine hemihydrochloride **115** (Scheme 4.6). This two-step, one pot reaction produced the DHEA O-(carboxymethyl)oxime **116** in 88% yield over the two steps as a single diastereomer.

There is limited characterisation data reported for this oxime **116** with the exception of the optical rotation which matched the measured rotation perfectly.¹⁴⁸ The NMR data fits perfectly with the proposed structure of DHEA O-(carboxymethyl)oxime **116**. Parallel with the other synthesised DHEA analogues, the ^1H spectrum of the DHEA O-(carboxymethyl)oxime **116** (attached in the example spectra) looks similar to the DHEA **55** NMR spectrum except with an added oxime environment. A large singlet at 4.42 ppm,

Steroid solubilisation strategy

integrating to two protons, corresponded to the methylene of the newly installed oxime. The ^{13}C spectrum depicted the correct number of carbon signals and included new peaks at 171 ppm and 70 ppm respectively assigned to the carboxylic acid and methylene carbon of the oxime moiety.



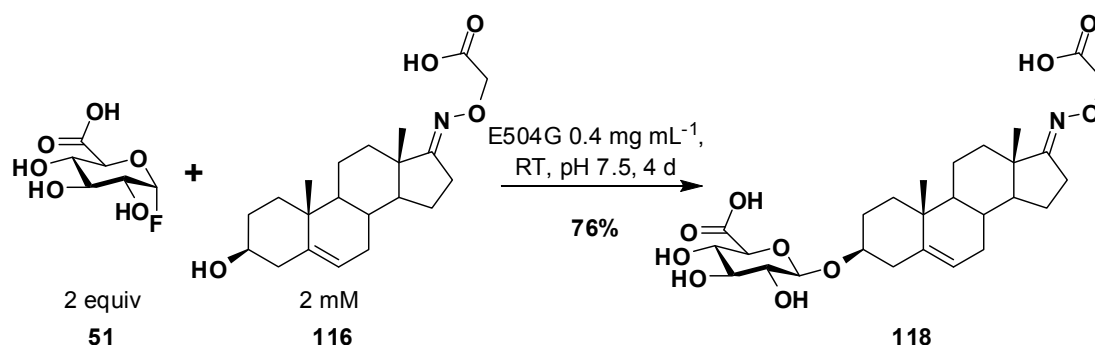
Scheme 4.6. Synthesis of DHEA O-(carboxymethyl)oxime 116.

The solubility of these DHEA oxime analogues in 100 mM phosphate buffer, pH 7.5 was tested against DHEA **55** and the hydrazone analogues. The DHEA oxime **114** displayed the same solubility (0.05 mM) as the DHEA 2'-pyridylhydrazone **113**. The DHEA oxime **114** does not become ionised like the DHEA hydrazone **112** which may compromise its water solubility. The DHEA O-(carboxymethyl)oxime **116** was soluble at 2 mM which was the best solubility enhancement result observed. This was a hundred-fold improvement on the solubility of DHEA **55**. It was of great interest to see if this more soluble DHEA analogue was prone to glucuronylation in a glucuronylsynthase reaction.

4.3.3 Glucuronylsynthesis of DHEA O-(carboxymethyl)oxime 116

The development of a range of DHEA **55** analogues with improved water solubility was hoped to replace the high concentration of detergents and co-solvents and the harsh, denaturing effects they impose on the glucuronylsynthase enzyme. The DHEA O-(carboxymethyl)oxime **116** was the most soluble of these analogues and its participation in a glucuronylsynthase reaction was explored.

The glucuronylsynthase reaction was performed on a 2 mM concentration of DHEA O-(carboxymethyl)oxime **116** using 0.4 mg mL⁻¹ of the glucuronylsynthase enzyme at room temperature. Elevated temperatures were not used for this reaction so a direct comparison could be made between the glucuronylsynthesis of DHEA **55** (Scheme 4.1) which was also performed at room temperature. A new spot was observed by TLC after an hour, but after a couple of days, the reaction seemed to have stopped. Uncertain if the α -D-glucuronyl fluoride **51** had degraded, another equivalent was added. To our amazement, the DHEA O-(carboxymethyl)oxime β -D-glucuronide **118** was isolated in an impressive 76% yield after 4 days (Scheme 4.7). This was over three times that reported from the best DHEA **55** glucuronylsynthase reaction.



Scheme 4.7. Glucuronylsynthase reaction of DHEA O-(carboxymethyl)oxime **116**

With no previous report of this glucuronide reported in literature, a thorough characterisation of this compound was undertaken. High resolution mass spectrometry reported a peak at m/z 536.2495 which is consistent with the formula C₂₇H₃₈NO₁₀ that corresponds to the parent molecule minus a proton. A peak at m/z of 558.2302 was also observed that can be assigned as the di-anion of the molecule plus a sodium cation (C₂₇H₃₇NO₁₀Na).

Comparing the IR spectrum of DHEA O-(carboxymethyl)oxime **116** to its glucuronide **118**, subtle changes in absorption confirm glucuronide conjugation. Most noticeable is the more intense and broad absorption at 3423 cm⁻¹ corresponding with the additional O-H stretches from the glucuronyl residue. The additional carboxylic acid from the glucuronyl residue produces a broader carbonyl stretch that peaks at 1745 cm⁻¹ as opposed to the 1680 cm⁻¹ produced from the combined C=N and C=O stretches of the DHEA O-(carboxymethyl)oxime **116**. But possibly the most information is provided in

Steroid solubilisation strategy

the NMR spectra (Figure 4.2). The alkenic proton occurs at 5.51 ppm and the oxime methylene protons occur as a singlet at 4.38 ppm. The glucuronosyl protons integrate correctly and appear in the 3-4 ppm region. The anomeric glucuronyl proton is observed as a doublet at 4.59 ppm with a coupling constant of 7.3 Hz consistent with axial-axial coupling with the adjacent proton. This coupling interaction implies an alpha-positioned proton which confirms a beta-linked glucuronide product. The ^{13}C spectrum was also consistent with glucuronide conjugation due to the appearance of 6 new carbon environments. The carboxylic acid carbon of the glucuronide appears at 178.4 ppm, the anomeric carbon at 101.2 ppm, and the remaining 4 glucuronyl carbons occurring in the region 80.6-73.9 ppm.

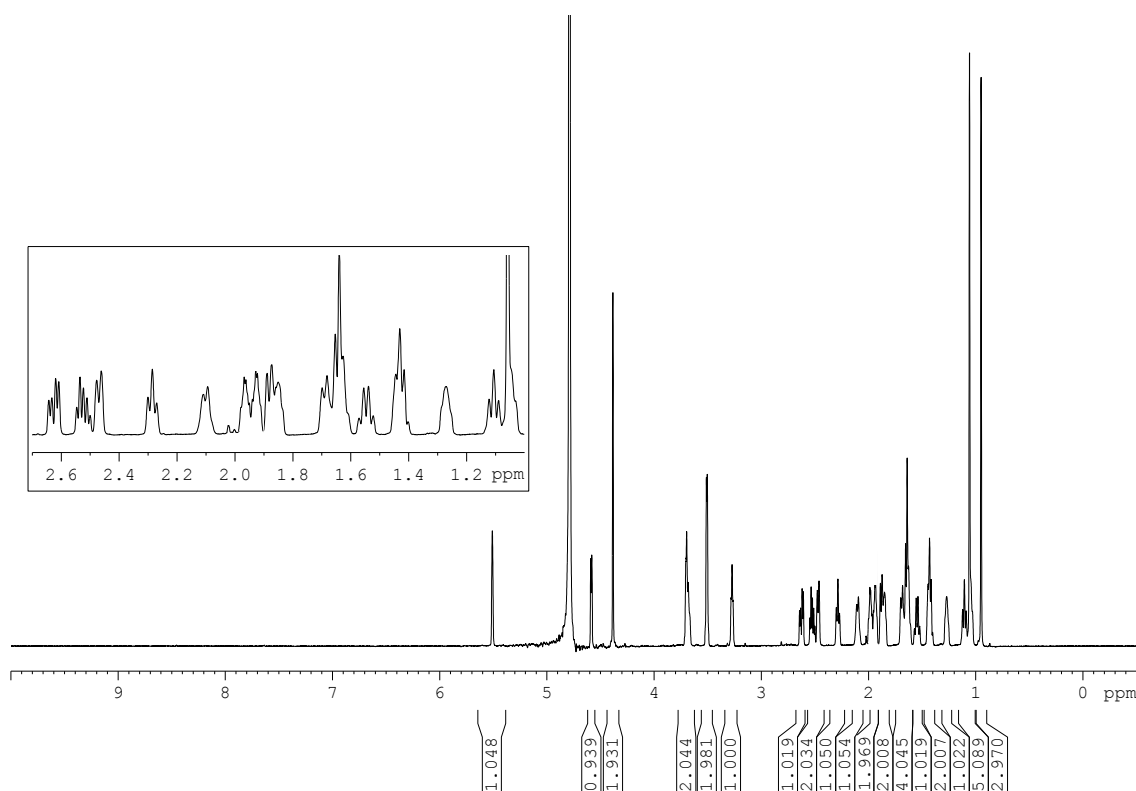


Figure 4.2. ^1H NMR spectrum (800 MHz, D_2O) of DHEA O-(carboxymethyl)oxime β -D-glucuronide **118** (Full page spectrum attached in example spectra).

To authenticate the synthesis of the proposed glucuronide **118** and remove any doubts of stereochemistry, crystals of the DHEA O-(carboxymethyl)oxime β -D-glucuronide **118** were grown for single x-ray crystal analysis. Successful recrystallisation of the DHEA O-(carboxymethyl)oxime β -D-glucuronide **118** from ethyl acetate, methanol, and water formed translucent crystals upon

cooling overnight at 4 °C. The di-sodium salt of DHEA O-(carboxymethyl)oxime β -D-glucuronide **118** was determined (Figure 4.3). The relative stereochemistry was consistent with spectral data and shows the *E*-configuration of the oxime substituent and the β -linked glycosidic bond.

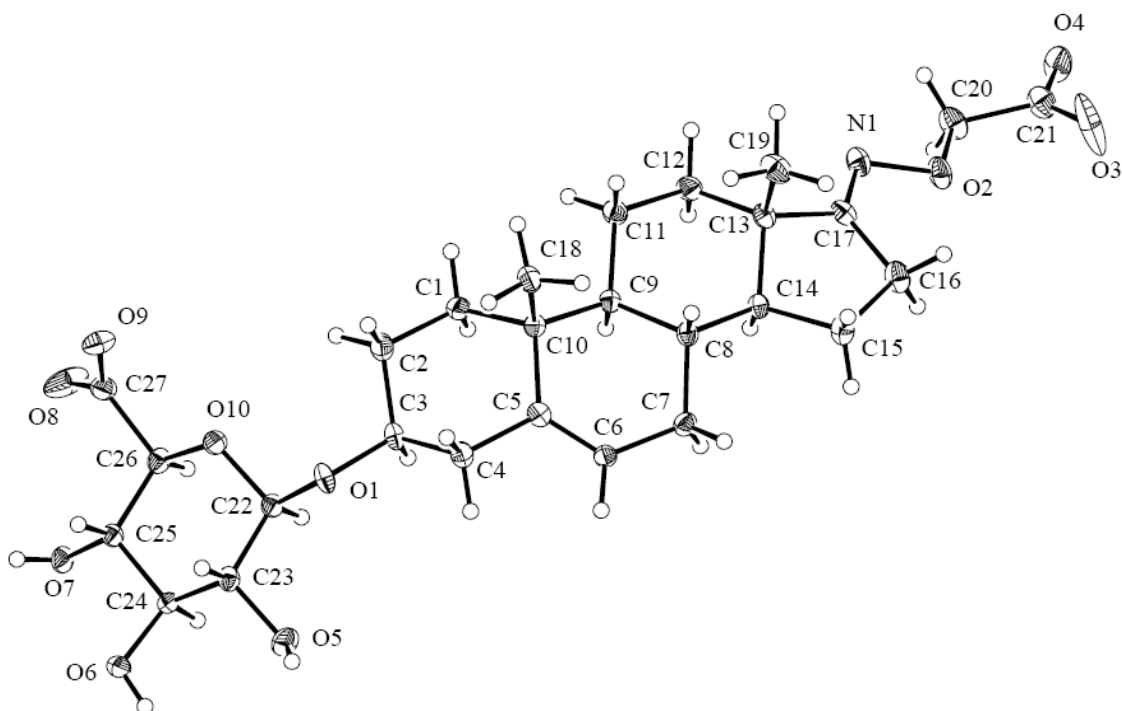
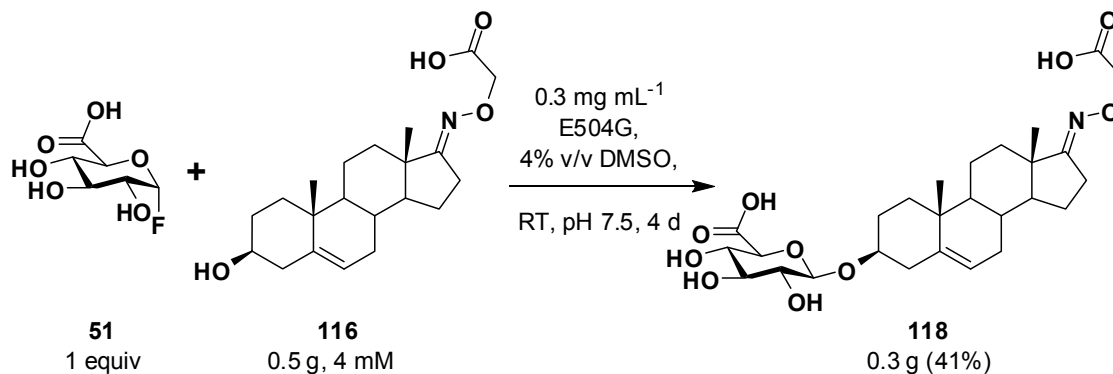


Figure 4.3. Crystal structure of one DHEA O-(carboxymethyl)oxime β -D-glucuronide **118** di-anion molecule with labelling of selected atoms. Anisotropic displacement ellipsoids show 30% probability levels. Hydrogen atoms are drawn as circles with small radii. The CIF file is reported in appendix 2.

Given the impressive yield of 76% for the DHEA O-(carboxymethyl)oxime **116** glucuronylsynthase reaction, the reaction was repeated on a larger scale to prove the practicality of large scale glucuronylsynthase reactions with steroids. A large scale glucuronylsynthase reaction has already been demonstrated on 2-phenylethanol **45**, but a large scale steroid reaction would demonstrate the practical applications of this enzyme and surmount the limitations of alternative means of enzymatic glucuronylation. A reaction with 0.5 g of DHEA O-(carboxymethyl)oxime **116** was prepared, but due to an unforeseen low expression batch of glucuronylsynthase, the DHEA analogue **116** had to be used at a more concentrated level. This was to ensure enzyme concentrations were high enough to sufficiently convert the large amount of material in a reasonable time. A concentration of 4 mM of DHEA O-

Steroid solubilisation strategy

(carboxymethyl)oxime **116** was achieved by the addition of 5% v/v DMSO. After swirling for 4 days at room temperature, only 0.3 g (41%) of the DHEA O-(carboxymethyl)oxime β -D-glucuronide **118** was obtained.



Scheme 4.8. Large scale glucuronylsynthase reaction on DHEA O-(carboxymethyl)oxime **116.**

There were three possible factors that could be associated with this drop in yield. The first factor was the concentration of DHEA O-(carboxymethyl)oxime **116**. The large scale reaction had twice the concentration of aglycon, than the previous reaction. If substrate inhibition exists for DHEA O-(carboxymethyl)oxime **116**, then the large scale reaction could have suffered reduced reaction rates that resulted in a lower yield. The equivalent of α -D-glucuronyl fluoride **51** was also different in each reaction. Unlike the first reaction, an additional equivalent of α -D-glucuronyl fluoride **51** was not added to the large scale reaction. And the final factor is the addition of DMSO as an additive to the large scale reaction. The effect of co-solvents and detergents on the activity and stability of the WT β -glucuronidase has been explored, but no studies have been directed to the glucuronylsynthase enzyme. In order to determine the effect that each of these three factors place on the DHEA O-(carboxymethyl)oxime **116** glucuronylsynthase reactions, it was necessary to revisit the HPLC kinetics. However, with copious quantities of the DHEA O-(carboxymethyl)oxime β -D-glucuronide **118** in hand, the discovery of a de-oximating procedure was deemed more important. Without an efficient de-oximation step, the synthesis sequence would have hit a dead end and the optimisation of the glucuronylsynthase step would be futile.

4.4 De-oximation of the O-(carboxymethyl)oxime

The appendage of carboxymethoxylamine **115** to DHEA **55** created the oxime analogue **116** that has vastly improved solubility in water. The DHEA O-(carboxymethyl)oxime **116** was successfully converted to its glucuronide **118** in 76% yield under un-optimised conditions. The final step of the improved steroid solubilisation strategy was to cleave the oxime to reform the ketone of DHEA **55** in the presence of the attached glucuronide residue. To begin this study, de-oximation of DHEA O-(carboxymethyl)oxime **116** was tried first before attempting de-oximation of the subsequent glucuronide.

4.4.1 De-oximation of DHEA O-(carboxymethyl)oxime **116**

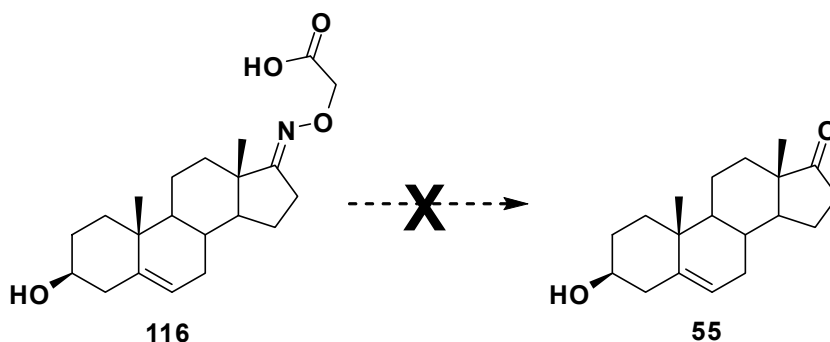
A long list of oxime cleavage procedures exist with the majority operating through an acid/metal activated hydrolysis or reduction/oxidation of the oxime. With the ultimate goal of removing the oxime from DHEA O-(carboxymethyl)oxime β -D-glucuronide **118** (Scheme 4.9), the reaction procedure needed to be mild so it did not hydrolyse the glycosidic bond of the glucuronide. As a result, the use of strong acids was cast aside in fear they would degrade the labile glucuronide moiety. The conditions would also need to be selective to avoid any side reactions with other functional groups present in the molecule such as the alcohols on the glucuronide or the alkene in DHEA **55**. Oxidative cleavage seemed an unlikely procedure in light of these concerns.

Many of the de-oximation procedures use non-polar organic solvents as the reaction solvent. With the exception of only a few polar organic solvents, such as methanol and DMSO, the DHEA O-(carboxymethyl)oxime β -D-glucuronide **118** is water soluble. The ideal procedure would be a mild and stereoselective procedure, preferably performed in an aqueous media.

An acid-mediated hydrolysis is the most commonly used procedure but refluxing is generally required to achieve higher yields even with unsubstituted oximes.¹⁴⁹ The combination of heat and acid would surely degrade the glucuronide **118** and may also lead to by-products through the Beckmann rearrangement (see Scheme 4.5 for an example).¹⁵⁰ A metal-mediated hydrolysis was hoped to provide improved activation to avoid unnecessary

Steroid solubilisation strategy

heating. Cupric chloride is commonly utilised for the hydrolysis of hydrazones in an aqueous media with good yields obtained within hours of reaction at room temperature.¹⁵¹⁻¹⁵³ It has also been used in the hydrolysis of oximes, but to a lesser effect.¹⁵⁴ Given the mild, aqueous reaction conditions, this was attempted in the de-oximation of DHEA O-(carboxymethyl)oxime **116** (Scheme 4.9A). After 24 hours of stirring DHEA O-(carboxymethyl)oxime **116** in the presence of 50 mM cupric chloride in phosphate buffer at pH 7.5, no new spots were observed by TLC.



Conditions

A: 50 mM CuCl₂, phosphate buffer pH 7.5, RT, 24 h

B: Mo(CO)₆, acetonitrile/phosphate buffer pH 7.5, RT, 24 h

C: Fe(NO₃)₃·9H₂O, H₃PW₁₂O₄₀·6H₂O, solvent-free, 40-45 °C, 24 h

Scheme 4.9. De-oximation of the DHEA O-(carboxymethyl)oxime **116**.

The hydrolysis of the oxime was then attempted with an aqueous solution of molybdenum hexacarbonyl.¹⁵⁵ Molybdenum hexacarbonyl had previously been used in the cleavage of isoxazolidines¹⁵⁶, but only recently been proven to mediate oxime hydrolysis.¹⁵⁵ The procedure recommended refluxing in aqueous acetonitrile, but to commence, the molybdenum hexacarbonyl was stirred in a pH 7.5 buffered solution of the DHEA O-(carboxymethyl)oxime **116** (Scheme 4.9B). After 3 hours, no new spots were observed by TLC, so acetonitrile was added to aid solubility of the DHEA O-(carboxymethyl)oxime **116** and possibly the molybdenum reagent also. After 24 hours, no new products were observed by TLC. The published procedure only reported yields for the unsubstituted oximes upon refluxing.¹⁵⁵ So it was no surprise that our attempt of de-oximating a substituted oxime at room temperature would fail. The discovery of a hydrolysis procedure without heating was preferential and so an alternative procedure was explored.

Iron(III) nitrate has also been reported as a mild oxidant for deoxygenation.¹⁵⁷⁻¹⁶² In some instances, it was used in a solvent-free system which may reduce the possibility of hydrolysis occurring to the glucuronide. The solvent-free method reported by Firouzabadi *et al* was attempted (Scheme 4.9C).¹⁶⁰ It involved stirring a dry mixture of iron(III) nitrate nonahydrate (0.5 equiv) and phosphotungstic acid hexahydrate (0.5 equiv) with the oxime (1 equiv). After an hour, a sample of the stirring dry powder was dissolved in chloroform and analysed by TLC. No new spots were observed, so the solvent-free reaction was heated to 40 °C with stirring. The reaction was analysed by TLC once again after 24 hours and showed no evidence of DHEA **55** formation. The published procedure only reports yields for the unsubstituted oxime and observes the release of a red gas. It appears that iron(III) nitrate oxidises the unsubstituted oxime ultimately to nitrogen dioxide which is replaced with water to reform the carbonyl. Unfortunately, iron(III) nitrate was too mild to oxidatively cleave the *O*-(carboxymethyl)oxime. It appeared that the search for a mild de-oximation procedure would have to be refined to substituted oximes.

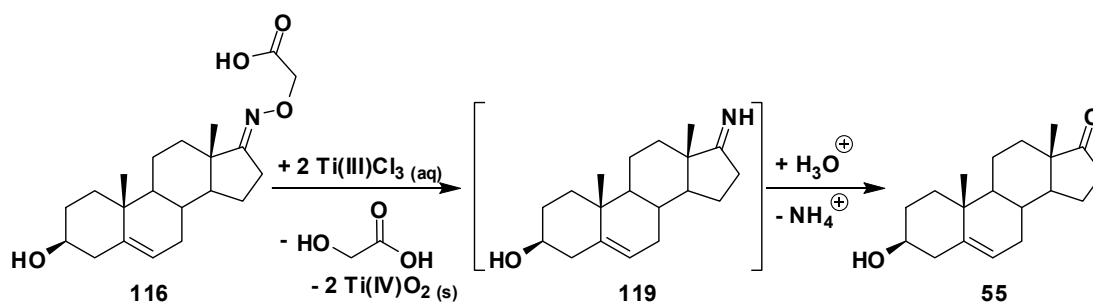
Corey and Richman published a mild de-oximation procedure with chromous acetate.¹⁶³ The procedure is reported to work better on oxime acetates than the unsubstituted oxime. Unfortunately, alkyl oximes (such as our oxime) required heating in order to react. Heating in the presence of a Lewis acid (Cr^{2+}) may hydrolyse the glycosidic bond of the glucuronide. It seemed most published procedures for substituted oxime removal required harsh reaction conditions; or at least harsh in respect to our substrate. These were conditions we had hoped to avoid.

Timms and Wildsmith developed a mild de-oximation procedure using titanium(III) chloride during their synthesis of erythromyclamine.¹⁶⁴ Whilst their paper reports the de-oximation of an unsubstituted oxime, their procedure has also been effective against substituted oximes.¹⁶⁵ A 20 mg reaction of the DHEA *O*-(carboxymethyl)oxime **116** was attempted according to the procedure. Upon addition of the solution of titanium(III) chloride, the reaction solution turned immediately black-violet and the reaction left to stir at room temperature under a nitrogen atmosphere. The reaction was conveniently followed by a colour change with the reaction solution fading to a light blue and

Steroid solubilisation strategy

the formation of titanium dioxide observed as a white precipitate. After an hour, a complete conversion to DHEA **55** was observed by TLC but only 33% was isolated upon work-up. The remaining mass was unaccounted for and possibly lost during workup. Nevertheless, this was the first de-oximation observed, with the product isolated matching the spectral data for DHEA **55**.

Timms describes how the anhydrous reaction yields the imine intermediate implying a reductive N-O cleavage is achieved from titanium(III) chloride (Scheme 4.10).¹⁶⁴ This suggests that two titanium (III) atoms are oxidised in the process. With the exception of the imine **119**, the intermediates of this reaction have not been isolated, and a detailed mechanism is unknown. The reaction solution is buffered at an acidic pH with acetate to ensure the titanium(III) does not readily undergo oxidation with oxygen and the imine product **119** formed is hydrolysed to its corresponding ketone **55**.



Scheme 4.10. De-oximation of DHEA O-(carboxymethyl)oxime **116** and its imine intermediate **119**.

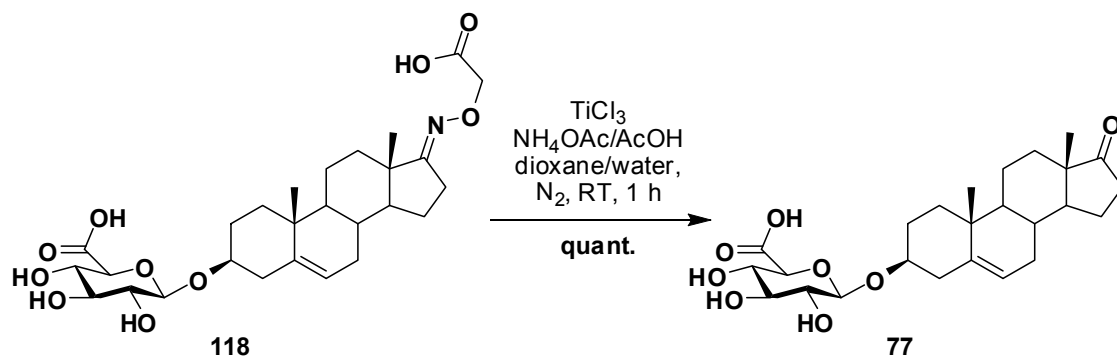
The successful de-oximation of DHEA O-(carboxymethyl)oxime **116** was achieved using titanium(III) chloride under mild conditions that avoided the use of heat or strong inorganic acids. Next it was time to attempt the de-oximation of the oxime in the presence of the glucuronyl residue.

4.4.2 De-oximation of the DHEA O-(carboxymethyl)oxime β -D-glucuronide **118**

The DHEA O-(carboxymethyl)oxime **116** was synthesised as more soluble analogue of DHEA **55** which resulted in superior yields in the glucuronylsynthase reactions. However, the DHEA O-(carboxymethyl)oxime β -D-glucuronide **118** is not a glucuronide metabolite of interest. The cleavage of the oxime functionality would restore the ketone to produce the DHEA β -D-glucuronide **77** which is a metabolite of interest. Titanium(III) chloride was shown to successfully cleave the oxime from DHEA O-(carboxymethyl)oxime

116, so the procedure was attempted in the presence of the glucuronyl residue.

The addition of a solution of titanium(III) chloride to an acetate buffered solution of the DHEA *O*-(carboxymethyl)oxime β -D-glucuronide **118** produced a violet-black solution that progressively lightened over time. After an hour, a single spot was observed on TLC that matched the retention factor of DHEA β -D-glucuronide **77**. The reaction mixture was also run against DHEA **55** and DHEA *O*-(carboxymethyl)oxime **116** standards on the TLC to assess if any glucuronide degradation had occurred. To our delight, no spots were observed for these degradation products. After purification, a quantitative yield was achieved for this de-oximation (Scheme 4.11).



Scheme 4.11. De-oximation of DHEA *O*-(carboxymethyl)oxime β -D-glucuronide **118**

Characterisation of the de-oximated product matched the spectral data for DHEA β -D-glucuronide **77**. High resolution mass spectrometry value matched the calculated value with a difference of only 0.9 ppm. The ^1H NMR spectrum (Figure 4.4) is missing the singlet which corresponded to the two methylene protons of the *O*-(carboxymethyl)oxime moiety in the 4-5 ppm region. All glucuronide protons are accounted for with the anomeric proton present as a doublet (J 7.7 Hz) at 4.45 ppm, the proton adjacent to the glucuronyl carboxylic acid present as a doublet (J 9.6 Hz) at 3.80 ppm and the remaining protons as triplets in the 3.7-3.1 ppm region. With the exception of the doublet at 5.43 ppm (J 4.2 Hz) corresponding to the alkene, the steroidal protons are difficult to assign, but integrate correctly. The ^{13}C spectrum provided good evidence of ketone regeneration with the C17 carbon shifting almost 50 ppm downfield from an oxime (177 ppm) to the ketone (226 ppm). The signals for the

Steroid solubilisation strategy

carboxylic acid and methylene carbons from the oxime moiety were absent from this spectrum.

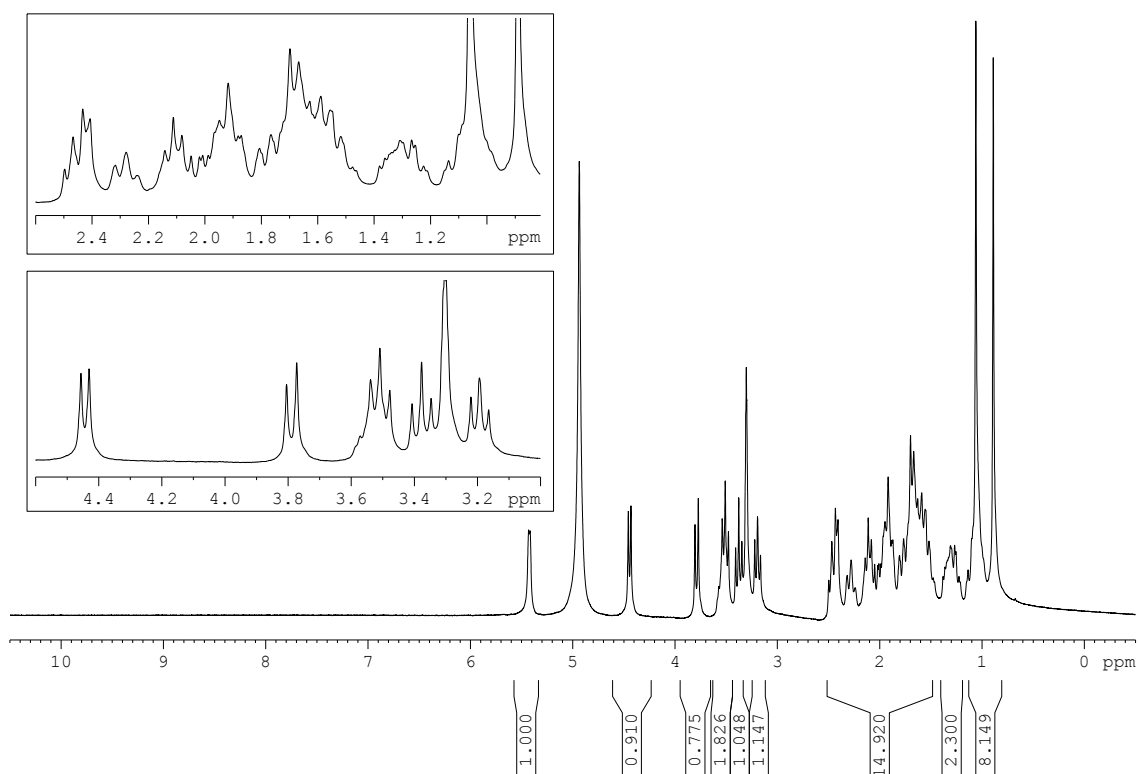
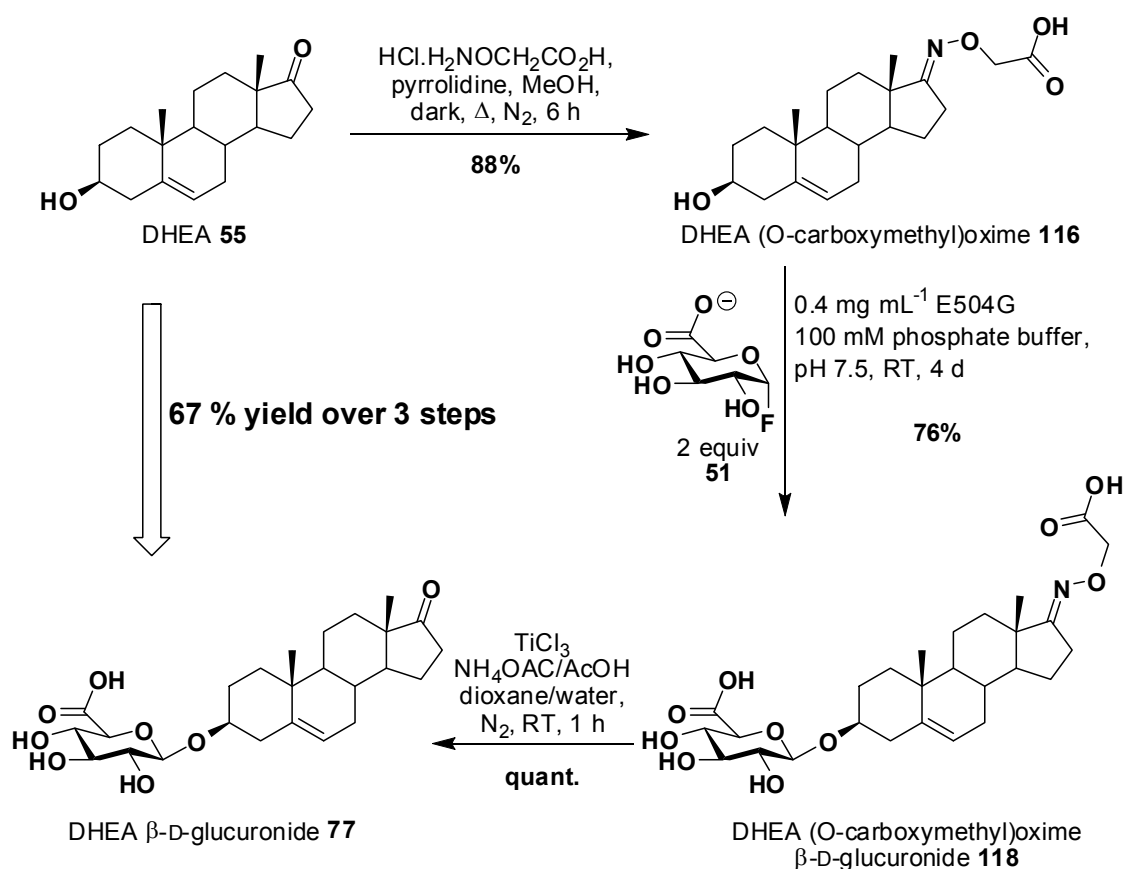


Figure 4.4. ^1H NMR spectrum (800 MHz, MeOD) for the de-oximated product: DHEA β -D-glucuronide **77** (full page spectrum attached in example spectra).

The quantitative yield for the de-oximation step provides a high yield overall for the 3 step solubility strategy (Scheme 4.12). A total yield of 67% was achieved over the three steps which provided an improvement in yield of over 2.5 times the best yield obtained from the direct glucuronysynthesis of DHEA **55**. The 3 step sequence is a vast improvement on the reported Koenigs-Knorr procedure which provides a yield of only 20% over two steps.²⁰ With the successful application to DHEA **55**, it would be of great interest to expand the strategy to other steroids with alternative functional arrangements. A good example would be testosterone **7** whose glucuronide **6** was only obtained in 12% yield from direct glucuronysynthesis. This yield is likely attributed to a combination of poor water solubility and the more sterically-hindered position of the alcohol on the C17 carbon. Of particular interest for testosterone **7** is whether the three step sequence will succeed with an unsaturated ketone. But before other steroids are studied with the three step solubility sequence, it

seems appropriate that the optimised conditions of this sequence be determined first.



Scheme 4.12. The 3 step solubility strategy for DHEA 55.

The lowest yield in the three step sequence was the glucuronylsynthase reaction. The two attempts at this reaction had only a couple of varied reaction conditions which caused a large difference in the yield obtained (35% difference). With the exception of scale, the only difference between the two reactions was the equivalents of α -D-glucuronyl fluoride **51**, the concentration of the DHEA O-(carboxymethyl)oxime **116** and the addition of DMSO to aid solubility. The HPLC assay could be used to investigate the effect that these 3 factors have on the glucuronylsynthesis of DHEA O-(carboxymethyl)oxime **116** which may improve the overall yield of the 3 step sequence.

4.5 Investigation the reaction variables of the DHEA O-(carboxymethyl)oxime glucuronylsynthase reaction.

The glucuronylsynthesis of DHEA O-(carboxymethyl)oxime **116** has been performed twice with two very different yields obtained (76% versus 41%). It was of great interest to understand what reaction variables caused such a change in yield and whether the conditions could be optimised to improve the yield further. The three factors, other than scale, that differed between the two reactions were the substrate concentration of DHEA O-(carboxymethyl)oxime **116** and α -D-glucuronyl fluoride **51** and the presence of DMSO. A study on each of these factors was performed using the HPLC kinetic assay. The kinetic parameters of DHEA O-(carboxymethyl)oxime **116** were determined first. A comparison of the kinetic parameters of DHEA O-(carboxymethyl)oxime **116** will be made against the simple acceptor alcohols tested previously in the HPLC kinetic study. Of particular interest, is the existence of substrate inhibition present in many of the other acceptor alcohols.

4.5.1 Kinetic parameters of DHEA O-(carboxymethyl)oxime 116

The kinetic parameters of DHEA O-(carboxymethyl)oxime **116** were explored by the developed HPLC assay (chapter 3.5). The calibration curve for DHEA O-(carboxymethyl)oxime β -D-glucuronide **118** was generated between 0-10 μ M using previously synthesised material. Due to the hydrophobicity of DHEA O-(carboxymethyl)oxime **116** relative to previous substrates, the concentration of acetonitrile in the HPLC mobile phase had to be increased to 30% v/v. With this altered mobile phase, the glucuronide **118** had a retention time of 5.7 min. Thirteen reactions were monitored at 21 °C with a saturating concentration of α -D-glucuronyl fluoride **51** (1 mM) and varied concentrations (0 – 1.95 mM) of DHEA O-(carboxymethyl)oxime **116**. The initial velocities of these reactions were plotted against their respective concentration of DHEA O-(carboxymethyl)oxime **116**, to develop a curve that showed substrate inhibition at high substrate concentrations (Figure 3.16).

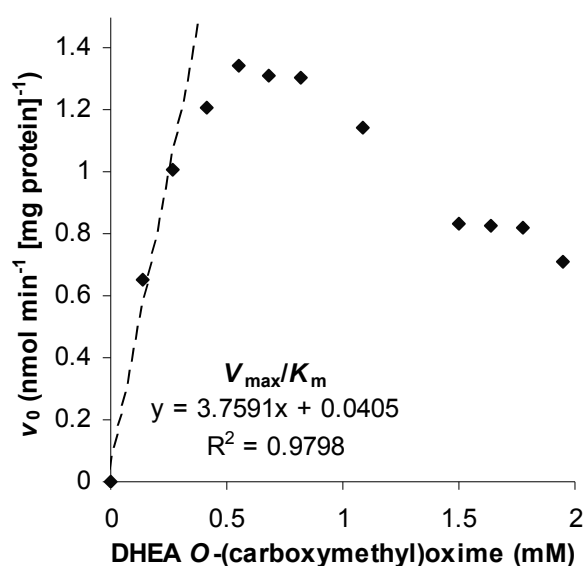


Figure 4.5. Initial velocity vs. concentration plot of varying DHEA O-(carboxymethyl)oxime 116 acceptor with constant saturating (1 mM) α -D-glucuronyl fluoride 51 donor (21 °C, 100 mM phosphate buffer, pH 7.5). Broken line represents the initial slope of the curve used for k_{cat}/K_m calculations (n = 3) with its linear regression analysis denoted as R^2 .

Fitting the data to the substrate inhibition kinetic model (refer to section 3.5.6, equation 19), a good fit ($R^2 > 0.97$) is obtained for the curve, but the errors associated with the kinetic parameters were large (100-280%). The V_{max} was extrapolated as $32 \pm 87 \text{ nmol min}^{-1} [\text{mg protein}]^{-1}$, the K_m as $7 \pm 19 \text{ mM}$ and the K_{si} was $0.1 \pm 0.1 \text{ mM}$. The V_{max} equates to a k_{cat} of 0.037 s^{-1} which is fast relative to the other aglycons studied (Table 3.2). The calculated substrate specificity (k_{cat}/K_m) of $5.3 \text{ M}^{-1} \text{ s}^{-1}$ is over three times greater than the substrate specificity calculated for 3-methoxybenzyl alcohol 47.

Due to substrate inhibition, the maximum observed velocity occurs at 0.55 mM and provides a maximum velocity of $1.3 \text{ nmol min}^{-1} [\text{mg protein}]^{-1}$ which equates to a k_{cat} of $1.4 \times 10^{-3} \text{ s}^{-1}$. Using the initial slope of the kinetic curve at very low substrate concentration, the substrate specificity constant (k_{cat}/K_m) was determined as $4.3 \text{ M}^{-1} \text{ s}^{-1}$. This observed value is only marginally lower than the calculated specificity constant and is the highest specificity constant reported for the glucuronylsynthase enzyme so far. The k_{cat} of the substrate falls in line with other aglycons studied suggesting that the higher substrate specificity arises from a lower K_m value. The larger surface area of the DHEA

Steroid solubilisation strategy

O-(carboxymethyl)oxime **116** molecule may provide more favourable interactions with the enzyme binding site which helps lower the K_m value.

The substrate inhibition may be a factor as to why the large scale DHEA O-(carboxymethyl)oxime **116** reaction of 4 mM provided a lower yield than the higher yielding 2 mM reaction. In the large scale reaction, the reaction velocity is more hindered by substrate inhibition on an account of DHEA O-(carboxymethyl)oxime **116** being more concentrated. A lower turnover means less product is formed over time. So it is likely that by doubling the concentration of DHEA O-(carboxymethyl)oxime **116**, the yield of glucuronide **118** was reduced. Next it was time to determine what effect the α -D-glucuronyl fluoride **51** concentration had on the DHEA O-(carboxymethyl)oxime **116** glucuronylsynthase reaction.

4.5.2 Equivalents of α -D-glucuronyl fluoride **51**

A second equivalent of α -D-glucuronyl fluoride **51** was added to the DHEA O-(carboxymethyl)oxime **116** glucuronylsynthase reaction that achieved a yield of 76%. To observe if this extra equivalent had any effect on the yield, a series of identical DHEA O-(carboxymethyl)oxime **116** glucuronylsynthase reactions with various equivalents of α -D-glucuronyl fluoride **51** were monitored by the HPLC assay over 40 hours at 37 °C. One equivalent of α -D-glucuronyl fluoride **51** produced a 48% yield in 40 hours which is similar to the yield (41%) achieved in the large scale reaction with only one equivalent of α -D-glucuronyl fluoride **51**. What is strange about this particular reaction profile is that after 14 hours, the reaction appeared to halt. This was observed as a plateau in product formation after 14 hours (Figure 4.6). The addition of two equivalents of α -D-glucuronyl fluoride **51** produced a yield of 77% which coincidentally matched the yield (76%) of the DHEA O-(carboxymethyl)oxime **116** glucuronylsynthase reaction where an additional equivalent was added midway through the reaction. A third, fourth and fifth equivalent of α -D-glucuronyl fluoride **51** was also monitored and we were delighted to observe near quantitative conversion (98%) of DHEA O-(carboxymethyl)oxime **116** to its glucuronide **118**. This was a drastic improvement in yield for the glucuronylsynthesis of DHEA O-(carboxymethyl)oxime **116**. This meant that

the overall yield for DHEA β -D-glucuronide **77** in the three step steroid solubility sequence (Scheme 4.12) could be upgraded from 67% to 86% over three steps.

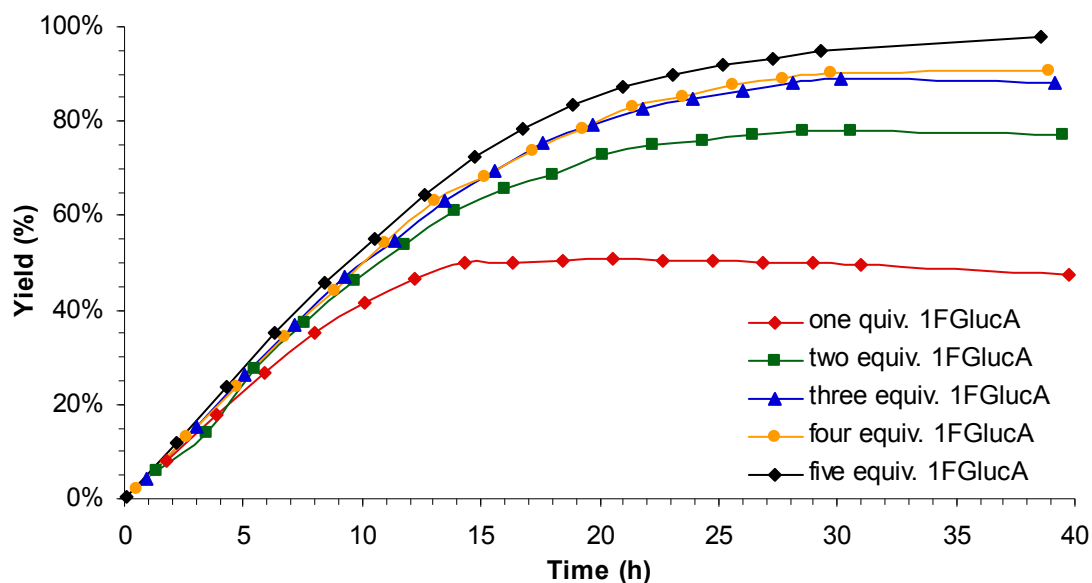


Figure 4.6. Reaction yield (%) against time for reaction of DHEA O-(carboxymethyl)oxime **116** acceptor (1.4 mM) and varying equivalents of α -D-glucuronyl fluoride **51** donor (37 °C, 100 mM phosphate buffer, pH 7.5).

Initially there were concerns of the quality of the α -D-glucuronyl fluoride **51** synthesised, despite characterisation validating purity. However, doubling the equivalents of α -D-glucuronyl fluoride **51** did not lead to a doubling of the yield. An uncertainty existed on the stability of the α -D-glucuronyl fluoride **51** in these reactions over time. During the synthesis of α -D-glucuronyl fluoride **51**, it was observed that this glycosyl fluoride was particularly sensitive to heat with discolouration observed within only a couple of hours of heating at 40 °C. It was proposed that by heating the reaction at 37 °C to improve glucuronylsynthase activity, it was at the cost of increased α -D-glucuronyl fluoride **51** degradation. The concentration of α -D-glucuronyl fluoride **51** could not be measured by the reversed phase HPLC assay, so its degradation could not be monitored.

4.5.3 Non-enzymatic hydrolysis of the α -D-glucuronyl fluoride **51**

A ^1H NMR kinetic experiment was performed to determine the extent of α -D-glucuronyl fluoride **51** degradation (Figure 4.7). The degradation of α -D-

Steroid solubilisation strategy

glucuronyl fluoride **51** involves the non-enzymatic hydrolysis to glucuronic acid **3** (analogous to Scheme 3.7a). Both anomers of glucuronic acid **3** were observed in the ^1H NMR spectrum. The anomeric proton of α -D-glucuronyl fluoride **51** was observed as a doublet of doublets over the region 5.8-5.9 ppm. The anomeric protons of the hydrolysis products, β -glucuronic acid β -**3** and α -glucuronic acid α -**3**, were observed at 5.4 ppm and 5.6 ppm respectively.

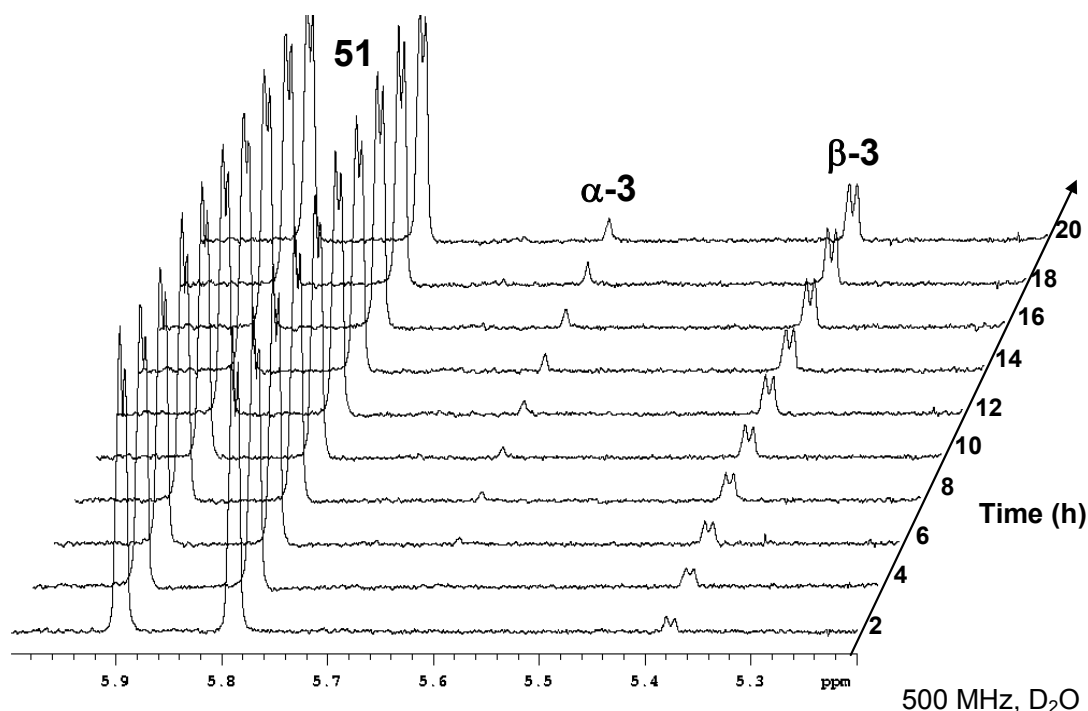


Figure 4.7. ^1H NMR analysis of α -D-glucuronyl fluoride **51** non-enzymatic hydrolysis at 37 °C in D_2O (500 MHz). Signals correspond to α -D-glucuronyl fluoride **51** (doublet of doublets), α -D-glucuronic acid α -**3** (singlet) and β -D-glucuronic acid β -**3** (doublet).

A 130 mM solution of α -D-glucuronyl fluoride **51** was made with D_2O , and scanned every hour over 21 hours at a probe temperature of 37 °C. By eye, it is difficult to observe the α -D-glucuronyl fluoride **51** peaks shrinking, but the formation of the glucuronic acid **3** anomers is evident. Plotting the peak integration over time, a linear degradation is observed at a rate of $0.6 \mu\text{mol h}^{-1}$ (Figure 4.8). The non-enzymatic hydrolysis of the glycosyl fluoride donor has been reported in other glycosynthase studies in which all state a first-order hydrolysis.^{104,166,167} Assuming the same ordered kinetics apply to α -D-glucuronyl fluoride **51**, a hydrolysis rate constant (k_{H}) of $1.3 \times 10^{-6} \text{ s}^{-1}$ is calculated. This is of equivalent magnitude to the other reported non-

enzymatic hydrolysis of glycosyl fluorides. This hydrolysis rate is 1000-fold lower than the k_{cat} of the DHEA O-(carboxymethyl)oxime **116** glucuronylsynthase reaction ($1.4 \times 10^{-3} \text{ s}^{-1}$) suggesting that something else was responsible for slowing the reaction. This suggested the operation of competitive product inhibition increasing over the course of the reaction, a phenomenon that could be overcome with increasing concentrations of α -D-glucuronyl fluoride **51** donor.

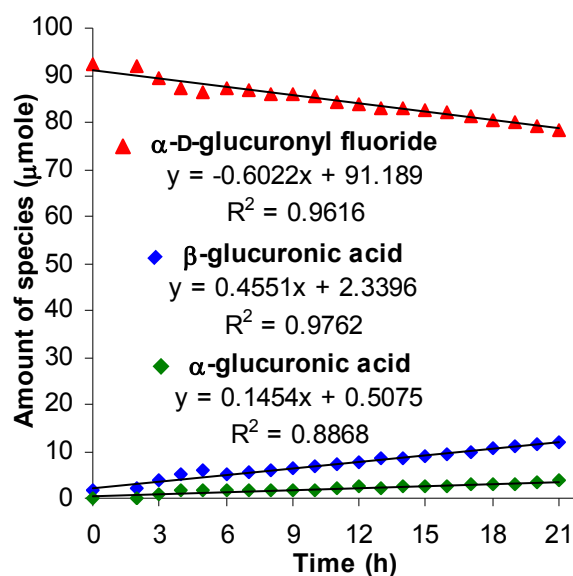


Figure 4.8. The rate of non-enzymatic hydrolysis of α -D-glucuronyl fluoride **51** (\blacktriangle) and the rate of formation of the glucuronic acid anomers (α -D-glucuronic acid **3** \blacklozenge and β -D-glucuronic acid **3** \blacklozenge) as a percentage of total components. R^2 values were calculated using linear regression analysis.

4.6 Product inhibition

Competitive product inhibition is suspected of causing incomplete conversion of DHEA O-(carboxymethyl)oxime **116** into its glucuronide **118**. This is credible considering the glucuronide products are the natural substrate of the original WT β -glucuronidase enzyme from which glucuronylsynthase was engineered. Furthermore, this inhibition appears to be overcome by the addition of excess α -D-glucuronyl fluoride **51** which signifies its competitive nature. An investigation to verify the existence of product inhibition and its magnitude in the glucuronylsynthase reactions was performed.

Steroid solubilisation strategy

4.6.1 A review of product inhibition

For a single-substrate system, there are two pure forms of inhibition that can be applied to an enzyme. The first is competitive inhibition, whereby the inhibitor will compete with the substrate for the active site of the enzyme (Figure 4.9). The formation of E.I is a dead-end complex; therefore its concentration is given by a true equilibrium constant termed the *competitive inhibitor constant* (K_{ic}). This equilibrium would be observed by an increase in the K_m , but not the limiting velocity (V_{max}), as a higher substrate concentration is seen to overcome the inhibition.

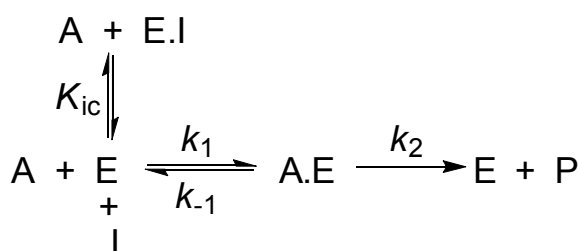


Figure 4.9. Schematic diagram of a single substrate system undergoing competitive inhibition. A = substrate, I = inhibitor and E = enzyme.

The second form of inhibition is uncompetitive inhibition, which mechanistically is the converse of competitive inhibition. The inhibitor binds to the enzyme-substrate complex only and not the free enzyme (Figure 4.10). The formation of A.E.I is the dead-end complex in this system and similarly its concentration is given by a true equilibrium constant termed the *uncompetitive inhibitor constant* (K_{iu}). This equilibrium reduces the effective concentration of the enzyme-substrate complex (E.A) which forces more substrate to combine with the enzyme through Le Chatelier's principle. This is observed as an improvement in the binding affinity of the substrate to the enzyme (reduces K_m). But with the enzyme-substrate complex locked up with the inhibitor, the turnover is reduced (lower V_{max}) regardless of how much substrate is added.

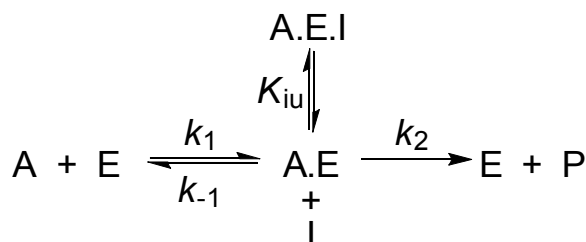


Figure 4.10. Schematic diagram of a single substrate system undergoing uncompetitive inhibition. A = substrate, I = inhibitor and E = enzyme.

Mixed inhibition is the common form of inhibition that arises from the combination of competitive and uncompetitive inhibition (Figure 4.11). The schematic diagram in Figure 4.11 can be used generally to represent the two cases of inhibition based on the size of the equilibrium constants. In competitive inhibition, $K_{iu} = \infty$, so the complex A.E.I never forms. In uncompetitive inhibition, $K_{ic} = \infty$, so the complex E.I never forms.

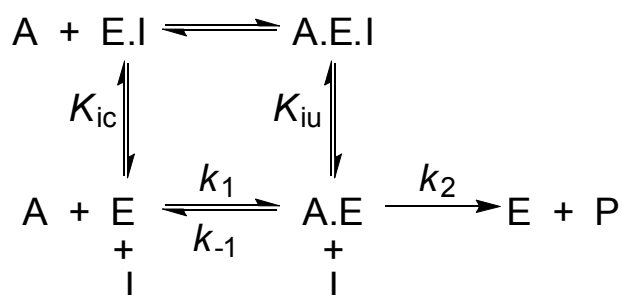


Figure 4.11. Schematic diagram of a single substrate system undergoing mixed inhibition. A = substrate, I = inhibitor and E = enzyme.

Non-competitive inhibition is a rare case of mixed inhibition whereby the inhibitor binds with equal affinity to the enzyme and enzyme-substrate complex at a different location to the active site. This would be represented in Figure 4.11 by the two inhibition constants being equal ($K_{ic} = K_{iu}$). The non-competitive inhibitor does not change how the substrate binds to the enzyme, so K_m remains unchanged. With binding affinity unchanged, there is no reason why mechanistically the substrate should not bind with the inhibitor-enzyme (E.I) complex to form A.E.I. This form of inhibition is observed as a reduction in the limiting rate (V_{max}). However, in most cases inhibition cases, $K_{ic} \neq K_{iu}$ and standard mixed inhibition is observed. This mixed inhibition model (Figure 4.11) is depicted by the single-substrate rate equation:

$$v = \frac{V_{max} a}{K_m (1 + 1/K_{ic}) + a (1 + 1/K_{iu})} \tag{20}$$

In 1953, Dixon deduced a method to determine the extent of inhibition on enzymes using inverse plots.¹⁶⁸ This was complemented by Cornish-Bowden's graphical means of determining the type and extent of enzyme inhibition in 1974 (Figure 4.12).¹⁶⁹ Curves of the inverse velocity plotted against inhibitor concentration (Dixon plot) intersect at a common place when competitive inhibition exists. The x-axis value of this intersection point represents the $-K_{ic}$

Steroid solubilisation strategy

value, the competitive inhibition constant. If a similar approach is taken to the substrate concentration over velocity (a/v) vs. inhibition concentration (i) curve, a common intersect point is observed for uncompetitive inhibition. The x-axis value of this intersection determines the uncompetitive inhibition constant (K_{iu}). In the pure forms of these inhibitions, the curves will intersect in only one of the graphs (Dixon or a/v vs. i) with parallel curves observed in the other. However, intersecting curves in both graphs (Dixon and a/v vs. i) is indicative of mixed inhibition. Non-competitive inhibition is identified by the intersection of both graphs occurring on the x-axis.

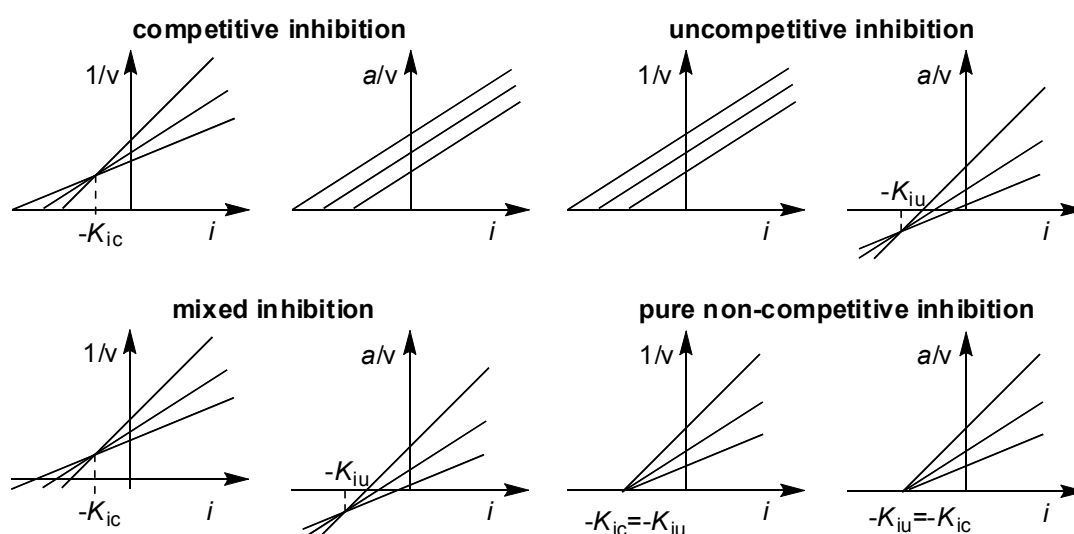


Figure 4.12. Characteristic plots for the different inhibition types and the determination of the inhibition constants K_{ic} and K_{iu} .

The use of inverse ordinate variables such $1/v_0$ used in the Dixon plot have long been known to distort the appearance of the experimental data to such a degree that the plot gives a false impression of the best-fit.¹⁷⁰ The corresponding distortion applied by using a/v_0 as an ordinate variable is much less.¹⁷¹ The uncompetitive inhibition parameter (K_{iu}) can be determined with good confidence, but the accuracy of the competitive inhibition parameter (K_{ic}) is questionable.

Recently, Cornish-Bowden deduced the relationship between inhibition parameters and the inhibitor concentration that imposes 50% inhibition ($i_{0.5}$) commonly referred to in biochemical and pharmacological applications.¹⁷² Manipulation of the Michaelis-Menten equation incorporating the inhibition

parameters (equation 20), Cornish-Bowden *et al* defined the line in a plot of a/v_0 against i as:

$$\frac{a}{v} = \frac{K_m}{V_{\max}} \left(1 + \frac{i}{K_{ic}} \right) + \frac{a}{V_{\max}} \left(1 + \frac{i}{K_{iu}} \right) \quad (21)$$

where a is substrate concentration, v is the initial reaction velocity, K_m is the Michaelis constant, V_{\max} is the limiting rate, i is the inhibitor concentration, K_{ic} is the competitive inhibition constant and K_{iu} is the uncompetitive inhibition constant.

The plot of a/v vs. inhibition concentration (i) intersects the y-axis at a/v_0 where the velocity (v) is the uninhibited velocity (v_0). Being a reciprocal, doubling the value of the y-intercept gets the value for half the uninhibited velocity ($2a/v_0 = a/0.5v_0$). Given that the $i_{0.5}$ value is defined as the concentration of inhibitor required to reduce the reaction rate by half, the inhibitor concentration (i) to achieve this $2a/v_0$ value, from the plot of a/v vs. inhibition concentration (i), is the $i_{0.5}$ concentration (Figure 4.13). Rather than attempting to solve equation 19 for the inhibitor concentration (i) that provides $2a/v_0$, the simple geometrical proof regarding two congruent triangles demonstrates that the x-intercept is equal to $-i_{0.5}$. So for every plot of a/v against i , the x-intercept is the $-i_{0.5}$ value for that specific concentration of substrate (a).

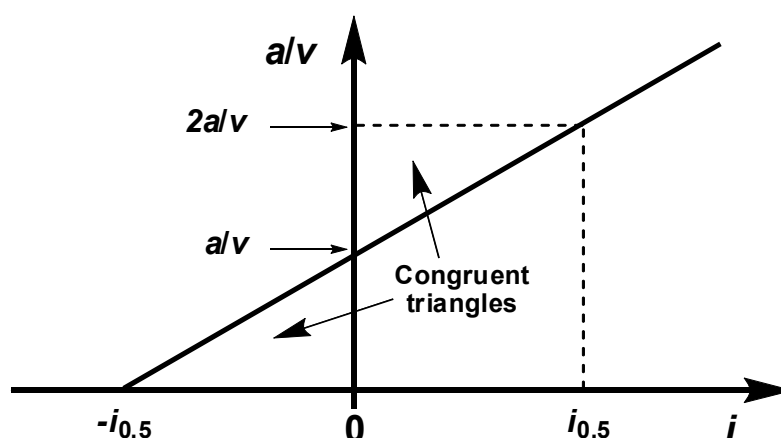


Figure 4.13. Geometrical proof for determining $i_{0.5}$ from the plot a/v vs. inhibitor concentration (i).

Cornish-Bowden *et al* also devised a relationship between $i_{0.5}$ and the normalised rate of the uninhibited reaction.¹⁷² A normalised rate is the ratio of

Steroid solubilisation strategy

the uninhibited reaction rate over the limiting reaction rate (v_0/V_{\max}). Its relationship to the $i_{0.5}$ value is defined as:

$$\frac{1}{i_{0.5}} = \frac{1}{K_{ic}} + \frac{v_0}{V_{\max}} \left(\frac{1}{K_{iu}} - \frac{1}{K_{ic}} \right) \quad (22)$$

Thus a plot of the inverse $i_{0.5}$ against the normalised rate of uninhibited reaction (v_0/V_{\max}) has a y-intercept of $1/K_{ic}$. This is reported to provide a more accurate determination of the competitive inhibition parameter than a Dixon plot. This is because it is a secondary plot derived from the plot a/v versus i whereas the Dixon plot uses the less accurate inverse ordinate variable, $1/v$. The slope of the secondary plot $1/i_{0.5}$ versus v_0/V_{\max} (equation 22) is $(1/K_{iu} - 1/K_{ic})$ which indicates that the gradient is determined by the size of each inhibition constant. As a result, the different types of inhibition can be determined by the angle of the slope (Figure 4.14). This secondary plot provides the values for all inhibition parameters and has a slope that defines the different types of inhibition. The implementation of this analysis will be presented in the inhibition studies.

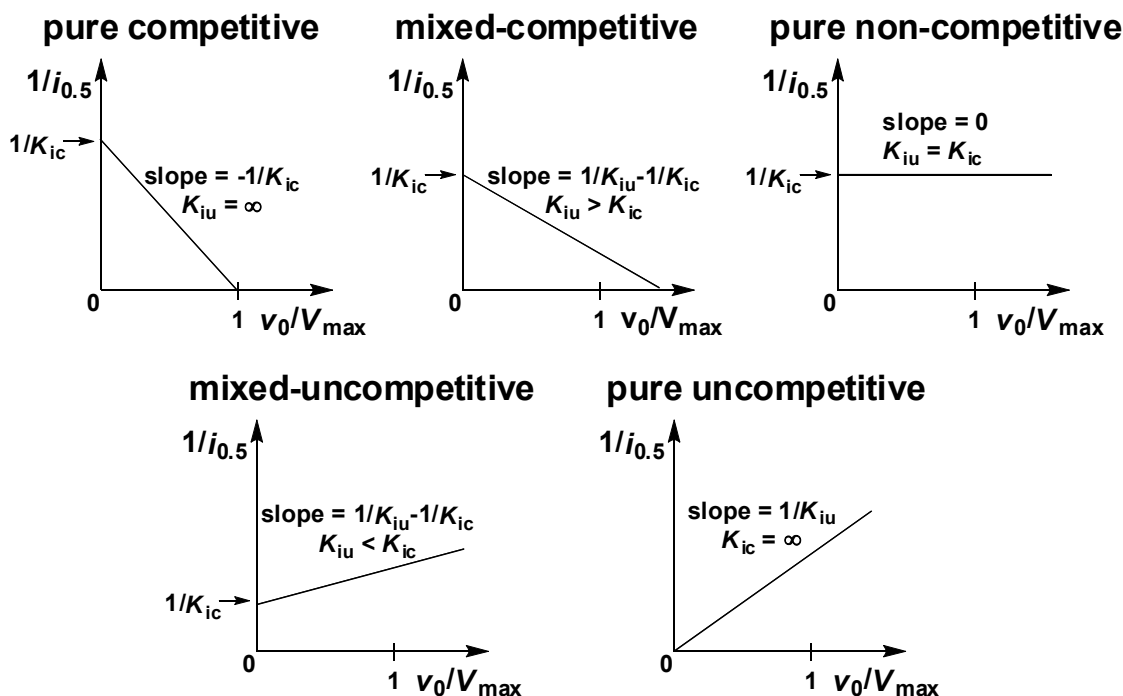


Figure 4.14. Determination of the inhibition types and the inhibition constants from the dependence of $1/i_{0.5}$ on v_0/V_{\max}

4.6.2 Determining the inhibition by DHEA O-(carboxymethyl)oxime β -D-glucuronide **118**

A study of the amount of α -D-glucuronyl fluoride **51** donor added to the DHEA O-(carboxymethyl)oxime **116** glucuronylsynthase reaction suggested product inhibition may be preventing full conversion to the glucuronide **118**. The observation that the reaction seemed to stall when the concentration of DHEA O-(carboxymethyl)oxime β -D-glucuronide **118** to α -D-glucuronyl fluoride **51** was approximately a 1:1 ratio was made. Product inhibition was suggested from the improved yields through the addition of extra equivalents of α -D-glucuronyl fluoride **51**

To investigate this product inhibition, the initial velocity of a series of glucuronylsynthase reactions in the presence of increasing concentration of DHEA O-(carboxymethyl)oxime β -D-glucuronide **118** would need to be determined. However, monitoring the effect of product inhibition on the DHEA O-(carboxymethyl)oxime **116** glucuronylsynthase reaction would provide complications as the product peak would be masked by the large quantities of the same glucuronide added as an inhibitor to each reaction. An attempt at monitoring a small change in the area of a large peak is less accurate than monitoring peaks developing from the baseline. As a result, the proposed inhibition effect of DHEA O-(carboxymethyl)oxime β -D-glucuronide **118** was tested against the 2-phenylethanol **45** glucuronylsynthase reaction. The glucuronylsynthesis of 2-phenylethanol **45** is free from substrate inhibition and was the fastest glucuronylsynthase reaction to monitor meaning a small effect on reaction velocity should be easier and more accurately detected. Furthermore, the retention time of the DHEA O-(carboxymethyl)oxime β -D-glucuronide **118** does not co-elute with the 2-phenylethyl β -D-glucuronide **68** peak which was monitored to determine initial reaction velocity.

Three series of 2-phenylethanol **45** glucuronylsynthase reactions were studied with 2-phenylethanol **45** at a fixed and sub-saturating concentration of 88 mM and the α -D-glucuronyl fluoride **51** donor at concentrations near its K_m^{app} (5 μ M, 10 μ M and 20 μ M). For each concentration of α -D-glucuronyl fluoride **51** used, six glucuronylsynthase reactions were performed in the

Steroid solubilisation strategy

presence of DHEA *O*-(carboxymethyl)oxime β -D-glucuronide **118** (0 – 101 μ M). A plot of the initial velocity of the 2-phenylethanol **45** glucuronylsynthase reaction against DHEA *O*-(carboxymethyl)oxime β -D-glucuronide **118** concentration depicts a decrease in velocity as the glucuronide concentration is increased for all concentrations of α -D-glucuronyl fluoride **51** (Figure 4.15). The reduction in initial velocity as a result of DHEA *O*-(carboxymethyl)oxime β -D-glucuronide **118** concentration already suggested inhibition was taking place.

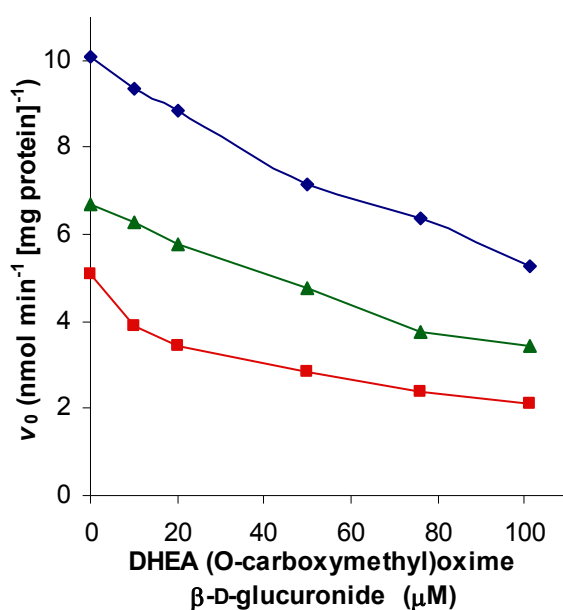


Figure 4.15. Inhibitory effect of different DHEA *O*-(carboxymethyl)-oxime β -D-glucuronide **118** concentrations (0-101 μ M) on the initial rate (v_0) of the glucuronylsynthase reaction involving sub-saturating 2-phenylethanol **45** (88 mM) and α -D-glucuronyl fluoride **51** (5 μ M ■, 10 μ M ▲, and 20 μ M ◆) at 21 °C in 100 mM phosphate buffer, pH 7.5

Estimations of the inhibition parameters were calculated from Dixon and a/v vs. i plots (Figure 4.16). The Dixon plot (Figure 4.16a) depicts the three series of 2-phenylethanol **45** reactions as linear plots ($R^2 > 0.97$) that all intersect above the x-axis at approximately 73 μ M. This denoted either competitive or mixed inhibition with a competitive inhibition parameter (K_{ic}) of 73 ± 6 μ M. The a/v versus i plot (Figure 4.16b) of the three series of 2-phenylethanol **45** reactions also shows a linear relationship ($R^2 > 0.97$) with a common point of intersect below 190 μ M. This common intersect provides an uncompetitive

inhibition parameter (K_{iu}) of $190 \pm 2 \mu\text{M}$. Intersecting curves on both plots denotes mixed predominately competitive inhibition.

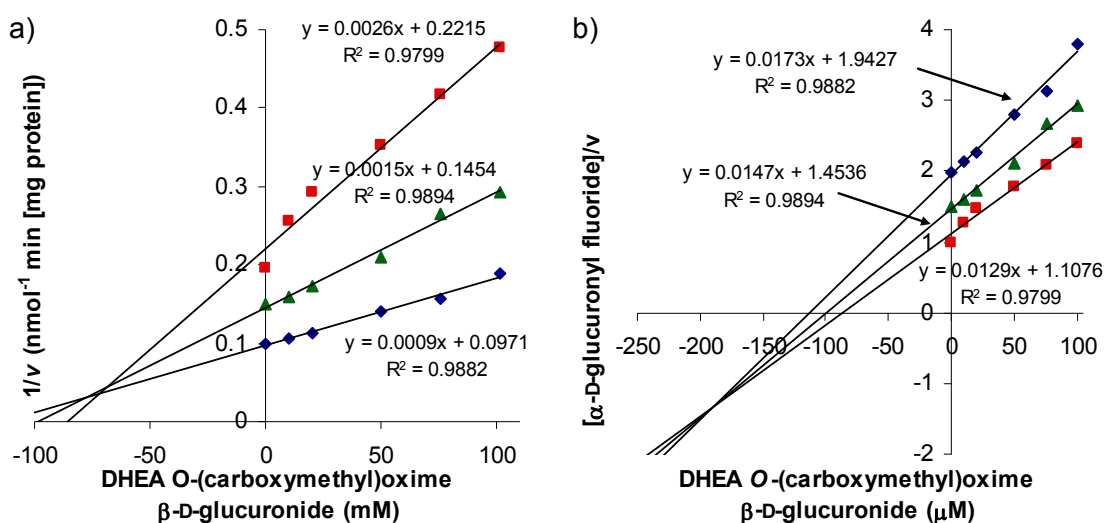


Figure 4.16. a) Dixon plot of $1/v$ against the concentration of DHEA O-(carboxymethyl)oxime β -D-glucuronide 118; and b) the plot of α -D-glucuronyl fluoride 51 concentration over initial velocity ($[\alpha\text{-D-glucuronyl fluoride 51}]/v$) against the concentration of DHEA O-(carboxymethyl)oxime β -D-glucuronide 118. The glucuronylsynthase reaction involved sub-saturating 2-phenylethanol 45 (88 mM) and α -D-glucuronyl fluoride 51 (5 μM ■, 10 μM ▲, and 20 μM ◆) at 21 °C in 100 mM phosphate buffer, pH 7.5. R^2 values were calculated using linear regression analysis.

To provide a more accurate determination of the inhibition parameters, the $i_{0.5}$ concentrations were determined from the x-axis intercepts of the a/v versus i plot (Figure 4.16b) and plotted against the normalised velocity (v_0/V_{max}) of their uninhibited reaction (Figure 4.17). The plot has a negative slope that crosses the x-axis at a point greater than one which signifies mixed predominately competitive inhibition. The competitive inhibition parameter (K_{ic}) was determined from the inverse of the y-intercept which equated to 71 μM . This value corresponds well with the K_{ic} value of 73 μM determined from the Dixon plot (Figure 4.16a). The K_{ic} value was substituted into the equation $(1/K_{iu} - 1/K_{ic})$ that defines the slope of the curve to solve for K_{iu} .¹⁷² K_{iu} was determined to be 180 μM which again agrees well with the value (190 μM) determined from the a/v versus i plot (Figure 4.16b).

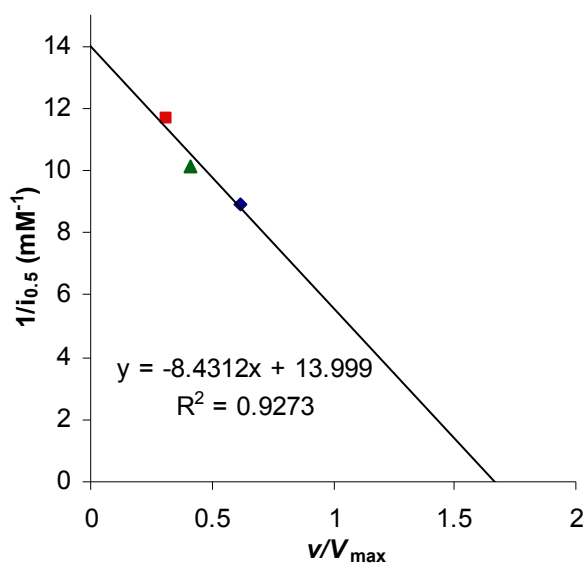


Figure 4.17. The plot of $1/i_{0.5}$ vs. v/V_{\max} exhibiting mixed (predominantly competitive) inhibition by DHEA O-(carboxymethyl)oxime β -D-glucuronide **118** in the glucuronylsynthase reaction involving sub-saturating 2-phenylethanol **45** (88 mM) and α -D-glucuronyl fluoride **51** (5 μM ■, 10 μM ▲, and 20 μM ◆) at 21 °C in 100 mM phosphate buffer, pH 7.5. R^2 was calculated using linear regression analysis.

The observation of DHEA O-(carboxymethyl)oxime β -D-glucuronide **118** inhibition in the 2-phenylethanol **45** glucuronylsynthase reaction strongly suggests that product inhibition is occurring in DHEA O-(carboxymethyl)oxime **116** glucuronylsynthase reaction. DHEA O-(carboxymethyl)oxime β -D-glucuronide **118** exerts mixed inhibition to the glucuronylsynthase enzyme that is predominately through competitive inhibition. The competitive inhibition parameter was determined as 73 μM with the use of a Dixon plot and 71 μM using the secondary plot of $1/i_{0.5}$ versus v/V_{\max} . This is a moderately strong inhibition value that suggested that the binding affinity of the DHEA O-(carboxymethyl)oxime β -D-glucuronide **118** is much stronger than the binding affinity of DHEA O-(carboxymethyl)oxime **116** which was estimated in the millimolar range (refer to section 4.5.1). Fortunately, the α -D-glucuronyl fluoride **51** K_m^{app} 0.15 μM is significantly lower which means a considerable amount of conversion can be achieved before the competitive product inhibition becomes a problem. By keeping the concentration of α -D-glucuronyl fluoride **51** high, by the addition of extra equivalents, the concentration does not approach K_m^{app} thus overcoming the effects of product inhibition. A

significant amount of uncompetitive inhibition was also discovered and determined to be 190 μM from the a/v versus i plot and 180 μM using the secondary plot of $1/i_{0.5}$ versus v/V_{max} . The combination of the two inhibition types was able to stop the glucuronylsynthase reaction of DHEA O-(carboxymethyl)oxime **116** at approximately 50% conversion in the presence of one equivalent of α -D-glucuronyl fluoride **51**. The glucuronylsynthesis of 2-phenylethanol **45** achieves 96% conversion with 1.2 equivalents of α -D-glucuronyl fluoride **51**. We were interested if product inhibition existed for this glucuronylsynthase reaction.

4.6.3 Determining the inhibition by 2-phenylethyl β -D-glucuronide **68**

Product inhibition of the DHEA O-(carboxymethyl)oxime **116** glucuronylsynthase reaction is responsible for incomplete conversion to the glucuronide **118**. The hypothesis that glucuronide yield might be directly proportional to the strength of product inhibition was proposed. The glucuronylsynthase reaction of 2-phenylethanol **45** achieves near quantitative yields with only one equivalent of α -D-glucuronyl fluoride **51**. We were interested in whether product inhibition was present in this reaction, and if so, to what degree.

The assay to measure the inhibition of 2-phenylethyl β -D-glucuronide **68** was conducted for the DHEA O-(carboxymethyl)oxime **116** glucuronylsynthase reaction. The DHEA O-(carboxymethyl)oxime β -D-glucuronide **118** produced in the reaction would not co-elute with the 2-phenylethyl β -D-glucuronide **68** added to the reaction mix. Initially, a reaction of DHEA O-(carboxymethyl)oxime **116** (0.6 mM; the concentration at the maximum observed velocity) with α -D-glucuronyl fluoride **51** (20 μM) was monitored with 5 concentrations of 2-phenylethyl β -D-glucuronide **68** in the micromolar range (0-100 μM). However, it appeared that the initial velocity did not reduce with an increase of 2-phenylethyl β -D-glucuronide **68** concentration (Figure 4.18). So the investigation was repeated with the same DHEA O-(carboxymethyl)oxime **116** reactions but with 2-phenylethyl β -D-glucuronide **68** concentrations in the millimolar range (0-100 mM). Once again, a decrease in initial velocity was not observed with increasing 2-phenylethyl β -D-glucuronide

Steroid solubilisation strategy

68 (Figure 4.18). With no observed inhibition in these glucuronylsynthase reactions, it was deemed meaningless to assay the inhibition at alternative α -D-glucuronyl fluoride **51** concentrations.

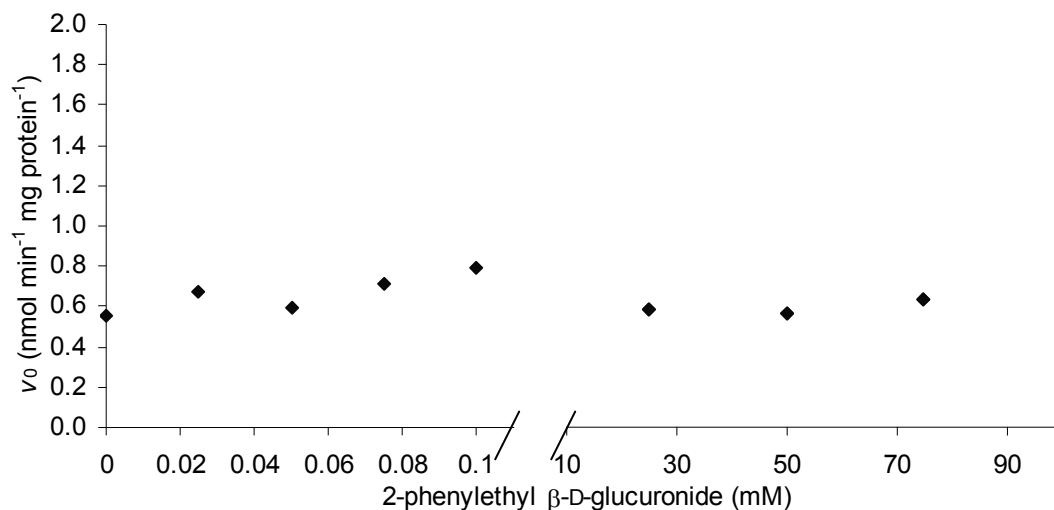


Figure 4.18. Effect of 2-phenylethyl β -D-glucuronide **68** (0-100 mM) on the initial rate (v_0) of the glucuronylsynthase reaction involving DHEA *O*-(carboxymethyl)oxime **116** (0.6 mM) and α -D-glucuronyl fluoride **51** (20 μ M) at 21 $^{\circ}$ C in 100 mM phosphate buffer, pH 7.5.

An average velocity of 0.6 ± 0.2 nmol min⁻¹ [mg protein]⁻¹ was observed for all concentrations of 2-phenylethyl β -D-glucuronide **68** up to 100 mM. It appeared that inhibition is either non-existent or too small to be detected by the assay. This is consistent with the findings from the ITC study (refer to section 3.4.3). In the ITC study, the 2-phenylethyl β -D-glucuronide **68** was also found to bind very weakly to the enzyme.

The β -D-glucuronidase is a promiscuous enzyme that binds with a range of glucuronides in the micromolar, if not low millimolar range. It can be assumed that with only a single amino acid change, an equivalent affinity to a range of glucuronides may be observed for the glucuronylsynthase. The underlying reason why 2-phenylethyl β -D-glucuronide **68** does not bind well and inhibit the glucuronylsynthase is a mystery. Kinetic studies using the wild-type β -glucuronidase could be used to determine the kinetic parameters, but due to the absence of a visible chromophore, the assay would not be simple to perform. Perhaps when a crystal structure is obtained of the *E. coli* β -D-

glucuronidase, or better yet, of the glucuronylsynthase, a structure-activity relationship can be devised.

The absence of both product and substrate inhibition in the 2-phenylethanol **45** glucuronylsynthase reaction may suggest why near quantitative yields can be achieved with only one equivalent of α -D-glucuronyl fluoride **51**. In contrast, the glucuronylsynthesis of DHEA O-(carboxymethyl)oxime **116**, where its glucuronide product **118** imposes strong inhibitory binding, only achieves ~50% yield with one equivalent of α -D-glucuronyl fluoride **51**. It would be of considerable interest to determine if product inhibition exists in some of the other glucuronylsynthase reactions performed to date. Further to this, if product inhibition is proven in these cases, what is the extent of the inhibition in these reactions? And finally, is there a relationship between the strength of product inhibition and the yields obtained in these glucuronylsynthase reactions with one equivalent of α -D-glucuronyl fluoride **51**?

The discovery of mixed, predominately competitive product inhibition and the ability to overcome it with additional equivalents of α -D-glucuronyl fluoride **51** has been a defining moment in the optimisation of the DHEA O-(carboxymethyl)oxime **116** glucuronylsynthase reaction. It has boosted the yield of the three step steroid solubilisation strategy by an additional 20%. It was of great interest to see if the success of this 3-step solubility strategy could be extended to other classes of steroidal substrates such as testosterone **7**.

4.7 Solubility strategy with testosterone

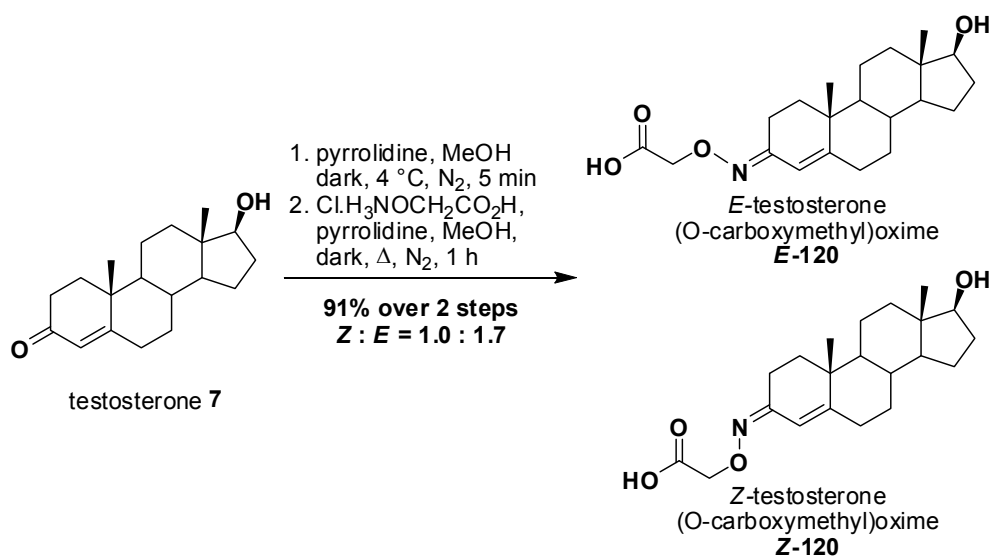
Testosterone **7** is a 17β -hydroxy steroid which suffers from poor solubility and low yields (12%) in the direct glucuronylsynthase reaction. It was hoped to overcome the issue of poor solubility and low yield by subjecting testosterone **7** to the three step steroid solubilisation strategy. Unlike DHEA **55**, testosterone **7** has an unsaturated ketone that is present in a range of steroids such as boldenone and gestrinone. It was of particular interest to see if the steroid solubilisation strategy would work with unsaturated ketones.

Steroid solubilisation strategy

4.7.1 Oximation of testosterone 7

The first step of the steroid solubility sequence was to attach the ionisable functional group onto testosterone **7**. The oximation of testosterone **7** with carboxymethoxylamine **115** was performed according to the procedure of Philomin.¹⁴⁷ Activation of the unsaturated ketone with pyrrolidine was rapid with the yellow testosterone pyrrolidinium species formed within 5 minutes as reported in literature. Refluxing this intermediate with carboxymethoxylamine hemihydrochloride **115** for an hour produced testosterone *O*-(carboxymethyl)oxime **120** in 91% yield and as a mixture (1.0 : 1.7) of *Z* and *E* isomers (Scheme 4.13). The ratio of isomers varied with each attempt at the synthesis with another attempt providing a yield of 65% and a *Z* : *E* ratio of 1.0 : 4.9. The major product (*E*-isomer) in each synthesis attempt was always the same isomer.

The 17-ketone of DHEA **55** required an hour to form the pyrrolidinium intermediate **117**, then over 6 hours to form the *O*-(carboxymethyl)oxime **116**. The reaction with testosterone **7** was much more rapid with a reaction time of only 5 min for the pyrrolidinium formation and only an hour for the *O*-(carboxymethyl)oxime **120** conversion. The discrepancy in reaction rates is likely due to steric factors with the ketone of DHEA **55** being adjacent to a quaternary carbon.



Scheme 4.13. Oximation of testosterone **7** with carboxymethoxylamine **115**.

Two distinct isomers were observed in the ¹H NMR spectrum (Figure 4.19). The NMR data for the reaction yielding a *Z* : *E* ratio of 1.0 : 4.9 was used in the

NMR analysis so that peaks could be easily assigned to each isomer based on signal intensity. There were two signals for the oxymethylene protons of the *O*-(carboxymethyl)oxime moiety as a result of the two isomers. The major isomer appears as a singlet at 4.54 ppm and the minor isomer at 4.51 ppm. The olefinic proton of the testosterone *O*-(carboxymethyl)oxime **120** isomers is present at 6.45 ppm for the minor isomer and 5.74 ppm for the major isomer.

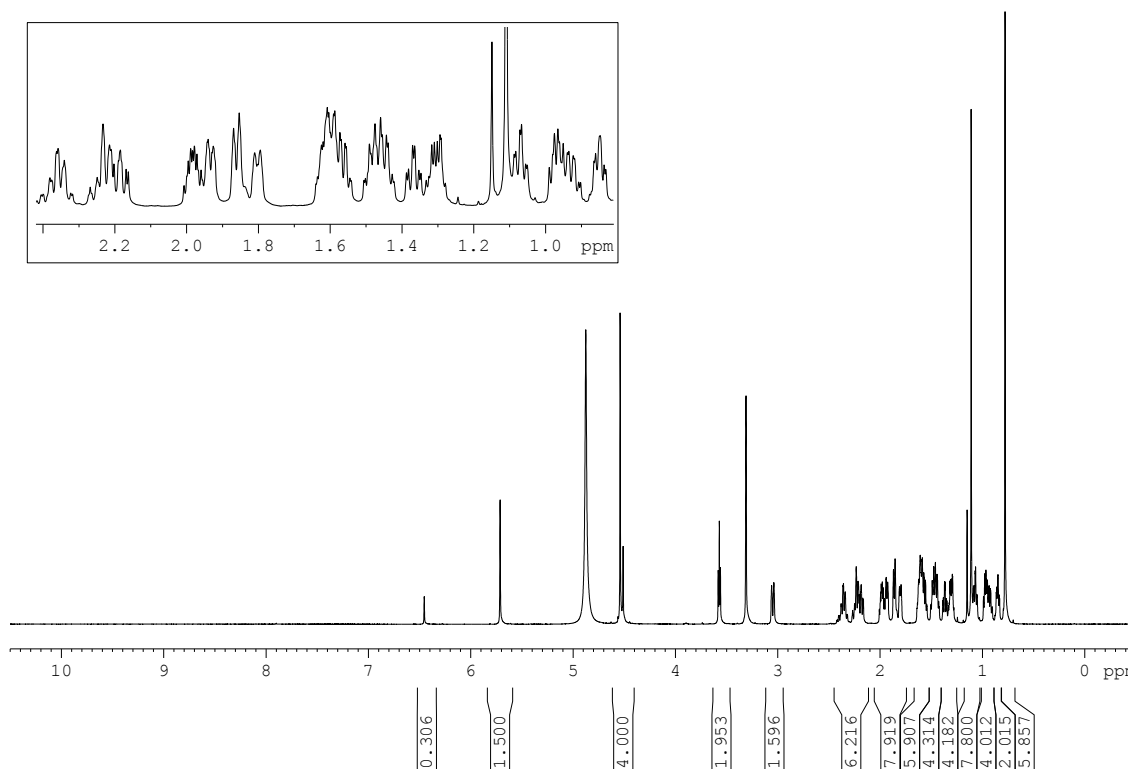


Figure 4.19. ¹H NMR (800 MHz, MeOD) of the diastereomeric mixture of testosterone *O*-(carboxymethyl)oxime **120** (full page spectrum attached in example spectra)

Differentiation of the isomers could not be determined by NOESY experimentation. The numerous studies on unsaturated oximes and testosterone oximes all report that the olefinic proton shifts downfield in the ¹H NMR spectrum for the *Z* isomer relative to the *E* isomer.¹⁷³⁻¹⁷⁶ Assuming this is true for our system, the olefinic proton for the minor product appears furthest downfield suggesting that the *E* oxime was the major product. This oxime group would be removed in the final step, so the stereochemistry of the testosterone *O*-(carboxymethyl)oxime **120** would have made no difference to the final product. The only exception may be if the glucuronylsynthase enzyme was selective for one isomer over the other.

Steroid solubilisation strategy

The ^{13}C NMR spectrum (attached example spectra) contained 41 environments as a result of the two isomers, with only a single carbon peak overlapping or obstructed. Fortunately, the 1 : 5 ratio of the sample analysed allowed the individual peaks to be assigned to their respective isomer based on peak intensity. The introduction of the *O*-(carboxymethyl)oxime moiety was verified by the addition of a carboxylic acid (174.07 and 173.99 ppm) and an oxymethylene (71.0 and 70.8 ppm) carbon resonance in the spectrum. In addition, the C3 carbon of testosterone shifted upfield from 200 ppm as an unsaturated ketone **7** to 157 ppm as an unsaturated oxime.

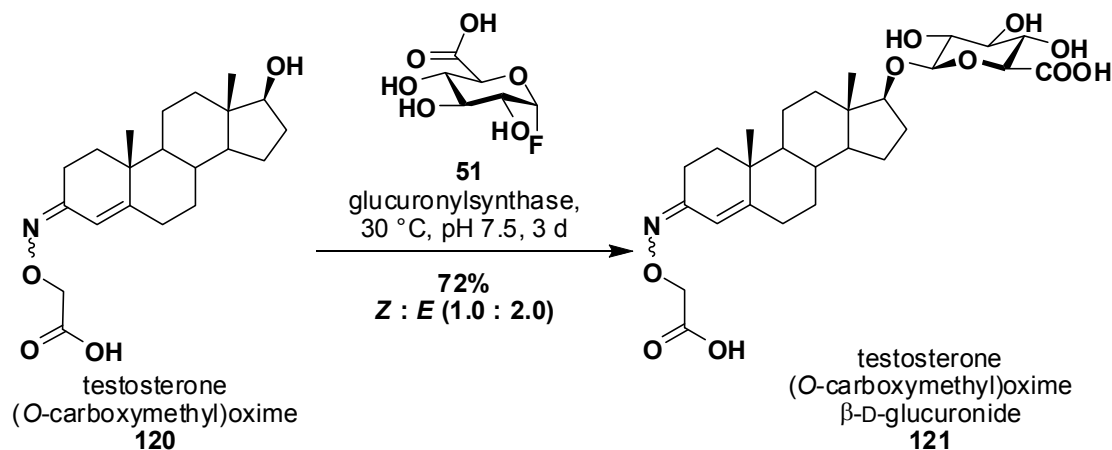
The melting point and optical rotation agreed with the literature.¹⁷⁷ But these values would be dependent on the ratio of isomers present and this was not specified in previous work. The high resolution mass spectroscopy ESI value matched the exact mass of the testosterone *O*-(carboxymethyl)oxime **120** anion.

The solubility of the testosterone *O*-(carboxymethyl)oxime **120** was tested against the solubility of testosterone **7** in 100 mM phosphate buffer at pH 7.5. Testosterone **7** appeared to dissolve at a concentration of 0.02 mM. The testosterone *O*-(carboxymethyl)oxime **120** was completely dissolved at a concentration of 10 mM which is a 500-fold increase in solubility. In contrast, only a 5 mM concentration of testosterone **7** was achieved when 2% DDM is used to aid solubility. This concentration was doubled without the need of additives through the use of the ionisable oxime group. Next it was time to see what this enhanced solubility had on the glucuronysynthesis of testosterone **7**.

4.7.2 Testosterone *O*-(carboxymethyl)oxime **120 glucuronysynthase reaction**

With testosterone *O*-(carboxymethyl)oxime **120** in hand, the testosterone **7** analogue was subjected to glucuronysynthesis using optimised conditions developed for the DHEA *O*-(carboxymethyl)oxime **116**. Testosterone *O*-(carboxymethyl)oxime **120** (10 mM) was reacted with three equivalents of α -D-glucuronyl fluoride **51** and glucuronysynthase (0.2 mg mL⁻¹, Scheme 4.14). After four days at 30 °C, the testosterone *O*-(carboxymethyl)oxime β -D-glucuronide **121** was isolated in a yield of 72% as a mixture of isomers. This yield is six times the yield obtained from the direct glucuronysynthesis of

testosterone **7** (12% yield). In addition to this, 23% of unreacted testosterone *O*-(carboxymethyl)oxime **120** was recovered from the column making the total yield 94% based on recovered starting materials.



**Scheme 4.14. Glucuronylsynthase reaction on testosterone
O-(carboxymethyl)oxime **120****

There is no previously reported synthesis or spectral data for testosterone *O*-(carboxymethyl)oxime β -D-glucuronide **121**. The high resolution mass spectrum exhibited a molecular anion consistent with the desired molecular formula $C_{27}H_{38}NO_{10}$. The infrared spectrum of the glucuronide **121** showed a broad absorption at 3370 cm^{-1} that corresponds to the alcohols of the installed glucuronyl residue. An absorption at 1732 and 1630 cm^{-1} denotes the existence of carboxylic acid carbonyls and oxime carbons ($C=N$) respectively.

The ^1H NMR spectrum (Figure 4.20) depicts the existence of two glucuronide isomers resulting from the diastereomeric mixture of oximes. The olefinic protons of the two isomers occur at 6.45 ppm (minor) and 5.71 ppm (major). The *E* isomer is once again the major isomer formed in a diastereomeric ratio 2.0 : 1.0. This ratio arises from the testosterone *O*-(carboxymethyl)oxime **120** *E* : *Z* ratio of 1.7 : 1.0. It appears the glucuronylsynthase had no strong selectivity of one isomer over the other. The *O*-(carboxymethyl)oxime segment is also present as two singlets as a result of the two isomers. The oxymethylene protons of this group appear at 4.54 ppm (major) and 4.52 ppm (minor).

The protons of the installed glucuronide residue are present in the spectrum and integrate perfectly. The spatial distance between the glucuronide and site

Steroid solubilisation strategy

of isomerisation is large enough that the glucuronyl environments are accidentally equivalent for the two isomeric species. The anomeric proton exists as a doublet at 4.38 ppm (J 7.2 Hz) whilst the remaining pyranose resonances appear in the 3-4 ppm region along with the steroidal H17 proton. The large coupling constant of the anomeric proton denotes axial-axial coupling with the adjacent proton which implies a β -glycosidic bond has formed between the testosterone alcohol and the glucuronide residue.

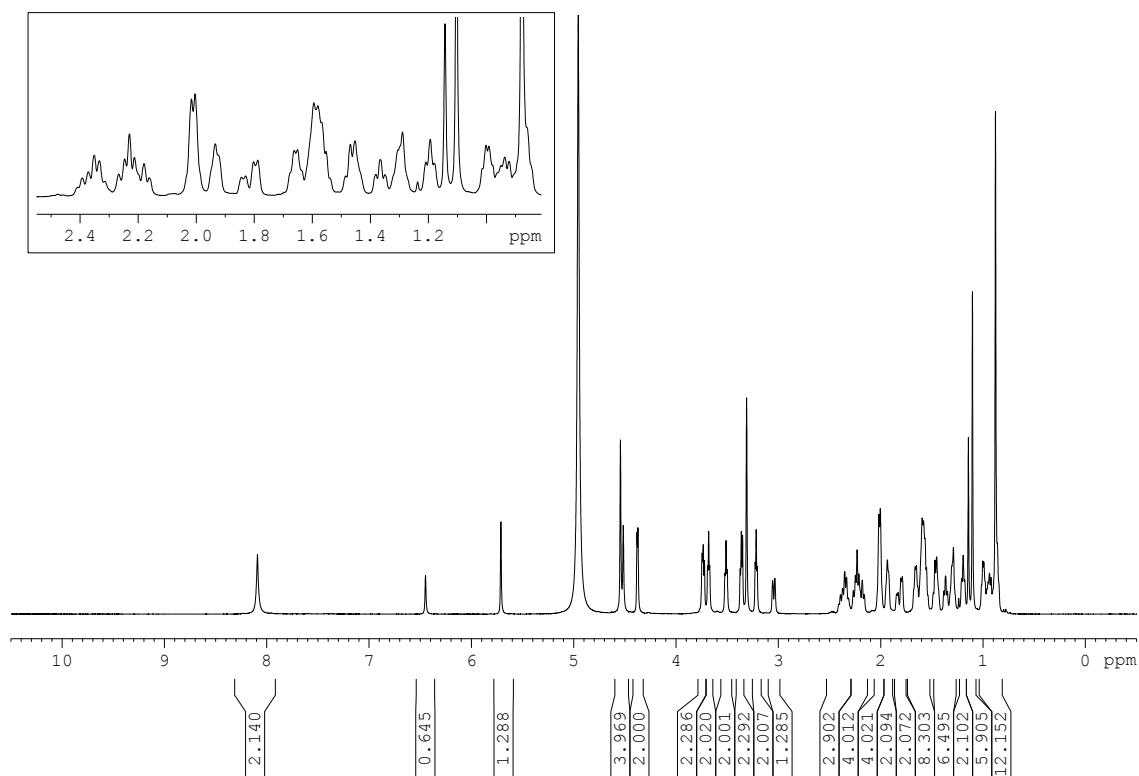


Figure 4.20. ^1H NMR (800 MHz, MeOD) of the diastereomeric mixture of testosterone *O*-(carboxymethyl)oxime β -D-glucuronide **121**.

The ^{13}C NMR spectrum was complex due to the existence of the two isomers but verified the introduction of the glucuronyl residue. A total of 46 environments were present in the spectrum with 8 carbons overlapping including the six glucuronyl carbons. The glucuronyl resonances occur at 172.7 ppm (carboxylic carbonyl), 105.1 ppm (anomeric) and 77.5, 76.6, 75.0 and 73.2 ppm for the remaining carbons of the pyranose ring. The 2 : 1 ratio of isomers allowed the carbon resonances to be assigned to their respective isomers based on their intensity.

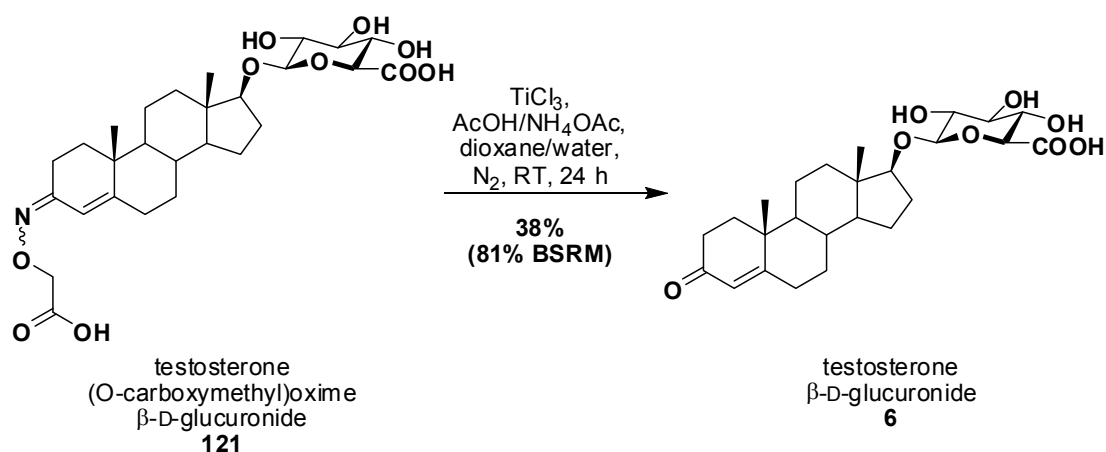
Attempts at recrystallising the testosterone *O*-(carboxymethyl)oxime β -D-glucuronide **121** were unsuccessful. With limited time left for research, focus

was made towards the de-oximation of testosterone *O*-(carboxymethyl)oxime β -D-glucuronide **121**.

4.7.3 De-oximation

Testosterone **7** was oximated in high yields then subjected to glucuronylsynthesis in good yield to synthesise the testosterone *O*-(carboxymethyl)oxime β -D-glucuronide **121**. The final step of the steroid solubilisation strategy would be to remove the oxime to yield testosterone β -D-glucuronide **6**.

Testosterone *O*-(carboxymethyl)oxime β -D-glucuronide **121** was subjected to the mild titanium(III) chloride conditions used on the DHEA *O*-(carboxymethyl)oxime β -D-glucuronide **118** (Scheme 4.15). The de-oximation took longer than the hour taken to de-oximate the DHEA derivative **118** possibly due to the extended conjugation present in testosterone *O*-(carboxymethyl)oxime β -D-glucuronide **121**. After 24 hours, the initial violet colour of the reaction had lightened to a greyish-blue and the reaction was worked-up. Unreacted testosterone *O*-(carboxymethyl)oxime β -D-glucuronide **121** was recovered in 53% yield with testosterone β -D-glucuronide **6** isolated in 38% yield (81% brsm).



Scheme 4.15. De-oximation of testosterone *O*-(carboxymethyl)oxime β -D-glucuronide **121**.

The high resolution mass spectrum of testosterone β -D-glucuronide **6** exhibited the molecular anion (m/z 463.2329) consistent with the desired molecular formula $\text{C}_{25}\text{H}_{35}\text{O}_8$. The IR depicts a broad absorbance at 3416 cm^{-1} confirming the presence of the hydroxyl groups from the glucuronyl moiety.

Steroid solubilisation strategy

The absorbance at 1666 cm^{-1} substantiates the reformation of the unsaturated ketone in the testosterone **7** moiety.

The ^1H NMR spectrum (Figure 4.21) confirms the oxime removal by the absence of the oxymethylene protons at 4.5 ppm and the formation of a single isomer once again. The olefinic proton is represented by a singlet at 5.71 ppm which provides evidence that testosterone β -D-glucuronide **6** was not over-reduced to a saturated ketone. Aqueous titanium(III) has been reported to reduce enediacarbonyl compounds to their saturated dicarbonyl form (Scheme 4.16).¹⁷⁸ But the spectral data confirms that only the unsaturated ketone is generated in this reaction.

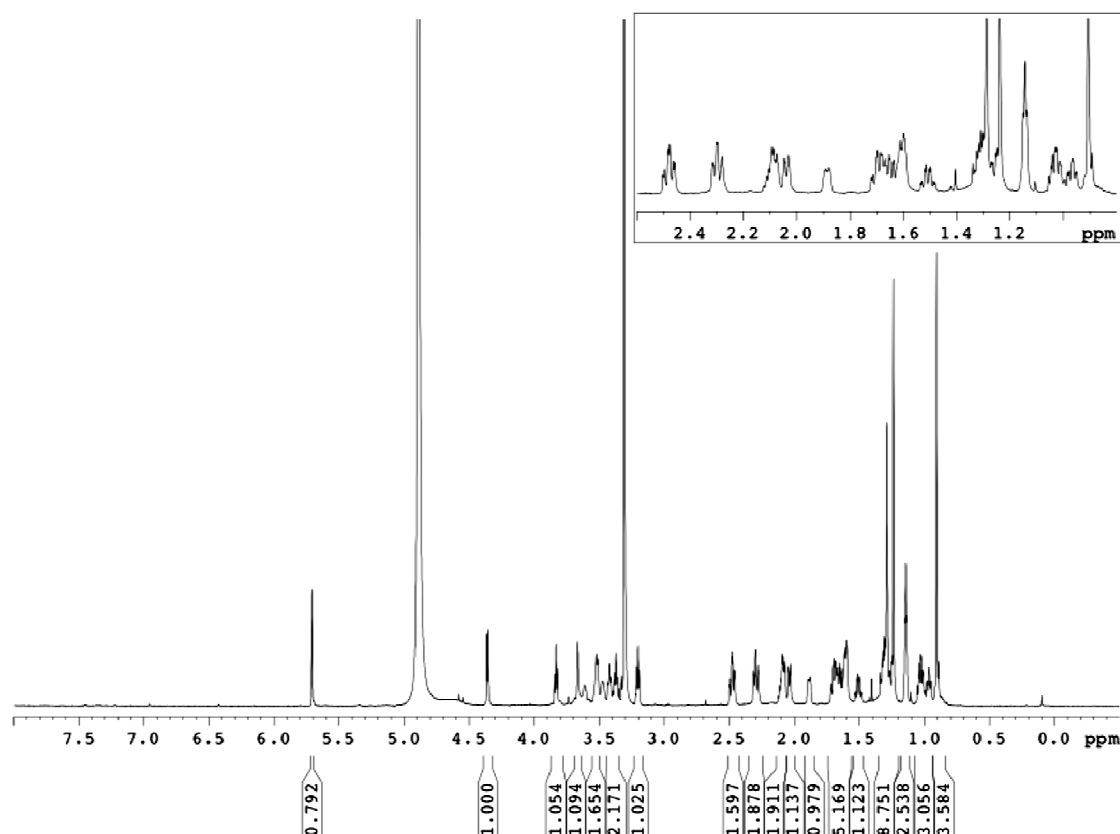
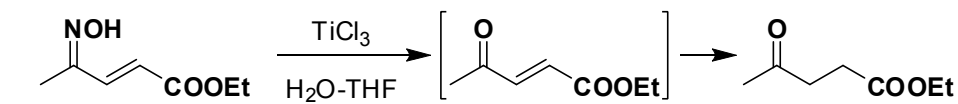


Figure 4.21. ^1H NMR (800 MHz, MeOD) of testosterone β -D-glucuronide **6**.

The glucuronyl moiety is also present with the anomeric proton appearing as a doublet at 4.36 ppm (J 7.8 Hz), the proton alpha to the carboxylic acid appearing at 3.52 ppm (J 8.7 Hz) and the remaining 3 pyranose protons appearing as triplets in the 3.5 - 3.2 ppm region. Once again, the large coupling constant of the anomeric proton is indicative of a β -glycosidic linkage of the glucuronyl residue.



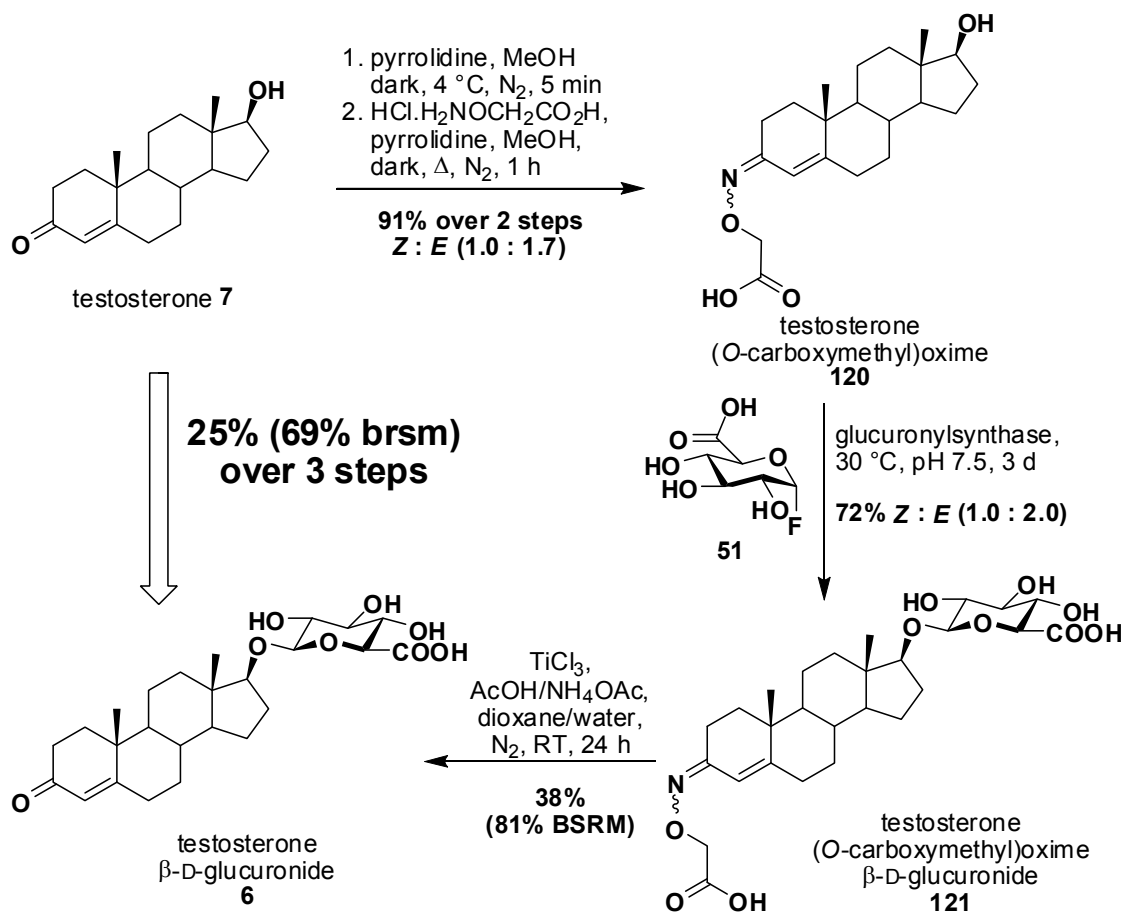
Scheme 4.16. Reduction of an enediacarbonyl species by titanium(III) chloride.¹⁷⁸

The ^{13}C NMR spectrum also confirms a single isomer as a result of oxime removal and shows 25 carbon environments consistent with the proposed structure. The oxime cleavage was also confirmed by the absence of the carboxylic acid (174 ppm) and oxymethylene carbon (71 ppm) of the oxime moiety. This is also confirmed by the downfield shift of the steroidal C3 carbon from 157 ppm as an oxime to 202 ppm as an unsaturated ketone.

The reaction time was not sufficient to completely convert the oxime glucuronide **121** to testosterone β -D-glucuronide **6**. Given a longer reaction time, a greater yield could potentially have been generated. Oxidation of titanium(III) was also observed over this extended reaction time which may have also contributed to lower conversions. A greater excess of titanium(III) may be needed or its continuous addition over time may improve conversions. Alternately, improved reaction conditions such as the degassing of solvents, the use of argon gas or optimising the buffer concentration and pH may help reduce the degradation of titanium(III). Nevertheless, the testosterone β -D-glucuronide **6** was synthesised from testosterone **7** in 25% over three steps (Scheme 4.17). This is still over double the yield from the direct glucuronysynthesis of testosterone **7** (12% yield) and an improvement on literature preparation via the Koenigs-Knorr procedure (17% over two steps).²⁰ Better yet, a yield of 69% over three steps is achieved if based on recovered starting materials.

Little improvement is envisaged for the oximation and glucuronysynthase step. Unlike the near-quantitative glucuronysynthesis of the DHEA O-(carboxymethyl)oxime **116**, the lower yield for testosterone O-(carboxymethyl)oxime **120** must arise from the substrate not binding in the necessary way (perhaps from steric hindrance associated with neopentyl alcohol). The de-oximation step is the lowest yielding step of the sequence and its optimisation will see a drastic improvement to the three step steroid solubilisation strategy for testosterone **7** and other steroids bearing unsaturated ketones.

Steroid solubilisation strategy



Scheme 4.17. The three step solubility strategy for testosterone 7.

4.8 Conclusions

The expansion of the glucuronylsynthase library was branched into the field of steroidal substrates as glucuronyl acceptors. The glucuronylsynthase enzyme was able to produce the glucuronides of a small range of steroid substrates by direct glucuronylsynthesis. The best yield of 26% was achieved with DHEA **55** when 2% DDM was used to aid its solubility. This yield was greater than the reported 20% yield of DHEA β-D-glucuronide **77** obtained over two steps from the Koenigs-Knorr reaction.²⁰

High concentrations of additives to aid steroid solubility only seem to provide small improvements. Improved solubility of DHEA **55** was investigated through the temporary interconversion of the ketone group to a hydrazone or oxime functionality. Four DHEA analogues were synthesised, but the DHEA O-(carboxymethyl)oxime **116** brought about the greatest solubility enhancement (100-fold the solubility of DHEA **55**). DHEA O-(carboxymethyl)oxime β-D-

glucuronide **118** was isolated in 76% from the glucuronylsynthase reaction of DHEA O-(carboxymethyl)oxime **116**. The cleavage of the oxime was achieved in quantitative yield from a mild, titanium(III) reduction.¹⁶⁴ This three step sequence for obtaining DHEA β -D-glucuronide **77** from DHEA **55** yielded 67% over three steps (Scheme 4.12). This 3-step solubility strategy was also applied to the synthesis of testosterone β -D-glucuronide **6** (Scheme 4.17). The testosterone β -D-glucuronide **6** was synthesised from testosterone **7** in 25% over three steps (69% brsm).

The kinetics of the glucuronylsynthase enzyme with DHEA O-(carboxymethyl)oxime **116** as a substrate were investigated with the HPLC assay. Substrate inhibition was observed for this substrate which provided a calculated K_m of 7 ± 19 mM and a k_{cat} of $1.4 \times 10^{-3} \text{ s}^{-1}$. Compared to the other alcohol accepters tested to date (Table 3.2), the K_m for DHEA O-(carboxymethyl)oxime **116** is the smallest reported whilst its catalytic turnover is the slowest. The specificity constant (k_{cat}/K_m) was the largest exhibited for an acceptor alcohol tested so far with a value of $4.3 \text{ M}^{-1} \text{ s}^{-1}$. It is hypothesised that the greater binding and specificity is due to the large size of the molecule available to make contact (bind) with the active site.

A study on the equivalents of α -D-glucuronyl fluoride **51** added to the DHEA O-(carboxymethyl)oxime **116** glucuronylsynthase reaction flagged the presence of product inhibition. Using HPLC kinetic studies, DHEA O-(carboxymethyl)oxime β -D-glucuronide **118** was proven to be an inhibitor displaying mixed predominately competitive inhibition. The competitive inhibition constant (K_{ic}) was determined as $73 \pm 6 \mu\text{M}$ and the weaker uncompetitive inhibition constant (K_{iu}) as $190 \pm 2 \mu\text{M}$. Conversely, 2-phenylethyl β -D-glucuronide **68** did not show any signs of inhibition. The product inhibition in the DHEA O-(carboxymethyl)oxime **116** glucuronylsynthase reaction was responsible for the moderate yields. Overcoming the product inhibition with extra equivalents of α -D-glucuronyl fluoride **51** achieved near quantitative yields of the DHEA O-(carboxymethyl)oxime β -D-glucuronide **118** (98% with 5 equivalents of **51**). This improvement in yield for the DHEA O-(carboxymethyl)oxime **116**

Steroid solubilisation strategy

glucuronylsynthase reaction improved the steroid solubilisation strategy for DHEA β -D-glucuronide **77** synthesis to 86% over three steps.

DHEA **55** and testosterone **7** were two examples that demonstrated the successful application of the steroid solubility sequence regardless of ketone position (3-keto and 17-keto shown), alcohol position (3- β and 17- β shown) or ketone type (saturated or α,β -unsaturated shown). As a result, this steroid solubilisation strategy is anticipated to be extended to a wide variety of saturated or unsaturated keto-steroids.

~ Chapter 5 ~

**Extension of the
glucuronylsynthase
methodology to
other steroids**

5.1 Introduction

The glucuronylsynthase enzyme has proven to synthesise a select range of steroids with good to moderate yields. The three step solubility strategy (chapters 4.3 and 4.7) has improved the yields of glucuronides for keto-steroids. To expand the steroid substrate repertoire for the glucuronylsynthase, a steroid screen is warranted. The application of the three step solubility sequence would be arduous and time-consuming task to apply in a screen and may not be applicable to some steroids (i.e. steroids without carbonyl functionality). The three step solubility strategy could be used for a preparative glucuronide synthesis at a later stage if required. To improve the solubility of the steroids in the screen, the use of additives to aid solubility were investigated by HPLC on the DHEA O-(carboxymethyl)oxime **116** glucuronylsynthase reaction. The design of a steroid substrate screen utilising solid phase extraction procedures will be discussed and some preliminary screening results will be presented.

5.2 Effects of additives on the glucuronylsynthase reactions

5.2.1 Effect of additives on glucuronylsynthase activity

The effect of a selection of detergents and co-solvents has already been determined on the activity and stability of the WT β -glucuronidase.⁵⁸ DMSO and DDM were considered the best additives to use with the WT β -glucuronidase. Differing by only one amino acid, it was assumed that the additives would have similar effects on the glucuronylsynthase enzyme. But given the large reduction in yield as a consequence of using DMSO in the DHEA O-(carboxymethyl)oxime **116** glucuronylsynthase reaction, it was important to investigate the effect that a selection of additives had on the glucuronylsynthase reactions.

The DHEA O-(carboxymethyl)oxime **116** glucuronylsynthase reaction rate is lower than most of the other acceptors (chapter 4.5). So any decrease in velocity, as a result of an additive, would be more difficult to assess than a

Extension of the glucuronylsynthase methodology to other steroids

change in a faster reaction, such as with 2-phenylethanol **45**. As a result, the effect of different additives on the initial velocity of the enzyme was determined at a saturating concentration of α -D-glucuronyl fluoride **51** donor (1 mM) and a high sub-saturating concentration of 2-phenylethanol **45** acceptor (94 mM). The co-solvents were tested at 5% and 10% v/v and included DMSO, ethanol (EtOH), *tert*-butanol (*t*BuOH), and glycerol. The detergents were tested at 1% and 2% w/v and included *n*-dodecyl maltoside (DDM), Triton X-100 (TX-100) and Brij-56. Also of interest was the protein extraction reagent BugBuster[®] which consists of a proprietary formulation of detergents and salts. It is used for cell lysis in the directed evolution screens and we wanted to ensure that full enzyme activity was sustained in this solution. It was tested at concentrations of 2% and 10% w/v which is equivalent to the concentration used in the screens and the supplied stock concentration respectively. Given the length of time to complete this investigation (2 days), another reaction without additives (control 2) was performed at the end of the investigation to account for activity loss over this time.

As expected, all the reactions with additives demonstrated a decrease in enzyme activity (Figure 5.1). Detergents maintained the highest activity with similar activities exhibited for each and no velocities falling below 70% of the control (no additives). The exception being the Bug Buster which was analysed at a greater concentration than the other detergents tested. Co-solvents were more detrimental to the enzyme albeit *tert*-butanol and glycerol which demonstrated enzymatic activities greater than 80% of the control. Based on the initial velocity of 2-phenylethanol **45**, all detergents are suitable at either 1% or 2% w/v concentration. If a co-solvent is used, glycerol is best suited at 5% or 10% v/v concentration or *tert*-butanol at 5% v/v concentration. DMSO essentially halved the initial rate of the 2-phenylethanol **45** glucuronylsynthase reaction. If an equivalent effect occurs with the DHEA O-(carboxymethyl)oxime **116** reaction, it would help explain the reduction in yield of the large scale reaction containing DMSO.

Extension of the glucuronylsynthase methodology to other steroids

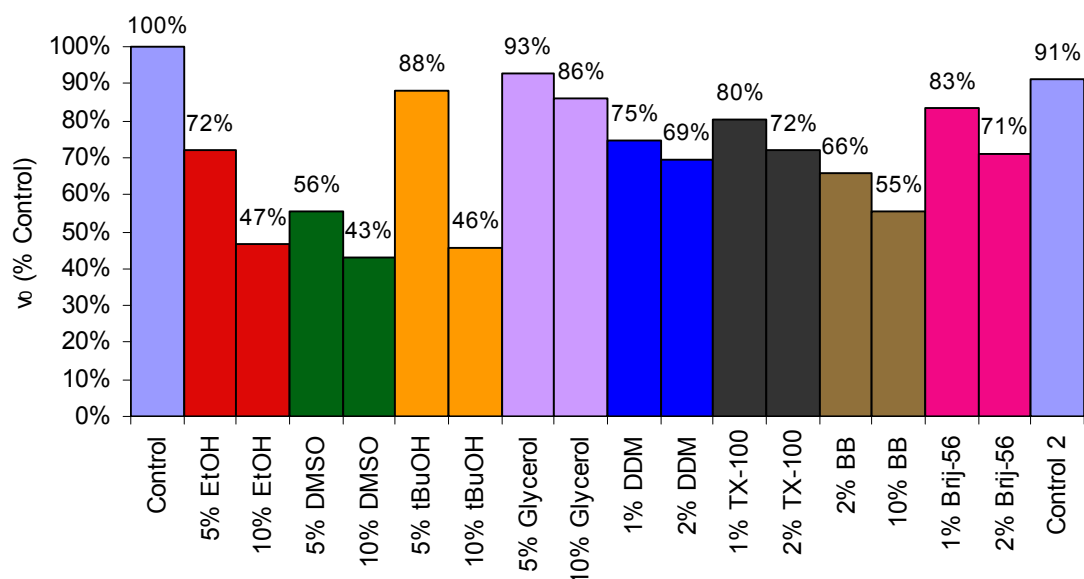


Figure 5.1. Effect of additives on the initial rate (v_0 , as a percentage of the initial velocity for the control) for reaction of 2-phenylethanol 45 acceptor (94 mM) and α -D-glucuronyl fluoride 51 (21 °C in 100 mM phosphate buffer, pH 7.5).

5.2.2 Effect of additives on glucuronylsynthase yields

In addition to knowing the effect of additives on the glucuronylsynthase activity, it was beneficial to investigate the stability of the glucuronylsynthase in these reactions over time. The DHEA O-(carboxymethyl)oxime **116** glucuronylsynthase reaction was used to explore the effect of additives on its yield. The study commenced with six identical 2 mM DHEA O-(carboxymethyl)oxime **116** glucuronylsynthase reactions prepared in HPLC vials that differed only by the additive. These reactions included 5% *tert*-butanol, 5% DMSO, 5% glycerol, 1% DDM, 1% TX-100 and one without additives (control). Three equivalents of α -D-glucuronyl fluoride **51** was used to overcome the product inhibition. The reactions were monitored at 37 °C over 60 hours with an injection taken every 5 hours (Figure 5.2).

The reaction profiles of the reactions with additives looked very similar to the control reaction with the exception of 1% DDM and 5% *tert*-butanol. The reaction containing 1% DDM was much slower than the other reactions resulting in a yield ~30% lower than the control. The reaction containing 5% *tert*-butanol reaction exhibited a faster production of product and achieved a higher yield than the control reaction. A decrease in glucuronide product **118** was observed for all reactions over an extended time which may be due to

Extension of the glucuronylsynthase methodology to other steroids

instrumental error or possible non-enzymatic hydrolysis occurring at these elevated temperatures (37 °C).

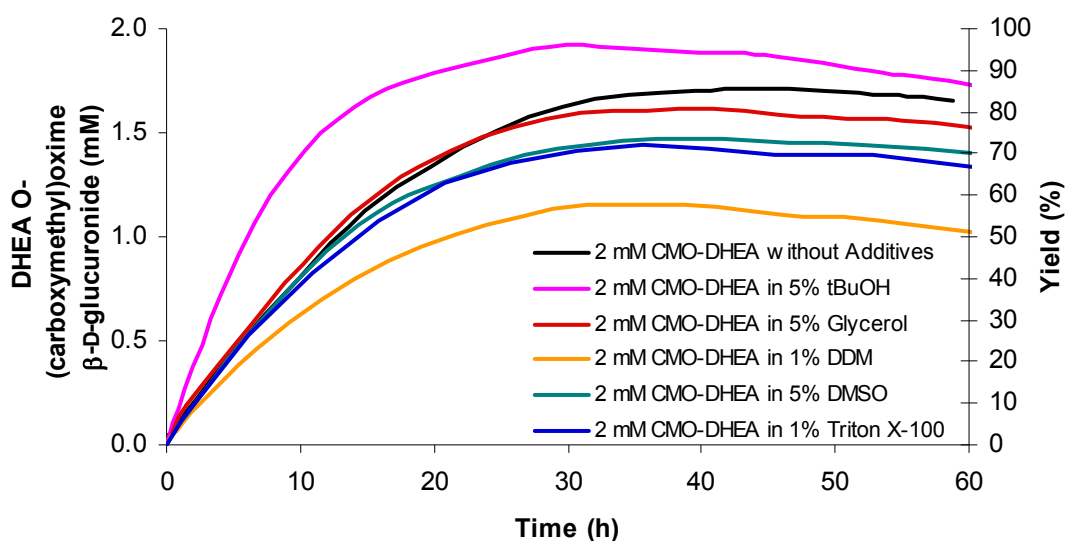


Figure 5.2. Reaction profiles for the reaction of DHEA O-(carboxymethyl)oxime (CMO-DHEA) **116** acceptor (2 mM) and α -D-glucuronyl fluoride **51** donor (6 mM) with glucuronylsynthase (0.4 mg mL^{-1}) in the presence of additive (37 °C, 100 mM phosphate buffer, pH 7.5). The reaction progress is depicted in terms of concentration (mM) of DHEA O-(carboxymethyl)oxime β -D-glucuronide **118** produced (left y-axis) and the yield (%) of the reaction (right y-axis).

The purpose of using additives is to increase the concentration of DHEA O-(carboxymethyl)oxime **116** and other steroids in the glucuronylsynthase reactions. So the effect of the additives was monitored on a 5 mM reaction of DHEA O-(carboxymethyl)oxime **116** using the same concentration of glucuronylsynthase. Six reactions of concentrated DHEA O-(carboxymethyl)oxime **116** glucuronylsynthase reactions were prepared in HPLC vials and monitored at 37 °C over 60 hours with an injection taken every 5 hours (Figure 5.3). Given the enhanced effect of 5% *tert*-butanol, a 10% v/v *tert*-butanol solution was prepared and monitored with a 5 mM concentration of DHEA O-(carboxymethyl)oxime **116**. The remaining reactions contained 5% *tert*-butanol, 5% DMSO, 5% glycerol, 1% DDM, or 1% TX-100. A control reaction could not be performed at 5 mM due to limitations in its solubility.

Unfortunately, the HPLC vial containing the reaction with 1% TX-100 had its seal ruptured during the assay and at 37 °C the solvent evaporated. Consequently, its results were omitted from the study. Given the reaction of 2

Extension of the glucuronylsynthase methodology to other steroids

mM DHEA *O*-(carboxymethyl)oxime **116** in the presence of 1% TX-100 yielded 15% less product than the control, it was deemed unnecessary to repeat this reaction. Evaluating the remainder of the additives, the reactions containing 5% DMSO and 1% DDM had approximately a 20% improvement in the yield of DHEA *O*-(carboxymethyl)oxime β -D-glucuronide **118**. The reactions containing *tert*-butanol and glycerol, exhibited similar yields achieved in the 2 mM DHEA *O*-(carboxymethyl)oxime **116** glucuronylsynthase reactions. However there is little room for improvement with *tert*-butanol as the reactions containing 5% and 10% *tert*-butanol both achieved a 97% yield.

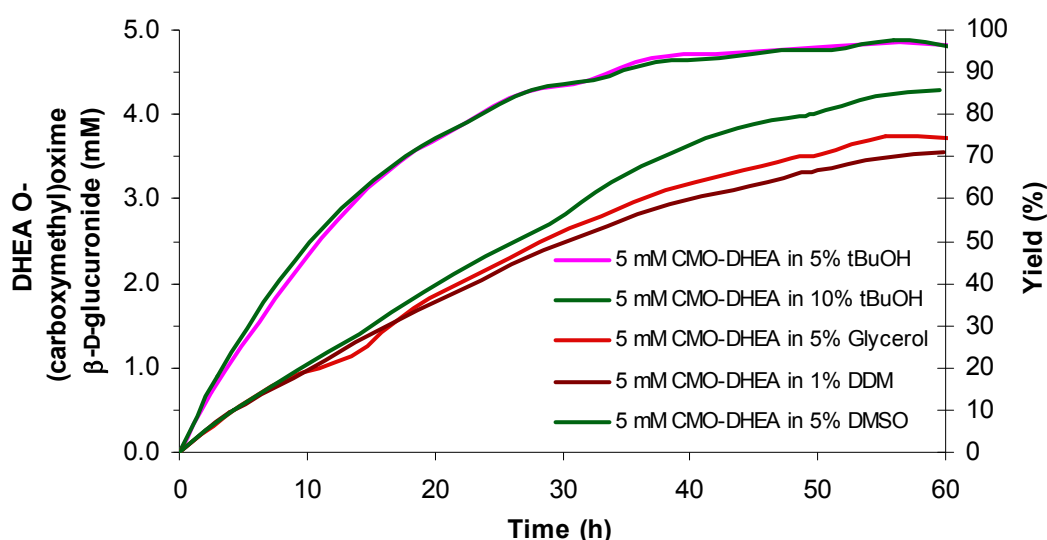


Figure 5.3. Reaction profiles for the reaction of DHEA *O*-(carboxymethyl)oxime **116** acceptor (5 mM) and α -D-glucuronyl fluoride **51** donor (15 mM) with glucuronylsynthase (0.4 mg mL^{-1}) in the presence of additive ($37 \text{ }^\circ\text{C}$, 100 mM phosphate buffer, pH 7.5). The reaction progress is depicted in terms of concentration (mM) of DHEA *O*-(carboxymethyl)oxime β -D-glucuronide **118** produced (left y-axis) and the yield (%) of the reaction (right y-axis).

The reaction rate in the presence of *tert*-butanol was clearly greater than in the presence of the other additives. The concentration of *tert*-butanol seemed to have no effect on the reaction rate and yield of the glucuronylsynthase reaction. The reaction profile for the 5 mM DHEA *O*-(carboxymethyl)oxime **116** glucuronylsynthase reaction in the presence of 5% and 10% *tert*-butanol were essentially identical.

A general improvement in the yield of DHEA *O*-(carboxymethyl)oxime β -D-glucuronide **118** was observed when the glucuronylsynthase reaction was

Extension of the glucuronylsynthase methodology to other steroids

performed with a more concentrated solution of DHEA O-(carboxymethyl)oxime **116**. To assess if the yield could be increased further, a study using a 10 mM solution of DHEA O-(carboxymethyl)oxime **116** was performed. Unfortunately, only 10% *tert*-butanol was capable of achieving complete dissolution of a 10 mM solution of DHEA O-(carboxymethyl)oxime **116**. A 76% yield of product was obtained after 60 hours, but it is worthy to note that the same concentration of enzyme (0.4 mg mL^{-1}) was used in all the reaction profiles monitored. Basic Michaelis-Menten kinetics states that velocity is not linear with substrate concentration (except at very low substrate concentrations) so a longer reaction time may still be required to process double the quantity of substrate in an equal volume of buffer.

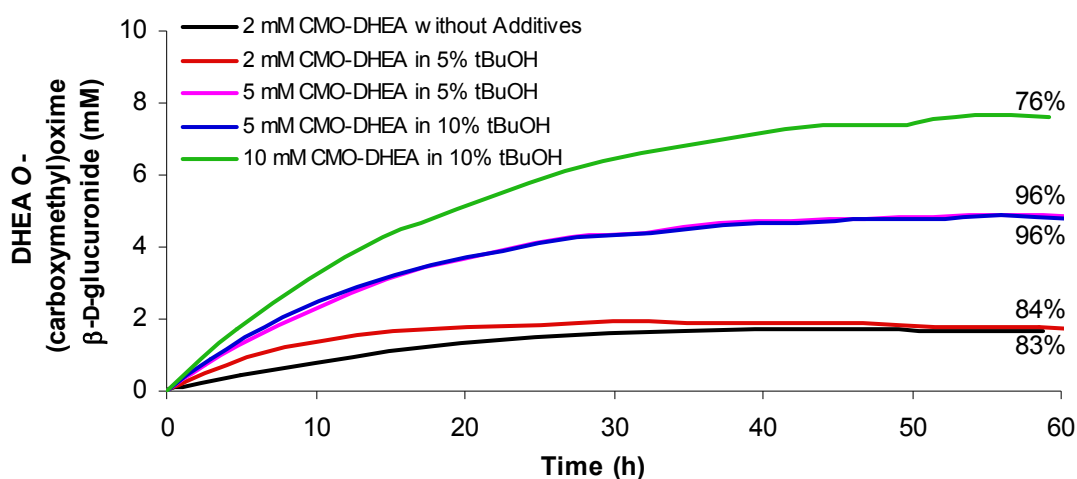


Figure 5.4. Reaction profiles (product formation, mM) for the reaction of DHEA O-(carboxymethyl)oxime **116** acceptor (2 mM, 5 mM or 10 mM) and α -D-glucuronyl fluoride **51** donor (3 equiv) with glucuronylsynthase (0.4 mg mL^{-1}) in the presence of *tert*-butanol (0%, 5% and 10%) and 100 mM phosphate buffer, pH 7.5 at 37 °C. Final reaction yields are displayed at the end of the curves.

With no other 10 mM reactions to compare against, the reaction profile of the 10 mM DHEA O-(carboxymethyl)oxime **116** reaction performed with 10% *tert*-butanol was compared against the other reactions containing *tert*-butanol and the control (Figure 5.4). When assessing the amount of product **118** formed, more glucuronide **118** is produced in the 10 mM DHEA O-(carboxymethyl)oxime **116** reaction (7.6 mM of **118**) than the 5 mM DHEA O-(carboxymethyl)oxime **116** reaction (4.8 mM of **118**) containing 10% *tert*-butanol given the same amount of time and enzyme.

Extension of the glucuronylsynthase methodology to other steroids

The reaction rate of the 10 mM DHEA O-(carboxymethyl)oxime **116** reaction is faster than the 5 mM reaction with the same 10% concentration of *tert*-butanol. A reaction with 2 mM DHEA O-(carboxymethyl)oxime **116** containing 10% *tert*-butanol was performed for comparative reasons, but due to a seal rupture in its assay, a final yield was never obtained.

The increasing reaction rate with increasing substrate concentration contradicts the notion of substrate inhibition observed in the DHEA O-(carboxymethyl)oxime **116** kinetic study (refer to section 4.5.1). If substrate inhibition exists, the reaction rate should be decreasing with increasing DHEA O-(carboxymethyl)oxime **116** concentration. To better assess reaction rate, the initial velocity of each DHEA O-(carboxymethyl)oxime **116** glucuronylsynthase reaction was estimated from the reaction profiles (Figure 5.5). The initial velocity of the DHEA O-(carboxymethyl)oxime **116** at 37 °C without additives is 3.3 nmol min⁻¹ [mg protein]⁻¹. This initial velocity is almost five times the rate of the 2 mM DHEA O-(carboxymethyl)oxime **116** reaction performed at 21 °C in the kinetic study. All the additives, except *tert*-butanol, exhibited initial velocities (2.6 – 4.1 nmol min⁻¹ [mg protein]⁻¹) similar to this rate in both 2 mM and 5 mM DHEA O-(carboxymethyl)oxime **116** reactions.

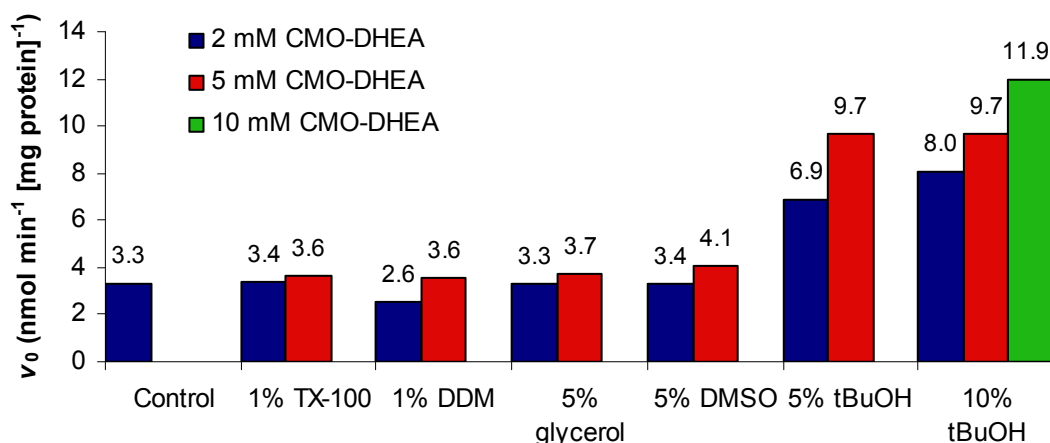


Figure 5.5. Estimated initial velocity (v_0) for the reaction of DHEA O-(carboxymethyl)oxime (CMO-DHEA) **116** acceptor (2 mM, 5 mM or 10 mM) and α -D-glucuronyl fluoride **51** donor (3 equiv) with glucuronylsynthase (0.4 mg mL⁻¹) in the presence of in the presence of additive (37 °C, 100 mM phosphate buffer, pH 7.5, n = 2). Numbers above the bars represent the initial velocity (nmol min⁻¹ [mg protein]⁻¹).

As suggested in their reaction profiles, the reactions containing *tert*-butanol exhibited enhanced initial velocities. The addition of 5% or 10% *tert*-butanol to

Extension of the glucuronylsynthase methodology to other steroids

a 2 mM DHEA O-(carboxymethyl)oxime **116** glucuronylsynthase reaction doubled the initial velocity of the reaction. The initial velocity was improved further when the DHEA O-(carboxymethyl)oxime **116** concentration was increased. A reaction with 5 mM of DHEA O-(carboxymethyl)oxime **116** had triple the initial velocity of the 2 mM control reaction for concentrations of 5% and 10% *tert*-butanol. Furthermore, the reaction with 10 mM of DHEA O-(carboxymethyl)oxime **116**, dissolved in 10% *tert*-butanol, had four times the initial velocity of the 2 mM control reaction.

Just how much *tert*-butanol can be added to the reactions before the glucuronylsynthase activity and stability is compromised is unknown. A future study that determines the limitation of *tert*-butanol concentration is needed as a greater *tert*-butanol concentration should provide a more concentrated steroid concentration. A greater concentration may increase the reaction rate and yield for DHEA O-(carboxymethyl)oxime **116** which may possibly extend to other steroid substrates.

This enhanced velocity with *tert*-butanol was not observed in the additives study with 2-phenylethanol **45**. Just the addition of *tert*-butanol to the DHEA O-(carboxymethyl)oxime **116** reaction doubled the reaction rate compared to when no additives were present. Conversely, a decrease in reaction rate (46-88% of control) was observed in the reaction of 2-phenylethanol **45**. Perhaps *tert*-butanol has some way of overcoming the substrate inhibition observed with DHEA O-(carboxymethyl)oxime **116**. This could easily be determined by repeating a study of initial rate vs. concentration of DHEA O-(carboxymethyl)oxime **116** in the presence of *tert*-butanol. Unfortunately, time restrictions did not allow for this study to take place. If proven however, it would be of considerable interest to see if the substrate inhibition is alleviated in the other substrates demonstrating substrate inhibition.

The conclusion from the addition of co-solvents and detergents to the DHEA O-(carboxymethyl)oxime **116** glucuronylsynthase reactions is unambiguous. The addition of DDM, DMSO, glycerol and TX-100 to the DHEA O-(carboxymethyl)oxime **116** glucuronylsynthase reaction to aid with solubility provided no additional benefits. Reaction rates and yields were similar for all cases. The addition of *tert*-butanol however, drastically improves the reaction

Extension of the glucuronylsynthase methodology to other steroids

rate and yields of the DHEA O-(carboxymethyl)oxime **116** glucuronylsynthase reaction. Greater concentrations of DHEA O-(carboxymethyl)oxime **116** dissolved in *tert*-butanol had enhanced reaction rates and yields. The influence that *tert*-butanol has on the DHEA O-(carboxymethyl)oxime **116** glucuronylsynthase reactions is unknown.

5.3 Additives Conclusion

With the three step steroid solubilisation strategy not applicable to every steroid, a study on the effects of additives to the glucuronylsynthase reaction was explored on the DHEA O-(carboxymethyl)oxime **116** glucuronylsynthase reaction. Monitoring the reaction with HPLC, it was observed that the yield and reaction rate were not greatly improved nor reduced by the addition of co-solvents and detergents. The exception being *tert*-butanol, which doubled the reaction rate compared to when no additives were present. This enhancement of enzyme activity as the concentration of organic solvent is increased is a phenomenon being studied by numerous research groups. Research by Dordick and Klivanov has seen the integration of enzymes into pure organic solvents with enzyme activities and thermostability beyond what is capable in a aqueous media.^{179,180} Furthermore, as the concentration of DHEA O-(carboxymethyl)oxime **116** was increased in the presence of *tert*-butanol, the reaction rate and yield improved further. The concentration of *tert*-butanol did not seem to affect the reaction with similar reaction profiles being observed with both 5% and 10% *tert*-butanol. It is proposed that the addition of *tert*-butanol alleviates substrate inhibition. Kinetic studies of the DHEA O-(carboxymethyl)oxime **116** glucuronylsynthase reaction in the presence of *tert*-butanol would be able to validate the statement. If true, the removal of substrate inhibition imposed on other acceptor alcohols may be possible. With an understanding of some of the additional variables in the glucuronylsynthase reactions, it was now time to expand the application of the methodology by investigating more steroid substrates.

5.4 Expansion of the steroid library

The optimum conditions for the glucuronylsynthase reactions have been determined and the solubility of steroids has been enhanced by the addition of *tert*-butanol. The substrate repertoire for the glucuronylsynthase enzyme was ready to be expanded by screening against a library of steroids. But the task of purifying each reaction would still be a lengthy process. To save time in this area, the use of solid-phase extraction cartridges were explored to quickly separate the components of the glucuronylsynthase reactions.

5.4.1 Principles of solid-phase extraction

Solid-phase extraction (SPE) is similar to chromatography in which a mixture of components is adsorbed onto a stationary phase. However, unlike chromatography which separates the components based on their retention through a column of solid media, SPE elutes one or more components from a small amount of sorbent using different types of mobile phases. As a result, structurally and chemically similar molecules (e.g. DHEA **55** and testosterone **7**) would elute in the same portion whilst chemically different molecules (e.g. DHEA **55** and DHEA β -D-glucuronide **77**) would be quickly and easily separated by different washes. The sorbent can be comprised of normal-phase, reverse-phase, ion-exchange or a combination of each media. The strategy behind SPE is to assess the chemical make-up of your desired product and how it differs from the other components in your mixture, just as you would in a liquid-liquid separation.

Solid phase extraction is routinely used in the sports drug testing industry to isolate the unconjugated steroids, steroid glucuronides and steroid sulphates from a competitor's urine sample. The Australian Racing Forensic Laboratory utilise Waters Oasis[®] WAX branded SPE cartridges to analyse steroid metabolites in urine samples.¹⁸¹ The WAX cartridge is a reverse phase sorbent with polar and weak anion exchange residues capable of separating unconjugated steroids, steroid glucuronides, and steroid sulphates from a urine matrix consisting of salts and other renal waste. Piperazine residues provide the weak anion exchange used to selectively elute the weakly acidic glucuronides over the strong acidic sulphates. The successful isolation of

Extension of the glucuronylsynthase methodology to other steroids

steroid glucuronides from such a complex mixture would suggest the isolation of the steroid glucuronide from the limited components in the glucuronylsynthase reactions would be easily achieved by SPE.

The components of the glucuronylsynthase reactions comprise of the steroid glucuronide, unreacted steroid, unreacted α -D-glucuronyl fluoride **51**, phosphate buffer salts and possibly some glucuronic acid **3** from the degradation of **51**. Assessing the chemical properties of each of these components (Figure 5.6), it can be seen that a combination of ionic and lipophilic interactions can be used to isolate steroid glucuronides from the crude reactions. With the absence of steroid sulphates from the reaction mixture, the use of the Waters Oasis[®] MAX SPE cartridges could also be used. Oasis[®] MAX cartridges are similar to the WAX cartridges but differ only by the ionic residue. The MAX cartridges have a quaternary amine (instead of the ionisable piperazine residue in the WAX) to produce a stronger ionic interaction that provides a better retention.

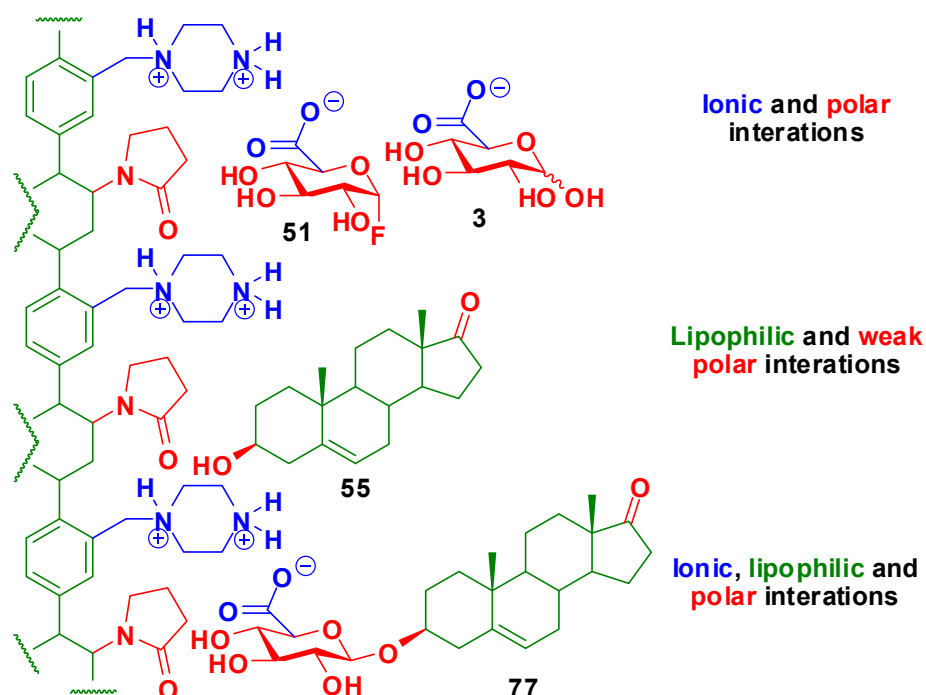


Figure 5.6. The interactions of the components from the DHEA 55 glucuronylsynthase reaction with the Waters Oasis[®] WAX sorbent. Lipophilic residues are coloured green, hydrophilic residues are red and ionic residues are coloured blue.

An investigation was undertaken to assess if solid phase extraction cartridges could separate the individual components of the glucuronylsynthase

to quickly isolate the steroid glucuronide. A quantitative study was also undertaken to measure the recovery of material from these extractions.

5.4.2 Method development

The Australian Racing Forensics Laboratory (ARFL) have isolated steroid glucuronides using the Oasis[®] WAX SPE cartridges and have developed their own method for glucuronide extraction (Figure 5.7). This procedure differs from the manufacturer's method (Figure 5.8) and so it was of interest to know which procedure worked best at isolating pure glucuronide with the highest recovery. Both Oasis[®] SPE cartridges (WAX and MAX) were tested with each extraction procedure to determine which combination provided the best separation and recovery. To establish these results, the isolation of DHEA O-(carboxymethyl)oxime β -D-glucuronide **118** from the crude DHEA O-(carboxymethyl)oxime **116** glucuronylsynthase reaction was used.

The HPLC conditions to separate and quantify the components of the DHEA O-(carboxymethyl)oxime **116** glucuronylsynthase reaction have already been developed (chapter 4.5). As a result, HPLC was utilised as a quantitative tool to determine the recovery of DHEA O-(carboxymethyl)oxime β -D-glucuronide **118** from SPE extraction. A glucuronylsynthase reaction of DHEA O-(carboxymethyl)oxime **116** was performed and after 5 days, the crude reaction was analysed by HPLC. Equal known volumes of the reaction were loaded onto two Oasis[®] WAX and two Oasis[®] MAX SPE cartridges. From HPLC analysis, it was determined that 2.72 μ mol of DHEA O-(carboxymethyl)oxime β -D-glucuronide **118** was loaded onto each cartridge.

The manufacturer's recommended extraction procedure (Figure 5.8) was performed on one of the Oasis[®] WAX cartridges and one of the Oasis[®] MAX cartridges. The ARFL's extraction procedure (Figure 5.7) was performed on the remaining WAX and MAX cartridge. Every fraction from the two SPE procedures were collected and subjected to HPLC analysis to determine the quantity of DHEA O-(carboxymethyl)oxime β -D-glucuronide **118** in each fraction (Table 7.2, Table 7.3, Table 7.4 and Table 7.5).

Extension of the glucuronylsynthase methodology to other steroids

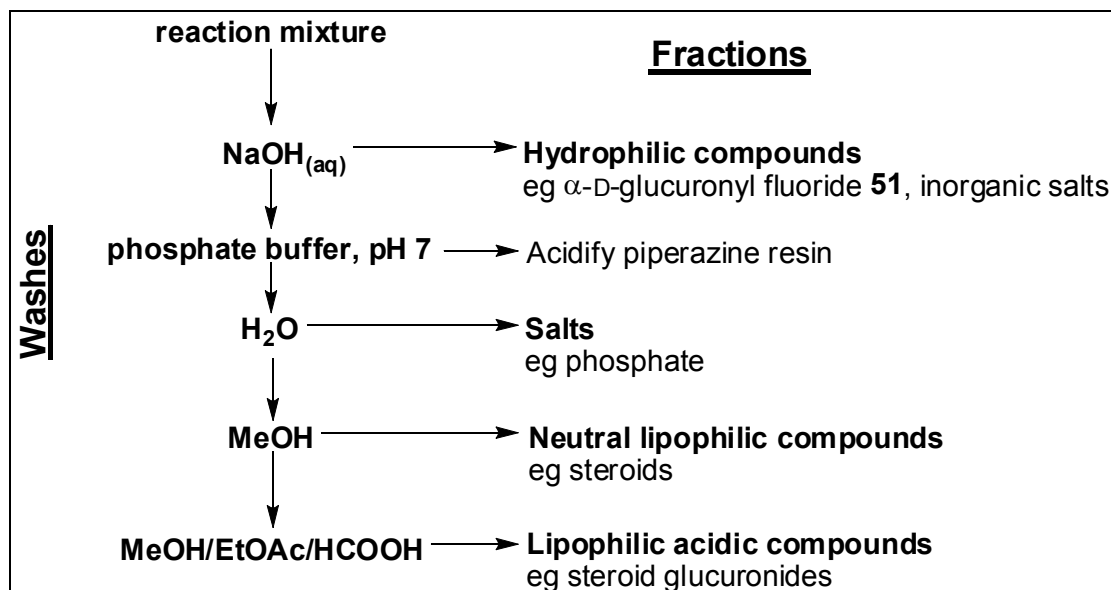


Figure 5.7. Schematic diagram of the ARFL SPE procedure used for both Oasis MAX and WAX SPE cartridges.

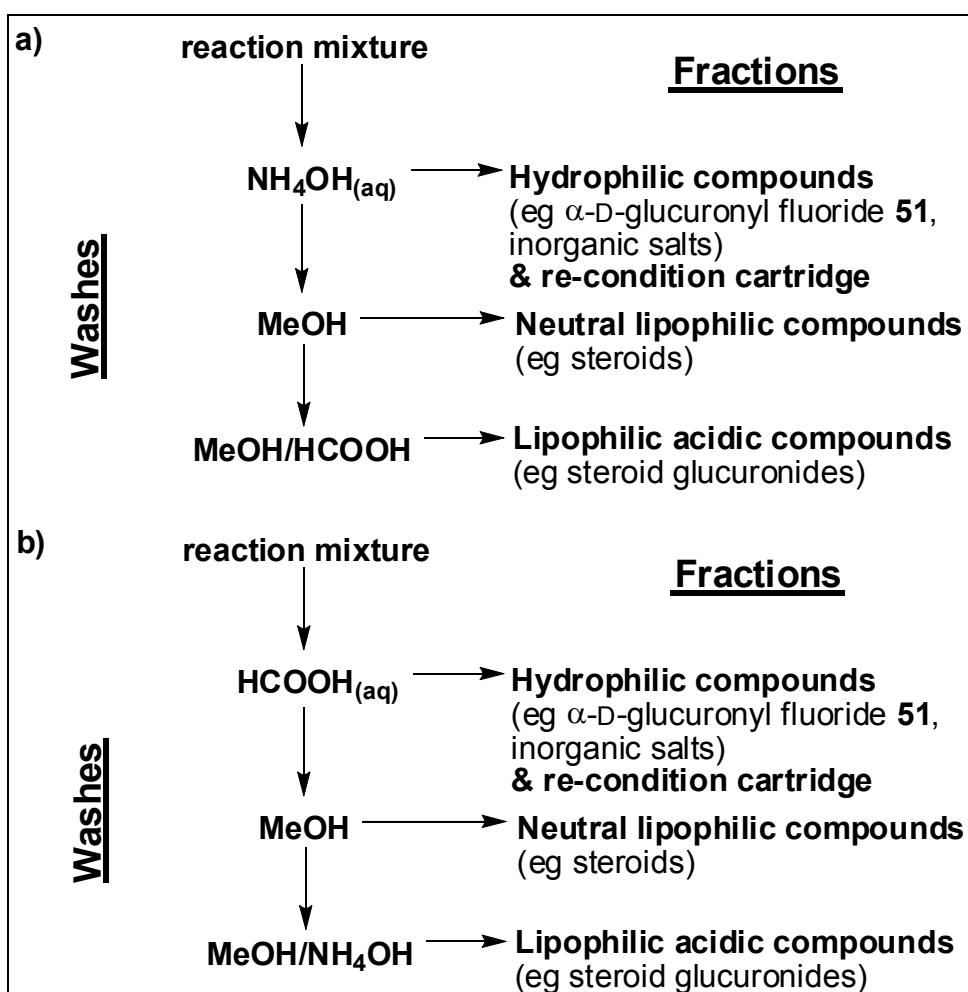


Figure 5.8. Schematic diagram of the Oasis SPE procedure for a) MAX and b) WAX cartridges

Extension of the glucuronylsynthase methodology to other steroids

The manufacturer's extraction procedure worked very well for both cartridges with 96% and 97% of the glucuronide recovered from the Oasis[®] WAX and MAX cartridges respectively in the final elution. A small quantity (1%) of the glucuronide **118** leached out in the methanol wash from the Oasis WAX cartridge. The methanol wash is supposed to extract out the unconjugated steroid whilst the glucuronide remains bound to the resin through ionic interactions. The weak anion exchange of the WAX cartridge failed to retain all of the glucuronide whereas the strong ionic interaction of the MAX cartridge successfully withheld all of the glucuronide.

The ARFL's extraction procedure worked the best for the Oasis MAX SPE cartridge. Approximately 99% of the DHEA *O*-(carboxymethyl)oxime β -D-glucuronide **118** was recovered from the MAX cartridge. Unfortunately, when the same procedure was applied to the Oasis WAX SPE cartridge, 83% of glucuronide **118** was washed out in the initial basic aqueous wash used to wash out the sugars and salts from the resin. This high loss is probably the result of using DHEA *O*-(carboxymethyl)oxime **116** as the steroid. The basic wash would have deprotonated the carboxylic acid of the oxime and glucuronide making the molecule **118** di-anionic and therefore highly hydrophilic. The di-anion **118** would not retain well in the lipophilic resin, which would normally retain steroid glucuronides, and was washed out from the cartridge. The remainder of the glucuronide **118** (14%) was reclaimed in the appropriate glucuronide wash which still accounts for a total recovery of 97% for the glucuronide **118**. Unfortunately, the majority of the glucuronide **118** which eluted in the first fraction would contain buffer salts and sugars. It is unlikely that the same would happen to a non-ionisable steroid nucleus such as DHEA **55**.

Reviewing the four different extraction combinations it appears that all are feasible procedures with greater than 97% recovery for all. The exception being the ARFL extraction procedure with the Oasis WAX cartridge which did not work well with DHEA *O*-(carboxymethyl)oxime **116**. But this is likely due to the ionisation of this steroid with literature evidence pointing to the success of this protocol. SPE has been successfully applied to workup small scale glucuronylsynthase reactions and isolate pure steroid glucuronide. The use of

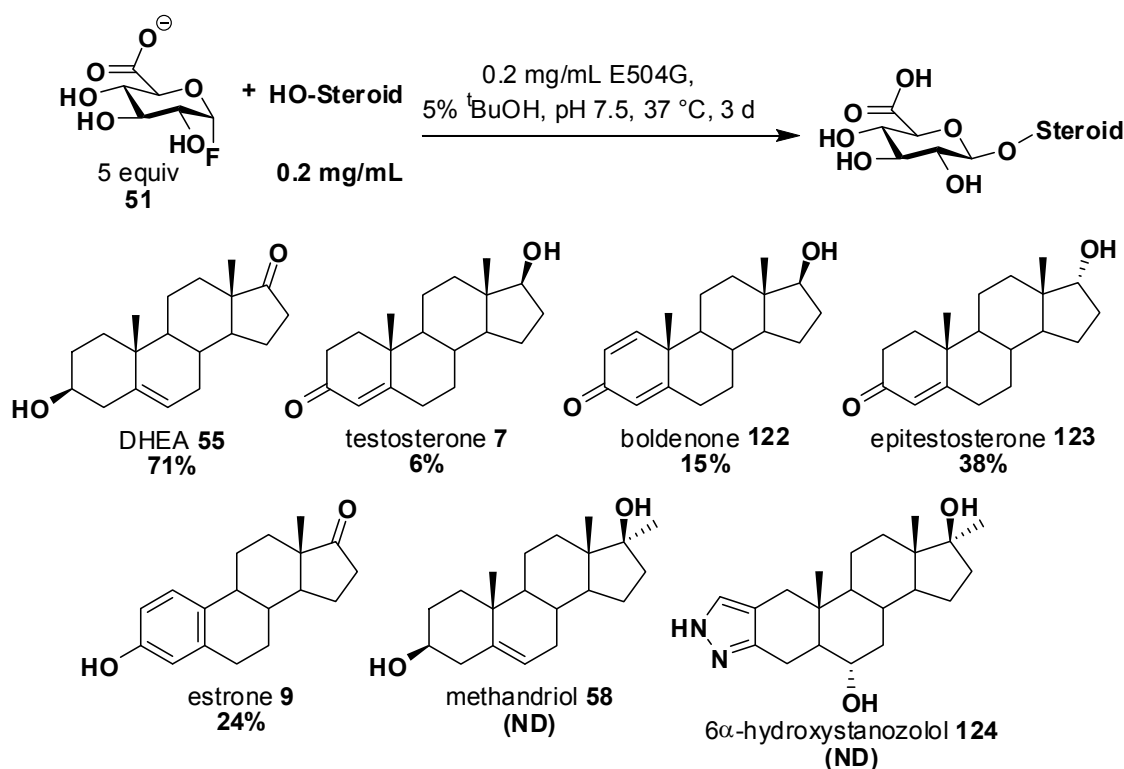
Extension of the glucuronylsynthase methodology to other steroids

SPE will save time in glucuronylsynthase steroid screens by providing a rapid and universal means of isolating steroid glucuronides.

5.4.3 Initial steroid screen

The optimum glucuronylsynthase reaction conditions have been identified and solid phase extraction has provided a rapid means of isolating the steroid glucuronides. Accordingly, a small steroid screen was performed to illustrate the practicality of the screen on a selection of different steroids.

DHEA **55**, testosterone **7**, boldenone **122**, epitestosterone **123**, estrone **9**, methandriol **58**, and 6 α -hydroxystanozolol **124** were used in the screen (Scheme 5.1). Using the optimised glucuronylsynthase conditions, a milligram of steroid was dissolved in phosphate buffer pH 7.5 with 5% *tert*-butanol to aid solubility. Five equivalents of α -D-glucuronyl fluoride **51** were added and the reaction incubated with 0.2 mg mL⁻¹ glucuronylsynthase at 37 °C. After 3 days, each of the crude reactions were analysed by HPLC and the peak area ratios were used to estimate a yield for the reaction. The glucuronides were isolated by solid phase extraction and then re-analysed by HPLC. The purified samples were also analysed by ESI-MS.



Scheme 5.1. Screening of steroid substrates for the glucuronylsynthase reaction.

Yields were determined from HPLC peak ratios and are reported below the structures.

Extension of the glucuronylsynthase methodology to other steroids

A remarkable improvement on the direct glucuronylsynthesis of DHEA **55** was observed (71%) with an almost tripling of the yield previously achieved by direct glucuronylsynthesis (26%). This yield even exceeds the 67% yield achieved over the three steps of the steroid solubilisation strategy. The purification of the DHEA β -D-glucuronide **77** can be visually observed by the HPLC chromatograms before (Figure 5.9) and after (Figure 5.10) solid phase extraction.

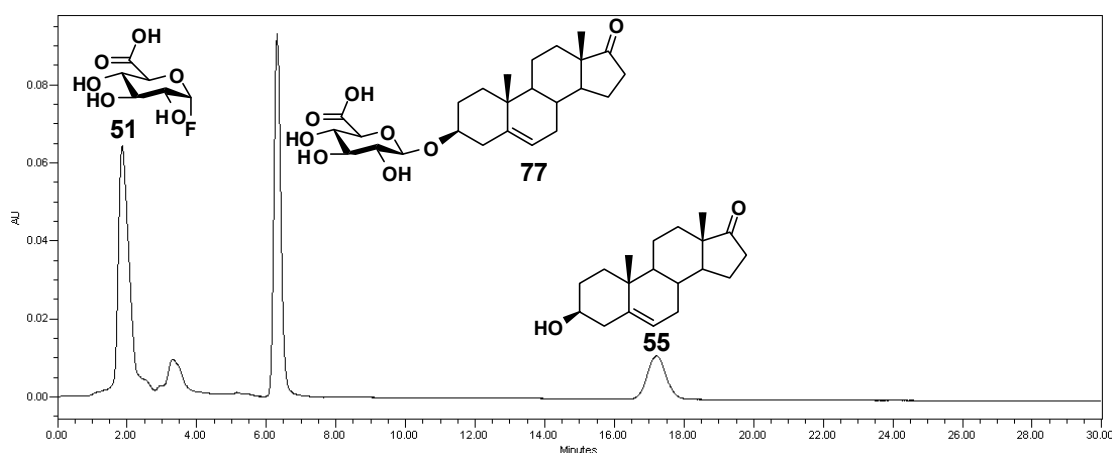


Figure 5.9. HPLC chromatogram of the crude glucuronylsynthase reaction of DHEA **55**.

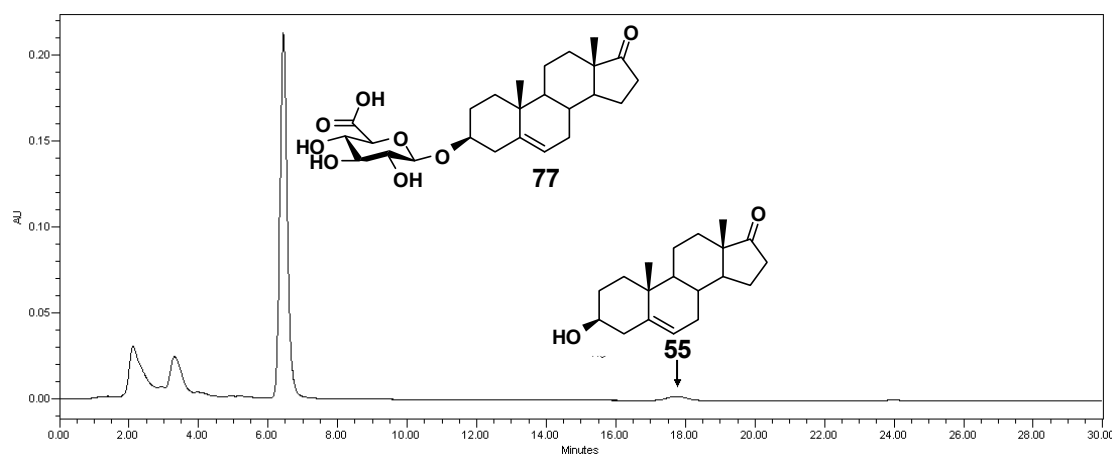


Figure 5.10. HPLC chromatogram of the purified DHEA β -D-glucuronide **77** using SPE

The testosterone β -D-glucuronide **6** was only achieved in 6% yield which is lower than the 12% yield achieved from the direct glucuronylsynthesis with DMSO co-solvent present. But this may just be an abnormality as the boldenone β -D-glucuronide **125**, which is structurally similar, was achieved in a yield of 15%. The less sterically-hindered epimer of testosterone **7**, epitestosterone **123**, provided a good yield of 38% for its respective

Extension of the glucuronylsynthase methodology to other steroids

glucuronide **126**. The glucuronylsynthesis of phenols has been proven to occur in low yields. It was therefore remarkable to obtain a yield of 24% for the estrone **9** glucuronylsynthase reaction.

The methandriol β -D-glucuronide **127** was observed in the high resolution mass spectrum and HPLC, but its yield could not be determined by HPLC due to the absence of a chromophore in the aglycon. An alternative means of detection, such as evaporative light scattering detection (ELSD), is needed to quantify the conversion of methandriol **58** and related steroids screened in glucuronylsynthase reactions. The 6α -hydroxystanozolol β -D-glucuronide **128** was also seen in the high resolution mass spectrum, but due to the ionisable pyrazole ring, both the glucuronide **128** and aglycon **124** co-eluted in the solvent front of the HPLC chromatogram. A normal phase HPLC method is required to analyse this steroid and other ionisable analogues.

Methandriol **58** and 6α -hydroxystanozolol **124** have two sites at which glucuronylation can occur. The mass spectrum did not show any evidence of glucuronylation occurring twice on these steroids. But the regioselectivity could not be determined either given such small quantities of glucuronide were available. Larger scale glucuronylsynthase reactions with methandriol **58** and 6α -hydroxystanozolol **124** would have to be conducted to determine yields and regioselectivity.

The glucuronylsynthase enzyme catalysed the glucuronylation of all the steroids subjected to the screen. Yields varied from exceptional to poor, but it is the universal application of this enzyme that is of most interest. The large range of substrate tolerance may open the doors for previously unachievable syntheses of glucuronides and provide the means of creating glucuronides for novel steroids always emerging in the sports drug testing. Subjecting the glucuronylsynthase enzyme to a larger screen of steroids will help build a profile for the enzyme and determine limitations of the enzyme.

~ Chapter 6 ~

**Conclusions and
Future Work**

6.1 Comparative study

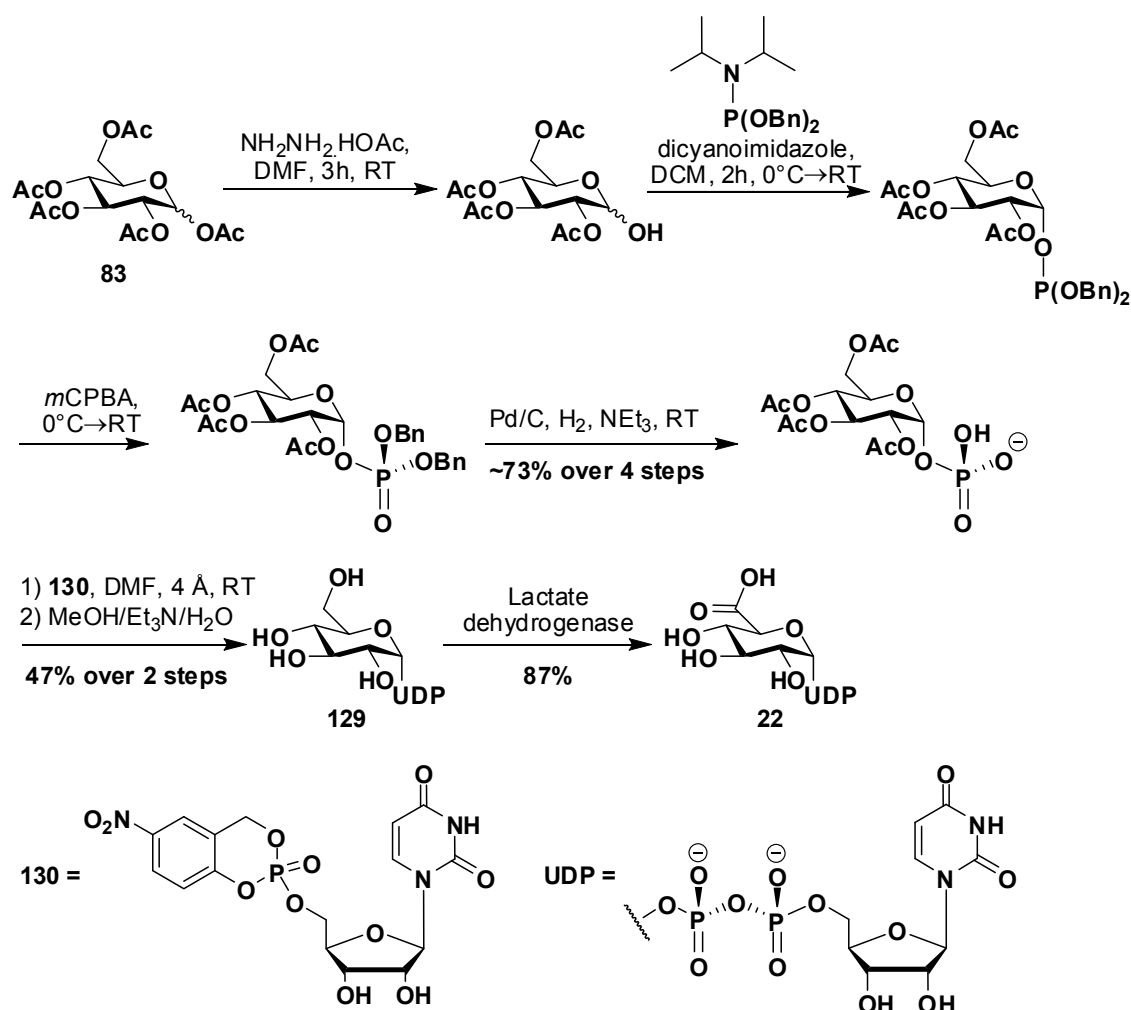
The glucuronylsynthase-mediated reaction provides is a novel procedure for glucuronide synthesis. The alternative procedures for glucuronide synthesis (using the UDP-glucuronosyltransferase, Koenigs-Knorr reaction and related reactions) were introduced earlier (chapter 1.5) and the characteristics of each were highlighted. In light of the results from this research, it seemed appropriate to re-evaluate the optimised methodology with the other glucuronylation procedures available in greater detail. In this comparative review, the procedure for preparing the substrates and enzyme/catalyst will be disclosed and the details of the reactions (yield, selectivity, reaction time, etc) will be scrutinised.

6.1.1 Preparation of the glucuronyl donors

A common attribute of all the glucuronylation procedures is the use of an activated glucuronyl donor. The glycosyl donor for the glucuronylsynthase reaction is the α -D-glucuronyl fluoride **51**. As discussed previously (chapter 2.4), it is prepared from cheap and commercially available D-glucose **82** in 39% (over 4 steps) or 69% (over 3 steps) from the per-acetylated glucose **83** (Scheme 2.2). A crystal structure (Figure 2.8) was obtained during this study which validated its preparation and relative stereochemistry.

The glucuronyl donor for the UDP-glucuronosyltransferase is the uridine 5'-diphosphate α -D-glucuronic acid **22**. With the exception of the synthesis by Roseman,¹⁸² every reported synthesis of UDP α -D-glucuronic acid **22** incorporates at least one enzymatic step in the synthetic sequence. The enzymatic step is commonly used for the oxidation of UDP α -D-glucose **129** to UDP α -D-glucuronic acid **22** or the phosphorylation of glucose.^{183,184} One of the latest reported synthesis of UDP-glucose **129** was published by Meier et al (Scheme 6.1).¹⁸⁵ Meier incorporates 5-nitro-cycloSal-uridine monophosphate **130** to synthesise UDP-glucose **129**. The UDP-glucose **129** obtained from the Meier's synthesis could be oxidised by lactate dehydrogenase.¹⁸⁴ This synthetic sequence is seven steps with an overall yield of 30% from the per-acetylated glucose **83**. A similar synthesis of UDP-glucose **129** has also been reported by Timmons.¹⁸⁶ It follows a similar sequence to the Meier sequence albeit the use of trifluoroacetic anhydride and *N*-methylimidazole to activate

uridine mono-phosphate instead of the cycloSal reagent **130** to achieve UDP-glucose **129** in 35% yield in that single coupling step.



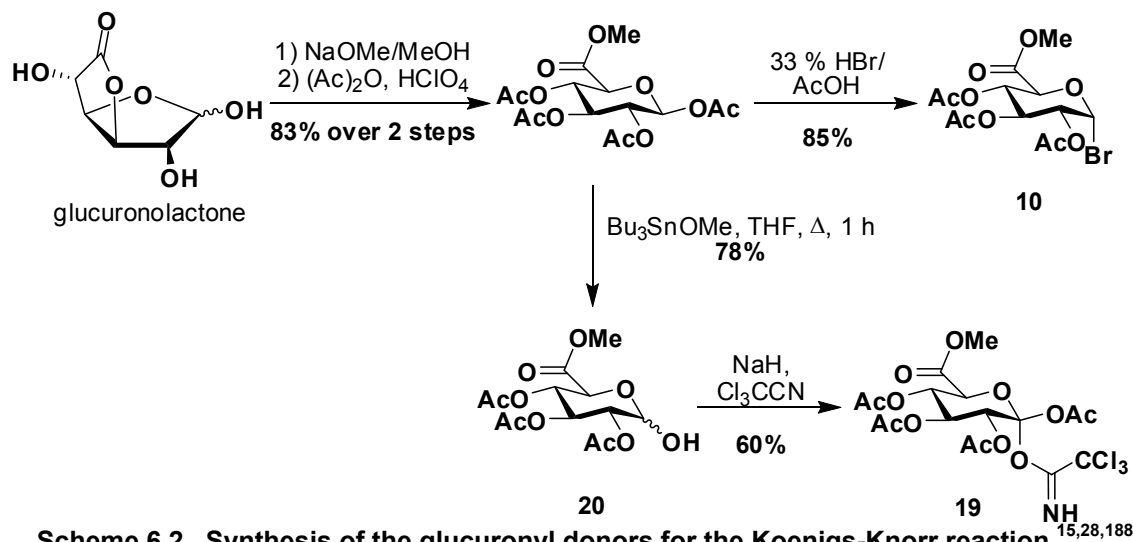
Scheme 6.1. Synthesis of UDP-glucuronic acid **22**.

Unlike the enzymatic procedures, the Koenigs-Knorr reaction and its related reactions do not require a specific glucuronyl donor. They only require an activated glucuronyl donor with protected alcohols. These protected glucuronyl donors come in the form of a α -D-glucuronyl halide (e.g. **10**)^{12,15}, α -D-glucuronyl trichloroacetimidate (e.g. **19**)²⁶ or α -D-glucuronyl silyl ether (produced *in situ* from **20**)²⁸. The synthesis of the glucuronyl donors (Scheme 6.2) range from 39% (over 4 steps) for the trichloroacetimidate sugar **19** to 71% (over 3 steps) for the glucuronyl bromide **10**.

The synthesis of the glucuronyl donor for the glucuronylsynthase and the Koenigs-Knorr procedure are similar in the synthetic route, yield and number of steps. Both procedures achieve the final glucuronyl donor in a short synthesis (3-4 steps) and high yields (~70% overall). The synthesis of UDP-glucuronic acid **22** required for UDP-glucuronosyltransferase is clearly the most complicated synthesis with only 30% achieved over 7 steps which usually

Conclusions and future work

incorporates an enzymatic step. This challenging synthesis makes the UDP-glucuronic acid **22** an expensive substrate to purchase (Sigma-Aldrich price for 100 mg of the tri-sodium salt is in excess of USD200)¹⁸⁷. The synthesis of the α -D-glucuronyl fluoride **51**, required for the glucuronylsynthase reactions, is therefore equally the highest yielding and easiest prepared substrate of the glucuronylation procedures.



Scheme 6.2. Synthesis of the glucuronyl donors for the Koenigs-Knorr reaction.

6.1.2 Preparation and properties of the reaction activator

Each glucuronylation procedure requires activation to promote the reaction between the acceptor alcohol and the glucuronyl donor. In the glucuronylsynthase and UDP-glucuronosyltransferases procedures, activation is achieved catalytically with the aid of an enzyme. The Koenigs-Knorr reaction uses stoichiometric amounts of metal salts whereas the trichloroacetimidate only uses catalytic protic or Lewis acids. The preparation of the reaction activator will be compared for each glucuronylation procedure.

The glucuronylsynthase enzyme is expressed in high yields (2.5% w/w cell) from a β -glucuronidase-deficient strain of *E. coli* and is easily purified by nickel-affinity chromatography. It takes approximately a week to obtain purified glucuronylsynthase enzyme from a sample of plasmid DNA. On average, 50 mg of purified enzyme is obtained from a litre of broth. At present, the glucuronylsynthase enzyme is not commercially available or expressed from a natural source which limits the accessibility of the enzyme to other researchers. However, given the widespread commercial availability of the WT β -glucuronidase enzyme, it can be assumed that the glucuronylsynthase enzyme could be made equally available. The low cost and high availability of the *E.*

coli WT β -glucuronidase enzyme can be attributed to the properties of the enzyme. The water-soluble enzyme allows easy preparation and handling and its homotetrameric quaternary structure provides robust thermal, pH and storage stability. These properties were reflected in this study for the glucuronylsynthase enzyme.

The UDP-glucuronosyltransferase is not expressed in prokaryotic cells and as a result animal sacrifice is usually required to obtain the enzyme. The purified UDP-glucuronosyltransferase is isolated in a yield of only 0.27% w/w from rat liver.¹⁸⁹ UDP-glucuronosyltransferases have many isoforms that are selective towards different classes of acceptor alcohols and phenols so it is essential that the correct isoform is isolated for the substrate glucuronylation. To avoid this complication, the enzyme is usually used from a crude microsomal extract from bovine, porcine, rabbit or rat liver. However, to complicate matters further, research shows that the UDP-glucuronosyltransferase activity also varies amongst different organisms.¹⁹⁰ So the UDP-glucuronosyltransferase obtained from a certain species may provide low yields of the required glucuronide, if any at all.

The purified, recombinant human UDP-glucuronosyltransferase enzyme expressed from insect cells is commercially available, but is valued at over 50 times the price of the *E. coli* WT β -glucuronidase for an identical mass.¹⁸⁷ The cost of this enzyme is due to difficulties in its preparation, expression and handling. The UDP-glucuronosyltransferase enzyme is membrane bound so the purified enzyme requires the use of co-solvents or detergents for stability.¹⁹¹ Most forms of the enzyme exhibit low stability towards pH and heat with a moderate pH range of 6.0-8.5 reported for the human UGT1A7 enzyme.¹⁹² The common optimum temperature of the enzyme across all species is 37 °C, however, the long-term stability of the enzyme is poor with the rat UDP-glucuronosyltransferase enzyme losing over 10% activity after only a week stored at 0-4 °C.¹⁹³ Finally, a divalent metal such as calcium or magnesium is required as a co-factor to activate the enzyme.^{191,194}

The Koenigs-Knorr reaction uses a different activator for each class of glycosyl donor used. When glycosyl halides are utilised (e.g. **10**), various halophilic metal salts are used to promote the activation of the halide leaving group. The most common metals include silver, cadmium and mercury which are typically used as the carbonates, oxides or perchlorates. When the triflate

Conclusions and future work

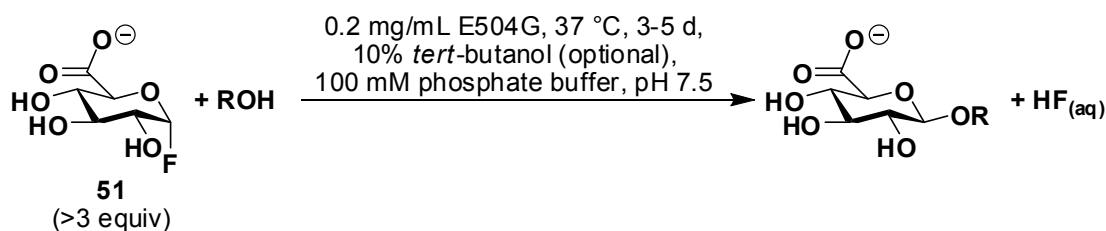
procedure is used for glucuronylation, trimethylsilyl triflate is used to silylate the anomeric alcohol of the glucuronyl donor **20** which provides a better leaving group. When the trichloroimidate glucuronyl donor **19** is used, a strong Lewis acid such as boron trifluoride etherate is used to promote the reaction. All these activators are commercially available (albeit most are expensive) or easily prepared in the laboratory within minutes.¹⁹⁵ However, these activators are moisture-sensitive so their storage stability is dependent on their exposure to water.

In terms of the complexity and duration of the preparation, the activator in the Koenigs-Knorr procedure is the simplest. The only disadvantages present are the high costs and poor stability of the Koenigs-Knorr activators. The UDP-glucuronosyltransferase is the worse activator to prepare due to the difficulties in expressing and purifying a membrane-bound enzyme that is harvested from animals. The glucuronylsynthase enzyme appears to be the most stable activator out of the glucuronylation procedures. It has a long storage stability and tolerates high temperatures and a wide range pHs over an extended amount of time. Its preparation appears to only be inferior to the Koenigs-Knorr preparation due to the time taken to express and purify the enzyme (~ 1 week). This is a small drawback that is outweighed by the many other advantages of this system.

6.1.3 The Reaction

The glucuronylation reactions can be sorted into two classes of reactions. The Koenigs-Knorr and its related reactions are a chemical synthesis approach whereas the UDP-glucuronosyltransferase and glucuronylsynthase procedures can be classed as enzyme-assisted reactions. There are pros and cons associated with each procedure which will be weighed up against the respective yields from these reactions.

The optimised conditions for the glucuronylsynthase reaction were determined in this study (Scheme 6.3). The ideal reaction conditions call for a pH 7.5 buffered solution at 37 °C for 3-5 days depending on the concentration of enzyme and turnover of the substrate (e.g. phenols and sterically-hindered alcohols react slowly). A concentration of 0.2 mg mL⁻¹ of glucuronylsynthase enzyme was frequently used in this research and found to be more than sufficient to catalyse glucuronide conjugation of any substrate within 5 days, especially at 37 °C.



Scheme 6.3. Optimised reaction conditions for the glucuronylsynthase reaction

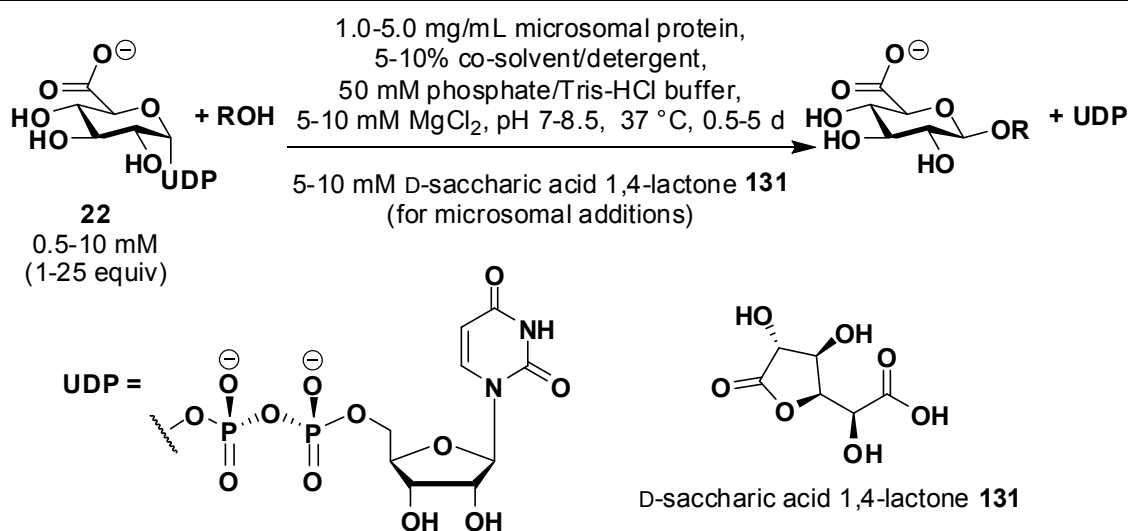
At least three equivalents of α -D-glucuronyl fluoride **51** is required to sufficiently overcome the possibility of product inhibition. From the product inhibition study on DHEA O-(carboxymethyl)oxime **116**, it was shown that >3 equivalents of α -D-glucuronyl fluoride **51** would further improve yield but by smaller quantities with each addition.

The addition of *tert*-butanol (up to 10% v/v) aids the solubility of hydrophobic substrates. However, further investigation into the effects of *tert*-butanol is needed to explain its effect on enhancing the reaction with DHEA O-(carboxymethyl)oxime **116** whilst hindering the reaction involving 2-phenylethanol **45**.

With the exception of the α -D-glucuronyl fluoride **51** hydrolysis (analogous to Scheme 3.7), no by-products have been observed in the glucuronylsynthase reaction to date. The resulting reaction mixture consists of the β -glucuronide product, glucuronic acid **3** (from the hydrolysis of α -D-glucuronyl fluoride **51**) and unreacted starting materials. The stereochemical outcome of the glucuronylsynthase reaction is stereospecific for the β -anomer as determined by its mechanism (Scheme 1.9).

The reaction conditions for the UDP-glucuronosyltransferase are very similar to the glucuronylsynthase (Scheme 6.4).^{40,190,196-199} Briefly, the UDP-glucuronosyltransferase is added to a buffered solution of alcohol and excess glucuronyl donor (UDP-glucuronic acid **22**) at 37 °C for a few days. Also essential to the reaction is magnesium chloride (activity modulator)²⁰⁰ and a co-solvent or detergent (to aid the solubility of the enzyme). DMSO is most commonly used but dimethylformamide, ethanol and Triton X-100 have also been used. When liver microsomal extracts are used, it can contain other metabolising enzymes such as cytochromes or β -glucuronidase. To maximise yields, D-saccharic acid 1,4-lactone **131** (a β -glucuronidase inhibitor) is added to the microsomal extracts.¹²⁰

Conclusions and future work



Scheme 6.4. General reaction conditions for the UDP-glucuronosyltransferase

Once again, the reaction time is dependent on the amount of enzyme added to the reaction with a typical reaction ($> 1 \text{ mg mL}^{-1}$) using over 5 times the concentration of glucuronylsynthase enzyme used (0.2 mg mL^{-1}). It is difficult to accurately compare the enzyme kinetic parameters between UDP-glucuronosyltransferase (Table 6.1) and the glucuronylsynthase enzyme (Table 6.2) due to the large number of isoforms and species from which UDP-glucuronosyltransferase can be obtained from. In addition to this, kinetic data was not available for the aglycons investigated in this research. Nevertheless, a general comparison of the kinetic parameters does provide some insight into the catalytic performance of these two enzymes. From the specific activity, it can be observed that the glucuronylsynthase catalyses the glucuronylation reaction of alkyl alcohols faster than the UDP-glucuronosyltransferase. However, UDP-glucuronosyltransferases are able to catalyse the conjugation of phenolic aglycons more rapidly. The glucuronylsynthase has a lower K_m for its glucuronyl donor ($K_m^{\text{app}} 15 \text{ }\mu\text{M}$) than UDP-glucuronosyltransferase ($K_m 260 \text{ }\mu\text{M}$). This binding affinity does not change much between different glucuronosyltransferase isoforms or between species with most Michaelis constants falling in the range of 0.2-0.7 mM.²⁰¹ It is interesting to note that the UDP-glucuronosyltransferase K_m values for the aglycon substrates are approximately three orders of magnitude lower than for glucuronylsynthase. This illustrates, once again, the role of β -glucuronidase in hydrolysing the glucuronic acid **3** residue non-selectively from a wide range of aglycons. Conversely, UDP-glucuronosyltransferases are a superfamily of enzymes with

each isoform being selective towards certain classes of aglycons. Therefore, a moderate affinity for the aglycon substrates is required for this selectivity.

Table 6.1. Examples of kinetic parameters for UDP-glucuronosyltransferase.

Substrate	Enzyme origin	K_m (mM)	Specific activity (nmol⁻¹ min⁻¹ [mg protein]⁻¹)
UDP-glucuronic acid 22 ²⁰²	Recombinant human 1A6 WT	0.26 ^{a)}	2.46 ^{a)}
phenol 52 ²⁰³	Rat liver microsome	N/A	10.6
DHEA 55 ¹⁹⁹	Recombinant human 2B7 WT	N/A	0.0021
Testosterone 7 ¹⁹⁸	Recombinant human 2B17 WT	0.010	1.0
Estrone 9 ²⁰⁴	Recombinant human 1A10 WT	0.042	7.9

^{a)} Reaction with 1-naphthol (50 mM)

Table 6.2. Kinetic parameters for the glucuronylsynthase enzyme

Substrate	K_m (mM)	Specific activity (nmol⁻¹ min⁻¹ [mg protein]⁻¹)
α -D-glucuronyl fluoride 51	0.015 ^{a)}	20.3 ^{a)}
2-phenylethanol 45	144	42.8
3-methoxybenzyl alcohol 47	43	64
4-fluorobenzyl alcohol 50	40	27
DHEA O-(carboxymethyl)oxime 116	7	32
phenol 52	20	5

^{a)} Apparent parameter from the reaction with 2-phenylethanol 45 (107 mM)

Conclusions and future work

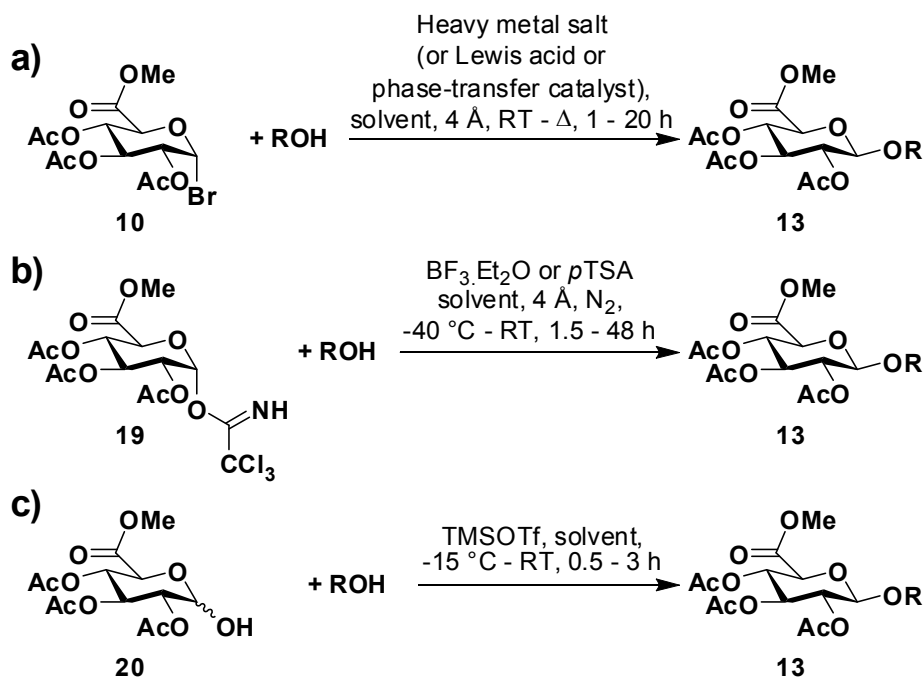
The mechanism for UDP-glucuronosyltransferase is stereospecific and involves an S_N2 reaction facilitated by the enzyme (similar to the glucuronosyltransferase mechanism).²⁰⁵ Reactions utilising pure UDP-glucuronosyltransferase do not report any by-products except for D-glucuronic acid **3** from the hydrolysis of the UDP-glucuronic acid **22**. However, when liver microsomes are used in reactions, the presence of other metabolising enzymes (such as cytochromes) can produce phase 1 by-products by oxidation (e.g. Scheme 1.1). The UDP-glucuronosyltransferase procedure requires more exertion to set-up than the glucuronosyltransferase reactions. Additional components (such as detergent, magnesium chloride and D-saccharic acid 1,4-lactone **131**) are essential for the operation of the UDP-glucuronosyltransferase compared to the glucuronosyltransferase system which only requires the substrates and buffer to operate in.

Only a small number of reaction components are required for the Koenigs-Knorr procedure. It essentially involves stirring or refluxing the glucuronyl donor and acceptor alcohol in the presence of a heavy metal salt, Lewis acid or phase-transfer catalyst (Scheme 6.5a).^{13-18,20} Despite the large range of reaction conditions, there is no generalised rule that states what conditions (i.e. which metal salts) should be used for certain substrates. Unless the reaction has been previously reported, conditions are usually chosen on a “trial-by-error” basis.

In the trichloroacetimidate procedure, the glucuronyl trichloroacetimidate **19** is stirred with the acceptor alcohol and boron trifluoride etherate under inert conditions at sub-zero to room temperatures (Scheme 6.5b).^{18,25-27} Longer and warmer reactions generally provide the α -anomer selectively (thermodynamic product), whereas short and chilled reactions are selective for β -glucuronide formation (kinetic).²⁶ The reaction conditions for the triflate procedure are similar to the imidate procedure albeit the addition of trimethylsilyl triflate to produce the activated glucuronyl donor *in situ* (Scheme 6.5c).^{18,28}

Despite the simplicity of the reaction components required, the presence of water is detrimental to the yields obtained from the Koenigs-Knorr reaction. As a result, laborious measures must be made to ensure that substrates, metal salts, solvents and glassware are all dry prior to use; an unnecessary step in the UDP-glucuronosyltransferase and glucuronosyltransferase procedures. Special

care must also be taken for the handling and disposal of the toxic heavy metals employed in this procedure.



Heavy metal salt: AgOTf, Ag₂O, Ag₂CO₃, AgNO₃, AgClO₄, CdCO₃, HgI₂, HgCl₂, HgBr₂, Hg(CN)₂

Lewis acids: Sn(OTf)₂, Sn(OTf)-collidine, Sn(OTf)₂·TMU, SnCl₄, TrCl·ZnCl₂

Phase-transfer catalysts: (Bu₄N)Br, (Et₃NCH₂Ph)Br, (Et₃NCH₂Ph)Cl

Solvent: dichloromethane, cyclohexane, petroleum ether, benzene, dichloroethane, toluene

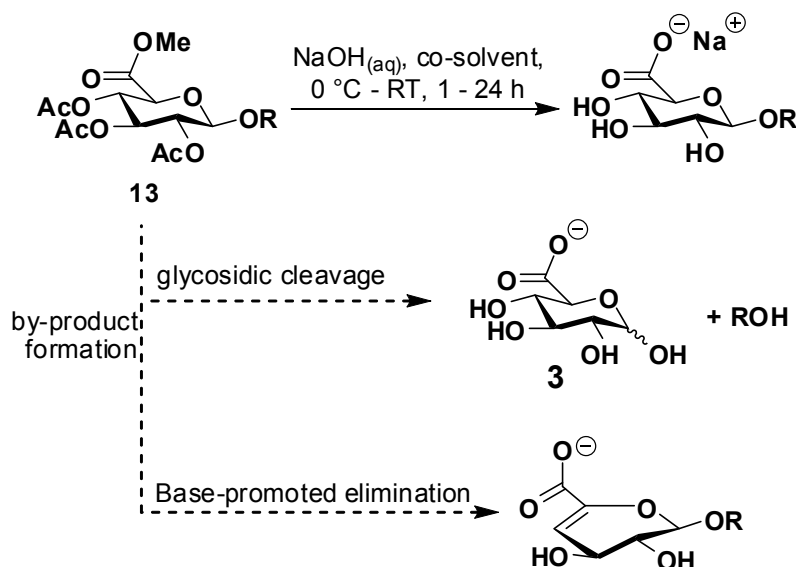
Scheme 6.5. General procedures for the a) Koenigs-Knorr, b) trichloroacetimidate and c) triflate glucuronylation reactions.

Unlike the stereospecific mechanism of the enzyme-assisted glucuronylation procedure, the Koenigs-Knorr reaction (and its derivatives) is only stereoselective (Scheme 1.4).²¹ The α linkage can result from the S_N1 pathway and the presence of anchimeric assistance can lead to a formation of the ortho ester **17** by-product. The profusion of mechanistic pathways is responsible for the majority of low yields reported for the Koenigs-Knorr reaction. The overall yield of the glucuronide product is reduced further by a deprotection step that is not present for the enzyme-assisted procedures.

The deprotection step generally involves saponification of acyl-protecting groups in a water-miscible solvent, such as methanol or ethanol, to aid the solubility of the protected glucuronide (Scheme 6.6).^{13-16,20,25,27,206} Dilute concentrations of hydroxide and low temperatures are used to prevent hydrolysis of the glycosidic linkage and/or base promoted elimination within the pyranose ring. The extra step in the Koenigs-Knorr reaction means that 2-3 days are required to go from the steroid aglycon to the final steroid glucuronide.

Conclusions and future work

Therefore, the Koenigs-Knorr and enzyme-mediated glucuronylation procedures are similar in preparation time.



Scheme 6.6. Saponification of the glucuronide triacetate **13** and possible side-reactions.

Possibly the most important factor to compare amongst the different glucuronylation procedures is the reaction yield. The yields obtained from the glucuronylation of various steroids (With the exception of estrone **9**, the UDP-glucuronosyltransferase provided consistently good yields (77%). However, it is important to note that in each UDP-glucuronosyltransferase synthesis that less than 10 mg of product is obtained which illustrates a major limitation of this procedure. The yields of the Koenigs-Knorr reaction are reported as yields over two steps and rarely achieve yields greater than 50%. This is due to the production of by-products (such as the ortho ester **17**) formed in the reaction (Scheme 1.4) and the additional deprotection step required after conjugation.

Table 6.3) were compared due to the lack of data available for the simple alcohols. The glucuronylsynthase provides the highest yields for the direct glucuronylsynthesis of DHEA **55** and epiandrosterone **56**. However, the yields for the more sterically hindered 17-positioned steroids were either on par with the other procedures (e.g. testosterone **7** and epitestosterone **123**) or worse off (e.g. nandrolone **108** and boldenone **118**). The yield of nandrolone β -D-glucuronide **110** was obtained from un-optimised conditions. The yield of epiandrosterone β -D-glucuronide **109** almost doubled (from 21% to 38%) when subjected to the optimised conditions. Alternatively, the use of the 3-step solubility strategy vastly improved the yields of DHEA **55** and testosterone **7**

and would be envisaged to have the same effects on the other 17-hydroxy steroid series.

With the exception of estrone **9**, the UDP-glucuronosyltransferase provided consistently good yields (77%). However, it is important to note that in each UDP-glucuronosyltransferase synthesis that less than 10 mg of product is obtained which illustrates a major limitation of this procedure. The yields of the Koenigs-Knorr reaction are reported as yields over two steps and rarely achieve yields greater than 50%. This is due to the production of by-products (such as the ortho ester **17**) formed in the reaction (Scheme 1.4) and the additional deprotection step required after conjugation.

Table 6.3. Yields for the glucuronylation of various steroid aglycons using different glucuronylation procedures.

Substrate	yields (%)		
	direct glucuronylsynthase	UDP-glucuronosyltransferase	Koenigs-Knorr ^a
DHEA 55	71% (86%) ^b	N/A	20% ²⁰
testosterone 7	12% (69%) ^b	77% (6.5 mg) ^{d,196}	17% ²⁰
epiandrosterone 56	21% (38%) ^c	N/A	19% ¹³
nandrolone 108	6%	77% (3.5 mg) ^{d,196}	N/A
estrone 9	24% ^c	17% ²⁰⁷	45% ¹⁴ (39%) ^{e,27}
epitestosterone 123	38% ^c	N/A	21-41% ²⁰⁶
boldenone 118	15% ^c	N/A	77% ¹⁶

^{a)} Yield over two steps; ^{b)} yield from 3-step solubility strategy; ^{c)} yield from HPLC trace; ^{d)} isolated mass; e) yield obtained from the trichloroimidate procedure.

The three glucuronylation procedures (glucuronylsynthase, UDP-glucuronosyltransferase and Koenigs-Knorr) were reviewed on their use for glucuronide preparation. The procedures were scrutinised from substrate costs and preparation through to reaction procedures and yield. Overall, it appears the glucuronylsynthase has many advantages over the alternative means of glucuronylation. The substrates and enzyme are easier to prepare than the UDP-glucuronosyltransferase procedure and it can be scaled up to multi-gram scale. The reaction conditions for the glucuronylsynthase reaction are milder

Conclusions and future work

and safer than the Koenigs-Knorr reaction which allows recovery of unconsumed starting material and avoids the additional deprotection step afterwards. But possibly the most significant advantage is the large diversity of substrates that have been applied without the need of modifying the reaction conditions albeit the addition of *tert*-butanol to aid solubility. The glucuronylsynthase has matched and surpassed the attractive attributes of these procedures and secured its role as a novel procedure for glucuronide synthesis.

6.2 Conclusions

The glucuronylsynthase is the latest glycosynthase engineered from the *E. coli* β -glucuronidase. The methodology for its expression and its application in glucuronylsynthase reactions was developed and optimised in this study. This was achieved through enzyme kinetic investigations performed with HPLC.

The enzyme kinetic studies (chapter 3.5) revealed a low K_m^{app} for the α -D-glucuronyl fluoride **51** (15 μM) and higher K_m (millimolar) for the alcohol acceptors. The presence of substrate inhibition was observed for all acceptor substrates except for 2-phenylethanol **45**. In addition to this, mixed predominately competitive product inhibition (K_{ic} 71 μM , K_{iu} 190 μM) was observed in the 2-phenylethanol **45** glucuronylsynthase reaction with DHEA O-(carboxymethyl)oxime β -D-glucuronide **118** as the inhibitor (chapter 4.6). The inhibition is two orders of magnitude stronger than the estimated substrate inhibition constant for DHEA O-(carboxymethyl)oxime **116** alone (K_{si} 0.1 mM). This is consistent with the β -glucuronidase's substrate promiscuity. The primary recognition of a glucuronide conjugate by β -glucuronidase is expected for the target carbohydrate moiety over the variable aglycon portion. Overcoming this predominately competitive product inhibition and maintaining high concentrations of α -D-glucuronyl fluoride **51** ($>K_m^{\text{app}}$) saw yields for the glucuronylation of DHEA O-(carboxymethyl)oxime **116** (section 4.5.2) rise dramatically from 48% (1 equiv) to 98% (5 equiv).

Further optimisation of the glucuronylsynthase reaction was achieved by scrutinising the reaction variables (chapter 3.6 and 5.2). The effect of reaction pH, temperature enzyme concentration and additives in the glucuronylsynthase kinetics were investigated by enzyme kinetics. The results of the study were

combined to develop the ideal reaction conditions for the glucuronylsynthase reaction (Scheme 6.3). The optimisation of reaction variables saw a marked improvement in yields. For example, phenyl β -D-glucuronide **76** was isolated in 43% yield compared to the previously un-optimised reaction yield of 13% and epiandrosterone **56** obtained in 38% HPLC yield from its un-optimised yield of 21%.

With a deeper understanding of the enzyme kinetics and the optimised conditions identified, the research was directed towards the glucuronylsynthesis of steroids which is the anticipated role for this enzyme in industry. The glucuronides of DHEA **55**, epiandrosterone **56**, testosterone **7**, and nandrolone **108** were successfully synthesised from glucuronylsynthase reactions (chapter 4.2). But the solubility of steroids in water required high concentrations of co-solvents or detergents which were harmful to the enzyme and very dilute reactions which required large quantities of enzyme. To overcome this problem, the steroids were made more water soluble through a temporary chemical modification.

Carboxymethoxylamine **115** was reacted with DHEA **55** and testosterone **7** to synthesise ionisable oxime analogues that were 100 and 500 times more water soluble than the parent steroid respectively (chapters 4.3 and 4.7). These steroid oximes were then subjected to glucuronylsynthase reactions under optimised conditions to achieve 98% yield of the DHEA O-(carboxymethyl)oxime β -D-glucuronide **118** and 72% yield of the testosterone O-(carboxymethyl)oxime β -D-glucuronide **121**. The oxime moiety was removed via a titanium(III)-mediated reduction of the N-O bond in the presence of the glucuronyl residue. The subsequent imine was hydrolysed *in situ* to form the DHEA β -D-glucuronide **77** in quantitative yields, but the testosterone β -D-glucuronide **6** in only 38% yield (81% brsm).

With the optimised reaction conditions determined for steroid glucuronylsynthesis, a small screen was trailed with the glucuronylsynthase enzyme (chapter 5.4). Solid phase extraction was used to quickly isolate the products from this screen. The screen contained steroids of different structural configurations, including phenols, pyrazoles and diols. Evidence of glucuronide formation was observed for all of the steroids subjected to the screen.

The growing substrate repertoire demonstrates the universal application of the glucuronylsynthase enzyme which is one of many aspects that makes it such an

Conclusions and future work

attractive method of glucuronylation. Another important attribute is the scalability of the reaction which was demonstrated by the large scale glucuronysynthesis on 2-phenylethanol **45** (300 mg, refer to section 2.5.2) and DHEA O-(carboxymethyl)oxime **116** (500 mg, refer to section 4.3.3). In many ways, the glucuronysynthase surpasses the attributes of the alternative means of glucuronylation and simultaneously overcomes many of their downfalls.

6.3 Future work

This research determined the optimised reaction conditions for the glucuronysynthase reactions (Scheme 6.3). It would be valuable to repeat the glucuronysynthase reactions on previously attempted substrates to see what improvement could be made on the un-optimised yields. In addition to this, the optimised conditions could be used to expand the collection of substrates that successfully undergo the glucuronysynthase reaction. Glucuronide formation was observed for all substrates involved in the small steroid screen (although no yield was determined for some of the steroids). A larger library will present the true value of the glucuronysynthase system in terms of its universal application as well as pose any limitations the procedure may have. The reaction with pharmaceutical substrates could also be re-explored with the glucuronysynthesis of morphine **2**, codeine **1** and chloramphenicol **87** producing no glucuronide under un-optimised conditions.

During the reaction optimisation with additives, the use of *tert*-butanol was determined to aid the solubility of hydrophobic substrates (chapter 5.2). It also demonstrated an unusual effect of enhancing the reaction rate for DHEA O-(carboxymethyl)oxime **116** glucuronysynthesis. It is still unknown whether *tert*-butanol imparts allosteric activation, represses substrate inhibition or has another role altogether at enhancing the reaction rate. Temperature was another variable changed in these investigations (21 °C vs. 37 °C) and may be responsible for the apparent altered kinetic parameters. Further investigations into the effects of *tert*-butanol and temperature on the glucuronysynthase reactions needs to be explored with a kinetic study.

The existence of product inhibition by DHEA O-(carboxymethyl)oxime β -D-glucuronide **118** in the 2-phenylethanol **45** glucuronysynthase reaction was proven in this research (refer to section 4.6.2). The yields achieved in the glucuronysynthase reactions using one equivalent of α -D-glucuronyl fluoride **51**

may be related to the binding affinity of the product. This could be investigated by the addition of the glucuronides derived from other alcohols (e.g. 3-methoxybenzyl alcohol **47** and 4-fluorobenzyl alcohol **50**) to a single glucuronylsynthase reaction (e.g. DHEA *O*-(carboxymethyl)oxime **116** or 2-phenylethanol **45** glucuronylsynthase reaction) to indirectly investigate the existence and extent of product inhibition. A relationship may exist between the binding affinity of the product (K_i) and the yield of the reactions given a single equivalent of α -D-glucuronyl fluoride **51**.

A simple means of detecting product inhibition would also be to repeat the same glucuronylsynthase reaction with increasing quantities of α -D-glucuronyl fluoride **51** and determine the yield from each (analogous to section 4.5.2). This would not provide the inhibition parameters but would provide a pointer toward competitive product inhibition that would warrant further investigation.

A three step steroid solubilisation strategy was developed that improved the overall synthesis of DHEA β -D-glucuronide **77** and testosterone β -D-glucuronide **6** (chapters 4.3 and 4.7). The synthesis sequence worked well for DHEA **55**, but the de-oximation of testosterone *O*-(carboxymethyl)oxime β -D-glucuronide **121** did not go to completion. Oxidation of titanium(III) was observed over the extended reaction time needed to cleave the oxime moiety. A greater excess of titanium(III) may be needed or its continuous addition over time may improve conversions. Alternately, improved reaction conditions such as the degassing of solvents, the use of argon gas or optimising the buffer concentration and pH may help reduce the degradation of titanium(III). Optimisation of this step will drastically improve the synthesis of testosterone β -D-glucuronide **6** via the three step steroid sequence.

The largest problem that exists for the glucuronylsynthase is its slow catalytic turnover. Despite its apparent catalytic superiority over UDP-glucuronosyltransferase (refer to section 6.1.3), the glucuronylsynthase is possibly the slowest glycosynthase reported to date. Reaction times extend for days for a glucuronylsynthase reaction unless large quantities of enzyme are used. The 3-methoxybenzyl alcohol **47** glucuronylsynthase recorded the fastest observed catalytic turnover of only 0.023 s^{-1} .

Previously reported glycosynthase activities have been improved through the use of directed evolution.^{91,96,121,124,134} Progress has already been made in this field with multiple high-throughput assays already been developed and trialled.

Conclusions and future work

Assays such as the fluoride-selective assay (refer to section 3.7.4) and the pH-dependent assay (refer to section 3.7.5) failed to work due to the minute amount of enzyme activity available in the cell lysate studies. Future work involves the directed evolution of the WT β -glucuronidase which has an appreciable and readily detectable activity. Site-directed mutagenesis of the catalytic residue would then be applied to the evolved WT gene to create the glucuronylsynthase gene. A marginally improved glucuronylsynthase enzyme could then be subjected to previously attempted directed evolution to improve the activity further. The ELISA assay (refer to section 3.7.6) is also an option but requires extensive biochemical procedures to develop the antibodies for the assay.

Further to this molecular biology work, the enzyme crystal structure of β -glucuronidase and glucuronylsynthase has not been determined. The crystal structure would help rationalise the findings in the mutagenic studies as well as provide structure-activity relationships to determine why some substrates react better than others. Attempts at growing an enzyme crystal (chapter 1.1) has achieved no sizable crystal to date.

The yields of the glucuronylsynthase reactions are continually improving as more is understood about the glucuronylsynthase system such as the findings presented in this research. Enzyme kinetic studies and complimentary strategies, such as the three step steroid solubilisation strategy, have aided the yields of steroid glucuronylation with the glucuronylsynthase enzyme. The future success of the enzyme relies on the improved catalytic turnover through the use of directed evolution technology. This would lead to more efficient syntheses and increased accessibility of glucuronide conjugates required in analytical studies such as sports drug testing and the pharmaceutical industry. The glucuronylsynthase shows great promise for the rapid synthesis of a variety of known glucuronide conjugates and those not yet obtainable via current methodologies.

~ Chapter 7 ~

Experimental

7.1 General Experimental

7.1.1 Equipment

Melting points were determined using a Reichart heating stage with microscope (USyd) or an Optimelt Automated Melting Point System MPA100 (ANU) and are uncorrected.

Optical activity was measured on a PolAAR 2001 polarimeter (USyd) or Perkin-Elmer Polarimeter 241MC (ANU) set at the 589.3 nm sodium D line, in a 0.25 dm or 1.00 dm cell. Data is expressed as $[\alpha]_D^T$ R (C, S), where T is temperature (°C), R is the calculated degree of rotation (10^{-1} deg $\text{cm}^2 \text{g}^{-1}$), C is the concentration of solution ($\text{g } 100 \text{ mL}^{-1}$), and S is the solvent used.

Infrared absorption (IR) spectra were obtained using with a Biorad FTS-40 series (USyd), Perkin Elmer 1600 series (USyd) or Perkin-Elmer Spectrum One (ANU) FTIR spectrometer. Compounds were homogenised (10% w/w) in anhydrous potassium bromide and measured directly from IR cups (KBr powder) or pressed into a disc (KBr disc). Alternatively, the compound was dried as a thin film onto sodium chloride plates (NaCl). Significant absorbance bands are reported in wavenumbers (cm^{-1}) and are described by the abbreviations: br = broad, s = strong, m = medium, w = weak. Where applicable, bands are also assigned their respective functional group.

^1H Nuclear Magnetic Resonance (^1H NMR) spectra were obtained on a Bruker Avance 200 (200 MHz, USyd), Bruker Avance 300 (300 MHz, USyd), Mercury 300 (300 MHz, ANU), Mercury 400 (400 MHz, ANU) or Bruker Avance 800 (800 MHz, ANU) at 300 K unless otherwise stated. Chemical shift data is expressed in ppm relative to $\delta_{\text{TMS}} = 0$, using residual protons in deuterated solvent as an internal reference. The data is reported as chemical shift (δ), relative integral, multiplicity (s = singlet, d = doublet, dd = doublet of doublets, ddd = doublet of doublet of doublets, dt = doublet of triplets, quint = quintet, m = multiplet), coupling constant(s) (J Hz) and assignment. All multiplicities and coupling constants are apparent.

^{13}C Nuclear Magnetic Resonance (^{13}C NMR) spectra were obtained on a Bruker Avance 200 (50 MHz, USyd), Bruker Avance 300 (75 MHz, USyd), Mercury 300 (75 MHz, ANU), Mercury 400 (100 MHz, ANU) or Bruker Avance 800 (200 MHz, ANU) at 300 K with complete proton decoupling unless otherwise stated. Chemical shift data is expressed in ppm relative to $\delta_{\text{TMS}} = 0$,

using deuterated solvent as an internal reference. ^{13}C spectra acquired in deuterium oxide were calibrated by the addition of a drop of methanol. The data is reported as chemical shift (δ) and assignment. Heteronuclear ^{13}C - ^{19}F coupling, where present, are denoted with multiplicity (d = doublet) and coupling constant (J Hz). The protonicity (CH_3 = primary, CH_2 = secondary, CH = tertiary, C_q = quaternary carbon) is provided where supported by a DEPT135 experiment.

Low resolution mass spectra (LRMS) was obtained from a ThermoQuest Finnigan LCQ Deca ion trap (USyd) or Micromass–Waters LC-ZMD single-stage quadrupole (ANU) mass spectrometer with electro-spray ionisation in either positive (+ESI) or negative (-ESI) mode. A VG Autospec Quattro II triple quadrupole mass spectrometer (ANU) was used to obtain electron impact spectra. Data is expressed as observed mass (m/z), assignment (M = molecular ion), and relative intensity (%).

High resolution mass spectroscopy (HRMS) was recorded on a Spectrospin 7T FTICR (UNSW) or Waters LCT Premier XE (ANU) mass spectrometer, using positive (+ESI) or negative (-ESI) electro-spray ionisation. Data is expressed as observed mass (m/z), assignment (M = molecular ion), and relative intensity (%).

Elemental analysis was determined using a Carlo Erba CE1106 automatic analyser (carbon, hydrogen and nitrogen), Diowex DX-120 ion-chromatograph (sulfur) and Varian spectraAA-30 (metals) and are uncorrected.

Isothermal Titration Calorimetry (ITC) experiments were performed on a MicroCal VP-ITC® Microcalorimeter. MicroCal® Origin software was used to determine the equilibrium constant (K_A). Solutions were made with identical degassed buffer.

Fast Protein Liquid Chromatography (FPLC) for protein purification was performed on a Waters ATKA purifier 10 series equipped with a P-900 pump, UV-900 UV detector (280 nm) and Frac-900 Fractionator. Eluting solvents and samples were filtered through a 0.45 μm membrane prior to use.

Centrifugal filtration was performed with Millipore Amicon Ultra 15 mL 10,000 MW cut-off centrifugal filter devices centrifuged at 5000g until acquiring the appropriate volume.

SDS-PAGE was run at 40 mV for ~3 h in glycine running buffer. Mark 12 wide-range protein standard was used as a reference standard. The gel was

Experimental

stained with glycine “Coomassie Blue” gel stain (1 h) then de-stained with glycine destain solution.

High Performance Liquid Chromatography with Ultra Violet detection (HPLC-UV) for the glucuronylsynthase assay was performed on Waters 2695 Separations module equipped with the Waters Alliance Series Column Heater (set at 30 °C) and Water 2996 Photodiode Array (PDA) Detector. Data acquisition and processing was performed with the Waters Empower 2 software.

UV spectroscopy was performed on a Cary 1 UV-VIS spectrometer set at 280 nm using Eppendorf UVettes with a path length of 1 cm. Enzyme solutions were centrifuged at 12,000 rpm for two minutes prior to reading.

Fluorescence was performed on a Cary Eclipse spectrometer with quartz cuvettes and at ambient temperatures. Fluorescence was measured using the Cary Eclipse Kinetics Application version 1.1.

Analytical thin layer chromatography (TLC) was performed using 0.2 mm thick, aluminium-backed, pre-coated silica gel plates (Merck Silica gel 60 F₂₅₄). Compounds were visualised by short and long wavelength ultra-violet fluorescence and by staining with 10% sulfuric acid in methanol or Goofy’s dip (15 g phosphomolybdic acid, 15 mL conc. sulfuric acid, 485 mL water and 2.5 g cerium sulfate).

Normal-phase Flash chromatography was performed using Merck Silica gel 60 (230 – 400 mesh ASTM), under a positive pressure of nitrogen, with the indicated solvents. Solvent compositions were mixed volume per volume (v/v) as specified.

Reversed-phase Flash Chromatography was performed with Davisil C18 silica (cat #633NC18E), under a positive pressure of air, with the indicated solvents. Solvent compositions were mixed volume per volume (v/v) as specified.

Ion exchange chromatography was performed using Dowex 1x8, 200-400, MeshCI resin. All solutions were made from MilliQ water and the resin was re-conditioned before every use. Resin was re-conditioned with 1 M hydrochloric acid (2 column volumes), then water until neutral, 1 M sodium hydroxide (2 column volumes), then water until neutral, 1 M ammonium bicarbonate (2 column volumes), then finally water (≥ 5 column volumes).

Evaporation or concentration under reduced pressure refers to evaporation using a rotary evaporator connected to a vacuum pump. Removal of residual

solvent when necessary was achieved by evacuation (0.01 - 0.1 mm Hg) with a high stage oil sealed vacuum pump.

All solvents and reagents were dried and purified when necessary according to published standard procedures.¹⁹⁵ Hexanes refers to hexanes (bp 65 – 69 °C) and brine refers to saturated aqueous sodium chloride solution. Moisture sensitive reactions were carried out in oven dried glassware under a dry inert atmosphere of nitrogen or argon. Reaction temperatures were controlled using ice : water (0 – 5 °C) cooling baths or oil heating baths (> room temperature). Room temperature ranges from 18-25 °C.

7.1.2 Biochemical solutions

Formulae for biochemical solutions are as follows. Solutions are made with MilliQ water with % concentration in g (100 mL)⁻¹ unless otherwise stated.

Binding Buffer

Sodium dihydrogen phosphate (20 mM), sodium chloride (0.5 M), imidazole (20 mM), MilliQ water, adjusted to pH 7.4.

Bromophenol Blue (BPB) loading buffer

Bromophenol blue (0.05%), glycerol (75%), Tris buffer (2.5 mM, pH 8.0)

Buffer H (10X)

Tris-HCl (0.5 M), sodium chloride (1 M), magnesium chloride (100 mM), dithioerythritol (10 mM), pH 7.5 (at 37 °C).

Eluting Buffer

Sodium phosphate (20 mM), sodium chloride (0.5 M), imidazole (500 mM), MilliQ water, adjusted to pH 7.4.

Extraction Buffer

Sodium dihydrogen phosphate (50 mM), β-mercaptoethanol (10 mM), Triton X-100 (0.1%), water (MilliQ), adjusted to pH 7.4.

Glycine “Coomassie Blue” Gel Stain

Coomassie Brilliant Blue R (0.125%), methanol (40% v/v), acetic acid (7% v/v), water (MilliQ).

Experimental

Glycine Destain Solution

Acetic acid (10% v/v), methanol (30% v/v), water (MilliQ).

Glycine Running Buffer

Tris Buffer (0.25 M), glycine (1.92 M), sodium dodecyl sulfate (SDS, 1%), water (MilliQ), adjusted to pH 8.3.

Glycine SDS-PAGE Resolving Gel

Acrylamide (15%), Tris buffer pH 8.8 (0.36 M), sodium dodecyl sulfate (SDS, 0.10%), ammonium persulfate (APS, 0.05%), water (MilliQ), *N,N,N',N'*-tetramethylethylenediamine (TEMED, 0.10%).

Glycine SDS-PAGE Stacking Gel

Acrylamide (4%), Tris buffer pH 8.8 (0.19 M), sodium dodecyl sulfate (SDS, 0.05%), ammonium persulfate (APS, 0.03%), water (MilliQ), *N,N,N',N'*-tetramethylethylenediamine (TEMED, 0.07%).

KCM

Potassium chloride (100 mM), calcium chloride (30 mM), magnesium chloride (50 mM)

Luria Burtani (LB) Media

Peptone (1%), yeast extract (0.5%), sodium chloride (0.5%), water (MilliQ).

Luria Burtani (LB) Agar Media

Agar (1.5%), peptone (1%), yeast extract (0.5%), sodium chloride (0.5%), water (MilliQ).

Luria Burtani with Kanamycin **78** (LB_{kan}) Media

Peptone (1%), yeast extract (0.5%), sodium chloride (0.5%), kanamycin **78** (0.005%), water (MilliQ).

Lysis Buffer

Tris buffer pH 8.0 (50 mM), sodium chloride (50 mM), Triton X-100 (1%), phenylmethanesulfonyl fluoride (PMSF, 1.4 mM), β -mercaptoethanol (1.4 mM), water (MilliQ).

Phosphate Buffered Saline (PBS) Buffer

Sodium chloride (0.8%), potassium chloride (0.02%), sodium hydrogen phosphate (0.144%), potassium dihydrogen phosphate (0.024%), water (MilliQ), adjusted to pH 7.4, autoclaved.

Resuspension buffer

LB media (pH 6.1), PEG 3350 or PEG 8000 (10%), DMSO (5% v/v), magnesium chloride (10 mM), magnesium sulfate (10 mM), glycerol (10%).

SDS-PAGE Loading Buffer (Glycine Gel)

Tris buffer pH 6.8 (0.31 M), sodium dodecyl sulfate (SDS, 10%), glycerol (50%), β -mercaptoethanol (25%), bromophenol blue (0.5%), water (MilliQ).

SOC Media

Yeast (0.5%), tryptone (2%), sodium chloride (10 mM), potassium chloride (2.5 mM), magnesium chloride (10 mM), magnesium sulfate (10 mM), autoclaved, then glucose **82** (20 mM).

Sodium Borate Buffer

Sodium hydroxide (0.04%), boric acid (0.225%)

YenB Media

Yeast extract (0.75%), nutrient broth (0.8%), water (MilliQ).

7.2 Glucuronylsynthase expression

7.2.1 DNA SDS-PAGE

The DNA sodium dodecylsulfate-polyacrylamide gel electrophoresis (SDS-PAGE) gels were prepared by using heat and stirring to dissolve agarose (0.8% w/v) in sodium borate buffer (refer to section 7.1.2). Once the molten agarose had cooled to pouring temperature (50-55 °C), ethidium bromide (final concentration 5 $\mu\text{g mL}^{-1}$) was added. Gels were poured onto 125 mm wide by 80 mm long flat glass plates, with surface tension allowing gels of up to 5 mm thickness to be cast. Wells (5mm wide x 1 mm long x 4 mm deep) were cast with a 20-lane comb during the pouring process, resulting in wells capable of holding 15 μL of sample. Samples (7.5 μL) were prepared for loading by the addition of Bromophenol Blue (BPB) loading buffer (2.5 μL , 3.3) unless otherwise stated. A 1 kB DNA ladder (New England Biolabs) was used as a

Experimental

standard and prepared to the manufacturer's instructions by dilution with BPB loading buffer.

Electrophoresis occurred with the gel slightly submerged in sodium borate buffer (refer to section 7.1.2) in a Wide Mini Sub tank at a constant current of 150 mA and voltage of 150 V. DNA was visualised by use of 254 nm UV light and images captured by UVI Pro electronic photography system.

7.2.2 Protein SDS-PAGE

The protein SDS-PAGE protocol²⁰⁸ consisted of hand-casted mini-gels (0.75 mm) with a 50 mm glycine SDS-PAGE resolving gel region (refer to section 7.1.2) and a 10 mm glycine SDS-PAGE stacking gel region (refer to section 7.1.2).

The acrylamide, Tris buffer pH 8.8, and sodium dodecyl sulfate, were prepared in advanced and stored at 4°C with fresh batches made monthly. Polymerisation of the gel was initiated by the addition of ammonium persulfate (APS) and N,N,N',N'-tetramethylethylenediamine (TEMED).

Gels were cast with either 10 or 15 lanes. When cast with 10 lanes each lane was approximately 5 mm wide and was loaded with 15 μL of sample. In 15 lane gels each lanes was approximately 3.5 mm wide and was loaded with 10 μL of sample.

The low-range molecular weight standard (Bio-Rad) provided 100 ng μL^{-1} of protein in each of six bands: 97.4, 66.2, 45.0, 31.0, 21.5 and 14.4 kDa. Alternatively, the Mark 12TM wide-range protein standard (Invitrogen) provided twelve bands: 200, 116.3, 97.4, 66.3, 55.4, 36.5, 31.0, 21.5, 14.4, 6.0, 3.5, and 2.5 kDa. Protein standards were prepared according to manufacturers instructions.

Gels were immersed in glycine running buffer (refer to section 7.1.2) in water-cooled Mighty Small gel tanks with a current maintained at 40 mV (~3 h). The gel was stained with glycine "Coomassie Blue" gel stain (1 h, refer to section 7.1.2) then de-stained with glycine destain solution (refer to section 7.1.2).

7.2.3 Optical Density Measurements

The optical density to determine culture size was performed at 600 nm ($A_{600\text{nm}}$). For the pre-induction aliquots, the $A_{600\text{nm}}$ was measured on the

undiluted aliquot. The post-induction samples underwent a 1:4 dilution with LB media prior to the $A_{600\text{nm}}$ measurement.

7.2.4 Determining protein concentration

Enzyme concentrations were estimated from UV absorption (280 nm) using the extinction coefficient of wild-type *E. coli* β -glucuronidase ($\epsilon = 2.049 \text{ (mg mL}^{-1}\text{)}^{-1} \text{ cm}^{-1}$).²⁰⁹ Concentrations were determined from assays run as duplicates or triplicates.

7.2.5 Selection for the recombinant *E. coli*

LB agar media (100 mL, refer to section 7.1.2) was autoclaved then allowed to cool to $\sim 55 \text{ }^\circ\text{C}$ at which point kanamycin **78** (100 μL , 50 mg mL^{-1}), X-gluc **79** (8 mg), and IPTG **81** (1 M, 50 μL) were added. The media was immediately distributed into four Petri dishes and allowed to cool. The four GMS407(DE3) *E. coli* strains with the recombinant glucuronidase enzyme (E504A, E504G, E504S, and WT) were streaked separately onto each of the dishes which were then incubated ($37 \text{ }^\circ\text{C}$) overnight. The WT strain was selected from a blue-coloured colony whilst the E504A, E504G, and E504S mutants were selected from colonies free from blue discoloration.

7.2.6 Heat-shock competent cells general procedure

A single host colony is picked from an LB AGAR plate (refer to section 7.1.2) and grown overnight ($37 \text{ }^\circ\text{C}$) in sterile LB media (10 mL, refer to section 7.1.2). An aliquot of the overnight broth (4 mL) was used to inoculate SOC media (400 mL, refer to section 7.1.2) and the culture grown ($37 \text{ }^\circ\text{C}$) to A_{600} 0.4. All subsequent steps were undertaken at $4 \text{ }^\circ\text{C}$. The culture was centrifuged (4000 rpm, 5 min, $4 \text{ }^\circ\text{C}$) with the cell pellet resuspended in a resuspension buffer (20 mL, refer to section 7.1.2). The resuspended culture was distributed into aliquots (220 μL), snap-frozen with liquid nitrogen and stored at $-80 \text{ }^\circ\text{C}$ until transformation.

7.2.7 Heat-shock general procedure

Heat-shock competent *E. coli* host cells (50 μL , refer to section 7.2.6) were thawed on ice then added to concentrated pET28a(+) vector (1 μL) in KCM (50 μL , refer to section 7.1.2). The solution was mixed gently and kept on ice (15 min) before subjecting to heat shock ($42 \text{ }^\circ\text{C}$, 90 s). LB media (200 μL , refer to section 7.1.2) was immediately added to the culture and then incubated ($37 \text{ }^\circ\text{C}$,

Experimental

1 h) without agitation. The culture was plated on LB agar plates (refer to section 7.2.5) with a sterile loop and incubated (37 °C) overnight.

7.2.8 Electro-competent cells general procedure⁶³

A single host colony is picked from an LB AGAR plate (refer to section 7.1.2) and grown overnight (37 °C) in sterile YENB media (2 mL, refer to section 7.1.2). An aliquot of the overnight broth (1 mL) was used to inoculate YENB media (100 mL, refer to section 7.1.2) and the culture grown (37 °C) to A₆₀₀ 0.8 (~3 h). All steps subsequent were undertaken at 4 °C. Cells were harvested by centrifugation (4,000 g, 10 min, 4 °C) with the cell pellet washed with water (2 x 40 mL) then sterile glycerol (10% v/v, 40 mL). The cell pellet was resuspended in a sterile glycerol (10% v/v, 200 µL), distributed into aliquots (50 µL), snap-frozen with liquid nitrogen and stored at -80 °C until transformation.

7.2.9 Electroporation transformation general procedure

Electro-competent *E. coli* host cells (50 µL, refer to section 7.2.6) were thawed on ice before the addition of concentrated pET28a(+)-E504G vector (1 µL). The mixture was left to stand (1 min) before being transferred into a 0.2 mm electrode cuvette and subjected to an electric field potential (2.5 kV, 5 ms) using a Micropulser.

YENB media (1 mL, refer to section 7.1.2) was immediately added to the cells which were then incubated (37 °C, 1 h) without agitation. Cells were streaked onto LB agar plates (refer to section 7.2.5) with a sterile loop and incubated (37 °C) overnight.

7.2.10 Plasmid Amplification in *E. coli* NEB5α cells

The pET28a(+)-E504G vector (0.5 µL) was diluted with water (25 µL) before its addition to *E. coli* NEB5α [fhuA2Δ(argF-lacZ)U169 phoA glnV44 Φ80 Δ(lacZ)M15 gyrA96 recA1 relA1 endA1 thi-1 hsdR17] cells (40 µL) in 10% glycerol. The cells were transformed via electroporation (4.2.5). A single colony from the agar plate was used to inoculate sterile LB_{kan} media (2 mL, refer to section 7.1.2) which was then incubated (37 °C) overnight. The culture was centrifuged (13000 rpm, 2 min) and the supernatant was removed. Plasmid was isolated and purified using a QIAprep Spin Miniprep Kit (Qiagen) as per the manufacturer's instructions.²¹⁰

7.2.11 Plasmid sequencing

A single digestion solution was created by combining Buffer H (10X, 1 μ L, refer to section 7.1.2), XhoI restriction enzyme (0.5 μ L, Roche) and water (3.5 μ L). A double digestion solution was created by combining Buffer H (10X, 1 μ L, refer to section 7.1.2), XhoI restriction enzyme (0.5 μ L, Roche), NdeI restriction enzyme (0.5 μ L, Roche) and water (3 μ L). Concentrated plasmid (5 μ L, refer to section 7.2.10) was combined with a single digestion mixture (5 μ L) or double digestion mixture (5 μ L) and incubated (37 °C) for 2 h. The reaction was ceased by the addition of Bromophenol Blue (BPB) loading buffer (2 μ L, refer to section 7.1.2). The samples were subjected to DNA SDS-PAGE (refer to section 7.2.1). Single digestion lanes showed a single band at approximately 6 kB. Double digestion lanes exhibited a band at 5 kB and 1-2 kB.

7.2.12 Induction

A colony of transformed *E. coli* GMS407(DE3) cells (refer to section 7.2.7 or section 7.2.9) was picked from the selection LB agar plate and placed in an aliquot of LB_{kan} media (10 mL, refer to section 7.1.2). The samples were incubated (37 °C) overnight with shaking at 180 rpm.

The overnight culture (5 mL) was used to inoculate sterile LB_{kan} media (500 mL, refer to section 7.1.2) and cultures were incubated (37 °C) with shaking. At $A_{600nm} \sim 0.7$ (3 h), cells were induced with IPTG **81** (1 M, 200 μ L, 0.2 mol) and incubated further (37 °C, 3 h). Cultures were harvested by centrifugation (5000 rpm, 10 min, 4 °C). The pellet was resuspended in PBS buffer (100 mL, refer to section 7.1.2) and centrifugation was repeated. The cell pellet (~1 g) was stored at -80 °C until required.

7.2.13 Chemical Bacterial Cell Lysis

Bacterial cells (~1 g) were resuspended in lysis buffer (10 mL, refer to section 7.1.2) and DNase (100 μ L, 10 mg mL⁻¹) and lysosymes (100 μ L, 100 mg mL⁻¹) were added. The solution was subjected to five cycles of snap-freezing in liquid nitrogen and warming to room temperature. The cell suspension was centrifuged (13000 rpm, 10 min, 4 °C) and the supernatant was collected and stored at -80 °C until required.

Experimental

7.2.14 Pressurised Bacterial Cell Lysis

All subsequent steps were done at 4 °C. Bacterial cells (~1 g) were resuspended in binding buffer (15 mL, refer to section 7.1.2), lysed three times using a French Pressure Cell Press (20,000 kPa) and centrifuged (40,000 *g*, 45 min, 4 °C). The supernatant was immediately subjected to FPLC.

7.2.15 FPLC Enzyme purification

Lysed bacterial extracts were purified by FPLC equipped with a 5 mL HisTrap™ column (GE Healthcare). The backpressure controlled flow rate was used at 0.3 MPa with a maximum flow rate of 5 mL min⁻¹ used. The HisTrap™ was pre-conditioned with water (5 column volumes) and then binding buffer (5 column volumes) prior to loading the sample directly onto the column via syringe equipped with a 0.45 μM membrane filter. The sample was washed with binding buffer until a baseline response was observed (~10 column volumes) by UV (*A*_{280nm}). A linear gradient to 100% eluting buffer over 25 column volumes was applied and then maintained until a baseline response was regained. A retention time for mutant strains was first determined by purifying the His-tagged WT glucuronidase. A strong UV absorbing peak (280 nm) was observed and verified by mixing a droplet from the UV peak fractions with a droplet of *p*-nitrophenyl-β-D-glucuronide **25** (10 mM) - a rapid yellow colour change confirming WT β-glucuronidase. A strong UV absorbing peak with an equal retention time was observed for the other glucuronylsynthase strains. Fractions were concentrated and the buffer solution changed to 50 mM phosphate buffer pH 7.4 using centrifugal filtration.

Samples were tested for purity by diluting an aliquot (5 μL) from each sample with SDS-PAGE loading buffer (glycine gel) (10 μL, refer to section 7.1.2) and subjecting them to glycine SDS-PAGE (refer to section 7.2.2).

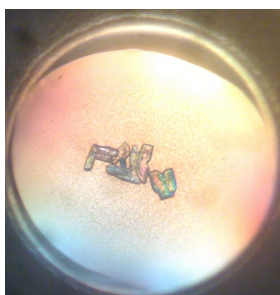
After use, the HisTrap™ was washed with water (5 column volumes) and then aqueous ethanol (20%, 5 column volumes) before being stored at 4 °C.

7.2.16 Enzyme crystallisation screens

High through-put screening for appropriate protein crystallisation conditions were performed with a Cartesian Honeybee Crystallisation Robot (Genomic Solutions) using the Hampton Research® Crystal Screen™ (Hampton Research, Laguna Hills, CA), Hampton Research® Index Screen™ (Hampton Research, Laguna Hills, CA) and QIAGEN® PEGS Suite™ (QIAGEN Sciences,

Germantown, MD). Crystal screens were performed as microbatches in Intelli-plates™ 96-3 LVR 96-well plates (Hampton Research, Laguna Hills, CA). Each well consisted of three reservoirs. In the first reservoir, screening solutions were mixed with a droplet of glucuronylsynthase (41 mg mL⁻¹). In the second reservoir, screening solutions were mixed with a droplet of glucuronylsynthase (41 mg mL⁻¹) and α -D-glucuronyl fluoride **51** (350 mM). In the final reservoir, screening solutions were mixed with glucuronylsynthase (41 mg mL⁻¹) and *p*-nitrophenyl- β -D-glucuronide **25** (10 mM). Wells were covered with para-film™ and stored at 4 °C. Reservoirs were examined under microscope for the presence of crystallisation. Crystals were observed in the following conditions:

Hampton Research Crystal Screen (Well B2.2)

**Contents:**

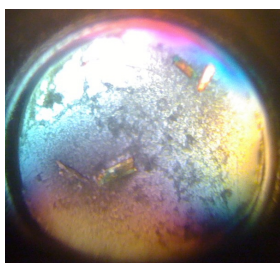
E504G (41 mg mL⁻¹) + α -D-glucuronyl fluoride **51** (350 mM)

Conditions:

calcium chloride dehydrate (0.2 M),

Tris.HCl (0.1 M, pH 8.5), polyethylene glycol 400 (30% v/v).

Qiagen PEG Screen (Well G1.2)

**Contents:**

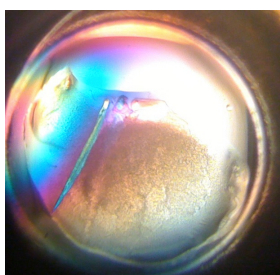
E504G (41 mg mL⁻¹) + α -D-glucuronyl fluoride **51** (350 mM)

Conditions:

magnesium acetate (0.2 M),

polyethylene glycol 3350 (20% w/v)

Qiagen PEG Screen (Well H4.1)

**Contents:**

E504G (41 mg mL⁻¹)

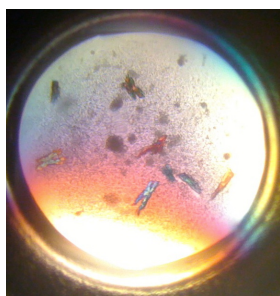
Conditions:

di-sodium phosphate (0.2 M),

polyethylene glycol 3350 (20% w/v)

Experimental

Qiagen PEG Screen (Well F8.2)



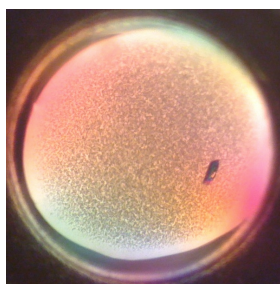
Contents:

E504G (41 mg mL⁻¹) + α -D-glucuronyl fluoride **51** (350 mM)

Conditions:

magnesium formate (0.2 M),
polyethylene glycol 3350 (20% w/v)

Hampton Research Index Screen (Well G1.2)



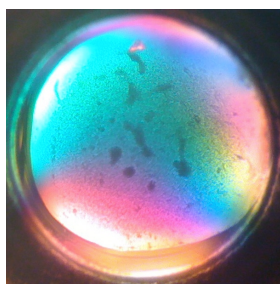
Contents:

E504G (41 mg mL⁻¹) + α -D-glucuronyl fluoride **51** (350 mM)

Conditions:

sodium chloride (0.2 M), Tris (0.1 M, pH 8.5),
polyethylene glycol 3350 (25% w/v)

Hampton Research Index Screen (Well G2.2)



Contents:

E504G (41 mg mL⁻¹) + α -D-glucuronyl fluoride **51** (350 mM)

Conditions:

lithium sulfate monohydrate (0.2 M),
bis-Tris (0.1 M, pH 5.5), polyethylene glycol 3350 (25% w/v)

Hampton Research Index Screen (Well B6.2 + B6.3)



Contents:

E504G (41 mg mL⁻¹) + α -D-glucuronyl fluoride **51** (350 mM)

(top)

41 mg mL⁻¹ E504G + *p*-nitrophenyl- β -D-glucuronide **25** (10 mM) (bottom)

Conditions:

Tris (0.1 M, pH 6.9), di-potassium phosphate (0.91 M),
mono-sodium phosphate monohydrate (0.49 M)

Hampton Research Index Screen (Well D8.2)



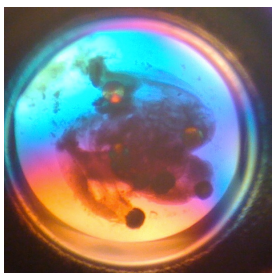
Contents:

E504G (41 mg mL⁻¹) + α -D-glucuronyl fluoride **51** (350 mM)

Conditions:

HEPES (0.1 M, pH 7.5), polyethylene glycol 3350 (25% w/v)

Hampton Research Index Screen (Well D9.2)



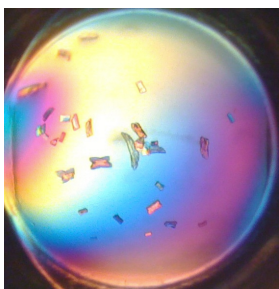
Contents:

E504G (41 mg mL⁻¹) + α -D-glucuronyl fluoride **51** (350 mM)

Conditions:

Tris (0.1 M, pH 8.5), polyethylene glycol 3350 (25% w/v)

Hampton Research Index Screen (Well B9.1)



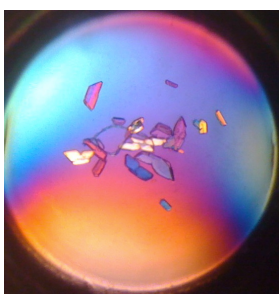
Contents:

E504G (41 mg mL⁻¹)

Conditions:

Tri-ammonium citrate (1.8 M, pH 7.0)

Hampton Research Index Screen (Well B9.2)



Contents:

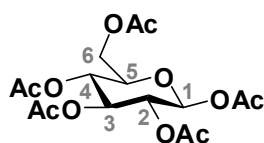
E504G (41 mg mL⁻¹) + α -D-glucuronyl fluoride **51** (350 mM)

Conditions:

Tri-ammonium citrate (1.8 M, pH 7.0)

7.3 Synthesis of α -D-glucuronyl fluoride 51

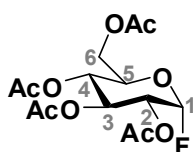
7.3.1 1,2,3,4,6-Penta-O-acetyl β -D-glucopyranoside **83**²¹¹



Acetic anhydride (100 mL, 1.06 mol) was added to D-glucose **82** (20.0 g, 0.111 mol) and sodium acetate (16.0 g, 0.195 mol) and the solution heated to 100 °C for 2.5 h. The reaction was cooled to RT and poured onto ice with stirring to give a colourless suspension in water. The solid was filtered, washed with water (1 L) and dried at the pump, then overnight over potassium hydroxide. Recrystallisation from methanol yielded the title compound **83** as white crystals (24.4 g, 56.4%, α : β 1:17).

mp 164-167 °C (Lit. mp 176-178 °C); $[\alpha]_D^{24} +7.8$ (4.5, CHCl₃) [lit.²¹² $[\alpha]_D^{23} +4.5$ (4.6, CHCl₃)]; IR (NaCl): 2958 (m, C-H), 1747 (s, C=O), 1433, 1367, 1220, 1078, 1039, 910 cm⁻¹; ¹H NMR (300 MHz, CDCl₃): δ 5.70 (1H, d, J_{H1-H2} 8.2, H1), 5.24 (1H, t, $J_{H1-H2} \approx J_{H2-H3}$ 9.3, H2), 5.19-5.05 (2H, m, H3, H4), 4.28 (1H, dd, $^2J_{H6a-H6b}$ 12.5, $^3J_{H5-H6a}$ 4.4, H6a), 4.09 (1H, dd, $^2J_{H6a-H6b}$ 12.5, $^2J_{H5-H6b}$ 1.7, H6b), 3.84 (1H, ddd, J_{H4-H5} 9.9, J_{H5-H6a} 4.2, J_{H5-H6b} 2.0, H5), 2.17-2.01 (15H, m, 5 x CH₃); ¹³C NMR (300 MHz CDCl₃): δ 170.7 (C=O), 170.2 (C=O), 169.5 (C=O), 169.3 (C=O), 169.0 (C=O), 91.83 (C1), 72.9, 70.4, 70.0, 67.9, 61.6, 20.9 (2 x CH₃), 20.7 (3 x CH₃).

7.3.2 2,3,4,6-Tetra-O-acetyl α -D-glucopyranosyl fluoride **84**^{69,213}

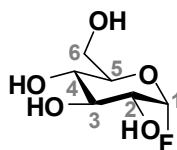


Hydrogen fluoride-pyridine (70%, 7.0 mL) was added to 1,2,3,4,6-penta-O-acetyl β -D-glucopyranoside **83** (3.500 g, 8.967 mmol) in dichloromethane (5.5 mL) at RT and under nitrogen atmosphere. The reaction was stirred for 7 h at RT, then poured into a solution of ether (30 mL) and aqueous potassium fluoride (10%, 80 mL). The organic layer was collected and the aqueous layer was washed with ether: hexane (3:1, 3 x 90 mL). The organic layers were combined and washed with aqueous potassium fluoride (10%, 2 x 60 mL), saturated sodium bicarbonate (30 mL) and then brine (30 mL). The solvent was

dried over anhydrous magnesium sulphate, filtered and removed under reduced pressure at 40 °C. The residue was dissolved in minimal chloroform and subjected to flash chromatography (chloroform : ethyl acetate, 9:1) to yield the target compound **84** (2.576 g, 82%) as a white crystalline solid.

mp 95-98 °C (lit.²¹³ mp 108 °C); $[\alpha]_D^{24}$ +86.0 (3.0, CHCl₃) [lit.²¹³ $[\alpha]_D^{20}$ +90.1 (3.0, CHCl₃)]; **R_f** 0.71 (5:2 ethyl acetate : ethanol); **IR** (KBr powder): 2963 (C-H), 1755 (C=O), 1370, 1224, 1162, 1043, 924, 771; **¹H NMR** (300 MHz, CDCl₃): δ 5.75 (1H, dd, J_{H1-F} 52.9, J_{H1-H2} 2.7, H1), 5.49 (1H, t, $J_{H3-H4} \approx J_{H4-H5}$ 9.9, H4), 5.15 (1H, t, $J_{H2-H3} \approx J_{H3-H4}$ 10.0, H3), 4.95 (1H, ddd, J_{H2-F} 24.2, J_{H1-H2} 2.8, J_{H2-H3} 10.2, H2), 4.31-4.12 (3H, m, H5, H6), 2.10 (3H, s, Ac), 2.09 (3H, s, Ac), 2.04 (3H, s, Ac), 2.02 (3H, s, Ac); **¹³C NMR** (75 MHz, CDCl₃): δ 170.7 (C=O), 170.1 (C=O), 170.0 (C=O), 169.5 (C=O), 103.9 (d, $^1J_{C1-F}$ 229.6, C1), 70.4 (d, $^2J_{C2-F}$ 24.6, C2), 69.9 (d, $^3J_{C3-F}$ 4.2, C3), 69.6 (C5), 67.5 (C4), 61.4 (C6), 20.8 (Ac), 20.7 (3C, 3 x Ac).

7.3.3 α -D-Glucopyranosyl fluoride **32**²¹⁴

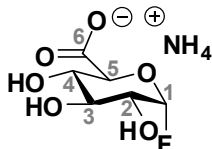


Sodium methoxide in methanol (0.6 mL, 1 M, 0.6 mmol) was added dropwise to 2,3,4,6-tetra-O-acetyl- α -D-glucopyranosyl fluoride **84** (1.02 g, 2.91 mmol) dissolved in dry methanol (28.5 mL) on ice under nitrogen atmosphere. The reaction was stored overnight (18 h) at 4 °C then quenched by the addition of silica gel (4.5 g). The solvent was evaporated at 30 °C and the resulting residue dry-loaded onto a flash silica column. Flash chromatography (ethyl acetate: ethanol 5:2) afforded the target compound **32** (0.512 g, 96.6%) as a white powder.

mp 190-200 °C (decomp); $[\alpha]_D^{22}$ +91.4 (1.0, H₂O) [lit.²¹⁵ $[\alpha]_D^{25}$ +90 (1, H₂O)]; **R_f** 0.40 (5:2 ethyl acetate : ethanol); **IR** (KBr powder): 3313 (broad, OH), 2935 (C-H), 1344, 1236, 1167, 894, 775; **¹H NMR** (300 MHz, D₂O): δ 5.72 (1H, dd, J_{H1-F} 53.5, J_{H1-H2} 2.8, H1), 3.92-3.37 (6H, m, H2, H3, H4, H5, H6); **¹³C NMR** (75 MHz, D₂O): δ 107.8 (d, J_{C1-F} 223, C1), 74.6, (C5), 72.8 (C3), 71.4 (d, $^2J_{C2-F}$ 25, C2), 69.0 (C4), 60.5 (C6).

Experimental

7.3.4 Ammonium α -D-glucopyranuronyl fluoride **51**²¹⁶



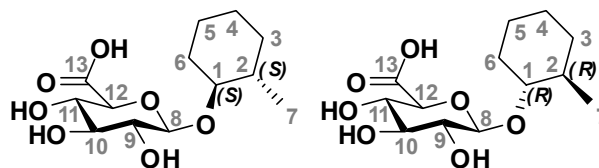
TEMPO (77 mg, 0.49 mmol) was added to α -D-glucopyranosyl fluoride **32** (1.67 g, 9.15 mmol) dissolved in MilliQ water (80 mL) on ice. The pH was adjusted to ~ 9 before the drop wise addition of sodium hypochlorite (1 M, 18.5 mL, 18.5 mmol). The addition of sodium hypochlorite was maintained at a rate such that the reaction pH was maintained at 9.5 ± 0.5 . After the addition of sodium hypochlorite, the pH of the reaction was maintained at 9.5 ± 0.5 by the addition of sodium hydroxide (1 M) until pH was steady. Upon completion (~ 3 h), the pH was lowered to 7 by the addition hydrochloric acid (1 M), and the crude reaction subjected to anion-exchange chromatography (Dowex® 1x8, 200-400, meshCl resin). The column was eluted with MilliQ water (4 column volumes), then 0.1 M ammonium bicarbonate (2 column volumes), then 0.2 M ammonium bicarbonate until complete elution of target compound **51**. Fractions were combined and evaporated under reduced pressure at 30 °C. The white residue was stored overnight under vacuum to remove residual ammonium bicarbonate, resulting in the off-white powder of the target compound **51** (1.87 g, 96%). Rapid recrystallisation from aqueous ethanol (70%) afforded the target compound **51** as colourless, dendritic crystals (1.70 g, 87%).

mp 97-150 °C (decomp), $[\alpha]_D^{24}$ +46.6 (c 1.1, H₂O); **R_f** 0.47 (5:2:1 ethyl acetate : methanol : water); **IR** (NaCl): 3219 (broad, OH), 1597 (CO₂⁻), 1422 (CO₂⁻), 1310, 1162, 1109, 1077, 1034, 1011, 946, 880, 622; **¹H NMR** (300 MHz, D₂O): δ 5.72 (1H, dd, J_{H1-F} 53.4, J_{H1-H2} 2.5, H1), 4.10 (1H, d, J_{H4-H5} 10.1, H5), 3.81-3.50 (3H, m, H2, H3, H4); **¹³C NMR** (75 MHz, D₂O): δ 176.1 (C6), 107.8, (d, J_{C2-F} 223.8, C1), 74.6 (C5), 72.9 (C3), 71.7 (C4), 71.3 (C2).

Crystals for single crystal x-ray diffraction (Figure 2.8) were grown by dissolving the crude product in boiling 70% aqueous ethanol, and then adding acetone drop wise until cloudiness was almost persistent. The solution was allowed to cool slowly to room temperature before chilling at 4 °C overnight.

7.4 Revised glucuronylsynthase reactions

7.4.1 *trans*-2-Methylcyclohexyl β -D-glucuronide **64**

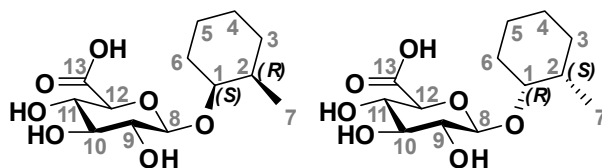


Glucuronylsynthase (E504G, 25 mg mL⁻¹, 280 μ L, final concentration 0.40 mg mL⁻¹) was added to α -D-glucuronyl fluoride **51** (187 mg, 0.877 mmol, final concentration 50 mM), *trans*-2-methylcyclohexanol **39** (100 mg, 0.876 mmol, final concentration 50 mM) and DMSO (876 μ L, final concentration 5.0% v/v) in sodium phosphate buffer (100 mM, 16.36 mL, pH 7.5). The reaction was swirled continuously (100 rpm) under ambient conditions for 4 days then dried onto silica. The residue was subjected to flash chromatography (ethyl acetate : methanol : water, 7:2:1) to obtain the glucuronide product **64** as a mixture of diastereomers (103.4 mg, 40.7%).

mp decomposes; $[\alpha]_D^{20}$ -59 (c 0.78, MeOH); R_f 0.37 (7:2:1 ethyl acetate : methanol : water); **IR** (neat): 3358 (broad, OH), 2928 (C-H), 2857 (C-H), 1605 (CO₂H), 1418 (CO₂H), 1376, 1297, 1167, 1038; **¹H NMR** (800 MHz, MeOD): δ 4.40 (2H, d, J_{H1-H2} 7.8, H8), 3.77 (1H, d, $J_{H11-H12}$ 9.8, H5 minor isomer), 3.75 (1H, d, $J_{H11-H12}$ 9.8, H5 major isomer), 3.55 (1H, t, J 9.4, major isomer), 3.52 (1H, t, J 9.5, minor isomer), 3.40 (1H, t, J 9.2, major isomer), 3.55 (1H, obstructed, minor isomer), 3.26-3.20 (3H, m), 3.12 (1H, m, minor isomer), 2.11 (1H, m, minor isomer), 2.06 (1H, m, major isomer), 1.80-1.68 (4H, m), 1.60 (2H, m), 1.50-1.39 (2H, m), 1.34-1.15 (6H, m), 1.05 (3H, d, J_{H6-H7} 6.4, H7 minor isomer), 1.02 (2H, obstructed), 0.98 (3H, d, J_{H6-H7} 6.6, H7 major isomer); **¹³C NMR** (75 MHz, D₂O): 176.3 (C6), 100.0 (C1), 84.3 (C1'), 76.7, 76.4, 73.6, 72.5, 37.7, 33.9, 31.6, 25.4, 24.9, 18.8 (C7'); **LRMS (+ESI)** m/z: 959 ([3M-3H+4Na]⁺, 52.5), 647 ([2M-2H+3Na]⁺, 100), 335 ([M-H+2Na]⁺, 51.5), 313 ([M+Na]⁺, 17); **HRMS (+ESI)** m/z: 335.1081 ([M-H+2Na]⁺, C₁₃H₂₁O₇Na₂⁺ gives 335.1078);

Experimental

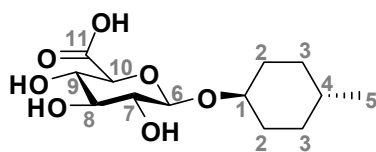
7.4.2 *cis*-2-Methylcyclohexyl β -D-glucuronide **65**



Glucuronylsynthase (E504G, 27 mg mL⁻¹, 60 μ L, final concentration 0.2 mg mL⁻¹) was added to α -D-glucuronyl fluoride **51** (104 mg, 0.488 mmol, final concentration 59.5 mM), *cis*-2-methylcyclohexanol **38** (50 μ L, 46.8 mg, 0.410 mmol, final concentration 50 mM) and DMSO (820 μ L, final concentration 10.0% v/v) in sodium phosphate buffer (100 mM, 7.27 mL, pH 7.5). The reaction was swirled continuously (100 rpm) under ambient conditions for 4 days then dried onto silica. The residue was subjected to flash chromatography (ethyl acetate : methanol : water, 7:2:1) to obtain the glucuronide product **65** as a mixture of diastereomers (71.3 mg, 59.9%).

mp decomposes; **R_f** 0.15 (7:2:1 ethyl acetate : methanol : water); **IR** (neat): 3370 (broad, OH), 2928 (C-H), 2863 (C-H), 1607 (CO₂H), 1416 (CO₂H), 1376, 1298, 1163, 1028, 935; **¹H NMR** (300 MHz, D₂O): δ 4.55 (1H, m, H8), 3.90 (1H, m, H12), 3.90 (1H, m, H11), 3.60-3.45 (2H, m, H10, H1), 3.45-3.25 (1H, m, H9), 2.1-1.2 (10H, m, H2-H6), 0.96 (3H, d, J_{H2-H7} 6.9, H7); **¹³C NMR** (75 MHz, D₂O): 176.4 (C13), 100.7 (C8), 80.2 (C1), 76.7, 76.3, 73.5, 72.5, 34.7, 30.1, 27.7, 23.1, 22.2, 15.5 (C7); **LRMS (+ESI)** m/z: 959 ([3M-3H+4Na]⁺, 74), 647 ([2M-2H+3Na]⁺, 100), 335 ([M-H+2Na]⁺, 46), 313 ([M+Na]⁺, 10); **HRMS (+ESI)** m/z: 335.1076 ([M-H+2Na]⁺, C₁₃H₂₁O₇Na₂⁺ gives 335.1078);

7.4.3 *trans*-4-Methylcyclohexyl β -D-glucuronide **66**

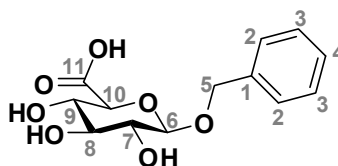


Glucuronylsynthase (E504G, 27 mg mL⁻¹, 52 μ L, final concentration 0.20 mg mL⁻¹) was added to α -D-glucuronyl fluoride **51** (45 mg, 0.21 mmol, final concentration 30 mM), *trans*-4-methylcyclohexanol **41** (22 μ L, 20 mg, 0.18 mmol, final concentration 26 mM) and DDM (39 mg, final concentration 0.56% w/v) in sodium phosphate buffer (100 mM, 6.95mL, pH 7.5). The reaction was swirled continuously (100 rpm) under ambient conditions for 4 days then dried onto silica. The residue was subjected to flash chromatography (ethyl acetate :

methanol : water, 7:2:1) to obtain the glucuronide product **66** as a mixture of diastereomers (71.3 mg, 59.9%).

mp decomposes; $[\alpha]_D^{19}$ -72 (c 0.52, MeOH); R_f 0.28 (7:2:1 ethyl acetate : methanol : water); **IR** (neat): 3358 (broad, OH), 2948 (C-H), 2926 (C-H), 2866 (C-H), 1607 (CO₂H), 1451, 1418 (CO₂H), 1372, 1297, 1162, 1107, 1034, 941, 890; **¹H NMR** (300 MHz, D₂O): δ 4.60 (1H, d, J_{H6-H7} 8.0, H6), 3.81-3.68 (2H, m, H10, H1), 3.53 (1H, m, H9), 3.50 (1H, m, H8), 3.27 (1H, m, H7), 2.04 (2H, m, H2), 1.74 (2H, m, H2), 1.44-1.21 (3H, m, H3, H4), 1.07-0.94 (2H, m, H3), 0.88 (3H, d, J_{H4-H5} 6.5, H5); **¹³C NMR** (75 MHz, D₂O): 176.4 (C11), 100.8 (C6), 79.9 (C10), 76.8, 76.3, 73.6, 72.5, 33.5, 33.4, 33.2, 32.0, 31.9 (C4), 21.8 (C5); **LRMS (+ESI)** m/z: 647 (100), 641 (79.5), 393 (81), 335 ([M-H+2Na]⁺, 56), 313 ([M+Na]⁺, 43); **HRMS (+ESI)** m/z: 313.1267 ([M+Na]⁺, C₁₃H₂₂O₇Na⁺ gives 313.1258).

7.4.4 Benzyl β -D-glucuronide **69**⁵⁷



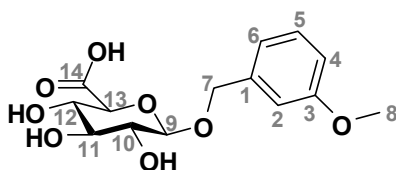
Glycosynthase (E504G, 27 mg mL⁻¹, 41 μ L, final concentration 0.20 mg mL⁻¹) was added to α -D-glucuronyl fluoride **51** (72 mg, 0.33 mmol, final concentration 59 mM), benzyl alcohol **46** (30 mg, 0.28 mmol, final concentration 50 mM) in sodium phosphate buffer (100 mM, 5.51 mL, pH 7.5). The reaction was swirled continuously under ambient conditions for 4 days then dried onto silica. The residue was subjected to flash chromatography (ethyl acetate : methanol : water, 7:2:1) to obtain benzyl β -D-glucuronide **69** (46 mg, 58%) as a white powder.

mp decomposes; $[\alpha]_D^{20}$ -89 (c 0.53, MeOH); R_f 0.19 (7:2:1 ethyl acetate : methanol : water); **IR** (neat): 3389 (broad, O-H), 2892 (C-H), 1605 (C=O), 1418, 1370, 1285, 1158, 1046, 946, 795, 737, 701; **¹H NMR** (400 MHz, MeOD): δ 7.47-7.23 (5H, m, H2-4), 5.00 (1H, d, $^2J_{H5a-H5b}$ 11.6, H5a), 4.66 (1H, d, $J_{H5a-H5b}$ 12.0, H5b), 4.38 (1H, d, J_{H6-H7} 7.6, H6), 3.62 (1H, d, J_{H9-H10} 9.6, H10), 3.49 (1H, t, $J_{H8-H9} \approx J_{H9-H10}$ 9.2, H9), 3.41 (1H, t, $J_{H7-H8} \approx J_{H8-H9}$ 9.0, H8), 3.50-3.27 (1H, obscured, H7); **¹³C NMR** (75 MHz, D₂O): 176.3 (C_q, C11), 137.2 (C_q, C1), 129.4 (2 x CH), 129.3 (2 x CH), 129.0 (CH, C4), 101.6 (CH, C6), 76.6 (CH, C20), 76.2 (CH), 73.6 (CH), 72.4 (CH), 71.9 (CH₂, C5); **LRMS (+ESI)** m/z: 941

Experimental

([3M-3H+4Na]⁺, 100), 635 ([2M-2H+3Na]⁺, 95), 329 ([M-H+2Na]⁺, 31); **HRMS (+ESI)** m/z: 329.0602 ([M-H+2Na]⁺, C₁₃H₁₅O₇Na₂ gives 329.0608).

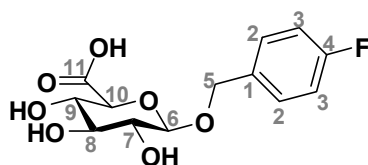
7.4.5 3-Methoxybenzyl β-D-glucuronide 71



Glycosynthase (E504G, 14.5 mg mL⁻¹, 50 μL, final concentration 0.20 mg mL⁻¹) was added to α-D-glucuronyl fluoride **51** (77 mg, 0.36 mmol, final concentration 100 mM), 3-methoxybenzyl alcohol **47** (50 mg, 0.36 mmol, final concentration 100 mM) in sodium phosphate buffer (100 mM, 3.57 mL, pH 7.5). The reaction was swirled continuously under ambient conditions for 4 days then dried onto silica. The residue was subjected to flash chromatography (ethyl acetate : methanol : water, 7:2:1) to obtain benzyl β-D-glucuronide **71** (73 mg, 64%) as a white powder.

mp decomposes; [α]_D²⁰ -72 (c 1.0, MeOH); **R_f** 0.19 (7:2:1 ethyl acetate : methanol : water); **IR** (neat): 3355 (broad, OH), 2914 (C-H), 1597 (CO₂H), 1433 (CO₂H), 1267, 1157, 1038; **¹H NMR** (300 MHz, MeOD): δ 7.22 (1H, t, *J*_{H4-H5} ≈ *J*_{H5-H6} 7.8, H5), 7.05 (1H, d, ²*J*_{H2-H4} 1.8, H2), 6.97 (1H, d, *J*_{H5-H6} 7.5, H6), 6.82 (1H, dd, *J*_{H4-H5} 8.0, *J*_{H2-H4} 2.3, H4), 4.95 (1H, d, ²*J*_{H7-H7} 12.0, H7), 4.65 (1H, d, ²*J*_{H7-H7} 12.0, H7), 4.38 (1H, d, *J*_{H9-H10} 7.8, H9), 3.79 (3H, s, H8), 3.63 (1H, d, *J*_{H12-H13} 9.3, H13), 3.50 (1H, t, H12), 3.42 (1H, t, H11), 3.35-3.23 (1H, obscured by solvent peak, H10); **¹³C NMR** (75 MHz, MeOD): 176.7 (C14), 161.2 (C3), 140.6 (C1), 130.2 (C5), 121.3 (C6), 114.5, 114.4, 103.3 (C9), 77.8, 76.2 (C13), 74.9, 73.7, 71.7 (C7) 55.7 (C8); **LRMS (-ESI)** m/z: 649 ([2M-2H+Na]⁻, 12), 627 ([2M-H]⁻, 10.5), 313 ([M-H]⁻, 100); **HRMS (+ESI)** m/z: 359.0699 ([M-H+2Na]⁺, C₁₄H₁₇O₈Na₂⁺ gives 359.0713), 337.0898 ([M+Na]⁺, C₁₄H₁₈O₈Na⁺ gives 337.0894); **HRMS (-ESI)** m/z: 313.0920 ([M-H]⁻, C₁₄H₁₇O₇⁻ gives 313.0929).

7.4.6 4-Fluorobenzyl β-D-glucuronide 73⁵⁷

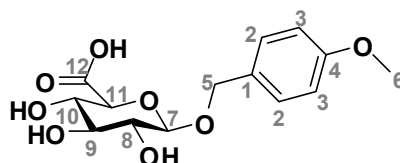


Glucuronylsynthase (E504G, 27 mg mL⁻¹, 47.0 μL, final concentration 0.20 mg mL⁻¹) was added to α-D-glucuronyl fluoride **51** (41 mg, 0.19 mmol, final concentration 30 mM), 4-fluorobenzyl alcohol **50** (20 mg, 0.16 mmol, final

concentration 25 mM) and *n*-dodecyl β -maltoside (32 mg, final concentration 0.5% w/v) in sodium phosphate buffer (50 mM, 6.34 mL, pH 7.5). The reaction was swirled continuously under ambient conditions for 4 days then dried onto silica. The residue was subjected to flash chromatography (ethyl acetate : methanol : water, 7:2:1) to obtain the glucuronide product **73** (24.1 mg, 50%) as a white powder.

mp decomposes; $[\alpha]_D^{20}$ -91 (c 0.52, MeOH); **R_f** 0.24 (7:2:1 ethyl acetate : methanol : water); **IR** (neat): 3362 (broad, O-H), 2887 (C-H), 1605 (C=O), 1512, 1418, 1367, 1292, 1227, 1155, 1038, 947, 827; **¹H NMR** (300 MHz, D₂O): δ 7.50 (2H, dd, ³J_{H2-H3} 8.3, ²J_{H2-F} 5.9, H2), 7.19 (2H, t, ⁴J_{H3-F} \approx ³J_{H2-H3} 8.9, H2), 4.95 (1H, d, ²J_{H5a-H5b} 11.7, H5a), 4.73 (1H, d, ²J_{H5a-H5b} 11.7, H5b), 4.54 (1H, d, J_{H6-H7} 8.1, H6), 3.73 (1H, d, J_{H9-H10} 9.0, H10), 3.53 (2H, m, H8, H9), 3.36 (1H, t, J_{H7-H8} \approx J_{H6-H7} 8.3, H7); **¹³C NMR** (100 MHz, MeOD): 176.9 (C_q, C11), 163.8 (C_q, d, ¹J_{C4-F} 244.0, C4), 135.2 (C_q, d, ⁴J_{C1-F} 2.8, C1), 131.2 (2xCH, d, ³J_{C2-F} 8.0, C2), 115.9 (2xCH, d, ²J_{C3-F} 21.5, C3), 103.3 (CH, C6), 77.8 (CH, C8), 76.0 (CH, C10), 74.9 (CH, C7), 73.7 (CH, C9), 71.1 (CH₂, C5); **LRMS (+ESI)** m/z: 671 ([2M-2H+3Na]⁺, 100), 347 ([M-H+2Na]⁺, 73); **HRMS (+ESI)** m/z: 347.0519 ([M-H+2Na]⁺, C₁₃H₁₄FO₇Na₂ gives 347.0514).

7.4.7 4-Methoxybenzyl β -D-glucuronide **72**⁵⁷



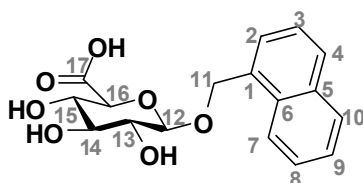
Glycosynthase (E504G, 27 mg mL⁻¹, 42.9 μ L, final concentration 0.20 mg mL⁻¹) was added to α -D-glucuronyl fluoride **51** (37 mg, 0.17 mmol, final concentration 29 mM), 4-methoxybenzyl alcohol **48** (20 mg, 0.14 mmol, final concentration 26 mM) and *n*-dodecyl β -maltoside (119 mg, final concentration 2.1% w/v) in sodium phosphate buffer (50 mM, 5.79 mL, pH 7.5). The reaction was swirled continuously under ambient conditions for 4 days then dried onto silica. The residue was subjected to flash chromatography (ethyl acetate : methanol : water, 7:2:1) to obtain 4-methoxybenzyl β -D-glucuronide **72** (20 mg, 45%) as a white powder.

mp decomposes; $[\alpha]_D^{20}$ -90 (c 0.56, MeOH); **R_f** 0.22 (7:2:1 ethyl acetate : methanol : water); **IR** (neat): 3360 (broad, O-H), 2909 (C-H), 2838 (C-H), 1613 (C=O), 1514, 1416, 1368, 1302, 1250, 1158, 1032, 822; **¹H NMR** (300 MHz,

Experimental

D₂O): δ 7.45 (2H, d, J_{H2-H3} 8.4, H2), 7.05 (2H, d, J_{H2-H3} 8.7, H3) 4.92 (1H, d, $^2J_{H5a-H5b}$ 11.4, H5a), 4.69 (1H, d, $^2J_{H5a-H5b}$ 11.1, H5b), 4.52 (1H, d, J_{H7-H8} 7.8, H7), 3.87 (3H, s, H6), 3.72 (1H, d, $J_{H10-H11}$ 9.2, H11), 3.52 (2H, m, H9, H10), 3.35 (1H, t, $J_{H8-H9} \approx J_{H7-H8}$ 8.1, H8); **¹³C NMR** (75 MHz, D₂O): 176.3 (C_q, C12), 159.5 (C_q, C4), 131.2 (2 x CH, C2), 129.8 (C_q, C1), 114.7 (2 x CH, C3), 101.4 (CH, C7), 76.7 (CH, C11), 76.3 (CH), 73.6 (CH), 72.5 (CH), 71.5 (CH₂, C5), 56.0 (CH₃, C6); **LRMS (+ESI)** m/z: 714 (100), 695 ([2M-2H+3Na]⁺, 47), 359 ([M-H+2Na]⁺, 17.5); **HRMS (+ESI)** m/z: 359.0705 ([M-H+2Na]⁺, C₁₄H₁₇O₈Na₂ gives 359.0714).

7.4.8 1-Naphthalenemethyl β -D-glucuronide **75**⁵⁷

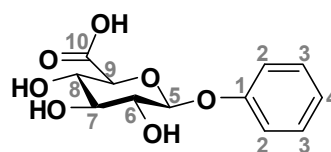


Glycosynthase (E504G, 33 mg mL⁻¹, 65 μ L, final concentration 0.20 mg mL⁻¹) was added to α -D-glucuronyl fluoride **51** (32 mg, 0.15 mmol, final concentration 14 mM), 1-naphthalenemethanol **43** (21 mg, 0.13 mmol, final concentration 12 mM) and *n*-dodecyl β -maltoside (107 mg, final concentration 1% w/v) in sodium phosphate buffer (50 mM, 10.7 mL, pH 7.5). The reaction was swirled continuously under ambient conditions for 4 days then dried onto silica. The residue was subjected to flash chromatography (ethyl acetate : methanol : water, 7:2:1) to obtain 1-O-(1'-naphthalenemethyl) β -D-glucopyranuronic acid **75** (21 mg, 48%) as a white powder.

mp decomposes; $[\alpha]_D^{20}$ -65 (c 0.63, MeOH); R_f 0.30 (7:2:1 ethyl acetate : methanol : water); **IR** (neat): 3370 (broad, O-H), 3050 (C-H), 2922 (C-H), 1613 (C=H), 1422, 1289, 1169, 1063, 1034, 946, 793, 777; **¹H NMR** (300 MHz, D₂O): δ 8.15 (1H, d, J 7.8), 7.99-7.84 (2H, m), 7.68-7.44 (4H, m), 5.33 (1H, d, $^2J_{H11a-H11b}$ 11.7, H11a), 5.04 (1H, d, $^2J_{H11a-H11b}$ 11.7, H11b), 4.50 (1H, d, $J_{H12-H13}$ 7.8, H12), 3.71 (1H, d, $J_{H15-H16}$ 9.6, H16), 3.56 (1H, t, $J_{H14-H15} \approx J_{H15-H16}$ 7.2, H15), 3.45 (1H, t, $J_{H13-H14} \approx J_{H14-H15}$ 9.0, H14), 3.34 (1H, t, $J_{H12-H13} \approx J_{H13-H14}$ 8.6, H13); **¹³C NMR** (75 MHz, D₂O): 176.4 (C17), 134.0 (C1), 132.5 (Cq), 132.0 (Cq), 129.9 (CH), 129.1 (CH), 128.7 (CH), 127.3 (CH), 126.8 (CH), 126.1 (CH), 124.6 (CH), 101.5 (C12), 76.7 (C16), 76.2 (C14), 73.5 (C13), 72.4 (C15), 70.0 (C11); **LRMS (+ESI)** m/z: 735 ([2M-2H+3Na]⁺, 100), 379 ([M-H+2Na]⁺, 55), 356

($[M+Na]^+$, 20); **HRMS (+ESI)** m/z : 379.0762 ($[M-H+2Na]^+$, $C_{17}H_{17}O_7Na_2$ gives 379.0765).

7.4.9 Phenyl β -D-glucuronide **76**⁵⁷

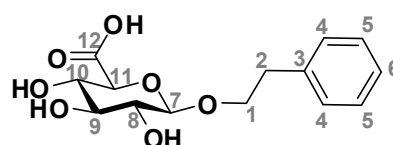


Glycosynthase (E504G, 1.35 mg mL⁻¹, 4.89 mL, final concentration 0.50 mg mL⁻¹) was added to α -D-glucuronyl fluoride **51** (113 mg, 0.53 mmol, final concentration 40 mM), phenol **52** (50 mg, 0.53 mmol, final concentration 40 mM) in sodium phosphate buffer (100 mM, 4.89 mL pH 7.5). The reaction was incubated at 30 °C without agitation for 3 days then acidified to pH 2 and dried onto reverse-phase flash silica. The residue was subjected to reverse-phase flash chromatography (18% aqueous acetonitrile + 0.1% acetic acid) to obtain phenyl β -D-glucopyranuronic acid **76** (61 mg, 43%) as a white powder.

mp 158-160 °C (lit. 160-161 °C)²¹⁷; $[\alpha]_D^{20}$ -78.4 (c 1.9, MeOH) [lit. $[\alpha]_D^{20}$ -87.5 (c 2.10, H₂O)]²¹⁷; **R_f** 0.27 (7:2:1 ethyl acetate : methanol : water); **IR** (NaCl): 3351 (broad, OH), 2922 (C-H), 1601 (C=O), 1495, 1416, 1295, 1229, 1109, 1063, 755, 693; **¹H NMR** (400 MHz, D₂O+AcOH spike): δ 7.38 (2H, t, J 8.0), 7.17-7.06 (3H, m), 5.10 (1H, d, J_{H5-H6} 7.0, H5), 3.86 (1H, d, J_{H8-H9} 9.1, H9), 3.64-3.53 (3H, m, H2-H4); **¹³C NMR** (100 MHz, D₂O+AcOH spike): 173.4 (C10), 154.6 (C1), 127.9 (2C, C3), 121.3 (C4), 114.6 (2C, C2), 98.1 (C5), 74.2, 73.3, 70.7, 69.7; **LRMS (+ESI)** m/z : 899 ($[3M-3H+4Na]^+$, 76), 607 ($[2M-2H+3Na]^+$, 88), 315 ($[M-H+2Na]^+$, 100); **HRMS (+ESI)** m/z : 315.0446 ($[M-H+2Na]^+$, $C_{12}H_{13}O_7Na_2$ gives 315.0452).

7.5 Large scale glucuronylsynthase reaction

7.5.1 Large scale synthesis of 2-phenylethyl β -D-glucuronide **68**⁵⁷



Glycosynthase (E504G, 27 mg mL⁻¹, 185 μ L, final concentration 0.20 mg mL⁻¹) was added to α -D-glucuronyl fluoride **51** (0.63 g, 3.0 mmol, final concentration 120 mM), 2-phenylethanol **45** (0.30 g, 2.5 mmol, final concentration 100 mM) in sodium phosphate buffer (100 mM, 24.8 mL, pH 7.5).

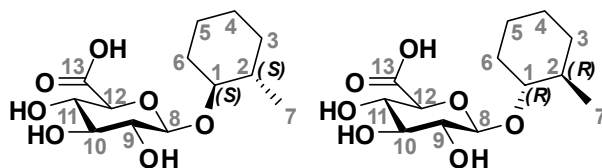
Experimental

The reaction was swirled continuously under ambient conditions for 4 days then dried onto silica. The residue was subjected to flash chromatography (ethyl acetate : methanol : water, 7:2:1) to obtain 2-phenylethyl β -D-glucuronide **68** (718 mg, 96%) as a white powder. Characterisation data was identical to previously characterised material.

R_f 0.22 (ethyl acetate : methanol : water, 7:2:1); $^1\text{H NMR}$ (300MHz, D_2O): δ 7.47-7.28 (5H, m, H4-H6), 4.49 (1H, d, $J_{\text{H}7-\text{H}8}$ 8.1, H7), 4.20, (1H, dt, $^2J_{\text{H}1\text{a}-\text{H}1\text{b}}$ 10.2, $^3J_{\text{H}1\text{a}-\text{H}2}$ 6.9, H1a), 3.94 (1H, dt, $^2J_{\text{H}1\text{a}-\text{H}1\text{b}}$ 10.2, $^3J_{\text{H}1\text{b}-\text{H}2}$ 7.0, H1b), 3.70 (1H, m, H11), 3.53 (1H, m, H10), 3.50 (1H, m, H9), 3.30 (1H, m, H8), 3.00 (2H, t, $J_{\text{H}1-\text{H}2}$ 6.9, H2); $^{13}\text{C NMR}$ (75 MHz, D_2O): 176.4 (C_q , C12), 139.4 (C_q , C3), 129.7 (2xCH), 129.3 (2xCH), 127.2 (CH, C6), 102.7 (CH, C7), 76.7 (CH, C11), 76.2 (CH), 73.5 (CH), 72.4 (CH), 71.3 (CH_2 , C1), 35.7 (CH_2 , C2).

7.6 Kinetic resolution of racemic *trans*-2-methylcyclohexanol **39**

7.6.1 Glucuronysynthesis of *trans*-2-methylcyclohexanol **39**⁵⁷



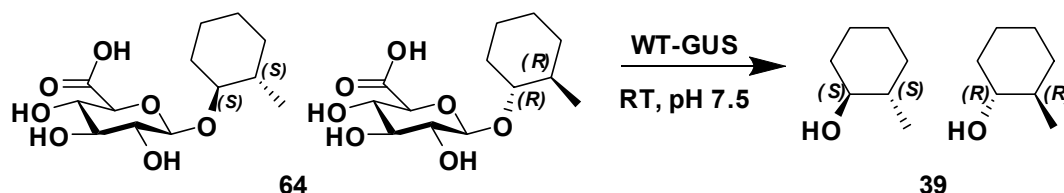
trans-2-Methylcyclohexanol **39** (50 mg, 0.44 mmol, final concentration 50 mM) and α -D-glucuronyl fluoride **51** (93 mg, 0.44 mmol, final concentration 50 mM) were dissolved in 100 mM sodium phosphate buffer (100 mM, 8.3 mL, pH 7.5) and DMSO (400 μL , final concentration 4.5% v/v). Glucuronysynthase (32.6 mg mL^{-1} , 53.7 μL , final concentration 0.2 mg mL^{-1}) was added to the solution and the mixture was swirled (120 rpm) at RT for 7 d. The unreacted alcohol was extracted from the crude reaction with ethyl acetate (3 x 20 mL), and washed with saturated sodium bicarbonate (20 mL). The organic layer was dried over sodium sulphate and evaporated to dryness under weak vacuum (>100 mm Hg, 30 $^\circ\text{C}$) to reclaim crude unreacted *trans*-2-methylcyclohexanol **39** (23 mg, 46%) as a colourless oil.

The aqueous crude reaction layer and sodium bicarbonate washes were combined and silica (~0.5 g) was added. The water was removed under reduced pressure (40 $^\circ\text{C}$) and the resulting white residue was dry loaded on top of a flash silica column. Ethyl acetate : methanol (5:2) was used to elute the

DMSO, then ethyl acetate : methanol : water (7:2:1) was used to elute the target compound. Removal of the solvent by evaporation yielded *trans*-2-methylcyclohexyl β -D-glucuronide **64** (44 mg, 34%) as a mixture of diastereomers.

Spectra was identical to previously synthesised material (refer to section 7.4.1).

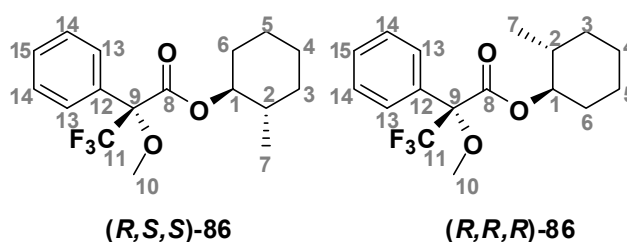
7.6.2 Enzymatic hydrolysis of the *trans*-2-methylcyclohexyl β -D-glucuronide **64**



trans-2-Methylcyclohexyl β -D-glucuronide **64** (44 mg, 0.15 mmol) was dissolved in sodium phosphate buffer (100 mM, 1 mL, pH 7.5) and wild-type β -D-glucuronidase (1.2 mg mL⁻¹, 200 μ L, final concentration 0.2 mg mL⁻¹) was added. The reaction was swirled (150 rpm) under ambient conditions until complete hydrolysis was observed (2 h) by TLC (ethyl acetate: methanol : water, 7:2:1).

The free alcohol was extracted with ethyl acetate (3 x 5 mL), washed with sodium hydroxide (1 M, 5 mL), and dried over sodium sulphate. The solvent was removed under gentle vacuum (>100 mm Hg, 30 °C) to yield *trans*-2-methylcyclohexanol **39** (11.7 mg, 68%) as a colourless oil.

7.6.3 General Mosher's esterification procedure⁷¹



Freshly distilled oxalyl chloride (4 mmol) was added to a stirring solution of (*R*)-(+)- α -methoxy- α -(trifluoromethyl)phenylacetic acid (3.9 mmol) in dichloromethane (15 mL) on ice. Dimethylformamide was added drop wise until effervescence commenced and the reaction was warmed to RT and stirred for a further 30 min.

This solution was then transferred *via* cannula (14 mL dichloromethane washing) to a stirred solution of *trans*-2-methylcyclohexanol **39** (1 mmol), diisopropylethylamine (8 mmol) and 4-*N,N'*-dimethylaminopyridine (1 mmol) in

Experimental

dichloromethane (15 mL). The reaction was stirred at RT until complete consumption was observed (18 h) by TLC analysis (ethyl acetate : hexane, 1 : 19). The reaction was quenched with saturated sodium bicarbonate (275 mL) and extracted with diethyl ether (3 x 275 mL). The organic extracts were combined and washed with brine (275 mL), dried over anhydrous magnesium sulphate, filtered, and concentrated under reduced pressure to a colourless oil. The crude oil was subjected to flash chromatography (ethyl acetate : hexane, 1:19) to yield the pure *trans* Mosher esters **86**.

¹H NMR (300 MHz, CDCl₃): δ 7.73-5.33 (10H, m, H13-H15), 5.35-5.12 (2H, m, H1), 3.69-3.46 (6H, m, H10), 2.12-1.87 (2H, m, H2), 1.86-1.15 (16H, m, H3-H6), 0.94 (3H, d, *J*_{H2-H7} 6.4, H7), 0.78 (3H, d, *J*_{H2-H7} 6.5, H7); ¹³C NMR (75 MHz, CDCl₃)⁷⁵: δ 166.0 (C8), 165.9 (C8), 132.3 (C12), 132.1 (C12), 129.2 (2C, s, C15), 128.04 (C14), 128.01 (C14), 127.1 (C13), 126.90 (C13), 123.13 (d, *J*_{C11-F} 287, C11), 123.07 (d, *J*_{C11-F} 287, C11), 81.3 (C1), 81.2 (C1), 76.5 (2C, d, ³*J*_{C9-F} 34, C9), 55.2 (C10), 55.1 (C10), 36.5 (C2), 35.3 (C2), 33.14 (C6), 33.08 (C6), 31.2 (C3), 30.6 (C3), 24.77 (C4), 24.67 (C4), 24.30 (C5), 24.16 (C5), 18.3 (C7), 17.9 (C7).

7.6.4 Determination of the diastereomeric ratio

Analytical normal-phase HPLC was used to determine the diastereomeric ratio using a Waters Sunfire column (5 μM, 4.4 x 150 mm) and an ethyl acetate : hexane (0.2% v/v, 0.5 mL min⁻¹) solvent system. The column module was heated at 30 °C and the detection of the *trans* Mosher esters **86** (11.7 min and 12.2 min) was measured by UV (A_{260nm}). Peak areas were determined using Empower 2 software.

7.6.5 Mosher's esterification on the starting material

The general procedure (refer to section 7.6.3) was used with commercially supplied *trans*-2-methylcyclohexanol **39** (25 mg, 0.22 mmol) to generate the (2-methylcyclohexyl) (R)-3,3,3-trifluoro-2-methoxy-2-phenylpropanoate **86** (61 mg, 84%). Ratio of diastereomers was 1.0 : 1.1 by HPLC, equating to 4.8% ee.

7.6.6 Mosher's esterification on the hydrolysed glucuronide product

The general procedure (refer to section 7.6.3) was used with *trans*-2-methylcyclohexanol **39** (12 mg, 0.11 mmol) obtained from 4.3.2 to generate the (2-methylcyclohexyl) (R)-3,3,3-trifluoro-2-methoxy-2-phenylpropanoate **86** (4.0 mg, 11%). Ratio of diastereomers was 1.0 : 13.2 by HPLC, equating to 86% ee.

7.7 ^1H NMR assay

7.7.1— ^1H NMR General

NMR spectra were taken with a Bruker Avance 800 instrument (800.1 MHz for ^1H). Kinetic experiments were run simultaneously through the use of an autosampler and conducted at room temperature (21 ± 1 °C). A “Jump and Return” sequence¹⁰³ was used with a delay d_2 of 160 μs .

The baseline was corrected at the regions 5.9-5.4 ppm (anomeric proton of α -D-glucuronyl fluoride **51**), 4.5-4.3 ppm (anomeric proton of the glucuronide product **68**) and 3.1-2.7 ppm (benzylic protons of 2-phenylethanol **45** and the glucuronide product **68**).

7.7.2— ^1H NMR Michaelis-Menten kinetics of α -D-glucuronyl fluoride **51**

Glucuronylsynthase (32.6 mg mL^{-1} , $15.3 \mu\text{L}$, final concentration 1.0 mg mL^{-1}) was added to 2-phenylethanol **45** (final concentration 100 mM), deuterium oxide (final concentration 10% v/v) and α -D-glucuronyl fluoride **51** (final concentrations 2.4 mM, 12 mM, 24 mM, 60 mM, 119 mM, 239 mM, and 500 mM) pre-incubated at 21 °C in sodium phosphate buffer (50 mM, $485 \mu\text{L}$, pH 7.5). The reaction was immediately subjected to ^1H NMR analysis. Seven scans were made to monitor the initial velocity of the reactions at 22.5 min intervals on average (Figure 3.4). Data points (minimum 4 points, 0.6-15% conversion) that encompassed the initial linear velocity were used to plot initial velocities against the α -D-glucuronyl fluoride **51** concentration to provide the Michaelis-Menten plot (Figure 3.5). The result from the reaction with α -D-glucuronyl fluoride **51** at 2.4 mM was not used due to the reaction reaching 23% conversion at the second data point.

7.7.3— ^1H NMR Michaelis-Menten kinetics of 2-phenylethanol **45**

Glucuronylsynthase (32.6 mg mL^{-1} , $18 \mu\text{L}$, final concentration 1.0 mg mL^{-1}) was added to α -D-glucuronyl fluoride **51** (final concentration 100 mM), deuterium oxide (final concentration 10% v/v) and 2-phenylethanol **45** (final concentrations 1 mM, 5 mM, 10 mM, 25 mM, 50 mM, 77 mM, and 104 mM) pre-incubated at 21 °C in sodium phosphate buffer (50 mM, $482 \mu\text{L}$, pH 7.5). The reaction was immediately subjected to ^1H NMR analysis. Eight scans were made to monitor the initial velocity of the reactions at 18.7 min intervals on average (Figure 3.6). Data points (8 points, 1.8-3.5% conversion) that

Experimental

encompassed the initial linear velocity were used to plot initial velocities against the 2-phenylethanol **45** concentration to provide the Michaelis-Menten plot (Figure 3.7).

7.8 Isothermal titration calorimetry (ITC) assay

7.8.1 Isothermal titration calorimetry for α -D-glucuronyl fluoride **51**

Isothermal microcalorimetry experiments were performed on a MicroCal VP-ITC® microcalorimeter and were conducted at 21 °C with each titration consisting of 59 successive injections (1 × 0.5 μ L, 60 × 5 μ L) of a degassed solution of α -D-glucuronyl fluoride **51** (3 mM) in sodium phosphate buffer (100 mM, pH 7.5). The titrant was injected into a thermostatted reaction cell containing a known volume (1.44 mL) of the E504G (50 μ M) in identical degassed buffer. Injection duration was 5.4 s every 240 s and the solutions were stirred at 300 rpm. Independent heat of dilution experiments were conducted and used to correct the binding experiments. The equilibrium constant (K_A) of 1130 M^{-1} was obtained which equates to a dissociation constant (K_D) of 0.88 mM. The experiment was repeated with α -D-glucuronyl fluoride **51** (6.7 mM) and E504G (125 μ M) to obtain a K_A of 780 M^{-1} equating to K_D of 1.3 mM.

7.8.2 Isothermal titration calorimetry for 2-phenylethyl β -D-glucuronide **68**

Isothermal microcalorimetry experiments were performed on a MicroCal VP-ITC® microcalorimeter and were conducted at 21 °C with each titration consisting of 59 successive injections (1 × 0.5 μ L, 60 × 5 μ L) of a degassed solution of 2-phenylethyl β -D-glucuronide **68** (1 mM) in sodium phosphate buffer (100 mM, pH 7.5). The titrant was injected into a thermostatted reaction cell containing a known volume (1.44 mL) of the E504G (50 μ M) in identical degassed buffer. Injection duration was 5.4 s every 240 s and the solutions were stirred at 450 rpm. Independent heat of dilution experiments were conducted and used to correct the binding experiments. An equilibrium constant (K_A) could not be determined from this experiment. The experiment was repeated with 2-phenylethyl β -D-glucuronide **68** (10 mM and 100 mM) and E504G (50 μ M) with no equilibrium constant resulting.

7.9 HPLC-UV assay

7.9.1 HPLC general

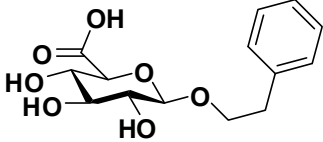
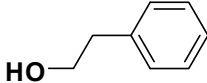
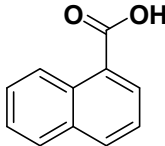
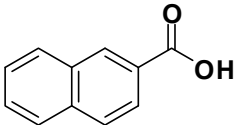
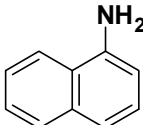
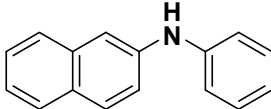
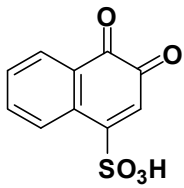
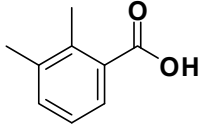
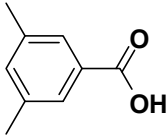
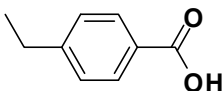
Enzyme kinetics was directly and continuously monitored by HPLC using a Waters Alliance E2695 Separations Module equipped with thermostatted autosampler and a Waters 2998 Photodiode Array detector. Reaction injections (25 μ L unless otherwise stated) were resolved on a Waters XterraMS C₁₈ 5 μ m column (2.1 x 150 mm) using an acetonitrile : sodium phosphate buffer (100 mM, pH 2.0) mobile phase. The column module was heated at 30 °C whilst the sample compartment was kept at 21 °C unless otherwise stated. Detection of product glucuronide was measured at 211 nm unless otherwise stated. Reactions were performed in sodium phosphate buffer (100 mM, pH 7.5) unless otherwise stated. Reactions rates were extrapolated using Empower 2 software and data analysis was performed with Microsoft Excel and Kleidograph 4.0.2.

7.9.2 Internal Standard Screen

Compounds trialled as potential internal standards include 1-naphthoic acid **132**, 2-naphthoic acid **133**, naphthalenamine **134**, *N*-phenylnaphthalen-2-amine **135**, 1,2-naphthoquinone-4-sulfonic acid **90**, 2,6-diacetoxynaphthalene **136**, 2,6-naphthalenedisulfonic acid **137**, 2,3-dimethylbenzoic acid **138**, 3,5-dimethylbenzoic acid **139**, 4-ethylbenzoic acid **140**, 4-propylbenzoic acid **141**, 4-*tert*-butylbenzoic acid **142**, 2-acetylbenzoic acid **143**, 2-methoxybenzoic acid **91**, 4-methoxybenzoic acid **92**, 3,4-dimethoxybenzoic acid **93**, 2-nitrobenzoic acid **94**, 3-nitrobenzoic acid **95**, and 4-nitrobenzoic acid **144**. The compound (~1 mg) was added to sodium phosphate buffer (50 mM, 1 mL, pH 7.5) and sonicated (5 min, 30 °C) before being filtered (0.45 μ m membrane) into a HPLC vial. Samples were subjected to the reported HPLC conditions (refer to section 7.9) using a mobile phase of 23% acetonitrile in sodium phosphate buffer (100 mM, pH 2.0). Their retention times and λ_{max} are reported in Table 7.1.

Experimental

Table 7.1 Library of compounds to potentially use as an internal standard for monitoring the glucuronysynthesis of 2-phenylethanol 45 via HPLC.

Compound	Structure	Retention time (min)	λ_{\max} (nm)
solvent front	N/A	~2	
2-phenylethyl β -D-glucuronide 68		4.2	260
2-phenylethanol 45		7.2	260
1-naphthoic acid 132		32.1	217, 294
2-naphthoic acid 133		37.7	236, 281
naphthalenamine 134		2.0	221, 285
<i>N</i> -phenylnaphthalen-2-amine 135		2.0 & 3.0	227, 275
1,2-naphthoquinone-4-sulfonic acid 90		2.5	252, 361
2,3-dimethylbenzoic acid 138		19.7	254, 281
3,5-dimethylbenzoic acid 139		31.0	239, 287
4-ethylbenzoic acid 140		30.7	241

Compound	Structure	Retention time (min)	λ_{\max} (nm)
4-propylbenzoic acid 141		75.9	241
4- <i>tert</i> -butylbenzoic acid 142		116.8	241
2-acetylbenzoic acid 143		4.7	232, 272
2-methoxybenzoic acid 91		5.5	235, 296
4-methoxybenzoic acid 92		8.1	235, 294
3,4-dimethoxybenzoic acid 93		5.3	220, 261, 292
2-nitrobenzoic acid 94		6.3	210, 261
3-nitrobenzoic acid 95		9.3	221, 261
4-nitrobenzoic acid 144		10.2	271
2,6-diacetoxynaphthalene 136		7.8	239, 274
2,6-naphthalenedisulfonic acid 137		1.8	225, 275

7.9.3 Effect of internal standard

A solution of 2-phenylethanol **45** (final concentration 100 mM) and α -D-glucuronyl fluoride **51** (final concentration 100 mM) in sodium phosphate buffer

Experimental

(100 mM, pH 7.5) was divided (1460 μL each) into two separate vials. To the first vial (the control), sodium phosphate buffer (100 mM, 20 μL , pH 7.5) was added. To the second vial (internal standard), 2-methoxybenzoic acid **91** (75 mM) in sodium phosphate buffer (100 mM, 20 μL , pH 7.5) was added. Glucuronylsynthase (15 mg mL^{-1} , 20 μL) was added to each vial and the reaction rate monitored by the HPLC assay (refer to section 7.9) at 22 min intervals over 27 h ($\sim 6\%$ conversion). A mobile phase of 23% acetonitrile in sodium phosphate buffer (100 mM, pH 2.0) provided a retention time of 4.8 min for 2-phenylethanol **45** and 5.8 min for 2-methoxybenzoic acid **91**. The plot of the glucuronide product peak area against time was linear ($R^2 > 0.99$) over the studied time frame (Figure 3.12). The reaction without 2-methoxybenzoic acid **91** (control) provided an initial velocity of 15865 arbitrary units (au) min^{-1} whilst the reaction containing 1 mM 2-methoxybenzoic acid **91** (internal standard) provided an initial velocity of 15401 arbitrary units (au) min^{-1} (97% of control). At concentrations below 1 mM, 2-methoxybenzoic acid **91** did not affect the rate of the glucuronylsynthase reactions and so was adopted at 0.5 mM as an internal standard for monitoring the kinetics of these reactions by HPLC.

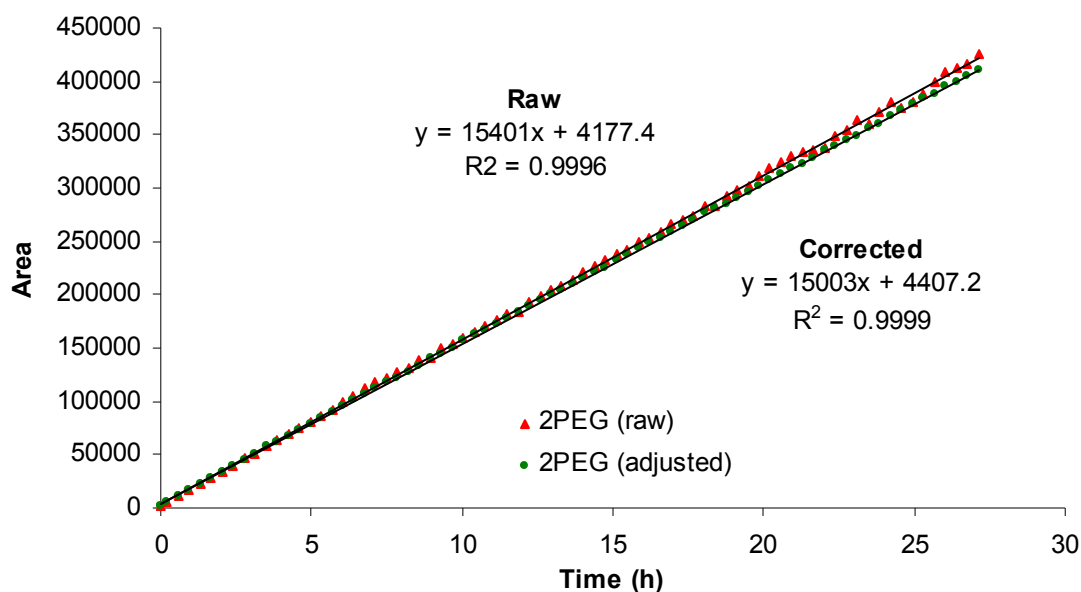
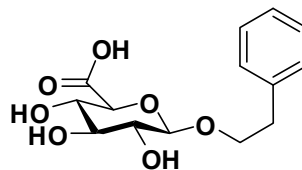


Figure 7.1. Reaction profiles for the glucuronylsynthase reaction between 2-phenylethanol **45** acceptor (100 mM) with α -D-glucuronyl fluoride **51** donor (100 mM) in the presence of 2-methoxybenzoic acid **91** raw data (\blacktriangle) and corrected with the internal data (\bullet) (21°C in 100 mM phosphate buffer, pH 7.5). Line represents line of best fit with its linear regression analysis.

7.9.4 Calibration of 2-phenylethyl β -D-glucuronide **68**



A solution of 2-phenylethyl β -D-glucuronide **68** (final concentrations 2 μ M, 4 μ M, 6 μ M, 8 μ M, 10 μ M, 15 μ M, 20 μ M, 25 μ M, 30 μ M, 40 μ M, 50 μ M, 75 μ M, and 100 μ M) in sodium phosphate buffer (100 mM, pH 7.5) was prepared and subjected to the HPLC assay (refer to section 7.9) in duplicate. A mobile phase of 23% acetonitrile in sodium phosphate buffer (100 mM, pH 2.0) provided a retention time of 4.8 min. The area was plotted against the concentration to provide the absorption co-efficient of 42846 au μ M⁻¹ for 2-phenylethyl β -D-glucuronide **68** under the specified conditions.

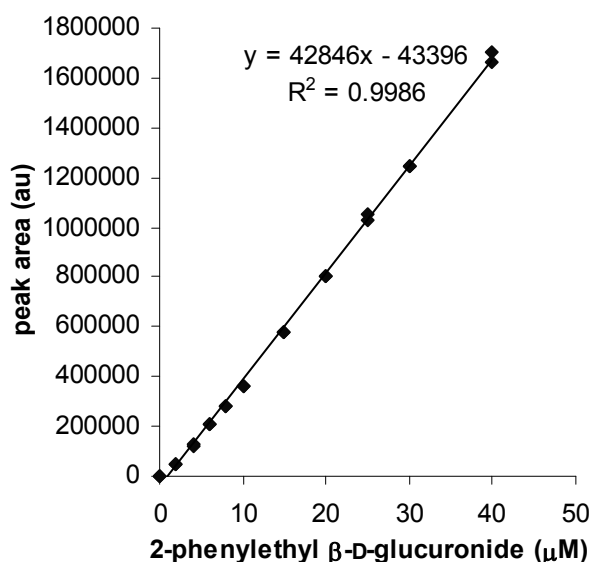
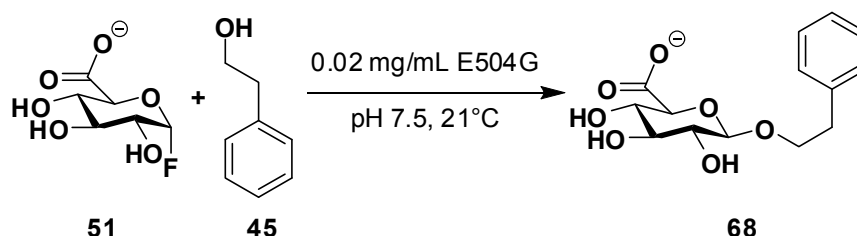


Figure 7.2. Calibration curve of 2-phenylethyl β -D-glucuronide **68** (211 nm, 21 $^{\circ}$ C, 100 mM sodium phosphate, pH 7.5). R^2 was calculated using linear regression analysis.

7.9.5 Michaelis-Menten kinetics of α -D-glucuronyl fluoride **51**

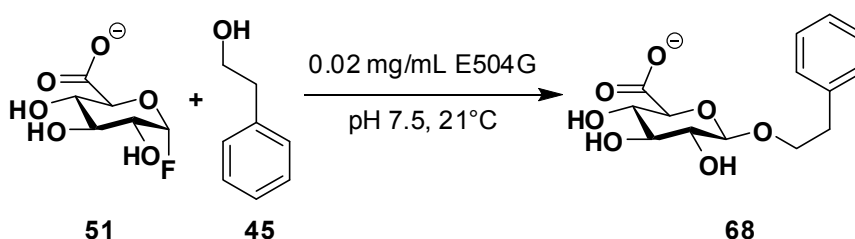


Glucuronylsynthase (1.2 mg mL⁻¹, 20 μ L) was added to 2-phenylethanol **45** (final concentration 97 mM) and α -D-glucuronyl fluoride **51** (final concentrations 0 μ M, 2 μ M, 4 μ M, 6 μ M, 8 μ M, 10 μ M, 15 μ M, 20 μ M, 25 μ M, 30 μ M, 40 μ M, 50 μ M, 75 μ M, and 100 μ M) pre-incubated at 21 $^{\circ}$ C in sodium phosphate buffer

Experimental

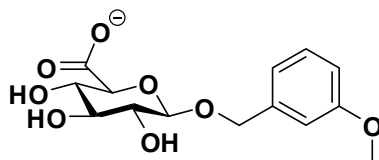
(100 mM, 1480 μ L, pH 7.5). The reaction was immediately subjected to HPLC (refer to section 7.9) with a mobile phase of 23% acetonitrile in sodium phosphate (100 mM, pH 2.0). Six injections were made to monitor the initial velocity of the reactions at 11 min intervals. Data points (minimum 3 points, 15–34% conversion) that encompassed the initial linear velocity ($R^2 > 0.99$) were used to plot initial velocities against the α -D-glucuronyl fluoride **51** concentration to provide the Michaelis-Menten plot (Figure 3.13).

7.9.6 Michaelis-Menten kinetics of 2-phenylethanol **45**



Glucuronylsynthase (2.8 mg mL⁻¹, 20 μ L,) was added to α -D-glucuronyl fluoride **51** (final concentration 1 mM) and 2-phenylethanol **45** (final concentrations 0 mM, 2 mM, 6 mM, 10 mM, 15 mM, 37 mM, 55 mM, 73 mM, 92 mM, and 107 mM) pre-incubated at 21 °C in sodium phosphate buffer (100 mM, 1480 μ L, pH 7.5). The reaction was immediately subjected to HPLC (refer to section 7.9) with a mobile phase of 23% acetonitrile in sodium phosphate buffer (100 mM, pH 2.0). Five injections were made to monitor the initial velocity of the reactions (<4% conversion) at 14 min intervals. Data points (5 points) that encompassed the initial linear velocity ($R^2 > 0.99$) were used to plot initial velocities against the 2-phenylethanol **45** concentration to provide the Michaelis-Menten plot (Figure 3.14).

7.9.7 Calibration of 3-methoxybenzyl β -D-glucuronide **71**



A solution of 3-methoxybenzyl β -D-glucuronide **71** (final concentration 5 μ M, 10 μ M, 20 μ M, 30 μ M, 40 μ M, 50 μ M, 75 μ M, and 100 μ M) in sodium phosphate buffer (100 mM, pH 7.5) was prepared and subjected to the HPLC assay (refer to section 7.9) in duplicate. A mobile phase of 23% acetonitrile in sodium phosphate buffer (100 mM, pH 2.0) provided a retention time of 3.7 min. The peak area was plotted against the concentration to provide the absorption co-

efficient as $48062 \text{ au } \mu\text{M}^{-1}$ for 3-methoxybenzyl β -D-glucuronide **71** under the specified conditions.

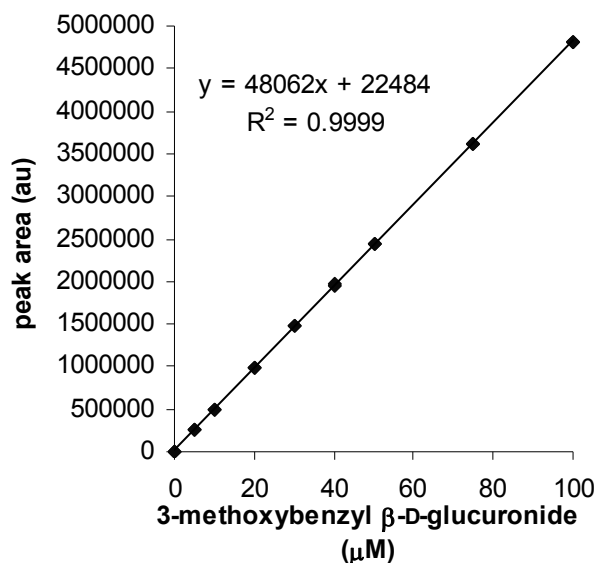
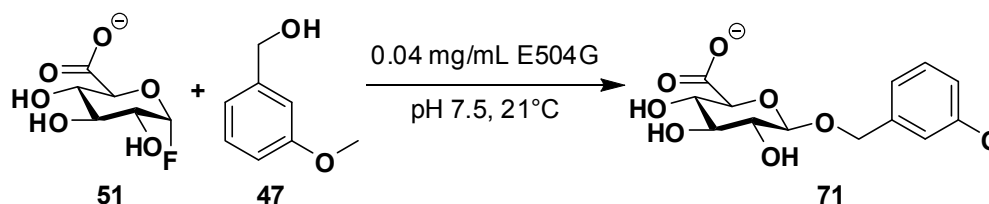


Figure 7.3. Calibration curve of 3-methoxybenzyl β -D-glucuronide **71** (211 nm, 21 °C, 100 mM sodium phosphate, pH 7.5). R^2 was calculated using linear regression analysis.

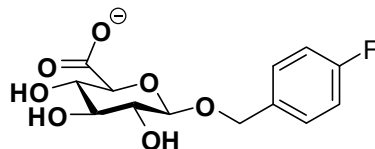
7.9.8 Michaelis-Menten kinetics of 3-methoxybenzyl alcohol **47**



Glucuronylsynthase (2.9 mg mL^{-1} , $20 \mu\text{L}$) was added to α -D-glucuronyl fluoride **51** (final concentration 1 mM) and 3-methoxybenzyl alcohol **47** (final concentrations 0 mM, 2 mM, 6 mM, 10 mM, 15 mM, 22 mM, 37 mM, 55 mM, 73 mM, 90 mM, and 107 mM) pre-incubated at 21 °C in sodium phosphate buffer (100 mM, 1480 μL , pH 7.5). The reaction was immediately subjected to HPLC (refer to section 7.9) with a mobile phase of 23% acetonitrile in sodium phosphate (100 mM, pH 2.0). Five injections were made to monitor the initial velocity of the reactions (<4% conversion) at 13 min intervals. Data points (5 points) that encompassed the initial linear velocity ($R^2 > 0.99$) were used to plot initial velocities against the 3-methoxybenzyl alcohol **47** concentration to provide the Michaelis-Menten model (Figure 3.15). The data did not fit a standard Michaelis-Menten curve, so the kinetic parameters were determined by taking the tangent of the initial slope ($k_{\text{cat}}/K_m = 1.25 \text{ M}^{-1} \text{ s}^{-1}$) and the local maximum velocity ($\text{max } k_{\text{cat}} = 0.022 \text{ s}^{-1}$ at 55 mM) from the Michaelis-Menten plot.

Experimental

7.9.9 Calibration of 4-fluorobenzyl β -D-glucuronide **73**



A solution of 4-fluorobenzyl β -D-glucuronide **73** (final concentration 1 μ M, 2.5 μ M, 5 μ M, 7.5 μ M, 10 μ M, 22.5 μ M, 35 μ M, 47.5 μ M, 60 μ M and 74 μ M) in sodium phosphate buffer (100 mM, pH 7.5) was prepared and subjected to the HPLC assay (refer to section 7.9) in duplicate. A mobile phase of 23% acetonitrile in sodium phosphate buffer (100 mM, pH 2.0) provided a retention time of 4.9 min. The peak area was plotted against the concentration to provide the absorption co-efficient of 39739 au μ M⁻¹ for 4-fluorobenzyl β -D-glucuronide **73** for the specified conditions.

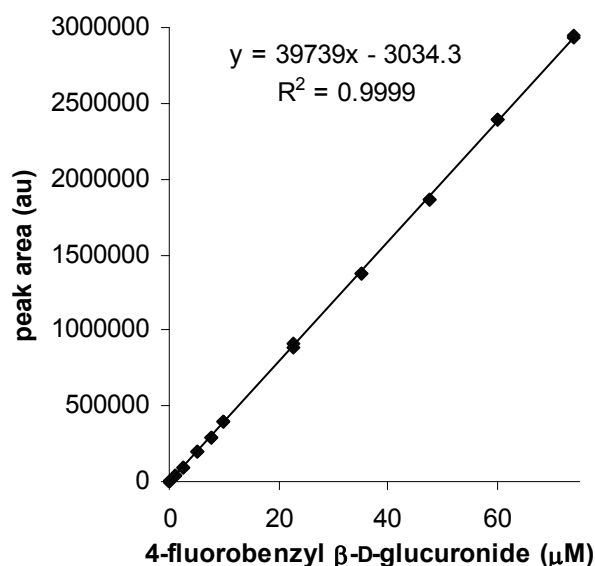
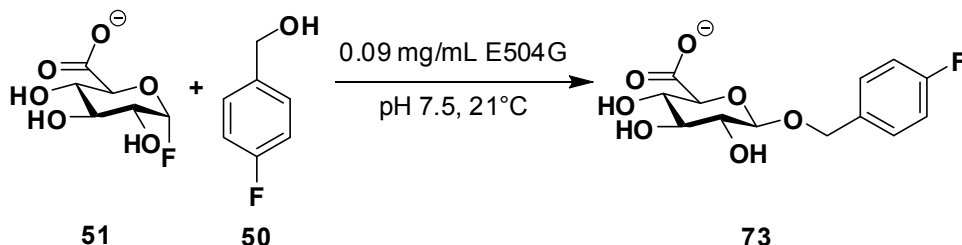


Figure 7.4. Calibration curve of 4-fluorobenzyl β -D-glucuronide **73** (211 nm, 21 $^{\circ}$ C, 100 mM sodium phosphate, pH 7.5). R^2 was calculated using linear regression analysis.

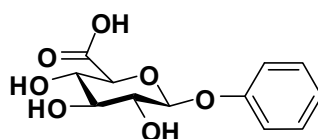
7.9.10 Michaelis-Menten kinetics of 4-fluorobenzyl alcohol **50**



Glucuronylsynthase (6.5 mg mL⁻¹, 20 μ L) was added to α -D-glucuronyl fluoride **51** (final concentration 1 mM) and 4-fluorobenzyl alcohol **50** (final concentrations 0 mM, 2 mM, 4 mM, 6 mM, 10 mM, 15 mM, 26 mM, 37 mM, 55 mM, 73 mM and 107 mM) pre-incubated at 21 $^{\circ}$ C in sodium phosphate buffer (100 mM, 1480 μ L, pH 7.5). The reaction was immediately subjected to HPLC

(refer to section 7.9) with a mobile phase of 23% acetonitrile in sodium phosphate buffer (100 mM, pH 2.0). Five injections were made to monitor the initial velocity of the reactions (<4% conversion) at 15 min intervals. Data points (5 points) that encompassed the initial linear velocity ($R^2 > 0.99$) were used to plot initial velocities against the 4-fluorobenzyl alcohol **50** concentration to provide the Michaelis-Menten plot (Figure 3.16). The data did not fit a standard Michaelis-Menten model, so the kinetic parameters were determined by taking the tangent of the initial slope ($k_{cat}/K_m = 0.59 \text{ M}^{-1} \text{ s}^{-1}$) and the local maximum velocity (max $k_{cat} = 0.081 \text{ s}^{-1}$ at 37 mM) from the Michaelis-Menten plot.

7.9.11 Calibration of phenyl β -D-glucuronide **76**



A solution of phenyl β -D-glucuronide **76** (final concentration 2 μM , 4 μM , 6 μM , 8 μM , 10 μM , 20 μM , 40 μM , 60 μM , 80 μM and 100 μM) in sodium phosphate buffer (100 mM, pH 7.5) was prepared and subjected to the HPLC assay (refer to section 7.9) in duplicate. A mobile phase of 18% acetonitrile in sodium phosphate buffer (100 mM, pH 2.0) provided a retention time of 4.2 min. The area was plotted against the concentration to provide the absorption co-efficient of 30292 au μM^{-1} for phenyl β -D-glucuronide **76** for the specified conditions.

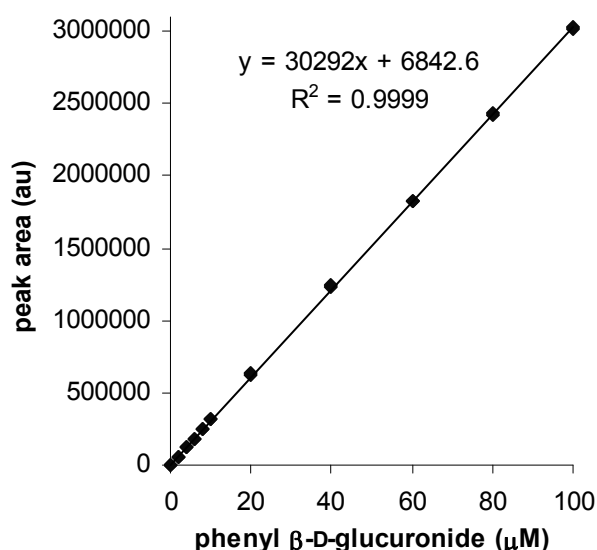
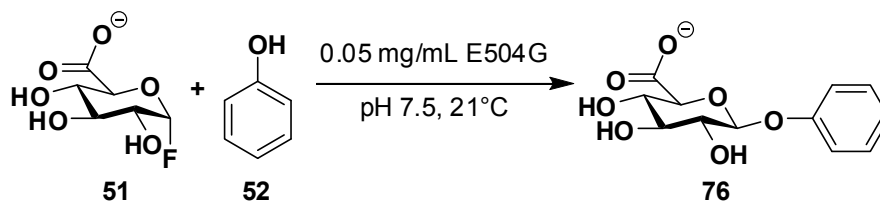


Figure 7.5. Calibration curve of phenyl β -D-glucuronide **76** (211 nm, 21 $^{\circ}\text{C}$, 100 mM sodium phosphate, pH 7.5). R^2 was calculated using linear regression analysis.

Experimental

7.9.12 Michaelis-Menten kinetics of phenol **52**



Glucuronylsynthase (1.45 mg mL^{-1} , $50 \text{ }\mu\text{L}$) was added to α -D-glucuronyl fluoride **51** (final concentration 1 mM) and phenol **52** (final concentrations 0 mM , 2 mM , 4 mM , 6 mM , 8 mM , 10 mM , 12 mM , 16 mM , 20 mM , 30 mM , 40 mM , 80 mM , 160 mM and 240 mM) pre-incubated at $21 \text{ }^\circ\text{C}$ in sodium phosphate buffer (100 mM , $1450 \text{ }\mu\text{L}$, $\text{pH } 7.5$). The reaction was immediately subjected to HPLC (refer to section 7.9) with a mobile phase of 18% acetonitrile in sodium phosphate buffer (100 mM , $\text{pH } 2.0$). Five injections were made to monitor the initial velocity of the reactions ($<1\%$ conversion) at 16 min intervals. Data points (5 points) that encompassed the initial linear velocity ($R^2 > 0.99$) were used to plot initial velocities against the phenol **52** concentration to provide the Michaelis-Menten plot (Figure 3.17). The data did not fit a standard Michaelis-Menten model, so the kinetic parameters were determined by taking the tangent of the initial slope ($k_{\text{cat}}/K_m = 0.21 \text{ M}^{-1} \text{ s}^{-1}$) and the local maximum velocity (max $k_{\text{cat}} = 0.0029 \text{ s}^{-1}$ at 30 mM) from the Michaelis-Menten plot.

7.10 Reaction optimisation

7.10.1 pH optimisation

Glucuronylsynthase (2.0 mg mL^{-1} , $20 \text{ }\mu\text{L}$) was added to α -D-glucuronyl fluoride **51** (final concentration 1 mM) and 2-phenylethanol **45** (final concentration 107 mM) pre-incubated at $21 \text{ }^\circ\text{C}$ in sodium phosphate buffer (100 mM , $1480 \text{ }\mu\text{L}$) adjusted to $\text{pH } 3.0$, 4.0 , 5.0 , 6.0 , 7.0 , 8.0 , 9.0 , 10.0 , or 11.0 . The reaction was immediately subjected to HPLC (refer to section 7.9) with a mobile phase of 23% acetonitrile in sodium phosphate buffer (100 mM , $\text{pH } 2.0$). Five injections were made at 16 min intervals to determine the initial reaction velocity. After 5 days, the reactions were re-subjected to HPLC to determine the yield of the reactions based on the limiting amount of α -D-glucuronyl fluoride **51** added (Figure 3.18).

7.10.2 Temperature optimisation

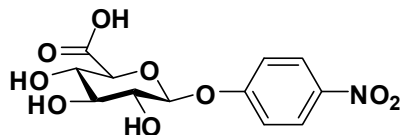
Glucuronylsynthase (1.7 mg mL^{-1} , $20 \text{ }\mu\text{L}$) was added to α -D-glucuronyl fluoride **51** (final concentration 89 mM) and 3-methoxybenzyl alcohol **47** (final concentration 89 mM) pre-incubated at either $4 \text{ }^\circ\text{C}$, $11 \text{ }^\circ\text{C}$, $18 \text{ }^\circ\text{C}$, $24 \text{ }^\circ\text{C}$, $30 \text{ }^\circ\text{C}$, or $37 \text{ }^\circ\text{C}$ in sodium phosphate buffer (100 mM , $1480 \text{ }\mu\text{L}$, $\text{pH } 7.5$). The reaction was immediately subjected to HPLC (refer to section 7.9) with a mobile phase of 23% acetonitrile in sodium phosphate buffer (100 mM , $\text{pH } 2.0$). Five injections were made at 16 min intervals to determine the initial reaction velocity. Reactions were stored at their corresponding temperatures and re-tested after day 4 and 13. Reaction yields were determined by the removal of aliquots ($20 \text{ }\mu\text{L}$) which were diluted in sodium phosphate buffer (100 mM , $180 \text{ }\mu\text{L}$, $\text{pH } 7.5$) then subjected to the HPLC assay (Figure 3.19).

7.10.3 Effect of Enzyme Concentration

A solution of 2-phenylethanol **45** (final concentration 94 mM) and α -D-glucuronyl fluoride **51** (final concentration 1 mM) in sodium phosphate buffer (100 mM , $1350 \text{ }\mu\text{L}$, $\text{pH } 7.5$) was distributed into six separate HPLC vials. The solutions were equilibrated at $21 \text{ }^\circ\text{C}$ for 5 min then glucuronylsynthase ($150 \text{ }\mu\text{L}$, final concentrations $0.0257 \text{ mg mL}^{-1}$, 0.129 mg mL^{-1} , 0.257 mg mL^{-1} , 0.643 mg mL^{-1} , 1.29 mg mL^{-1} , and 1.93 mg mL^{-1}) was added and the reactions were immediately subjected to HPLC (refer to section 7.9) with a mobile phase of 23% acetonitrile in sodium phosphate buffer (100 mM , $\text{pH } 2.0$). The reactions were monitored individually by HPLC by a further 4 injections at 16 min intervals. Data points (2-5 points, 4-42% conversion) that encompassed the initial linear velocity ($R^2 > 0.99$ where applicable) were used to plot initial velocities per mg enzyme against the glucuronylsynthase concentration (Figure 3.20). A linear relationship ($R^2 > 99\%$) exists between the initial velocity per mg enzyme and the concentration of glucuronylsynthase.

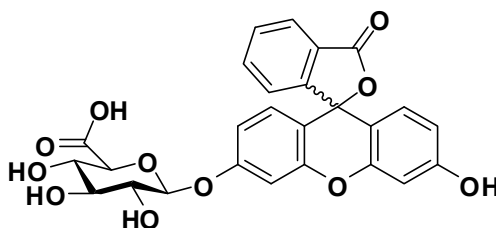
7.11 In vitro chromo-ablative assay for directed evolution

7.11.1 Small scale *p*-nitrophenyl- β -D-glucuronide **25**⁴⁰



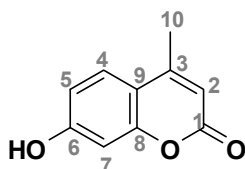
Glucuronylsynthase (22.5 mg mL⁻¹, 8 μ L, final concentration 0.5 mg mL⁻¹) was added to *p*-nitrophenol **54** (5 mg, 36 μ mol, final concentration 100 mM) and α -D-glucuronyl fluoride **51** (7.7 mg, 36 μ mol, final concentration 100 mM) in sodium phosphate buffer (100 mM, 351 μ L, pH 7.5) and swirled at RT for 4 d. No product was observed by TLC analysis (ethyl acetate : methanol : water, 7 : 2 : 1) but a weak signal consistent with the formation of product **25** was detected by LRMS (-ESI); **LRMS (-ESI):** *m/z* 314 ([M-H]⁻, <10%)

7.11.2 Small scale fluorescein- β -D-glucuronide



Glucuronylsynthase (22.5 mg mL⁻¹, 10 μ L, final concentration 0.2 mg mL⁻¹) was added to fluorescein sodium salt **96** (2 mg, 5 μ mol, final concentration 5 mM) and α -D-glucuronyl fluoride **51** (1.1 mg, 5 μ mol, final concentration 5 mM) in sodium phosphate buffer (100 mM, 1.069 mL, pH 7.5) and swirled at RT for 4 d. No product was observed by TLC analysis (ethyl acetate : methanol : water, 7 : 2 : 1) or LRMS (-ESI).

7.11.3 Synthesis of 7-hydroxy-4-methylumbelliferone **97**¹²⁷

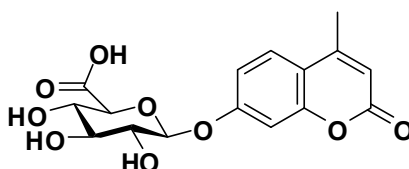


Resorcinol **99** (2.236g, 20.31 mmol), ethyl acetoacetate (2.70 g, 20.7 mmol) and Amberlite IR-120+ resin (2.0 g) in toluene (20 mL) were refluxed (2 h) under Dean-Stark conditions. The mixture was cooled to RT, then warm methanol (40 mL) was added and the Amberlite resin removed by filtration. The filtrate was

evaporated under reduced pressure and the residue was recrystallised from methanol/water and dried overnight under vacuum to produce the white crystals of 7-hydroxy-4-methylumbelliferone **97** (1.36 g, 38.0%).

mp 183-185 °C [lit.²¹⁸ mp 186-187 °C]; **IR** (KBr disc): 3497 (m, O-H), 3127 (Ar C-H), 1673 (s, O-H), 1604 (C=C), 1453, 1392, 1276, 1068, 846, 806, 583, 477; **¹H NMR** (400 MHz, MeOD): δ 10.42 (1H, singlet, O-H), 7.45 (1H, d, J_{H4-H5} 8.7, H4), 6.68 (1H, dd, $^3J_{H4-H5}$ 8.7, $^4J_{H5-H7}$ 2.4, H5), 6.58 (1H, d, $^4J_{H5-H7}$ 2.3, H7), 5.99 (1H, d, J_{H2-H10} 1.0, H2), 2.23 (3H, d, $^4J_{H2-H10}$ 1.0, H10); **¹³C NMR** (100 MHz, MeOD): 170.7 (C1), 169.8, 164.3, 163.0, 136.1, 122.4, 121.5, 119.8, 111.7, 27.6 (C10); **LRMS (+ESI) *m/z***: 199 ([M+Na]⁺, 10%), 177 ([M+H]⁺, 100%); **HRMS (+ESI) *m/z***: 177.0552 (C₁₀H₉O₃ gives 177.0552).

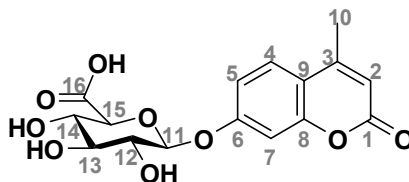
7.11.4 Small scale 4-methylumbellifer-7-yl β-D-glucuronide **100**



Glucuronylsynthase (22.5 mg mL⁻¹, 63 μL, final concentration 0.5 mg mL⁻¹) was added to 7-hydroxy-4-methylumbelliferone **97** (5 mg, 28 μmol, final concentration 10 mM), α-D-glucuronyl fluoride **51** (6.0 mg, 28 μmol, final concentration 10 mM) and DMSO (284 μL, final concentration 10% v/v) in sodium phosphate buffer (100 mM, 2.491 mL, pH 7.5) and swirled at RT for 4 d. Product was observed by TLC analysis (ethyl acetate : methanol : water, 7 : 2 : 1) and confirmed by LRMS (-ESI).

LRMS (-ESI): *m/z* 351 ([M-H]⁻, 25%)

7.11.5 Preparative scale 4-methylumbellifer-7-yl-β-D-glucuronide **100**^{219,220}



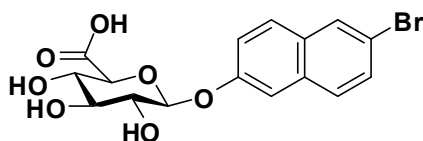
Glucuronylsynthase (22.5 mg mL⁻¹, 757 μL, final concentration 0.48 mg mL⁻¹) was added to 7-hydroxy-4-methylumbelliferone **97** (60 mg, 0.34 mmol, final concentration 10 mM), α-D-glucuronyl fluoride **51** (72 mg, 0.34 mmol, final concentration 10 mM) and DMSO (3.4 mL, final concentration 9.7% v/v) in sodium phosphate buffer (100 mM, 31.04 mL, pH 7.5) and swirled at RT for 5 d. The crude reaction was dried onto silica which was subjected to flash

Experimental

chromatography (ethyl acetate : methanol : water, 7 : 2 : 1). The 4-methylumbellifer-7-yl β -D-glucuronide **100** (49 mg, 41%) was obtained as a white powder. Spectral data was identical to reported literature.²²¹

¹H NMR (300 MHz, D₂O): δ 7.06 (1H, d, J_{H4-H5} 9.0, H4), 6.63 (1H, d, J_{H4-H5} 8.7, H5), 6.47 (1H, s, H7), 5.64 (1H, s, H2), 4.88 (1H, d, $J_{H11-H12}$ 6.3, H11), 3.71 (1H, d, $J_{H14-H15}$ 8.7, H15), 4.10-3.20 (3H, m, obscured, H12-14), 1.90 (3H, s, H10).

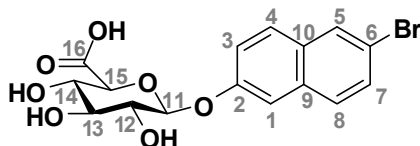
7.11.6 Small scale 6-bromo-2-naphthyl β -D-glucuronide **101**²²²



Glucuronylsynthase (22.5 mg mL⁻¹, 50 μ L, final concentration 0.5 mg mL⁻¹) was added to 6-bromo-2-naphthol **98** (6 mg, 27 μ mol, final concentration 12 mM), α -D-glucuronyl fluoride **51** (6 mg, 28 μ mol, 12 mM) and DMSO (224 μ L, final concentration 10% v/v) in sodium phosphate buffer (100 mM, 1.972 mL, pH 7.5) and swirled at RT for 4 d. Product was observed by TLC analysis (ethyl acetate : methanol : water, 7 : 2 : 1) and confirmed by LRMS (-ESI).

LRMS (-ESI): m/z 397 ([M-H]⁻, 25%), 399 ([M-H]⁻, 25%).

7.11.7 Preparative scale 6-bromo-2-naphthyl β -D-glucuronide **101**²²²



Glucuronylsynthase (22.5 mg mL⁻¹, 598 μ L, final concentration 0.48 mg mL⁻¹) was added to 6-bromo-2-naphthol **98** (61 mg, 0.27 mmol, final concentration 9.7 mM), α -D-glucuronyl fluoride **51** (58 mg, 0.27 mmol, final concentration 9.7 mM) and DMSO (2.69 mL, final concentration 9.7% v/v) in sodium phosphate buffer (100 mM, 24.47 mL, pH 7.5) and swirled at RT for 5 d. The crude reaction was dried onto silica which was subjected to flash chromatography (ethyl acetate : methanol : water, 7 : 2 : 1). The 6-bromo-2-naphthyl β -D-glucuronide **101** (74 mg, 69%) was obtained as a white powder.

¹H NMR (300 MHz, D₂O): δ 7.10-6.70 (6H, m, H1, H3-H5, H7, H8), 4.76 (1H, obscured, H11), 3.80-3.30 (4H, m, H12-H15).

7.11.8 Excitation and emission of 7-hydroxy-4-methylumbelliferone **97**²²³ and 6-bromo-2-naphthol **98**²²⁴

Fluorescence was carried out at room temperature (25 ± 5 °C) with an excitation slit of 2.5 nm and an emission slit of 2.5 nm. Data was collected at a rate of 600 nm min^{-1} with a resolution of 1 nm. The excitation spectra (Figure 3.23 and Figure 3.24) were collected between 280-440 nm and the emission spectra was collected between 400-700 nm. Sodium phosphate (100 mM, pH 7.5) was used to blank the instrument prior to solutions (1 mM) of 7-hydroxy-4-methylumbelliferone **97** and 6-bromo-2-naphthol **98** in sodium phosphate (100 mM, pH 7.5) being scanned. 7-Hydroxy-4-methylumbelliferone **97** showed an excitation maximum (λ_{ex}) of 389 nm and an emission maximum (λ_{em}) of 447 nm (Figure 7.6). 6-Bromo-2-naphthol **98** showed an excitation maximum (λ_{ex}) of 257 nm and an emission maximum (λ_{em}) of 367 nm (Figure 7.7).

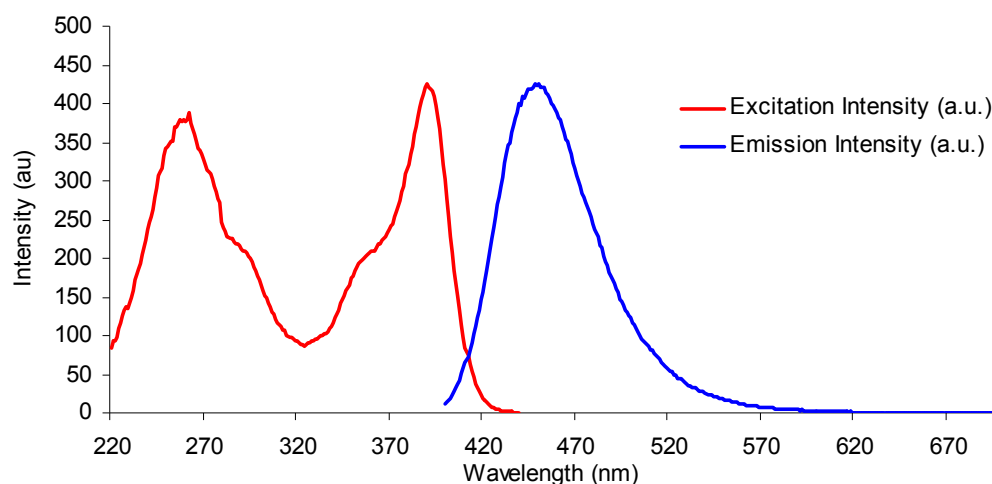


Figure 7.6. Excitation and emissions spectrum of 1 mM 7-hydroxy-4-methylumbelliferone **97** in 100 mM sodium phosphate, pH 7.5

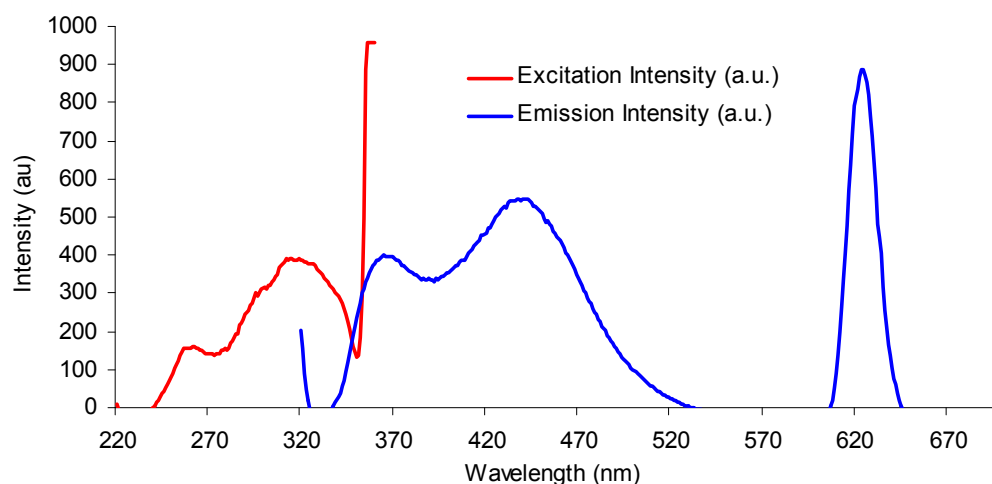


Figure 7.7. Excitation and emissions spectrum of 1 mM 6-bromo-2-naphthol **98** in 100 mM sodium phosphate, pH 7.5

Experimental

7.11.9 Calibration of 7-hydroxy-4-methylumbelliferone **97**

A solution of 7-hydroxy-4-methylumbelliferone **97** (final concentration 0.1 mM, 0.2 mM, 0.3 mM, 0.4 mM, and 0.5 mM) in sodium phosphate buffer (100 mM, pH 7.5) was analysed by fluorometry. An excitation of 389 nm was used with the emission intensity observed at 449 nm plotted against the concentration (Figure 7.8) to provide the absorption co-efficient of 805 au mM⁻¹.

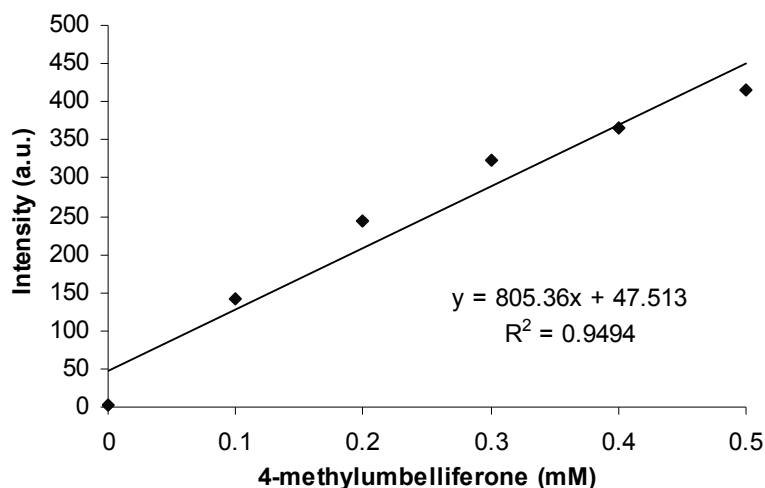


Figure 7.8. Calibration curve of 7-hydroxy-4-methyl-umbelliferone **97** in 100 mM sodium phosphate, pH 7.5 obtained from fluorometry ($\lambda_{\text{ex}} = 389 \text{ nm}$, $\lambda_{\text{em}} = 449 \text{ nm}$). R^2 was calculated using linear regression analysis.

7.11.10 Calibration of 6-bromo-2-naphthol **98**

A solution of 6-bromo-2-naphthol **98** (final concentration 0.04 mM, 0.08 mM, 0.12 mM, 0.16 mM, and 0.20 mM) in sodium phosphate buffer (100 mM, pH 7.5) was analysed by fluorometry. An excitation of 257 nm was used with the emission intensity observed at 367 nm plotted against the concentration (Figure 7.9) to provide the absorption co-efficient of 1691 au mM⁻¹.

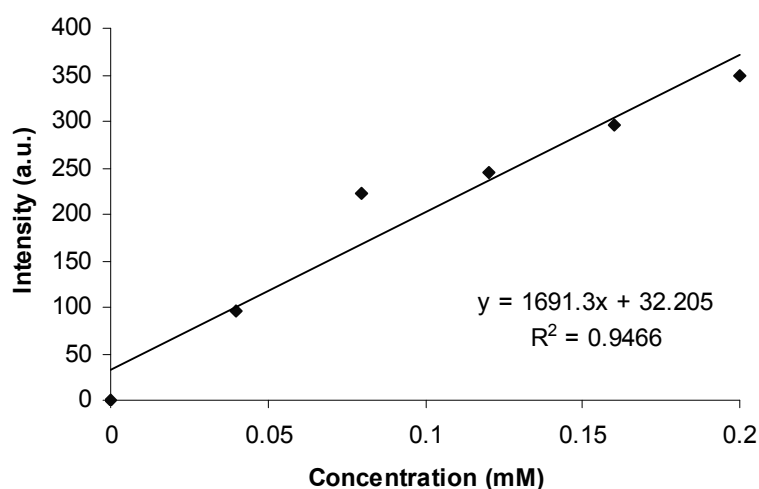
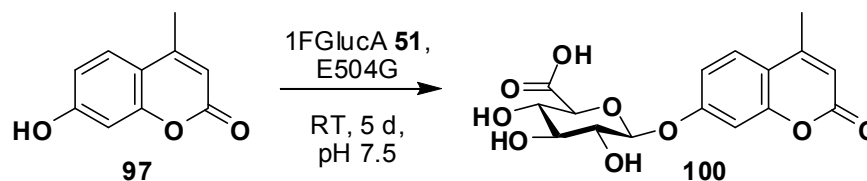
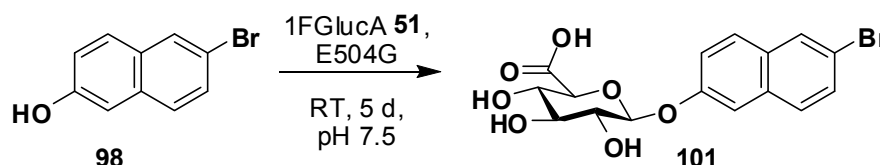


Figure 7.9. Calibration curve of 6-bromo-2-naphthol **98** in 100 mM sodium phosphate, pH 7.5 obtained from fluorometry ($\lambda_{\text{ex}} = 257 \text{ nm}$, $\lambda_{\text{em}} = 367 \text{ nm}$). R^2 was calculated using linear regression analysis.

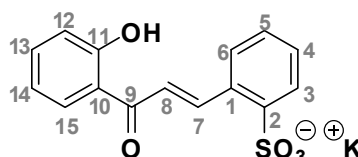
7.11.11 In vitro assay of 7-hydroxy-4-methylumbelliferone **97**

Glucuronylsynthase (22.5 mg mL^{-1} , $113 \text{ }\mu\text{L}$, final concentration 0.85 mg mL^{-1}) was added to 7-hydroxy-4-methylumbelliferone **97** (0.26 mg , $1.5 \text{ }\mu\text{mol}$, final concentration 0.5 mM) and α -D-glucuronyl fluoride **51** (6.4 mg , 0.03 mmol , final concentration 10 mM) in sodium phosphate buffer (100 mM , 2.887 mL , $\text{pH } 7.5$) in a quartz cuvette. The reaction was left untouched for 5 days in the fluorometer with the emission at 449 nm (excitation 389 nm) scanned every 10 min . The reaction was repeated in the absence of enzyme.

7.11.12 In vitro assay of 6-bromo-2-naphthol **98**

Glucuronylsynthase (22.5 mg mL^{-1} , $113 \text{ }\mu\text{L}$, final concentration 0.85 mg mL^{-1}) was added to 6-bromo-2-naphthol **98** (0.13 mg , $0.57 \text{ }\mu\text{mol}$, final concentration 0.19 mM) and α -D-glucuronyl fluoride **51** (6.4 mg , 0.03 mmol , final concentration 10 mM) in sodium phosphate buffer (100 mM , 2.887 mL , $\text{pH } 7.5$) in a quartz cuvette. The reaction was left untouched for 5 days in the fluorometer with the emission at 367 nm (excitation 257 nm) scanned every 10 min . The reaction was repeated in the absence of enzyme.

7.12 In vitro fluoride-selective assay for directed evolution

7.12.1 Synthesis of potassium 2'-hydroxychalcone-2-sulfonate **105**²²⁵

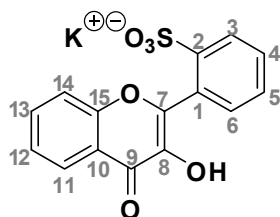
Potassium hydroxide (5 M , 7.5 mL , 37.5 mmol) was added to *o*-hydroxyacetophenone **103** (1.36 g , 10.0 mmol) in methanol (9 mL). Sodium 2-formylbenzenesulfonate **104** (2.09 g , 10.0 mmol) was dissolved in a minimal volume of water ($\sim 10 \text{ mL}$) and added dropwise to the stirring, basic acetophenone solution at RT. After stirring at RT for 30 h , a yellow-orange

Experimental

precipitate had formed and a new spot was visible by TLC (ethyl acetate : methanol, 5 : 2 + 0.1% formic acid). The reaction mixture was acidified to pH 2 with concentrated hydrochloric acid and the yellow precipitate was collected by filtration. Recrystallisation from aqueous methanol (50% v/v) produced shiny, yellow flakes of 2'-hydroxychalcone-2-sulfuric acid hemihydrate **105** (3.47 g, 99%).

mp 307-311 °C (decomp.); **IR** (KBr): 3480 (O-H), 3077 (Ar-H), 3057 (Ar-H), 1650 (C=O), 1593 (C=C), 1490, 1343 ($\nu_{\text{as}}\text{SO}_2$), 1205 ($\nu_{\text{s}}\text{SO}_2$), 1017, 750, 744 (C-S); **$^1\text{H NMR}$** (800 MHz, d_6 -DMSO): δ 12.58 (1H, s, OH), 8.96 (1H, d, $J_{\text{H7-H8}}$ 15.7, H7), 8.26 (1H, d, J 7.8), 8.06 (1H, d, J 7.0), 7.92-7.84 (2H, m, H8), 7.57 (1H, t, J 7.5), 7.43 (2H, m,), 7.04-6.97 (2H, m,); **$^{13}\text{C NMR}$** (100 MHz, d_6 -DMSO): 194.0 (C9), 162.0, 147.9, 144.81, 136.3, 131.8, 131.0, 129.8, 129.1, 127.4, 127.2, 121.9, 120.7, 119.2, 117.8; **LRMS (-ESI)** m/z : 303 ([M-K]⁻, 100); **HRMS (-ESI)** m/z : 303.0324 (C₁₅H₁₁O₅S gives 303.0327); **Anal.** Calcd. for C₁₅H₁₁KO₅S·½H₂O: C, 51.27; H, 3.44; K, 11.13; S, 9.12. Found: C, 51.21; H, 3.58; K, 11.73; S 9.15.

7.12.2 Synthesis of potassium flavonol-2-sulfate **102**²²⁵



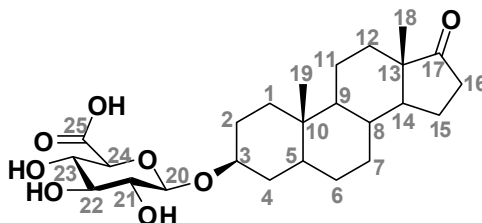
Potassium hydroxide (40% m/v, 3.7 mL) was added to potassium 2'-hydroxychalcone-2-sulfate hemihydrate **105** (1.13 g, 3.22 mmol) dissolved in aqueous methanol (50% v/v, 37 mL). The mixture was cooled on ice and then hydrogen peroxide (30% w/w, 1.11 mL) was added. After 2 h stirring on ice, the solution was neutralised with hydrochloric acid (1 M) and solvent removed under reduced pressure. The residue was subjected to reverse-phase flash chromatography (100% water to 100% methanol gradient). Recrystallisation from water produced tan crystals of potassium flavonol-2-sulfate hydrate **102** (0.43 g, 36%).

mp 311-321 °C (decomp.); **IR** (KBr): 3438 (O-H), 1629 (C=O), 1611, 1565 (C=C), 1469, 1421, 1345 ($\nu_{\text{as}}\text{SO}_2$), 1201 ($\nu_{\text{s}}\text{SO}_2$), 1129, 1095, 1023, 901, 766, 757 (C-S), 615; **$^1\text{H NMR}$** (800 MHz, d_6 -DMSO): δ 8.79 (1H, s, OH), 8.12 (1H, dd, 3J 7.9, 4J 1.0), 7.94 (1H, d, J 7.8), 7.74 (1H, dt, J 7.7, 4J 1.3), 7.59-7.48 (4H, m), 7.45 (1H, t, J 7.5); **$^{13}\text{C NMR}$** (200 MHz, d_6 -DMSO): 169.3 (C9), 151.0,

147.7, 142.6, 133.9, 129.1, 126.7, 125.7, 124.8, 124.2, 123.5, 120.8, 120.2, 118.8, 114.5; **LRMS (-ESI)** m/z : 317 ($[M-K]^+$, 100); **HRMS (-ESI)** m/z : 317.0120 ($C_{15}H_9O_6S$ gives 317.0120).

7.13 Steroid glucuronylsynthase reactions

7.13.1 Epiandrosterone β -D-glucuronide **109**¹³

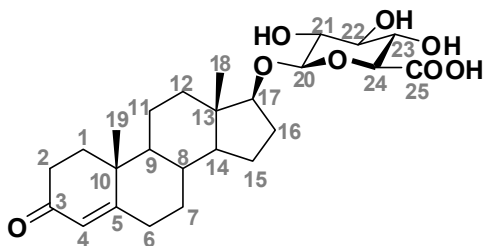


Glycosynthase (E504G, 27 mg mL⁻¹, 204 μ L, final concentration 0.22 mg mL⁻¹) was added to α -D-glucuronyl fluoride **51** (36 mg, 0.17 mmol, final concentration 7 mM), epiandrosterone **56** (40 mg, 0.14 mmol, final concentration 5.7 mM) and *n*-dodecyl β -maltoside (490 mg, final concentration 2% w/v) in sodium phosphate buffer (50 mM, pH 7.5, final volume 24.5 mL). The reaction was swirled continuously under ambient conditions for 4 days then dried onto silica. The crude product over silica was subjected to flash chromatography (ethyl acetate : methanol : water, 7:2:1) to reclaim unreacted epiandrosterone **56** (30 mg, 75%) and obtain 17-oxo-androst-5 α -an-3-yl β -D-glucuronide **109** (14 mg, 21%) as a white powder.

mp >200 °C (decomp); **R_f** 0.26 (ethyl acetate : methanol : water, 7:2:1); **IR** (NaCl): 3339 (O-H), 2924, C-H), 2850 (C-H), 1728 (C=O), 1607, 1415, 1031, 562; **¹H NMR** (400 MHz, MeOD): δ 4.44 (1H, d, $J_{H20-H21}$ 7.8, H20), 3.73 (1H, m, H3), 3.65 (1H, d, $J_{H23-H24}$ 8.3, H24), 3.54-3.37 (2H, m, H22, H23), 3.19, (1H, t, $J_{H20-H21} \approx J_{H21-H22}$ 8.1, H21), 2.43 (1H, dd, J 19.1, J 8.6) 2.21-0.68 (21H, m), 0.88 (3H, s, CH₃), 0.87 (3H, s, CH₃); **¹³C NMR** (100 MHz, MeOD): 224.1 (C17), 102.0 (C20), 79.2, 77.7, 76.2, 74.8, 73.6, 55.9, 52.7, 46.0, 38.2, 36.9, 36.7, 36.4, 35.3, 32.8, 32.1, 30.2, 29.7, 22.7, 21.6, 14.2, 12.7, C25 is unresolved and one carbon obscured; **LRMS (+ESI)** m/z : 511 ($[M-H+2Na]^+$, 70%), 489 ($[M+Na]^+$, 100%); **HRMS (+ESI)** m/z : 489.2463 ($[M+Na]^+$, C₂₅H₃₈O₈Na gives 489.2464).

Experimental

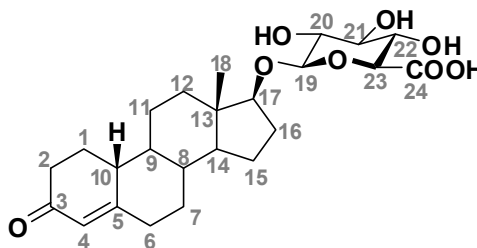
7.13.2 Testosterone β -D-glucuronide **6**^{20.206}



Glycosynthase (E504G, 33 mg mL⁻¹, 175 μ L, final concentration 0.22 mg mL⁻¹) was added to α -D-glucuronyl fluoride **51** (36 mg, 0.17 mmol, final concentration 6 mM), testosterone **7** (42 mg, 0.15 mmol, final concentration 5 mM) and *n*-dodecyl β -maltoside (568 mg, final concentration 2% w/v) in sodium phosphate buffer (50 mM, 28.9 mL, pH 7.5). The suspension was swirled continuously under ambient conditions for 4 days then dried onto silica. The crude product over silica was subjected to flash chromatography (ethyl acetate : methanol : water, 7:2:1) to reclaim unreacted testosterone **7** (30 mg, 71%) and obtain 3-oxo-androst-4-en-17 β -yl β -D-glucopyranosiduronic acid **6** (8 mg, 12%) as a white powder.

mp 240 °C (decomp); $[\alpha]_{\text{D}}^{20}$ +4.5 (*c* 0.22, MeOH); **R_f** 0.28 (ethyl acetate : methanol : water, 7:2:1); **IR** (KBr disc): 3416 (O-H), 2933 (C-H), 2848 (C-H), 1666 (unsat. C=O), 1614 (C=O), 1430, 1162, 1069, 1053, 1027, 958, 684; **¹H NMR** (800 MHz, MeOD): δ 5.71, (1H, s, H4), 4.36 (1H, d, $J_{\text{H20-H21}}$ 7.8, H20), 3.83 (1H, t, $J_{\text{H16-H17}}$ 8.6, H17), 3.52 (1H, d, $J_{\text{H23-H24}}$ 8.7, H24), 3.42 (1H, t, $J_{\text{H22-H23}} \approx J_{\text{H23-H24}}$ 9.0, H23), 3.37 (1H, $J_{\text{H21-H22}} \approx J_{\text{H22-H23}}$ 8.7, H22), 3.20 (1H, t, $J_{\text{H20-H21}} \approx J_{\text{H21-H22}}$ 8.3, H21), 2.51-2.44 (2H, m), 2.33-2.25 (2H, m), 2.13-2.01 (3H, m, H16a), 1.89 (1H, m), 1.73-1.55 (4H, m, H16b), 1.51 (1H, ddd, 2J 26.1, 3J 13.0, 3J 3.8), 1.39-1.20 (3H, m, obscured), 1.24 (3H, s, CH₃), 1.06-0.93 (3H, m), 0.91 (3H, s, CH₃); **¹³C NMR** (200 MHz, MeOD): 202.4 (C3), 175.3 (C25), 170.4 (C5), 124.1 (C4), 104.5 (C20), 89.2 (C17), 77.9 (C22), 76.4 (C24), 75.3 (C21), 73.7 (C23), 55.4, 51.7, 44.2, 40.0, 38.5, 36.8, 36.7, 34.7, 33.9, 32.8, 29.5, 24.1, 21.8, 17.7, 12.0; **LRMS (-ESI)** *m/z*: 463 ([M-H]⁻, 100%); **HRMS (-ESI)** *m/z*: 463.2329 ([M-H]⁻, C₂₅H₃₅O₈ gives 463.2332)

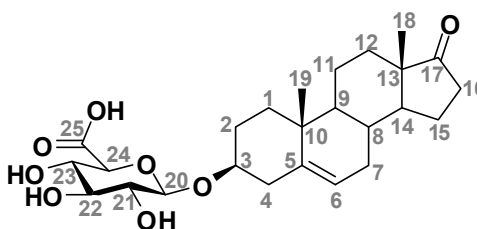
7.13.3 Nandrolone β -D-glucuronide **110**²⁰⁶



Glycosynthase (E504G, 33 mg mL⁻¹, 89 μ L, final concentration 0.22 mg mL⁻¹) was added to α -D-glucuronyl fluoride **51** (38 mg, 0.18 mmol, final concentration 12 mM), nandrolone **108** (40 mg, 0.15 mmol, final concentration 10 mM) and *n*-dodecyl β -maltoside (294 mg, final concentration 2% w/v) in sodium phosphate buffer (50 mM, pH 7.5, final volume 14.7 mL). The reaction was swirled continuously under ambient conditions for 4 days then dried onto silica. The crude product over silica was subjected to flash chromatography (ethyl acetate : methanol : water, 7:2:1) to reclaim unreacted nandrolone **108** (37 mg, 93%) and obtain the 3-oxo-estr-4-en-17 β -yl β -D-glucopyranosiduronic acid **110** (4 mg, 6%) as a white powder.

mp >200 °C (decomp); **R_f** 0.28 (ethyl acetate : methanol : water, 7:2:1); **IR** (NaCl): 3369 (O-H), 2916 (C-H), 2850 (C-H), 1661 (C=O), 1610 (C=O), 1415, 1051, 1028; **¹H NMR** (400 MHz, MeOD): δ 5.80, (1H, s, H4), 4.36 (1H, d, $J_{H19-H20}$ 7.8, H19), 3.85 (1H, t, $J_{H16-H17}$ 8.6, H17), 3.65-3.35 (3H, m, H21-23), 3.20 (1H, t, $J_{H19-H20} \approx J_{H20-H21}$ 8.3, H20), 2.50 (1H, m), 2.41-2.25 (4H, m), 2.25-2.00 (3H, m), 1.91-1.82 (2H, m), 1.73-1.25 (7H, m), 1.15-1.00 (2H, m), 0.92 (3H, s, H18), 0.87 (1H, m); **LRMS (+ESI)** *m/z*: 495 ([M-H+2Na]⁺, 50%), 473 ([M+Na]⁺, 100%); **HRMS (+ESI)** *m/z*: 473.2151 ([M+Na]⁺, C₂₄H₃₄O₈Na gives 473.2151).

7.13.4 Direct glucuronidation of DHEA **55** with DMSO⁵⁷



Glycosynthase (E504G, 28 mg mL⁻¹, 200 μ L, final concentration 0.20 mg mL⁻¹) was added to α -D-glucuronyl fluoride **51** (36 mg, 0.17 mmol, final concentration 6 mM), DHEA **55** (41 mg, 0.14 mmol, final concentration 5 mM) and DMSO (6.8 mL, final concentration 25% v/v) in sodium phosphate buffer (50 mM, 27.5 mL, pH 7.5). The reaction was swirled continuously under

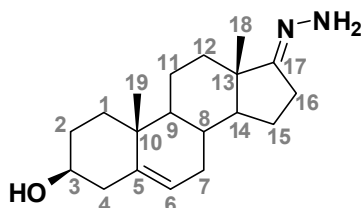
Experimental

ambient conditions for 4 days then filtered prior to drying onto silica. The filtration residue was washed with ethyl acetate (2 x 5 mL) to reclaim unreacted DHEA **55** (19 mg, 46%). The crude product over silica was subjected to flash chromatography (ethyl acetate : methanol : water, 7:2:1) to reclaim further unreacted DHEA **55** (8 mg, 20%) and obtain 17-oxo-androst-5-en-3-yl β -D-glucuronide **77** (11 mg, 17%) as a white powder.

mp 188 °C (dec.); $[\alpha]_D^{20}$ -29 (0.70, MeOH), [lit.²⁰ $[\alpha]_D^{25}$ -35.5 (1, EtOH)]; **R_f** 0.25 (7:2:1 ethyl acetate : methanol : water); **IR** (NaCl): 3369 (O-H), 2938 (C-H), 2903 (C-H), 1733 (C=O), 1636, 1436, 1373, 1259, 1218, 1161, 1089, 1049, 1020; **¹H NMR** (300 MHz, MeOD): δ 5.43 (1H, d, J_{H6-H7} 4.2, H6), 4.45 (1H, d, $J_{H20-H21}$ 7.7, H20), 3.80 (1H, d, $J_{H23-H24}$ 9.6, H24), 3.64-3.44 (2H, m, H3, H23), 3.38 (1H, t, $J_{H21-H22} \approx J_{H22-H23}$ 9.1, H22), 3.20 (1H, t, $J_{H21-H22} = J_{H20-H21}$ 8.3, H21), 2.60-1.44 (15H, m), 1.43-1.20 (2H, m), 1.19-0.82 (2H, m), 1.05 (3H, s), 0.90 (3H, s); **¹³C NMR** (100 MHz, MeOD): 223.9 (C17), 177.1 (C25), 142.2 (C5), 122.2 (C6), 102.2 (C20), 79.5 (C3), 77.8, 76.3, 74.9, 73.7, 53.0, 51.8, 39.6, 38.5, 38.0, 36.7, 32.8, 32.7, 31.9, 30.5, 22.8, 21.5, 19.9, 13.9, one carbon overlapping or obscured; **LRMS (-ESI)** m/z : 927 ([2M-H]⁻, 43%), 463 ([M-H]⁻, 100%); **HRMS (-ESI)** m/z : 463.2342 ([M-H]⁻, C₂₅H₃₅O₈ gives 463.2338).

7.14 DHEA Derivatives

7.14.1 DHEA hydrazone **112**¹⁴⁴

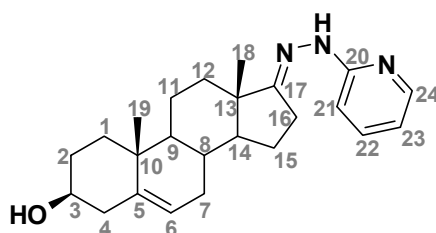


Triethylamine (400 μ L, 2.9 mmol) and aqueous hydrazine hydrate solution (~25%, 80 μ L, 0.41 mmol) were added to a solution of DHEA **55** (103 mg, 0.36 mmol) in aqueous ethanol (95%, 1.0 mL). The mixture was refluxed with stirring for 4 h, cooled to RT, and then precipitated from solution by the addition of water (6 mL). The precipitate was collected by filtration and washed with water (5 x 1 mL) to afford 3 β -hydroxy-androst-5-en-17-one hydrazone **112** (88 mg, 81%) as white prisms.

mp 206-211 °C (decomp) [lit.¹⁴⁴ mp 208-213 °C]; $[\alpha]_D^{20}$ -45 (1.0, CHCl₃); **IR** (NaCl): 3369 (broad, O-H), 2938, 2903 (C-H), 1733 (C=N), 1636, 1436, 1373,

1259, 1089, 1049, 1020; **¹H NMR** (800 MHz, DMSO-*d*₆): δ 5.33 (2H, s, broad, NH₂), 5.28 (1H, d, *J*_{H6-H7} 5.0, H6), 4.63 (1H, s, broad, OH), 3.25 (1H, m, H3), 2.19 (2H, m), 2.07 (2H, m), 1.99 (1H, m, H7), 1.77 (3H, m), 1.67 (1H, m), 1.57 (2H, m), 1.48 (1H, ddt, *J* 10.7, *J* 10.7, *J* 5.2), 1.41 (1H, ddt, *J* 13.2, *J* 13.0, *J* 4.0), 1.33 (2H, m), 1.21 (1H, dt, *J* 13.1, *J* 4.0), 0.98 (3H, m), 0.96 (3H, s, CH₃), 0.75 (3H, s, CH₃); **¹³C NMR** (200 MHz, DMSO-*d*₆): δ 161.4 (C17), 141.5 (C5), 120.3 (C6), 70.0 (C3), 53.8, 50.1, 43.1, 42.3, 36.9, 36.3, 34.4, 31.5, 31.0, 30.9, 24.3, 23.1, 20.3, 19.2, 17.0; **LRMS (+ESI)** *m/z*: 303 ([M+H]⁺, 100%); **HRMS (+ESI)** *m/z*: 303.2436 (C₁₉H₃₁N₂O gives 303.2436).

7.14.2 DHEA 2'-pyridylhydrazone **113**



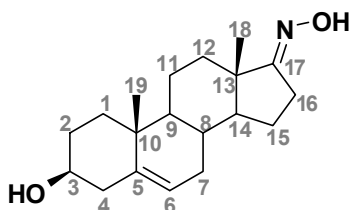
Triethylamine (171 μL, 1.2 mmol) and 2-pyridylhydrazine (88 mg, 0.81 mmol) were added to a solution of DHEA **55** (101 mg, 0.350 mmol) in absolute ethanol (1.0 mL). The mixture was refluxed with stirring for 4 h, then cooled to RT, and finally precipitated from solution by the addition of water (6 mL). The precipitate was collected by filtration and washed with water (5 x 1 mL) to afford 3β-hydroxy-androst-5-en-17-one 2-(2-pyridyl)hydrazone **113** (98 mg, 74%) as off-white prisms and a single diastereomer.

mp 271-274 °C (decomp); **[α]_D²⁰** +15 (1.0, CHCl₃); **IR** (NaCl): 3312 (O-H), 2926 (C-H), 1598 (C=N), 1577 (C=C), 1522, 1444, 1373, 1324, 1273, 1136, 1060, 771; **¹H NMR** (800 MHz, DMSO-*d*₆): δ 8.85 (1H, s, NH), 7.97 (1H, d, ³*J*_{H23-H24} 4.1, ⁴*J*_{H22-H24} 0.8, H24), 7.48 (1H, dt, ³*J*_{H21-H22} ≈ ³*J*_{H22-H23} 7.7, ⁴*J*_{H22-H24} 1.3 H22), 6.96 (1H, d, *J*_{H21-H22} 8.4, H21), 6.60 (1H, dd, *J*_{H22-H23} 6.4, *J*_{H23-H24} 5.4, H23), 5.23 (1H, d, *J*_{H6-H7} 4.8, H6), 4.59 (1H, d, *J* 4.6, O-H), 3.19 (1H, m, H3), 2.47-2.42 (1H obscured, m), 2.22 (1H, quin, *J* 9.1), 2.10 (1H, m), 2.03 (1H, m), 1.94 (1H, m), 1.87 (1H, m), 1.78-1.69 (2H, m), 1.62 (1H, m), 1.59-1.49 (2H, m), 1.46 (1H, ddt, *J* 10.7, *J* 10.7, *J* 5.1); 1.40 (1H, ddt, *J* 13.1, *J* 13.0, *J* 4.1), 1.36-1.23 (3H, m), 1.04 (1H, m), 0.97-0.87 (2H, m), 0.91 (3H, s, CH₃), 0.78 (3H, s, CH₃); **¹³C NMR** (200 MHz, DMSO-*d*₆): δ 162.9 (C17), 158.2 (C20), 147.5 (C24), 141.5 (C5), 137.6 (C22), 120.3 (C6), 114.3 (C23), 106.1 (C21), 70.1 (C3), 53.5, 50.1, 43.7, 42.3, 37.0, 36.3, 31.2, 31.5, 31.0, 30.9, 26.0, 23.3, 20.3, 19.3, 17.0;

Experimental

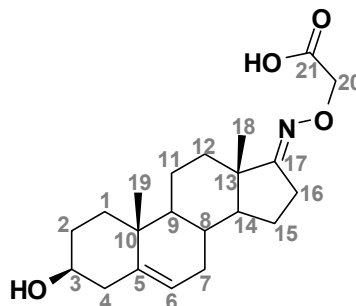
LRMS (+ESI) m/z : 380 ($[M+H]^+$, 100%), 402 ($[M+Na]^+$, 15%); **HRMS (+ESI) m/z :** 380.2701 ($[M+H]^+$, $C_{24}H_{34}N_3O$ gives 380.2702).

7.14.3 DHEA oxime **114**¹⁴⁵



Sodium acetate (98 mg, 1.2 mmol) and hydroxylamine hydrochloride (43 mg, 0.62 mmol) were dissolved in methanol (100 mL) and refluxed for 10 min. DHEA **55** (173 mg, 0.60 mmol) was added to the hot solution and the reaction was stirred for 2 h at 4 °C. The reaction mixture was then diluted with water (65 mL) and extracted with ethyl acetate (4 x 65 mL). The organic phase was washed with brine (2 x 65 mL) then dried over magnesium sulphate. The solution was filtered and evaporated to dryness, resulting in an off-white solid. Recrystallisation from aqueous ethanol (50%) produced 3 β -hydroxy-androst-5-en-17-one oxime **114** (94 mg, 52%) as a mixture of E and Z diastereomers (1.9 : 1.0 respectively).

mp 192-195 °C (decomp) [lit.¹⁴⁵ mp 200-202 °C]; $[\alpha]_D^{20}$ -60 (0.47, $CHCl_3$); **IR** (NaCl): 3252 (O-H), 2930 (C-H), 1679 (C=N), 1429, 1373, 1019, 948, 923, 797, 725; **¹H NMR** (800 MHz, $DMSO-d_6$): δ 10.06 (1H, s N-OH *E*-isomer), 9.78 (1H, s N-OH *Z*-isomer), 5.28 (2H, s, H6), 4.72-4.51 (2H, m, C3-OH), 3.25 (2H, m, H3), 2.39-2.22 (4H, m), 2.20-2.04 (4H, m), 2.02-1.92 (2H, m), 1.87-1.63 (8H, m), 1.62-1.39 (8H, m), 1.38-1.19 (7H, m), 1.09 (1H, dt, J 11.9, J 6), 1.01-0.89 (13H, m), 0.83 (3H, s, *E*-isomer); **¹³C NMR** (200 MHz, $DMSO-d_6$): δ 167.9 (C17, *E*-isomer), 165.6 (C17, *Z*-isomer), 141.4 (C5, both isomers), 120.2 (C6, both isomers), 70.0 (C3, both isomers), 54.7 (*Z*-isomer), 53.7 (*E*-isomer), 49.9 (*E*-isomer), 49.7 (*Z*-isomer), 44.5 (*Z*-isomer), 42.9 (*E*-isomer), 42.24 (*E*-isomer), 42.22 (*Z*-isomer), 36.91 (*E*-isomer), 36.87 (*Z*-isomer), 36.25 (*E*-isomer), 36.22 (*Z*-isomer), 34.9 (*Z*-isomer), 34.1 (*E*-isomer), 31.44 (*E*-isomer), 31.43 (*Z*-isomer), 30.87 (*E*-isomer), 30.85 (*Z*-isomer), 30.83 (*E*-isomer), 30.4 (*Z*-isomer), 28.4 (*Z*-isomer), 24.9 (*E*-isomer), 23.6 (*Z*-isomer), 22.9 (*E*-isomer), 20.3 (*Z*-isomer), 20.2 (*E*-isomer), 19.2 (*E*-isomer), 19.1 (*Z*-isomer), 17.0 (*E*-isomer), 13.3 (*Z*-isomer); **LRMS (+ESI) m/z :** 304 ($[M+H]^+$, 100%); **HRMS (+ESI) m/z :** 304.2275 ($[M+H]^+$, $C_{19}H_{30}NO_2$ gives 304.2277).

7.14.4 DHEA O-(carboxymethyl)oxime **116**¹⁴⁸

Pyrrolidine (600 μ L, 7.19 mmol) was added to DHEA **55** (1.00 g, 3.47 mmol) dissolved in dry methanol (40 mL) on ice under a nitrogen atmosphere in the dark. After one hour, the solution had turned yellow. Carboxymethoxylamine hemihydrochloride **115** (800 mg, 7.32 mmol) was dissolved in a dry solution of methanol (10 mL) and pyrrolidine (600 μ L, 7.19 mmol) under nitrogen atmosphere and transferred to the DHEA **55** reaction via cannula with methanol washing (5 mL). The solution went immediately clear and was heated to reflux. The reaction was monitored by TLC (methanol : dichloromethane, 1 : 9) and was complete after 6 h. The solvent was evaporated under reduced pressure and water (100 mL) was added to the residue. The pH was adjusted to 2 with hydrochloric acid (2 M) and the white precipitate was extracted with ethyl acetate until all precipitate had dissolved (5 x 150 mL with sonication required). The organic extracts were combined, washed with water (200 mL), dried over magnesium sulphate, and then evaporated under reduced pressure.

The yellow-white residue (1.15 g) was washed with cold chloroform (5 mL, then 2 x 3 mL) to afford 3 β -hydroxy-androst-5-en-17-one O-(carboxymethyl)oxime **116** (1.10 g, 88%) as a colourless solid.

mp 215-217 $^{\circ}$ C (decomp.); $[\alpha]_D^{20}$ -36 (1.0, DMSO) [lit.¹⁴⁸ $[\alpha]_D^{24}$ -37.9 (1, EtOH)]; **R_f** 0.38 (7:2:1 ethyl acetate : methanol : water); **IR** (KBr): 3351 (broad, O-H), 2946, 2910, 2865, 2505 (C-H), 1680 (s, C=O), 1377, 1348, 1284, 1090, 1071, 1040, 849; **¹H NMR** (800 MHz, *d*₆-DMSO): δ 5.28 (1H, s, H6), 4.61 (1H, s, broad, OH), 4.42 (2H, s, OCH₂COO), 3.26 (1H, obscured, m, H3), 2.46 (1H, dd, ²*J*_{H16a-H16b} 18.9, ³*J*_{H15-H16a} 9.0, H16a), 2.38 (1H, m, H16b), 2.16 (1H, dd, ²*J*_{H4a-H4b} 12.8, ³*J*_{H3-H4a} 2.3, H4a), 2.09 (1H, t, ²*J*_{H4a-H4b} \approx ³*J*_{H3-H4b} 12.1, H4b), 1.98 (1H, m, H7a), 1.82-1.70 (3H, m), 1.67 (1H, d, *J* 12.2), 1.58 (2H, m, H7b), 1.51 (1H, dquart, *J* 10.5, *J* 5.2), 1.42 (1H, dquart, *J* 13.2, *J* 3.4), 1.38-1.28 (3H, m), 1.12 (1H, m), 1.02-0.91 (2H, m), 0.96 (3H, s, CH₃), 0.85 (3H, s, CH₃), COOH not observed; **¹³C NMR** (200 MHz, *d*₆-DMSO): 171.3 (C21), 170.6 (C17), 141.4

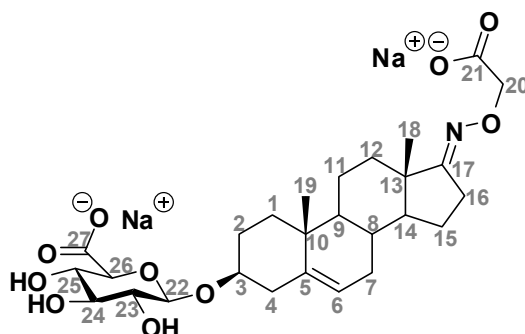
Experimental

(C5), 120.1 (C6), 70.0 (C3), 69.8 (C20), 53.5, 49.8, 43.5, 42.2 (C4), 36.9, 36.2, 33.8, 31.4, 30.82, 30.78, 25.7 (C16), 22.8, 20.2, 19.2 (CH₃), 16.8 (CH₃); **LRMS (+ESI)** *m/z*: 384 ([M+Na]⁺, 100); **LRMS (-ESI)** *m/z*: 360 ([M-H]⁻, 100); **HRMS (+ESI)** *m/z*: 384.2151 ([M+Na]⁺, C₂₁H₃₁NO₄Na gives 384.2151).

7.14.5 Solubility of DHEA derivatives

Solutions (10 mM) of DHEA **55**, DHEA hydrazone **112**, DHEA 2'-pyridylhydrazone **113**, DHEA oxime **114**, and DHEA O-(carboxymethyl)oxime **116** were made with sodium phosphate buffer (100 mM, pH 7.5). Solutions were sonicated (10 min, 30 °C) prior to solubility being determined by eye. If complete dissolution was not achieved, the solution was diluted further with sodium phosphate (100 mM, pH 7.5). Dilutions were made such that the final concentration employed were 5 mM, 2 mM, 1 mM, 0.75 mM, 0.5 mM, 0.3 mM, 0.1 mM and 0.05 mM.

7.14.6 DHEA O-(carboxymethyl)oxime β-D-glucuronide **118**



Reaction at room temperature

Glucuronylsynthase (22.5 mg mL⁻¹, 521 μL, final concentration 0.42 mg mL⁻¹) was added to a solution containing DHEA O-(carboxymethyl)oxime **116** (20.1 mg, 0.056 mmol, final concentration 2.0 mM) and α-D-glucuronyl fluoride **51** (11.9 mg, 0.056 mmol, final concentration 2.0 mM) in sodium phosphate buffer (100 mM, 27.1 mL, pH 7.5). The reaction was swirled at room temperature for 2 days then a further addition of α-D-glucuronyl fluoride **51** (11.9 mg, 0.056 mmol) was added. Silica gel (~100 mg) was added and the solution was evaporated to dryness by rotary evaporation. The dried residue was subjected to flash chromatography with ethyl acetate : ethanol (5:2) to recover unreacted oxime **116**, then ethyl acetate : methanol : water (7:2:1) to isolate pure 17-carboxymethoximino-androst-5-en-3-yl β-D-glucuronide **118** (22.8 mg, 76%) as a colourless solid.

Large scale reaction

Glucuronylsynthase (110 mg, final concentration 0.32 mg mL⁻¹) was added to a solution containing DHEA O-(carboxymethyl)oxime **116** (500 mg, 1.38 mmol, final concentration 3.97 mM), α -D-glucuronyl fluoride **51** (298 mg, 1.40 mmol, final concentration 4.03 mM) and DMSO (15 mL, final concentration 4.3% v/v) in sodium phosphate buffer (100 mM, 27.1 mL, pH 7.5). Silica gel (~1 g) was added and the solution was evaporated to dryness by rotary evaporation. The dried residue was subjected to flash chromatography with ethyl acetate : ethanol (5:2) to recover unreacted oxime **116**, then ethyl acetate : methanol : water (7:2:1) to isolate pure 17-carboxymethoximino-androst-5-en-3-yl β -D-glucuronide **118** (0.293 mg, 41%) as a colourless solid.

Reaction at 37 °C

Glucuronylsynthase (1.45 mg mL⁻¹, 4.14 mL, final concentration 0.21 mg mL⁻¹) was added to a solution containing DHEA O-(carboxymethyl)oxime **116** (20 mg, 0.055 mmol, final concentration 1.9 mM) and α -D-glucuronyl fluoride **51** (57.5 mg, 0.270 mmol, final concentration 9.3 mM) in sodium phosphate buffer (100 mM, 25 mL, pH 7.5). The reaction was incubated at 37 °C without agitation for 3 days then dried onto reverse-phase silica. The dried residue was subjected to reverse-phase flash chromatography (25% aqueous acetonitrile + 0.1% formic acid) to isolate pure 17-carboxymethoximino-androst-5-en-3-yl β -D-glucuronide **118** (29 mg, 98%) as a colourless solid.

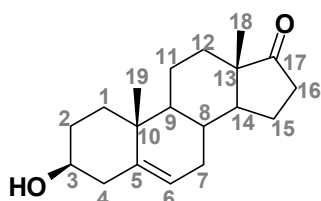
mp decomp.; $[\alpha]_D^{20}$ -62 (1.0, DMSO); **R_f** 0.02 (ethyl acetate : methanol : water, 7:2:1); **IR** (KBr): 3423 (O-H), 2942 (C-H), 1745 (C=O), 1436, 1373, 1367, 1226, 1167, 1109, 1092, 1070, 1049, 1021; **¹H NMR** (800 MHz, D₂O): δ 5.51 (1H, s, H6), 4.59 (1H, d, $J_{H22-H23}$ 7.3, H22), 4.38 (2H, s, H20), 3.73-3.64 (2H, m, H3, H26), 3.54-3.47 (2H, m, H24, H25), 3.27 (1H, t, $J_{H22-H23} \approx J_{H23-H24}$ 7.1, H23), 2.63 (1H, dd, $J_{H16a-H16b}$ 19.2, $J_{H15-H16}$ 8.3, H16a), 2.52 (1H, m, H16b), 2.47 (1H, d, $J_{H4a-H4b}$ 12.6, H4a), 2.29 (1H, t, $J_{H3-H4} \approx J_{H4a-H4b}$ 12.0, H4b), 2.10 (1H, d, J 11.3, H7a), 1.99-1.91 (2H obscured, m, H2a), 1.91-1.81 (2H, m, H14), 1.72-1.60 (4H, m, H2b, H7b), 1.55 (1H, quart, J 13.0), 1.48-1.38 (2H, m, H15), 1.27 (1H, m), 1.10 (1H, t, J 13.0), 1.06 (3H, s, CH₃), 1.04 (1H, m), 0.95 (3H, s, CH₃); **¹³C NMR** (200 MHz, D₂O): 181.7 (C21), 178.4 (C27), 176.8 (C17), 142.7 (C5), 122.9 (C6), 101.2 (C22), 80.6 (C26), 77.2 (C3), 76.6 (C24), 73.9 (C23), 72.8 (C20), 72.4 (C25), 54.5, 50.7, 45.1 (quart. C), 39.0 (C4), 37.6, 37.5 (quart. C),

Experimental

34.4, 31.8 (C7), 29.8 (C2), 27.3 (C16), 23.8, 23.7, 21.1, 19.8, 17.2; **LRMS (-ESI)** m/z : 536 ($[M-H]^-$, 100%), 558 ($[M-2H+Na]^-$, 30%); **HRMS (-ESI)** m/z : 536.2495 ($[M-H]^-$, $C_{27}H_{38}NO_{10}$ gives 536.2496), 558.2302 ($[M-2H+Na]^-$, $C_{27}H_{37}NO_{10}Na$ gives 558.2315).

Recrystallisation was obtained from ethyl acetate & methanol with water used sparingly to achieve complete dissolution. Upon cooling overnight at 4 °C, the translucent crystals of disodium DHEA O-(carboxymethyl)oxime β -D-glucuronate were observed that were suitable for single crystal x-ray structure determination (Figure 4.3).

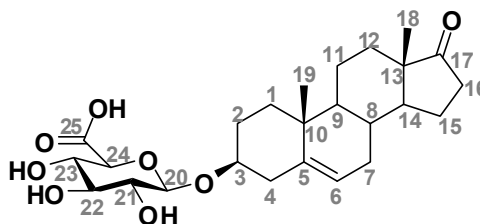
7.14.7 DHEA **55** from the deoxygenation of DHEA O-(carboxymethyl)oxime **116**



DHEA O-(carboxymethyl)oxime **116** (20 mg, 0.055 mmol) and ammonium acetate (55 mg, 0.71 mmol) were dried under vacuum, then purged with nitrogen, and dissolved in dioxane (0.5 mL) and aqueous acetic acid (50% v/v, 22 μ L). Aqueous titanium trichloride (9 mM) was freshly prepared and added (14 mL) dropwise to the reaction to which the solution turned violet-black. After one hour, the solution had lightened in colour to a light blue with a white-grey precipitate. TLC analysis (ethyl acetate : methanol : water, 50:2:1) showed significant conversion to a product with an equivalent R_f of DHEA **55**. The solution was filtered, and the residue washed with ethyl acetate (20 mL). The filtrate was washed with brine (10 mL), then saturated sodium bicarbonate (10 mL) and then water (10 mL). The organic layer was dried over anhydrous magnesium sulfate, then evaporated to dryness to yield crude DHEA **55** (5 mg, 33%).

Spectral data confirmed the removal of the oxime group and was identical to a DHEA **55** reference sample.

7.14.8 Dehydroepiandrosterone β -D-glucuronide **77**²⁰

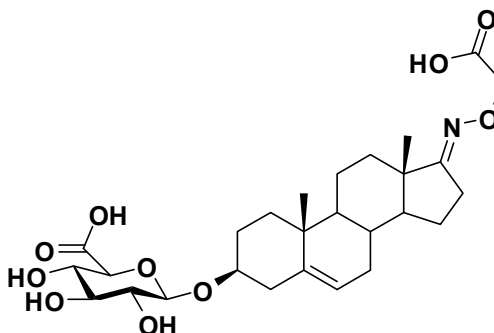


DHEA O-(carboxymethyl)oxime β -D-glucuronide **118** (50 mg, 0.093 mmol) and ammonium acetate (96 mg, 1.2 mmol) were purged with nitrogen gas, then dioxane (0.5 mL) and aqueous acetic acid (50%, 38 μ L) were added. In a second flask, anhydrous titanium trichloride (36 mg, 0.23 mmol) was purged with nitrogen gas before water (6 mL) was added. The aqueous titanium trichloride was added via cannula to the stirred DHEA O-(carboxymethyl)oxime β -D-glucuronide **118** solution at room temperature and under a nitrogen atmosphere. The reaction instantly turned black-violet upon addition and gradually changed to a white-grey as the reaction proceeded. After 2 h, the reaction was deemed complete by TLC (ethyl acetate : methanol : water, 7:2:1) so the reaction was acidified to pH 2 and dried onto silica. The dry residue was subjected to flash chromatography (ethyl acetate : methanol : water, 7:2:1 + 0.1% formic acid) to isolate pure 17-oxo-androst-5-en-3-yl β -D-glucopyranuronic acid **77** (44.8 mg, 100%) as a white solid.

Spectral data was identical to literature and previously synthesised material (refer to section 7.13.4).^{20,57}

7.15 Kinetics with DHEA O-(carboxymethyl)oxime

7.15.1 Calibration of DHEA O-(carboxymethyl)oxime β -D-glucuronide **118**



A solution of DHEA O-(carboxymethyl)oxime β -D-glucuronide **118** (final concentration 0.2 μ M, 0.4 μ M, 0.6 μ M, 0.8 μ M, and 10 μ M) in sodium phosphate buffer (100 mM, pH 7.5) was prepared and subjected to the HPLC assay (refer to section 7.9) in duplicate. A mobile phase of 30% acetonitrile in sodium

Experimental

phosphate buffer (100 mM, pH 2.0) provided a retention time of 5.7 min. The area was plotted against the concentration (Figure 7.10) to provide the absorption co-efficient of $10083 \text{ au } \mu\text{M}^{-1}$ for DHEA O-(carboxymethyl)oxime β -D-glucuronide **118** for the specified conditions.

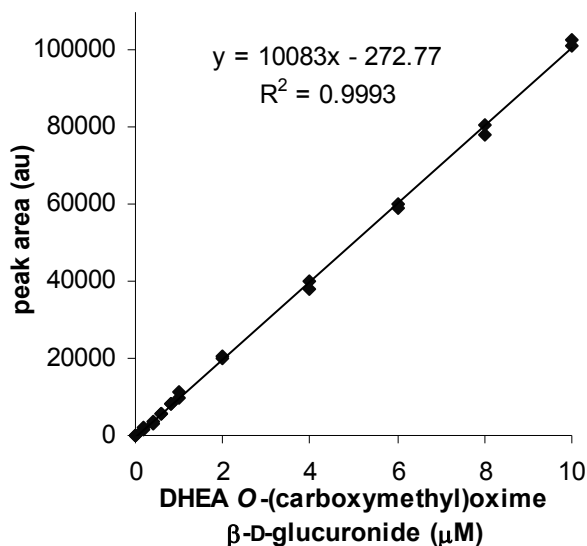
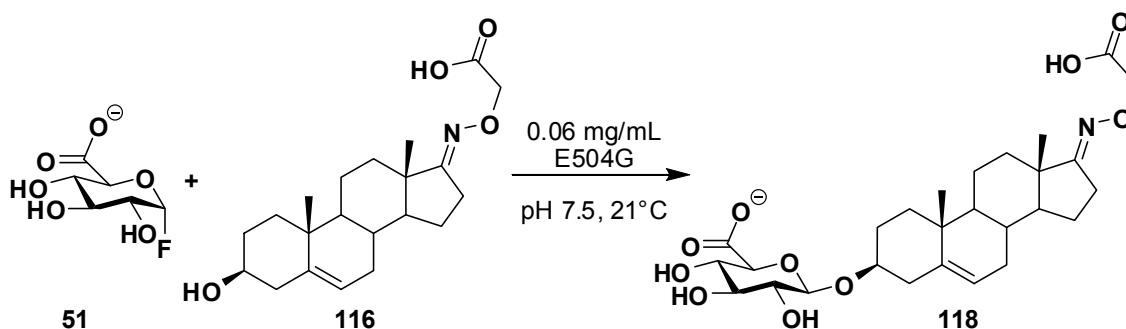


Figure 7.10. Calibration curve of DHEA O-(carboxymethyl)oxime β -D-glucuronide **118** (211 nm, 21 °C, 100 mM sodium phosphate, pH 7.5). R^2 was calculated using linear regression analysis.

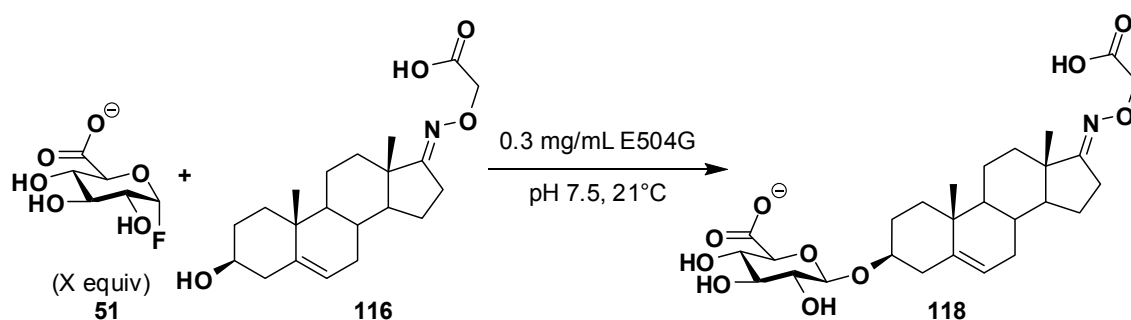
7.15.2 Michaelis-Menten kinetics of DHEA O-(carboxymethyl)oxime **116**



Glucuronylsynthase (1.77 mg mL^{-1} , $50 \mu\text{L}$) was added to α -D-glucuronyl fluoride **51** (final concentration 1 mM) and DHEA O-(carboxymethyl)oxime **116** (final concentrations 0 mM, 0.14 mM, 0.27 mM, 0.41 mM, 0.55 mM, 0.68 mM, 0.82 mM, 1.09 mM, 1.37 mM, 1.5 mM, 1.64 mM, 1.78 mM, and 1.95 mM) pre-incubated at 21 °C in sodium phosphate buffer (100 mM, $1450 \mu\text{L}$, pH 7.5). The reaction was immediately subjected to HPLC (refer to section 7.9) with a mobile phase of 30% acetonitrile in sodium phosphate buffer (100 mM, pH 2.0). Five injections were made to monitor the initial velocity of the reactions (<1% conversion) at 21 min intervals. Data points (5 points) that encompassed the

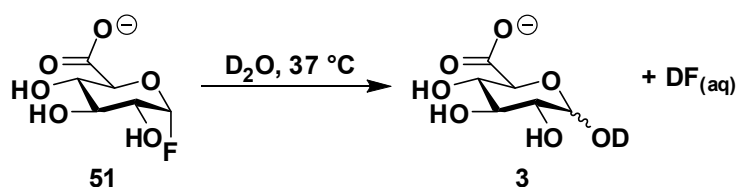
initial linear velocity ($R^2 > 0.99$) were used to plot initial velocities against the DHEA O-(carboxymethyl)oxime **116** concentration to provide the Michaelis-Menten plot (Figure 4.5). The data did not fit a standard Michaelis-Menten model, so the kinetic parameters were determined by taking the tangent of the initial slope ($k_{\text{cat}}/K_m = 5.0 \text{ M}^{-1} \text{ s}^{-1}$) and the local maximum velocity ($\text{max } k_{\text{cat}} = 0.0014 \text{ s}^{-1}$ at 0.55 mM) from the Michaelis-Menten plot.

7.15.3 Equivalents of α -D-glucuronyl fluoride **51** in the DHEA O-(carboxymethyl)oxime **116** glucuronylsynthase reaction



A stock solution of DHEA O-(carboxymethyl)oxime **116** (1.6 mM) in sodium phosphate buffer (100 mM, pH 7.5) was distributed into five separate HPLC vials (1.28 mL each). An aliquot (200 μL , 160 μL , 120 μL , 80 μL , and 40 μL) of α -D-glucuronyl fluoride **51** (52.5 mM) in sodium phosphate buffer (100 mM, pH 7.5) was added to each vial. The volume of the vial was made up to 1.48 mL using sodium phosphate buffer (100 mM, pH 7.5) and then equilibrated at 37 $^{\circ}\text{C}$ for 5 min. Glucuronylsynthase (22.5 mg mL^{-1} , 20 μL , final concentration 0.3 mg mL^{-1}) was added to each vial and the reactions were immediately subjected to HPLC (refer to section 7.9) with a mobile phase of 30% acetonitrile in sodium phosphate buffer (100 mM, pH 2.0). The reactions were monitored simultaneously by HPLC over 30 h with an injection taken every 2h.

7.15.4 Non-enzymatic hydrolysis of the α -D-glucuronyl fluoride **51** donor



α -D-Glucuronyl fluoride **51** (20 mg, 94 μmol) was dissolved in deuterium oxide (700 μL) at 37 $^{\circ}\text{C}$ and subjected to a timescale NMR (500 MHz) experiment whereby a proton spectrum was recorded every hour over a 21 h period (Figure 4.7). The hydrolysis was quantified through the integration of the anomeric

Experimental

proton of α -D-glucuronyl fluoride **51** (5.72 ppm) and the hydrolysis products α -glucuronic acid **3** (5.50 ppm) and β -glucuronic acid **3** (5.38 ppm). The rate of hydrolysis (Figure 4.8) was determined as a proportion to the sum of the integrations to provide a hydrolysis rate of 600 nmol h⁻¹. Assuming first-order kinetics, the rate constant of hydrolysis (k_H) is $1.8 \times 10^{-6} \text{ s}^{-1}$.

7.15.5 Estimation of inhibition constant for DHEA O-(carboxymethyl)oxime β -D-glucuronide **118**

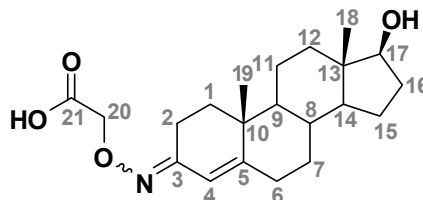
Glucuronylsynthase (1.9 mg mL⁻¹, 20 μ L) was added to 2-phenylethanol **45** (final concentration 88 mM), α -D-glucuronyl fluoride **51** (final concentration 20 μ M) and DHEA O-(carboxymethyl)oxime β -D-glucuronide **118** (final concentration 0 μ M, 10 μ M, 20 μ M, 50 μ M, 76 μ M, or 101 μ M) pre-incubated at 21 °C in sodium phosphate buffer (100 mM, 1480 μ L, pH 7.5). The reaction was immediately subjected to HPLC (refer to section 7.9) with a mobile phase of 23% acetonitrile in sodium phosphate buffer (100 mM, pH 2.0). Three injections were made at 26 min intervals to determine the initial reaction velocity. The procedure was repeated with 5 μ M and 10 μ M final concentrations of α -D-glucuronyl fluoride **51**.

7.15.6 Estimation of inhibition for 2-phenylethyl glucuronide **68**

Glucuronylsynthase (1.9 mg mL⁻¹, 20 μ L) was added to DHEA O-(carboxymethyl)oxime **116** (final concentration 0.6 mM), α -D-glucuronyl fluoride **51** (final concentration 20 μ M) and 2-phenylethyl glucuronide **68** (final concentration 0 mM, 25 μ M, 50 μ M, or 75 μ M, 100 μ M, 25 mM, 50 mM, 75 mM or 100 mM) pre-incubated at 21 °C in sodium phosphate buffer (100 mM, 1480 μ L, pH 7.5). The reaction was immediately subjected to HPLC (refer to section 7.9) with a mobile phase of 30% acetonitrile in sodium phosphate buffer (100 mM, pH 2.0). Three injections were made at 23 min intervals to determine the initial reaction velocity.

7.16 Steroid solubility strategy with testosterone

7.16.1 Testosterone O-(carboxymethyl)oxime **120**¹⁷⁷



Pyrrolidine (85 μ L, 1.0 mmol) was added to testosterone **7** (146 mg, 0.506 mmol) dissolved in dry methanol (8 mL) on ice under a nitrogen atmosphere in the dark. Within 5 min, the solution had turned yellow. The solution was heated to 50 $^{\circ}$ C and further pyrrolidine (85 μ L, 1.0 mmol) was added followed by carboxymethoxylamine hemihydrochloride **115** (117 mg, 1.07 mmol). The solution turned immediately clear and was monitored by TLC (methanol : dichloromethane, 1 : 9). After 1 h, the solvent was removed under reduced pressure and water (20 mL) was added to the residue. The pH was adjusted to 2 with hydrochloric acid (2 M) and the white precipitate was extracted with ethyl acetate until all precipitate had dissolved (3 x 15 mL with sonication required). The organic extracts were combined, washed with water (30 mL), dried over magnesium sulphate, and then evaporated to dryness by rotary evaporation. The yellow residue was subjected to flash chromatography (methanol : dichloromethane, 1:9) to yield an off-white solid. Discolouration was removed by washing with cold chloroform (2-3 mL), followed by filtration to yield the white powder of 17 β -hydroxy-androst-4-en-3-one O-(carboxymethyl)oxime **120** (166 mg, 91%) as a mixture of *E* and *Z* isomers (1.7:1.0 respectively).

mp 173-175 $^{\circ}$ C (decomp.) [lit.¹⁷⁷ mp 179-181 $^{\circ}$ C]; $[\alpha]_D^{20}$ +119 (1.0, MeOH) [lit.¹⁷⁷ $[\alpha]_D^{25}$ +144 (1.3, EtOH)]; **R_f** 0.38 (ethyl acetate : methanol : water, 7:2:1); **IR** (KBr): 3392 (O-H), 2934 (C-H), 1739 (C=O), 1689 (C=N), 1286, 1204, 1094, 1055, 1028, 753, 663; **¹H NMR** (800 MHz, MeOD): δ 6.45 (1H, s, H4 *Z*-isomer), 5.74 (1H, s, H4 *E*-isomer), 4.54 (2H, s, H20 *E*-isomer), 4.51 (2H, s, H20 *Z*-isomer), 3.57 (2H, t, $J_{H16-H17}$ 8.7, H17), 3.05 (2H, d, $J_{H6a-H6b}$ 17.3, H6a), 2.42-2.15 (6H, m, H6b), 2.01-1.75 (8H, m, H16a), 1.65-1.25 (14H, m, H16b), 1.20-0.70 (8H, m), 1.11 (6H, s, CH₃), 0.78 (6H, s, CH₃); **¹³C NMR** (200 MHz, MeOD): 174.07 (C21, *Z*-isomer), 173.99 (C21 *E*-isomer), 161.9 (C5, *Z*-isomer), 159.1 (C5, *E*-isomer), 158.4 (C3, *E*-isomer), 156.0 (C3, *Z*-isomer), 117.6 (C4, *E*-isomer), 112.0 (C4, *Z*-isomer), 82.4 (C17, *E*-isomer), 82.3 (C17, *Z*-isomer), 71.0

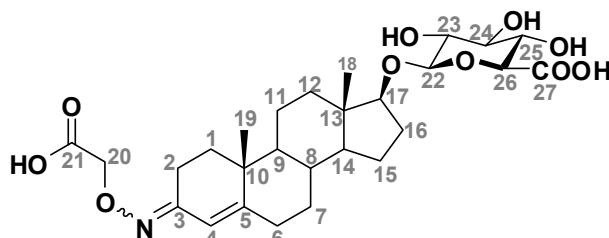
Experimental

(C20, *E*-isomer), 70.8 (C20, *Z*-isomer), 55.8 (*Z*-isomer), 55.5 (*E*-isomer), 52.0 (*E*-isomer), 51.9 (*Z*-isomer), 44.0 (*Z*-isomer), 43.9 (*E*-isomer), 40.1 (*Z*-isomer), 39.2 (*E*-isomer), 37.9 (*E*-isomer), 37.8 (*Z*-isomer), 37.4 (*Z*-isomer), 37.2 (*E*-isomer), 37.1 (*Z*-isomer), 35.9 (*E*-isomer), 34.0 (*Z*-isomer), 33.52 (*E*-isomer), 33.46 (*Z*-isomer), 33.1 (*E*-isomer), 30.6 (C16, *E*-isomer), 25.4 (*Z*-isomer), 24.29 (*E*-isomer), 24.27 (*Z*-isomer), 22.1, (*E*-isomer), 21.9 (*Z*-isomer), 20.5 (C6, *E*-isomer), 18.4 (*Z*-isomer), 18.2 (*E*-isomer), 11.59 (*Z*-isomer), 11.58 (*E*-isomer), one C obscured or overlapping; **LRMS (-ESI) m/z** : 360 ($[M-H]^-$, 100); **HRMS (-ESI) m/z** : 360.2175 ($[M-H]^-$, $C_{21}H_{30}NO_4$ gives 360.2175).

7.16.2 Solubility of testosterone *O*-(carboxymethyl)oxime **120**

Solutions (28 mM) of testosterone **7** and testosterone *O*-(carboxymethyl)oxime **120** were made with sodium phosphate buffer (100 mM, pH 7.5). Solutions were sonicated (10 min, 30 °C) prior to solubility being determined by eye. If complete dissolution was not achieved, the solution was diluted further with sodium phosphate (100 mM, pH 7.5). Dilutions were made such that the final concentration employed were 14 mM, 9.3 mM, 4.7 mM, 2.3 mM, 1.2 mM, 0.58 mM, 0.29 mM.

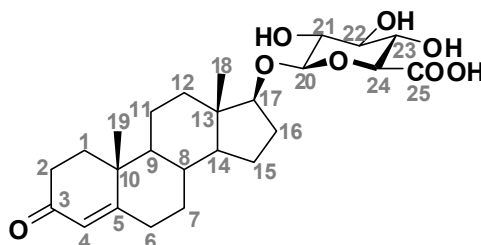
7.16.3 Testosterone *O*-(carboxymethyl)oxime β -D-glucuronide **121**



Glucuronylsynthase (21.6 mg mL⁻¹, 128 μ L, final concentration 0.21 mg mL⁻¹) was added to a solution containing testosterone *O*-(carboxymethyl)oxime **120** (52 mg, 0.14 mmol, final concentration 11 mM) and α -D-glucuronyl fluoride **51** (145 mg, 0.680 mmol, final concentration 38 mM) in sodium phosphate buffer 7.5 (100 mM, 13 mL, pH 7.5). The reaction was incubated at 30 °C without agitation for 3 days before being acidified to pH 2 and then dried onto reverse-phase silica. The dried residue was subjected to reverse-phase flash chromatography (25% aqueous acetonitrile + 0.1% formic acid) to isolate 3-carboxymethoximino-androst-4-en-17-yl β -D-glucuronide acid **121** (54 mg, 72%) as a colourless solid and a mixture of *anti* and *syn* isomers (2.0 : 1.0 respectively). Unreacted testosterone *O*-(carboxymethyl)oxime **120** was also recovered (12 mg, 23%).

mp decomp.; $[\alpha]_D^{20}$ +50.3 (1.0, MeOH); **IR** (NaCl): 3370 (O-H), 2935 (C-H), 1732 (C=O), 1630 (C=N), 1434, 1375, 1243, 1168, 1097, 1055, 1024; **¹H NMR** (800 MHz, MeOD): δ 6.45 (1H, s, H4 *Z*-isomer), 5.71 (1H, s, H4 *E*-isomer), 4.54 (2H, s, C20 *E*-isomer), 4.52 (2H, s, H20 *Z*-isomer), 4.38 (2H, d, $J_{H22-H23}$ 7.2, H22), 3.73 (2H, m H26), 3.68 (2H, t, $J_{H16-H17}$ 8.1, H17), 3.51 (2H, t, $J_{H24-H25} \approx J_{H25-H26}$ 8.8, H25), 3.36 (2H, t, $J_{H23-H24} \approx J_{H24-H25}$ 9.3, H24), 3.22 (2H, t, $J_{H22-H23} \approx J_{H23-H24}$ 8.1, H23), 3.04 (1H, d, $J_{H6a-H6b}$ 17.0, H6a), 2.42-2.12 (7H, m, H6b), 2.06-1.89 (6H, m, H16a), 1.87-1.76 (2H, m), 1.71-1.52 (8H, m, H16b), 1.51-1.25 (6H, m), 1.19 (2H, t, J 11.6), 1.14 (3H, s, H19 *Z*-isomer), 1.10 (3H, s, H19 *E*-isomer), 1.04-0.82 (6H, m), 0.88 (6H, s, H18); **¹³C NMR** (200 MHz, MeOD): 174.0 (2C, C21, *E+Z*-isomer), 172.7 (2C, C27, *E+Z*-isomer), 161.9 (C5, *Z*-isomer), 159.1 (C5, *E*-isomer), 158.3 (C3 *E*-isomer), 156.0 (C3, *Z*-isomer), 117.6 (C4 *E*-isomer), 112.0 (C4 *Z*-isomer), 105.1 (2C, C22, *E+Z*-isomer), 90.29 (C17, *E*-isomer), 90.24 (C17, *Z*-isomer), 77.5 (2C, C24, *E+Z*-isomer), 76.6 (2C, C26, *E+Z*-isomer), 75.0 (2C, C23, *E+Z*-isomer), 73.2 (2C, C25, *E+Z*-isomer), 71.0 (*E*-isomer), 70.8 (*Z*-isomer), 55.6 (*Z*-isomer), 55.3 (*E*-isomer), 51.73 (*E*-isomer), 51.67 (*Z*-isomer), 44.17 (*Z*-isomer), 44.13 (*E*-isomer), 40.1 (*Z*-isomer), 39.2 (*E*-isomer), 38.5 (*E*-isomer), 38.4 (*Z*-isomer), 37.4 (*Z*-isomer), 36.93 (*E*-isomer), 36.87 (*Z*-isomer), 35.8 (*E*-isomer), 34.0 (*Z*-isomer), 33.5 (*E*-isomer), 33.4 (*Z*-isomer), 33.0 (*E*-isomer), 29.8 (*E*-isomer), 25.3 (*Z*-isomer), 24.26 (*E*-isomer), 24.25 (*Z*-isomer), 22.1 (*E*-isomer), 21.9 (*Z*-isomer), 20.5 (*E*-isomer), 18.4 (C19, *Z*-isomer), 18.2 (C19, *E*-isomer), 11.99 (C18, *Z*-isomer), 11.98 (C18, *E*-isomer), one carbon obscured or overlapping; **LRMS (-ESI)** m/z : 558 ($[M-2H+Na]^+$, 94), 536 ($[M-H]^+$, 100); **HRMS (-ESI)** m/z : 558.2314 ($[M-2H+Na]^+$, $C_{27}H_{37}NO_{10}Na$ gives 558.2315), 536.2496 ($[M-H]^+$, $C_{27}H_{38}NO_{10}$ gives 536.2496).

7.16.4 Testosterone β -D-glucuronide **6**



Testosterone *O*-(carboxymethyl)oxime β -D-glucuronide **121** (30 mg, 0.056 mmol) and ammonium acetate (117 mg, 1.52 mmol) were purged with nitrogen gas, then dioxane (0.5 mL) and aqueous acetic acid (50%, 90 μ L) were added. Aqueous titanium trichloride (40 mg mL⁻¹, 0.54 mL, 0.18 mmol) was added to

Experimental

the stirred testosterone *O*-(carboxymethyl)oxime β -D-glucuronide **121** solution at room temperature and under a nitrogen atmosphere. The reaction instantly turned black-violet upon addition and gradually changed to a white-grey as the reaction proceeded. After 24 h, the reaction was acidified to pH 2 and dried onto silica. The dry residue was subjected to flash chromatography (ethyl acetate : methanol : water, 7:2:1 + 0.1% formic acid) to isolate a mixture of testosterone β -D-glucopyranuronic acid **6** and unreacted testosterone *O*-(carboxymethyl)oxime β -D-glucopyranuronic acid **121**. These were separated by prep TLC (ethyl acetate : methanol : water, 7:2:1 + 0.1% formic acid) to recover flash chromatography (25% aqueous acetonitrile + 0.1% formic acid) to isolate testosterone *O*-(carboxymethyl)oxime β -D-glucuronide **121** (16 mg, 53%) and obtain pure 3-oxo-androst-4-en-17-yl β -D-glucuronide **6** (10 mg, 38%) as a white solid.

Spectral data was identical to literature and previously synthesised material (refer to section 7.13.2).^{20,206}

7.17 Effect of additives on the glucuronylsynthase reactions

7.17.1 Effect of co-solvents on initial velocity

Co-solvents investigated include ethanol, DMSO, *tert*-butanol, and glycerol at a final concentration of 5% v/v and 10% v/v. Glucuronylsynthase (1.4 mg mL⁻¹, 50 μ L) was added to α -D-glucuronyl fluoride **51** (final concentration 1 mM), 2-phenylethanol **45** (final concentration 94 mM) and co-solvent pre-incubated at 21 °C in sodium phosphate buffer (100 mM, 1450 μ L, pH 7.5). The reaction was immediately subjected to HPLC (refer to section 7.9) with a mobile phase of 23% acetonitrile in sodium phosphate (100 mM, pH 2.0). An additional 3 injections were made at 16 min intervals.

7.17.2 Effect of detergents on initial velocity

Detergents investigated include dodecyl maltoside, Triton X-100, Bug Buster, and Brij-56 at a final concentration of 1% w/v and 2% w/v. Glucuronylsynthase (1.4 mg mL⁻¹, 50 μ L) was added to α -D-glucuronyl fluoride **51** (final concentration 1 mM), 2-phenylethanol **45** (final concentration 94 mM) and detergent pre-incubated at 21 °C in sodium phosphate buffer (100 mM, 1450 μ L, pH 7.5). The reaction was immediately subjected to HPLC (refer to section

7.9) with a mobile phase of 23% acetonitrile in sodium phosphate buffer (100 mM, pH 2.0). An additional 3 injections were made at 16 min intervals.

7.17.3 Effect of co-solvents on reaction yield

Co-solvents investigated include DMSO (5% v/v), *tert*-butanol (5% v/v and 10% v/v), and glycerol (5% v/v). Glucuronylsynthase (21.7 mg mL⁻¹, 20 μL, final concentration 0.4 mg mL⁻¹) was added to DHEA O-(carboxymethyl)oxime **116** (final concentration 2 mM, 5 mM or 10 mM), α-D-glucuronyl fluoride **51** (3 equiv), and co-solvent pre-incubated at 37 °C in sodium phosphate buffer (100 mM, 980 μL, pH 7.5). The reaction was immediately subjected to HPLC (5 μL injections, refer to section 7.9) with a mobile phase of 30% acetonitrile in sodium phosphate buffer (100 mM, pH 2.0). The reaction was monitored by injections (5 μL) every 5 h for 60 h. The reaction endpoint was determined to be 48 h.

7.17.4 Effect of detergents on reaction yield

Detergents investigated include dodecyl maltoside (1% w/v) and Triton X-100 (1% w/v). Glucuronylsynthase (21.7 mg mL⁻¹, 20 μL, final concentration 0.4 mg mL⁻¹) was added to DHEA O-(carboxymethyl)oxime **116** (final concentration 2 mM and 5 mM), α-D-glucuronyl fluoride **51** (3 equiv), and detergent pre-incubated at 37 °C in sodium phosphate buffer (100 mM, 980 μL, pH 7.5). The reaction was immediately subjected to HPLC (5 μL injection, refer to section 7.9) with a mobile phase of 30% acetonitrile in sodium phosphate buffer (100 mM, pH 2.0). The reaction was monitored by injections (5 μL) every 5 h for 60 h.

A reaction with DHEA O-(carboxymethyl)oxime **116** (5 mM) dissolved in a Triton X-100 (1% w/v) solution was also trialled, but due to the HPLC autosampler rupturing the vial seal, it was omitted from the study.

7.18 SPE methodology

7.18.1 Australian Racing Forensic Laboratories solid phase extraction procedure¹⁸¹

Solid phase extraction cartridge (3 cc, Oasis[®] MAX or Oasis[®] WAX, Waters Co.) was pre-conditioned with methanol (1 mL), then water (3 mL). The crude reaction was loaded into the cartridge and washed with sodium hydroxide (0.1 M, 3 mL), sodium phosphate buffer (0.05 M, 3 mL, pH 7.5), then water

Experimental

(3 mL). The cartridge was dried briefly under pressure and subsequently eluted with methanol (3 mL) and then a solution of methanol, ethyl acetate and formic acid (25:25:1 respectively, 3 mL).

7.18.2 Waters Oasis[®] MAX extraction procedure²²⁶

The Oasis[®] MAX solid-phase extraction cartridge (3 cc, Waters Co.) was pre-conditioned with methanol (1 mL), then water (3 mL). The crude reaction was loaded into the cartridge and washed with ammonium hydroxide (5% v/v, 3 mL), methanol (3 mL), then formic acid in methanol (2% v/v, 3 mL).

7.18.3 Waters Oasis[®] WAX extraction procedure²²⁶

The Oasis[®] WAX solid-phase extraction cartridge (3 cc, Waters Co.) was pre-conditioned with methanol (1 mL), then water (3 mL). The crude reaction was loaded into the cartridge and washed with formic acid (2% v/v, 3 mL), methanol (3 mL), then ammonium hydroxide in methanol (5% v/v, 3 mL).

7.18.4 Assessing the optimum SPE cartridge and SPE procedure.

Glucuronylsynthase (final concentration 0.3 mg mL⁻¹) was added to α -D-glucuronyl fluoride **51** (final concentration 10 mM) and DHEA O-(carboxymethyl)oxime **116** (final concentration 2 mM) in sodium phosphate buffer (50 mM, pH 7.5, final volume 5 mL). The reaction was incubated at 37 °C for 5 d without agitation. An aliquot (1 mL each) was loaded onto four SPE cartridges (2 x Oasis[®] MAX, 2 x Oasis[®] WAX) with the remainder used to determine the quantity of DHEA O-(carboxymethyl)oxime β -D-glucuronide **118** (2.7 μ mol) loaded onto each cartridge by HPLC (see section 5.2.12 for conditions).

The ARFL extraction procedure (refer to section 7.18.1) was applied to an Oasis[®] MAX and Oasis[®] WAX SPE cartridge and the remaining SPE cartridges were extracted with their respective protocols. Each procedure was eluted with the final wash twice more to ensure complete elution. Non-aqueous solutions were evaporated to dryness by a nitrogen jet, and then re-dissolved in sodium phosphate buffer (50 mM, pH 7.5) to their original volume. The quantity of DHEA O-(carboxymethyl)oxime β -D-glucuronide **118** (5.7 min) and DHEA O-(carboxymethyl)oxime **116** (13.7 min) were determined in every fraction by HPLC analysis (see section 7.15 for conditions).

Table 7.2. Recovery of DHEA O-(carboxymethyl)oxime β -D-glucuronide (CMO-DHEA Gluc) 118 and DHEA O-(carboxymethyl)oxime (CMO-DHEA) 116 (determined by HPLC) from Oasis[®] MAX SPE cartridge using the ARFL extraction procedure. Recovery is a percentage based on the amount of CMO-DHEA Gluc 118 loaded on the cartridge.

Reaction component	CMO-DHEA Gluc 118		CMO-DHEA 116	
	Quantity (μ mol)	Recovery (%)	Response (au)	Recovery (%)
Loading	2.72	100	3874233	100
NaOH	0	0	0	0
Phosphate buffer	0	0	0	0
Water	0	0	0	0
MeOH	0	0	0	0
MeOH/EtOAc/HCO ₂ H (Wash 1)	2.68	98.5	3251745	83.9
MeOH/EtOAc/HCO ₂ H (Wash 2)	0	0	0	0
MeOH/EtOAc/HCO ₂ H (Wash 3)	0	0	0	0
Unaccounted	0.04	1.5	622488	16.1

Table 7.3. Recovery of DHEA O-(carboxymethyl)oxime β -D-glucuronide (CMO-DHEA Gluc) 118 and DHEA O-(carboxymethyl)oxime (CMO-DHEA) 116 (determined by HPLC) from Oasis[®] WAX SPE cartridges using the ARFL extraction procedure. Recovery is a percentage based on the amount of CMO-DHEA Gluc 118 loaded on the cartridge.

Reaction component	CMO-DHEA Gluc 118		CMO-DHEA 116	
	Quantity (μ mol)	Recovery (%)	Response (au)	Recovery (%)
Loading	2.72	100	3874233	100
NaOH	2.26	83.1	0	0
Phosphate buffer	0.06	2.2	0	0
Water	0	0	0	0
MeOH	0	0	2013942	52.0
MeOH/EtOAc/HCO ₂ H (Wash 1)	0.37	13.6	1239216	32.0
MeOH/EtOAc/HCO ₂ H (Wash 2)	0	0	0	0
MeOH/EtOAc/HCO ₂ H (Wash 3)	0	0	0	0
Unaccounted	0.03	1.1	621075	16.0

Experimental

Table 7.4. Recovery of DHEA O-(carboxymethyl)oxime β -D-glucuronide (CMO-DHEA Gluc) 118 and DHEA O-(carboxymethyl)oxime (CMO-DHEA) 116 (determined by HPLC) from Oasis[®] MAX using the Waters Oasis[®] MAX extraction procedure. Recovery is a percentage based on the amount of CMO-DHEA Gluc 118 loaded on the cartridge.

Reaction component	CMO-DHEA Gluc 118		CMO-DHEA 116	
	Quantity (μ mol)	Recovery (%)	Response (au)	Recovery (%)
Loading	2.72	100	3874233	100
Aq. NH ₄ OH	0	0	0	0
MeOH	0	0	0	0
HCO ₂ H/MeOH (wash 1)	2.65	97.4	3847113	99.3
HCO ₂ H/MeOH (wash 1)	0.01	0.4	0	0
HCO ₂ H/MeOH (wash 1)	0	0	0	0
Unaccounted	0.06	2.2	27120	0.7

Table 7.5. Recovery of DHEA O-(carboxymethyl)oxime β -D-glucuronide (CMO-DHEA Gluc) 118 and DHEA O-(carboxymethyl)oxime (CMO-DHEA) 116 (determined by HPLC) from Oasis[®] WAX using the Waters Oasis[®] WAX extraction procedure. Recovery is a percentage based on the amount of CMO-DHEA Gluc 118 loaded on the cartridge.

Reaction component	CMO-DHEA Gluc 118		CMO-DHEA 116	
	Quantity (μ mol)	Recovery (%)	Response (au)	Recovery (%)
Loading	2.72	100	3874233	100
Aq. HCO ₂ OH	0	0	0	0
MeOH	0.03	1.1	2349012	60.6
NH ₄ OH/MeOH (wash 1)	2.61	96.0	1482323	38.3
NH ₄ OH/MeOH (wash 1)	0	0	0	0
NH ₄ OH/MeOH (wash 1)	0	0	0	0
Unaccounted	0.08	2.9	42898	1.1

7.18.5 General steroid screen with SPE

Steroid (1 mg, final concentration 0.2 mg mL⁻¹), α -D-glucuronyl fluoride **51** (5 equiv) and *tert*-butanol (final concentration 5% v/v) were combined in sodium phosphate (50 mM, pH 7.5) and sonicated (2 min, 30 °C). Glucuronylsynthase (final concentration 0.2 mg mL⁻¹) was added and the reaction was incubated at 37 °C without agitation for 3 days. The crude reaction was analysed by TLC

(ethyl acetate : methanol : water, 7 : 2 : 1) and HPLC (refer to section 7.9) with 30% acetonitrile in sodium phosphate buffer (100 mM, pH 2.0). The glucuronide product was isolated using Oasis® WAX SPE cartridge (3 cc) and the ARFL procedure. The purified glucuronide product was re-subjected to HPLC analysis and submitted for ESI-MS analysis.

Yields were estimated from the peak area % from HPLC analysis (where applicable) using the UV absorbance maximum of the largest peak common to steroid and steroid glucuronide and assuming equal absorbance co-efficients for the steroid and steroid glucuronide.

7.18.6 SPE with DHEA 55

The general steroid SPE procedure (refer to section 7.18.5) was applied to DHEA **55** to produce the DHEA β -D-glucuronide **77** (76%). The chromatogram was measured at 211 nm to provide a retention time of 17.2 min for DHEA **55** and 6.4 min for the DHEA β -D-glucuronide **77** (Figure 5.9). The target glucuronide **77** was purified by SPE (96% purity by HPLC, Figure 5.10).

λ_{\max} 211 nm; **LRMS (-ESI) m/z** : 463 ($[M-H]^-$, 100%); **HRMS (-ESI) m/z** : 463.2342 ($[M-H]^-$, $C_{25}H_{35}O_8$ gives 463.2332).

7.18.7 SPE with testosterone 7

The general steroid SPE procedure (refer to section 7.18.5) was applied to testosterone **7** to produce the testosterone β -D-glucuronide **6** (6%). The chromatogram was measured at 248 nm to provide a retention time of 14.5 min for testosterone **7** and 6.1 min for the testosterone β -D-glucuronide **6** (Figure 7.11). The target glucuronide **6** was purified by SPE (49% purity by HPLC, Figure 7.12).

λ_{\max} 248 nm; **LRMS (-ESI) m/z** : 463 ($[M-H]^-$, 100%); **HRMS (-ESI) m/z** : 463.2332 ($[M-H]^-$, $C_{25}H_{35}O_8$ gives 463.2332).

Experimental

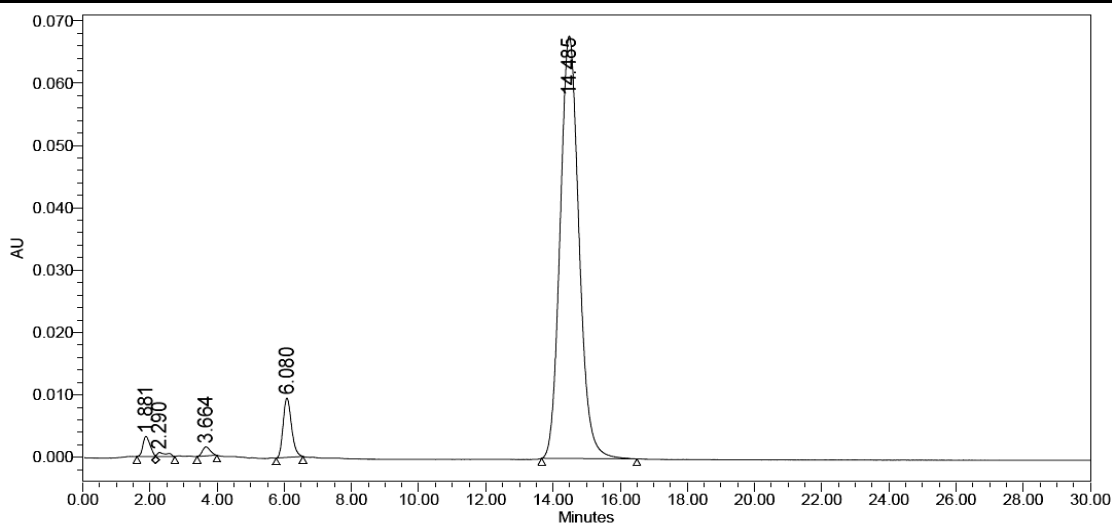


Figure 7.11. HPLC chromatogram of the crude glucuronylsynthase reaction of testosterone 7.

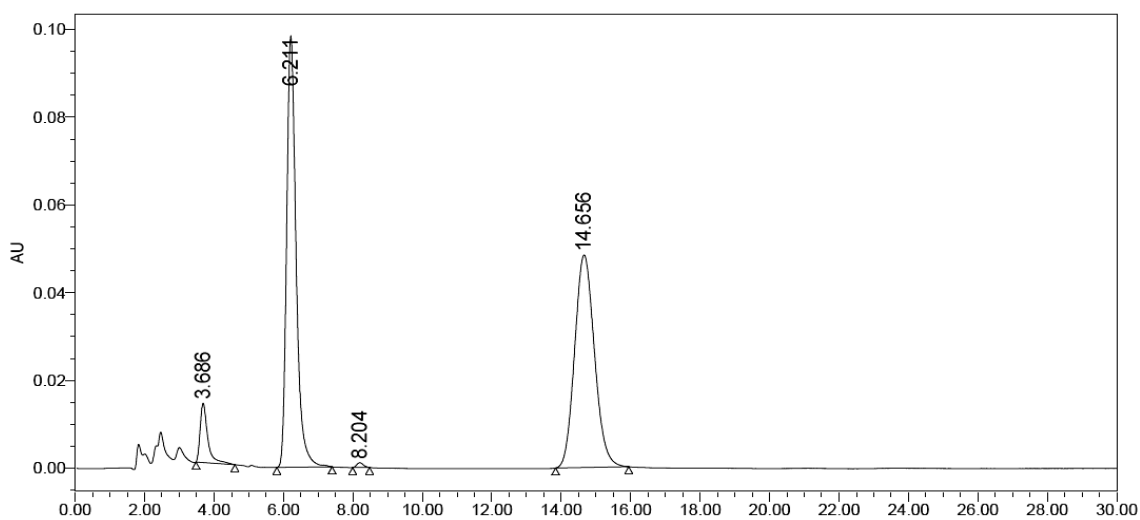


Figure 7.12. HPLC chromatogram of the purified testosterone β -D-glucuronide 6 using SPE

7.18.8 SPE with epitestosterone 123

The general steroid SPE procedure (refer to section 7.18.5) was applied to epitestosterone **123** to produce the epitestosterone β -D-glucuronide **126** (38%). The chromatogram was measured at 248 nm to provide a retention time of 19.5 min for epitestosterone **123** and 8.2 min for the epitestosterone β -D-glucuronide **126** (Figure 7.13). The target glucuronide **126** was purified by SPE (58% purity by HPLC, Figure 7.14). A second SPE step was performed to purify the glucuronide **126** further (96% purity by HPLC, Figure 7.15).

λ_{\max} 248 nm; **LRMS (-ESI) m/z** : 463 ($[M-H]^-$, 100%); **HRMS (-ESI) m/z** : 463.2338 ($[M-H]^-$, $C_{25}H_{35}O_8$ gives 463.2332).

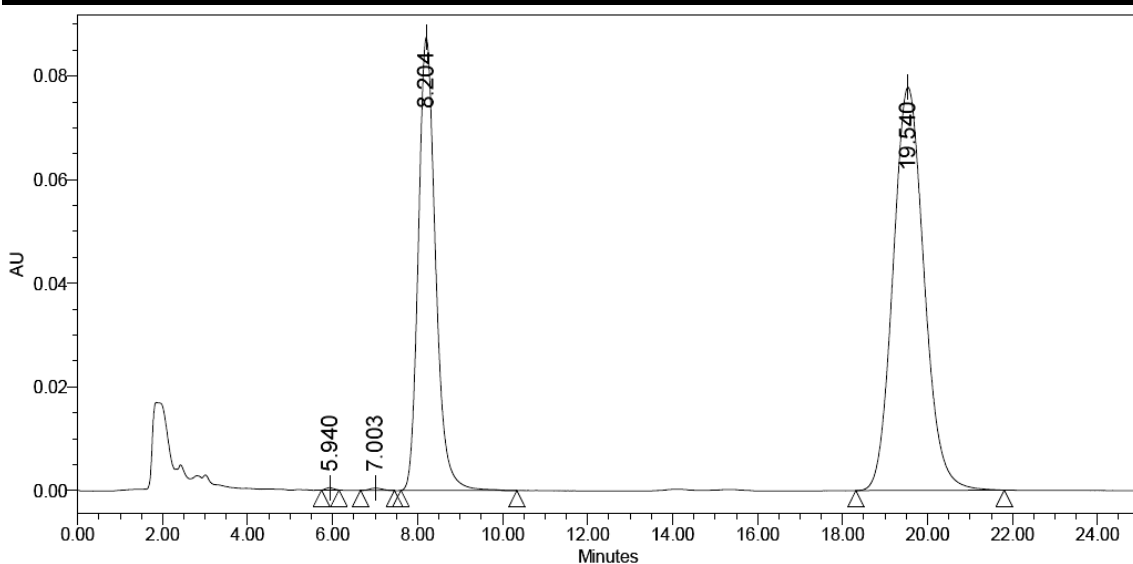


Figure 7.13. HPLC chromatogram of the crude glucuronylsynthase reaction of epitestosterone 123.

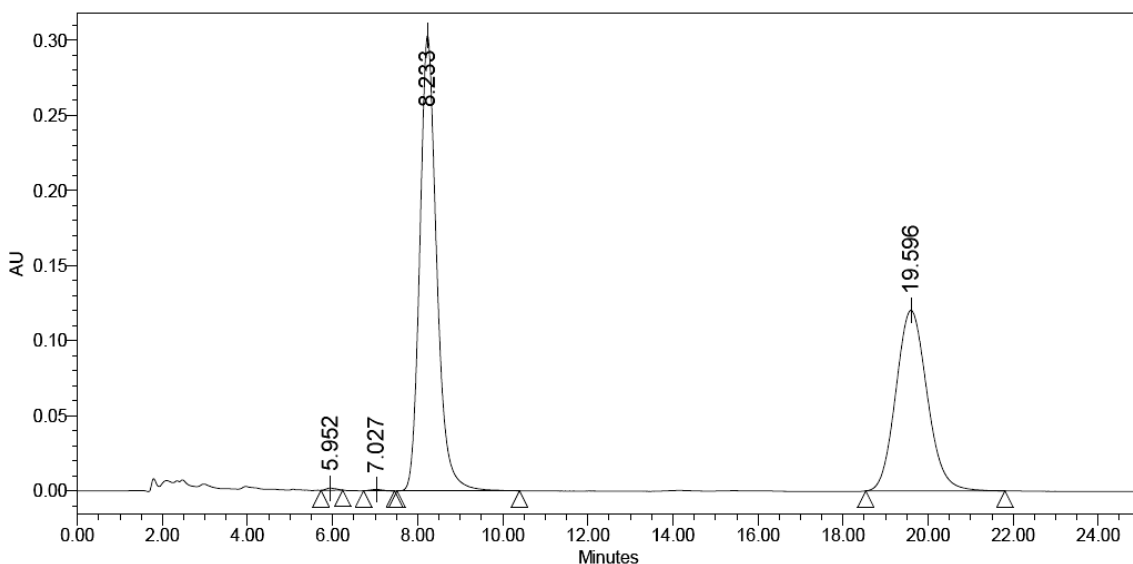


Figure 7.14. HPLC chromatogram of the purified epitestosterone β -D-glucuronide 126 after one round of SPE.

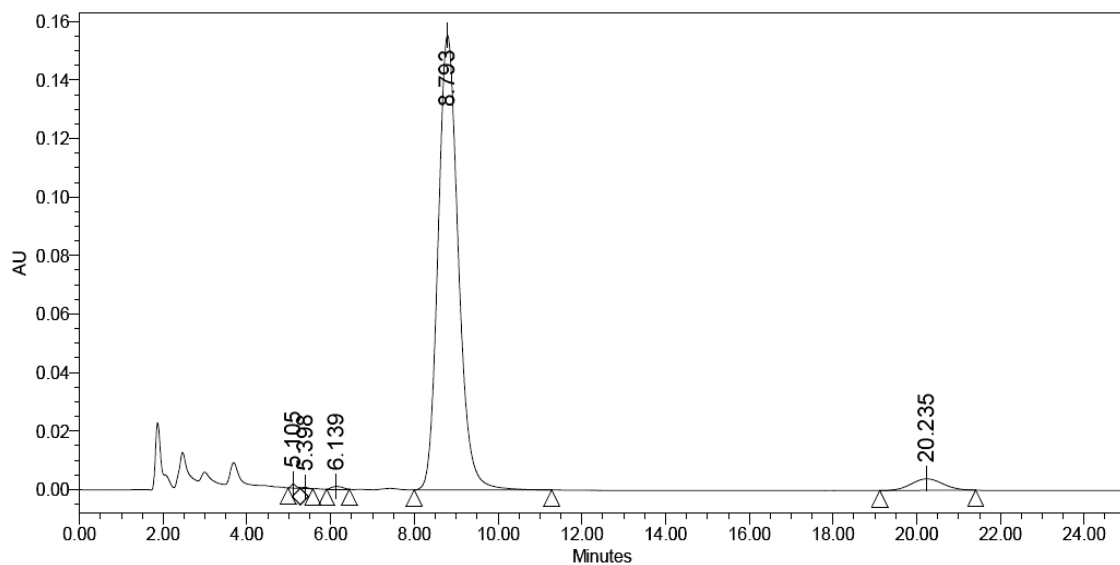


Figure 7.15. HPLC chromatogram of the purified epitestosterone β -D-glucuronide 126 after two rounds of SPE.

Experimental

7.18.9 SPE with boldenone **118**

The general steroid SPE procedure (refer to section 7.18.5) was applied to boldenone **118** to produce the boldenone β -D-glucuronide **125** (15%). The chromatogram was measured at 248 nm to provide a retention time of 9.9 min for boldenone **118** and 5.2 min for the boldenone β -D-glucuronide **125** (Figure 7.16). The target glucuronide **125** was purified by SPE (75% purity by HPLC, Figure 7.17). A second SPE step was performed to purify the glucuronide **125** further (99% purity by HPLC, Figure 7.18).

λ_{\max} 248 nm; **LRMS (-ESI) m/z** : 461 ($[M-H]^-$, 80%); **HRMS (-ESI) m/z** : 461.2184 ($[M-H]^-$, $C_{25}H_{33}O_8$ gives 461.2175).

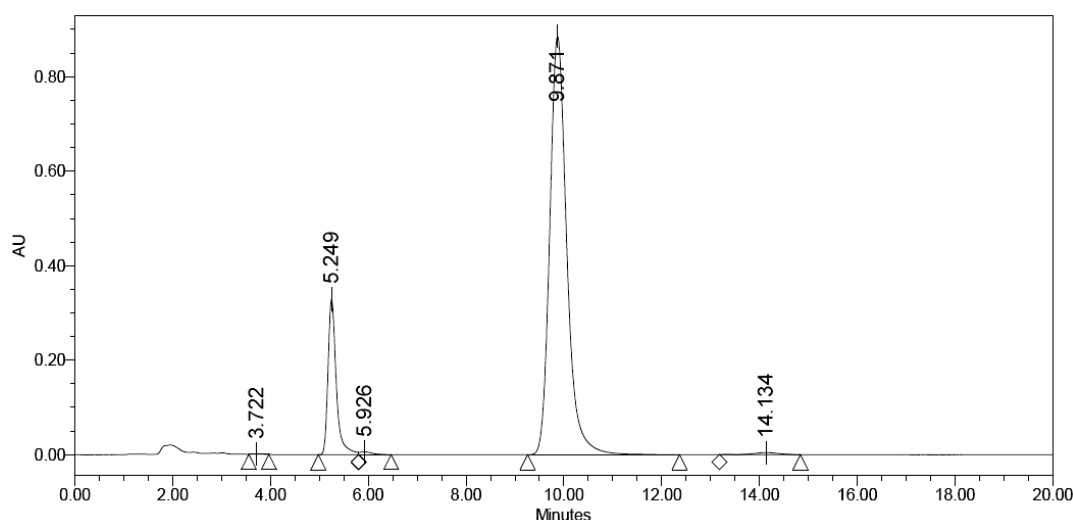


Figure 7.16. HPLC chromatogram of the crude glucuronylsynthase reaction of boldenone **118.**

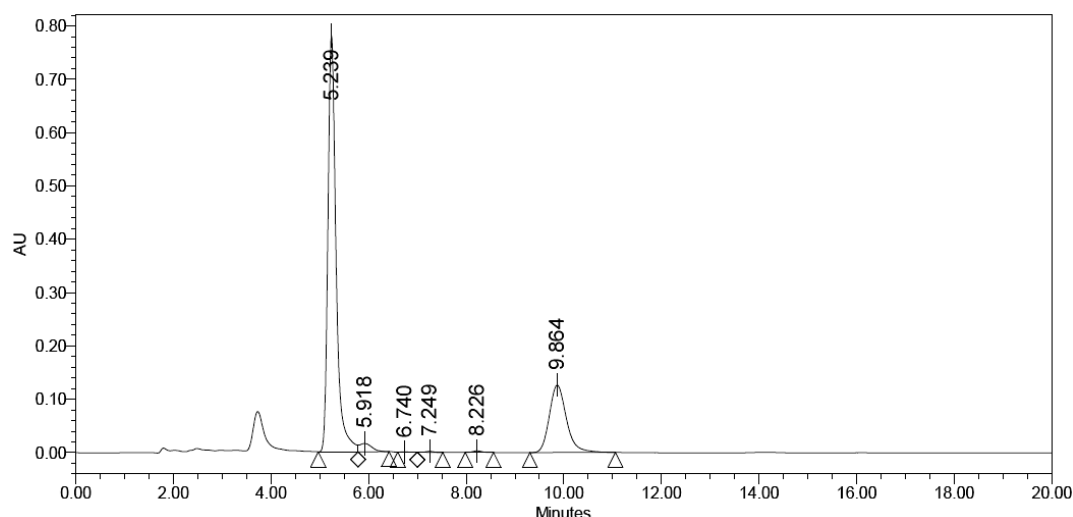


Figure 7.17. HPLC chromatogram of the purified boldenone β -D-glucuronide **125 after one round of SPE.**

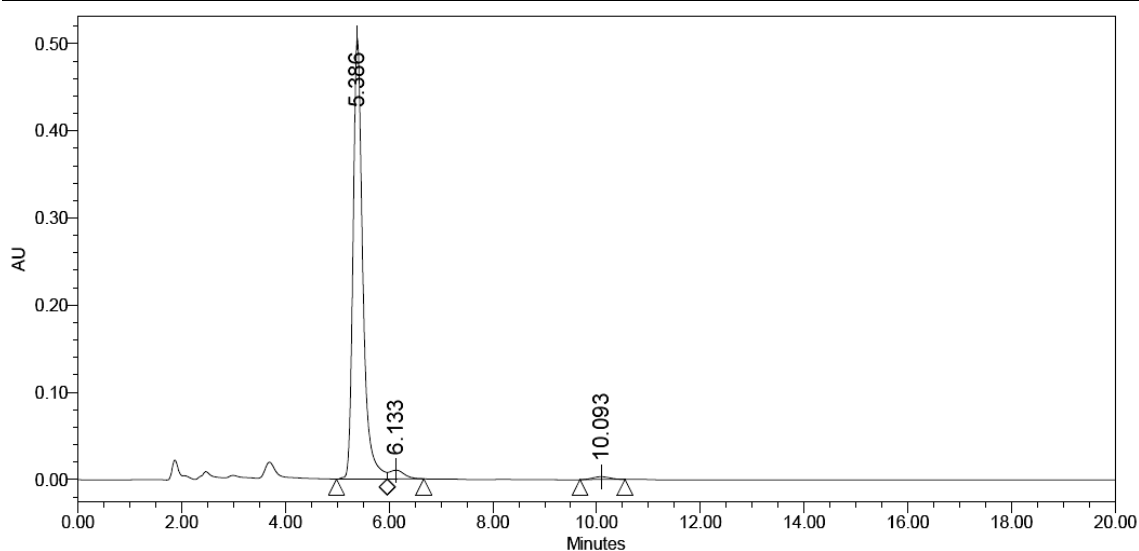


Figure 7.18. HPLC chromatogram of the purified boldenone β -D-glucuronide **125** after two rounds of SPE.

7.18.10 SPE with estrone **9**

The general steroid SPE procedure (refer to section 7.18.5) was applied to estrone **9** to produce the estrone β -D-glucuronide **12** (24%). The chromatogram was measured at 254 nm to provide a retention time of 20.2 min for estrone **9** and 6.0 min for the estrone β -D-glucuronide **12** (Figure 7.19). The target glucuronide **12** was purified by SPE (43% purity by HPLC, Figure 7.20).

λ_{\max} 254nm; LRMS (-ESI) m/z : 445 ($[M-H]^-$, 80%); HRMS (-ESI) m/z : 445.1862 ($[M-H]^-$, $C_{24}H_{29}O_8$ gives 445.1862).

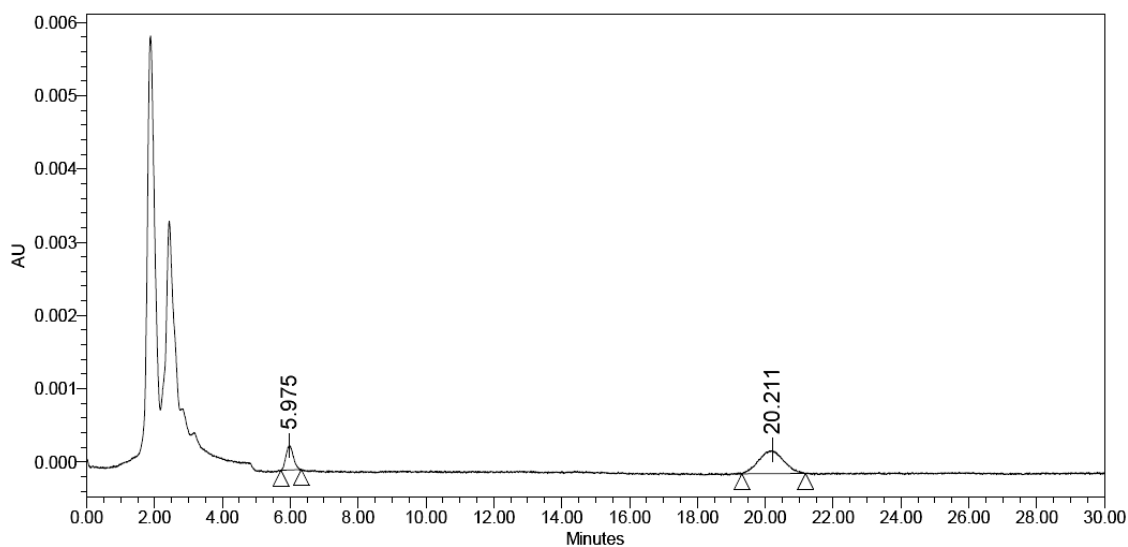


Figure 7.19. HPLC chromatogram of the crude glucuronylsynthase reaction of estrone **9**.

Experimental

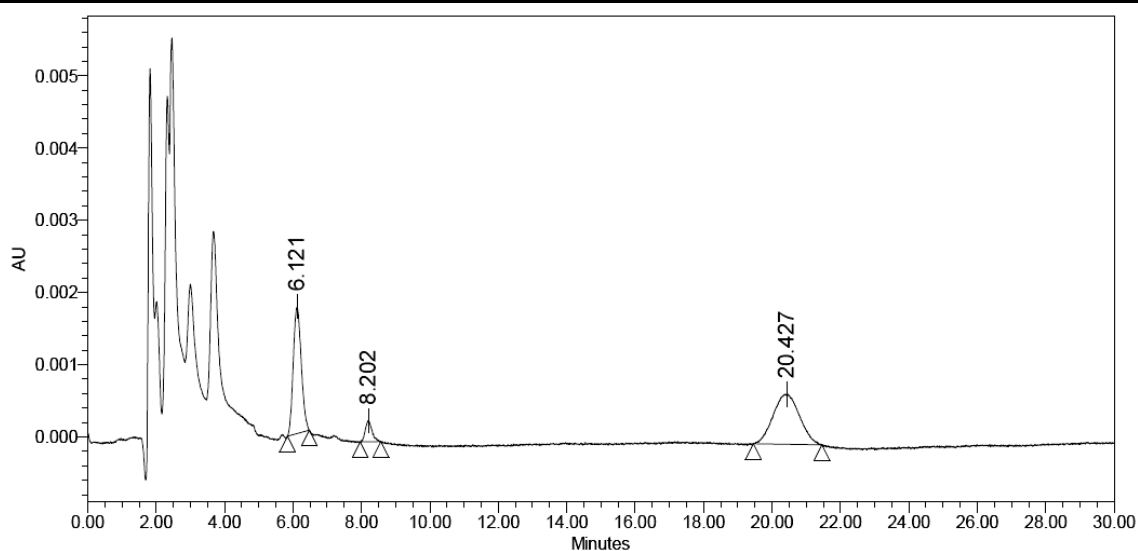


Figure 7.20. HPLC chromatogram of the purified estrone β -D-glucuronide **12** after one round of SPE.

7.18.11 SPE with methandriol **58**

The general steroid SPE procedure (refer to section 7.18.5) was applied to methandriol **58** to produce the methandriol β -D-glucuronide **127** (yield not determined). The chromatogram was measured at 211 nm to provide a retention time of 5.9 min for the methandriol β -D-glucuronide **127** (Figure 7.19) but no absorption for methandriol **58** (Figure 7.21).

λ_{\max} N/A; **LRMS (-ESI) m/z :** 479 ($[M-H]^-$, 65); **HRMS (-ESI) m/z :** 479.2645 ($[M-H]^-$, $C_{26}H_{39}O_8$ gives 479.2645).

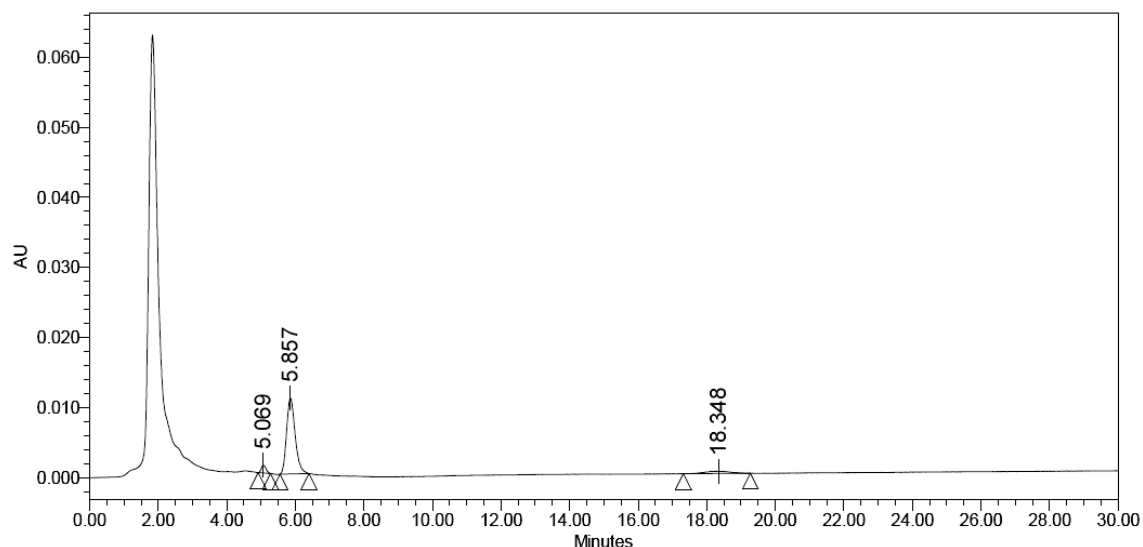


Figure 7.21. HPLC chromatogram of the crude glucuronylsynthase reaction of methandriol **58**.

7.18.12 SPE with 6 α -hydroxystanozolol **124**

The general steroid SPE procedure (refer to section 7.18.5) was applied to 6 α -hydroxystanozolol **124** to produce 6 α -hydroxystanozolol glucuronide **128**

(yield not determined). The chromatogram was measured at 229 nm but no resolution was obtained with the given HPLC procedure (Figure 7.22).

λ_{\max} 229 nm; LRMS (-ESI) m/z : 519 ($[M-H]^-$, 40%); HRMS (-ESI) m/z : 519.2691 ($[M-H]^-$, $C_{27}H_{39}N_2O_8$ gives 519.2706).

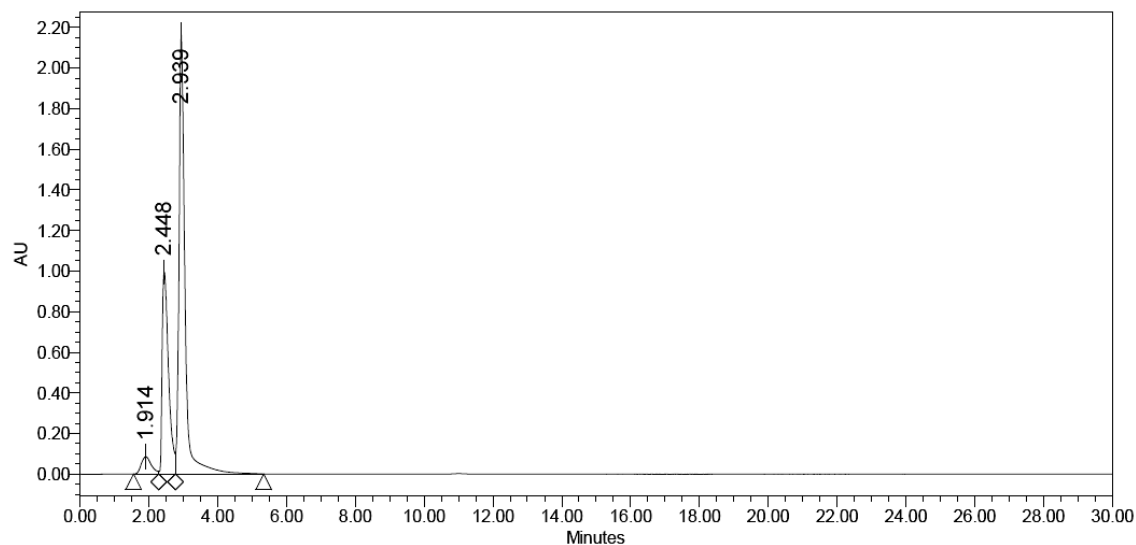
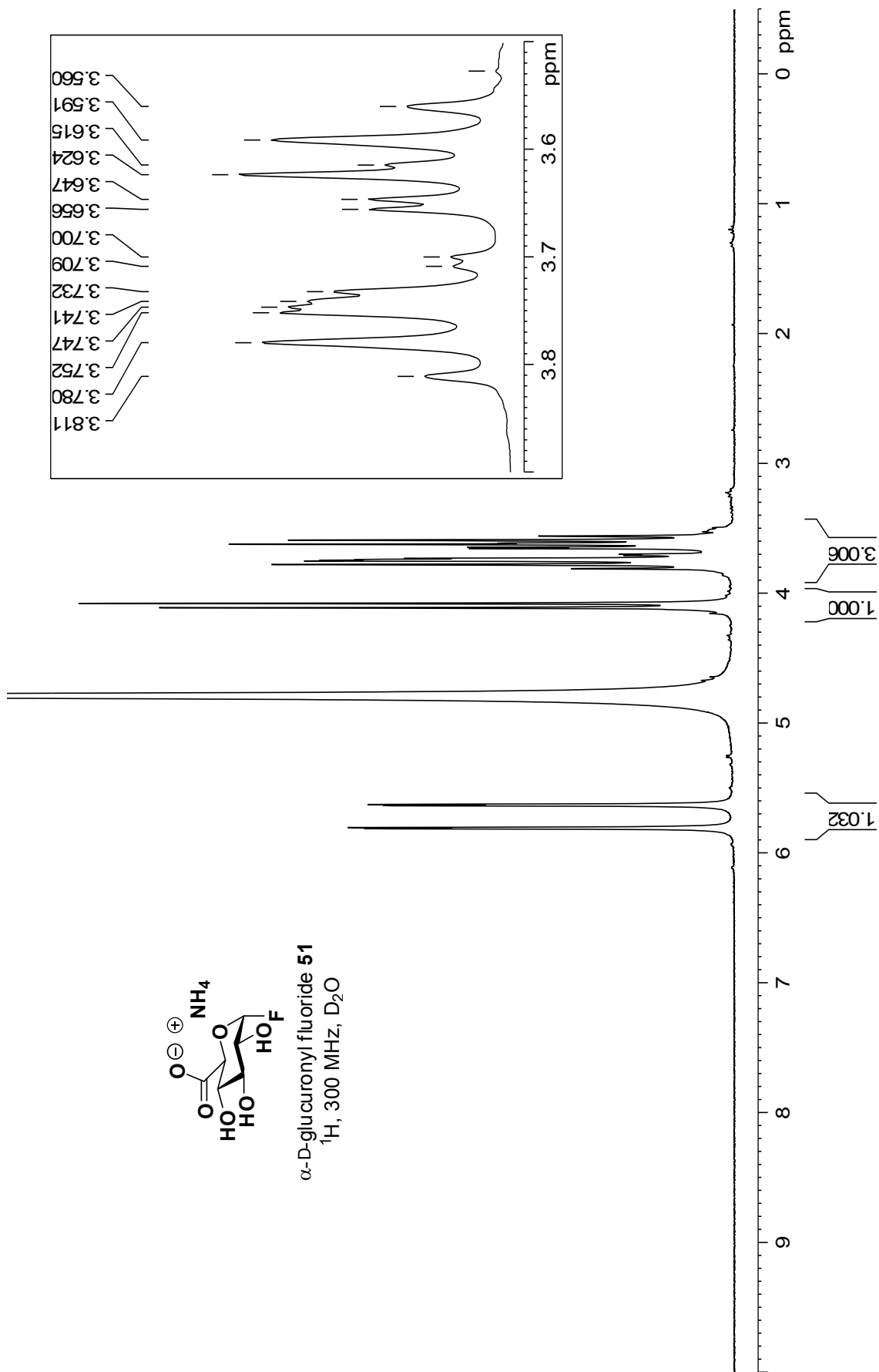
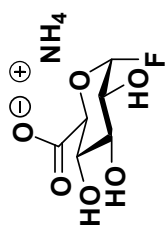
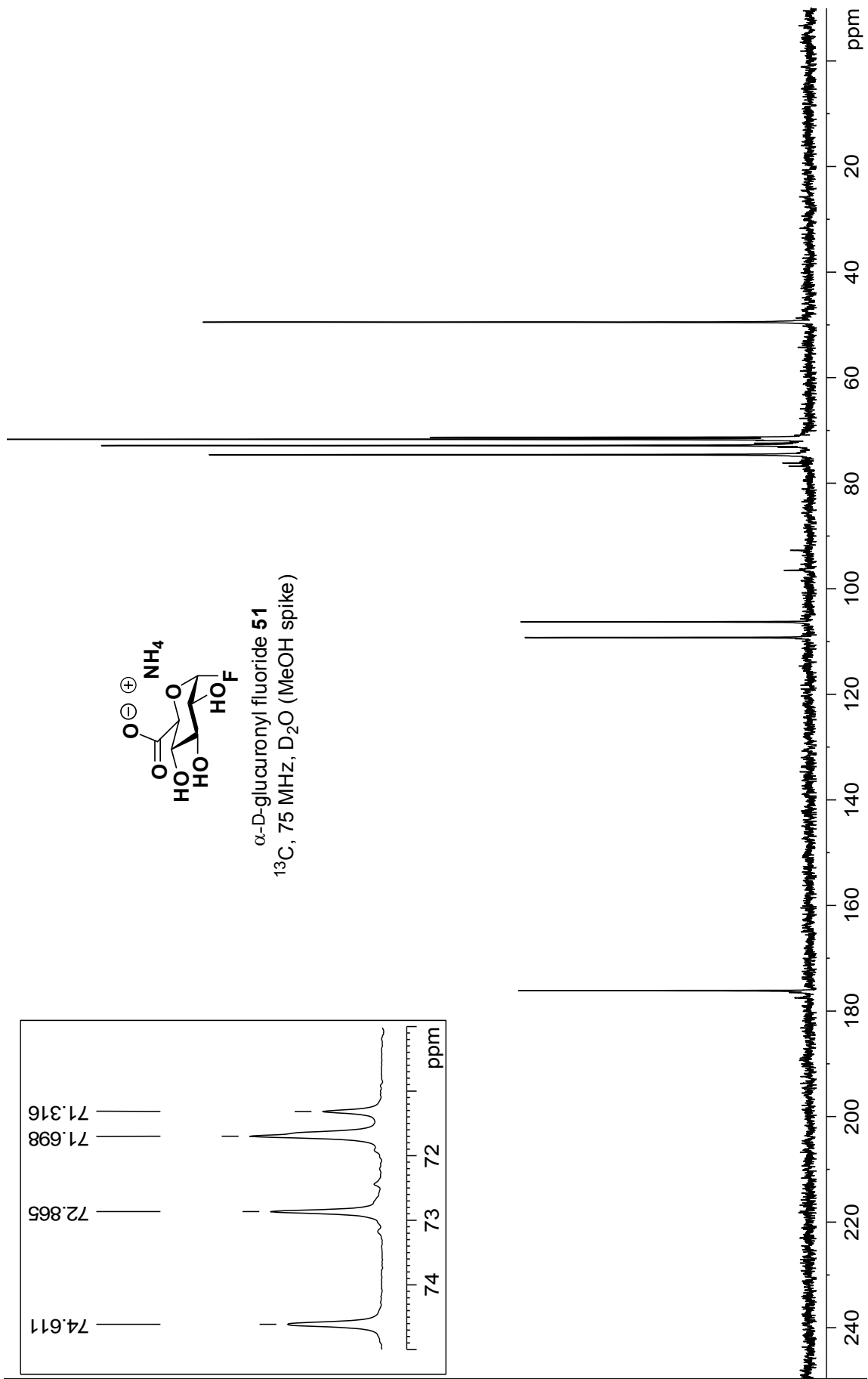


Figure 7.22. HPLC chromatogram of the crude glucuronylsynthase reaction of 6α -hydroxystanozolol 124.

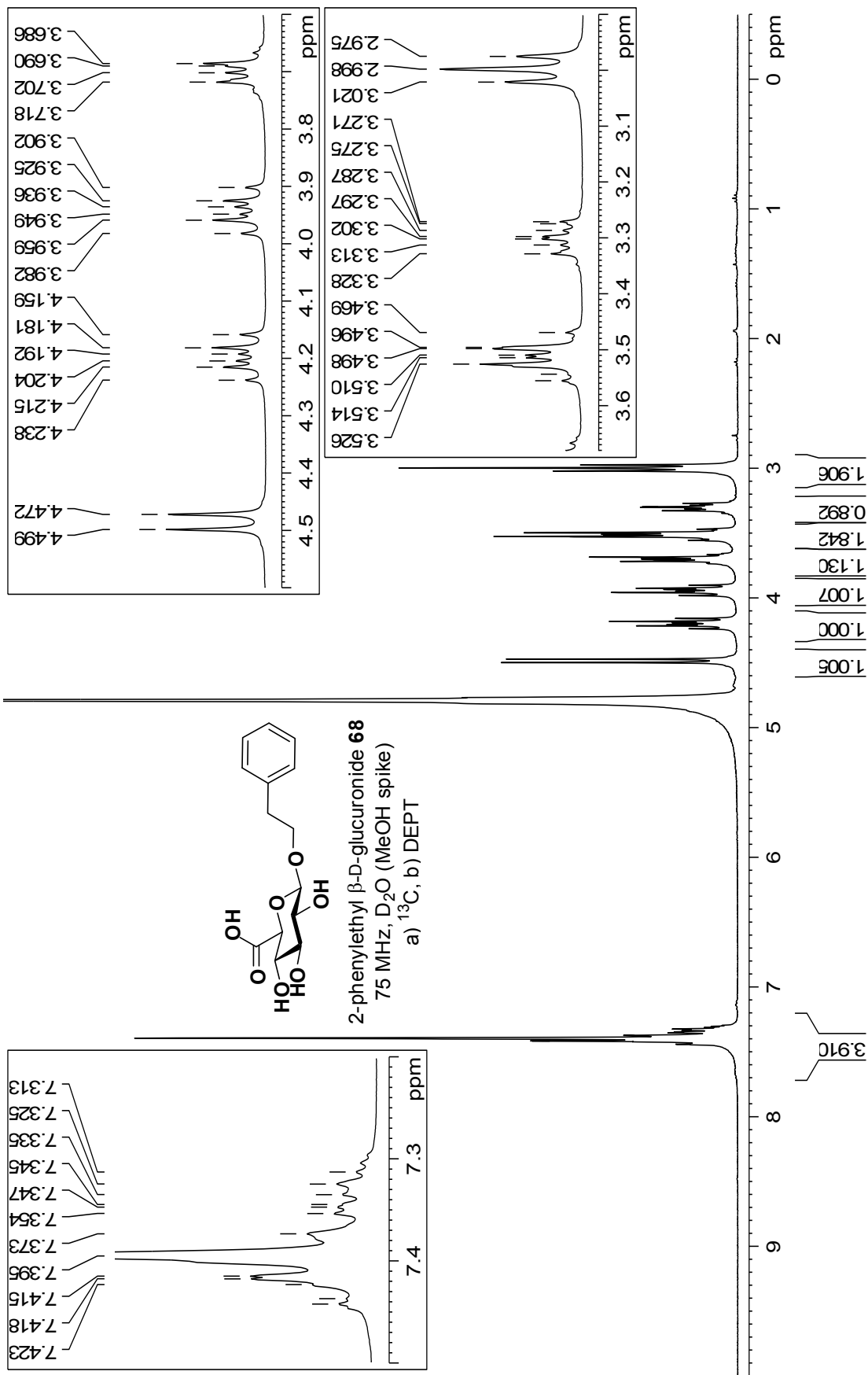
~ Chapter 8 ~

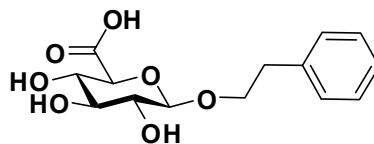
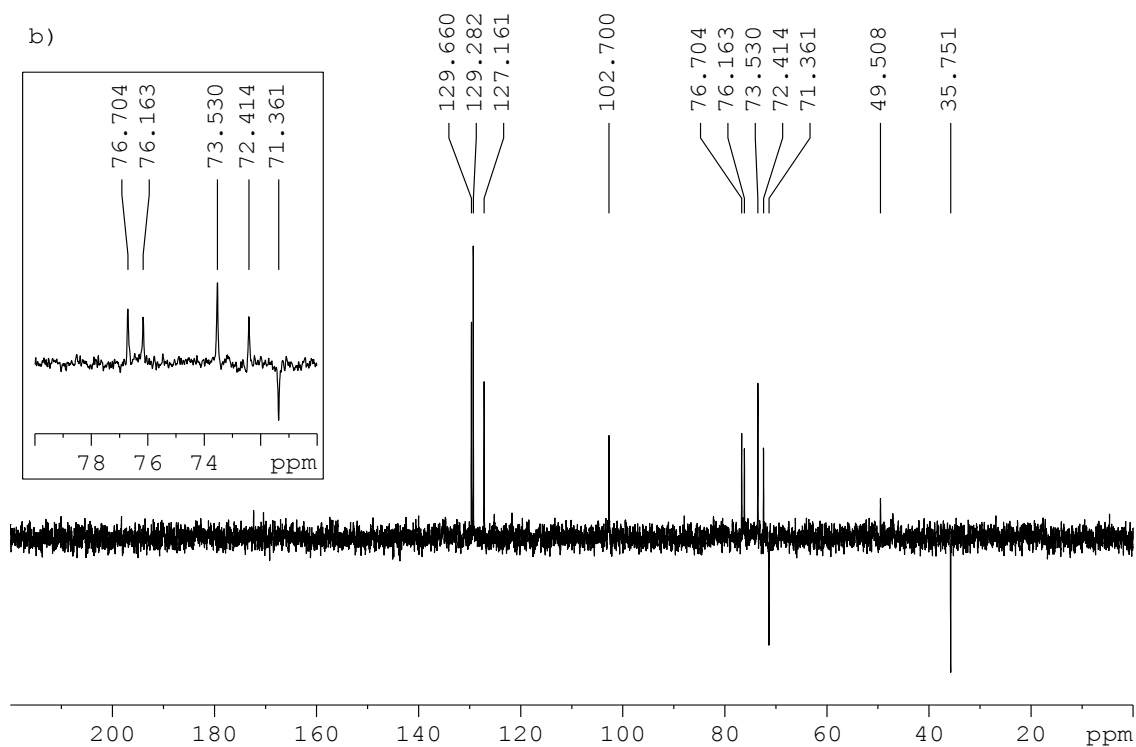
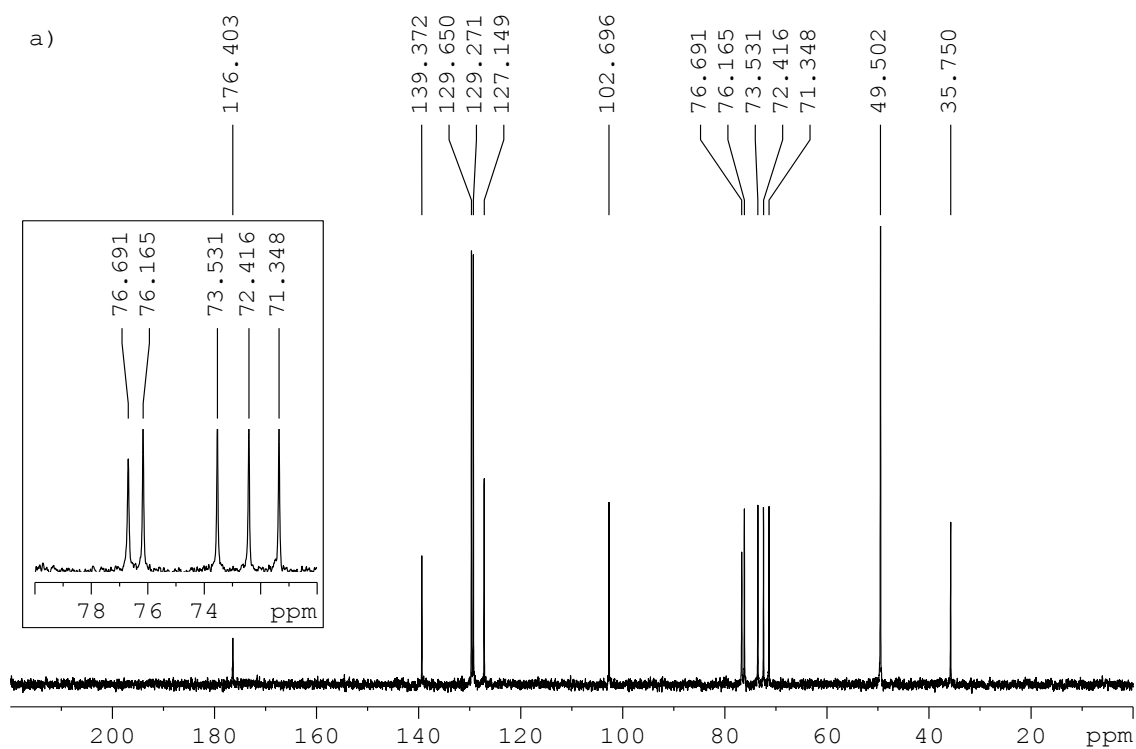
NMR spectra

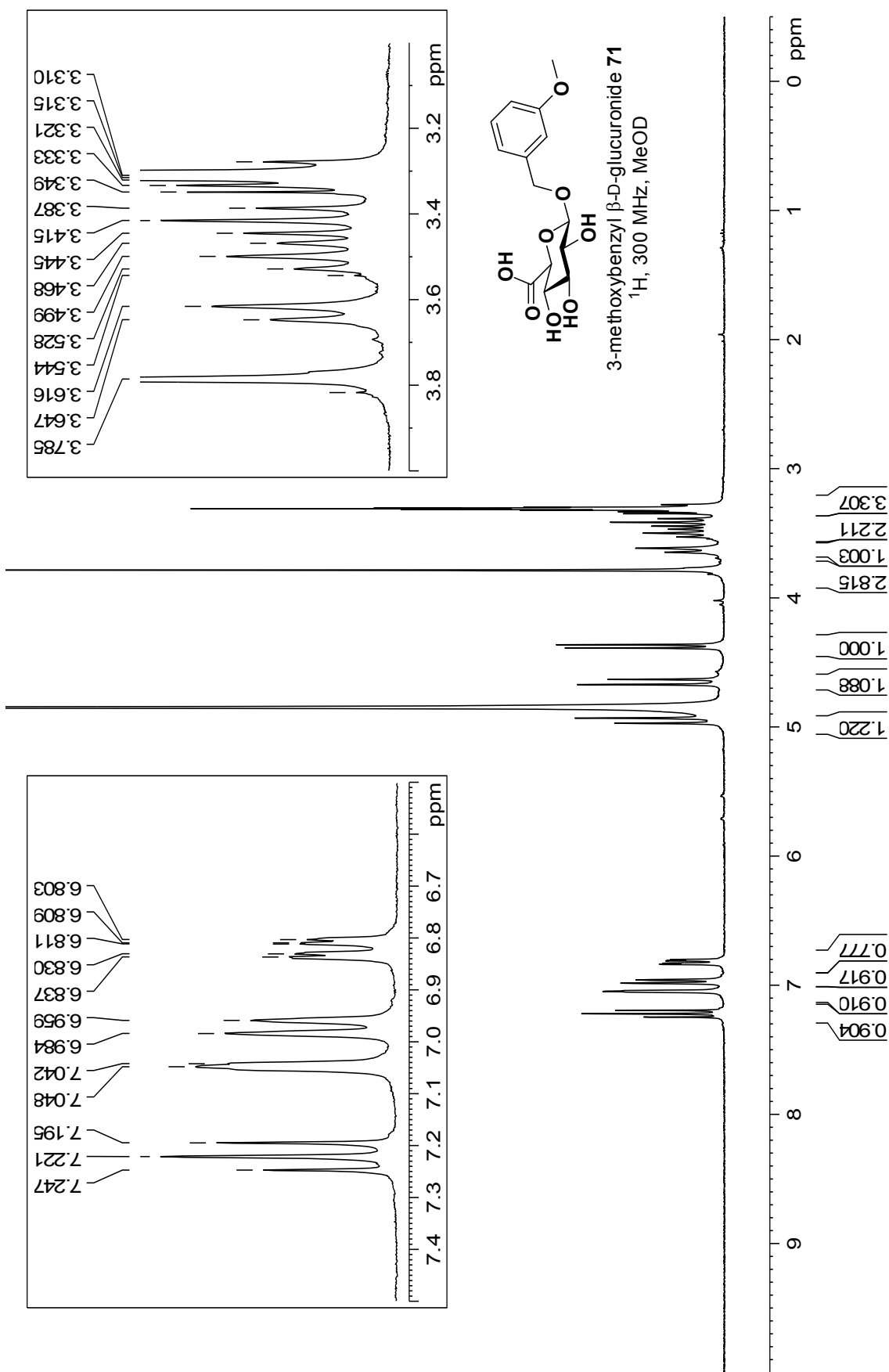


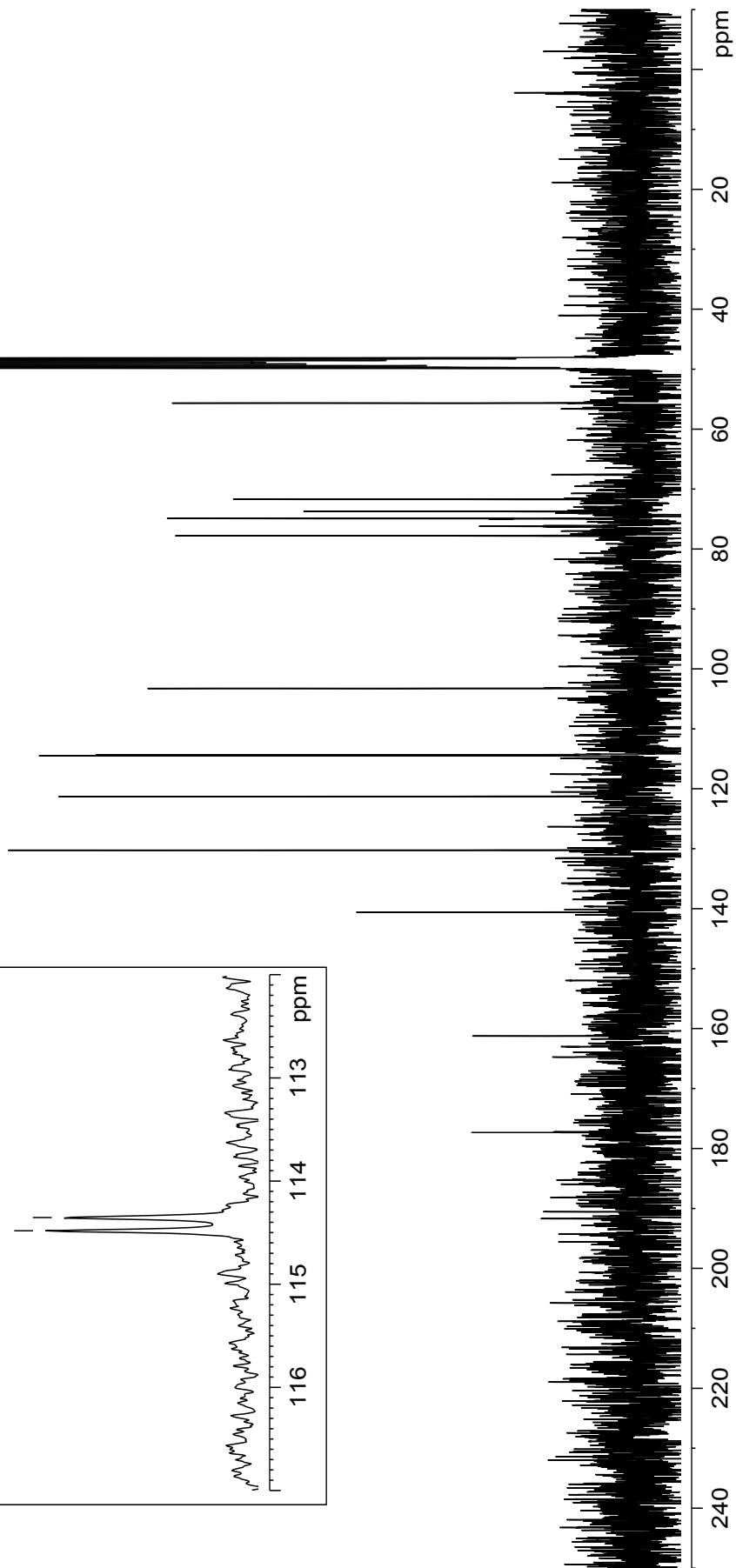
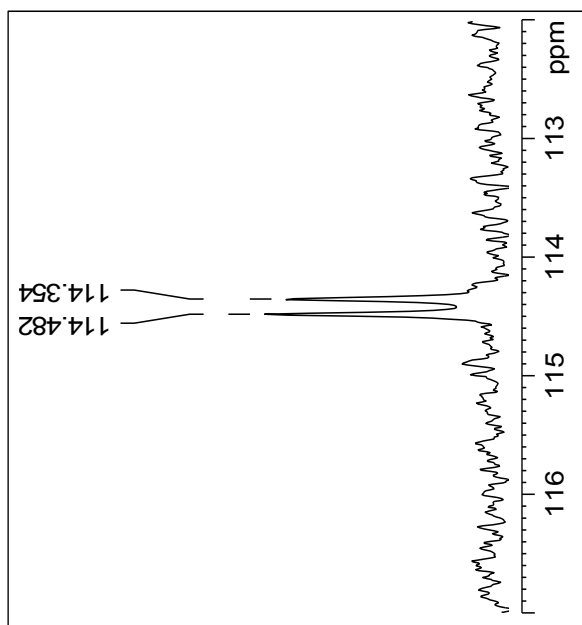
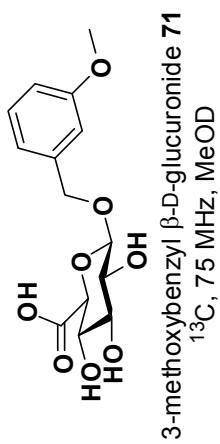


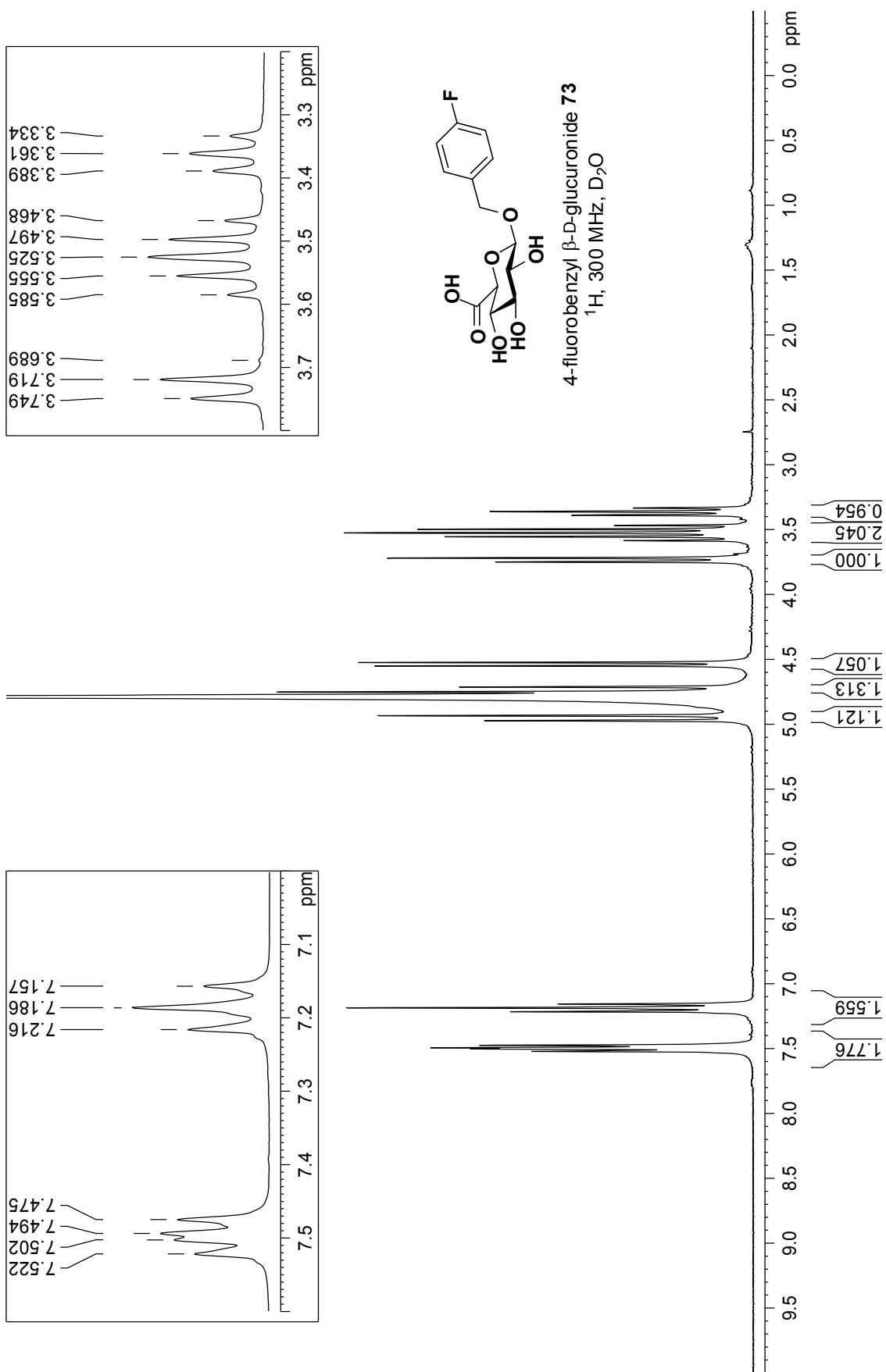
α -D-glucuronyl fluoride **51**
 ^{13}C , 75 MHz, D_2O (MeOH spike)

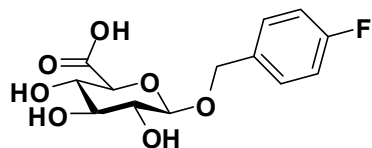


2-phenylethyl β -D-glucuronide **68**75 MHz, D₂O (MeOH spike)a) ¹³C, b) DEPT

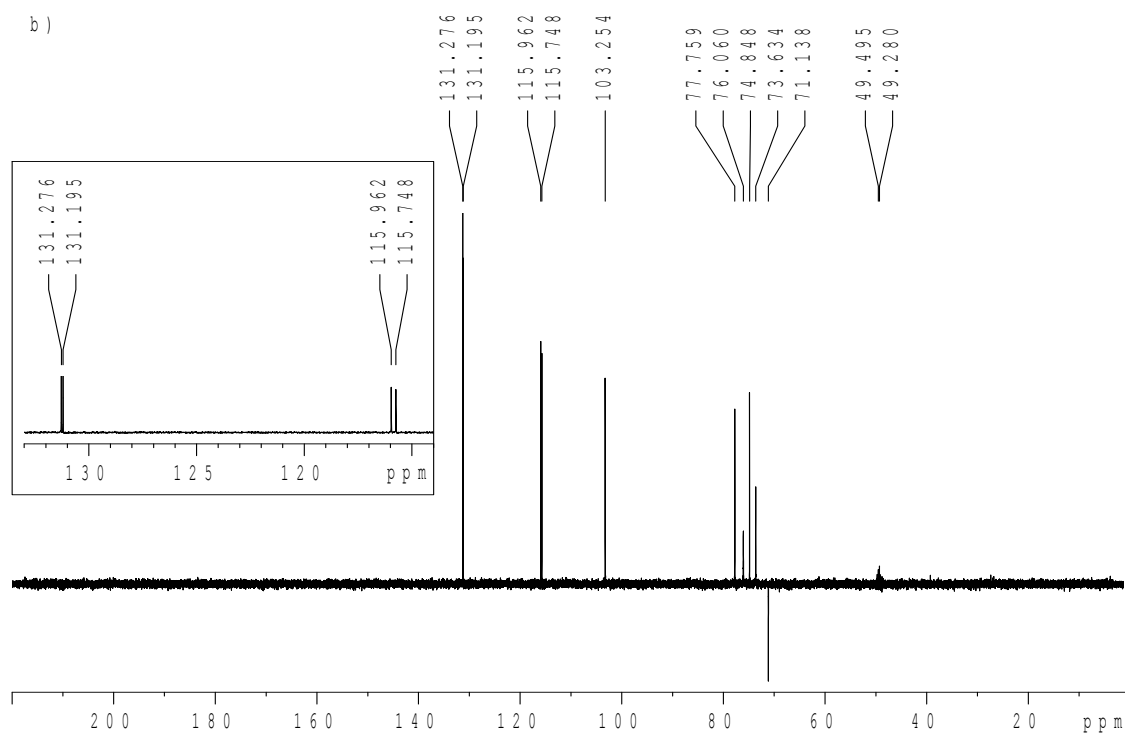
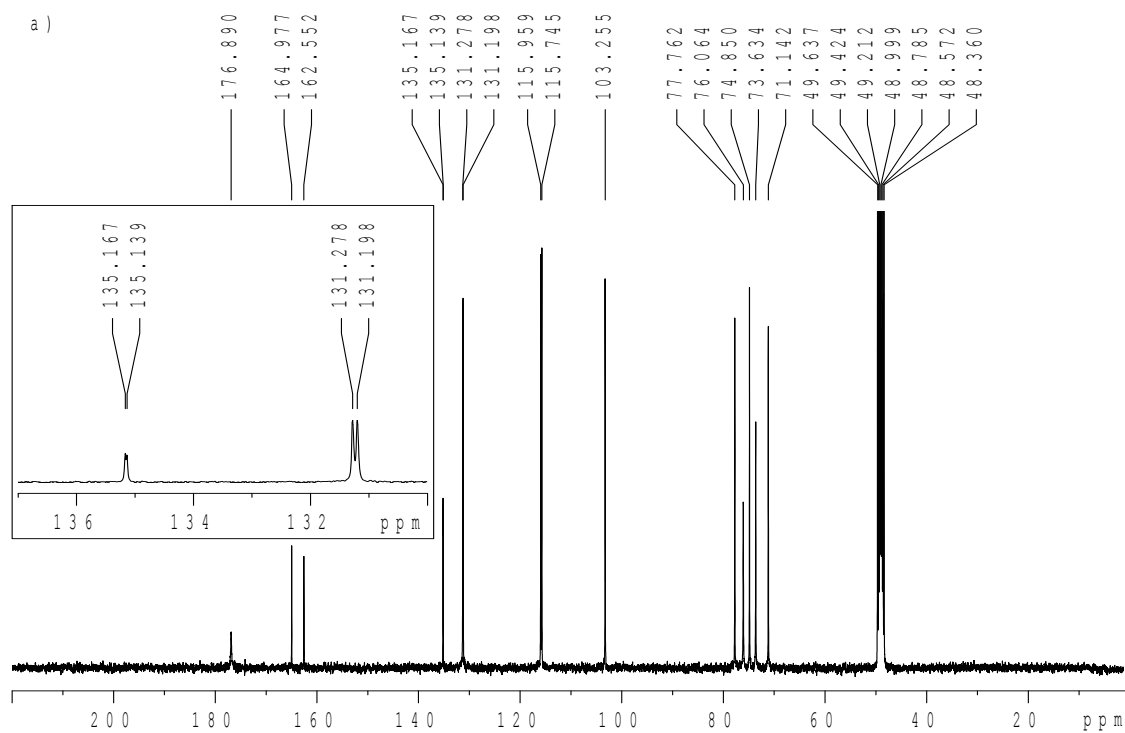


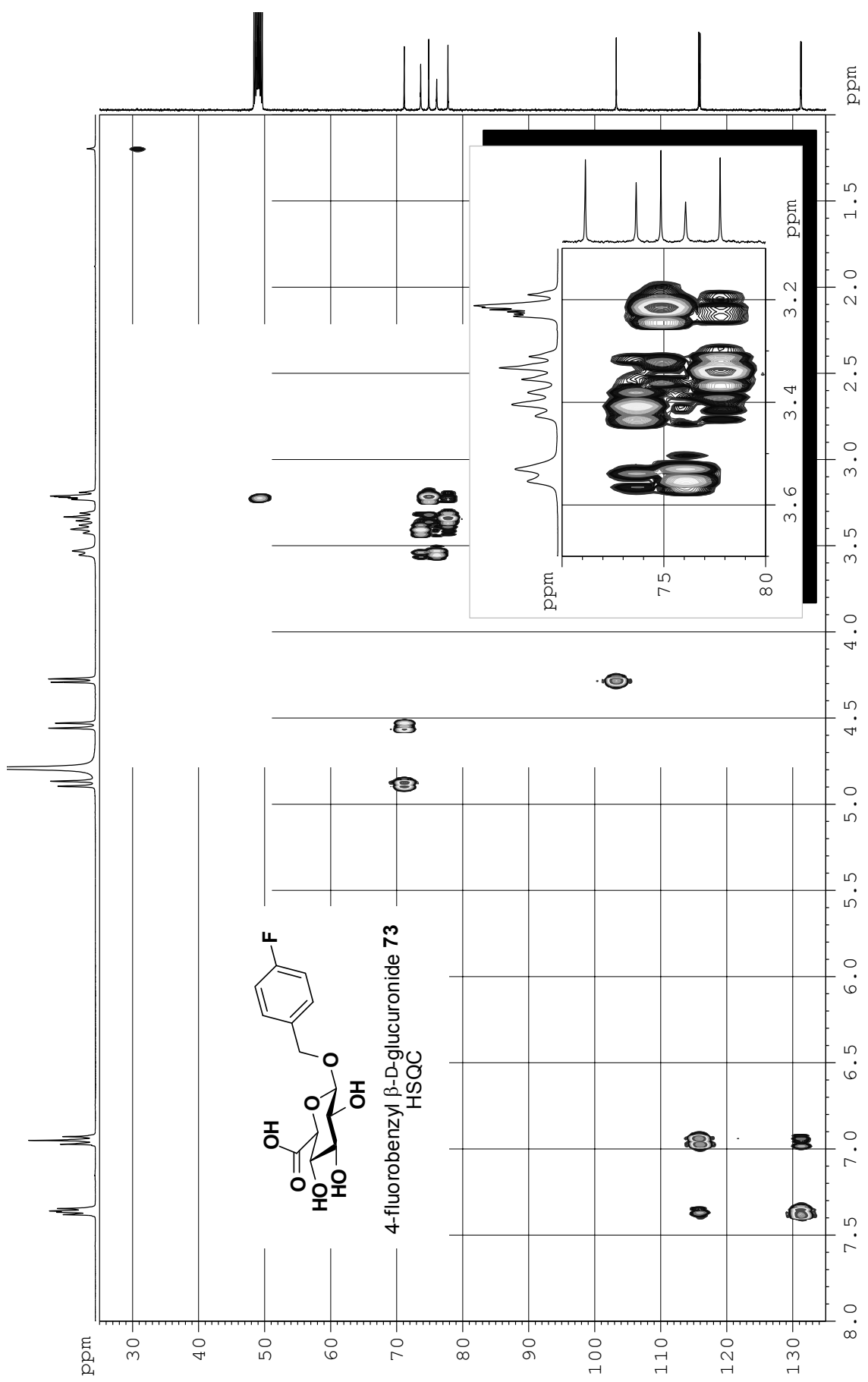


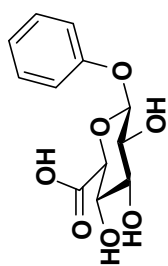


4-fluorobenzyl β -D-glucuronide **73**

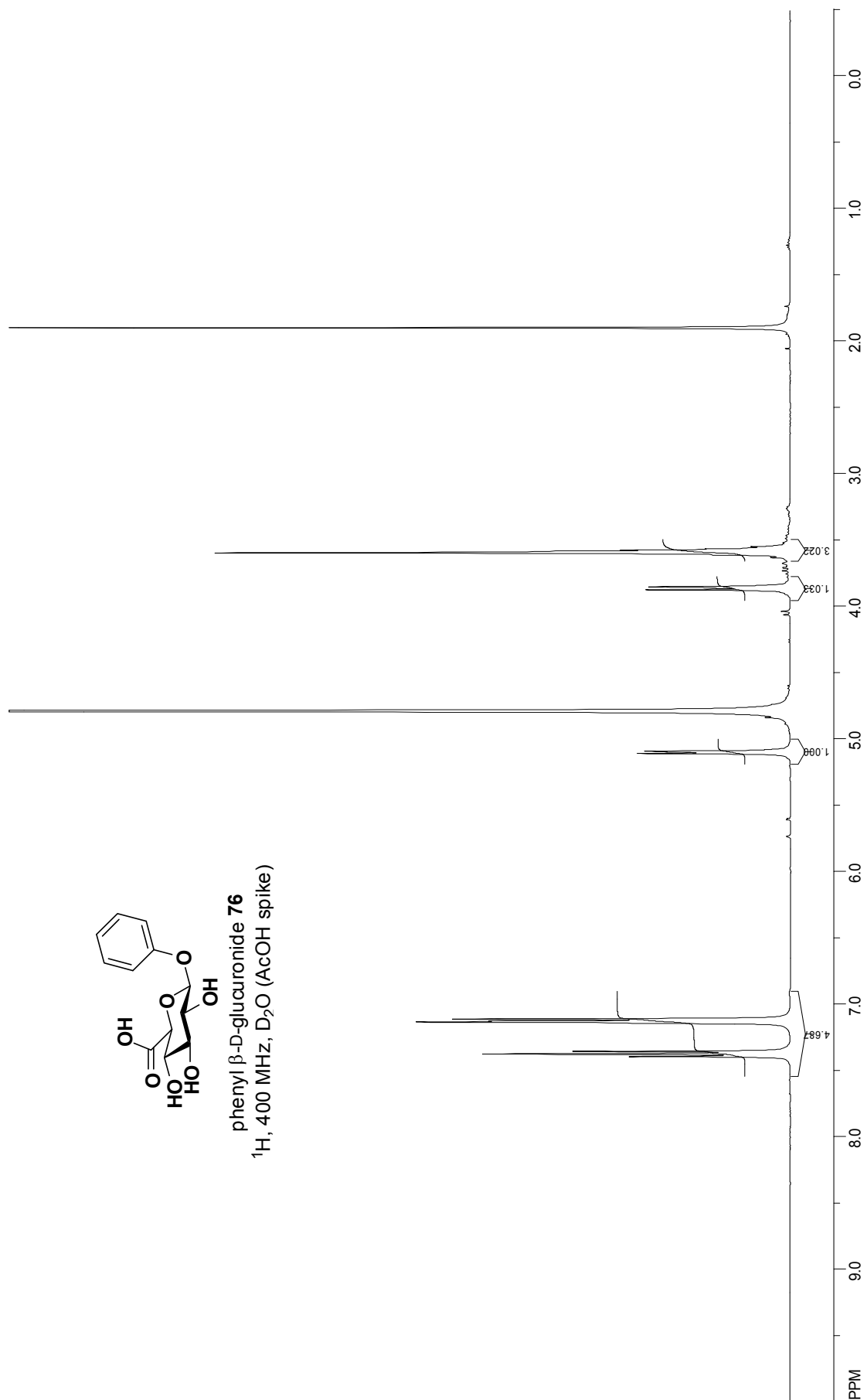
75 MHz, MeOD

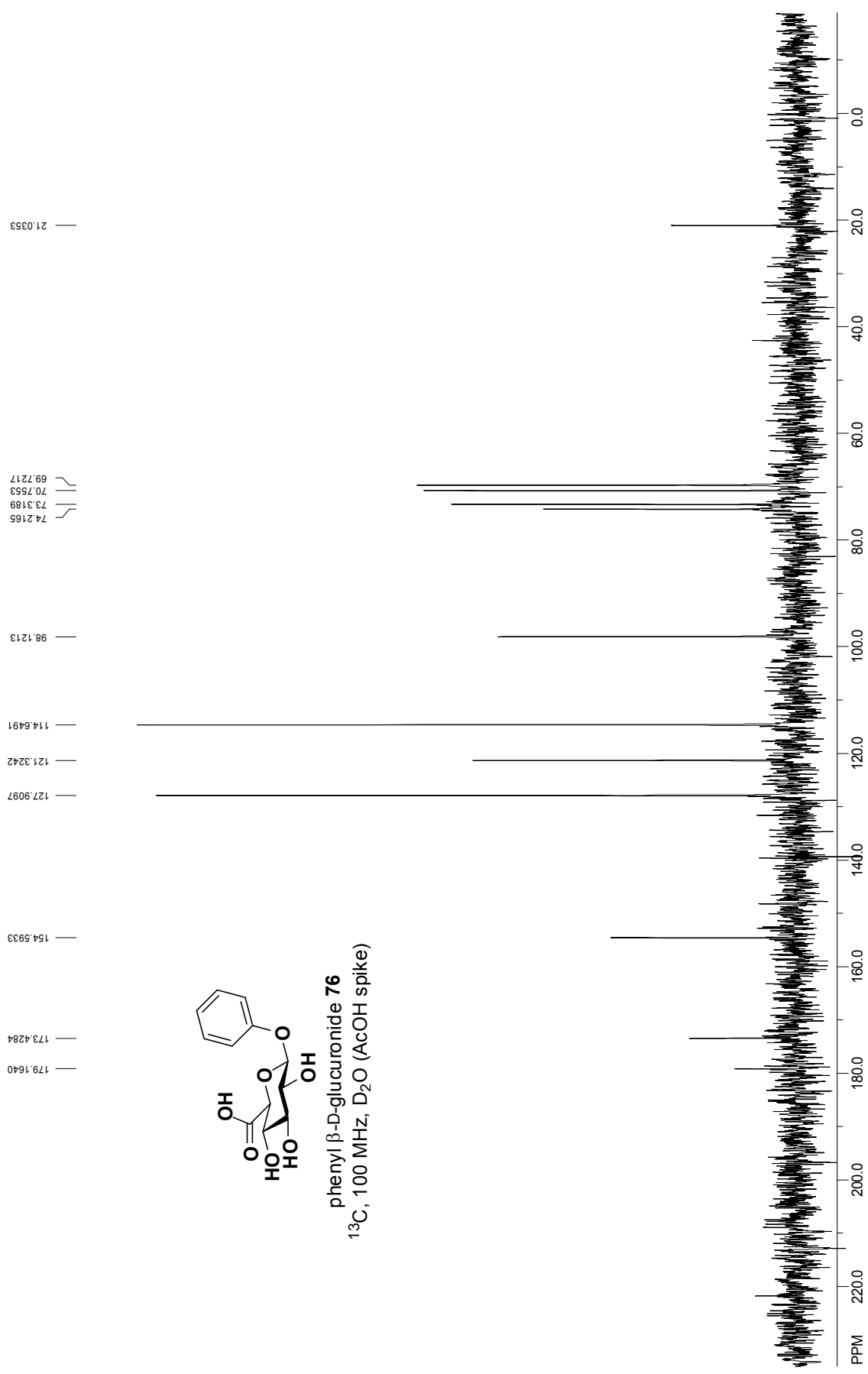
a) ^{13}C , b) DEPT

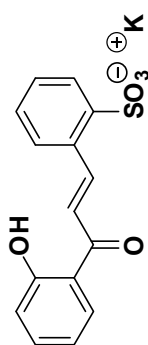




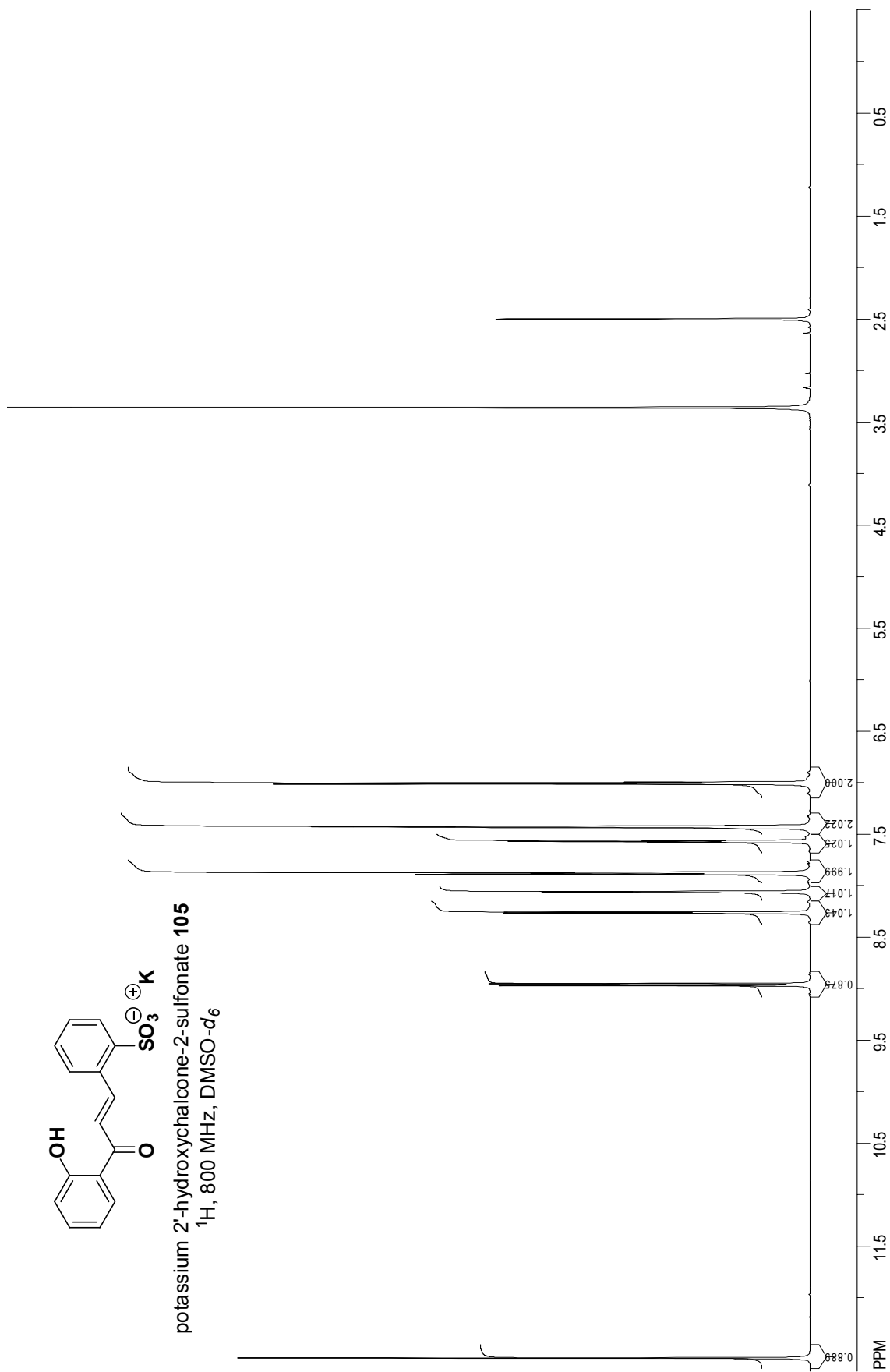
phenyl β -D-glucuronide **76**
 ^1H , 400 MHz, D_2O (AcOH spike)

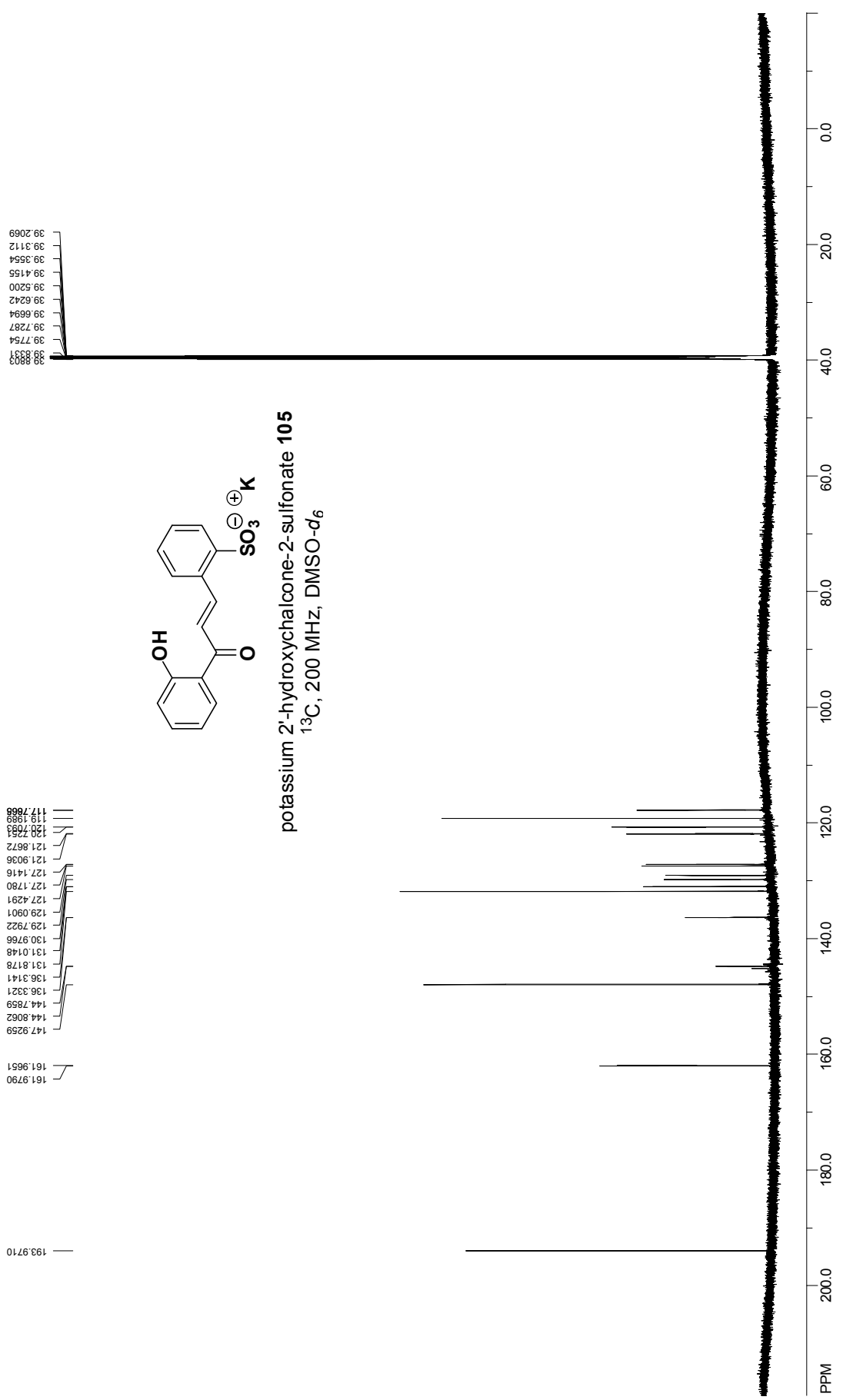


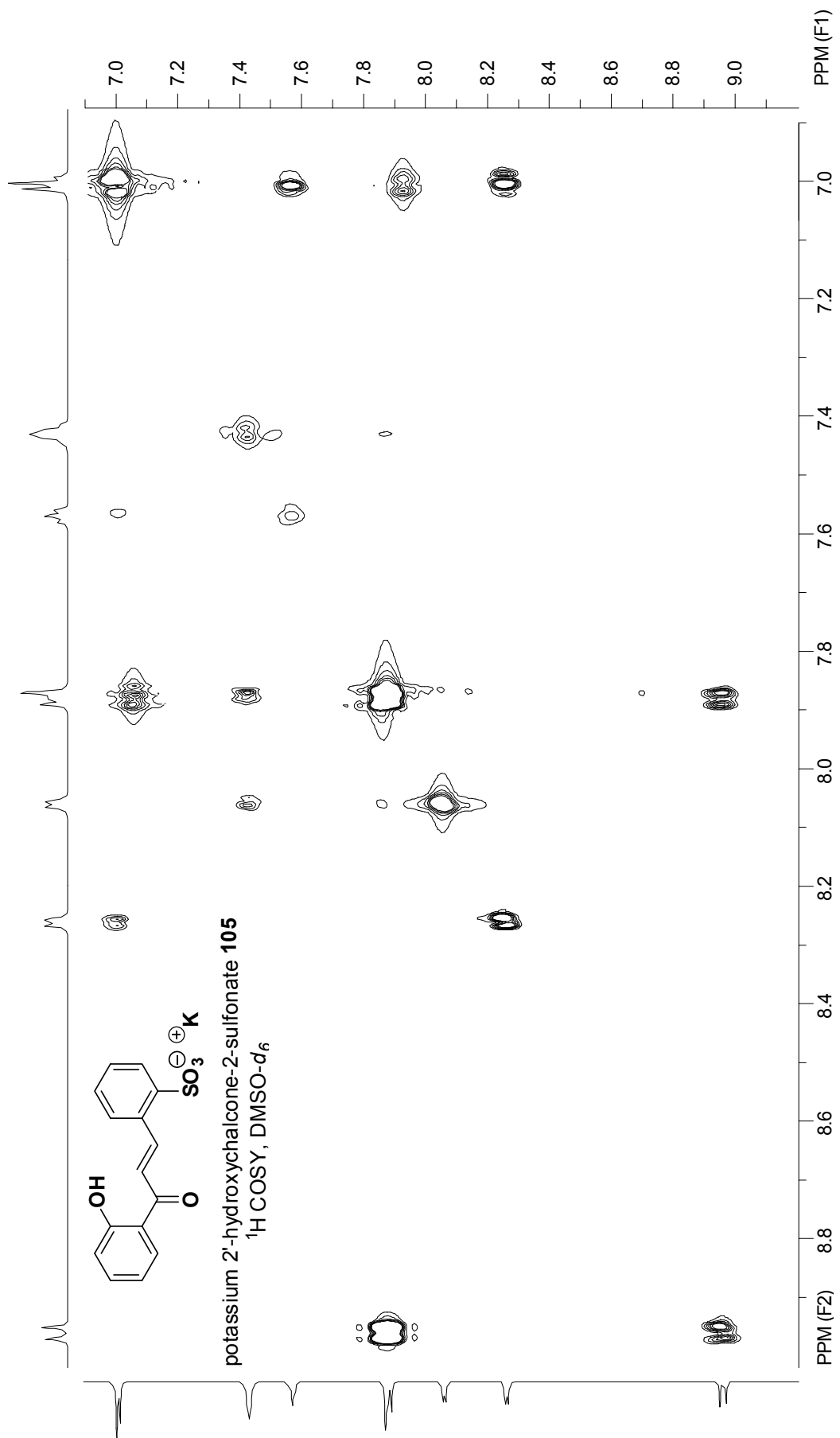


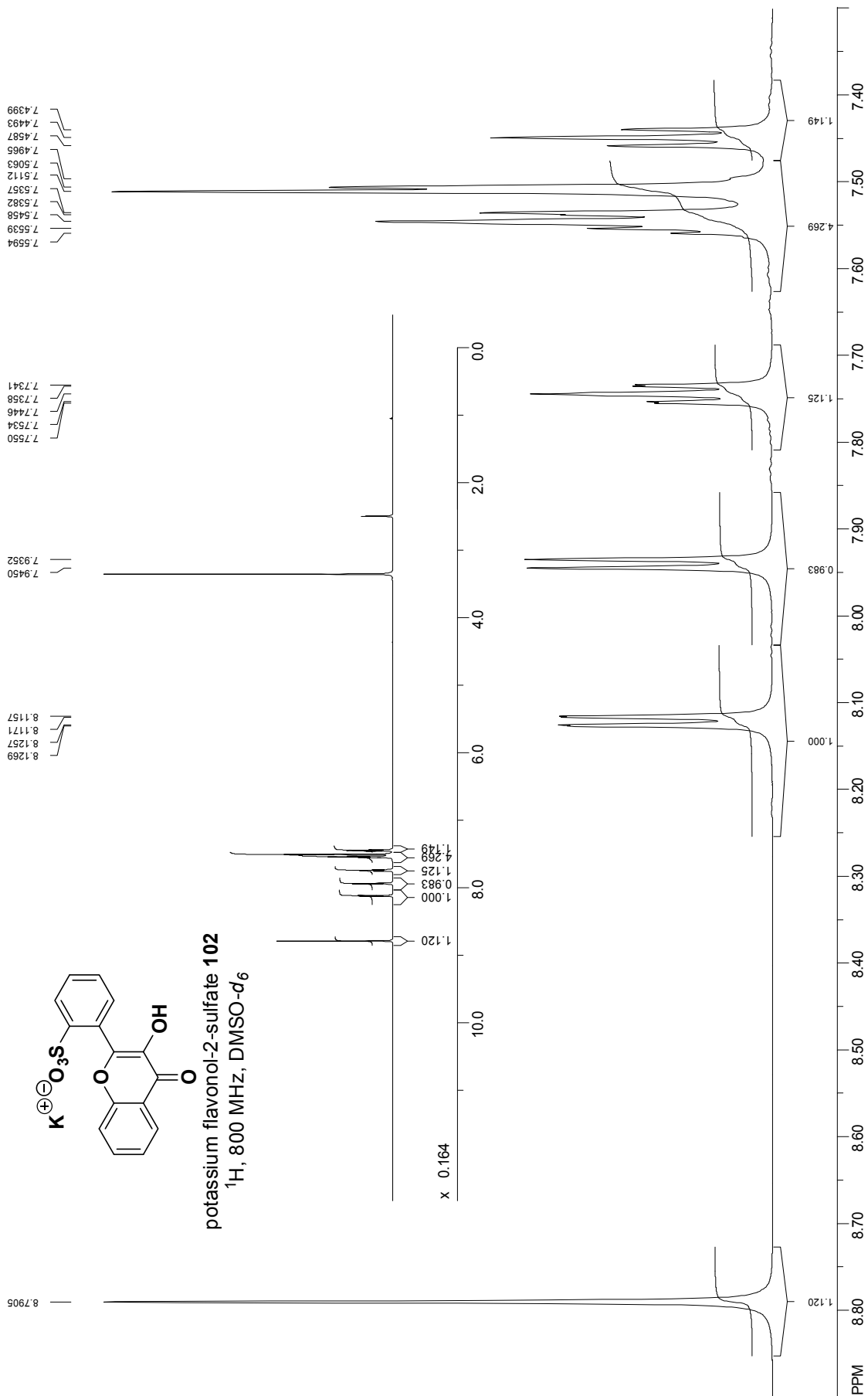


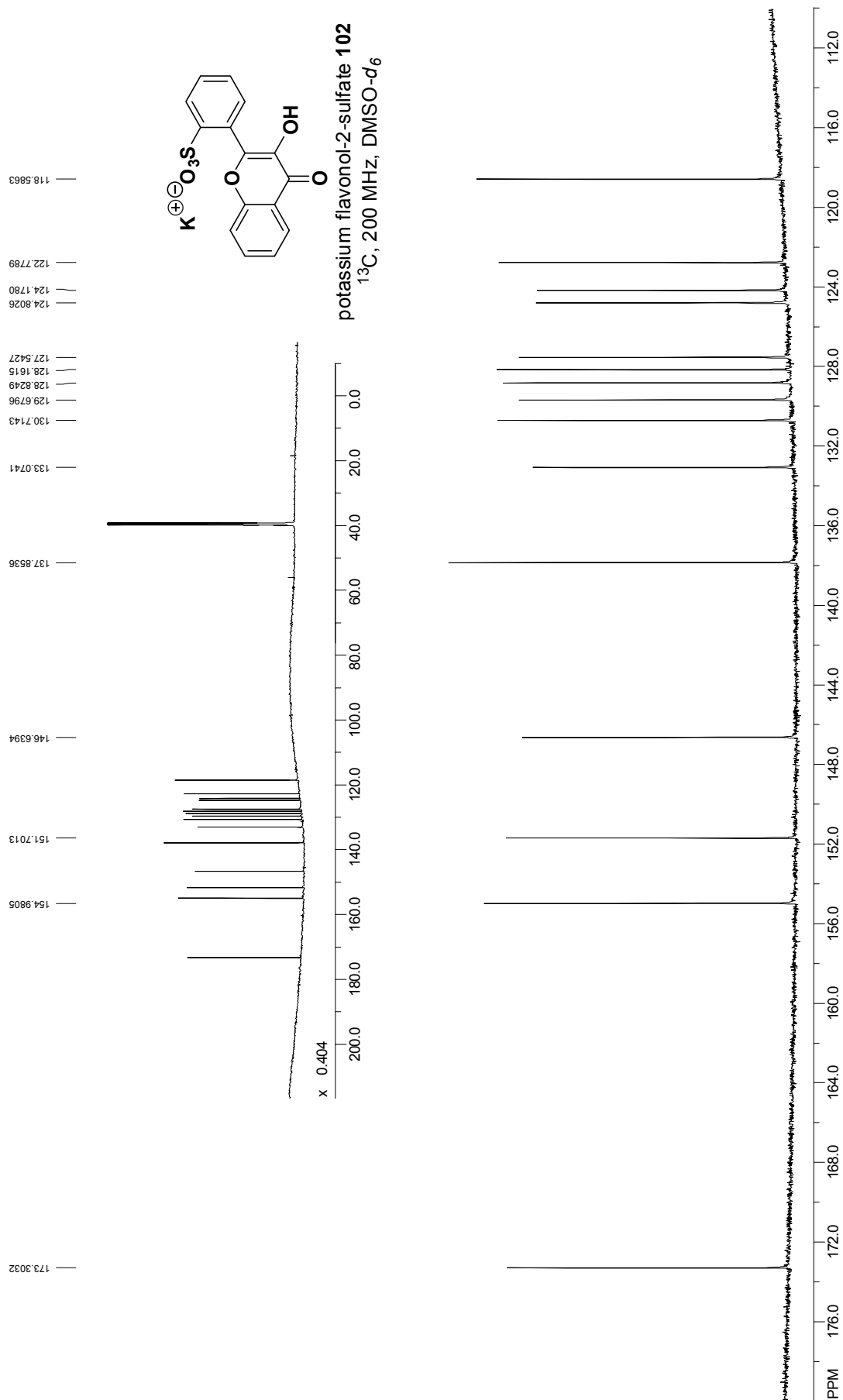
potassium 2'-hydroxychalcone-2-sulfonate **105**
¹H, 800 MHz, DMSO-d₆

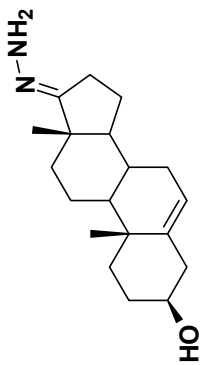




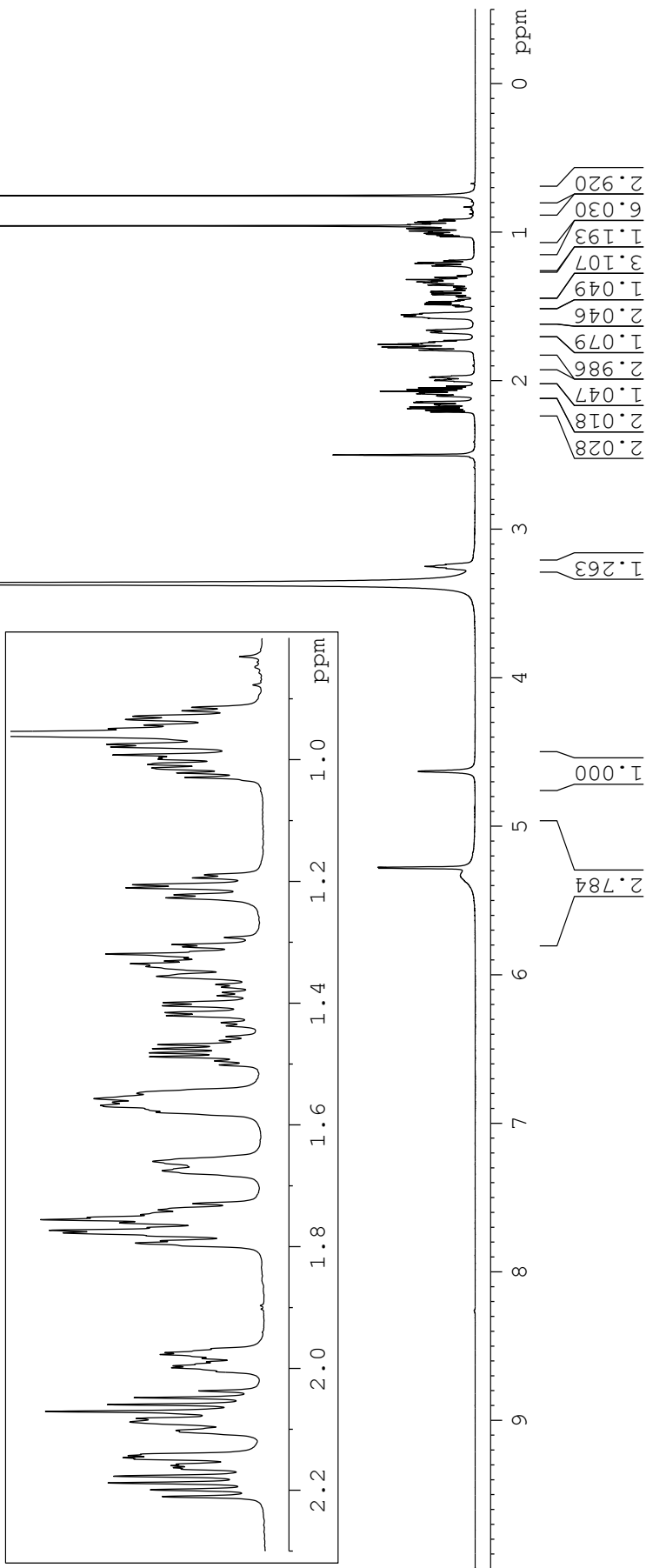


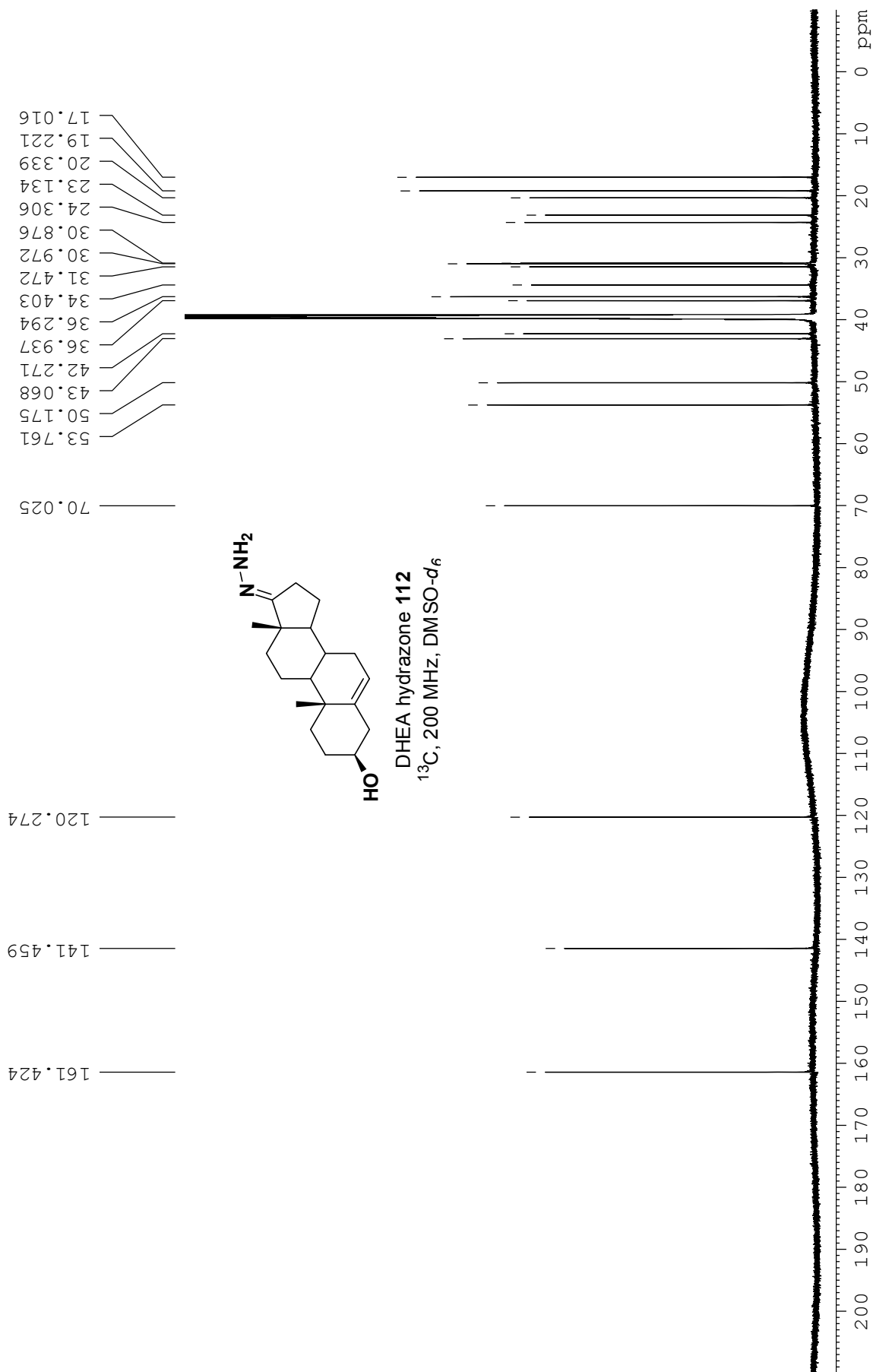


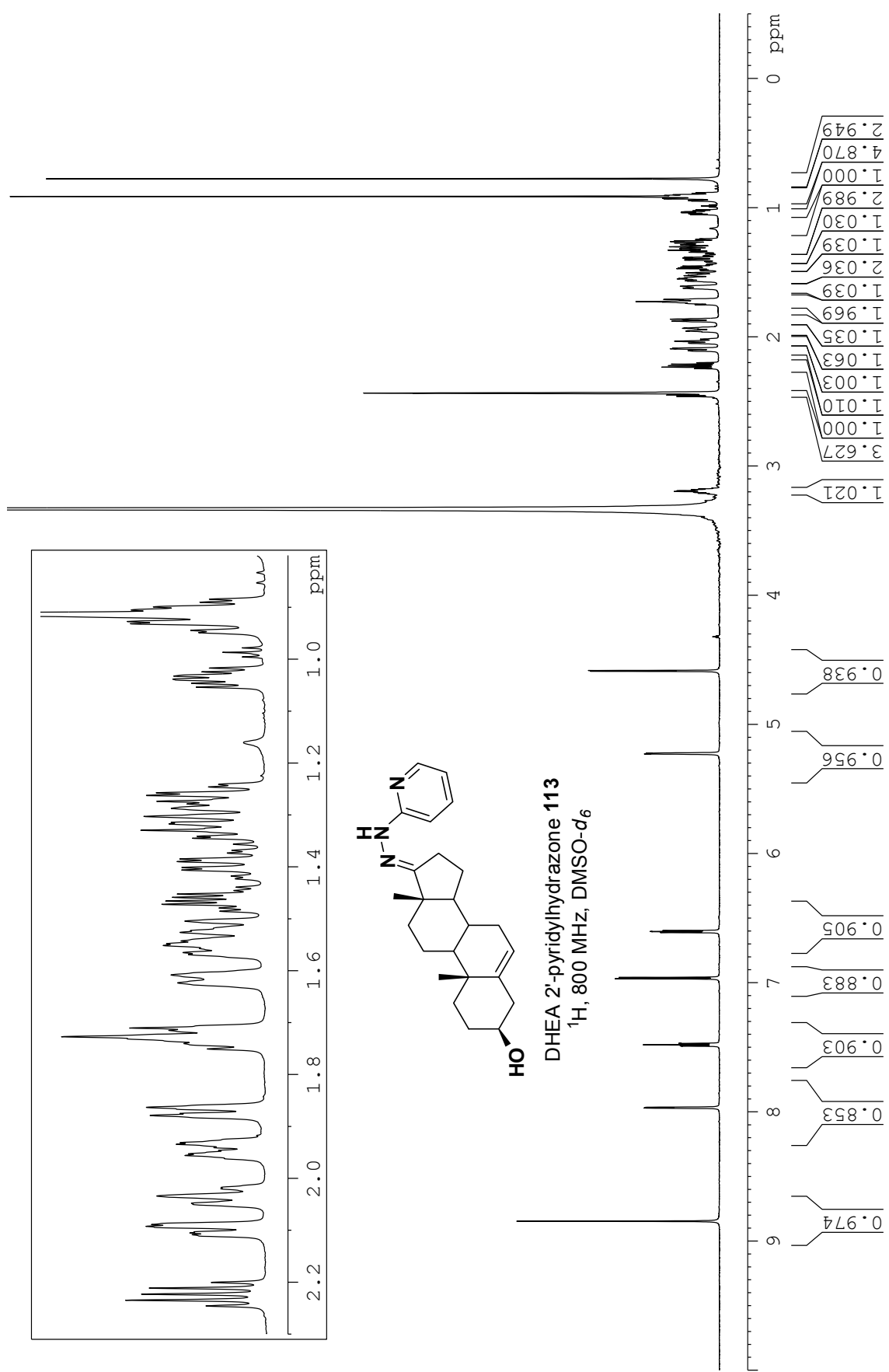


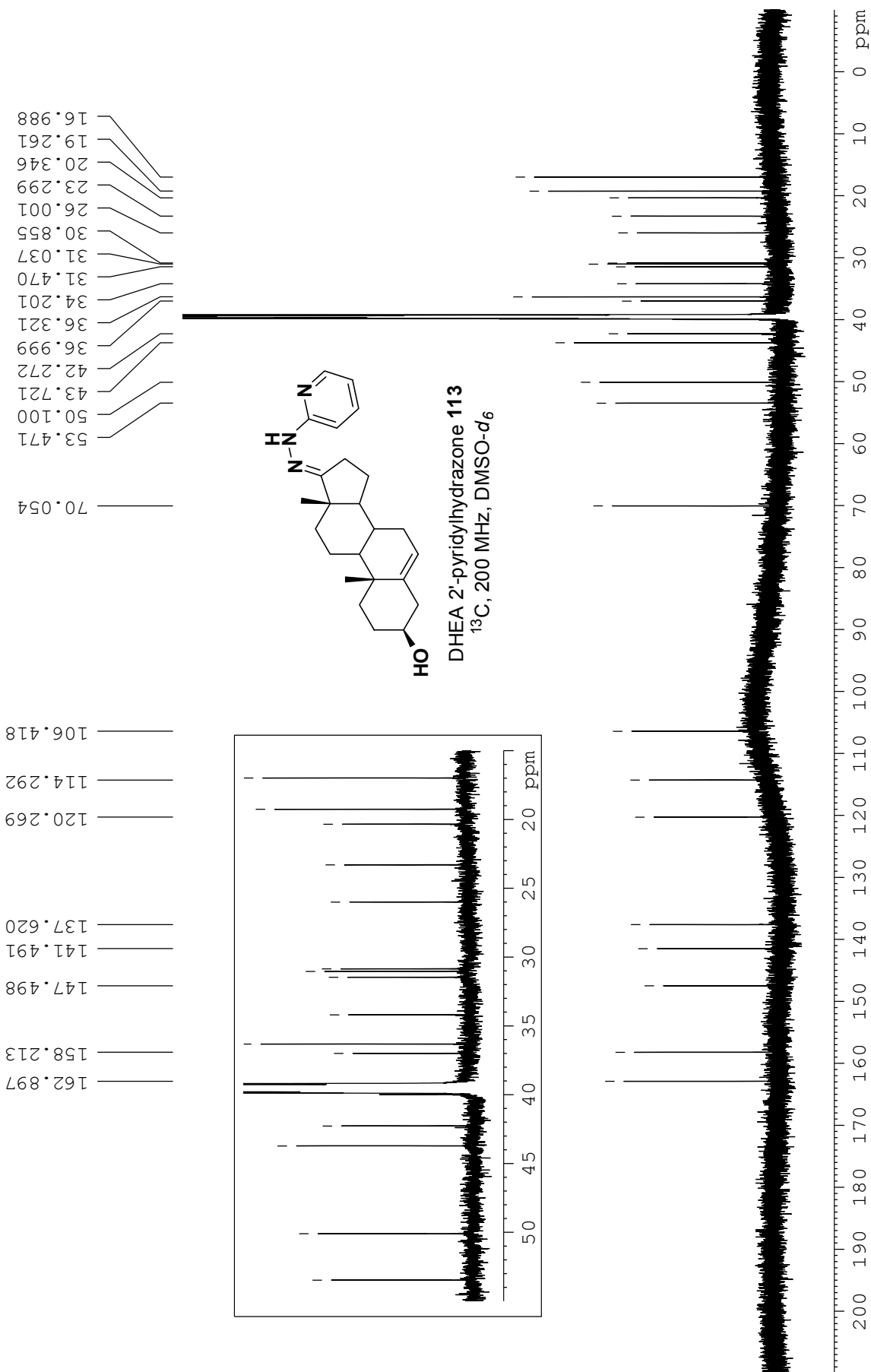


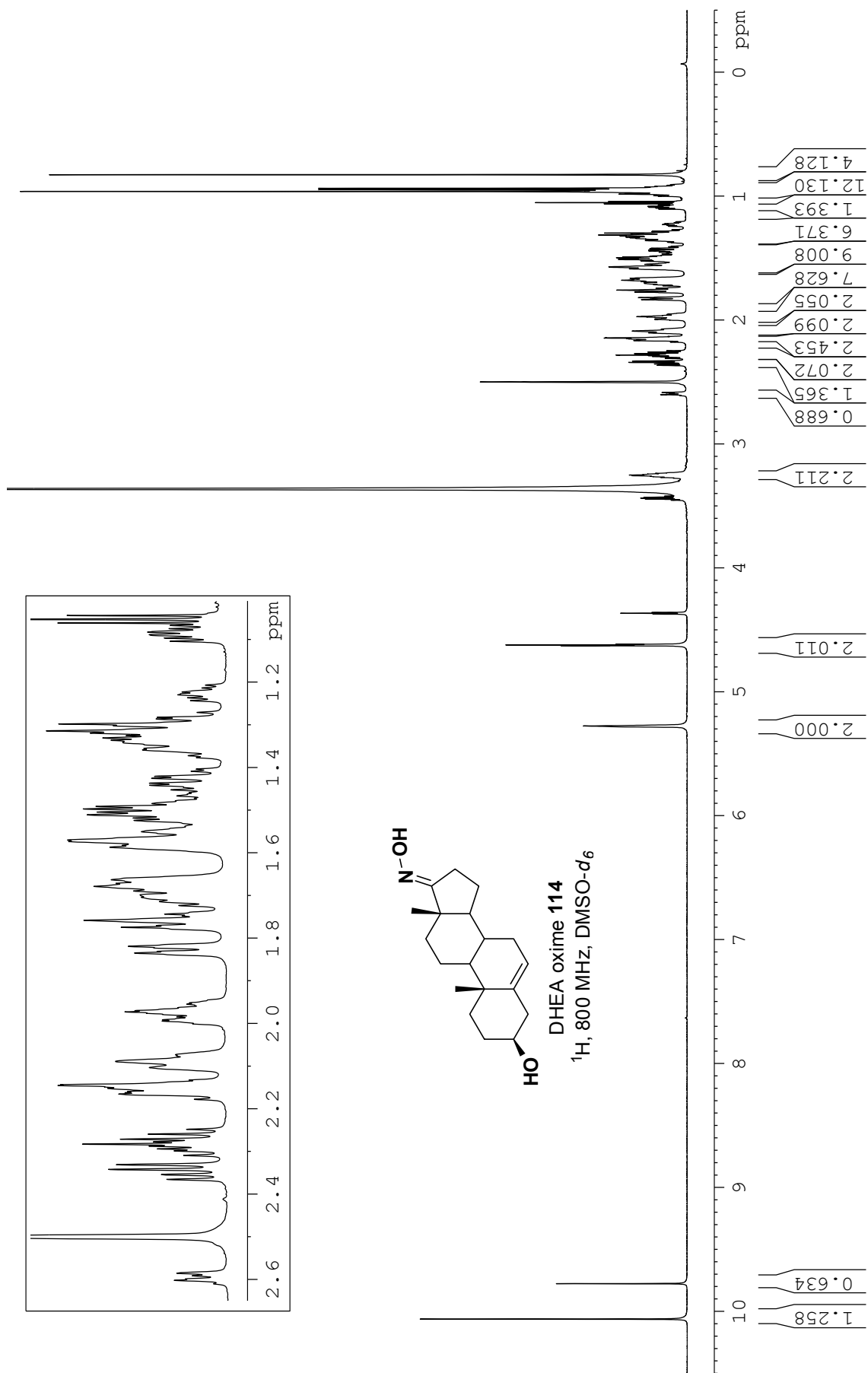
DHEA hydrazone 112
¹H, 800 MHz, DMSO-d₆

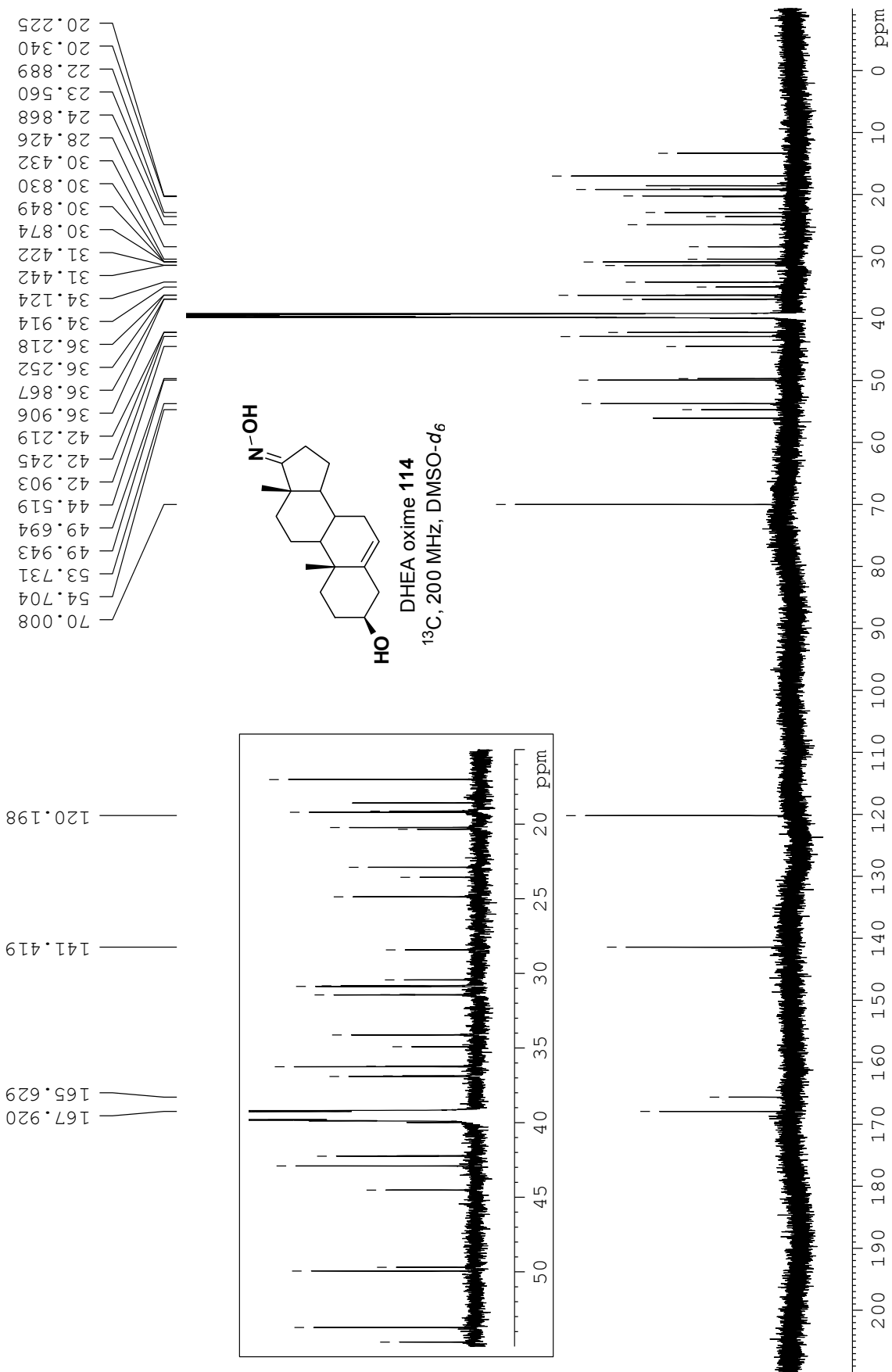


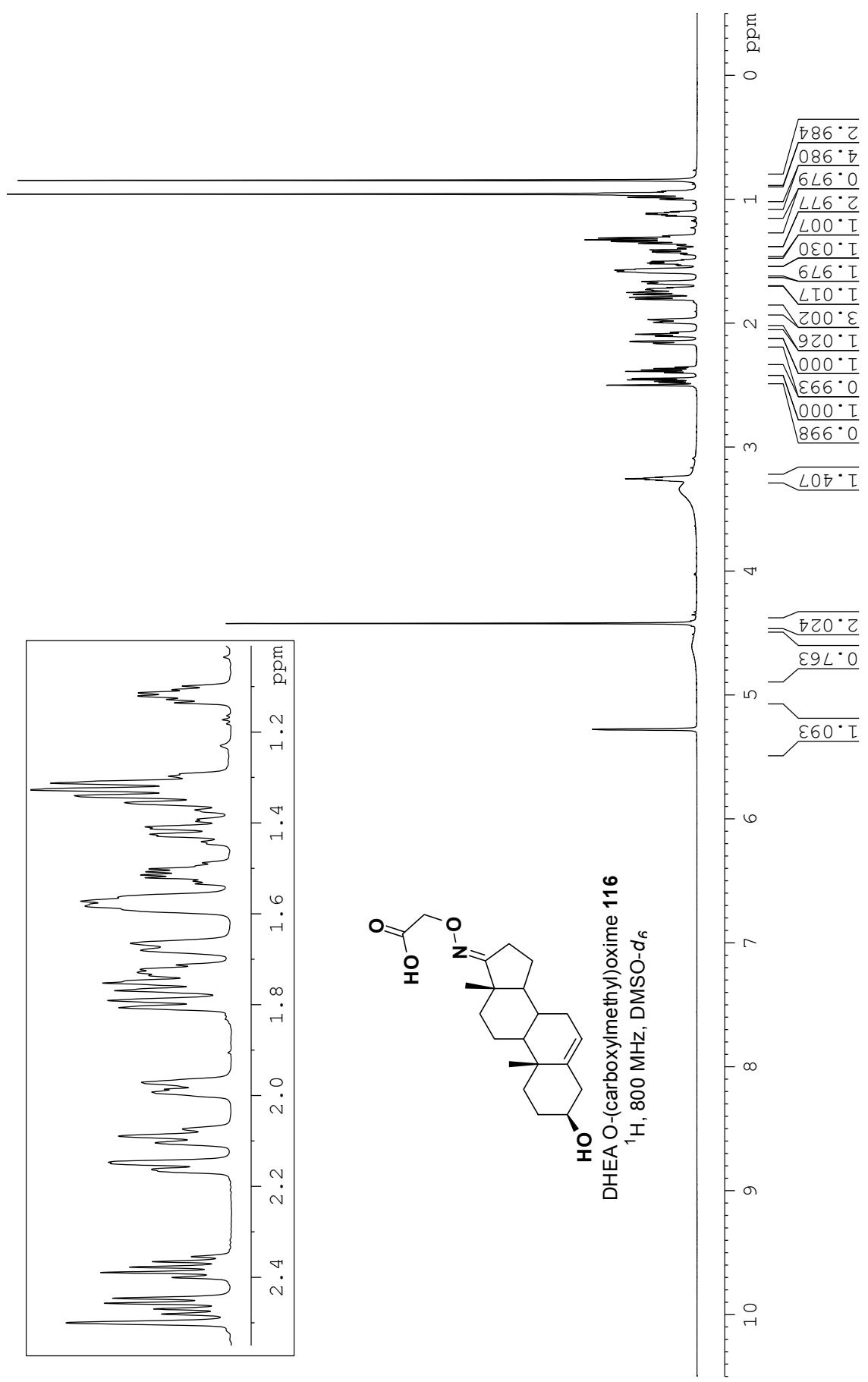


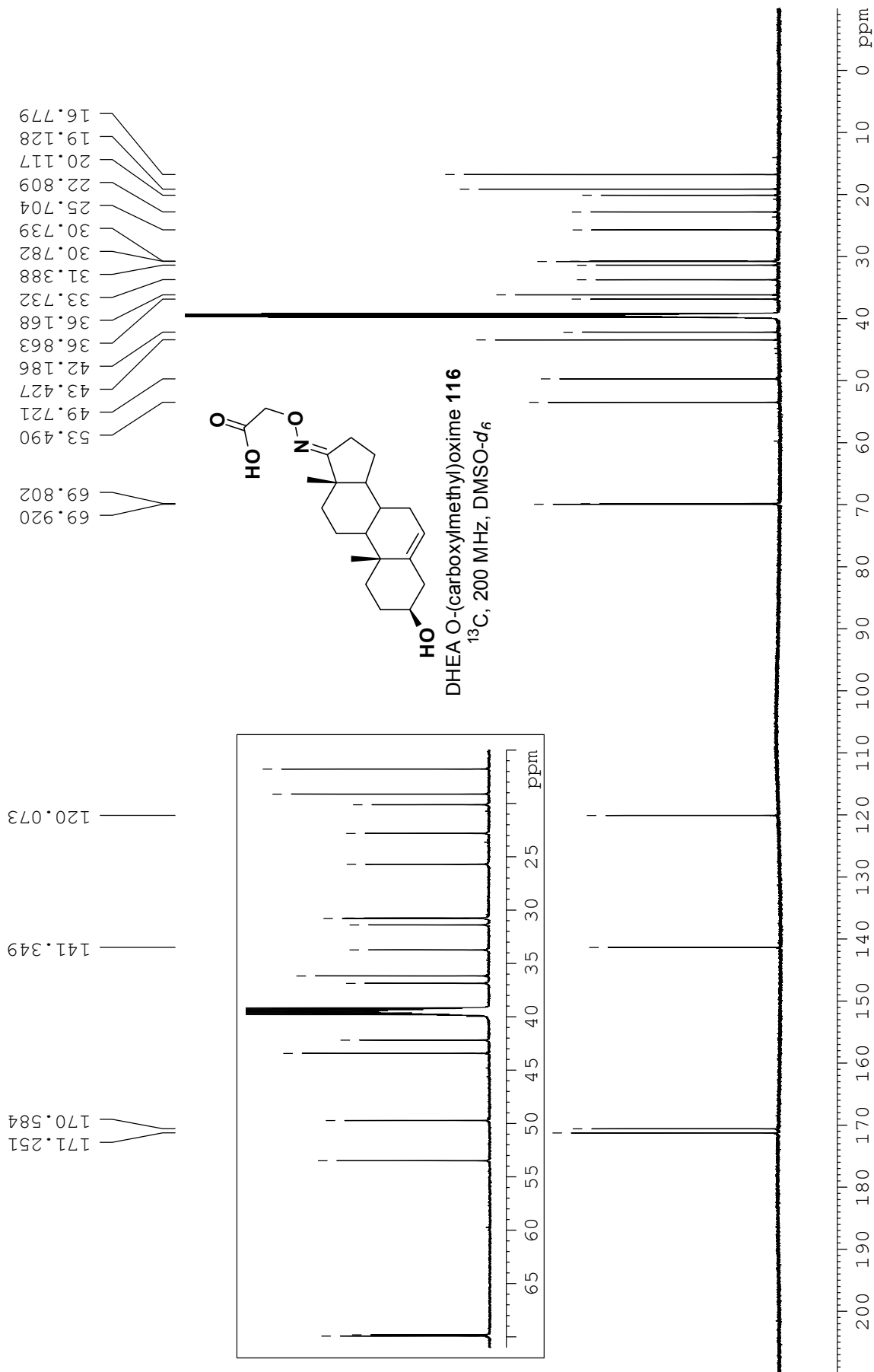


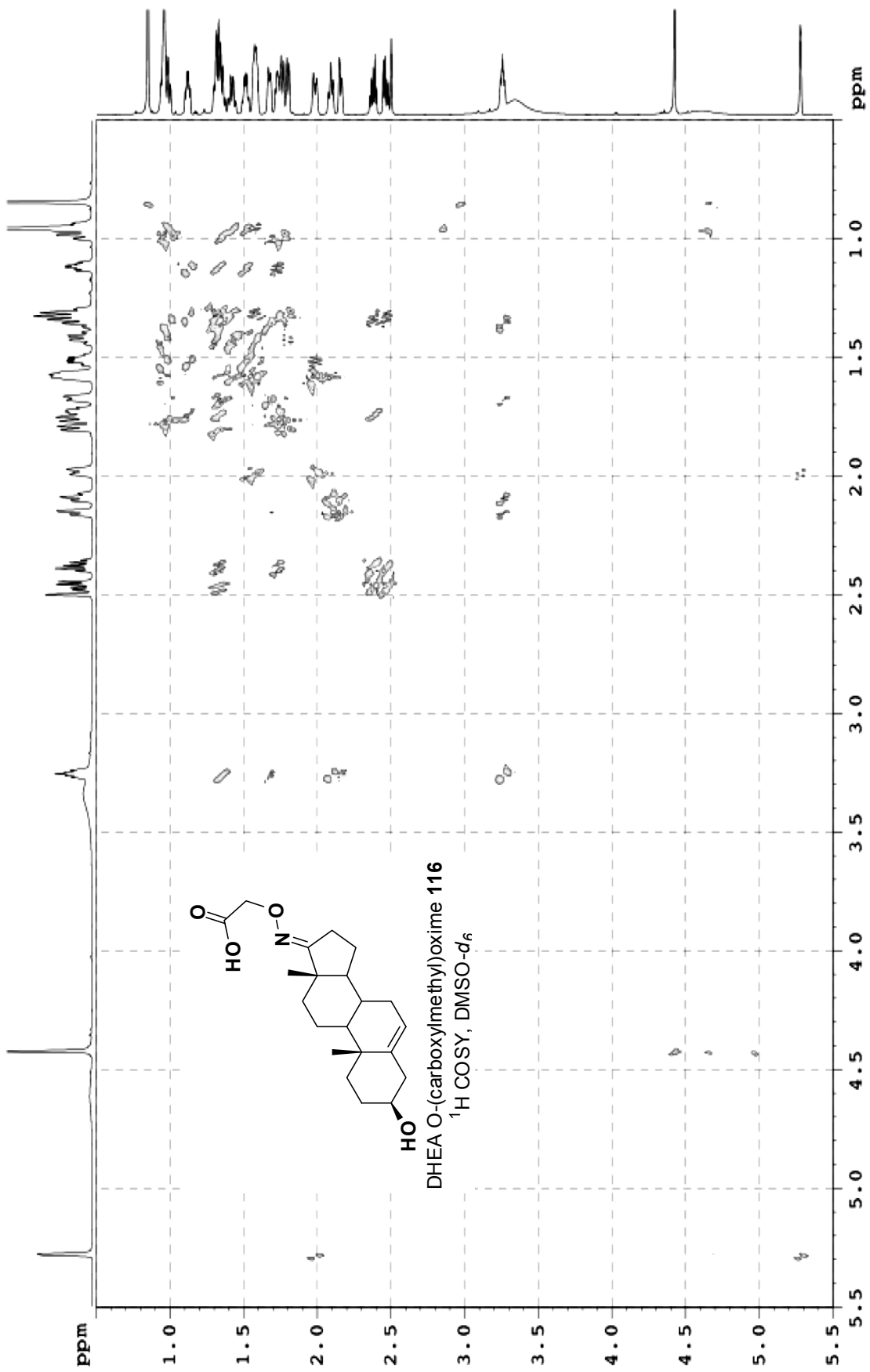


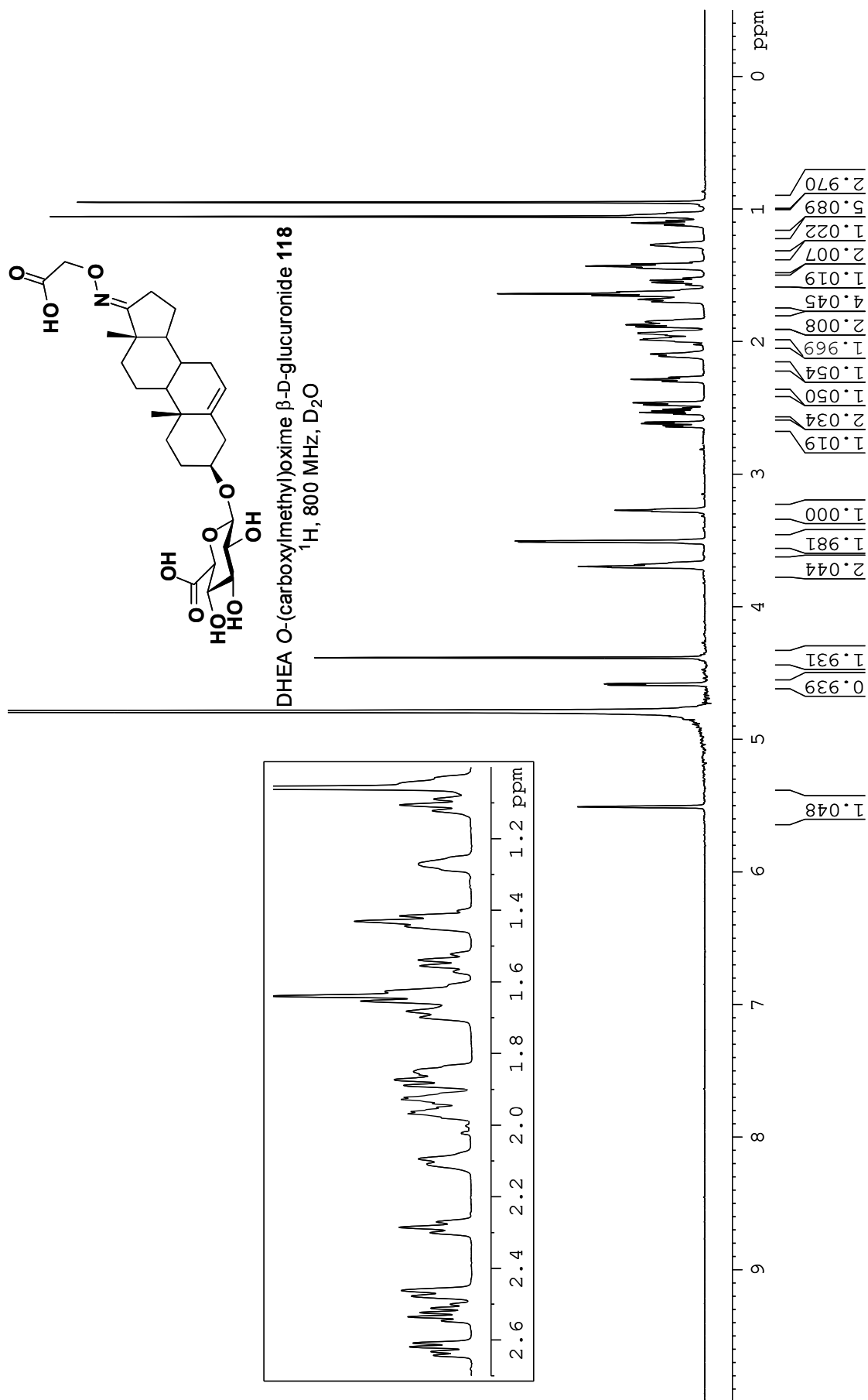


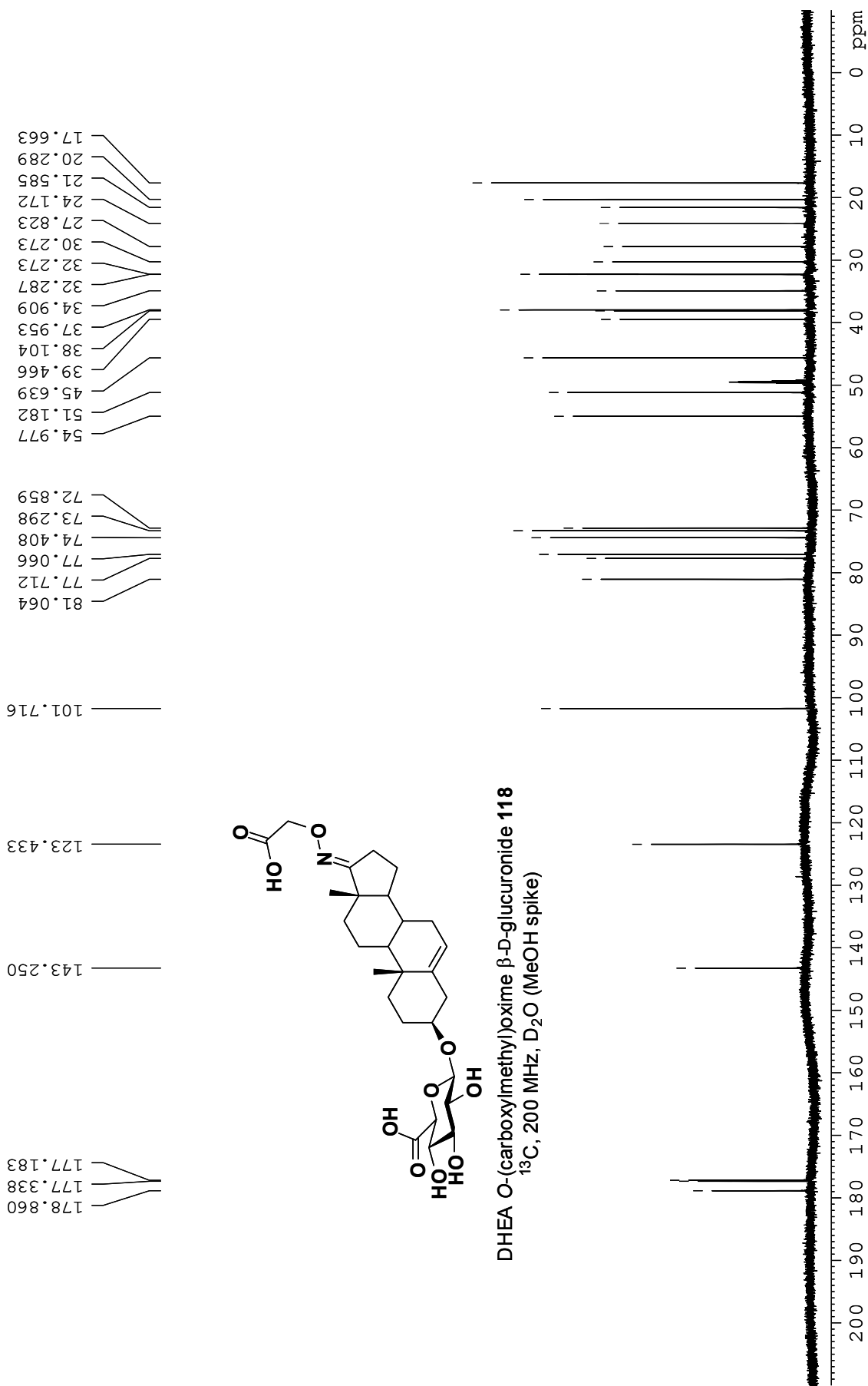


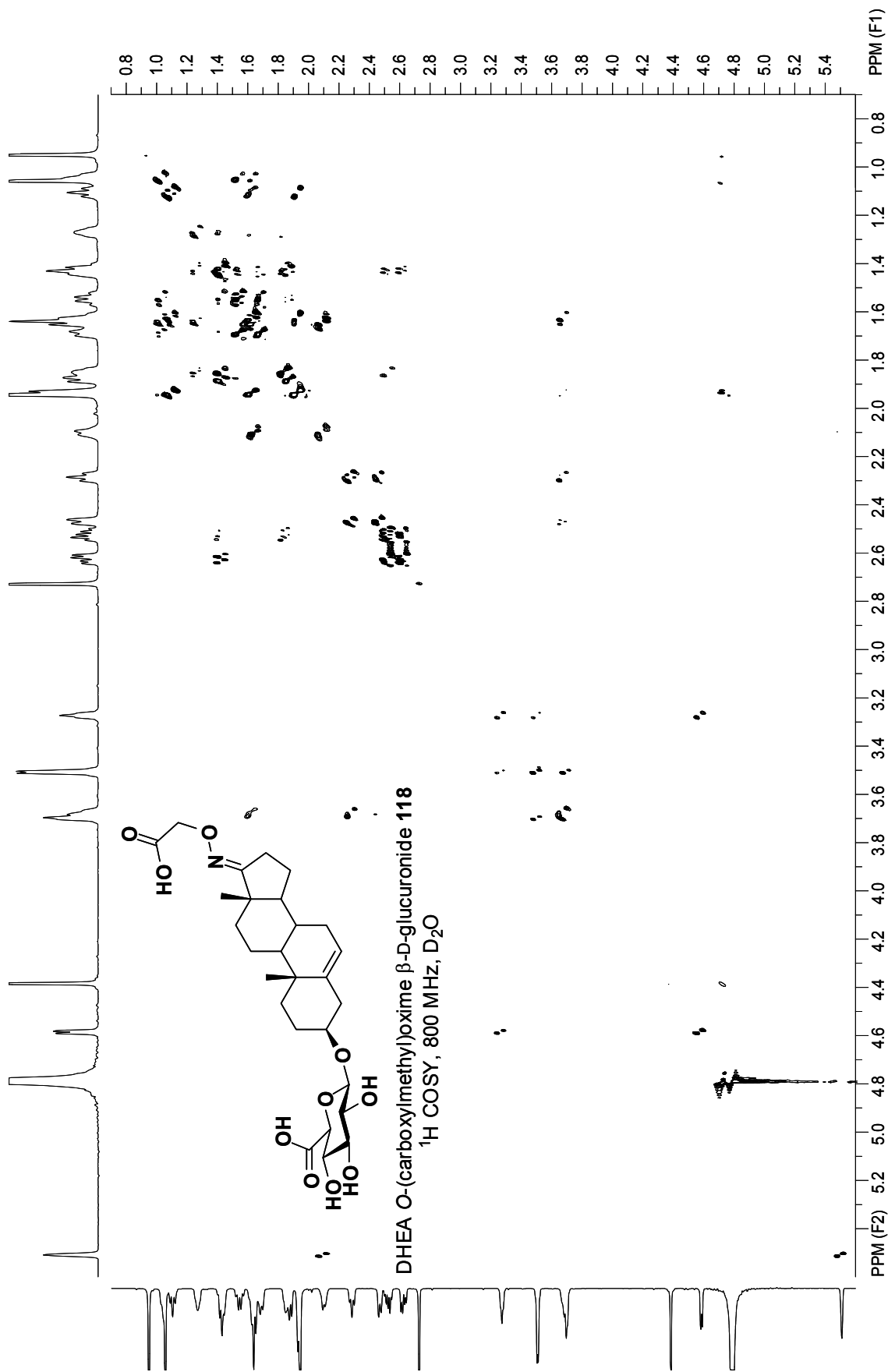


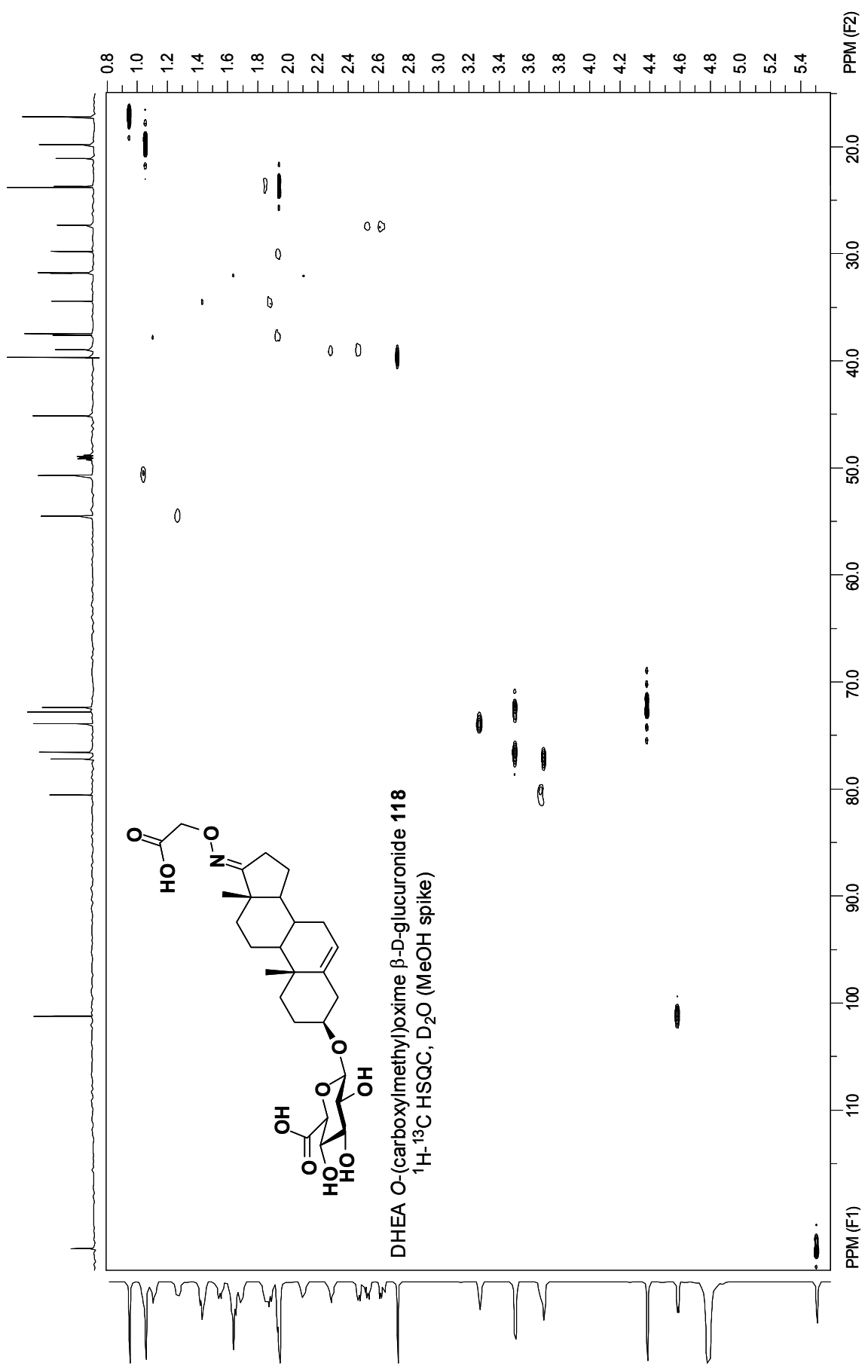


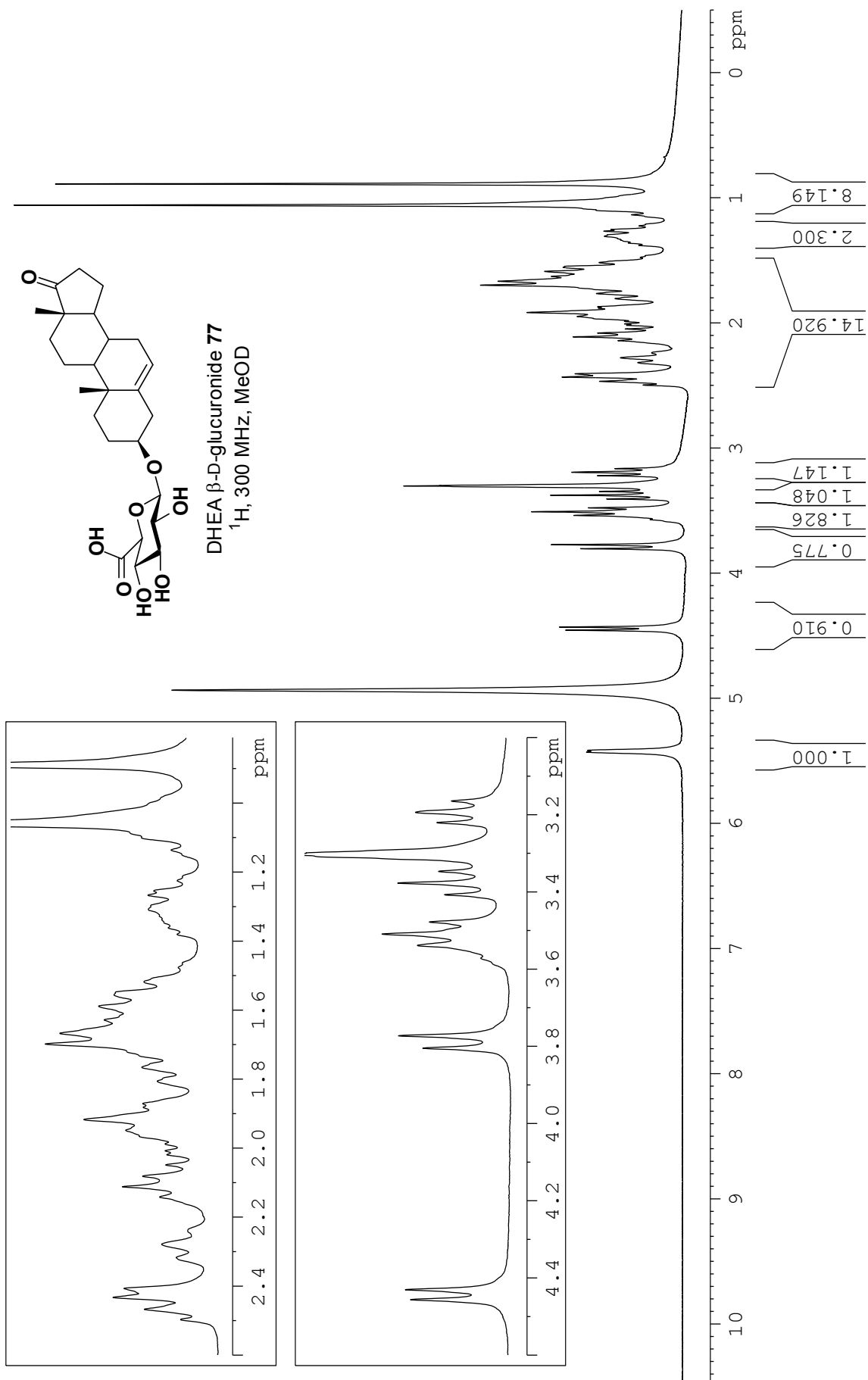




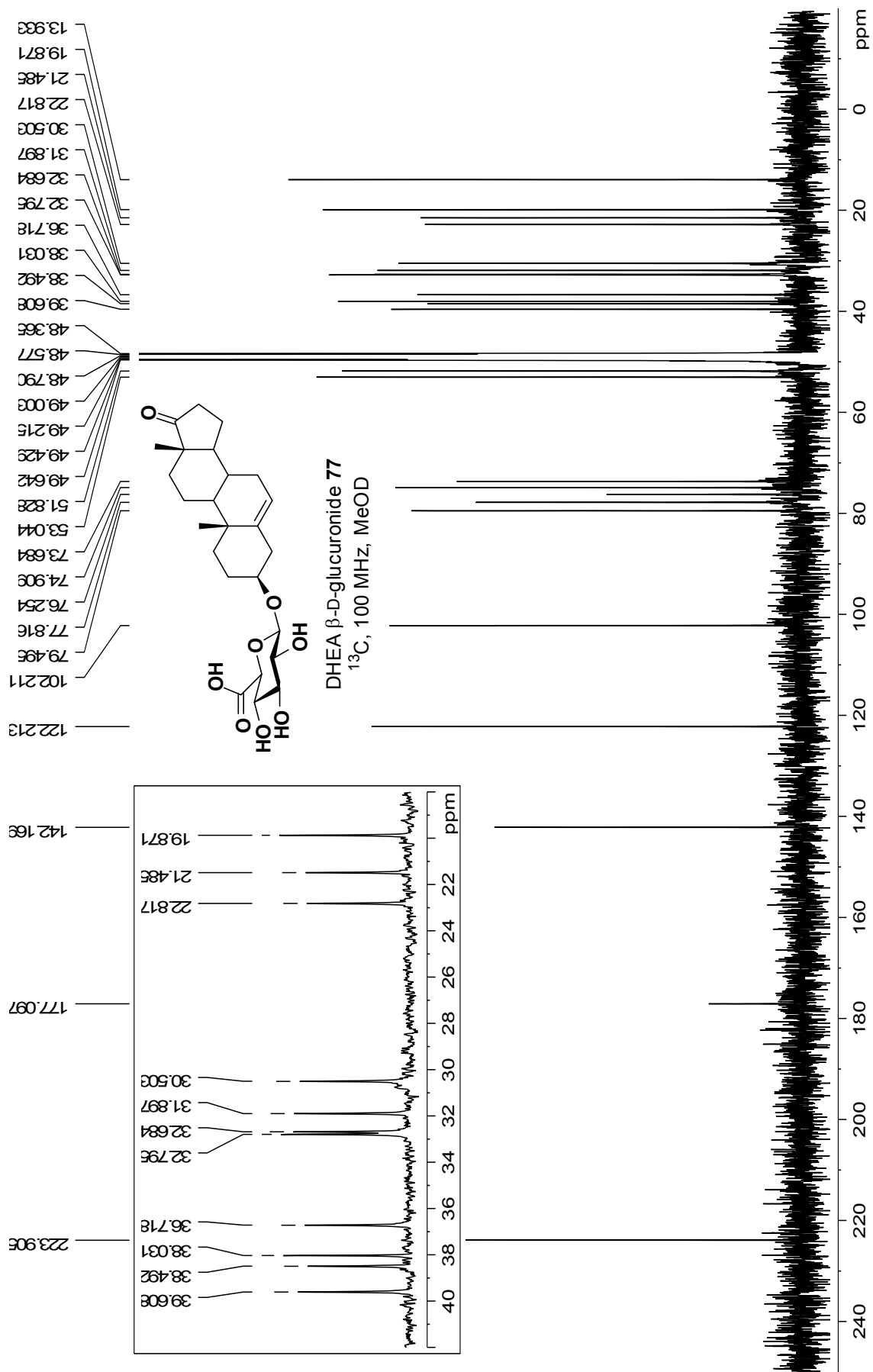


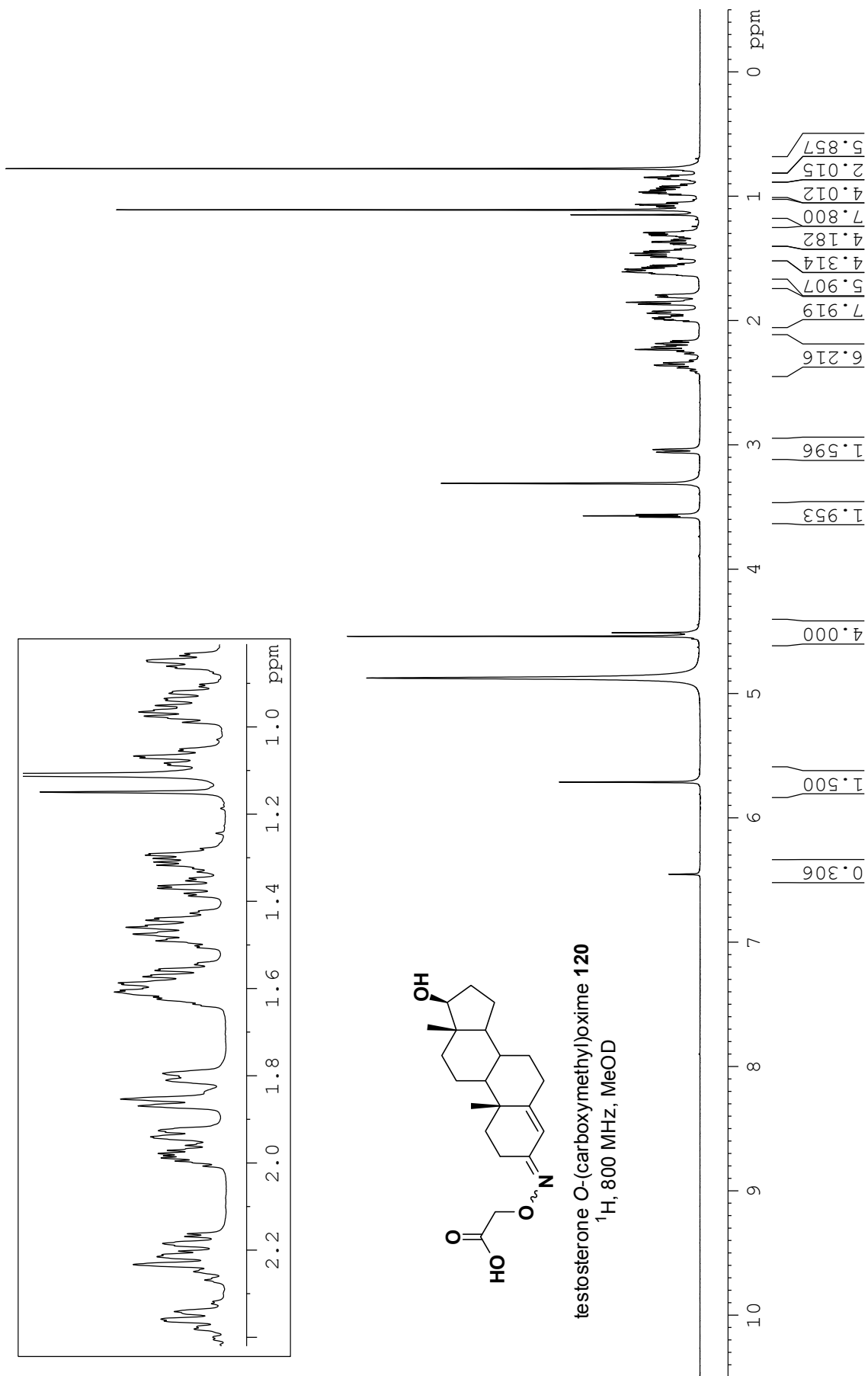


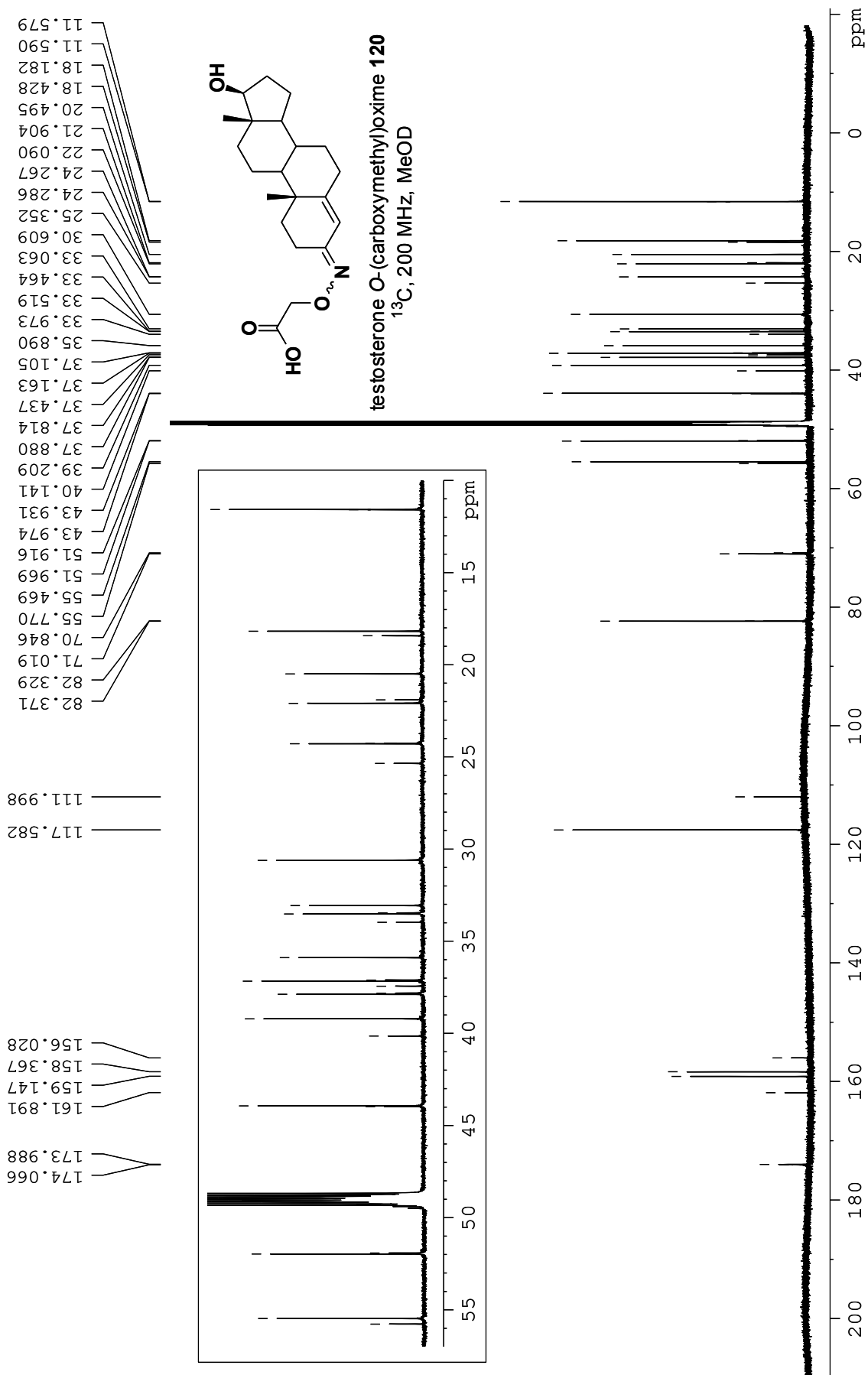


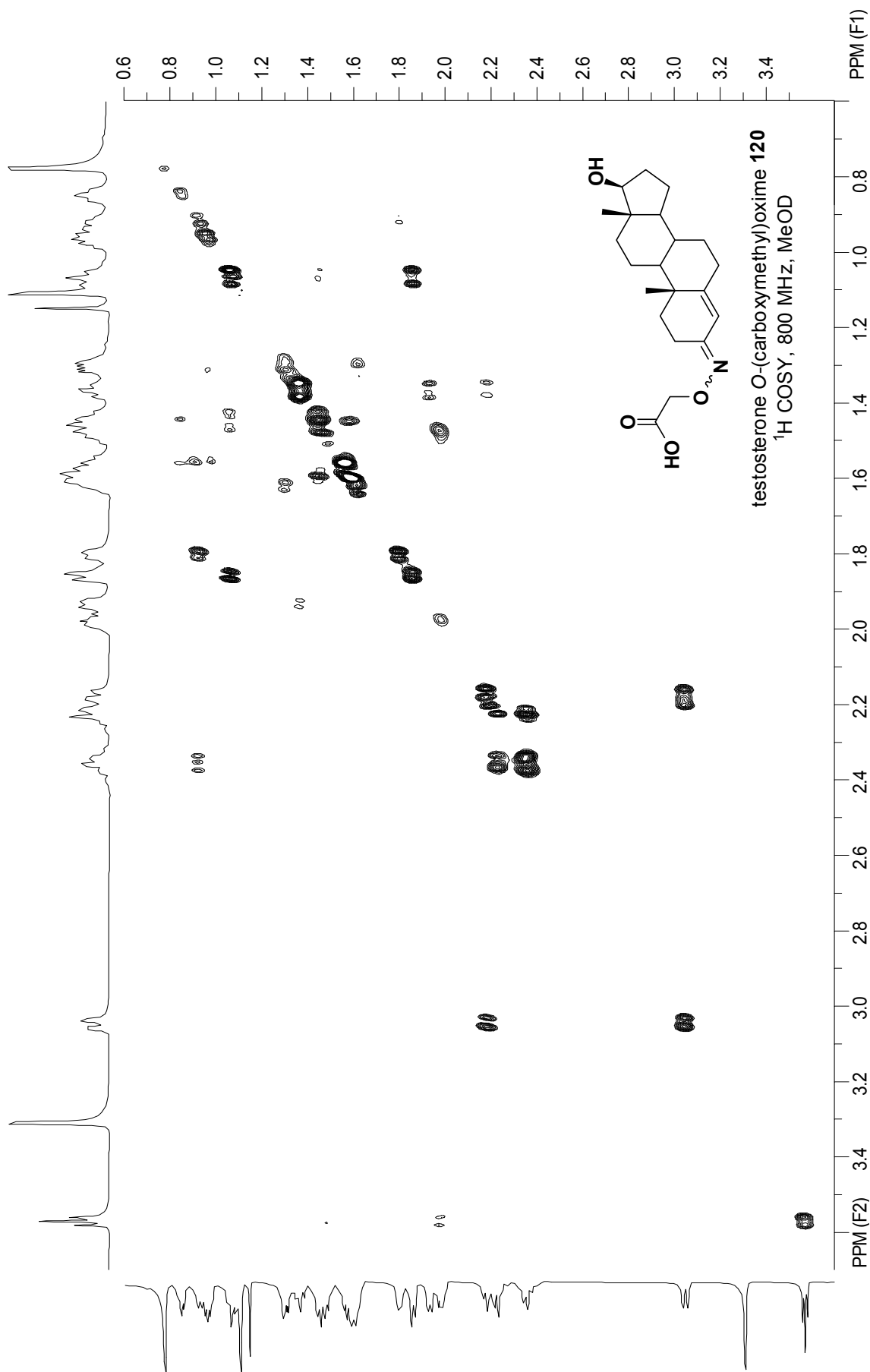


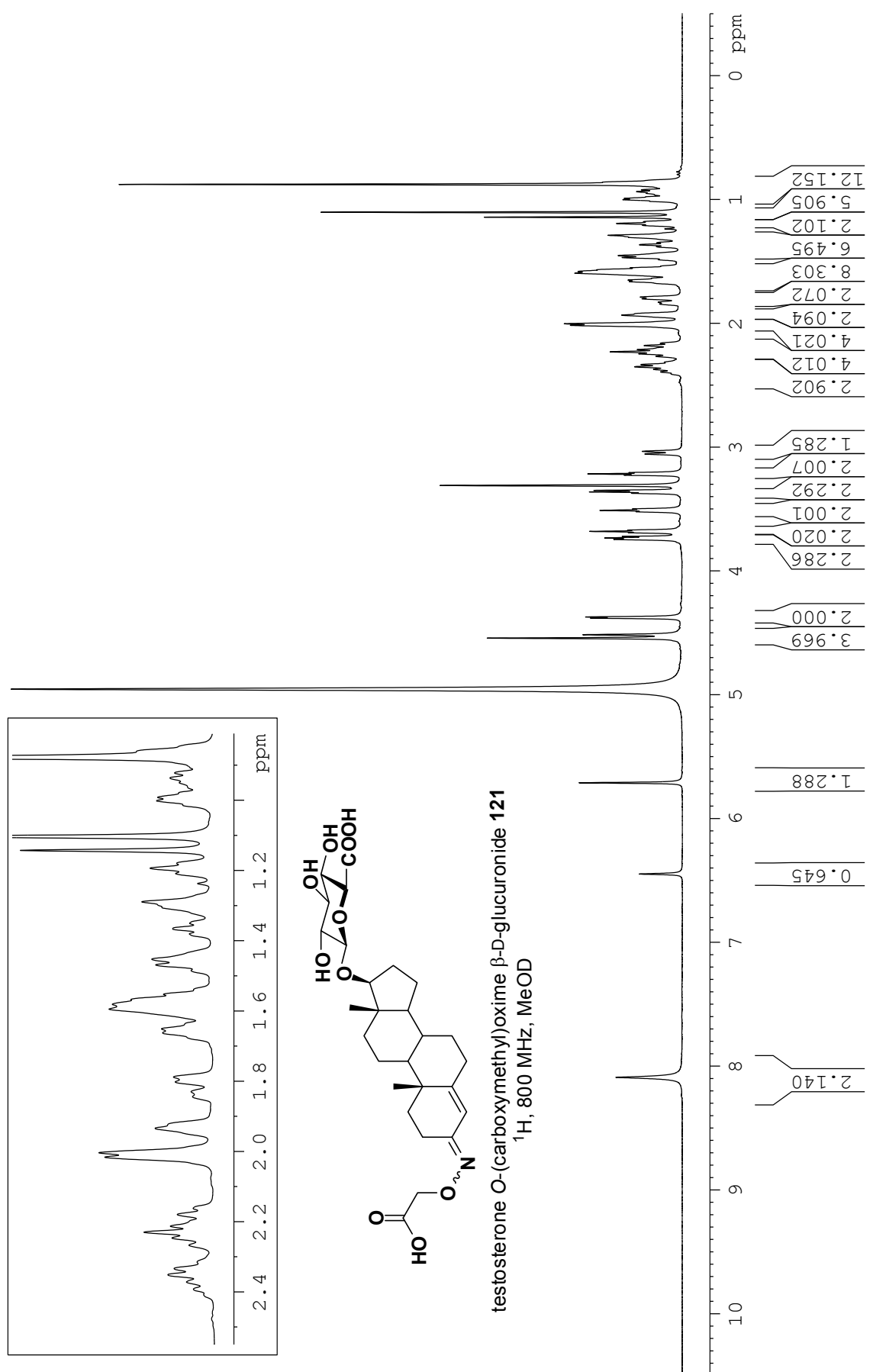
NMR Spectra

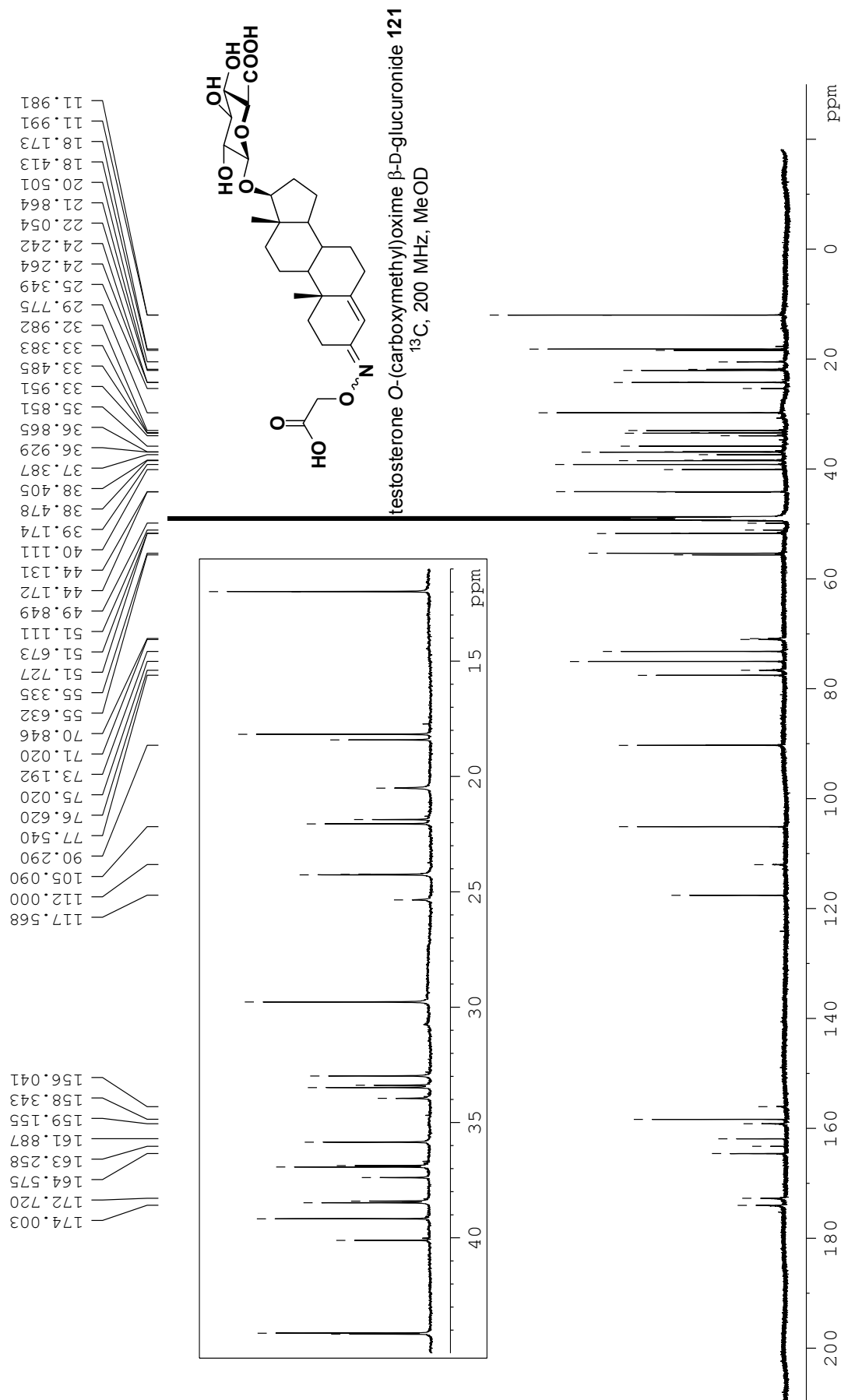


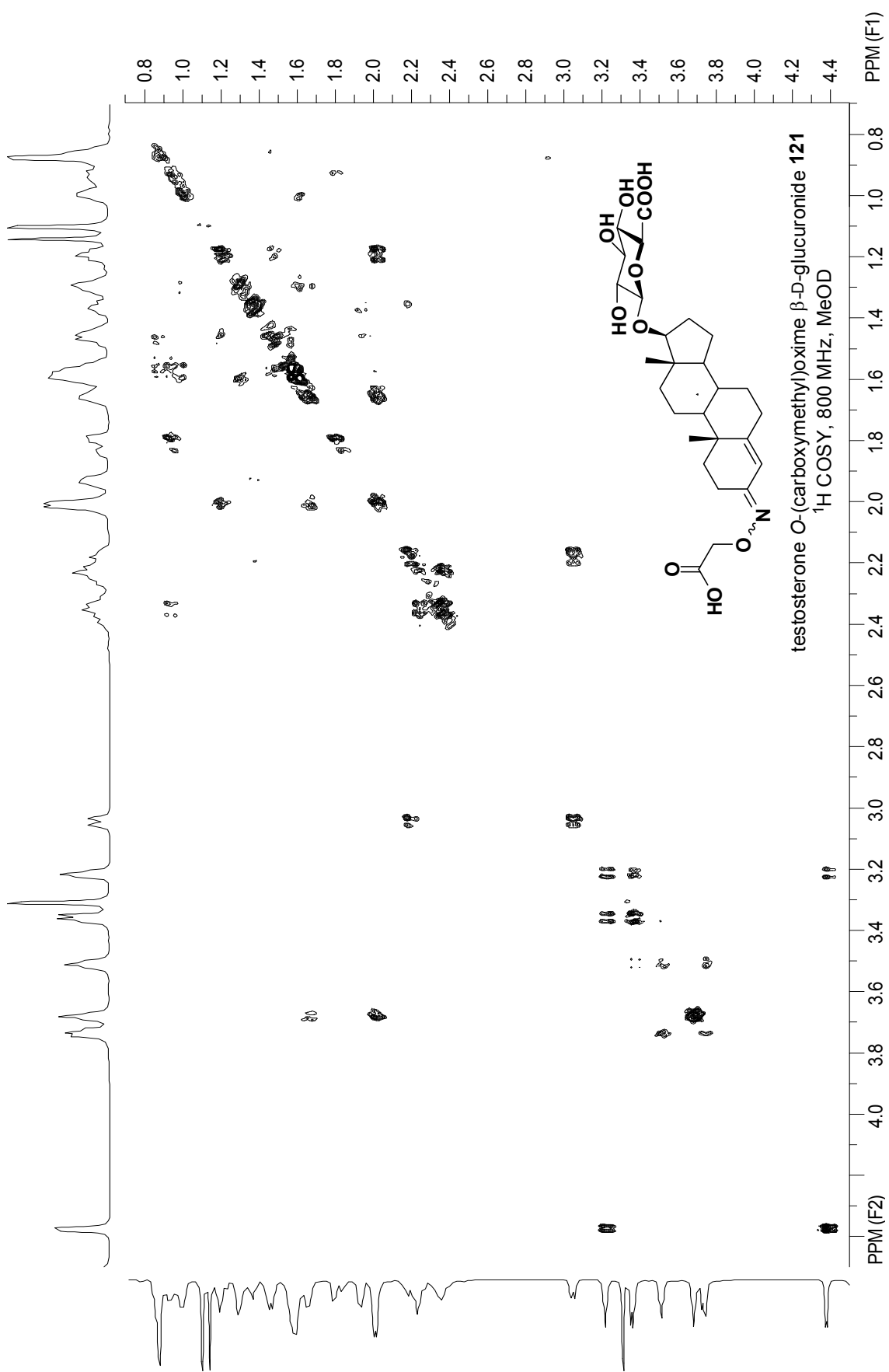


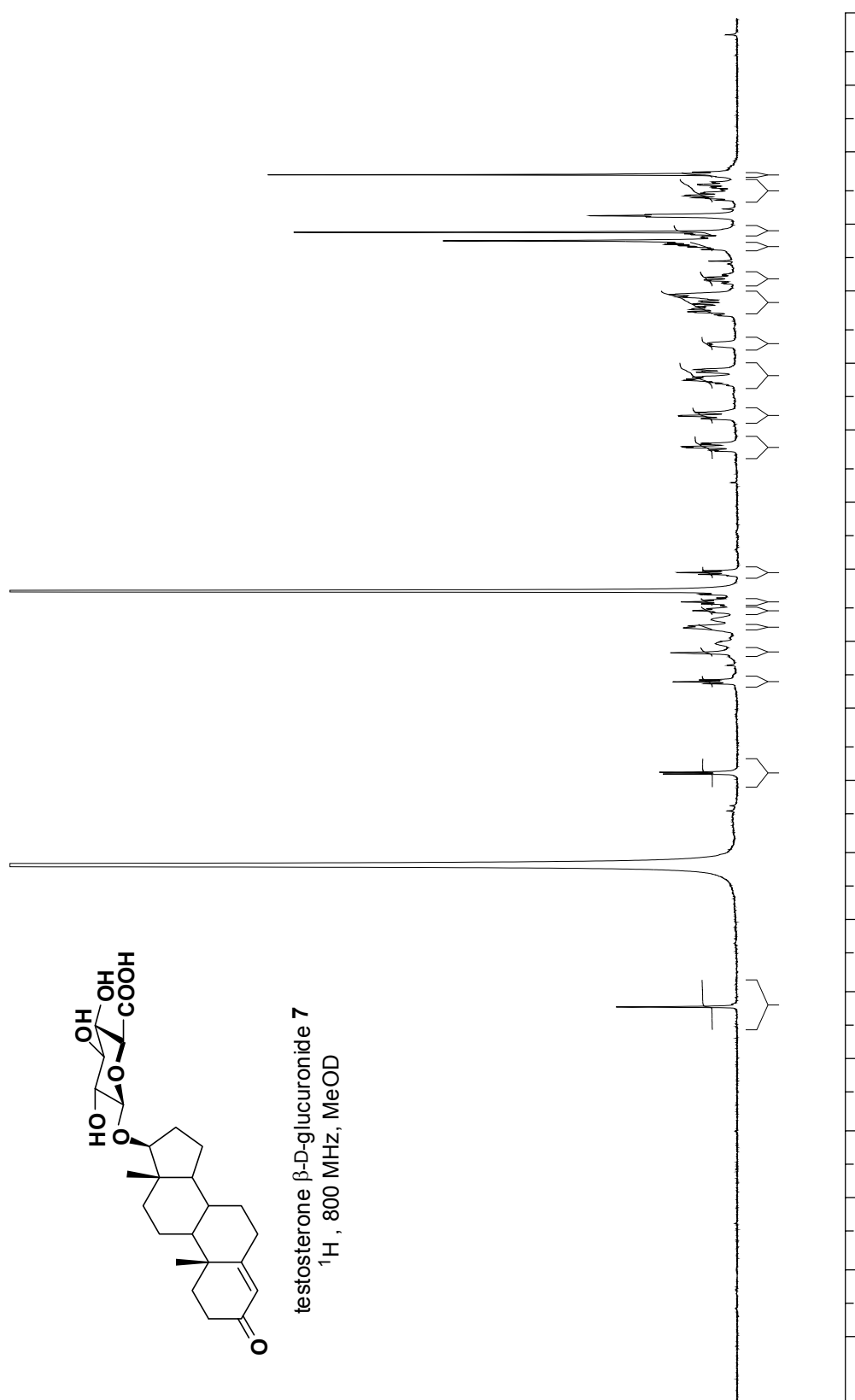


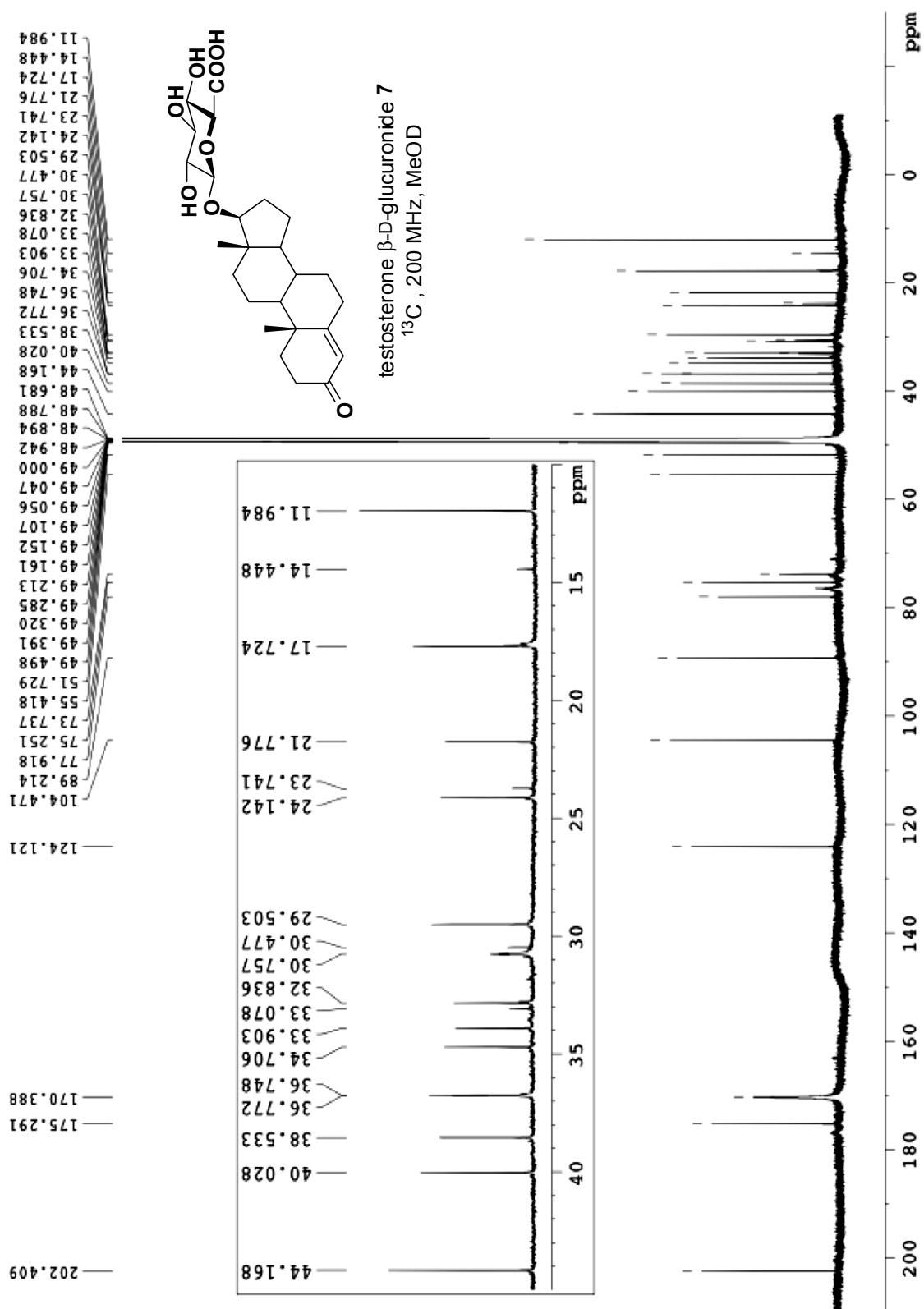












~ Chapter 9 ~

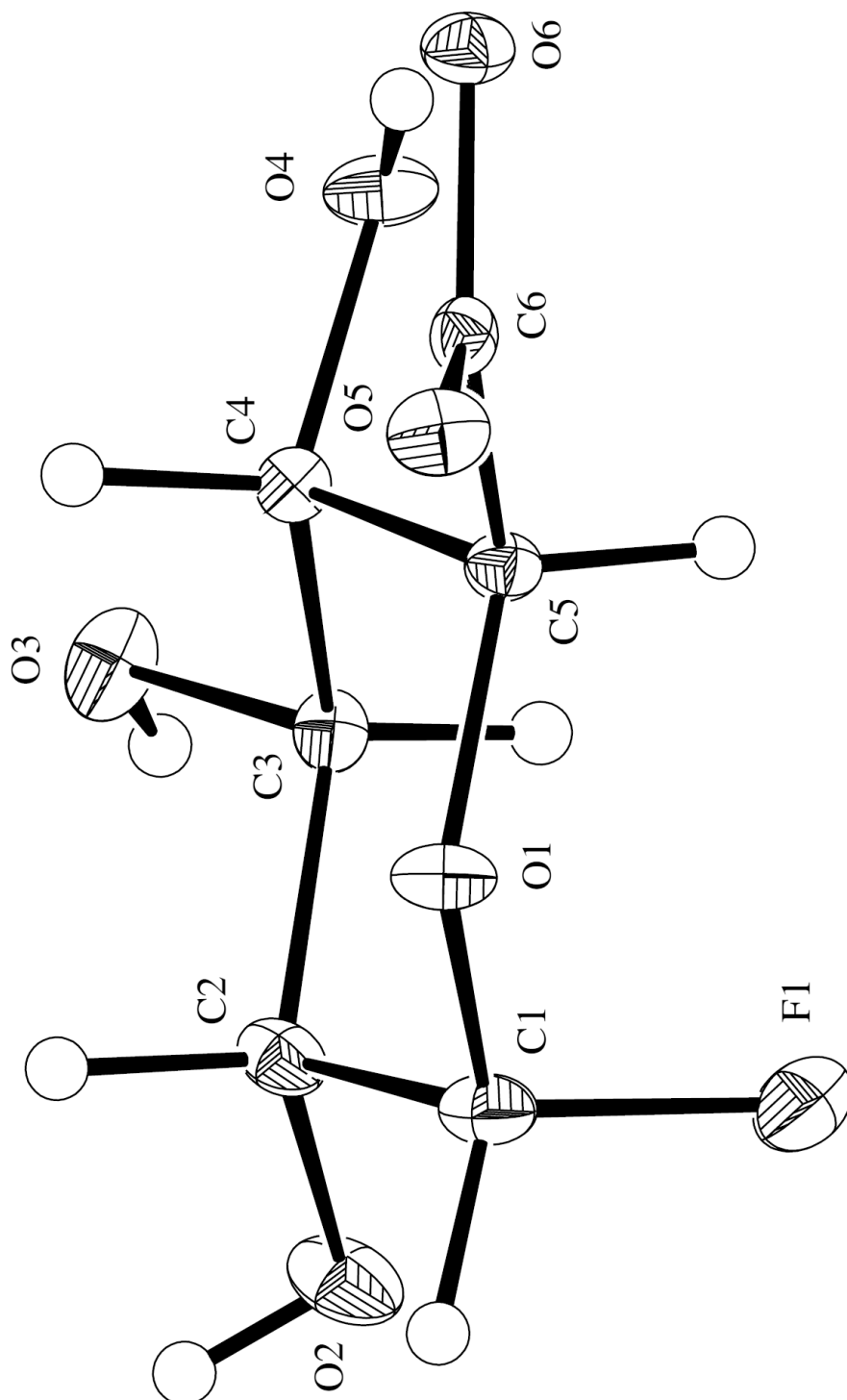
X-Ray Crystal Data

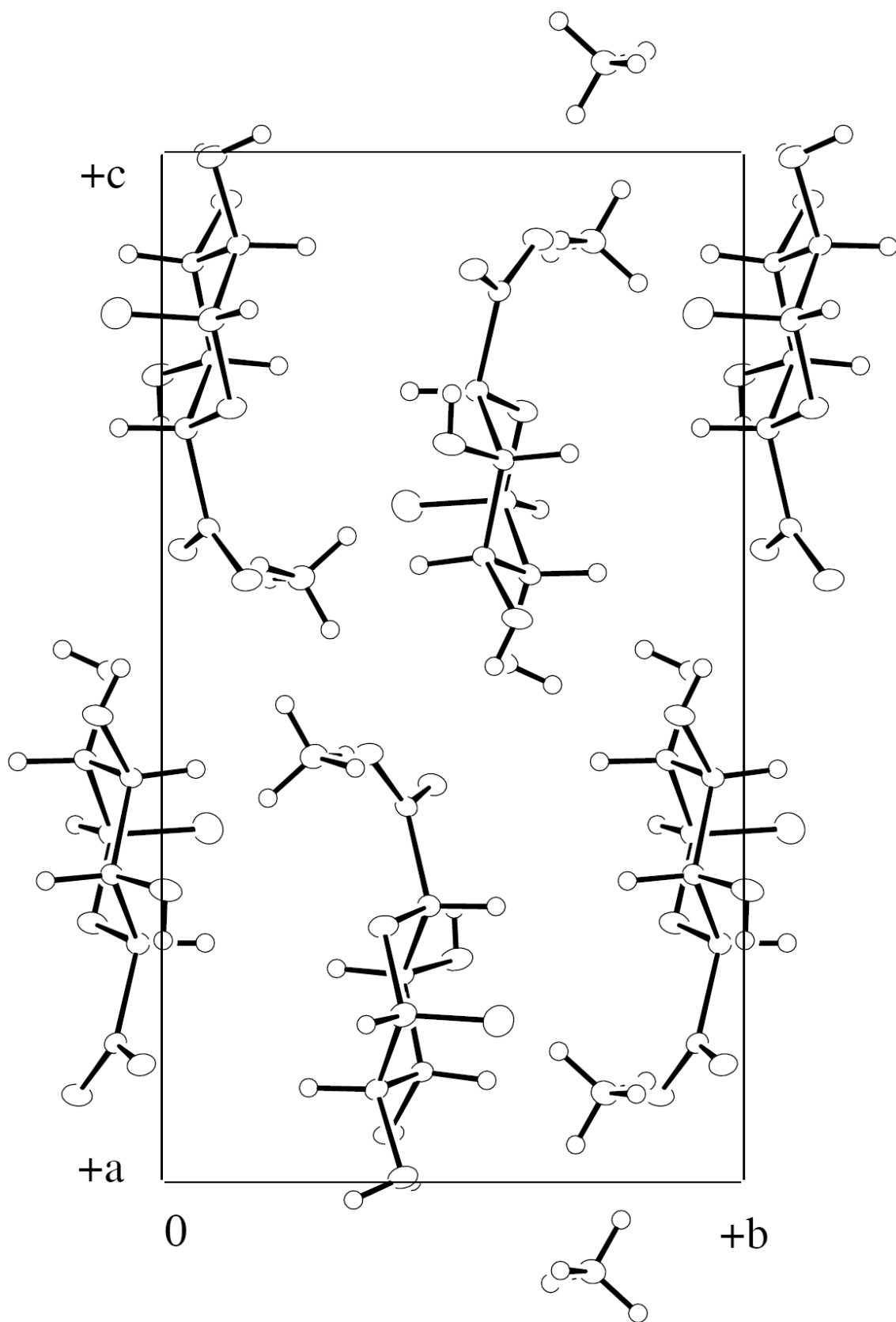
9.1 Crystal structure of $C_6H_{12}FNO_6$ — mcl0801

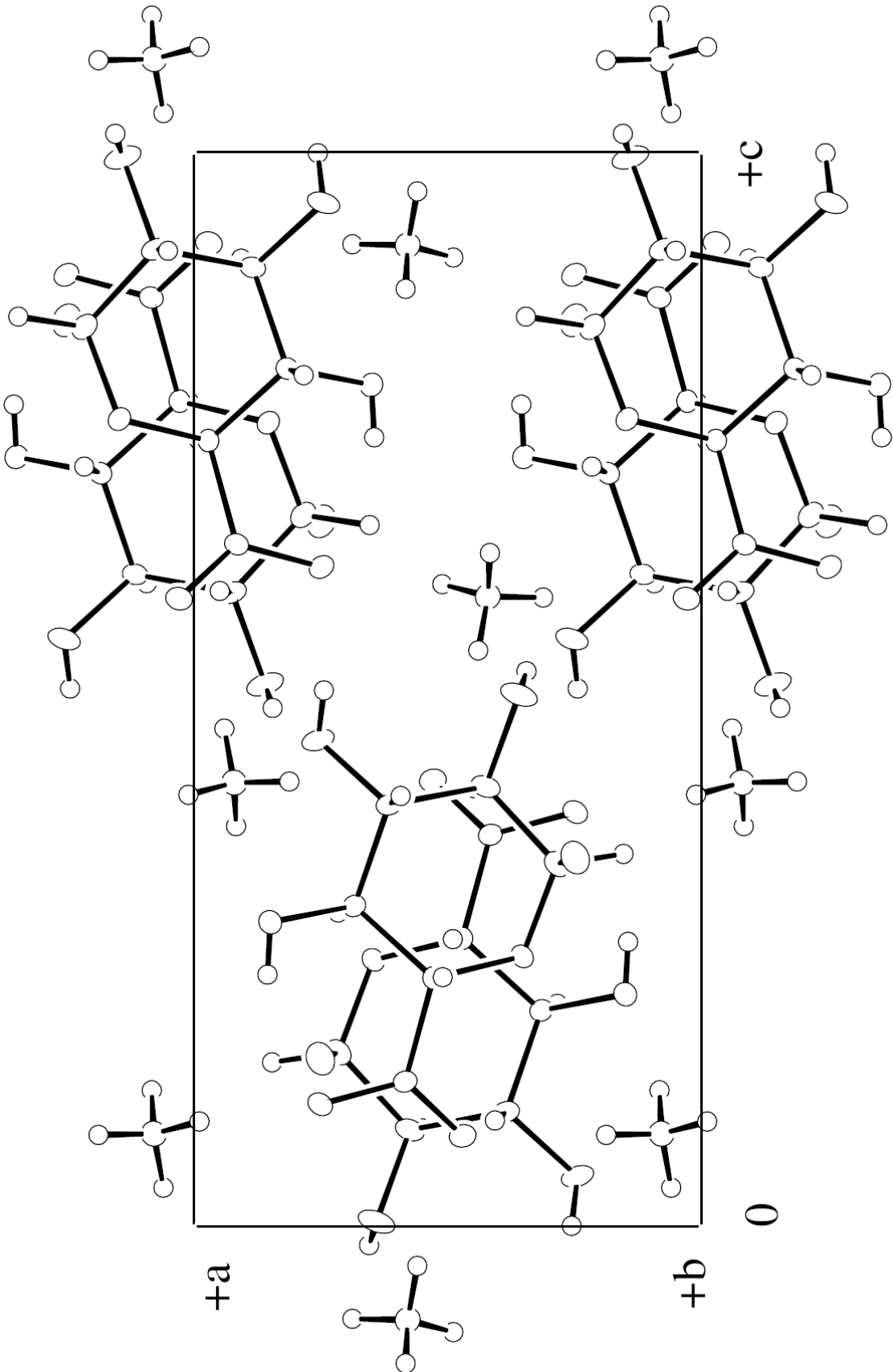
Shane M. Wilkinson, Malcolm D. McLeod and Anthony C. Willis

Research School of Chemistry, The Australian National University, Canberra, A. C. T.
0200, Australia

Correspondence email: willis@rsc.anu.edu.au







Abstract

The crystal structure of C₆H₁₂FNO₆ is reported.

Comment

The compound is enantiometrically pure but the anomalous dispersion terms are very low for all elements in the structure and so the absolute configuration can not be determined in this experiment. Consequently Friedel-pair reflections have been averaged and the Flack parameter has not been refined. The absolute configuration of the molecule has been assigned on the basis of the synthetic precursors.

The crystallographic asymmetric unit consists of one NH₄⁺ cation and one C₆H₈FO₆⁻ anion. There is extensive hydrogen-bonding between species within the unit cell.

Experimental

The compound was prepared by SMW and recrystallized from ethanol/water/acetone. The sample ID is SMW4B108.

Refinement

All hydrogen atoms were observed in difference electron density maps synthesized prior to their inclusion. They were included at these positions and then refined positionally with their displacement parameters held fixed at $U_{\text{iso}}(\text{H}) = 1.2 \times U_{\text{eq}}(\text{adjacent atom})$.

The final difference electron density map is essentially featureless, with the largest peaks being located between carbon atoms.

Computing details

Data collection: *COLLECT* (Nonius BV, 1997); cell refinement: *DENZO/SCALEPACK* (Otwinowski & Minor, 1997); data reduction: *DENZO/SCALEPACK* (Otwinowski & Minor, 1997); program(s) used to solve structure: *SIR92* (Altomare *et al.*, 1994); program(s) used to refine structure: *CRYSTALS* (Watkin *et al.* 2003); molecular graphics: *ORTEPII* (Johnson 1976) in *TEXSAN* (MSC, 1992-1997); software used to prepare material for publication: *CRYSTALS* (Watkin *et al.* 2003).

X-Ray crystal data

Crystal data

$\text{H}_4\text{N}^+\cdot\text{C}_6\text{H}_8\text{FO}_6^-$

$M_r = 213.16$

Orthorhombic, $P2_12_12_1$

$a = 7.0684$ (2) Å

$b = 8.4206$ (2) Å

$c = 14.9569$ (5) Å

$V = 890.24$ (4) Å³

$Z = 4$

$F_{000} = 448$

$D_x = 1.590$ Mg m⁻³

Mo $K\alpha$ radiation

$\lambda = 0.71073$ Å

Cell parameters from 6863 reflections

$\theta = 2.6$ – 27.5°

$\mu = 0.15$ mm⁻¹

$T = 200$ K

Block, colourless

$0.44 \times 0.33 \times 0.23$ mm

Data collection

Nonius KappaCCD diffractometer

Monochromator: graphite

$T = 200$ K

φ and ω scans with CCD

Absorption correction: integration via Gaussian method (Coppens, 1970) implemented in maXus (2000)

$T_{\min} = 0.950$, $T_{\max} = 0.977$

10200 measured reflections

1196 independent reflections

1100 reflections with $I > 2.0\sigma(I)$

$R_{\text{int}} = 0.035$

$\theta_{\max} = 27.5^\circ$

$\theta_{\min} = 2.7^\circ$

$h = -9 \rightarrow 9$

$k = -9 \rightarrow 10$

$l = -19 \rightarrow 19$

Refinement

Refinement on F^2

Least-squares matrix: full

$R[F^2 > 2\sigma(F^2)] = 0.026$

$wR(F^2) = 0.073$

$S = 0.99$

1196 reflections

163 parameters

Primary atom site location: structure-invariant direct methods

Hydrogen site location: inferred from neighbouring sites

Only H-atom coordinates refined

Method = Modified Sheldrick $w = 1/[\sigma^2(F^2) + (0.05P)^2 + 0.0P]$, where $P = (\max(F_o^2, 0) + 2F_c^2)/3$

$(\Delta/\sigma)_{\max} = 0.0003$

$\Delta\rho_{\max} = 0.21$ e Å⁻³

$\Delta\rho_{\min} = -0.17$ e Å⁻³

Extinction correction: None

Absolute structure: The enantiomer has been assigned by reference to an unchanging chiral centre in the synthetic procedure.

Fractional atomic coordinates and isotropic or equivalent isotropic displacement parameters (\AA^2)

	x	y	z	$U_{\text{iso}}^*/U_{\text{eq}}$
F1	0.75092 (15)	0.57835 (13)	0.15646 (7)	0.0330
O1	0.64661 (17)	0.38047 (15)	0.24833 (7)	0.0226
O2	0.6403 (2)	0.41398 (18)	0.00483 (8)	0.0323
O3	0.2445 (2)	0.38953 (15)	0.04701 (8)	0.0286
O4	0.15035 (17)	0.50600 (17)	0.21649 (8)	0.0254
O5	0.52940 (18)	0.35395 (15)	0.41541 (8)	0.0253
O6	0.24880 (17)	0.46453 (14)	0.38595 (8)	0.0227
N1	0.4209 (2)	0.23923 (19)	0.58663 (10)	0.0232
C1	0.7153 (3)	0.4142 (2)	0.16247 (11)	0.0236
C2	0.5746 (3)	0.36880 (19)	0.09024 (10)	0.0217
C3	0.3841 (2)	0.44694 (18)	0.10722 (10)	0.0186
C4	0.3160 (2)	0.41374 (19)	0.20132 (10)	0.0172
C5	0.4715 (2)	0.45872 (18)	0.26834 (10)	0.0172
C6	0.4159 (2)	0.41985 (18)	0.36479 (10)	0.0176
H2	0.655 (4)	0.329 (3)	-0.0171 (16)	0.0390*
H3	0.256 (4)	0.429 (3)	0.0009 (17)	0.0340*
H4	0.145 (3)	0.502 (3)	0.2652 (15)	0.0300*
H5	0.417 (3)	0.318 (3)	0.6271 (14)	0.0280*
H6	0.440 (3)	0.289 (3)	0.5364 (15)	0.0280*
H7	0.511 (3)	0.168 (3)	0.5980 (14)	0.0280*
H8	0.312 (3)	0.185 (3)	0.5856 (15)	0.0280*
H11	0.846 (3)	0.351 (3)	0.1530 (13)	0.0280*
H21	0.551 (3)	0.252 (2)	0.0917 (14)	0.0260*
H31	0.407 (3)	0.558 (2)	0.0990 (13)	0.0220*
H41	0.284 (3)	0.300 (2)	0.2075 (12)	0.0210*
H51	0.490 (3)	0.574 (2)	0.2677 (13)	0.0210*

Atomic displacement parameters (\AA^2)

	U^{11}	U^{22}	U^{33}	U^{12}	U^{13}	U^{23}
F1	0.0278 (6)	0.0346 (5)	0.0365 (6)	-0.0064 (5)	0.0051 (5)	0.0030 (5)
O1	0.0171 (6)	0.0331 (6)	0.0176 (5)	0.0068 (5)	0.0026 (4)	0.0027 (5)
O2	0.0459 (8)	0.0325 (6)	0.0184 (6)	0.0109 (7)	0.0117 (6)	0.0046 (5)
O3	0.0354 (8)	0.0345 (7)	0.0158 (5)	-0.0109 (7)	-0.0073 (5)	0.0037 (5)
O4	0.0178 (6)	0.0396 (7)	0.0188 (5)	0.0069 (6)	0.0013 (5)	0.0048 (6)
O5	0.0243 (6)	0.0340 (6)	0.0176 (5)	0.0017 (5)	-0.0017 (5)	0.0025 (5)
O6	0.0207 (6)	0.0297 (6)	0.0176 (5)	0.0009 (5)	0.0036 (5)	-0.0026 (5)

X-Ray crystal data

N1	0.0213 (8)	0.0268 (7)	0.0215 (7)	0.0020 (7)	-0.0006 (6)	0.0018 (6)
C1	0.0214 (8)	0.0276 (8)	0.0217 (8)	0.0045 (7)	0.0057 (7)	0.0034 (7)
C2	0.0288 (9)	0.0200 (7)	0.0164 (7)	0.0052 (7)	0.0054 (7)	0.0027 (6)
C3	0.0223 (8)	0.0189 (7)	0.0146 (7)	-0.0015 (6)	-0.0018 (6)	0.0010 (5)
C4	0.0173 (8)	0.0182 (7)	0.0160 (7)	0.0001 (6)	-0.0013 (6)	0.0011 (6)
C5	0.0148 (7)	0.0194 (7)	0.0174 (7)	0.0014 (6)	-0.0002 (6)	-0.0004 (6)
C6	0.0195 (8)	0.0177 (6)	0.0155 (7)	-0.0033 (6)	-0.0016 (6)	-0.0024 (6)

Geometric parameters (Å, °)

F1—C1	1.408 (2)	N1—H7	0.89 (2)
O1—C1	1.4021 (19)	N1—H8	0.90 (2)
O1—C5	1.4339 (19)	C1—C2	1.517 (2)
O2—C2	1.4114 (19)	C1—H11	1.07 (2)
O2—H2	0.79 (3)	C2—C3	1.520 (2)
O3—C3	1.4208 (19)	C2—H21	1.00 (2)
O3—H3	0.77 (3)	C3—C4	1.514 (2)
O4—C4	1.423 (2)	C3—H31	0.96 (2)
O4—H4	0.73 (2)	C4—C5	1.535 (2)
O5—C6	1.235 (2)	C4—H41	0.99 (2)
O6—C6	1.279 (2)	C5—C6	1.531 (2)
N1—H5	0.90 (2)	C5—H51	0.978 (19)
N1—H6	0.87 (2)		
F1...N1 ⁱ	2.972 (2)	O3...C2 ^{viii}	3.223 (2)
F1...O4 ⁱⁱ	3.025 (2)	O3...C6 ^{vii}	3.360 (2)
F1...C6 ⁱⁱⁱ	3.124 (2)	O3...N1 ^{vii}	3.390 (2)
F1...O5 ⁱⁱⁱ	3.235 (2)	O3...O5 ^{vii}	3.506 (2)
F1...O6 ⁱⁱⁱ	3.313 (2)	O4...N1 ^{vii}	2.937 (2)
F1...C4 ⁱⁱⁱ	3.567 (2)	O4...C1 ^{ix}	3.272 (2)
O1...N1 ^{iv}	3.297 (2)	O5...N1	2.842 (2)
O1...O4 ^v	3.504 (2)	O5...N1 ^{iv}	2.876 (2)
O2...O3 ^{vi}	2.770 (2)	O5...C3 ^v	3.498 (2)
O2...N1 ⁱⁱⁱ	3.092 (2)	O6...N1 ^x	2.913 (2)
O2...O5 ⁱ	3.325 (2)	O6...C3 ^{xi}	3.520 (2)
O2...O6 ^{vii}	3.431 (2)	N1...C3 ^{xi}	3.424 (2)
O3...O6 ^{vii}	2.705 (2)		
C1—O1—C5	113.40 (12)	C2—C3—O3	111.24 (13)
C2—O2—H2	100.1 (18)	C2—C3—C4	110.92 (12)
C3—O3—H3	110.2 (18)	O3—C3—C4	107.79 (13)
C4—O4—H4	100.0 (18)	C2—C3—H31	104.5 (13)

X-Ray crystal data

H5—N1—H6	103.5 (18)	O3—C3—H31	111.7 (12)
H5—N1—H7	112.9 (19)	C4—C3—H31	110.7 (12)
H6—N1—H7	112.2 (19)	C3—C4—O4	108.00 (12)
H5—N1—H8	111.1 (19)	C3—C4—C5	109.52 (13)
H6—N1—H8	111.3 (20)	O4—C4—C5	110.49 (12)
H7—N1—H8	105.8 (19)	C3—C4—H41	109.9 (11)
F1—C1—O1	108.62 (13)	O4—C4—H41	108.8 (12)
F1—C1—C2	108.60 (13)	C5—C4—H41	110.1 (11)
O1—C1—C2	111.96 (14)	C4—C5—O1	111.61 (12)
F1—C1—H11	109.0 (11)	C4—C5—C6	112.26 (12)
O1—C1—H11	108.5 (11)	O1—C5—C6	108.68 (12)
C2—C1—H11	110.1 (11)	C4—C5—H51	109.6 (12)
C1—C2—O2	111.14 (15)	O1—C5—H51	109.7 (12)
C1—C2—C3	110.65 (13)	C6—C5—H51	104.8 (11)
O2—C2—C3	109.03 (13)	C5—C6—O6	114.05 (13)
C1—C2—H21	110.0 (12)	C5—C6—O5	120.46 (14)
O2—C2—H21	109.9 (12)	O6—C6—O5	125.47 (15)
C3—C2—H21	105.9 (12)		
F1—C1—O1—C5	61.9 (2)	O3—C3—C4—O4	-65.3 (2)
F1—C1—C2—O2	55.8 (2)	O3—C3—C4—C5	174.4 (1)
F1—C1—C2—C3	-65.5 (2)	O4—C4—C3—C2	172.7 (1)
O1—C1—C2—O2	175.8 (1)	O4—C4—C5—C6	64.2 (2)
O1—C1—C2—C3	54.5 (2)	O5—C6—C5—C4	134.9 (1)
O1—C5—C4—O4	-173.5 (1)	O6—C6—C5—C4	-46.6 (2)
O1—C5—C4—C3	-54.7 (2)	C1—O1—C5—C4	58.4 (2)
O1—C5—C6—O5	10.9 (2)	C1—O1—C5—C6	-177.2 (1)
O1—C5—C6—O6	-170.5 (1)	C1—C2—C3—C4	-52.4 (2)
O2—C2—C3—O3	65.1 (2)	C2—C1—O1—C5	-58.1 (2)
O2—C2—C3—C4	-175.0 (1)	C2—C3—C4—C5	52.4 (2)
O3—C3—C2—C1	-172.4 (1)	C3—C4—C5—C6	-177.0 (1)

Symmetry codes: (i) $-x+3/2, -y+1, z-1/2$; (ii) $x+1, y, z$; (iii) $-x+1, y+1/2, -z+1/2$; (iv) $x+1/2, -y+1/2, -z+1$; (v) $-x+1, y-1/2, -z+1/2$; (vi) $x+1/2, -y+1/2, -z$; (vii) $-x+1/2, -y+1, z-1/2$; (viii) $x-1/2, -y+1/2, -z$; (ix) $x-1, y, z$; (x) $x-1/2, -y+1/2, -z+1$; (xi) $-x+1/2, -y+1, z+1/2$.

Hydrogen-bond geometry (Å, °)

<i>D</i> —H... <i>A</i>	<i>D</i> —H	H... <i>A</i>	<i>D</i> ... <i>A</i>	<i>D</i> —H... <i>A</i>
O2—H2...O3 ^{vi}	0.79 (3)	2.00 (3)	2.770 (2)	165 (3)
O3—H3...O6 ^{vii}	0.77 (3)	1.94 (3)	2.705 (2)	173 (3)
O4—H4...O6	0.73 (2)	1.97 (2)	2.651 (2)	154 (2)

X-Ray crystal data

N1—H5···O4 ^{xi}	0.90 (2)	2.05 (2)	2.937 (2)	168 (2)
N1—H6···O5	0.87 (2)	1.99 (2)	2.843 (2)	165 (2)
N1—H7···O6 ^{iv}	0.89 (2)	2.03 (2)	2.913 (2)	170 (2)
N1—H8···O5 ^x	0.90 (2)	2.02 (2)	2.877 (2)	159 (2)
N1—H5···F1 ^{xii}	0.90 (2)	2.54 (2)	2.972 (2)	110 (2)

Symmetry codes: (vi) $x+1/2, -y+1/2, -z$; (vii) $-x+1/2, -y+1, z-1/2$; (xi) $-x+1/2, -y+1, z+1/2$; (iv) $x+1/2, -y+1/2, -z+1$; (x) $x-1/2, -y+1/2, -z+1$; (xii) $-x+3/2, -y+1, z+1/2$.

References

Mackay, S., Gilmore, C. J., Edwards, C., Stewart, N. & Shankland, K. (2000). *maXus* Computer Program for the Solution and Refinement of Crystal Structures. Nonius, The Netherlands, MacScience, Japan & The University of Glasgow.

Coppens, P. (1970). *The Evaluation of Absorption and Extinction in Single-Crystal Structure Analysis. Crystallographic Computing*. F. R. Ahmed, S. R. Hall and C. P. Huber, eds., Munksgaard. Copenhagen. pp 255-270.

Altomare, A., Cascarano, G., Giacovazzo, C., Guagliardi, A., Burla, M. C., Polidori, G. & Camalli, M. (1994). *SIR92* – a program for automatic solution of crystal structures by direct methods. *J. Appl. Cryst.* (27), 435-435

Betteridge, P. W., Carruthers, J. R., Cooper, R. I., Prout, K. & Watkin, D. J. (2003). *J. Appl. Cryst.* 36, 1487–?.

Nonius BV, *COLLECT* Software, 1997-2001)

Otwinowski, Z. & Minor, W. (1996). Processing of X-ray Diffraction Data Collected in Oscillation Mode. *Methods Enzymol.* 276, 1997, 307–326. Ed Carter, C.W. & Sweet, R.M., Academic Press.

Molecular Structure Corporation. (1992–1997). *TEXSAN*. Single Crystal Structure Analysis Software. Version 1.8. MSC, 3200 Research Forest Drive, The Woodlands, TX 77381, USA.

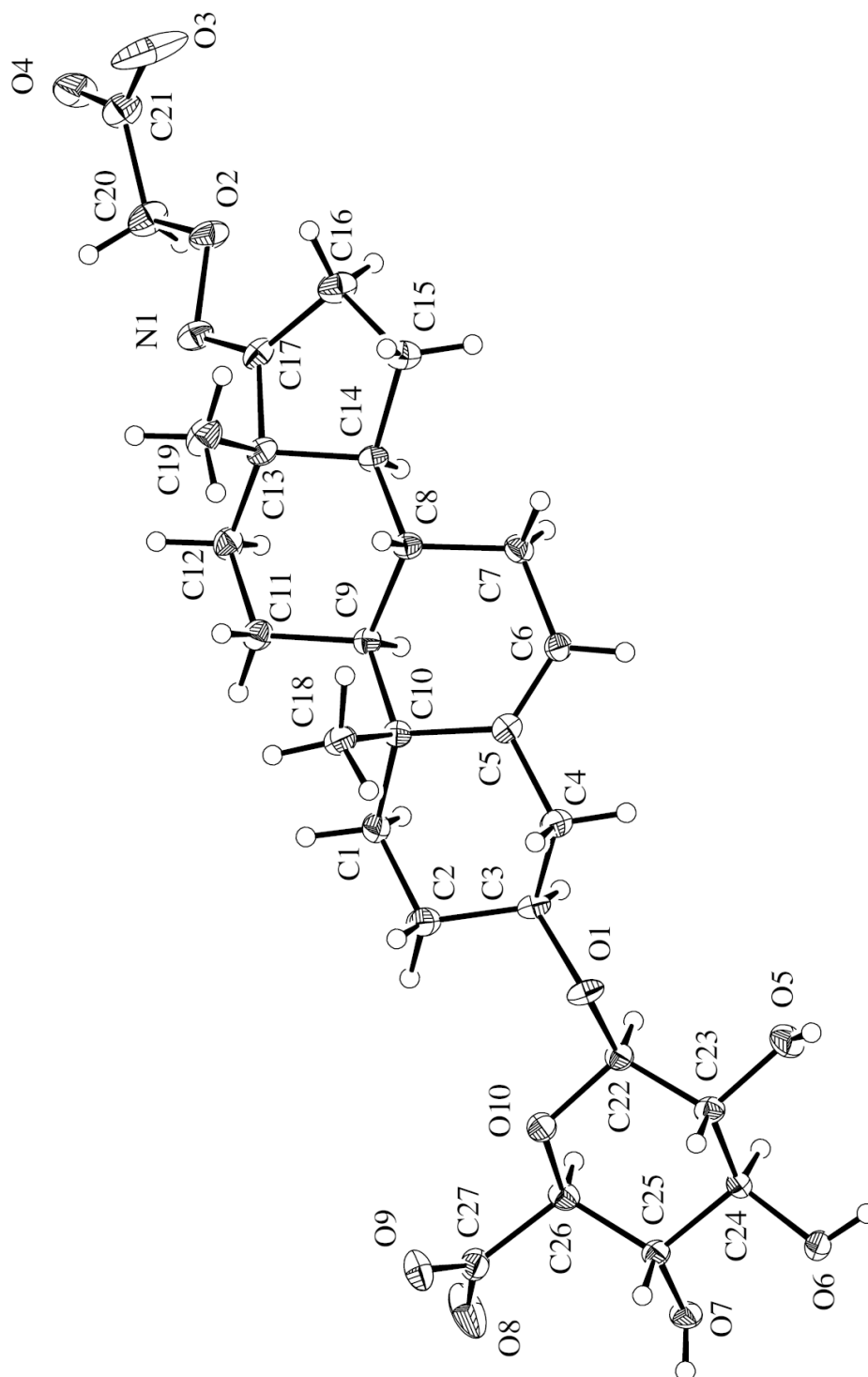
Johnson, C. K. (1976). *ORTEPII*, A Fortran Thermal-Ellipsoid Plot Program, Report ORNL-5138, Oak Ridge National Laboratory, Oak Ridge, Tennessee, USA.

9.2 Crystal structure of $\text{Na}_2\text{C}_{27}\text{H}_{37}\text{NO}_{10}\cdot\text{CH}_3\text{OH}$ — mcl0901

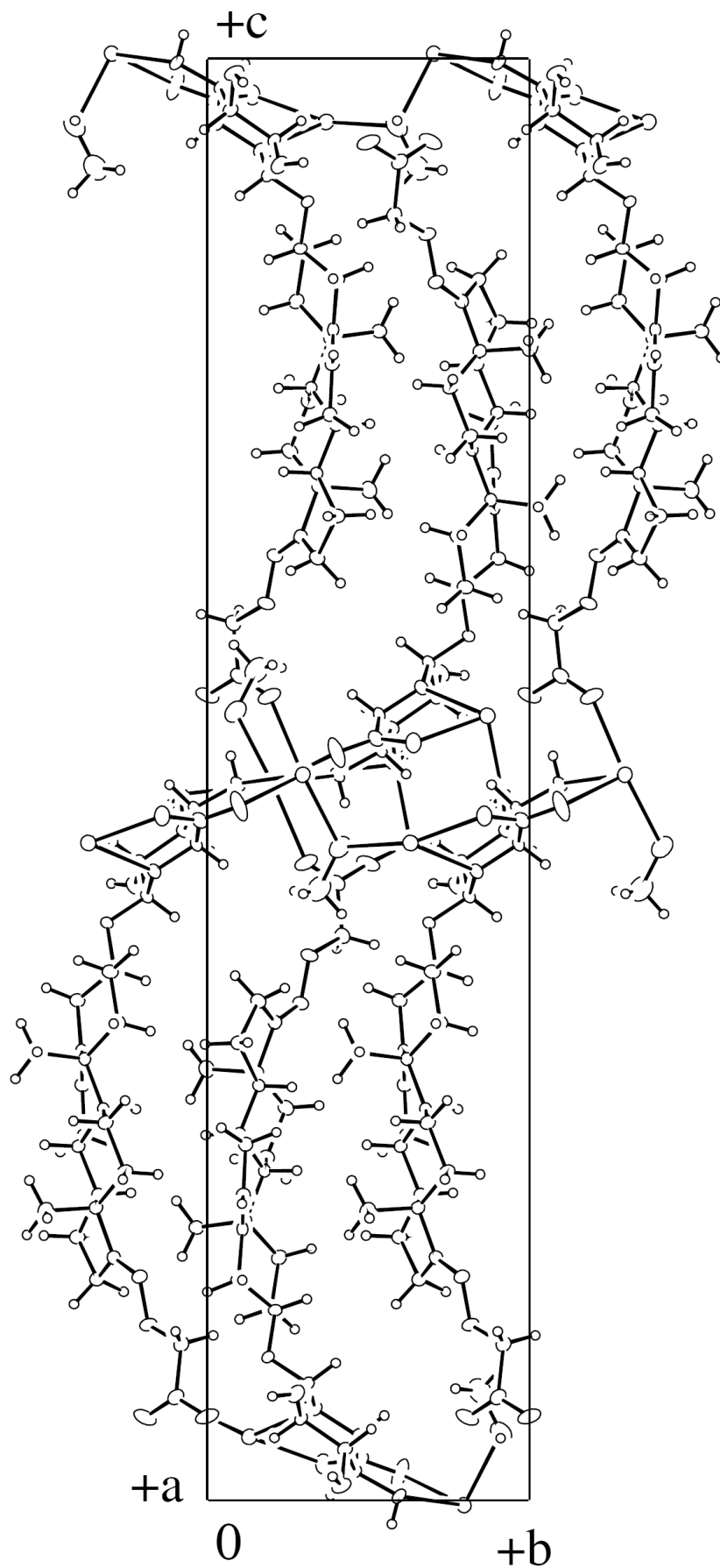
Shane M. Wilkinson, Malcolm D. McLeod and Anthony C. Willis

Research School of Chemistry, The Australian National University, Canberra, A. C. T.
0200, Australia

Correspondence email: willis@rsc.anu.edu.au



X-Ray crystal data



Abstract

The crystal structure of $\text{Na}_2\text{C}_{27}\text{H}_{37}\text{NO}_{10}\cdot\text{CH}_3\text{OH}$ is reported.

Comment

The compound is enantiometrically pure but the anomalous dispersion terms are very low for all elements in the structure and so the absolute configuration can not be determined in this experiment. Consequently Friedel-pair reflections have been averaged and the Flack parameter has not been refined. The absolute configuration of the molecule has been assigned on the basis of the synthetic precursors.

The crystallographic asymmetric unit consists of two Na^+ cations, one $\text{C}_{27}\text{H}_{37}\text{NO}_{10}^{2-}$ anion and one methanol molecule of crystallization. There is also a region of electron density isolated from the principal molecules which presumably arises from disordered solvate molecules, probably methanol and/or water. No sensible disordered model could be formulated which would match the observed electron density, so the computer program SQUEEZE within *PLATON* was used to account for the electron density in this region of the unit cell. [Sluis, P. van der and Spek, A.L. (1990) *Acta Crystallogr.*, Sect. A, 46, 194–201.] The program identified solvent accessible voids totalling 236.4 \AA^3 and 52 electrons per unit cell were recovered. The formula weight, density *etc.* listed in the Tables do not include any correction for the missing solvate.

Experimental

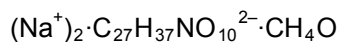
The compound was prepared by SMW and recrystallized from methanol/water/ethyl acetate. The sample ID is SMW34C46.

Computing details

Data collection: *COLLECT* (Nonius, 1997-2001).; cell refinement: *DENZO/SCALEPACK* (Otwinowski & Minor, 1997); data reduction: *DENZO/SCALEPACK* (Otwinowski & Minor, 1997); program(s) used to solve structure: *SIR92* (Altomare *et al.*, 1994); program(s) used to refine structure: *CRYSTALS* (Betteridge *et al.*, 2003), *SQUEEZE* (Spek *et al.*, 1990); molecular graphics: *ORTEPII* (Johnson 1976) in *TEXSAN* (MSC, 1992-1997); software used to prepare material for publication: *CRYSTALS* (Betteridge *et al.*, 2003).

X-Ray crystal data

Crystal data



$M_r = 613.61$

Orthorhombic, $P2_12_12_1$

$a = 7.8722$ (3) Å

$b = 9.2049$ (3) Å

$c = 41.2201$ (15) Å

$V = 2986.92$ (19) Å³

$Z = 4$

$F_{000} = 1304$

$D_x = 1.364$ Mg m⁻³

Mo $K\alpha$ radiation

$\lambda = 0.71073$ Å

Cell parameters from 65058 reflections

$\theta = 2.7$ – 25°

$\mu = 0.13$ mm⁻¹

$T = 200$ K

Plate, colourless

$0.37 \times 0.36 \times 0.05$ mm

Data collection

Area diffractometer

Monochromator: graphite

$T = 200$ K

φ and ω scans with CCD

Absorption correction: integration via Gaussian method (Coppens, 1970) implemented in maXus (2000)

$T_{\min} = 0.956$, $T_{\max} = 0.993$

3055 measured reflections

3055 independent reflections

2092 reflections with $I > 2.0\sigma(I)$

$R_{\text{int}} = 0.069$

$\theta_{\max} = 25.1^\circ$

$\theta_{\min} = 2.6^\circ$

$h = -9 \rightarrow 9$

$k = -10 \rightarrow 10$

$l = -48 \rightarrow 48$

Refinement

Refinement on F^2

Least-squares matrix: full

$R[F^2 > 2\sigma(F^2)] = 0.037$

$wR(F^2) = 0.092$

$S = 0.82$

3053 reflections

367 parameters

Primary atom site location: structure-invariant direct methods

Hydrogen site location: inferred from neighbouring sites

H-atom parameters constrained

Method = Modified Sheldrick $w = 1/[\sigma^2(F^2) + (0.05P)^2 + 0.0P]$,

where $P = (\max(F_o^2, 0) + 2Fc^2)/3$

$(\Delta/\sigma)_{\max} = 0.001$

$\Delta\rho_{\max} = 0.59$ e Å⁻³

$\Delta\rho_{\min} = -0.38$ e Å⁻³

Extinction correction: None

Absolute structure: The enantiomer has been assigned by reference to an unchanging chiral centre in the synthetic procedure.

Special details

Refinement. In addition to the cations, anion and solvate molecule identified, there is also a region of electron density isolated from the principal species which presumably arises from disordered solvate molecules, probably methanol and/or water. No sensible disordered model could be formulated which would match the observed electron density, so the computer program SQUEEZE within PLATON was used to account for the electron density in this region of the unit cell. [Sluis, P. van der and Spek, A.L. (1990) Acta Crystallogr., Sect. A, 46, 194–201.] The program identified solvent accessible voids totalling 236.4 Å³ and 52 electrons per unit cell were recovered. The formula weight, density etc. listed in the Tables do not include any correction for the missing solvate.

Hydrogen atoms attached to carbon atoms of the anion were introduced at calculated positions, and the other H atoms were located in difference electron density maps. They were initially refined with soft restraints on the bond lengths and angles to regularize their geometry (C—H in the range 0.93–0.98, O—H = 0.82 Å) and with $U_{\text{iso}}(\text{H})$ in the range 1.2–1.5 times U_{eq} of the parent atom, after which the positions were refined with riding constraints.

The displacement ellipsoids of O3 and C52 are noticeably elongated, suggesting some disorder of their positions arising from the variable nature of their surroundings dependent on the disordered solvate molecules which were not located. The largest peaks in the final difference electron density map lie between C52 and the region where SQUEEZE was applied.

Fractional atomic coordinates and isotropic or equivalent isotropic displacement parameters (Å²)

	x	y	z	$U_{\text{iso}}^*/U_{\text{eq}}$
Na1	0.6893 (2)	0.86909 (15)	0.54410 (3)	0.0395
Na2	0.5896 (2)	0.20364 (15)	0.49675 (3)	0.0442
O1	0.4075 (3)	0.8113 (2)	0.59946 (5)	0.0295
O2	0.8537 (3)	0.6830 (3)	0.87802 (5)	0.0384
O3	0.9002 (6)	0.6930 (4)	0.94238 (7)	0.0995
O4	1.0695 (4)	0.5004 (3)	0.94172 (6)	0.0537
O5	0.0878 (3)	0.7248 (3)	0.57391 (6)	0.0394

X-Ray crystal data

O6	0.1160 (3)	0.5835 (3)	0.51023 (5)	0.0359
O7	0.3911 (3)	0.4048 (2)	0.50303 (5)	0.0305
O8	0.7668 (4)	0.4014 (3)	0.51857 (8)	0.0681
O9	0.8028 (3)	0.6402 (3)	0.52542 (6)	0.0387
O10	0.5450 (3)	0.6646 (2)	0.56369 (5)	0.0280
O51	0.4985 (4)	0.0880 (4)	0.54701 (8)	0.0668
N1	0.9020 (4)	0.7101 (3)	0.84479 (7)	0.0349
C1	0.7251 (5)	0.7769 (4)	0.66845 (8)	0.0296
C2	0.6671 (5)	0.8011 (5)	0.63341 (8)	0.0338
C3	0.4745 (5)	0.7890 (4)	0.63195 (8)	0.0277
C4	0.3939 (5)	0.9032 (4)	0.65323 (8)	0.0303
C5	0.4533 (5)	0.8907 (4)	0.68822 (8)	0.0250
C6	0.3412 (5)	0.8882 (4)	0.71183 (8)	0.0263
C7	0.3814 (4)	0.8806 (4)	0.74700 (8)	0.0278
C8	0.5695 (5)	0.8997 (4)	0.75435 (7)	0.0254
C9	0.6787 (4)	0.8222 (4)	0.72859 (7)	0.0230
C10	0.6452 (4)	0.8805 (4)	0.69386 (8)	0.0235
C11	0.8668 (5)	0.8155 (4)	0.73799 (8)	0.0311
C12	0.8998 (5)	0.7557 (4)	0.77232 (8)	0.0320
C13	0.8007 (5)	0.8456 (4)	0.79695 (8)	0.0273
C14	0.6119 (5)	0.8398 (4)	0.78774 (7)	0.0241
C15	0.5214 (5)	0.9034 (4)	0.81734 (8)	0.0347
C16	0.6235 (5)	0.8412 (4)	0.84629 (8)	0.0370
C17	0.7867 (5)	0.7898 (4)	0.83162 (8)	0.0293
C18	0.7224 (5)	1.0336 (4)	0.68924 (8)	0.0316
C19	0.8726 (5)	1.0019 (4)	0.79920 (9)	0.0419
C20	0.9697 (6)	0.5804 (4)	0.89153 (8)	0.0397
C21	0.9794 (6)	0.5975 (5)	0.92827 (9)	0.0417
C22	0.3870 (5)	0.6872 (4)	0.58102 (8)	0.0254
C23	0.2438 (4)	0.7085 (4)	0.55679 (8)	0.0262
C24	0.2356 (4)	0.5722 (4)	0.53575 (8)	0.0259
C25	0.4040 (5)	0.5399 (4)	0.51986 (8)	0.0240
C26	0.5466 (5)	0.5339 (4)	0.54480 (9)	0.0268
C27	0.7220 (5)	0.5236 (4)	0.52842 (9)	0.0324
C52	0.5013 (12)	0.1533 (7)	0.57578 (14)	0.1545
H1	0.0322	0.7978	0.5722	0.0595*
H2	0.0186	0.6107	0.5166	0.0544*
H3	0.4051	0.4268	0.4837	0.0457*

X-Ray crystal data

H4	0.3941	0.0895	0.5432	0.1012*
H11	0.8469	0.7903	0.6694	0.0368*
H12	0.6934	0.6765	0.6746	0.0359*
H21	0.7035	0.8998	0.6256	0.0409*
H22	0.7189	0.7284	0.6187	0.0413*
H31	0.4393	0.6911	0.6396	0.0332*
H41	0.4212	0.9995	0.6446	0.0357*
H42	0.2724	0.8910	0.6528	0.0356*
H61	0.2273	0.8921	0.7057	0.0316*
H71	0.3195	0.9560	0.7584	0.0329*
H72	0.3445	0.7856	0.7553	0.0325*
H81	0.5963	1.0045	0.7534	0.0306*
H91	0.6387	0.7214	0.7287	0.0278*
H111	0.9133	0.9150	0.7368	0.0364*
H112	0.9264	0.7552	0.7227	0.0375*
H121	1.0220	0.7620	0.7774	0.0387*
H122	0.8606	0.6529	0.7739	0.0383*
H141	0.5847	0.7372	0.7867	0.0290*
H151	0.5312	1.0071	0.8163	0.0420*
H152	0.4023	0.8743	0.8175	0.0418*
H161	0.6441	0.9134	0.8639	0.0441*
H162	0.5667	0.7592	0.8553	0.0442*
H181	0.6858	1.0954	0.7077	0.0479*
H182	0.8440	1.0274	0.6890	0.0486*
H183	0.6810	1.0775	0.6692	0.0474*
H191	0.8144	1.0596	0.8158	0.0625*
H192	0.9925	0.9964	0.8043	0.0626*
H193	0.8610	1.0518	0.7781	0.0630*
H201	1.0795	0.5983	0.8828	0.0484*
H202	0.9352	0.4816	0.8855	0.0478*
H221	0.3651	0.6013	0.5953	0.0300*
H231	0.2639	0.7915	0.5434	0.0296*
H241	0.2006	0.4909	0.5495	0.0302*
H251	0.4278	0.6172	0.5037	0.0288*
H261	0.5324	0.4504	0.5589	0.0319*
H521	0.6155	0.2016	0.5794	0.2347*
H522	0.4818	0.0830	0.5933	0.2340*
H523	0.4139	0.2296	0.5775	0.2340*

X-Ray crystal data

Atomic displacement parameters (\AA^2)

	U_{11}	U_{22}	U_{33}	U_{12}	U_{13}	U_{23}
Na1	0.0490	0.0347	0.0348	-0.0097	0.0015	-0.0015
Na2	0.0681	0.0308	0.0338	0.0157	0.0071	0.0014
O1	0.0476 (16)	0.0219 (12)	0.0190 (12)	0.0008 (14)	-0.0051 (12)	-0.0031 (10)
O2	0.0514 (19)	0.0415 (15)	0.0224 (13)	0.0099 (15)	-0.0071 (13)	0.0064 (12)
O3	0.192 (5)	0.071 (2)	0.0350 (17)	0.075 (3)	-0.044 (2)	-0.0227 (18)
O4	0.054 (2)	0.075 (2)	0.0318 (15)	0.0292 (19)	0.0000 (16)	0.0192 (16)
O5	0.0331 (16)	0.0419 (16)	0.0433 (16)	0.0086 (14)	0.0079 (14)	-0.0127 (13)
O6	0.0234 (14)	0.0524 (17)	0.0320 (14)	0.0013 (14)	-0.0026 (12)	-0.0143 (13)
O7	0.0353 (15)	0.0276 (13)	0.0287 (13)	-0.0021 (13)	0.0046 (12)	-0.0113 (11)
O8	0.0383 (19)	0.0408 (18)	0.125 (3)	-0.0040 (16)	0.027 (2)	-0.039 (2)
O9	0.0256 (15)	0.0331 (16)	0.0574 (17)	-0.0024 (14)	0.0063 (14)	-0.0007 (14)
O10	0.0293 (15)	0.0254 (14)	0.0292 (13)	-0.0023 (12)	0.0009 (12)	-0.0052 (11)
O51	0.071 (2)	0.064 (2)	0.065 (2)	0.005 (2)	0.0164 (19)	0.019 (2)
N1	0.045 (2)	0.0347 (18)	0.0246 (16)	-0.0008 (19)	-0.0045 (16)	0.0036 (15)
C1	0.026 (2)	0.032 (2)	0.0305 (19)	-0.0024 (19)	0.0000 (18)	-0.0042 (17)
C2	0.038 (2)	0.038 (2)	0.026 (2)	0.006 (2)	-0.0003 (18)	-0.0024 (19)
C3	0.038 (2)	0.027 (2)	0.0181 (18)	0.000 (2)	-0.0018 (17)	-0.0005 (17)
C4	0.034 (2)	0.032 (2)	0.0251 (19)	0.004 (2)	-0.0019 (18)	-0.0017 (17)
C5	0.030 (2)	0.0177 (19)	0.0273 (19)	0.0030 (18)	-0.0027 (19)	0.0000 (16)
C6	0.023 (2)	0.029 (2)	0.026 (2)	0.0051 (18)	-0.0013 (17)	-0.0015 (17)
C7	0.026 (2)	0.029 (2)	0.028 (2)	0.003 (2)	0.0029 (18)	-0.0008 (17)
C8	0.030 (2)	0.0234 (19)	0.0225 (18)	-0.0007 (19)	0.0003 (17)	0.0011 (16)
C9	0.026 (2)	0.0198 (19)	0.0237 (18)	-0.0019 (17)	0.0004 (17)	-0.0008 (15)
C10	0.026 (2)	0.0207 (19)	0.0239 (18)	0.0007 (17)	0.0006 (16)	-0.0008 (16)
C11	0.031 (2)	0.034 (2)	0.028 (2)	0.004 (2)	-0.0037 (18)	0.0030 (17)
C12	0.029 (2)	0.036 (2)	0.031 (2)	0.003 (2)	-0.0043 (18)	0.0057 (17)
C13	0.032 (2)	0.026 (2)	0.0239 (19)	0.0011 (19)	-0.0038 (17)	0.0011 (16)
C14	0.030 (2)	0.0211 (19)	0.0212 (18)	0.0005 (18)	-0.0002 (17)	0.0013 (15)
C15	0.043 (2)	0.034 (2)	0.0274 (19)	0.009 (2)	0.0019 (19)	0.0001 (19)
C16	0.049 (3)	0.033 (2)	0.029 (2)	0.012 (2)	-0.005 (2)	0.0041 (18)
C17	0.034 (2)	0.026 (2)	0.0284 (19)	0.002 (2)	-0.0100 (18)	-0.0009 (17)
C18	0.038 (2)	0.031 (2)	0.0261 (19)	-0.007 (2)	-0.0019 (19)	0.0009 (16)
C19	0.049 (3)	0.034 (2)	0.042 (2)	-0.010 (2)	-0.011 (2)	0.0044 (19)
C20	0.053 (3)	0.032 (2)	0.034 (2)	0.011 (2)	-0.013 (2)	0.0043 (18)
C21	0.054 (3)	0.037 (3)	0.034 (2)	-0.001 (2)	-0.007 (2)	0.009 (2)
C22	0.028 (2)	0.0221 (19)	0.0258 (19)	-0.0049 (18)	0.0020 (18)	-0.0049 (16)
C23	0.031 (2)	0.0225 (18)	0.0248 (18)	-0.0009 (18)	0.0015 (18)	-0.0047 (17)
C24	0.021 (2)	0.032 (2)	0.0246 (19)	-0.0028 (18)	0.0030 (17)	-0.0038 (17)

X-Ray crystal data

C25	0.027 (2)	0.0208 (19)	0.0243 (18)	-0.0032 (18)	0.0007 (18)	-0.0057 (16)
C26	0.031 (2)	0.0200 (19)	0.0293 (19)	0.0002 (18)	0.0054 (19)	-0.0053 (16)
C27	0.027 (2)	0.034 (2)	0.036 (2)	0.001 (2)	-0.0026 (19)	-0.008 (2)
C52	0.298 (12)	0.078 (5)	0.088 (5)	0.056 (7)	0.091 (6)	0.019 (4)

Geometric parameters (Å, °)

Na1—O4 ⁱ	2.325 (3)	C7—H71	0.969
Na1—O6 ⁱⁱ	2.353 (3)	C7—H72	0.984
Na1—O51 ⁱⁱⁱ	2.517 (4)	C8—C9	1.541 (5)
Na1—O9	2.414 (3)	C8—C14	1.520 (4)
Na1—O10	2.342 (3)	C8—H81	0.988
Na2—O3 ^{iv}	2.436 (3)	C9—C10	1.551 (4)
Na2—O7 ^v	2.575 (3)	C9—C11	1.531 (5)
Na2—O6 ^v	2.667 (3)	C9—H91	0.980
Na2—O8 ^{vi}	2.791 (3)	C10—C18	1.547 (5)
Na2—O7	2.437 (3)	C11—C12	1.541 (4)
Na2—O8	2.464 (3)	C11—H111	0.987
Na2—O51	2.437 (3)	C11—H112	0.962
O1—C3	1.454 (4)	C12—C13	1.524 (5)
O1—C22	1.382 (4)	C12—H121	0.986
O2—N1	1.443 (3)	C12—H122	0.998
O2—C20	1.427 (4)	C13—C14	1.535 (5)
O3—C21	1.225 (5)	C13—C17	1.522 (5)
O4—C21	1.269 (5)	C13—C19	1.549 (5)
O5—C23	1.424 (4)	C14—C15	1.530 (5)
O5—H1	0.805	C14—H141	0.969
O6—C24	1.416 (4)	C15—C16	1.549 (5)
O6—H2	0.847	C15—H151	0.958
O7—C25	1.428 (4)	C15—H152	0.975
O7—H3	0.830	C16—C17	1.497 (5)
O8—C27	1.247 (4)	C16—H161	0.996
O9—C27	1.254 (4)	C16—H162	0.952
O10—C22	1.449 (4)	C18—H181	0.993
O10—C26	1.433 (4)	C18—H182	0.959
O51—C52	1.330 (6)	C18—H183	0.974
O51—H4	0.837	C19—H191	0.981
N1—C17	1.287 (5)	C19—H192	0.969
C1—C2	1.531 (5)	C19—H193	0.987
C1—C10	1.550 (5)	C20—C21	1.524 (5)

X-Ray crystal data

C1—H11	0.967	C20—H201	0.951
C1—H12	0.990	C20—H202	0.981
C2—C3	1.521 (5)	C22—C23	1.519 (5)
C2—H21	1.006	C22—H221	1.000
C2—H22	0.991	C23—C24	1.526 (5)
C3—C4	1.509 (5)	C23—H231	0.956
C3—H31	0.995	C24—C25	1.508 (5)
C4—C5	1.520 (4)	C24—H241	0.980
C4—H41	0.978	C25—C26	1.523 (5)
C4—H42	0.963	C25—H251	0.993
C5—C6	1.314 (5)	C26—C27	1.540 (5)
C5—C10	1.532 (5)	C26—H261	0.971
C6—C7	1.486 (5)	C52—H521	1.014
C6—H61	0.932	C52—H522	0.982
C7—C8	1.521 (5)	C52—H523	0.985
O2...C52 ^{vii}	3.393 (9)	O5...C21 ^{vii}	3.472 (5)
O2...C4 ^{viii}	3.477 (4)	O5...C20 ^{vii}	3.598 (4)
O3...O7 ^{ix}	3.124 (4)	O6...O9 ^x	2.597 (3)
O3...C52 ^{vii}	3.27 (1)	O6...O51 ^{vi}	2.986 (4)
O3...O51 ^{vii}	3.313 (6)	O6...O8 ^x	3.238 (4)
O3...O8 ^{ix}	3.514 (5)	O6...C27 ^x	3.238 (5)
O4...O7 ^{ix}	2.691 (3)	O6...O9 ^{xi}	3.285 (4)
O4...O5 ^{viii}	2.895 (4)	O7...O8 ^{vi}	3.114 (3)
O4...C25 ^{ix}	3.249 (4)	O9...C24 ^{xii}	3.490 (4)
O5...O9 ^x	3.104 (3)		
O4 ⁱ —Na1—O6 ⁱⁱ	110.06 (11)	C10—C9—H91	106.2
O4 ⁱ —Na1—O51 ⁱⁱⁱ	93.39 (12)	C11—C9—H91	105.7
O6 ⁱⁱ —Na1—O51 ⁱⁱⁱ	75.55 (10)	C5—C10—C1	109.6 (3)
O4 ⁱ —Na1—O9	103.39 (12)	C5—C10—C9	109.2 (3)
O6 ⁱⁱ —Na1—O9	87.08 (9)	C1—C10—C9	110.0 (3)
O51 ⁱⁱⁱ —Na1—O9	159.21 (12)	C5—C10—C18	108.2 (3)
O4 ⁱ —Na1—O10	136.64 (11)	C1—C10—C18	108.5 (3)
O6 ⁱⁱ —Na1—O10	111.00 (10)	C9—C10—C18	111.2 (3)
O51 ⁱⁱⁱ —Na1—O10	109.75 (11)	C9—C11—C12	114.2 (3)
O9—Na1—O10	65.68 (9)	C9—C11—H111	108.0
O3 ^{iv} —Na2—O7 ^v	97.14 (13)	C12—C11—H111	108.4
O3 ^{iv} —Na2—O6 ^v	106.58 (11)	C9—C11—H112	109.2
O7 ^v —Na2—O6 ^v	62.90 (8)	C12—C11—H112	108.2

X-Ray crystal data

O3 ^{iv} —Na2—O8 ^{vi}	87.54 (15)	H111—C11—H112	108.7
O7 ^v —Na2—O8 ^{vi}	134.89 (9)	C11—C12—C13	109.3 (3)
O6 ^v —Na2—O8 ^{vi}	72.73 (9)	C11—C12—H121	109.8
O3 ^{iv} —Na2—O7	79.75 (11)	C13—C12—H121	109.0
O7 ^v —Na2—O7	152.30 (10)	C11—C12—H122	110.4
O6 ^v —Na2—O7	144.53 (11)	C13—C12—H122	108.2
O8 ^{vi} —Na2—O7	72.75 (9)	H121—C12—H122	110.0
O3 ^{iv} —Na2—O8	91.64 (14)	C12—C13—C14	108.2 (3)
O7 ^v —Na2—O8	76.31 (9)	C12—C13—C17	118.6 (3)
O6 ^v —Na2—O8	136.70 (12)	C14—C13—C17	98.6 (3)
O8 ^{vi} —Na2—O8	148.66 (10)	C12—C13—C19	110.9 (3)
O7—Na2—O8	76.28 (9)	C14—C13—C19	113.6 (3)
O3 ^{iv} —Na2—O51	164.21 (16)	C17—C13—C19	106.5 (3)
O7 ^v —Na2—O51	95.70 (10)	C13—C14—C8	115.1 (3)
O6 ^v —Na2—O51	71.45 (10)	C13—C14—C15	103.9 (3)
O8 ^{vi} —Na2—O51	76.88 (12)	C8—C14—C15	118.7 (3)
O7—Na2—O51	93.01 (10)	C13—C14—H141	105.0
O8—Na2—O51	100.31 (13)	C8—C14—H141	105.4
C3—O1—C22	115.6 (3)	C15—C14—H141	107.8
N1—O2—C20	108.4 (3)	C14—C15—C16	103.4 (3)
Na2 ^{ix} —O3—C21	134.5 (3)	C14—C15—H151	108.0
Na1 ^{xiii} —O4—C21	158.8 (3)	C16—C15—H151	111.1
C23—O5—H1	121.0	C14—C15—H152	110.4
Na1 ^{xi} —O6—Na2 ^{vi}	95.76 (9)	C16—C15—H152	113.1
Na1 ^{xi} —O6—C24	123.9 (2)	H151—C15—H152	110.6
Na2 ^{vi} —O6—C24	93.4 (2)	C15—C16—C17	104.5 (3)
Na1 ^{xi} —O6—H2	117.4	C15—C16—H161	113.4
Na2 ^{vi} —O6—H2	104.8	C17—C16—H161	111.4
C24—O6—H2	113.2	C15—C16—H162	110.4
Na2—O7—Na2 ^{vi}	107.28 (9)	C17—C16—H162	108.1
Na2—O7—C25	131.9 (2)	H161—C16—H162	108.8
Na2 ^{vi} —O7—C25	113.7 (2)	C13—C17—C16	109.6 (3)
Na2—O7—H3	89.9	C13—C17—N1	122.5 (3)
Na2 ^{vi} —O7—H3	102.7	C16—C17—N1	127.9 (3)
C25—O7—H3	104.1	C10—C18—H181	108.3
Na2—O8—Na2 ^v	100.18 (9)	C10—C18—H182	109.8
Na2—O8—C27	128.7 (3)	H181—C18—H182	109.5
Na2 ^v —O8—C27	130.1 (3)	C10—C18—H183	110.5

X-Ray crystal data

Na1—O9—C27	121.9 (2)	H181—C18—H183	108.3
Na1—O10—C22	118.1 (2)	H182—C18—H183	110.4
Na1—O10—C26	118.88 (19)	C13—C19—H191	112.0
C22—O10—C26	113.3 (3)	C13—C19—H192	108.7
Na2—O51—Na1 ^{xiv}	97.67 (12)	H191—C19—H192	109.2
Na2—O51—C52	123.8 (4)	C13—C19—H193	110.2
Na1 ^{xiv} —O51—C52	113.2 (4)	H191—C19—H193	108.7
Na2—O51—H4	97.0	H192—C19—H193	107.9
Na1 ^{xiv} —O51—H4	126.2	O2—C20—C21	110.6 (3)
C52—O51—H4	100.2	O2—C20—H201	108.6
O2—N1—C17	108.2 (3)	C21—C20—H201	108.3
C2—C1—C10	115.3 (3)	O2—C20—H202	109.7
C2—C1—H11	108.4	C21—C20—H202	111.1
C10—C1—H11	107.2	H201—C20—H202	108.5
C2—C1—H12	107.6	C20—C21—O4	112.9 (4)
C10—C1—H12	107.4	C20—C21—O3	121.4 (4)
H11—C1—H12	111.0	O4—C21—O3	125.7 (4)
C1—C2—C3	108.9 (3)	O10—C22—O1	106.8 (3)
C1—C2—H21	110.5	O10—C22—C23	109.4 (2)
C3—C2—H21	109.7	O1—C22—C23	110.0 (3)
C1—C2—H22	110.8	O10—C22—H221	108.9
C3—C2—H22	109.6	O1—C22—H221	110.5
H21—C2—H22	107.3	C23—C22—H221	111.2
C2—C3—O1	112.8 (3)	C22—C23—O5	109.1 (3)
C2—C3—C4	110.2 (3)	C22—C23—C24	107.4 (3)
O1—C3—C4	106.5 (3)	O5—C23—C24	109.4 (3)
C2—C3—H31	109.4	C22—C23—H231	111.1
O1—C3—H31	108.6	O5—C23—H231	110.2
C4—C3—H31	109.3	C24—C23—H231	109.6
C3—C4—C5	111.7 (3)	C23—C24—O6	113.0 (3)
C3—C4—H41	109.2	C23—C24—C25	111.8 (3)
C5—C4—H41	110.2	O6—C24—C25	106.0 (3)
C3—C4—H42	108.9	C23—C24—H241	108.1
C5—C4—H42	108.4	O6—C24—H241	107.5
H41—C4—H42	108.4	C25—C24—H241	110.4
C4—C5—C6	119.9 (3)	C24—C25—O7	108.7 (3)
C4—C5—C10	116.9 (3)	C24—C25—C26	111.2 (3)
C6—C5—C10	123.3 (3)	O7—C25—C26	110.4 (3)

X-Ray crystal data

C5—C6—C7	125.5 (3)	C24—C25—H251	108.4
C5—C6—H61	116.4	O7—C25—H251	108.1
C7—C6—H61	118.1	C26—C25—H251	109.9
C6—C7—C8	113.3 (3)	C25—C26—O10	109.3 (3)
C6—C7—H71	109.4	C25—C26—C27	111.5 (3)
C8—C7—H71	108.1	O10—C26—C27	107.3 (3)
C6—C7—H72	108.6	C25—C26—H261	110.4
C8—C7—H72	108.7	O10—C26—H261	109.7
H71—C7—H72	108.7	C27—C26—H261	108.5
C7—C8—C9	110.7 (3)	C26—C27—O9	116.5 (3)
C7—C8—C14	110.6 (3)	C26—C27—O8	116.9 (4)
C9—C8—C14	109.5 (3)	O9—C27—O8	126.6 (4)
C7—C8—H81	108.2	O51—C52—H521	110.1
C9—C8—H81	107.8	O51—C52—H522	110.8
C14—C8—H81	110.0	H521—C52—H522	108.7
C8—C9—C10	112.4 (3)	O51—C52—H523	112.0
C8—C9—C11	112.6 (3)	H521—C52—H523	107.3
C10—C9—C11	114.3 (3)	H522—C52—H523	107.9
C8—C9—H91	104.7		
Na1—O4 ⁱ —C21 ⁱ —O3 ⁱ	-115.4 (7)	O10—Na1—O6 ⁱⁱ —C24 ⁱⁱ	-124.4 (3)
Na1—O4 ⁱ —C21 ⁱ —C20 ⁱ	67.7 (9)	O10—Na1—O9—C27	14.1 (3)
Na1—O6 ⁱⁱ —C24 ⁱⁱ —C23 ⁱⁱ	102.1 (3)	O10—C22—O1—C3	-89.8 (3)
Na1—O6 ⁱⁱ —C24 ⁱⁱ —C25 ⁱⁱ	-20.7 (4)	O10—C22—C23—C24	59.2 (3)
Na1—O9—C27—O8	177.2 (3)	O10—C26—C25—C24	-53.1 (4)
Na1—O9—C27—C26	-0.3 (4)	O51—Na1 ^{xiv} —O4 ^{xiii} —C21 ^{xiii}	31.7 (7)
Na1—O10—C22—O1	-37.7 (3)	O51—Na2—O6 ^v —C24 ^v	-158.1 (2)
Na1—O10—C22—C23	81.3 (3)	O51—Na2—O7—C25	86.4 (3)
Na1—O10—C26—C25	-85.6 (3)	O51—Na2—O7 ^v —C25 ^v	90.9 (2)
Na1—O10—C26—C27	35.5 (3)	O51—Na2—O8—C27	-84.2 (3)
Na2—O6 ^v —C24 ^v —C23 ^v	-158.6 (2)	N1—O2—C20—C21	154.3 (3)
Na2—O6 ^v —C24 ^v —C25 ^v	78.6 (2)	N1—C17—C13—C12	29.2 (5)
Na2—O7—Na2 ^{vi} —O6	179.3 (1)	N1—C17—C13—C14	145.4 (4)
Na2—O7—Na2 ^{vi} —O7 ^{vi}	-7.3 (1)	N1—C17—C13—C19	-96.7 (4)
Na2—O7—Na2 ^{vi} —O8 ^{vi}	-15.7 (1)	N1—C17—C16—C15	-168.3 (4)
Na2—O7—Na2 ^{vi} —O51 ^{vi}	-115.0 (1)	C1—C2—C3—C4	60.8 (4)
Na2—O7—C25—C24	-140.7 (2)	C1—C10—C5—C4	-42.3 (4)
Na2—O7—C25—C26	-18.5 (4)	C1—C10—C5—C6	137.2 (4)
Na2—O7 ^v —Na2 ^v —O6 ^{xii}	0.4 (2)	C1—C10—C9—C8	-167.0 (3)

X-Ray crystal data

Na2—O7 ^v —Na2 ^v —O7 ^{xii}	-169.5 (2)	C1—C10—C9—C11	63.2 (4)
Na2—O7 ^v —Na2 ^v —O8 ^v	-161.1 (1)	C2—C1—C10—C5	46.2 (4)
Na2—O7 ^v —Na2 ^v —O51 ^v	-61.2 (1)	C2—C1—C10—C9	166.3 (3)
Na2—O7 ^v —C25 ^v —C24 ^v	5.3 (3)	C2—C1—C10—C18	-71.8 (4)
Na2—O7 ^v —C25 ^v —C26 ^v	127.5 (2)	C2—C3—O1—C22	92.1 (4)
Na2—O8—C27—O9	-144.6 (3)	C2—C3—C4—C5	-57.7 (4)
Na2—O8—C27—C26	32.8 (5)	C3—O1—C22—C23	151.6 (3)
Na2—O51—Na1 ^{xiv} —O4 ^{xiii}	74.7 (1)	C3—C2—C1—C10	-56.6 (4)
O1—C3—C2—C1	179.7 (3)	C3—C4—C5—C6	-129.9 (4)
O1—C3—C4—C5	179.6 (3)	C3—C4—C5—C10	49.7 (4)
O1—C22—O10—C26	176.5 (2)	C4—C3—O1—C22	-146.8 (3)
O1—C22—C23—O5	-65.3 (4)	C4—C5—C6—C7	-178.2 (3)
O1—C22—C23—C24	176.2 (3)	C4—C5—C10—C9	-162.9 (3)
O2—N1—C17—C13	177.0 (3)	C4—C5—C10—C18	75.9 (4)
O2—N1—C17—C16	-3.5 (5)	C5—C6—C7—C8	9.1 (5)
O2—C20—C21—O3	-2.9 (6)	C5—C10—C9—C8	-46.7 (4)
O2—C20—C21—O4	174.2 (3)	C5—C10—C9—C11	-176.5 (3)
O4—Na1 ^{xiii} —O9 ^{xiii} —C27 ^{xiii}	149.5 (3)	C6—C5—C10—C9	16.7 (5)
O4—Na1 ^{xiii} —O10 ^{xiii} —C22 ^{xiii}	105.3 (2)	C6—C5—C10—C18	-104.5 (4)
O4—Na1 ^{xiii} —O10 ^{xiii} —C26 ^{xiii}	-110.9 (2)	C6—C7—C8—C9	-38.6 (4)
O5—C23—C22—O10	177.7 (3)	C6—C7—C8—C14	-160.1 (3)
O5—C23—C24—O6	66.8 (3)	C7—C6—C5—C10	2.3 (6)
O5—C23—C24—C25	-173.7 (3)	C7—C8—C9—C10	59.2 (4)
O6—Na1 ^{xi} —O9 ^{xi} —C27 ^{xi}	-100.5 (3)	C7—C8—C9—C11	-170.0 (3)
O6—Na1 ^{xi} —O10 ^{xi} —C22 ^{xi}	-94.4 (2)	C7—C8—C14—C13	176.7 (3)
O6—Na1 ^{xi} —O10 ^{xi} —C26 ^{xi}	49.4 (2)	C7—C8—C14—C15	-59.2 (4)
O6—Na2 ^{vi} —O7—C25	25.1 (2)	C8—C9—C10—C18	72.7 (4)
O6—Na2 ^{vi} —O7 ^{vi} —C25 ^{vi}	148.0 (2)	C8—C9—C11—C12	51.0 (4)
O6—Na2 ^{vi} —O8 ^{vi} —C27 ^{vi}	-158.0 (3)	C8—C14—C13—C12	-60.3 (4)
O6—Na2 ^{vi} —O51 ^{vi} —C52 ^{vi}	156.0 (5)	C8—C14—C13—C17	175.6 (3)
O6—C24—C23—C22	-174.9 (3)	C8—C14—C13—C19	63.3 (4)
O6—C24—C25—O7	-61.6 (3)	C8—C14—C15—C16	-168.2 (3)
O6—C24—C25—C26	176.6 (3)	C9—C8—C14—C13	54.6 (4)
O7—Na2—O6 ^v —C24 ^v	133.9 (2)	C9—C8—C14—C15	178.6 (3)
O7—Na2—O7 ^v —Na2 ^v	-7.3 (1)	C9—C11—C12—C13	-55.8 (4)
O7—Na2—O7 ^v —C25 ^v	-161.5 (2)	C10—C9—C8—C14	-178.7 (3)
O7—Na2—O8—C27	6.5 (3)	C10—C9—C11—C12	-179.2 (3)
O7—Na2—O51—C52	-56.6 (5)	C11—C9—C8—C14	-47.9 (4)

X-Ray crystal data

O7—Na2 ^{vi} —O6—C24	-51.3 (2)	C11—C9—C10—C18	-57.1 (4)
O7—Na2 ^{vi} —O7 ^{vi} —Na2 ^x	-169.5 (2)	C11—C12—C13—C14	57.5 (4)
O7—Na2 ^{vi} —O7 ^{vi} —C25 ^{vi}	-21.9 (3)	C11—C12—C13—C17	168.6 (3)
O7—Na2 ^{vi} —O8 ^{vi} —C27 ^{vi}	-177.6 (3)	C11—C12—C13—C19	-67.8 (4)
O7—Na2 ^{vi} —O51 ^{vi} —C52 ^{vi}	97.1 (5)	C12—C13—C14—C15	168.1 (3)
O7—C25—C24—C23	174.9 (3)	C12—C13—C17—C16	-150.4 (3)
O7—C25—C26—O10	-173.8 (3)	C13—C14—C15—C16	-38.8 (3)
O7—C25—C26—C27	67.7 (4)	C13—C17—C16—C15	11.3 (4)
O8—Na2—O6 ^v —C24 ^v	-72.8 (2)	C14—C13—C17—C16	-34.2 (4)
O8—Na2—O7—C25	-13.5 (3)	C14—C15—C16—C17	16.8 (4)
O8—Na2—O7 ^v —C25 ^v	-169.9 (2)	C15—C14—C13—C17	44.1 (3)
O8—Na2—O51—C52	20.0 (5)	C15—C14—C13—C19	-68.2 (3)
O8—C27—C26—O10	160.4 (3)	C16—C17—C13—C19	83.7 (4)
O8—C27—C26—C25	-80.0 (4)	C17—N1—O2—C20	172.9 (3)
O9—Na1—O4 ⁱ —C21 ⁱ	-160.6 (7)	C22—O10—C26—C25	59.8 (3)
O9—Na1—O6 ⁱⁱ —C24 ⁱⁱ	-61.9 (3)	C22—O10—C26—C27	-179.1 (3)
O9—Na1—O10—C22	-170.9 (2)	C22—C23—C24—C25	-55.4 (4)
O9—Na1—O10—C26	-27.1 (2)	C23—C22—O10—C26	-64.5 (3)
O9—C27—C26—O10	-21.9 (4)	C23—C24—C25—C26	53.1 (4)
O9—C27—C26—C25	97.8 (4)	C24—C25—C26—C27	-171.6 (3)
O10—Na1—O4 ⁱ —C21 ⁱ	-92.0 (7)		

Symmetry codes: (i) $-x+2, y+1/2, -z+3/2$; (ii) $x+1/2, -y+3/2, -z+1$; (iii) $x, y+1, z$; (iv) $-x+3/2, -y+1, z-1/2$; (v) $x+1/2, -y+1/2, -z+1$; (vi) $x-1/2, -y+1/2, -z+1$; (vii) $-x+1, y+1/2, -z+3/2$; (viii) $-x+1, y-1/2, -z+3/2$; (ix) $-x+3/2, -y+1, z+1/2$; (x) $x-1, y, z$; (xi) $x-1/2, -y+3/2, -z+1$; (xii) $x+1, y, z$; (xiii) $-x+2, y-1/2, -z+3/2$; (xiv) $x, y-1, z$.

Hydrogen-bond geometry (Å, °)

D—H...A	D—H	H...A	D...A	D—H...A
O5—H1...O4 ^{vii}	0.81	2.11	2.895 (5)	165
O6—H2...O9 ^x	0.85	1.76	2.597 (5)	169
O7—H3...O4 ^{iv}	0.83	1.87	2.692 (5)	173

Symmetry codes: (vii) $-x+1, y+1/2, -z+3/2$; (x) $x-1, y, z$; (iv) $-x+3/2, -y+1, z-1/2$.

References

Mackay, S., Gilmore, C. J., Edwards, C., Stewart, N. & Shankland, K. (2000). *maXus* Computer Program for the Solution and Refinement of Crystal Structures. Nonius, The Netherlands, MacScience, Japan & The University of Glasgow.

X-Ray crystal data

Coppens, P. (1970). *The Evaluation of Absorption and Extinction in Single-Crystal Structure Analysis. Crystallographic Computing*. F. R. Ahmed, S. R. Hall and C. P. Huber, eds., Munksgaard. Copenhagen. pp 255-270.

Altomare, A., Cascarano, G., Giacovazzo, C., Guagliardi, A., Burla, M. C., Polidori, G. & Camalli, M. (1994). *SIR92* – a program for automatic solution of crystal structures by direct methods. *J. Appl. Cryst.* (27), 435-435

Betteridge, P. W., Carruthers, J. R., Cooper, R. I., Prout, K. & Watkin, D. J. (2003). *J. Appl. Cryst.* 36, 1487.

Nonius BV, *COLLECT* Software, (1997-2001)

Otwinowski, Z. & Minor, W. (1996). Processing of X-ray Diffraction Data Collected in Oscillation Mode. *Methods Enzymol.* 276, 1997, 307-326. Ed Carter, C.W. & Sweet, R.M., Academic Press.

Molecular Structure Corporation. (1992–1997). *TEXSAN*. Single Crystal Structure Analysis Software. Version 1.8. MSC, 3200 Research Forest Drive, The Woodlands, TX 77381, USA.

Johnson, C. K. (1976). *ORTEPII*, A Fortran Thermal-Ellipsoid Plot Program, Report ORNL-5138, Oak Ridge National Laboratory, Oak Ridge, Tennessee, USA.

Sluis, P. van der & Spek, A. L. (1990). *Acta Crystallogr., Sect. A*, 46, 194-201.

~ Chapter 10 ~

References

References

- (1) Mulder, G. J. *Annu. Rev. Pharmacol. Toxicol.* **1992**, 32, 25.
- (2) Coffman, B. L.; Rios, G. R.; Tephly, T. R. *Drug Metab. Dispos.* **1996**, 24, 329.
- (3) Wang, H. M.; Loganathan, D.; Linhardt, R. J. *Biochem. J.* **1991**, 278 (Pt 3), 689.
- (4) Schänzer, W.; Donike, M. *Anal. Chim. Acta* **1993**, 275, 23.
- (5) Kuuranne, T.; Kotiaho, T.; Pedersen-Bjergaard, S.; Einar Rasmussen, K.; Leinonen, A.; Westwood, S.; Kostianen, R. *J. Mass Spectrom.* **2003**, 38, 16.
- (6) Masse, R.; Ayotte, C.; Dugal, R. *J. Chromatogr.* **1989**, 489, 23.
- (7) *Chemicals and public health: An information brochure on the assessment of toxicity*; Office of Chemical Safety, Therapeutic Goods Administration, Department of Health and Ageing, 2004.
- (8) Shipkova, M.; Wieland, E. *Clin. Chim. Acta* **2005**, 358, 2.
- (9) Smith, M. T.; Watt, J. A.; Cramond, T. *Life Sci.* **1990**, 47, 579.
- (10) Raloff, J. *Science News* **2002**, 161, 10.
- (11) Pellissier, H. *Tetrahedron* **2004**, 60, 5123.
- (12) Koenigs, W.; Knorr, E. *Ber. Dtsch. Chem. Ges.* **1901**, 34, 957.
- (13) Becker, J. F. *BBA-Gen Subjects* **1965**, 100, 574.
- (14) Bernstein, S.; Conrow, R. B. *J. Org. Chem.* **1971**, 36, 863.
- (15) Bollenback, G. N.; Long, J. W.; Benjamin, D. G.; Lindquist, J. A. *J. Am. Chem. Soc.* **1955**, 77, 3310.
- (16) Casati, S.; Ottria, R.; Ciuffreda, P. *Steroids* **2009**, 74, 250.
- (17) Elce, J. S.; Carpenter, J. G. D.; Kellie, A. E. *J. Chem. Soc. C.* **1967**, 542.
- (18) Rao, P. N.; Rodriguez, A. M.; Miller, D. W. *J. Steroid Biochem.* **1986**, 25, 417.
- (19) Schneider, J. J.; Bhacca, N. S. *J. Org. Chem.* **1969**, 34, 1990.
- (20) Wotiz, H. H.; Smakula, E.; Lichtin, N. N.; Leftin, J. H. *J. Am. Chem. Soc.* **1959**, 81, 1704.
- (21) Wallace, J. E.; Schroeder, L. R. *J. Chem. Soc., Perkin Trans. 2* **1977**, 795.

- (22) Kürti, L.; Czakó, B. *Strategic Applications of Named Reactions in Organic Synthesis*; Elsevier: Burlington, MA, USA, 2005.
- (23) Pougny, J.-R.; Sinaÿ, P. *Tetrahedron Lett.* **1976**, *17*, 4073.
- (24) Rees, M. D. *B Sc. (Hons)*, UNSW, 1999.
- (25) Harding, J. R.; King, C. D.; Perrie, J. A.; Sinnott, D.; Stachulski, A. V. *Org. Biomol. Chem.* **2005**, *3*, 1501.
- (26) Schmidt, R. R. *Angew. Chem., Int. Ed. Engl.* **1986**, *25*, 212.
- (27) Werschkun, B.; Gorziza, K.; Thiem, J. *J. Carbohydr. Chem.* **1999**, *18*, 629.
- (28) Fischer, B.; Nudelman, A.; Ruse, M.; Herzig, J.; Gottlieb, H. E.; Keinan, E. *J. Org. Chem.* **1984**, *49*, 4988.
- (29) Melvin, F.; McNeill, A.; Henderson, P. J. F.; Herbert, R. B. *Tetrahedron Lett.* **1999**, *40*, 1201.
- (30) Bouktaib, M.; Atmani, A.; Rolando, C. *Tetrahedron Lett.* **2002**, *43*, 6263.
- (31) Smith Iii, A. B.; Hale, K. J.; Rivero, R. A. *Tetrahedron Lett.* **1986**, *27*, 5813.
- (32) Juteau, H.; Gareau, Y.; Labelle, M. *Tetrahedron Lett.* **1997**, *38*, 1481.
- (33) Perrie, J. A.; Harding, J. R.; Holt, D. W.; Johnston, A.; Meath, P.; Stachulski, A. V. *Org. Lett.* **2005**, *7*, 2591.
- (34) Kiryu, T.; Kiso, T.; Nakano, H.; Murakami, H. *J. Appl. Glycosci.* **2009**, *56*, 277.
- (35) Nagatsuka, T.; Uzawa, H.; Asanuma, H.; Nishida, Y. *J. Carbohydr. Chem.* **2009**, *28*, 94.
- (36) Uzawa, H.; Nagatsuka, T.; Hiramatsu, H.; Nishida, Y. *Chem. Commun. (Cambridge, U. K.)* **2006**, 1381.
- (37) Langlois, V.; Parisot, J.; Bonnet, V.; Rabiller, C. *Tetrahedron: Asymmetry* **2002**, *13*, 2369.
- (38) Salleh, H. M.; Mullegger, J.; Reid, S. P.; Chan, W. Y.; Hwang, J.; Warren, R. A. J.; Withers, S. G. *Carbohydr. Res.* **2006**, *341*, 49.
- (39) Fialová, P.; Carmona, A. T.; Robina, I.; Ettrich, R.; Sedmera, P.; Prikrylová, V.; Petrásková-Husáková, L.; Kren, V. *Tetrahedron Lett.* **2005**, *46*, 8715.

References

- (40) Werschkun, B.; Wendt, A.; Thiem, J. *J. Chem. Soc., Perkin Trans. 1* **1998**, 3021.
- (41) Tukey, R. H.; Strassburg, C. P. *Annu. Rev. Pharmacol. Toxicol.* **2000**, *40*, 581.
- (42) Mackenzie, P. I.; Rodbourne, L.; Stranks, S. *J. Steroid Biochem. Mol. Biol.* **1992**, *43*, 1099.
- (43) Sasaki, K.; Taura, F.; Shoyama, Y.; Morimoto, S. *J. Biol. Chem.* **2000**, *275*, 27466.
- (44) Gadelle, D.; Raibaud, P.; Sacquet, E. *Appl. Environ. Microbiol.* **1985**, *49*, 682.
- (45) Blattner, F. R.; Plunkett, G., 3rd; Bloch, C. A.; Perna, N. T.; Burland, V.; Riley, M.; Collado-Vides, J.; Glasner, J. D.; Rode, C. K.; Mayhew, G. F.; Gregor, J.; Davis, N. W.; Kirkpatrick, H. A.; Goeden, M. A.; Rose, D. J.; Mau, B.; Shao, Y. *Science* **1997**, *277*, 1453.
- (46) Aiba, H.; Baba, T.; Hayashi, K.; Inada, T.; Isono, K.; Itoh, T.; Kasai, H.; Kashimoto, K.; Kimura, S.; Kitakawa, M.; Kitagawa, M.; Makino, K.; Miki, T.; Mizobuchi, K.; Mori, H.; Mori, T.; Motomura, K.; Nakade, S.; Nakamura, Y.; Nashimoto, H.; Nishio, Y.; Oshima, T.; Saito, N.; Sampei, G.-i.; Seki, Y.; Sivasundaram, S.; Tagami, H.; Takeda, J.-i.; Takemoto, K.; Takeuchi, Y.; Wada, C.; Yamamoto, Y.; Horiuchi, T. *DNA Res.* **1996**, *3*, 363.
- (47) Aich, S.; Delbaere, L. T.; Chen, R. *Protein Expr Purif* **2001**, *22*, 75.
- (48) Aich, S.; Delbaere, L. T.; Chen, R. *BioTechniques* **2001**, *30*, 846.
- (49) Matsumura, I.; Ellington, A. D. *J. Mol. Biol.* **2001**, *305*, 331.
- (50) Geddie, M. L.; Matsumura, I. *J. Biol. Chem.* **2004**, *279*, 26462.
- (51) Xiong, A. S.; Peng, R. H.; Cheng, Z. M.; Li, Y.; Liu, J. G.; Zhuang, J.; Gao, F.; Xu, F.; Qiao, Y. S.; Zhang, Z.; Chen, J. M.; Yao, Q. H. *Protein Eng Des Sel* **2007**, *20*, 319.
- (52) Zechel, D. L.; Withers, S. G. *Acc. Chem. Res.* **2000**, *33*, 11.
- (53) Mackenzie, L. F.; Wang, Q.; Warren, R. A. J.; Withers, S. G. *J. Am. Chem. Soc.* **1998**, *120*, 5583.
- (54) Williams, S. J.; Withers, S. G. *Aust. J. Chem.* **2002**, *55*, 3.
- (55) Planas, A.; Faijes, M. *Afinidad* **2002**, *59*, 295.
- (56) Faijes, M.; Planas, A. *Carbohydr. Res.* **2007**, *342*, 1581.

-
- (57) Wilkinson, S. M.; Liew, C. W.; Mackay, J. P.; Salleh, H. M.; Withers, S. G.; McLeod, M. D. *Org. Lett.* **2008**, *10*, 1585.
- (58) Wilkinson, S. M. *B Sc. (Hon)*, University of Sydney, 2006.
- (59) Novel, G.; Novel, M. *Mol Gen Genet* **1973**, *120*, 319.
- (60) Everett-Patriquin, M. B. *pET-28a-c(+)* TB074 10/98, 1998.
- (61) Mandel, M.; Higa, A. *J. Mol. Biol.* **1970**, *53*, 159.
- (62) Maniatis, T.; Fritsch, E. F.; Sambrook, J. *Molecular Cloning: A Laboratory Manual*; Cold Spring Harbor University Press, 1982.
- (63) Dower, W. J.; Miller, J. F.; Ragsdale, C. W. *Nucl. Acids Res.* **1988**, *16*, 6127.
- (64) Jacob, F.; Monod, J. *J. Mol. Biol.* **1961**, *3*, 318.
- (65) Novagen *pET System Manual*, 2006.
- (66) Kim, K. M.; Yi, E. C.; Baker, D.; Zhang, K. Y. *J. Acta Crystallogr., Sect. D: Biol. Crystallogr.* **2001**, *57*, 759.
- (67) Sayari, A.; Mosbah, H.; Verger, R.; Gargouri, Y. *J. Colloid Interface Sci.* **2007**, *313*, 261.
- (68) Paigen, K. *Prog. Nucleic Acid Res. Mol. Biol.*; Waldo, E. C., Kivle, M., Eds.; Academic Press: 1989; Vol. Volume 37, p 155.
- (69) Hayashi, M.; Hashimoto, S.-i.; Noyori, R. *Chem. Lett.* **1984**, *13*, 1747.
- (70) Zhao, M. M.; Li, J.; Mano, E.; Song, Z. J.; Tschaen, D. M.; Ghosh, A.; Sieser, J.; Cai, W.; Kelly, S. E. *Org. Synth.* **2009**, *Collective*, 107.
- (71) Ward, D. E.; Rhee, C. K. *Tetrahedron Lett.* **1991**, *32*, 7165.
- (72) Dale, J. A.; Mosher, H. S. *J. Am. Chem. Soc.* **1973**, *95*, 512.
- (73) Hirata, T.; Izumi, S.; Akita, K.; Yoshida, H.; Gotoh, S. *Tetrahedron: Asymmetry* **1993**, *4*, 1465.
- (74) Nishiyama, H.; Park, S.-B.; Itoh, K. *Tetrahedron: Asymmetry* **1992**, *3*, 1029.
- (75) Lemière, G. L.; Willaert, J. J.; Dommissse, R. A.; Lepoivre, J. A.; Alderweireldt, F. C. *Chirality* **1990**, *2*, 175.
- (76) Michaelis, L.; Menten, M. L. *Biochem. Z.* **1913**, *49*, 333.
- (77) Briggs, G. E.; Haldane, J. B. *Biochem. J.* **1925**, *19*, 338.
-

References

- (78) Cook, P. F.; Cleland, W. W. *Enzyme Kinetics and Mechanism*; Cook, P. F., Ed.; Taylor & Francis Group: New York, NY, 2007.
- (79) Cleland, W. W. *Biochim. Biophys. Acta* **1963**, *67*, 104.
- (80) King, E. L.; Altman, C. *J. Phys. Chem.* **1956**, *60*, 1375.
- (81) Cornish-Bowden, A. *Fundamentals of Enzyme Kinetics*; 3rd ed.; Portland Press Ltd: London, UK, 2004.
- (82) Cook, P. F.; Cleland, W. W. *Enzyme Kinetics and Mechanism*; Cook, P. F., Ed.; Taylor & Francis Group: New York, NY, 2007, p 78.
- (83) Igarashi, S.; Sode, K. *Mol. Biotechnol.* **2003**, *24*, 97.
- (84) Lu, L.-Y.; Chiang, H.-P.; Chen, W.-T.; Yang, Y.-S. *Drug Metab. Dispos.* **2009**, *37*, 1083.
- (85) Mei, G.; Di Venere, A.; Buganza, M.; Vecchini, P.; Rosato, N.; Finazzi-Agro, A. *Biochemistry* **1997**, *36*, 10917.
- (86) Hulme, E. C.; Tipton, K. F. *FEBS Lett.* **1971**, *12*, 197.
- (87) Shiio, I.; Sugimoto, S.-i. *J. Biochem. (Tokyo, Jpn.)* **1981**, *89*, 1483.
- (88) Ben-David, A.; Bravman, T.; Balazs, Y. S.; Czjzek, M.; Schomburg, D.; Shoham, G.; Shoham, Y. *ChemBioChem* **2007**, *8*, 2145.
- (89) Caines, M. E. C.; Vaughan, M. D.; Tarling, C. A.; Hancock, S. M.; Warren, R. A. J.; Withers, S. G.; Strynadka, N. C. J. *J. Biol. Chem.* **2007**, *282*, 14300.
- (90) Ducros, V. M. A.; Tarling, C. A.; Zechel, D. L.; Brzozowski, A. M.; Frandsen, T. P.; von Ossowski, I.; Schülein, M.; Withers, S. G.; Davies, G. J. *Chem. Biol.* **2003**, *10*, 619.
- (91) Hancock, S. M.; Rich, J. R.; Caines, M. E. C.; Strynadka, N. C. J.; Withers, S. G. *Nat. Chem. Biol.* **2009**, *5*, 508.
- (92) Hommalai, G.; Withers, S. G.; Chuenchor, W.; Cairns, J. R. K.; Svasti, J. *Glycobiology* **2007**, *17*, 744.
- (93) Honda, Y.; Kitaoka, M. *J. Biol. Chem.* **2006**, *281*, 1426.
- (94) Hrmova, M.; Imai, T.; Rutten, S. J.; Fairweather, J. K.; Pelosi, L.; Bulone, V.; Driguez, H.; Fincher, G. B. *J. Biol. Chem.* **2002**, *277*, 30102.
- (95) Jahn, M.; Stoll, D.; Warren, R. A. J.; Szabo, L.; Singh, P.; Gilbert, H. J.; Ducros, V. M.-A.; Davies, G. J.; Withers, S. G. *Chem. Commun. (Cambridge, U. K.)* **2003**, 1327.

- (96) Kim, Y.-W.; Lee, S. S.; Warren, R. A. J.; Withers, S. G. *J. Biol. Chem.* **2004**, *279*, 42787.
- (97) Piens, K.; Henriksson, A.-M.; Gullfot, F.; Lopez, M.; Faure, R.; Ibatullin, F. M.; Teeri, T. T.; Driguez, H.; Brumer, H. *Org. Biomol. Chem.* **2007**, *5*, 3971.
- (98) Sugimura, M.; Nishimoto, M.; Kitaoka, M. *Biosci. Biotechnol. Biochem.* **2006**, *70*, 1210.
- (99) *Fluoride selective electrode User Guide*; Thermo Fisher Scientific Inc.: Waltham, MA 2007.
- (100) *Fluoride Ion Selective Electrodes Operators Manual*; Omega Engineering Inc.: Stamford, CT, 1992.
- (101) *Technical Specifications for the Fluoride Ion-Selective Electrode*; Nico2000 Ltd: Middlesex, U.K.
- (102) *Fluoride ion selective electrode instruction manual*; HANNA instruments, Inc.: Woonsocket, RI, USA, 2002.
- (103) Plateau, P.; Gueron, M. *J. Am. Chem. Soc.* **1982**, *104*, 7310.
- (104) Faijes, M.; Perez, X.; Perez, O.; Planas, A. *Biochemistry* **2003**, *42*, 13304.
- (105) Faijes, M.; Saura-Valls, M.; Pérez, X.; Conti, M.; Planas, A. *Carbohydr. Res.* **2006**, *341*, 2055.
- (106) Christensen, J. J.; Izatt, R. M.; Hansen, L. D.; Partridge, J. A. *J. Phys. Chem.* **1966**, *70*, 2003.
- (107) Beaudette, N. V.; Langerman, N. *Anal. Biochem.* **1978**, *90*, 693.
- (108) Spink, C.; Wadso, I. *Methods Biochem Anal* **1976**, *23*, 1.
- (109) Wiseman, T.; Williston, S.; Brandts, J. F.; Lin, L.-N. *Anal. Biochem.* **1989**, *179*, 131.
- (110) Freire, E.; Mayorga, O. L.; Straume, M. *Anal. Chem.* **1990**, *62*, 950A.
- (111) Freyer, M. W.; Lewis, E. A. *Methods in Cell Biology*; Dr. John, J. C., Dr. H. William Detrich, III, Eds.; Academic Press: 2008; Vol. Volume 84, p 79.
- (112) Eatough, D. J.; Lewis, E. A.; Hansen, L. D. *Analytical Solution Calorimetry*; Grime, K., Ed.; John Wiley & Sons: New York, NY, 1985.
- (113) Cohlberg, J. A. *J. Chem. Educ.* **1979**, *56*, 512.
- (114) Fairweather, J. K.; Faijes, M.; Driguez, H.; Planas, A. *ChemBioChem* **2002**, *3*, 866.

References

- (115) Yang, M.; Davies, Gideon J.; Davis, Benjamin G. *Angew. Chem. Int. Ed.* **2007**, *46*, 3885.
- (116) Bain, J. H. *B Sc (Hons)*, University of Sydney, 2006.
- (117) Yang, M.; Brazier, M.; Edwards, R.; Davis, B. G. *ChemBioChem* **2005**, *6*, 346.
- (118) Liang, W. J.; Wilson, K. J.; Xie, H.; Knol, J.; Suzuki, S.; Rutherford, N. G.; Henderson, P. J.; Jefferson, R. A. *J. Bacteriol.* **2005**, *187*, 2377.
- (119) Bowers, L. D.; Johnson, P. R. *BBA-Enz* **1981**, *661*, 100.
- (120) Kim, D. H.; Jin, Y. H.; Jung, E. A.; Han, M. J.; Kobashi, K. *Biol. Pharm. Bull.* **1995**, *18*, 1184.
- (121) Lin, H.; Tao, H.; Cornish, V. W. *J. Am. Chem. Soc.* **2004**, *126*, 15051.
- (122) Tao, H.; Peralta-Yahya, P.; Decatur, J.; Cornish, V. W. *ChemBioChem* **2008**, *9*, 681.
- (123) Tao, H.; Peralta-Yahya, P.; Lin, H.; Cornish, V. W. *Bioorg. Med. Chem.* **2006**, *14*, 6940.
- (124) Mayer, C.; Jakeman, D. L.; Mah, M.; Karjala, G.; Gal, L.; Warren, R. A. J.; Withers, S. G. *Chem. Biol.* **2001**, *8*, 437.
- (125) Hiyama, K.; Okada, S. *J. Biochem. (Tokyo, Jpn.)* **1976**, *80*, 1201.
- (126) Rye, C. S.; Withers, S. G. *J. Am. Chem. Soc.* **2002**, *124*, 9756.
- (127) Hoefnagel, A. J.; Gunnewegh, E. A.; Downing, R. S.; van Bekkum, H. *J. Chem. Soc., Chem. Commun.* **1995**, 225.
- (128) Ahrland, S.; Karipides, D.; Norén, B. *Acta Chem. Scand.* **1963**, *17*.
- (129) Guyon, J. C.; Jones, B. E.; Britton, D. A. *Microchim. Acta* **1968**, *56*, 1180.
- (130) Takahashi, Y.; Tanaka, D. A. P.; Matsunaga, H.; Suzuki, T. M. *J. Chem. Soc., Perkin Trans. 2* **2002**, 759.
- (131) Alford, W.; Shapiro, L.; White, C. *Anal. Chem.* **1951**, *23*, 1149.
- (132) Matsunaga, H.; Kanno, C.; Yamada, H.; Takahashi, Y.; Suzuki, T. M. *Talanta* **2006**, *68*, 1000.
- (133) Watson, M.; McLeod, M. D.; Wilkinson, S. M. In *Unpublished work*; Australian National University: Canberra, ACT, 2010.
- (134) Ben-David, A.; Shoham, G.; Shoham, Y. *Chem. Biol.* **2008**, *15*, 546.

- (135) Hancock, S. M.; Tarling, C. A.; Withers, S. G. *Anal. Biochem.* **2008**, *382*, 48.
- (136) Lewis, J. G.; Clifford, J. K.; Elder, P. A. *Steroids* **1990**, *55*, 314.
- (137) Takei, H.; Mathumoto, M.; Kambegawa, A.; Toyoura, T.; Saisho, S. *Screening* **1994**, *3*, 153.
- (138) Cooke, D. G.; Binnie, J. E.; Blackwell, L. F. *Steroids* **2007**, *72*, 580.
- (139) Hungerford, N. L.; McKinney, A. R.; Stenhouse, A. M.; McLeod, M. D. *Org. Biomol. Chem.* **2006**, *4*, 3951.
- (140) Hungerford, N. L.; Sortais, B.; Smart, C. G.; McKinney, A. R.; Ridley, D. D.; Stenhouse, A. M.; Suann, C. J.; Munn, K. J.; Sillence, M. N.; McLeod, M. D. *J. Steroid Biochem. Mol. Biol.* **2005**, *96*, 317.
- (141) Laneri, S.; Sacchi, A.; di Frassello, E. A.; Luraschi, E.; Colombo, P.; Santi, P. *Pharm. Res.* **1999**, *16*, 1818.
- (142) McMurry, J. *Organic chemistry*; Brooks/Cole: Pacific Grove, CA, USA, 2000; Vol. 5th Ed.
- (143) Harnsberger, H. F.; Cochran, E. L.; Szmant, H. H. *J. Am. Chem. Soc.* **1955**, *77*, 5048.
- (144) Décréau, R. A.; Marson, C. M.; Smith, K. E.; Behan, J. M. *J. Steroid Biochem. Mol. Biol.* **2003**, *87*, 327.
- (145) Hartmann, R. W.; Hector, M.; Haidar, S.; Ehmer, P. B.; Reichert, W.; Jose, J. *J. Med. Chem.* **2000**, *43*, 4266.
- (146) Göndös, G.; Matkovics, B.; Kovács, Ö. *Microchem. J.* **1964**, *8*, 415.
- (147) Philomin, V.; Vessieres, A.; Gruselle, M.; Jaouen, G. *Bioconjugate Chem.* **1993**, *4*, 419.
- (148) Rosenfeld, R. S.; Rosenberg, B.; Kream, J.; Hellman, L. *Steroids* **1973**, *21*, 723.
- (149) DePuy, C. H.; Ponder, B. W. *J. Am. Chem. Soc.* **1959**, *81*, 4629.
- (150) Beckmann, E. *Ber. Dtsch. Chem. Ges.* **1886**, *19*, 988.
- (151) Corey, E. J.; Knapp, S. *Tetrahedron Lett.* **1976**, *17*, 3667.
- (152) Mino, T.; Fukui, S.; Yamashita, M. *J. Org. Chem.* **1997**, *62*, 734.
- (153) Enders, D.; Hundertmark, T.; Lazny, R. *Synth. Commun.* **1999**, *29*, 27
- (154) Singh, L.; Ram, R. N. *Synth. Commun.* **1993**, *23*, 3139

References

- (155) Geneste, F.; Racelma, N.; Moradpour, A. *Synth. Commun.* **1997**, *27*, 957
- (156) Cicchi, S.; Goti, A.; Brandi, A.; Guarna, A.; De Sarlo, F. *Tetrahedron Lett.* **1990**, *31*, 3351.
- (157) Heravi, M. M.; Bakhtiari, K.; Oskooie, H. A.; Hekmatshoar, R. *Russ. J. Org. Chem.* **2009**, *45*, 863.
- (158) Heravi, M. M.; Ajami, D.; Mohajerani, B.; Tabar-Hydar, K.; Ghassemzadeh, M. *Synth. Commun.* **2002**, *32*, 3325.
- (159) Ghorbani-Choghamarani, A.; Shiri, L.; Zeinivand, J. *Bull. Korean Chem. Soc.* **2008**, *29*, 2496.
- (160) Firouzabadi, H.; Iranpoor, N.; Amani, K. *Synth. Commun.* **2004**, *34*, 3587.
- (161) Dewan, S. K.; Singh, R. *Orient. J. Chem.* **2004**, *20*, 211.
- (162) Dewan, S. K.; Singh, R. *Mater. Sci. Res. India* **2003**, *1*, 91.
- (163) Corey, E. J.; Richman, J. E. *J. Am. Chem. Soc.* **1970**, *92*, 5276.
- (164) Timms, G. H.; Wildsmith, E. *Tetrahedron Lett.* **1971**, *12*, 195.
- (165) Nakano, A.; Ushiyama, M.; Iwabuchi, Y.; Hatakeyama, S. *Adv. Synth. Catal.* **2005**, *347*, 1790.
- (166) Zhang, Y.; Bommuwamy, J.; Sinnott, M. L. *J. Am. Chem. Soc.* **1994**, *116*, 7557.
- (167) Banait, N. S.; Jencks, W. P. *J. Am. Chem. Soc.* **1991**, *113*, 7951.
- (168) Dixon, M. *Biochem. J.* **1953**, *55*, 170.
- (169) Cornish-Bowden, A. *Biochem. J.* **1974**, *137*, 143.
- (170) Wilkinson, G. N. *Biochem. J.* **1961**, *80*, 324.
- (171) Dowd, J. E.; Riggs, D. S. *J. Biol. Chem.* **1965**, *240*, 863.
- (172) Cortés, A.; Cascante, M.; Cárdenas, M. L.; Cornish-Bowden, A. *Biochem. J.* **2001**, *357*, 263.
- (173) Mazur, R. H. *J. Org. Chem.* **1963**, *28*, 248.
- (174) Slomp, G.; Wechter, W. J. *Chem. Ind. (London, U. K.)* **1962**, 41.
- (175) Axelson, M.; Sjövali, J.; Drakenberg, T.; Forsén, S. *Anal. Lett.* **1978**, *11*, 229
- (176) Dvolaitzky, M.; Dreiding, A. S. *Helv. Chim. Acta* **1965**, *48*, 1988.

- (177) Erlanger, B. F.; Borek, F.; Beiser, S. M.; Lieberman, S. *J. Biol. Chem.* **1957**, *228*, 713.
- (178) Blaszczyk, L. C.; McMurry, J. E. *J. Org. Chem.* **1974**, *39*, 258.
- (179) Dordick, J. S. *Curr. Opin. Biotechnol.* **1991**, *2*, 401.
- (180) Klibanov, A. M. *Nature* **2001**, *409*, 241.
- (181) McKinney, A. *Boldenone Undecylenate in Canine Urine*, Australian Racing Forensic Laboratory, 2008.
- (182) Roseman, S.; Distler, J. J.; Moffatt, J. G.; Khorana, H. G. *J. Am. Chem. Soc.* **1961**, *83*, 659.
- (183) Wong, C. H.; Haynie, S. L.; Whitesides, G. M. *J. Org. Chem.* **1982**, *47*, 5416.
- (184) Toone, E. J.; Simon, E. S.; Whitesides, G. M. *J. Org. Chem.* **1991**, *56*, 5603.
- (185) Wolf, S.; Zismann, T.; Lunau, N.; Meier, C. *Chem. Eur. J.* **2009**, *15*, 7656.
- (186) Timmons, S. C.; Jakeman, D. L. *Carbohydr. Res.* **2008**, *343*, 865.
- (187) <http://www.sigmaaldrich.com>; Accessed July, 2010
- (188) Nudelman, A.; Herzig, J.; Gottlieb, H. E.; Keinan, E.; Sterling, J. *Carbohydr. Res.* **1987**, *162*, 145.
- (189) Burchell, B. *Biochem. J.* **1977**, *161*, 543.
- (190) Jäntti, S. E.; Kiriazis, A.; Reinilä, R. R.; Kostianen, R. K.; Ketola, R. A. *Steroids* **2007**, *72*, 287.
- (191) Nishimura, Y.; Maeda, S.; Ikushiro, S.-i.; Mackenzie, P. I.; Ishii, Y.; Yamada, H. *BBA-Gen Subjects* **2007**, *1770*, 1557.
- (192) Basu, N. K.; Ciotti, M.; Hwang, M. S.; Kole, L.; Mitra, P. S.; Cho, J. W.; Owens, I. S. *J. Biol. Chem.* **2004**, *279*, 1429.
- (193) Gregory li, D. H.; Strickland, R. D. *BBA-Enz* **1973**, *327*, 36.
- (194) Bock, K. W.; Josting, D.; Lilienblum, W.; Pfeil, H. *Eur. J. Biochem.* **1979**, *98*, 19.
- (195) Vogel, A. I.; Tatchell, A. R.; Furnis, B. S.; Hannaford, A. J.; Smith, P. W. G. *Vogel's Textbook of Practical Organic Chemistry*; 5th ed.; Prentice Hall, 1996.

References

- (196) Hintikka, L.; Kuuranne, T.; Aitio, O.; Thevis, M.; Schänzer, W.; Kostianen, R. *Steroids* **2008**, *73*, 257.
- (197) Luukkanen, L.; Elovaara, E.; Lautala, P.; Taskinen, J.; Vainio, H. *Pharmacology & Toxicology* **1997**, *80*, 152.
- (198) Sten, T.; Bichlmaier, I.; Kuuranne, T.; Leinonen, A.; Yli-Kauhaluoma, J.; Finel, M. *Drug Metab. Dispos.* **2009**, *37*, 417.
- (199) Turgeon, D.; Carrier, J.-S.; Levesque, E.; Hum, D. W.; Belanger, A. *Endocrinology* **2001**, *142*, 778.
- (200) Matern, H.; Matern, S.; Schelzig, C.; Gerok, W. *FEBS Lett.* **1980**, *118*, 251.
- (201) Schomburg, D. *BRENDA Enzyme Database 2010.2*; Technische Universität Braunschweig <http://www.brenda-enzymes.org/>
- (202) Iwano, H.; Yokota, H.; Ohgiya, S.; Yuasa, A. *Arch. Biochem. Biophys.* **1999**, *363*, 116.
- (203) Coughtrie, M. W. H.; Burchell, B.; Bend, J. R. *Anal. Biochem.* **1986**, *159*, 198.
- (204) Starlard-Davenport, A.; Xiong, Y.; Bratton, S.; Gallus-Zawada, A.; Finel, M.; Radomska-Pandya, A. *Steroids* **2007**, *72*, 85.
- (205) Yin, H.; Bennett, G.; Jones, J. P. *Chem.-Biol. Interact.* **1994**, *90*, 47.
- (206) Thevis, M.; Opfermann, G.; Schmickler, H.; Schänzer, W. *J. Mass Spectrom.* **2001**, *36*, 998.
- (207) Smith, E. R.; Breuer, H. *Biochem. J.* **1963**, *88*, 168.
- (208) Laemmli, U. K. *Nature* **1970**, *227*, 680.
- (209) Gasteiger, E.; Hoogland, C.; Gattiker, A.; Duvaud, S.; Wilkins, M. R.; Appel, R. D.; Bairoch, A. *The Proteomics Handbook*; Walker, J. M., Ed.; Humana Press: 2005, p 571.
- (210) Qiagen *QIAprep Miniprep Handbook*, 2006.
- (211) Vogel, A. I.; Tatchell, A. R.; Furnis, B. S.; Hannaford, A. J.; Smith, P. W. G. *Vogel's Textbook of Practical Organic Chemistry*; 5th ed.; Prentice Hall, 1996, 452.
- (212) Wolfrom, M. L.; Thompson, A.; Galkowski, T. T. *J. Am. Chem. Soc.* **1951**, *73*, 4093.
- (213) Brauns, D. H. *J. Am. Chem. Soc.* **1923**, *45*, 833.

- (214) Kitahata, S.; Brewer, C. F.; Genghof, D. S.; Sawai, T.; Hehre, E. J. *J. Biol. Chem.* **1981**, *256*, 6017.
- (215) Barnett, J. E. G. *Carbohydr. Res.* **1969**, *9*, 21.
- (216) Heeres, A.; van Doren, H. A.; Gotlieb, K. F.; Bleeker, I. P. *Carbohydr. Res.* **1997**, *299*, 221.
- (217) Tsou, K. C.; Seligman, A. M. *J. Am. Chem. Soc.* **1953**, *75*, 1042.
- (218) Keri, R.; Hosamani, K.; Seetharama Reddy, H. *Catal. Lett.* **2009**, *131*, 321.
- (219) López-López, M. A.; Balbuzano-Deus, A.; Rodríguez-Domínguez, J. C.; Hernández, M. M.; Villalobo, A. F.; Reyes, Y. I.; Kirsch, G. *Synlett* **2007**, *2007*, 0649.
- (220) Park, S.; Shin, I. *Org. Lett.* **2007**, *9*, 619.
- (221) Lopez-Lopez, M. A.; Balbuzano-Deus, A.; Rodriguez-Dominguez, J. C.; Hernandez, M. M.; Villalobo, A. F.; Reyes, Y. I.; Kirsch, G. *Synlett* **2007**, 649.
- (222) Seligman, A. M.; Tsou, K.-C.; Rutenburg, S. H.; Cohen, R. B. *J. Histochem. Cytochem.* **1954**, *2*, 209.
- (223) Chen, W.-T.; Liu, M.-C.; Yang, Y.-S. *Anal. Biochem.* **2005**, *339*, 54.
- (224) Escandar, G. M.; Boldrini, M. A. *Talanta* **2001**, *53*, 851.
- (225) Wurm, G.; Lachmann, C. *Arch. Pharm. (Weinheim, Ger.)* **1974**, *307*, 695.
- (226) *User Manual 716001391 Rev C*; Waters Corporation: Milford, MA, USA, 2008, p 1.

~ Chapter 11 ~

**Publications arising
from this work**

Escherichia coli Glucuronylsynthase: An Engineered Enzyme for the Synthesis of β -Glucuronides

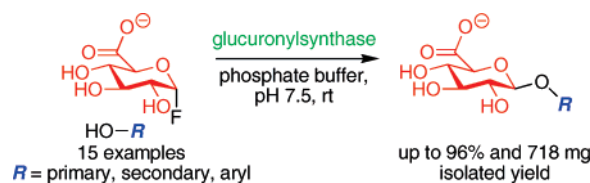
Shane M. Wilkinson,[†] Chu W. Liew,[‡] Joel P. Mackay,[‡] Hamzah M. Salleh,^{§,||}
Stephen G. Withers,[§] and Malcolm D. McLeod^{*,†}

School of Chemistry, University of Sydney, NSW 2006, Australia, School of Molecular and Microbial Biosciences, University of Sydney, NSW 2006, Australia, and Department of Chemistry, University of British Columbia, Vancouver, BC V6T 1Z1, Canada

m.mcleod@rsc.anu.edu.au

Received February 6, 2008

ABSTRACT



The glycosynthase derived from *E. coli* β -glucuronidase catalyzes the glucuronylation of a range of primary, secondary, and aryl alcohols with moderate to excellent yields. The procedure provides an efficient, stereoselective, and scalable single-step synthesis of β -glucuronides under mild conditions.

The formation of glucuronide conjugates during phase II metabolism is a major pathway for the elimination of xenobiotic and some endobiotic compounds from the body.¹ The identification, quantification, and pharmacological evaluation of these metabolites is essential in many fields including sports drug testing,² the detection of agricultural residues,³ and drug development,¹ leading to a significant demand for glucuronide standards.

The preparation of glucuronides presents significant challenges for existing methods of glucuronylation.⁴ Chemical methods⁵ of glucuronylation are based on the Koenigs–Knorr reaction or related procedures but often suffer from poor yields and side reactions due to the low reactivity of glucuronic acid derived glycosyl donors^{4,5} and require one or more deprotection steps to liberate free glucuronide. Enzymatic methods⁶ of synthesis employ uridine 5'-diphosphoglucuronosyl transferases (UGTs): a superfamily of

[†] School of Chemistry, University of Sydney. Current address: Research School of Chemistry, Australian National University, Canberra, ACT 0200, Australia.

[‡] School of Molecular and Microbial Biosciences, University of Sydney.
[§] University of British Columbia.

^{||} Current address: Department of Biotechnology Engineering, International Islamic University Malaysia, Kuala Lumpur, 53100, Malaysia.

(1) (a) Shipkova, M.; Wieland, E. *Clin. Chim. Acta* **2005**, *358*, 2. (b) Wells, P. G.; Mackenzie, P. I.; Chowdhury, J. R.; Guillemette, C.; Gregory, P. A.; Ishii, Y.; Hansen, A. J.; Kessler, F. K.; Kim, P. M.; Chowdhury, N. R.; Ritter, J. K. *Drug Metab. Dispos.* **2004**, *32*, 281.

(2) Schänzer, W.; Donike, M. *Anal. Chim. Acta* **1993**, *275*, 23.

(3) (a) Kim, H.-J.; Ahn, K. C.; Ma, S. J.; Gee, S. J.; Hammock, B. D. *J. Agric. Food Chem.* **2007**, *55*, 3750. (b) Hebestreit, M.; Flenker, U.; Buisson, C.; Andre, F.; Le Bizec, B.; Fry, H.; Lang, M.; Weigert, A. P.; Heinrich, K.; Hird, S.; Schanzer, W. *J. Agric. Food Chem.* **2006**, *54*, 2850.

(4) (a) Kaspersen, F. M.; Van Boeckel, C. A. A. *Xenobiotica* **1987**, *17*, 1451. (b) Stachulski, A. V.; Jenkins, G. N. *Nat. Prod. Rep.* **1998**, *15*, 173. (c) Stachulski, A. V.; Harding, J. R.; Lindon, J. C.; Maggs, J. L.; Park, B. K.; Wilson, I. D. *J. Med. Chem.* **2006**, *49*, 6931.

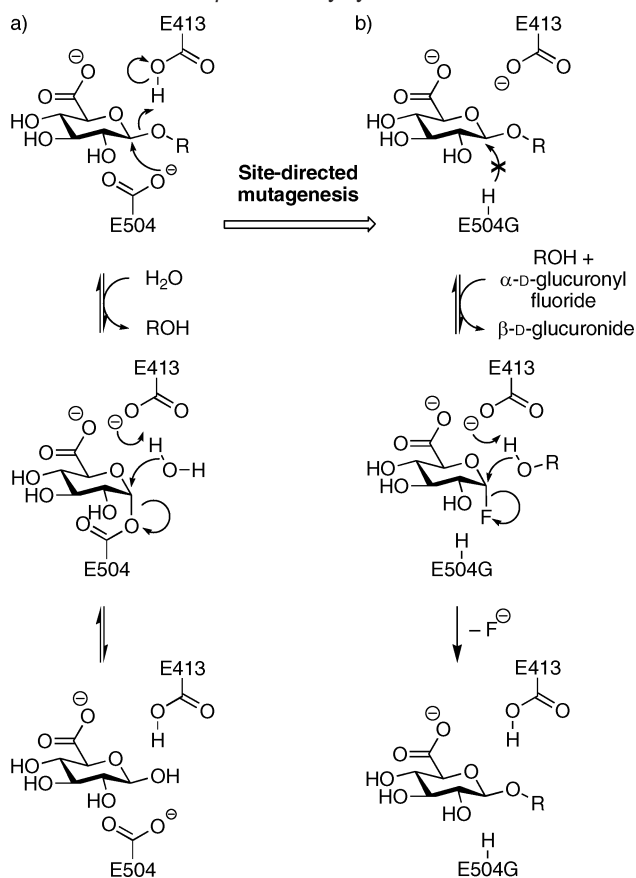
(5) For recent chemical synthesis, see: (a) Engstrom, K. M.; Daanen, J. F.; Wagaw, S.; Stewart, A. O. *J. Org. Chem.* **2006**, *71*, 8378. (b) Harding, J. R.; King, C. D.; Perrie, J. A.; Sinnott, D.; Stachulski, A. V. *Org. Biomol. Chem.* **2005**, *3*, 1501. (c) Poláková, M.; Pitt, N.; Tosin, M.; Murphy, P. V. *Angew. Chem., Int. Ed.* **2004**, *43*, 2518.

(6) For recent enzymic synthesis, see: (a) Jäntti, S. E.; Kiriazis, A.; Reinilä, R. R.; Kostiaainen, R. K.; Ketola, R. A. *Steroids* **2007**, *72*, 287. (b) Khymenets, O.; Joglar, J.; Clapés, P.; Parella, T.; Covas, M.-I.; de la Torre, R. *Adv. Synth. Catal.* **2006**, *348*, 2155. (c) Kuuranne, T.; Aitio, O.; Vahermo, M.; Elovaara, E.; Kostiaainen, R. *Bioconjugate Chem.* **2002**, *13*, 194.

enzymes responsible for glucuronylation in the body.^{7,8} This procedure provides a mild and stereospecific synthesis in a single step. However, UGTs are substrate-specific to the acceptor alcohol and practical considerations often limit this procedure to small scale syntheses. Given the limitations associated with existing methods, the development of improved glucuronylation protocols is an important goal.

Escherichia coli β -glucuronidase (EC 3.2.1.31) is a member of the retaining β -glycosidase family 2 and catalyzes the hydrolytic cleavage of terminal β -glucuronide residues. The enzyme has found application in the field of analytical chemistry for the deconjugation of a broad range of glucuronide metabolites. The enzyme active site contains two key catalytic residues. The side chain of glutamic acid 504 (E504)⁹ acts as a nucleophile, and glutamic acid 413 (E413) is responsible for general acid/base catalysis in a double-displacement mechanism (Scheme 1a). As demonstrated for

Scheme 1. Proposed Mechanism of Action of (a) *E. coli* WT β -Glucuronidase and (b) the *E. coli* E504G β -Glucuronylsynthase



a range of other retaining β -glycosidase enzymes,^{10,11} mutation of E504 to a non-nucleophilic glycine (E504G), alanine

(7) Mulder, G. J. *Annu. Rev. Pharmacol. Toxicol.* **1992**, 32, 25.

(8) Werschkun, B.; Wendt, A.; Thiem, J. J. *Chem. Soc., Perkin Trans. I* **1998**, 3021.

(9) Wong, A. W.; He, S.; Withers, S. G. *Can. J. Chem.* **2001**, 79, 510.

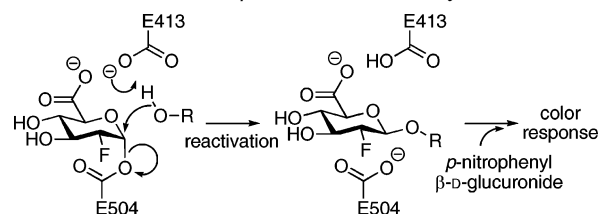
(10) Mackenzie, L. F.; Wang, Q.; Warren, R. A. J.; Withers, S. G. *J. Am. Chem. Soc.* **1998**, 120, 5583.

(E504A), or serine (E504S) residue disables the hydrolytic pathway (Scheme 1b). However, the resulting glycosynthase enzyme can catalyze the formation of glucuronide product from α -D-glucuronyl fluoride (**1**) and an acceptor alcohol substrate. In this paper, we report the development of a conceptually distinct approach, based on the glycosynthase^{10,11} derived from *E. coli* β -glucuronidase, for the mild, single-step synthesis of glucuronides that is liberated from the many drawbacks associated with contemporary procedures.

The E504G, E504A, and E504S glucuronylsynthase mutants were created using standard overlap mutagenesis, subcloned into the pET28a(+) expression vector and transformed into a β -glucuronidase-deficient strain of *E. coli* (GMS407(DE3)). The wild-type (WT) *E. coli* β -glucuronidase was also expressed in the same manner.

The aglycon specificity of *E. coli* glucuronidase and of the putative glycosynthase enzymes was determined using an established spectrophotometric screening protocol.^{12,13} This screen employs WT β -glucuronidase inactivated with 2-deoxy-2-fluoro- β -D-glucuronyl fluoride.¹⁴ A panel of 123 alcohol acceptors was evaluated in parallel for their ability to reactivate this inactivated enzyme by glucuronyl transfer (Scheme 2).¹² Surprisingly, of the 54 carbohydrate

Scheme 2. Acceptor Screening by Reactivation of Inactivated *E. coli* WT β -Glucuronidase Enzyme



acceptors screened, none gave significant reactivation of the inactivated enzyme relative to control. In contrast, thirteen of the 69 alcohol acceptors screened significantly enhanced reactivation rates (2–8 \times control). The thirteen alcohols identified by this screen included a range of primary and cyclic secondary aliphatic alcohols, substituted benzyl alcohols, and isomeric naphthalene methanols (Table 1, **2a–m**). The screening suggested an unusual preference for non-carbohydrate based acceptors to occupy the aglycon binding site of WT β -glucuronidase and glycosynthase enzymes.

Microgram scale reactions to identify glycosynthase activity were performed with the 13 alcohols (**2a–m**), α -D-glucuronyl fluoride **1**,¹⁵ and the three potential glucuronyl-

(11) For a review on glycosynthases, see: Williams, S. J.; Withers, S. G. *Aust. J. Chem.* **2002**, 55, 3.

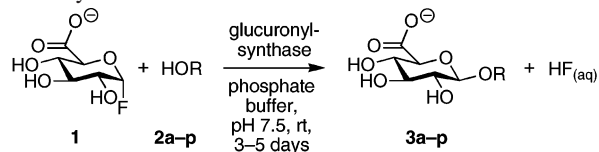
(12) Blanchard, J. E.; Withers, S. G. *Chem. Biol.* **2001**, 8, 627.

(13) The details of the screening protocol and the full list of alcohols used in the screen is reported in the Supporting Information.

(14) Wong, A. W.; He, S.; Grubb, J. H.; Sly, W. S.; Withers, S. G. *J. Biol. Chem.* **1998**, 273, 34057.

(15) Prepared by TEMPO-mediated oxidation of α -D-glucopyranosyl fluoride. Synthetic procedures and spectroscopic data are reported in the Supporting Information.

Table 1. *E. coli* Glucuronylsynthase-Catalyzed Glucuronylation



entry ^a	HOR 2	additive	yield of 3 (%) ^b
a		none	60
b		DMSO ^c	37
c		DMSO ^c	67
d		DMSO ^c	44
e		DMSO ^d	53
f		none none	93 96 ^e
g		none	59
h		DMSO ^c	71
i		none	84 (38)
j		DMSO ^d DDM ^f	39 42
k		none DDM ^g	40 50
l		DMSO ^d	67
m		DMSO ^d DDM ^h	42 (30) 48
n		none	NR
o		none	13
p		none ⁱ DMSO ^{d,i} DDM ^{k,j}	5 17 26

^a Reactions were performed using α -D-glucuronyl fluoride **1** (1.1–1.2 equiv), E504G glucuronylsynthase (0.1 mg mL⁻¹) in 50 mM sodium phosphate buffer, pH 7.5 unless otherwise stated. ^b Yield in parentheses denotes the yield obtained from the alanine glucuronylsynthase (E504A). ^c 12.5% v/v. ^d 25% v/v. ^e Reaction performed on a 2.5 mmol scale. ^f 2% w/v. ^g 0.5% w/v. ^h 1% w/v. ⁱ Saturated acceptor (1.4 mg mL⁻¹), E504G (0.2 mg mL⁻¹), and 100 mM sodium phosphate buffer, pH 7.5 was used. ^j 2.5% w/v.

synthase enzymes (E504A, E504G, and E504S). Glucuronide products **3a–m** were identified by ESI-MS for all 13 alcohols in the presence of the glycine (E504G) and alanine (E504A) mutants. No product formation was observed in the

absence of enzyme or for the serine mutant (E504S), which was not examined further.

To explore the synthetic potential of the glycosynthase enzymes, reactions involving the 13 alcohol acceptors (**2a–m**) were performed on a preparative scale (5–10 mg) in the presence of the E504G or E504A glucuronylsynthase mutants. The E504G mutant cleanly afforded the β -glucuronide products **3a–m** in 37–93% isolated yield (Table 1, entries a–m), with the E504A mutant affording lower yields in the cases examined (entries i and m). The low aqueous solubility of a number of acceptor alcohols was overcome in two ways. Dimethyl sulfoxide (DMSO) was used as cosolvent in concentrations of up to 25% v/v (entries b–e, h, j, l, m), with the enzyme retaining useful activity at these levels. The nonionic detergent, *n*-dodecyl β -maltoside (DDM), was also found to be effective at low concentrations resulting in improved yields (entries j, k, m). No oligomer formation was detected in these reactions, consistent with the observation that carbohydrates do not serve as efficient acceptors in the screen of aglycon specificity. The glucuronylation of phenylethanol **2f** on a large scale afforded the desired glucuronide **3f** in 96% yield (718 mg).

The synthesis reaction was also attempted with ethanol and phenol; two potential acceptors that formed part of the screen but that were not identified as hits. Indeed, ethanol failed to afford the glucuronide product (entry n), while a small quantity of phenyl β -D-glucuronide (**3m**) was isolated in 13% yield (entry o) using the E504G glucuronylsynthase. The low yield of this reaction can be rationalized by the poor nucleophilicity of phenol but also hints at a broader substrate scope for the glycosynthase mutants.

To further demonstrate the scope of the engineered glycosynthase enzyme, the reaction was performed on the steroid hormone dehydroepiandrosterone (DHEA, **2p**). This substrate was only partially soluble in 25% DMSO or 2.5% DDM solutions, so the reaction was performed with the steroid as a suspension (Table 1, entry p). The glucuronide (**3p**) was obtained in 5% yield in the absence of additives, 17% yield using DMSO and 26% using DDM with 73% recovery of residual starting material. Although of modest yield, these results illustrate the promise of the glucuronylsynthase enzyme for the synthesis of a range of important glucuronide products on a scale sufficient for modern analytical methods.

This glucuronylsynthase, the latest addition to the glycosynthase range, has been shown to catalyze the glucuronylation of a range of alcohols with moderate to excellent yields. This new procedure provides an efficient, stereoselective, and scalable single-step synthesis of β -glucuronides under mild conditions. It is envisaged that this alternative method of synthesis will assist to meet the demand for glucuronide standards required for analytical purposes. Further engineering will be directed to increasing the substrate scope and improving the catalytic efficiency of the glucuronylsynthase enzyme.

Acknowledgment. Dr. Kelvin Picker, School of Chemistry, University of Sydney, is acknowledged for assistance

with affinity chromatography and MS. We thank the University of Sydney and the Natural Sciences and Engineering Council of Canada for financial support.

Supporting Information Available: Protein expression procedures, experimental procedures, spectroscopic data and

^1H and ^{13}C NMR spectra for compounds **1** and **3a–p**. This material is available free of charge via the Internet at <http://pubs.acs.org>.

OL8002767

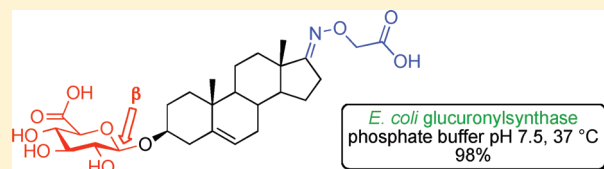
Experimental and Kinetic Studies of the *Escherichia coli* Glucuronylsynthase: An Engineered Enzyme for the Synthesis of Glucuronide Conjugates

Shane M. Wilkinson, Morgan A. Watson, Anthony C. Willis, and Malcolm D. McLeod*

Research School of Chemistry, Australian National University, Canberra, ACT 0200, Australia

Supporting Information

ABSTRACT: The detection and study of glucuronide metabolites is essential in many fields including pharmaceutical development, sports drug testing, and the detection of agricultural residues. Therefore, the development of improved methods for the synthesis of glucuronide conjugates is an important aim. The glycosynthase derived from *E. coli* β -glucuronidase provides an efficient, scalable, single-step synthesis of β -glucuronides under mild conditions. In this article we report on experimental and kinetic studies of the *E. coli* glucuronylsynthase, including the influence of acceptor substrate, pH, temperature, cosolvents, and detergents, leading to optimized conditions for glucuronide synthesis. Enzyme kinetics also reveals that both substrate and product inhibition may occur in glucuronylsynthase reactions but that these effects can be ameliorated through the judicious choice of acceptor and donor substrate concentrations. An investigation of temporary polar substituents was conducted leading to improved aqueous solubility of hydrophobic steroidal acceptors. In this way the synthesis of the steroidal metabolite dehydroepiandrosterone 3- β -D-glucuronide was achieved in three steps and 86% overall yield from dehydroepiandrosterone.



Conjugation with glucuronic acid during phase II metabolism is a major pathway for the elimination of hydrophobic xenobiotic and endogenous compounds in mammalian systems.¹ The identification, quantification, and pharmacological evaluation of these metabolites is essential for many fields including drug development,¹ sports drug testing,² and the detection of agricultural residues.³ This creates a significant demand for the synthesis of glucuronide conjugates **1** as standards.

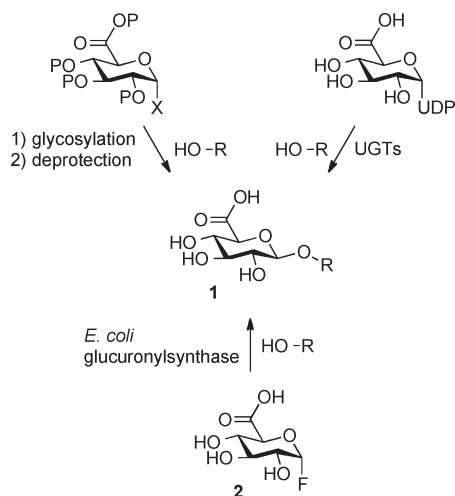
The preparation of glucuronides provides a significant challenge for existing methods of glucuronylation (Scheme 1).⁴ Chemical methods⁵ of glucuronylation based on the Koenigs–Knorr reaction or more recent procedures often suffer from poor yields and side reactions due to the low reactivity of glucuronic acid derived glycosyl donors^{4,5} and require one or more deprotection steps to liberate free glucuronide. Enzymatic methods⁶ of synthesis employ uridine 5'-diphosphoglucuronosyl transferases (UGTs), a superfamily of enzymes responsible for glucuronylation in the body.¹ This procedure provides a mild and stereospecific synthesis in a single step. However, UGTs are substrate-specific to the acceptor alcohol, and practical considerations often limit this procedure to small scale syntheses. Given the limitations associated with existing methods, the development of improved glucuronylation protocols is an important goal.

Recently we reported a distinct strategy for the synthesis of glucuronides based on the glycosynthase derived from *Escherichia coli* β -glucuronidase (EC 3.2.1.31).⁷ *Escherichia coli* β -glucuronidase is a member of the retaining β -glycosidase

family 2 and catalyzes the hydrolytic cleavage of terminal β -glucuronide residues. The enzyme displays substrate promiscuity and has been widely exploited in the field of analytical chemistry for the deconjugation of glucuronide metabolites.⁸ The enzyme active site contains two key catalytic residues. The side chain of glutamic acid 504 (E504)⁹ acts as a nucleophile, and glutamic acid 413 (E413) is responsible for general acid/base catalysis in a double displacement mechanism (Scheme 2a). As demonstrated for a range of other retaining β -glycosidase enzymes,^{10,11} mutation of the *E. coli* β -glucuronidase catalytic nucleophile to a non-nucleophilic glycine (E504G), alanine (E504A), or serine (E504S) residue disables the hydrolytic pathway (Scheme 2b). However, the resulting glycosynthase enzyme, or glucuronylsynthase, can catalyze the formation of glucuronide product **1** from α -D-glucuronyl fluoride **2** and an acceptor alcohol substrate. Our previous report⁷ detailed the application of a spectrophotometric screening protocol using the wild-type *E. coli* β -glucuronidase to identify likely acceptor alcohol substrates for the glycosynthase mediated reaction, expression of the enzyme, and confirmation of these screening hits with the *E. coli* glucuronylsynthase mutants. In this paper we report details of the glucuronylsynthase development together with a kinetic study of this enzyme mediated transformation and practical improvements to the process for the synthesis of steroidal glucuronides.

Received: October 7, 2010

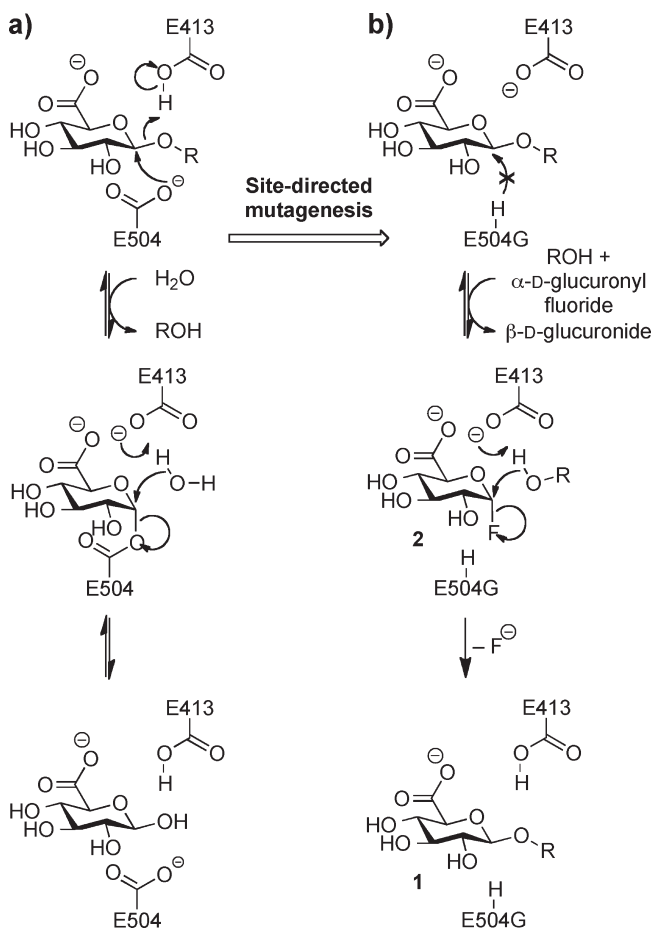
Scheme 1. Preparation of Glucuronide Conjugates 1



RESULTS AND DISCUSSION

The development of the *E. coli* glucuronylsynthase system required reliable access to both the mutant enzymes and the α -D-glucuronyl fluoride **2** donor sugar. The wild-type and three putative glycosynthase mutant enzymes, E504G, E504A, and E504S, were overexpressed in a glucuronidase deficient strain of *E. coli* (GMS407(DE3)) as previously described.⁷ A minor modification of replacing the method of cell lysis from freeze–thaw cycles to French pressure cell press improved the yield of purified protein from 18 to 25 mg L⁻¹ of culture. The enzymes produced by this protocol are histidine tagged (His₆), allowing for purification by nickel affinity chromatography. To assess if this modification has a deleterious effect on enzyme activity, the kinetic competence of the wild-type enzyme was investigated by colorimetric assay using *p*-nitrophenyl β -D-glucuronide as substrate and monitoring enzyme mediated hydrolysis at 410 nm.¹² The observed K_m of 0.17 ± 0.02 mM and k_{cat} of 38 ± 1 s⁻¹ (21 °C, 50 mM phosphate buffer, pH 7.5) compare well with reported literature values determined under similar conditions for hydrolysis by a similar histidine tagged glucuronidase construct ($K_m = 0.20$ mM, $k_{cat} = 68$ s⁻¹, Tris-HCl buffer, pH 7.6)¹³ and also purified native enzyme ($K_m = 0.22$ mM, 37 °C, 76 mM phosphate buffer, pH 7.0).¹⁴

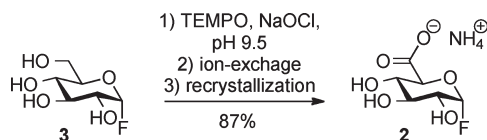
The second key component required for the glucuronylsynthase system is the α -D-glucuronyl fluoride **2** donor sugar. At the outset of this study one reported synthesis¹⁵ provided the potassium salt of this sugar in 65% yield and employed the TEMPO-mediated oxidation of the primary hydroxyl group of α -D-glucosyl fluoride **3**.¹⁶ Purification was achieved by ion exchange, followed by recrystallization to remove potassium acetate buffer salt. In our hands the recrystallization of the sugar from significant amounts of potassium acetate salt proved challenging. This difficulty was circumvented by the use of ammonium hydrogen carbonate as eluting buffer in the anion exchange chromatography, which was readily removed on lyophilization to afford the ammonium salt as an off-white powder. This was further purified by recrystallization from aqueous ethanol to give the α -D-glucuronyl fluoride **2** as the ammonium salt⁷ in 87% yield on a multigram scale (Scheme 3). The identity of sugar **2** was confirmed by single crystal X-ray analysis from

Scheme 2. Proposed Mechanism of Action of (a) *E. coli* Wild-Type β -Glucuronidase and (b) *E. coli* E504G Glucuronylsynthase

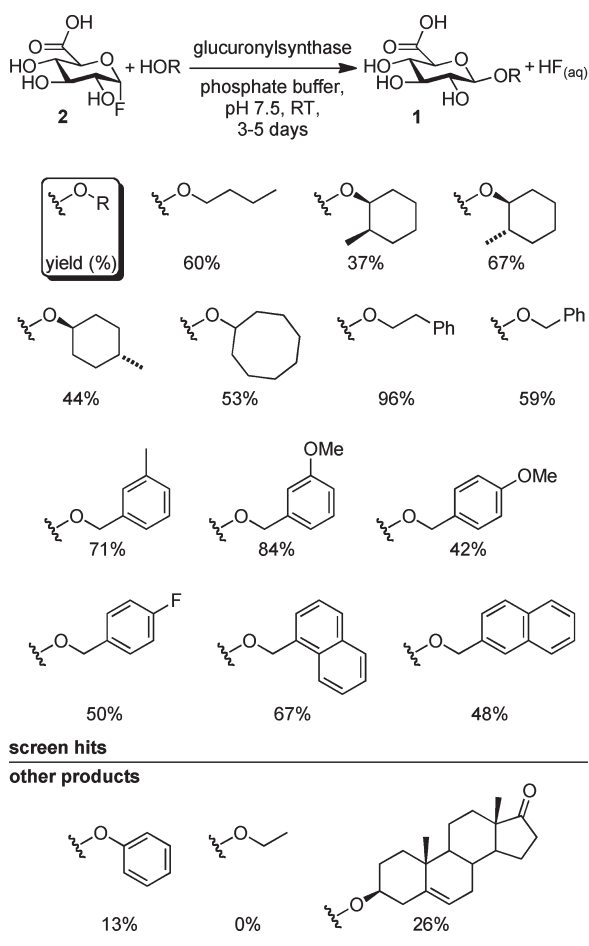
crystals grown in ethanol/water/acetone, which clearly showed the presence of the expected ammonium counterion.¹⁷ Analysis of the material by ¹³C NMR in D₂O solvent confirmed the absence of residual hydrogen carbonate buffer ($\delta \sim 160$).

In our previous investigations the aglycone specificity of the *E. coli* β -glucuronidase and of the putative glycosynthase enzymes was determined using an established spectrophotometric screening protocol against a panel of 123 alcohol acceptors.^{7,11} The 13 alcohols identified by this screen included a range of primary and cyclic secondary aliphatic alcohols, substituted benzyl alcohols, and isomeric naphthalene methanols. None of the 54 carbohydrates tested in the screen were identified as acceptors. Preparative scale synthesis of glucuronide conjugates was conducted from each of the 13 alcohol hits shown in Scheme 4. Of the three glucuronylsynthase mutants, the E504G proved most effective. The E504A mutant provided lower yields in the cases examined, and the E504S mutant did not promote glucuronide synthesis.

Reactions conducted on a small selection of alcohols not identified by the screen also hinted at a broader substrate scope. Phenol, an acceptor present in the initial screen but not identified as a hit, was glucuronylated in a low 13% yield (Scheme 4). Ethanol, an acceptor not included in the original screen, failed to afford detectable amounts of the glucuronide product. Of great

Scheme 3. Synthesis of α -D-Glucuronyl Fluoride 2

Scheme 4. Product Yields for E504G Glucuronylsynthase Mediated Synthesis



interest, the steroid dehydroepiandrosterone (DHEA), an acceptor not included in the original screen, was observed to give a modest 26% yield of the glucuronide product.

The isolated yields from these early experiments showed that the enzyme provided high yields of glucuronide products for some substrates, but this was not universal (Scheme 4). The yields varied considerably for some closely related acceptors such as 3-methoxybenzyl alcohol (84%) and 4-methoxybenzyl alcohol (42%). In a number of instances cosolvents or detergents were used to boost reaction yield for substrates with low aqueous solubility. However, the beneficial effects of cosolvents and detergents were not universally observed. Finally the variation of reaction variables such as substrate concentration provided some surprising results. In the case of 3-methoxybenzyl alcohol doubling the substrate concentration was expected to increase enzyme activity and therefore chemical yield. In fact doubling the

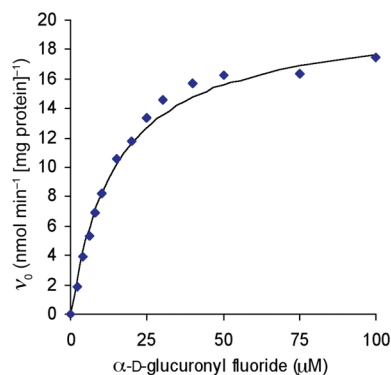


Figure 1. Plot of initial rate versus concentration for varying α -D-glucuronyl fluoride 2 donor with fixed (97 mM) 2-phenylethanol 4 acceptor (21 °C, 100 mM phosphate buffer, pH 7.5). The line represents the data fitted (least-squares) to the Michaelis–Menten equation.

substrate concentration led to a decrease in the isolated yield of glucuronide product from 84% to 64% based on the acceptor alcohol. In order to understand the factors governing this process and to optimize glucuronide synthesis, we embarked on a study of the kinetics of this enzyme catalyst.

The enzyme kinetics of the glucuronylsynthase reaction was conveniently investigated by an automatically sampled reverse-phase HPLC-UV assay monitored at 211 nm. Both alcohol acceptor and glucuronide product concentrations were determined relative to an internal standard over time to give a measure of initial rate (v_0). The first kinetic measurements were conducted at a fixed concentration of 2-phenylethanol 4 acceptor (97 mM), due to limited solubility of this substrate in the aqueous buffer, and a varying concentration of α -D-glucuronyl fluoride 2. At this concentration of alcohol acceptor, the α -D-glucuronyl fluoride 2 donor gave apparent values of $K_m^{\text{app}} = 15.0 \pm 1 \mu\text{M}$ and $k_{\text{cat}}^{\text{app}} = 0.024 \pm 0.01 \text{ s}^{-1}$ by least-squares fitting to the Michaelis–Menten equation (Figure 1). Because of the kinetically subsaturating concentration of the acceptor alcohol, the donor K_m^{app} and $k_{\text{cat}}^{\text{app}}$ values provide an estimate of the kinetic parameters for this substrate. Nevertheless, the donor K_m^{app} is low relative to other glycosynthase enzymes¹⁸ and well below the concentration required for preparative enzyme-mediated synthesis. The $k_{\text{cat}}^{\text{app}}$ or apparent turnover number for this donor, although an underestimate of k_{cat} , is also low relative to other glycosynthases, leaving considerable scope for improving the catalytic efficiency of the enzyme.¹⁸

The kinetic parameters for 2-phenylethanol 4 donor were also investigated at a fixed saturating concentration of α -D-glucuronyl fluoride 2 donor (1 mM). Under these conditions the acceptor alcohol did not kinetically saturate the enzyme due to the limited aqueous solubility of the acceptor alcohol. An estimate of the kinetic parameters for 2-phenylethanol 4 was obtained by fitting the available data to the Michaelis–Menten equation. This indicated a K_m of $140 \pm 10 \text{ mM}$, significantly higher than the highest acceptor substrate concentration tested (107 mM). An estimate of the specificity constant k_{cat}/K_m of $0.30 \pm 0.02 \text{ M}^{-1} \text{ s}^{-1}$ was obtained from the slope of the plot of initial rate against acceptor concentration at low acceptor concentration (Figure 2, Table 1).

The significant difference in estimated Michaelis constants (K_m) for the donor and acceptor substrates is noteworthy. This may reflect the binding interactions for glucuronide substrates at the wild-type β -glucuronidase and the role of this enzyme in

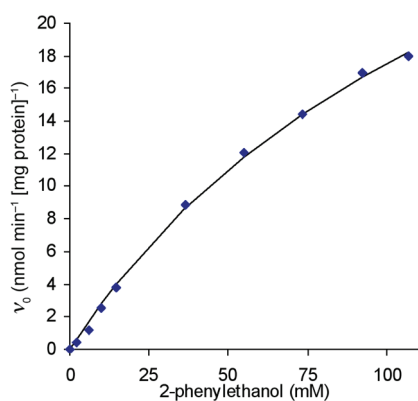
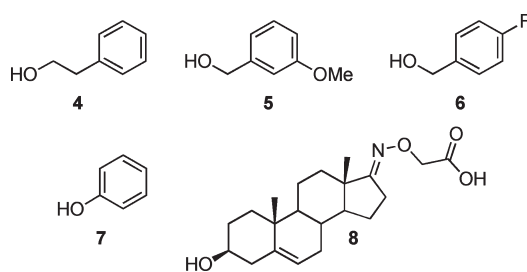


Figure 2. Plot of initial rate versus concentration for varying 2-phenylethanol 4 acceptor with fixed saturating (1 mM) α -D-glucuronyl fluoride 2 donor (21 °C, 100 mM phosphate buffer, pH 7.5). Line represents data fitted (least-squares) to the Michaelis–Menten equation.

Table 1. Estimated Kinetic Parameters for Alcohol Acceptors 4–8 with Constant Saturating (1 mM) α -D-Glucuronyl Fluoride 2 Donor^a



acceptor	k_{cat}/K_m ($\text{M}^{-1} \text{s}^{-1}$)	$k_{\text{cat}}^{\text{max}}$ (s^{-1})	$\text{concn}^{\text{max}}$ (mM)
4	0.30 ± 0.02	0.020	107 ^b
5	1.3 ± 0.1	0.023	55
6	0.62 ± 0.04	0.0081	37
7	0.22 ± 0.01	0.0029	30
8	4.3 ± 0.6	0.0014	0.55

^a 100 mM phosphate buffer, pH 7.5, 21 °C. ^b The solubility limit of 2-phenylethanol 4 in aqueous buffer at 21 °C.

E. coli, the producing organism. *Escherichia coli* is an enteric organism that employs a glucuronide transporter/ β -glucuronidase enzyme system to harvest the glucuronide residue as a carbon source from biliary metabolites excreted in the gut.¹⁹ These glucuronide conjugates are formed from a wide variety of xenobiotic and some endogenous compounds so the primary recognition of the glucuronide conjugate by wild-type β -glucuronidase is expected for the target carbohydrate residue over the variable aglycone portion. For the glucuronylsynthase enzyme, the function of the wild-type enzyme is reflected in a low apparent K_m for the α -D-glucuronyl fluoride 2 donor (K_m^{app} $15.0 \pm 1 \mu\text{M}$) and a much higher estimated K_m for the 2-phenylethanol acceptor 4 (K_m $140 \pm 10 \text{ mM}$).

Kinetic investigations on four additional acceptors 5–8 (Table 1) were conducted at a saturating concentration of α -D-glucuronyl fluoride 2 donor (1 mM). Each of these substrates showed a negative slope of initial rate against acceptor concentration

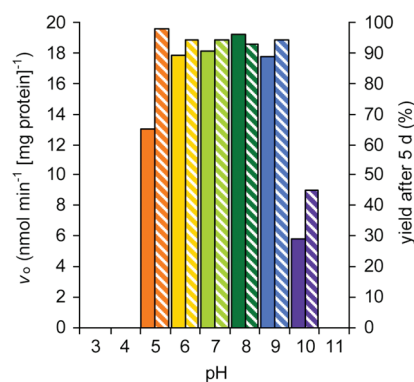


Figure 3. Dependence of initial rate (v_0 , solid bars) and HPLC yield after 5 d (%), lined bars) on pH for reaction of 2-phenylethanol 4 acceptor (107 mM) and α -D-glucuronyl fluoride 2 donor (1 mM) (100 mM phosphate buffer, 21 °C).

at high acceptor concentrations, consistent with substrate inhibition. Because of substrate inhibition the data could not be fitted to the Michaelis–Menten model. Kinetic parameters for these reactions (Table 1) were estimated in two ways. An estimate of acceptor specificity k_{cat}/K_m was obtained from the slope of the plot of initial rate against acceptor concentration at low acceptor concentration. A second measure of enzyme activity, the maximum observed k_{cat} ($k_{\text{cat}}^{\text{max}}$), was calculated from the initial velocity at the concentration of the local maximum ($\text{concn}^{\text{max}}$).¹² It was not possible to reliably estimate K_m from this data.

The kinetic parameters for acceptors 4–7 give some insight into the yields observed in previous synthetic work (Scheme 4).⁷ The observed yields parallel the maximum k_{cat} observed with the exception of 2-phenylethanol 4 ($k_{\text{cat}}^{\text{max}} = 0.020 \text{ s}^{-1}$, 96%), which afforded a yield greater than that of 3-methoxybenzyl alcohol 5 ($k_{\text{cat}}^{\text{max}} = 0.023 \text{ s}^{-1}$, 84%). Comparing estimated specificity constants (k_{cat}/K_m) for acceptor alcohols 4–7 gives 3-methoxybenzyl alcohol 5 ($1.3 \pm 0.1 \text{ M}^{-1} \text{ s}^{-1}$) highest, followed by 4-fluorobenzyl alcohol 6 ($0.62 \pm 0.04 \text{ M}^{-1} \text{ s}^{-1}$), 2-phenylethanol 4 ($0.30 \pm 0.02 \text{ M}^{-1} \text{ s}^{-1}$), and then phenol 7 ($0.22 \pm 0.01 \text{ M}^{-1} \text{ s}^{-1}$) as lowest. Interestingly 2-phenylethanol 4 substrate that provided the highest yield of product (96%) in previous work has among the lowest specificity constant (k_{cat}/K_m). The higher yield observed for 2-phenylethanol 4 can be attributed to the absence of substrate inhibition, which was relevant for all other acceptor alcohols under the high acceptor concentrations ($\sim 100 \text{ mM}$) used in preparative work. The kinetic observations also explain the reduction in yield based on acceptor alcohol that was observed on doubling the substrate concentration of acceptor 3-methoxybenzyl alcohol from 50 mM (84%) to 100 mM (64%). A higher yield is afforded by the reaction performed with substrate concentration close to the local maximum of enzyme activity ($\text{concn}^{\text{max}} = 55 \text{ mM}$). The lowest yielding acceptor phenol 7 (13%) gave the lowest values for $k_{\text{cat}}^{\text{max}}$ and k_{cat}/K_m of the four simple alcohol acceptors investigated. This study highlights the potential for substrate inhibition under the high acceptor alcohol concentrations usually employed for preparative purposes. It indicates that operating at lower substrate concentrations or employing slow addition of substrate may be beneficial for some glucuronylsynthase reactions.

To further improve the glucuronylsynthase reaction, variables such as pH, temperature, and the effect of additives were also investigated. The pH optimum of the enzyme was determined at a fixed concentration of α -D-glucuronyl fluoride 2 donor (1 mM)

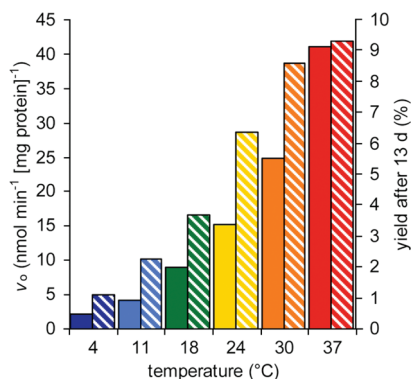


Figure 4. Dependence of initial rate (v_0 , solid bars) and HPLC yield after 13 d (%), lined bars) on temperature for reaction of 3-methoxybenzyl alcohol **5** acceptor (89 mM) and α -D-glucuronyl fluoride **2** donor (89 mM) (100 mM phosphate buffer, pH 7.5).

and 2-phenylethanol **4** acceptor (107 mM). Two measurements of enzyme activity were taken at each pH value. First, the initial rate (v_0) of reaction was measured at low conversion. Second, the reactions were incubated for 5 d, and the yield of product formed at end point was determined by HPLC. High yields were obtained at pH values of 5–9 with highest initial rates across a broad plateau between pH 6 and 9 (Figure 3). The enzyme showed an attenuated initial rate at pH 5 but maintained activity at this pH to afford a high yield of product after 5 d. Studies on the hydrolytic activity of wild-type β -glucuronidase shows a similar broad pH optimum.^{8,20}

Next, the enzyme activity was evaluated at several temperatures (4, 11, 18, 24, 30, 37 °C), at a fixed concentration of α -D-glucuronyl fluoride **2** donor (89 mM) and 3-methoxybenzyl alcohol **5** acceptor (89 mM). The use of 3-methoxybenzyl alcohol as acceptor alcohol and a reduced enzyme concentration (0.02 mg mL⁻¹) relative to typical synthesis experiments was also used to allow the observation of initial rates at higher temperatures and more keenly assess the influence of temperature on overall yield. Two measurements of enzyme activity were taken at each temperature value. First, the initial rate (v_0) of reaction was determined, and as expected there was an increase of initial rate with temperature (Figure 4). Second, the reactions were incubated for 13 d, and the yield of product formed was determined by HPLC. The reactions maintained at 30 and 37 °C gave similar yields after 13 d, suggesting that the higher initial reaction rate observed at the higher temperatures is attenuated over time by a higher rate of enzyme deactivation or α -D-glucuronyl fluoride **2** hydrolysis.^{21,22} The study indicated a temperature of 30–37 °C was preferred for the glucuronyl-synthase reactions.

Next the effect of different cosolvent and detergent additives was investigated. One limitation of the glucuronyl-synthase reaction is the low solubility of many of the hydrophobic acceptor alcohols relative to the glucuronide product. Additives such as detergents or cosolvents generally offer enhancement of substrate solubility but could also potentially have a deleterious effect on enzyme activity and stability.

The effect of different additives on the initial velocity of the enzyme was determined at a saturating concentration of α -D-glucuronyl fluoride **2** donor (1 mM) and a fixed concentration of 2-phenylethanol **4** acceptor (94 mM). All reactions with additives demonstrated a decrease in enzyme activity (Figure 5). Detergents maintained the highest activity with no velocities

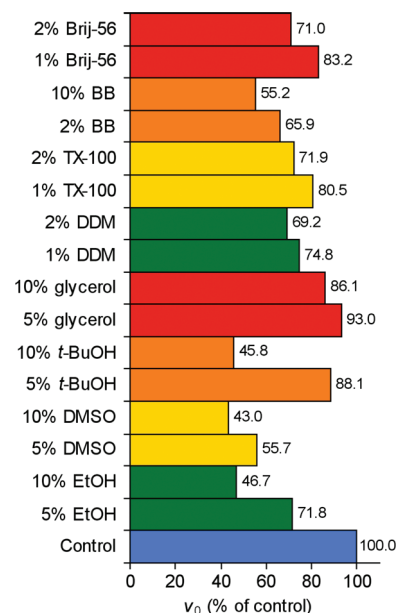
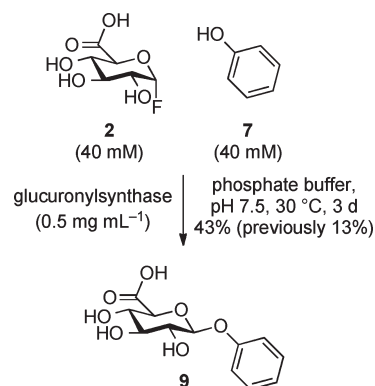


Figure 5. Effect of additives on the initial rate (v_0 as a percentage of the initial velocity for the control) for reaction of 2-phenylethanol **4** acceptor (94 mM) and α -D-glucuronyl fluoride **2** donor (1 mM) (100 mM buffer, pH 7.5, 21 °C). Brij-56, poly(ethylene glycol) hexadecyl ether; BB, commercial protein extraction reagent; TX-100, triton X-100; DDM, dodecyl β -D-maltoside.

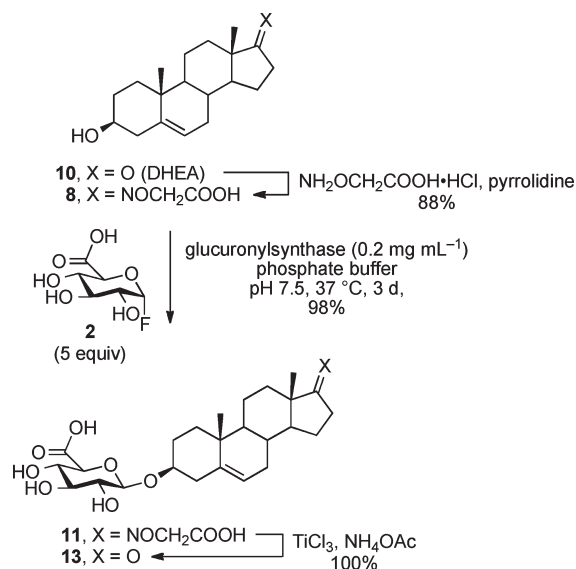
Scheme 5. Synthesis of Phenyl β -D-Glucuronide **9**



falling below 70% of the control (no additives). Organic cosolvents were more detrimental to the enzyme, albeit 5% *tert*-butanol and glycerol demonstrated enzymatic activities greater than 80% of the control.²³

It should be noted that in the cases where the higher acceptor concentrations can be achieved with the aid of cosolvents, this may occur at the cost of lower enzyme activity. Furthermore, high substrate concentrations may not always be advantageous given the observation of substrate inhibition. In summary, the optimal conditions of enzyme mediated synthesis of glucuronides occur at pH 6–9 and temperatures of 30–37 °C. Because of the influence of substrate inhibition, the kinetic behavior of individual acceptors must be investigated in order to optimize additional variables such as acceptor concentration or cosolvent composition.

The reaction of phenol **7** as acceptor alcohol was investigated to gauge the combined effect of the optimized conditions on the

Scheme 6. Synthesis of DHEA 3- β -Glucuronide 13

reaction outcome. This substrate served as a useful benchmark, as it was not identified by the spectrophotometric screening protocol used to identify potential acceptors and the previous synthetic procedure had provided phenyl glucuronide in a low 13% yield. Repeating this reaction with 40 mM substrate concentration, just above the local maximum of enzyme activity, and at 30 °C in pH 7.5 buffer afforded a phenyl β -D-glucuronide **9** in an improved yield of 43% (Scheme 5).

To further test the scope of the glucuronylsynthase reaction, we turned our attention to the synthesis of steroid glucuronides. In previous work the glucuronylation of dehydroepiandrosterone (**10**, DHEA) was achieved in 5% in phosphate buffer, 17% with 25% v/v DMSO cosolvent and 26% with 2.5% w/v dodecyl maltoside (DDM) nonionic detergent additive.⁷ However, in each case the reaction was performed as a suspension of DHEA **10** in the reaction mixture due to the low aqueous solubility of the hydrophobic steroid. The solubility of DHEA **10** has been estimated as 90 μM in aqueous buffer.²⁴

To address the challenge of working with hydrophobic acceptor alcohols, the temporary introduction of polar substituents was investigated as a strategy to boost solubility into a suitable range without the need for organic cosolvents or detergent additives. A three-step process was envisaged involving (1) introduction of a polar substituent, (2) enzyme catalyzed glucuronylation, and (3) cleavage of the polar substituent to give the steroid glucuronide. A range of derivatives were explored with the *O*-(carboxymethyl)oxime derivative appearing most suitable for this purpose.²⁵ The oxime unit is readily generated by condensation of commercially available *O*-(carboxymethyl) hydroxylamine reagent with a carbonyl compound promoted by pyrrolidine (Scheme 6). The charged derivative CMO-DHEA **8** thus formed in 88% had significantly greater solubility than the parent steroid and could be fully dissolved in aqueous buffer up to 2 mM at 21 °C.

The higher aqueous solubility allowed for completion of an enzyme kinetic study with a varying concentration of CMO-DHEA **8** and a saturating concentration of α -D-glucuronyl fluoride **2** donor (1 mM) (Table 1). In common with a number

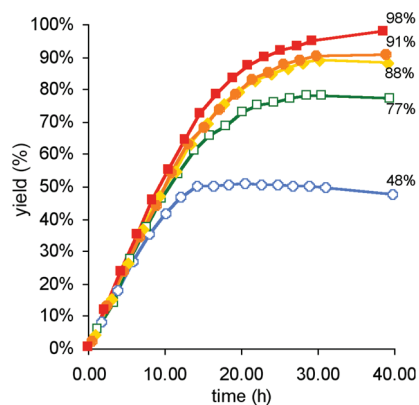


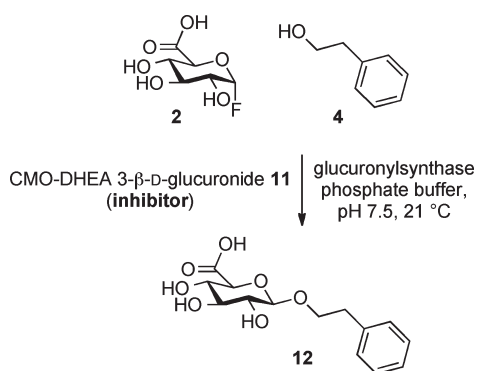
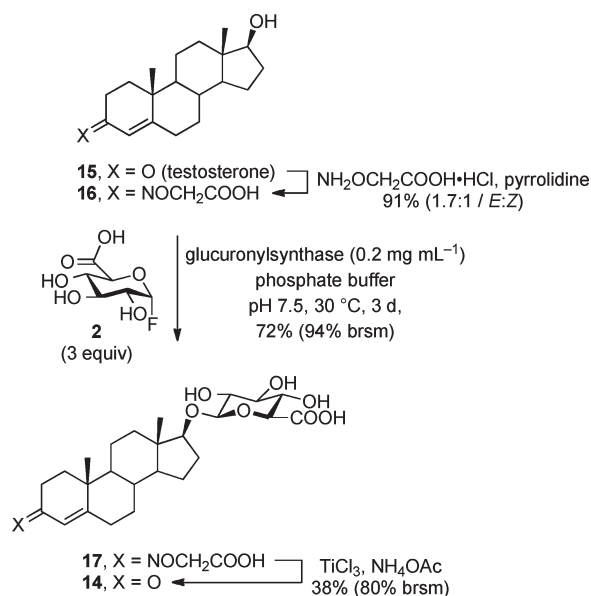
Figure 6. Reaction yield against time for reaction of CMO-DHEA **8** acceptor (1.4 mM) and varying equivalents of α -D-glucuronyl fluoride **2** donor (100 mM phosphate buffer, pH 7.5, 37 °C). (blue circles, 1 equiv; green squares, 2 equiv; yellow squares, 3 equiv; orange squares, 4 equiv; red squares, 5 equiv).

of the simple acceptor alcohols, a plot of initial rate against acceptor concentration showed a negative slope at high acceptor concentrations, consistent with substrate inhibition.¹² Relative to the simple alcohols this substrate gave the highest estimated k_{cat}/K_m ($4.3 \pm 0.6 \text{ M}^{-1} \text{ s}^{-1}$) and smallest $k_{\text{cat}}^{\text{max}}$ (0.0014 s^{-1}) at a concentration of 0.55 mM, with this local maximum occurring below the solubility limit (2 mM).

The CMO-DHEA **8** glucuronylation reaction was followed by HPLC. Using 1 equiv of α -D-glucuronyl fluoride **2** donor gave a reaction profile that reached a 48% HPLC yield (Figure 6). Increasing equivalents of α -D-glucuronyl fluoride **2** afforded higher yields of product with 5 equiv giving 98% HPLC yield. These observations suggested the operation of product inhibition at higher conversion, a phenomenon that could be overcome with increasing concentrations of α -D-glucuronyl fluoride **2** donor.²⁶

To assess this product inhibition, the influence of increasing concentrations of CMO-DHEA 3- β -D-glucuronide **11** as inhibitor on the glucuronylsynthase reaction between 2-phenylethanol **4** (88 mM) and α -D-glucuronyl fluoride **2** at several concentrations was investigated (Scheme 7). The analysis of reciprocal plots indicated mixed, predominantly competitive inhibition ($K_{\text{ic}} = 71 \mu\text{M}$, $K_{\text{iu}} = 180 \mu\text{M}$) for CMO-DHEA 3- β -D-glucuronide **11**.^{27,28} The observed competitive inhibition constant is higher than the apparent Michaelis constant ($K_m^{\text{app}} = 15 \pm 1 \mu\text{M}$) for α -D-glucuronyl fluoride **2**. The implication of this finding is that higher concentrations of α -D-glucuronyl fluoride **2** should successfully compete for occupancy of the enzyme active site and maintain enzyme activity as product concentration increases. This analysis is borne out in the results presented in Figure 6 with 5 equiv (7 mM) of α -D-glucuronyl fluoride **2** giving a 98% HPLC yield of CMO-DHEA 3- β -D-glucuronide **11**.

To further assess the potential for product inhibition in the glucuronylsynthase reaction, the reverse experiment was conducted. The inhibition derived from increasing concentrations of 2-phenylethyl β -D-glucuronide **12** on the glucuronylsynthase reaction involving CMO-DHEA **8** (0.6 mM) and α -D-glucuronyl fluoride **2** at several concentrations was investigated. In this instance no inhibition was observed for 2-phenylethyl β -D-glucuronide **12** between 0 and 75 mM.²⁹ Interestingly for the reaction of 2-phenylethanol **4** the absence of observable substrate and product inhibition correlates to a high yield of the 2-phenylethyl

Scheme 7. Study of Glucuronylsynthase Reaction Inhibition by CMO–DHEA 3- β -D-Glucuronide 11

Scheme 8. Synthesis of Testosterone 17- β -D-Glucuronide 14


β -D-glucuronide **12** product (96%) using 1.2 equiv of α -D-glucuronyl fluoride donor. For the reaction of CMO–DHEA **8** both substrate and product inhibition are observed in this study. In the former case this can be overcome by selection of a suitable substrate concentration and in the latter case by maintaining a high concentration of the α -D-glucuronyl fluoride donor **2**.

Performing the glucuronylation of CMO–DHEA **8** on a preparative scale under optimized conditions and using 5 equiv of α -D-glucuronyl fluoride donor and 1.9 mM acceptor alcohol gave the glucuronide product **11** in 98% yield (Scheme 6). A single crystal X-ray structure of the disodium salt of the glucuronide **11**, grown from ethyl acetate/methanol/water solution confirmed the expected structure.³⁰ The oxime exists solely as the *E*-isomer and the glycosidic linkage presents as the β anomer. Cleavage of the oxime unit was readily achieved using titanium(III) chloride in aqueous ammonium acetate buffer to regenerate the ketone and afford DHEA 3- β -D-glucuronide **13** in quantitative yield. This three-step sequence afforded the target glucuronide (**45** mg) in 86% yield, which compares favorably with the

previously reported single-step glucuronylsynthase mediated synthesis (26%).⁷ The reaction also compares favorably with the two-step Koenigs–Knorr glycosylation followed by base-promoted deprotection that is reported to afford DHEA 3- β -D-glucuronide **13** in 20% yield.³¹ The UGT catalyzed synthesis of DHEA 3- β -D-glucuronide **13** has not been reported.

The synthesis of testosterone 17- β -D-glucuronide **14** proceeded in a similar manner (Scheme 8). Testosterone **15** was converted to the oxime derivative **16** in 91% yield as a 1:1.7 mixture of *Z* and *E* (major) isomers. This charged derivative **16** had a solubility significantly greater than that of the parent steroid **15** and could be fully dissolved in aqueous buffer up to 10 mM at 21 °C. This smoothly underwent glucuronylation under optimized conditions and using 3 equiv of α -D-glucuronyl fluoride **2** to give the glucuronide product **17** in 72% yield. Partial cleavage of the oxime was achieved using titanium(III) chloride in aqueous ammonium acetate buffer to regenerate the ketone and afford testosterone 17- β -D-glucuronide **14** in 38% yield. The mild reaction conditions allowed recovery of unreacted oxime **17** (53%). No cleavage of the glycosidic bond was observed under the mild reaction conditions and no byproduct was observed from over-reduction of the unsaturated ketone or imine functionality.³² This three-step sequence afforded the target glucuronide in 25% yield. This contrasts with the two-step Koenigs–Knorr glycosylation followed by base-promoted deprotection, which is reported to afford testosterone 17- β -D-glucuronide **14** in 17% yield.³¹ The method can also be compared to a recent report that described the UGT-mediated synthesis of 11 steroid glucuronides.^{6a} The steroid glucuronides were afforded in 13–77% yield to provide 1.1–6.5 mg of product. Pertinent to this study was the synthesis of testosterone 17- β -D-glucuronide **14** in a yield of 77% (6.5 mg). However, drawbacks of this method include the high levels (1 mg mL⁻¹) of rat liver microsomal enzyme that is obtained through animal sacrifice. By contrast the glucuronylsynthase affords testosterone 17- β -D-glucuronide in a yield of 24% (16 mg) over three steps. Furthermore the method uses soluble enzyme (0.2 mg mL⁻¹) that is readily obtained on a large scale by standard methods of protein expression and nickel affinity purification.

CONCLUSION

Improved procedures for the glucuronylsynthase catalyzed synthesis of glucuronide conjugates have been developed. The influence of acceptor substrate, pH, temperature, cosolvents, and detergents on the enzyme activity has been investigated by HPLC/UV. Substrate inhibition was observed for the majority of acceptor alcohols investigated, indicating that the substrate concentration is an important consideration for optimizing enzyme activity. The operation of mixed, predominantly competitive inhibition was observed for the product CMO–DHEA 3- β -D-glucuronide **11** in the glucuronylsynthase reaction of 2-phenylethanol **4** as acceptor. This inhibition could be overcome through the use of higher concentrations of α -D-glucuronyl fluoride **2** donor. The temporary introduction of polar substituents was investigated as a way to increase the solubility of hydrophobic steroidal substrates. In this way the synthesis of DHEA 3- β -D-glucuronide **13** was achieved in three steps and in 86% overall yield from DHEA **10**. The glucuronylsynthase reaction provides a practical alternative to existing methods for the synthesis of glucuronide metabolites. Further engineering

will be directed to increasing the substrate scope and improving the catalytic efficiency of the glucuronylsynthase enzyme.

EXPERIMENTAL SECTION

17-Carboxymethoximino-dehydroepiandrosterone (CMO–DHEA) 8.³³ Pyrrolidine (600 μ L, 7.19 mmol) was added to DHEA 10 (1.00 g, 3.47 mmol) dissolved in dry methanol (40 mL) at 4 °C. After 1 h the solution had turned yellow. Carboxymethoxylamine hemihydrochloride (800 mg, 7.32 mmol) was dissolved in a dry solution of methanol (10 mL) and pyrrolidine (600 μ L, 7.19 mmol) and transferred to the DHEA mixture via cannula with methanol washing (5 mL). The solution immediately cleared and was heated to reflux. The reaction was complete after 6 h. The solvent was removed under reduced pressure, and water (100 mL) was added to the residue. The pH was adjusted to 2 with aqueous hydrochloric acid (2 M), and the white precipitate was extracted with ethyl acetate until all precipitate had dissolved (5 \times 150 mL with sonication required). The organic extracts were combined, washed with water (200 mL), dried over magnesium sulfate, and then evaporated to dryness. Cold chloroform (5 mL) was added to the resulting yellow-white residue (1.15 g). The white precipitate was filtered and washed with cold chloroform (2 \times 3 mL) to afford 17-carboxymethoximino-dehydroepiandrosterone **8** (1.10 g, 88%); mp 215–217 °C (decomp); [α]_D²⁰ –36 (c 1.0, DMSO) {lit.³³ [α]_D²⁴ –37.9 (c 1, EtOH)}; *R*_f 0.38 (7:2:1 ethyl acetate/methanol/water). IR (KBr): 3351 (broad, O–H), 2946, 2910, 2865, 2505 (C–H), 1680 (C=O). ¹H NMR (800 MHz, *d*₆-DMSO): δ 5.28 (1H, s), 4.61 (1H, s, broad), 4.42 (2H, s), 3.26 (1H, obscured, m), 2.46 (1H, dd, *J* = 18.9, 9.0 Hz), 2.38 (1H, m), 2.16 (1H, dd, *J* = 12.9, 2.4 Hz), 2.09 (1H, t, *J* = 12.1 Hz), 1.98 (1H, m), 1.82–1.70 (3H, m), 1.67 (1H, d, *J* = 12.2 Hz), 1.58 (2H, m), 1.51 (1H, m), 1.42 (1H, m), 1.38–1.28 (3H, m), 1.12 (1H, m), 1.02–0.91 (2H, m), 0.96 (3H, s), 0.85 (3H, s), COOH not observed. ¹³C NMR (200 MHz, *d*₆-DMSO): δ 171.3, 170.6, 141.4, 120.1, 70.0, 69.8, 53.5, 49.8, 43.5, 42.2, 36.9, 36.2, 33.8, 31.4, 30.82, 30.78, 25.7, 22.8, 20.2, 19.2, 16.8. LRMS (+ESI) *m/z*: 384 ([M + Na]⁺, 100%). LRMS (–ESI) *m/z*: 360 ([M – H][–], 100%); HRMS (+ESI) calcd for C₂₁H₃₁NO₄Na⁺ ([M + Na]⁺) 384.2151, found 384.2151.

CMO–DHEA 3- β -D-Glucuronide 11. Glucuronylsynthase (4.14 mL, 1.45 mg/mL) was added to a solution containing CMO–DHEA **8** (20 mg, 0.055 mmol, final concentration 1.9 mM) and α -D-glucuronyl fluoride **2** (57.5 mg, 0.270 mmol) in 100 mM sodium phosphate buffer pH 7.5 (25 mL). The reaction was incubated at 37 °C without agitation for 3 days and then dried onto reverse-phase silica. The dried residue was subjected to reverse-phase flash chromatography (25% aqueous acetonitrile + 0.1% formic acid) to isolate CMO–DHEA 3- β -D-glucuronide **11** (29 mg, 98%) as a colorless solid; [α]_D²⁰ –62 (c 1.0, DMSO); *R*_f 0.02 (7:2:1 ethyl acetate/methanol/water). IR (KBr): 3423 (O–H), 2942 (C–H), 1745 (C=O). ¹H NMR (800 MHz, D₂O): δ 5.51 (1H, s), 4.59 (1H, d, *J* = 7.3 Hz), 4.38 (2H, s), 3.72–3.69 (2H, m), 3.52–3.50 (2H, m), 3.27 (1H, t, *J* = 7.1 Hz), 2.63 (1H, dd, *J* = 19.2, 8.3 Hz), 2.52 (1H, m), 2.47 (1H, d, *J* = 12.6 Hz), 2.29 (1H, t, *J* = 12.0 Hz), 2.10 (1H, d, *J* = 11.3 Hz), 2.00–1.92 (2H, m), 1.90–1.84 (2H, m), 1.71–1.60 (4H, m), 1.55 (1H, m), 1.46–1.41 (2H, m), 1.27 (1H, m), 1.10 (1H, t, *J* = 13.0 Hz), 1.06 (3H, s), 1.06–1.02 (1H, m), 0.95 (3H, s). ¹³C NMR (200 MHz, D₂O): δ 178.9, 177.3, 177.2, 143.3, 123.4, 101.7, 81.0, 77.7, 77.7, 74.4, 73.3, 72.9, 55.0, 51.2, 45.6, 39.5, 38.1, 38.0, 34.9, 32.29, 32.27, 30.3, 27.8, 24.2, 21.6, 20.3, 17.7. LRMS (–ESI) *m/z*: 536 ([M – H][–], 100%), 558 ([M – 2H + Na][–], 30). HRMS (–ESI) calcd for C₂₇H₃₇NO₁₀ ([M – H][–]) 536.2496, found 536.2495; calcd for C₂₇H₃₇NO₁₀Na ([M – 2H + Na][–]) 558.2315, found 558.2302.

DHEA 3- β -D-Glucuronide 13.³¹ CMO–DHEA 3- β -D-glucuronide **11** (50 mg, 0.093 mmol) and ammonium acetate (96 mg, 1.2 mmol) were purged with nitrogen, and then dioxane (0.5 mL) and aqueous acetic acid (50%, 38 μ L) were added. In a second flask, titanium trichloride (36 mg, 0.23 mmol) was purged with nitrogen before water (6 mL) was

added. The aqueous titanium trichloride was added via cannula to the stirred CMO–DHEA 3- β -D-glucuronide solution at room temperature. The reaction instantly turned black-violet upon addition and gradually changed to a white-gray as the reaction proceeded. After 2 h, the reaction was deemed complete so the solution was acidified to pH 2 and dried onto silica. The dry residue was subjected to flash chromatography (7:2:1 ethyl acetate/methanol/water +0.1% formic acid) to isolate DHEA 3- β -D-glucuronide **13** (44.8 mg, 100%) as a colorless solid; [α]_D²⁰ –29 (c 0.70, MeOH), (lit.³¹ [α]_D²⁵ –35.5 (c 1, EtOH)); *R*_f 0.25 (7:2:1 ethyl acetate/methanol/water). IR (NaCl): 3369 (O–H), 2938, 2903 (C–H), 1733 (C=O), 1636. ¹H NMR (800 MHz, MeOD): δ 5.42 (1H, d, *J* = 4.9 Hz), 4.45 (1H, d, *J* = 7.8 Hz), 3.80 (1H, d, *J* = 9.7 Hz), 3.58–3.47 (2H, m), 3.38 (1H, t, *J* = 9.1 Hz), 3.20 (1H, t, *J* = 8.4 Hz), 2.48–1.43 (2H, m), 2.29 (1H, m), 2.16–2.07 (3H, m), 2.00–1.87 (3H, m), 1.78 (1H, m), 1.74–1.52 (5H, m), 1.40–1.23 (2H, m), 1.11–1.04 (2H, m), 1.07 (3H, s), 0.90 (3H, s). ¹³C NMR (75 MHz, MeOD/D₂O): δ 225.5, 169.8, 142.1, 122.2, 102.1, 79.7, 77.6, 74.7, 73.5, 72.5, 52.9, 51.6, 39.5, 38.3, 37.9, 36.8, 32.7, 32.5, 31.8, 30.4, 22.7, 21.4, 19.8, 13.9, one carbon overlapping or obscured. LRMS (–ESI) *m/z*: 927 ([2M – H][–], 43%), 463 ([M – H][–], 100). HRMS (–ESI) calcd for C₂₅H₃₅O₈ ([M – H][–]) 463.2338, found 463.2342.

ASSOCIATED CONTENT

S Supporting Information. CIF files for the X-ray crystal structures of α -D-glucuronyl fluoride **2** and CMO–DHEA 3- β -D-glucuronide **11**, protein expression procedures, experimental procedures, spectroscopic data and ¹H and ¹³C NMR spectra for compounds **2**, **8**, **9**, **11**, **13**, **14**, **16** and **17**. This material is available free of charge via the Internet at <http://pubs.acs.org>.

AUTHOR INFORMATION

Corresponding Author

*E-mail: malcolm.mcleod@anu.edu.au.

ACKNOWLEDGMENT

We thank the Australian Government Department of Health and Ageing Anti-Doping Research Program for financial support.

REFERENCES

- (1) (a) Lucaciu, R.; Ionescu, C. *Farmacia* **2005**, *53*, 10–19. (b) Shipkova, M.; Wieland, E. *Clin. Chim. Acta* **2005**, *358*, 2–23. (c) Wells, P. G.; Mackenzie, P. I.; Chowdhury, J. R.; Guillemette, C.; Gregory, P. A.; Ishii, Y.; Hansen, A. J.; Kessler, F. K.; Kim, P. M.; Chowdhury, N. R.; Ritter, J. K. *Drug Metab. Dispos.* **2004**, *32*, 281–290. (d) King, C. D.; Rios, G. R.; Green, M. D.; Tephly, T. R. *Curr. Drug Metab.* **2000**, *1*, 143–161. (e) Mulder, G. J. *Annu. Rev. Pharmacol. Toxicol.* **1992**, *32*, 25–49.
- (2) (a) Thörngren, J.-O.; Östervall, F.; Garle, M. *J. Mass Spectrom.* **2008**, *43*, 980–992. (b) Schulze, J. J.; Lundmark, J.; Garle, M.; Skilving, I.; Ekström, L.; Rane, A. *J. Clin. Endocrinol. Metab.* **2008**, *93*, 2500–2506. (c) Van Eenoo, P.; Lootens, L.; Spaerkeer, A.; Van Thuyne, W.; Deventer, K.; Delbeke, F. T. *J. Anal. Toxicol.* **2007**, *31*, 543–548. (d) Avois, L.; Mangin, P.; Saugy, M. *J. Pharm. Biomed. Anal.* **2007**, *44*, 173–179. (e) Spyridaki, M.-H.; Kiouisi, P.; Vonaparti, A.; Valavani, P.; Zonaras, V.; Zahariou, M.; Sianos, E.; Tsoupras, G.; Georgakopoulos, C. *Anal. Chim. Acta* **2006**, *573–574*, 242–249. (f) Jiménez, C.; Ventura, R.; Williams, J.; Segura, J.; de la Torre, R. *Analyst* **2004**, *129*, 449–455.
- (3) (a) Kim, H.-J.; Ahn, K. C.; Ma, S. J.; Gee, S. J.; Hammock, B. D. *J. Agric. Food Chem.* **2007**, *55*, 3750–3757. (b) Hebestreit, M.; Flenker, U.; Buisson, C.; Andre, F.; Le Bizec, B.; Fry, H.; Lang, M.; Weigert, A. P.; Heinrich, K.; Hird, S.; Schänzer, W. *J. Agric. Food Chem.* **2006**,

54, 2850–2858. (c) Hubert, T. D.; Bernardy, J. A.; Vue, C.; Dawson, V. K.; Boogaard, M. A.; Schreier, T. M.; Gingerich, W. H. *J. Agric. Food Chem.* **2005**, *53*, 5342–5346. (d) Llorach, R.; Tomás-Barberán, F. A.; Ferreres, F. *Eur. Food Res. Technol.* **2005**, *220*, 31–36.

(4) (a) Stachulski, A. V.; Harding, J. R.; Lindon, J. C.; Maggs, J. L.; Park, B. K.; Wilson, I. D. *J. Med. Chem.* **2006**, *49*, 6931–6945. (b) Stachulski, A. V.; Jenkins, G. N. *Nat. Prod. Rep.* **1998**, *15*, 173–186. (c) Kaspersen, F. M.; Van Boeckel, C. A. A. *Xenobiotica* **1987**, *17*, 1451–1471.

(5) For recent chemical synthesis, see: (a) Engstrom, K. M.; Daanen, J. F.; Wagaw, S.; Stewart, A. O. *J. Org. Chem.* **2006**, *71*, 8378–8383. (b) Harding, J. R.; King, C. D.; Perrie, J. A.; Sinnott, D.; Stachulski, A. V. *Org. Biomol. Chem.* **2005**, *3*, 1501–1057. (c) Poláková, M.; Pitt, N.; Tosin, M.; Murphy, P. V. *Angew. Chem., Int. Ed.* **2004**, *43*, 2518–2521. (d) Ferguson, J. R.; Harding, J. R.; Killick, D. A.; Lumbard, K. W.; Scheinmann, F.; Stachulski, A. V. *J. Chem. Soc., Perkin Trans. 1* **2001**, 3037–3041.

(6) For recent enzymic synthesis, see: (a) Hintikka, L.; Kuuranne, T.; Aitio, O.; Thevis, M.; Schänzer, W.; Kostianen, R. *Steroids* **2008**, *73*, 257–265. (b) Jäntti, S. E.; Kiriazis, A.; Reinilä, R. R.; Kostianen, R. K.; Ketola, R. A. *Steroids* **2007**, *72*, 287–296. (c) Khymentis, O.; Joglar, J.; Clapés, P.; Parella, T.; Covas, M.-I.; de la Torre, R. *Adv. Synth. Catal.* **2006**, *348*, 2155–2162. (d) Kuuranne, T.; Aitio, O.; Vahermo, M.; Elovaara, E.; Kostianen, R. *Bioconjugate Chem.* **2002**, *13*, 194–199. (e) Stevenson, D. E.; Hubl, U. *Enzyme Microb. Technol.* **1999**, *24*, 388–396. (f) Werschkun, B.; Wendt, A.; Thiem, J. *J. Chem. Soc., Perkin Trans. 1* **1998**, 3021–3024.

(7) Wilkinson, S. M.; Liew, C. W.; Mackay, J. P.; Salleh, H. M.; Withers, S. G.; McLeod, M. D. *Org. Lett.* **2008**, *10*, 1585–1588.

(8) (a) Gomes, R. L.; Meredith, W.; Snape, C. E.; Sephton, M. A. *J. Pharm. Biomed. Anal.* **2009**, *49*, 1133–1140. (b) Wakabayashi, M.; Fishman, W. H. *J. Biol. Chem.* **1961**, *236*, 996–1001.

(9) Wong, A. W.; He, S.; Withers, S. G. *Can. J. Chem.* **2001**, *79*, 510–518.

(10) Mackenzie, L. F.; Wang, Q.; Warren, R. A. J.; Withers, S. G. *J. Am. Chem. Soc.* **1998**, *120*, 5583–5584.

(11) For reviews on glycosynthases, see: (a) Rakić, B.; Withers, S. G. *Aust. J. Chem.* **2009**, *62*, 510–520. (b) Hancock, S. M.; Vaughan, M. D.; Withers, S. G. *Curr. Opin. Chem. Biol.* **2006**, *10*, 509–519. (c) Williams, S. J.; Withers, S. G. *Aust. J. Chem.* **2002**, *55*, 3–12.

(12) Plots of initial rate against substrate concentration are reported in Supporting Information.

(13) Geddie, M. L.; Matsumura, I. *J. Biol. Chem.* **2004**, *279*, 26462–26468.

(14) Kim, D.-H.; Jin, Y.-H.; Jung, E.-A.; Han, M.-J.; Kobashi, K. *Biol. Pharm. Bull.* **1995**, *18*, 1184–1188.

(15) Heeres, A.; van Doren, H. A.; Gotlieb, K. F.; Bleeker, I. P. *Carbohydr. Res.* **1997**, *299*, 221–227.

(16) Kitahata, S.; Brewer, C. F.; Genghof, D. S.; Sawai, T.; Hehre, E. J. *J. Biol. Chem.* **1981**, *256*, 6017–6026.

(17) The ORTEP diagram and CIF file for the α -D-glucuronyl fluoride **2** crystal structure (CCDC 793479) is provided in Supporting Information.

(18) Glycosynthases derived from *exo*-glycosidases: (a) Ben-David, A.; Bravman, T.; Balazs, Y. S.; Czjzek, M.; Schomburg, D.; Shoham, G.; Shoham, Y. *ChemBioChem* **2007**, *8*, 2145–2151. (b) Hommalai, G.; Withers, S. G.; Chuenchor, W.; Ketudat Cairns, J. R.; Svasti, J. *Glycobiology* **2007**, *17*, 744–753. (c) Fajjes, M.; Saura-Valls, M.; Pérez, X.; Conti, M.; Planas, A. *Carbohydr. Res.* **2006**, *341*, 2055–2065. (d) Nashiru, O.; Zechel, D. L.; Stoll, D.; Mohammadzadeh, T.; Warren, R. A. J.; Withers, S. G. *Angew. Chem., Int. Ed.* **2001**, *40*, 417–420. (e) Mayer, C.; Zechel, D. L.; Reid, S. P.; Warren, R. A. J.; Withers, S. G. *FEBS Lett.* **2000**, *466*, 40–44. Glycosynthases derived from *endo*-glycosidases: (f) Hancock, S. M.; Rich, J. R.; Caines, M. E. C.; Strynadka, N. C. J.; Withers, S. G. *Nat. Chem. Biol.* **2009**, *5*, 508–514. (g) Piens, K.; Henriksson, A.-M.; Gullfot, F.; Lopez, M.; Fauré, R.; Ibatullin, F. M.; Teeri, T. T.; Driguez, H.; Brumer, H. *Org. Biomol. Chem.* **2007**, *5*, 3971–3978. (h) Yang, M.; Davies, G. J.; Davis, B. G. *Angew. Chem.,*

Int. Ed. **2007**, *46*, 3885–3888. (i) Jahn, M.; Stoll, D.; Warren, R. A. J.; Szabó, L.; Singh, P.; Gilbert, H. J.; Ducros, V. M.-A.; Davies, G. J.; Withers, S. G. *Chem. Commun.* **2003**, 1327–1329.

(19) Liang, W.-J.; Wilson, K. J.; Xie, H.; Knol, J.; Suzuki, S.; Rutherford, N. G.; Henderson, P. J. F.; Jefferson, R. A. *J. Bacteriol.* **2005**, *187*, 2377–2385.

(20) (a) Goto, J.; Sato, A.; Suzuki, K.; Nambara, T. *Chem. Pharm. Bull.* **1981**, *29*, 1975–1980. (b) Bowers, L. D.; Johnson, P. R. *Biochim. Biophys. Acta* **1981**, *661*, 100–105.

(21) The first order rate constant for hydrolysis (k_H) of $1.8 \times 10^{-6} \text{ s}^{-1}$ was determined for α -D-glucuronyl fluoride **2** by ^1H NMR analysis (unbuffered D_2O , 37°C). Details are reported in Supporting Information. This hydrolysis rate constant (k_H) is of equivalent magnitude to other reported nonenzymatic glycosyl fluoride hydrolysis: (a) 3-O-cellobiosyl- α -D-glucosyl fluoride $k_H = 2.57 \times 10^{-6} \text{ s}^{-1}$ (50 mM maleate buffer, pH 7.0, 0.1 mM CaCl_2 35°C) Fajjes, M.; Pérez, X.; Pérez, O.; Planas, A. *Biochemistry* **2003**, *42*, 13304–13318. (b) α -D-glucopyranosyl fluoride $k_H = 8.42 \times 10^{-6} \text{ s}^{-1}$ (50 mM sodium acetate buffer, pH 6.0, 40°C) Zhang, Y.; Bommuswamy, J.; Sinnott, M. L. *J. Am. Chem. Soc.* **1994**, *116*, 7557–7563. (c) α -D-glucopyranosyl fluoride $k_H = 1.5 \times 10^{-6} \text{ s}^{-1}$ (5 mM potassium phosphate buffer, 30°C) Banait, N. S.; Jencks, W. P. *J. Am. Chem. Soc.* **1991**, *113*, 7951–7958. The hydrolysis of α -D-glucopyranosyl fluoride is catalyzed by phosphate buffer and is subject to isotope effects. (d) Banait, N. S.; Jencks, W. P. *J. Am. Chem. Soc.* **1991**, *113*, 7958–7963. We are currently investigating the influence of buffer composition on the hydrolysis of α -D-glucuronyl fluoride **2**.

(22) The HPLC reaction yields increased on average 3.1 times from day 4 to day 13 for each temperature regime. The HPLC yield of the reaction held at 37°C for 13 d was 2.9 times greater than that determined at 4 d. Details are reported in Supporting Information.

(23) A more comprehensive study of wild-type *E. coli* β -glucuronidase activity and stability in a wide range of cosolvents and detergents is reported in Supporting Information. Similar results are observed for the influence of cosolvent and detergent activity on both the wild-type glucuronidase and the glucuronylsynthase enzymes. For the effects of cosolvents on immobilized *E. coli* β -glucuronidase activity see ref 20b.

(24) Laneri, S.; Sacchi, A.; di Frassello, E. A.; Luraschi, E.; Colombo, P.; Santi, P. *Pharm. Res.* **1999**, *16*, 1818–1824.

(25) Derivatives investigated included: hydrazone, 2-(2-pyridyl)hydrazone, oxime, *O*-(carboxymethyl)oxime.

(26) Nonenzymatic hydrolysis of α -D-glucuronyl fluoride was excluded as a significant factor in the incomplete reactions on kinetic grounds. See ref 21.

(27) (a) Cortés, A.; Cascante, M.; Cárdenas, M. L.; Cornish-Bowden, A. *Biochem. J.* **2001**, *357*, 263–268. (b) Cornish-Bowden, A. *Biochem. J.* **1974**, *137*, 143–144. (c) Dixon, M. *Biochem. J.* **1953**, *55*, 170–171.

(28) Plots of $1/\nu_0$ against [CMO-DHEA 3- β -D-glucuronide] (Dixon plot), [α -D-glucuronyl fluoride]/ ν_0 against [CMO-DHEA 3- β -D-glucuronide], and $1/i_{0.5}$ against ν_0/V_{max} are reported in Supporting Information.

(29) A plot of initial rate against concentration of 2-phenylethyl β -D-glucuronide **12** (0–75 mM) for the glucuronylsynthase reaction of CMO-DHEA **8** and α -D-glucuronyl fluoride **2** is reported in Supporting Information.

(30) The ORTEP diagram and CIF file of the CMO-DHEA 3- β -D-glucuronide **11** crystal structure (CCDC 793480) is provided in Supporting Information.

(31) Wotiz, H. H.; Smakula, E.; Lichtin, N. N.; Leftin, J. H. *J. Am. Chem. Soc.* **1959**, *81*, 1704–1708.

(32) Blaszcak, L. C.; McMurry, J. E. *J. Org. Chem.* **1974**, *39*, 258–259.

(33) Rosenfeld, R. S.; Rosenberg, B.; Kream, J.; Hellman, L. *Steroids* **1973**, *21*, 723–733.